Bioresorbable Polymer Coated Metallic Stents and Fully Bioresorbable Scaffolds: Benefits and limitations in different coronary lesion subsets

-Clinical and intravascular imaging results-

Jiang Ming Fam

Printed by: Optima Grafische Communicatie, Rotterdam, The Netherlands

Layout by: Optima Grafische Communicatie, Rotterdam, The Netherlands

Cover design by: Jiang Ming Fam

ISBN 978-94-6361-110-7

Bioresorbable Polymer Coated Metallic Stents and Fully Bioresorbable Scaffolds: Benefits and limitations in different coronary lesion subsets

-Clinical and intravascular imaging results-

Bioresorbable polymeer gecoate metalen stents en volledig bioresorbable stents: Voordelen en beperkingen in verschillende subtypen coronaire letsels

-klinische en intravasculaire imaging resultaten-

Proefschrift

Ter verkrijging van de graad van doctor aan de

Erasmus Universiteit Rotterdam

Op gezag van de

rector magnificus

Prof.dr. H.A.P. Pols

en volgens besluit van het College voor Promoties.

De openbare verdediging zal plaatsvinden op

Vrijdag 25 Mei 2018 om 1330 uur

door

Jiang Ming Fam

geboren te Singapore

Erasmus University Rotterdam

Erasmus

Doctoral committee

Promotor: Prof. Dr. R,J M. van Geuns

Reading committee:

Prof. Dr. J. Deckers

Prof. Dr. J.J. Piek

Prof. Dr. G.P. Krestin

Co-promotor: Dr. Y. Onuma

To my family

TABLE OF CONTENTS

Chapter 1 **Introduction** 13

PART I **OPTICAL COHERENCE TOMOGRAPHY (OCT) FOR EVALUATION OF NEW THERAPIES AND IN CLINICAL PRACTICE**

Chapter 2 **Safety of optical coherence tomography in daily practice: a comparison with intravascular ultrasound.** 23
van der Sijde JN, Karanasos A, van Ditzhuijzen NS, Okamura T, van Geuns RJ, Valgimigli M, Ligthart JM, Witberg KT, Wemelsfelder S, **Fam JM**, Zhang B, Diletti R, de Jaegere PP, van Mieghem NM, van Soest G, Zijlstra F, van Domburg RT, Regar E.
Eur Heart J Cardiovasc Imaging. 2017 Apr 1; 18(4):467-474.

Chapter 3 **Optical Coherence Tomography is the way to go.** 33
Jiang Ming Fam, Nienke Simone van Ditzhuijzen, Jors van der Sjide, Antonis Karanasos, Robert-Jan van Geuns, Evelyn Regar.
Textbook on Bioresorbable Scaffolds: from basic concept to clinical application, Edited by Yoshinobu Onuma and Patrick W. Serruys Chapter 5.7 pages 177-187. (Textbook chapter)

Chapter 4 **Comparison of Acute Expansion of Bioresorbable Vascular Scaffolds Versus Metallic Drug-Eluting Stents in Different Degrees of Calcification - An Optical Coherence Tomography Study.** 47
Jiang Ming Fam, Jors N van Der Sjide, Antonis Karanasos, Roberto Dilleti, Nicolas van Mieghem, Marco Valgimigli, Floris Kauer, Peter de Jaegere, Felix Zijlstra, Robert Jan van Geuns, Evelyn Regar.
Catheter Cardiovasc Interv. 2017 Apr; 89 (5):798-810.

Chapter 5 **Differential thrombotic prolapse burden in either bioresorbable vascular scaffolds or metallic stents implanted during acute myocardial infarction: The snowshoe effect: Insights from the maximal footprint analysis.** 63
Diletti R, van der Sijde J, Karanasos A, **Fam JM**, Felix C, van Mieghem NM, Regar E, Rapoza R, Zijlstra F, van Geuns RJ.
Int J Cardiol. 2016 Oct 1; 220: 802-8.

Chapter 6 **OCT assessment of the mid-term vascular healing after everolimus-eluting bioresorbable scaffold implantation in STEMI (BVS-STEMI FIRST). A comparison with metallic drug-eluting stents.** 73
Antonis Karanasos, Nicolas M. Van Mieghem, Hector Garcia-Garcia, Roberto Diletti, Cordula Felix, Jors N. van der Sijde, Yuki Ishibashi, **Jiang Ming Fam,** Peter De Jaegere, Patrick W. Serruys, Yoshinobu Onuma, Felix Zijlstra, Evelyn Regar, Robert J van Geuns.
Submitted for publication.

Chapter 7 **Bioresorbable vascular scaffold for ST Elevation myocardial infarction: optical coherence tomography observations at the 2-year follow-up.** 121
Jiang Ming Fam, Antonis Karanasos, Evelyn Regar, Robert-Jan van Geuns.
Coron Artery Dis. 2015 Sep; 26 (6): 545-7.

Chapter 8 **Use of intracoronary imaging in ST Elevation Myocardial Infarction with coronary artery aneurysm and very late stent thrombosis.** 127
Jiang Ming Fam, Jors N van der Sijde, Antonis Karanasos, Buchun Zhang, Robert-Jan van Geuns, Evelyn Regar.
Int J Cardiol. 2015 Oct 15; 197: 296-9.

Chapter 9 **An Unusual Case of Stent- in-Stent thrombosis.** 133
Jiang Ming Fam, W. den Dekker, Paul de Graaf, Evelyn Regar.
JACC Cardiovasc Interv. 2015 Dec 28; 8 (15):e261-e262.

Chapter 10 **Optical Coherence Tomography in Grafts.** 137
AL-Qezweny M.N.A., van der Sijde J.N., **Fam J.M.**, Karanasos A., Zhang B., Regar E.
Optical Coherence Tomography in Grafts. (2016) In: Ţintoiu I., Underwood M., Cook S., Kitabata H., Abbas A. (eds) Coronary Graft Failure. Springer, Cham pp 539-554. (Textbook chapter)

PART II PERFORMANCE AND OUTCOMES OF NOVEL METALLIC STENTS FOR LEFT MAIN STENTING

Chapter 11 **Over-expansion capacity and stent design model: An update with contemporary DES platforms.** 157
Ng J, Foin N, Ang HY, **Fam JM**, Sen S, Nijjer S, Petraco R, Di Mario C, Davies J, Wong P.
Int J Cardiol. 2016 Oct 15; 221: 171-9.

Chapter 12 **Defining optimal stent overexpansion strategies for left main stenting: insights from bench testing.** 169
Jiang Ming Fam, Peter Mortier, Matthieu De Beule, Tim Dezutter, Nicolas van Mieghem, Roberto Diletti, Bert Everaert , Soo Teik Lim, Felix Zijlstra, Robert-Jan van Geuns.
AsiaIntervention 2017; 3: 111-120.

Chapter 13 **Left main stem bifurcation treatment with the Tryton side-branch stent: A prospective study with invasive imaging follow-up.** 199
Jiang Ming Fam, Pieter Stella, Joanna Wykrzykowska, Antonio L. Bartorelli, Guiseppe Tarantini, Eulogio Garcia, Indulis Kumsars, Michael Magro, Peter O'Kane, Robert-Jan van Geuns.
Submitted for publication.

PART III IMPLANTATION TECHNIQUE OF BIORESORBABLE VASCULAR SCAFFOLDS

Chapter 14 **Implantation Technique for Bioresorbable Scaffolds.** 237
Jiang Ming Fam, Robert-Jan van Geuns.
Cardiac Interventions Today January 2017.

Chapter 15 **Avoiding late acquired bioresorbable scaffold malapposition.** 245
Jiang Ming Fam; Antonis Karanasos, Robert-Jan van Geuns.
Submitted for publication.

Chapter 16 **Impact of postdilation on procedural and clinical outcomes in complex lesions treated with bioresorbable vascular scaffolds- a prospective registry study.** 277
Jiang Ming Fam, Cordula Felix, Yoshinobu Onuma, Roberto Diletti, Nicolas M Van Mieghem, Evelyn Regar, Peter De Jaegere, Felix Zijlstra, Robert J Van Geuns.
Submitted for publication.

PART IV TREATMENT OF CORONARY ARTERY DISEASE WITH BIORESORBABLE VASCULAR SCAFFOLDS- OUTCOMES AND LIMITATIONS IN DIFFERENT CLINICAL AND LESION SUBSETS

Chapter 17 **Expanded Clinical Use of Everolimus Eluting Bioresorbable Vascular Scaffolds for Treatment of Coronary Artery Disease.** 319
Roberto Diletti, Yuki Ishibashi, Cordula Felix, Yoshinobu Onuma, Shimpei Nakatani, Nicolas M. van Mieghem, Eveliyn Regar, Marco Valgimigli, Peter P. de Jaegere, Nienke van Ditzhuijzen, **Jiang Ming Fam**, Jurgen M.R. Ligthart, Mattie J. Lenzen, Patrick W. Serruys, Felix Zijlstra, Robert Jan van Geuns.
Catheter Cardiovasc Interv. 2017 Jul; 90 (1):58-69.

Chapter 18 **Coronary Stent Curvature Quantification in X-ray Angiography and Computed Tomography Angiography.** 333
Gerardo Dibildox, **Jiang Ming Fam**, Yoshinobu Onuma, Koen Nieman, Robert-Jan van Geuns, Theo van Walsum.
Submitted for publication.

Chapter 19 **Conformability in everolimus-eluting bioresorbable scaffolds compared with metal platform coronary stents in long lesions.** 359
Jiang Ming Fam, Yuki Ishibashi, Cordula Felix, Bu Chun Zhang, Roberto Diletti, Nicolas van Mieghem, Evelyn Regar, Ron van Domburg, Yoshinobu Onuma, Robert- Jan van Geuns.
Int J Cardiovasc Imaging. 2017 Dec; 33(12):1863-1871.

Chapter 20 **Are BVS suitable for ACS patients? Support from a large single center real live registry.** 371
Felix Cordula, Onuma Yoshinobu, **Fam Jiang Ming**, Diletti Roberto, Ishibashi Yuki, Karanasos Antonis, Everaert Bert, van Mieghem Nicolas M, Daemen Joost, de Jaegere Peter P, Zijlstra, Felix, Regar Evelyn, van Geuns Robert-Jan.
Int J Cardiol. 2016 Sep 1; 218: 89-97.

Chapter 21 **Initial experience with everolimus-eluting bioresorbable vascular scaffolds for treatment of patients presenting with acute myocardial infarction: a propensity-matched comparison to metallic drug eluting stents 18-month follow-up of the BVS STEMI first study.** 383
Fam Jiang Ming, Felix Cordula, van Geuns Robert-Jan, Onuma Yoshinobu, Van Mieghem Nicolas M, Karanasos Antonis, van der Sijde Jors, De Paolis Marcella, Regar Evelyn, Valgimigli Marco, Daemen Joost, de Jaegere Peter, Zijlstra Felix, Diletti Roberto.
EuroIntervention. 2016 May 17; 12(1):30-7.

Chapter 22 **Mid- to Long-Term Clinical Outcomes of Patients Treated With the Everolimus-Eluting Bioresorbable Vascular Scaffold: The BVS Expand Registry.** 393
Felix Cordula, **Fam Jiang Ming**, Diletti Roberto, Ishibashi Yuki, Karanasos Antonis, Everaert Bert, van Mieghem Nicolas M, Daemen Joost, de Jaegere Peter , Zijlstra Felix , Regar Evelyn, Onuma Yoshinobu, van Geuns Robert-Jan.
JACC Cardiovasc Interv. 2016 Aug 22; 9(16):1652-63.

Chapter 23 **Everolimus-eluting bioresorbable vascular scaffolds implanted in coronary bifurcation lesions: Impact of polymeric wide struts on side-branch impairment.** 409
De Paolis Marcella, Felix Cordula, van Ditzhuijzen Nienke, **Fam Jiang Ming**, Karanasos Antonis, de Boer Sanneke, van Mieghem Nicolas M, Daemen Joost, Costa Francesco, Bergoli Luis Carlos, Jurgen M.R. Ligthart, Regar Evelyn, de Jaegere Peter, Zijlstra Felix, van Geuns Robert-Jan, Diletti Roberto.
Int J Cardiol. 2016 Oct 15; 221: 656-64.

Chapter 24 **Everolimus-eluting bioresorbable vascular scaffolds for treatment of complex chronic total occlusions.** 421
Fam Jiang Ming, Ojeda S, Garbo R, Latib A, La Manna A, Vaquerizo B, Boukhris M, Vlachojannis GJ, van Geuns RJ, Ezhumalai B, Kawamoto H, van der Sijde J, Felix C, Pan M, Serdoz R, Boccuzzi GG, De Paolis M, Sardella G, Mancone M, Tamburino C, Smits PC, Di Mario C, Seth A, Serra A, Colombo A, Serruys P, Galassi AR, Zijlstra F, Van Mieghem NM, Diletti R.
EuroIntervention. 2017 Jun 20; 13(3):355-363.

Chapter 25 **Impact of calcium on procedural and clinical outcomes in lesions treated with bioresorbable vascular scaffolds- A prospective BRS registry study.** 433
Jiang Ming Fam, Cordula Felix, Yuki Ishibashi, Yoshinobu Onuma, Roberto Diletti, Nicolas M van Mieghem, Evelyn Regar, Peter de Jaegere, Felix Zijlstra, Robert J van Geuns.
Int J Cardiol. 2017 Dec 15; 249: 119-126.

Chapter 26 **Potentially increased incidence of scaffold thrombosis in patients treated with Absorb BVS who terminated DAPT before 18 months.** 443
Cordula M. Felix, Georgios J. Vlachojannis, Alexander J.J. IJsselmuiden, **Jiang Ming Fam,** Peter C. Smits, Wouter J. Lansink, Roberto Diletti, Felix Zijlstra, Evelyn S. Regar, Eric Boersma, Yoshinobu Onuma, Robert J.M. van Geuns.
EuroIntervention. 2017 Jun 2; 13(2):e177-e184.

Chapter 27 **Late and very late scaffold thrombosis.** 453
Antonis Karanasos, Bu-Chun Zhang, Jors van der Sijde, **Jiang Ming Fam**, Robert-Jan van Geuns, Evelyn Regar.
Textbook on Bioresorbable Scaffolds: from basic concept to clinical application, Edited by Yoshinobu Onuma and Patrick W. Serruy. Chapter 8.2 pages 421-430. (Textbook chapter)

Chapter 28 **Mid-term outcomes of the ABSORB BVS Versus Second-Generation DES: A Systematic Review and Meta-Analysis.** 465
Cordula Felix, Victor .J. van den Berg, Sanne .E. Hoeks, **Jiang Ming Fam**, Mattie. Lenzen, Eric Boersma, Peter C. Smits, Patrick. W. Serruys, Yoshinobu Onuma, Robert Jan M. van Geuns.
PLoS One (in press).

Chapter 29 **Mid-term CCTA Results for ABSORB Bioresorbable Vascular Scaffold in clinical practice- A BVS EXPAND project.** 509
Cordula Felix, Haroun. El Addouli, Adriaan. Coenen, Marissa M. Lubbers, Yoshinobu. Onuma, **Jiang Ming Fam**, Evelyn Regar, Roberto. Diletti, Felix Zijlstra, Ricardo PJ Budde, Koen Nieman, Robert-Jan.M. van Geuns.
Submitted for publication.

Chapter 30 **Summary and Conclusion** 541

Samenvatting en Conclusie 559

Curriculum Vitae 579

PhD Portfolio 583

List of publications 587

Acknowledgements 599

1

CHAPTER

INTRODUCTION

INTRODUCTION

Percutaneous coronary intervention (PCI) has become one of the mainstays of management of coronary heart disease. In disease subsets traditionally treated by surgery such as left main disease, PCI has even emerged to become a feasible and safe option for revascularisation [1-2]. The first generation drug eluting stents (DES) resulted in reduced rates of restenosis compared to bare metal stents. However first generation DES were associated with an increased risk of stent thrombosis due to delayed healing [3-4]. Newer DES led to further improvement in clinical results by reducing the risk of stent thrombosis rates reportedly as low as 0.4% per year [5-6]. Despite such good clinical results, contemporary drug eluting stents still face certain limitations such as risk of permanent strut failure, polymer induced vascular inflammation and antiproliferative drug related adverse effects, such that even the best metallic DES still have a 2-4% annual incidence of target vessel failure such as target vessel revascularisation [7-8]. Newer devices have since emerged such as newer generation DES with very thin struts with bioresorbable polymer as well as completely bioresorbable vascular scaffolds (BRS). The focus of this thesis is to investigate the outcomes and limitations of newer generation coronary devices such as DES with bioresorbable polymer and completely bioresorbable vascular scaffolds (BRS) in the different clinical and lesion subsets. For this purpose, I will use a combination of a) advanced imaging modality to evaluate coronary device performance in the background of specific clinical settings and b) clinical registries to study clinical outcomes post device implantation in relatively larger patient groups.

Outcomes associated with medical devices such as BRS may be affected by a variety of causes such as patient and device factors (such as the type, components and interactions among the biomaterials used), variation in operator technique and the use of adjunct technologies (such as choice of intravascular imaging). In addition, although medical devices

may be subject to similar risks of adverse outcomes, the root causes leading to the adverse outcomes may vary. Post approval medical device registries are thus important for the evaluation of device clinical outcomes and identification of factors which may affect these outcomes. The advantages of registry based studies are multifold. Firstly, medical device registries allow the monitoring of medical device performance in a real-world setting which may not be possible in clinical trials. Secondly, such post approval medical device registries can also be used for short- and long-term surveillance spanning a time period which may be longer than that covered in clinical trials unearthing outcomes not seen or reported in clinical trials and safety assessments of subpopulations which tend to be under-studied in initial clinical trials. Thirdly, since device registries incorporate data on large numbers of patients receiving care in diverse clinical settings and monitor clinical outcomes over time, they serve as an important platform for understanding the experience with a medical device throughout the device and patient lifespan. Thus, medical device registries play an increasingly important function in filling the data void between device performance in clinical trials and their use in routine practice over time.

In the first part of this thesis, we will investigate the safety and value of Optical Coherence Tomography (OCT), a new intravascular imaging technique with an exceptionally high resolution which can be used to evaluate the acute device performance and the healing process after implantation of metallic or bioresorbable devices. Such a methodology is ideal to evaluate the device performance in a relatively small series before larger patient registries provide information on the longer term clinical outcome.

The second part of the thesis focused on bench testing and clinical studies that were used to study the performance of metallic stents in left main stenting. Left main stenting frequently requires overexpansion of stents which can be performed by Proximal Optimisation technique (POT) or Final kissing balloon dilation (FKBD). For optimizing left main

procedures, I first performed bench testing for different novel DES with very thin strut and biodegradable polymers to gain insights into the potential strengths and limitations of the use of such devices in left main stenting and later report the clinical outcome of a dedicated bifurcation stent in left main stenting.

BRS represent a novel approach in the treatment of coronary artery disease, having the potential for device resorption and restoration of vascular physiology; thus at least partially overcoming the long term limitations of infinite vessel caging with permanent metallic DES such as impaired endothelial function, the reduced potential for vessel remodelling, interference with the normal arterial healing process, and the risk of occlusion of covered side branches by neointimal hyperplasia. In addition, interference with noninvasive imaging (cardiac computed tomography) during patient follow-up and possible impairment of future treatment options (recurrent PCI or coronary artery bypass surgery) are further drawbacks of permanent metallic stents [9-10]. The third part of the thesis focuses on the optimal implantation strategy for this group of novel BRS. The Absorb BVS® (Abbott Vascular, Santa Clara, CA, USA) provides transient vessel support and gradually elutes the antiproliferative drug everolimus. It remains the most widely used BRS in the world to date. If complete degradation of the polymer occurs in a process which may take approximately 2-3 years, no foreign material remains and the risk for developing very late scaffold thrombosis (ScT) is potentially reduced. The Absorb BVS® is composed of a backbone of bioresorbable poly-L-lactide (PLLA) polymer structured in a crystalline fashion and have unique structural characteristics such as limited overexpansion capabilities and larger strut thickness. Thus traditional metallic DES implantation strategies may not be suitably applied to BRS in view of such limitations.

The fourth and final section aims to address the outcomes and limitations physicians may face in the use of BRS in various clinical scenarios such as STEMI or involving complex

lesions such as chronic total occlusions (CTOs), bifurcations, or calcified lesions. We studied if the clinical presentation or nature of lesion may have an impact on the clinical result and device performance of the Absorb BVS®. The feasibility and outcomes of the use of BRS in different clinical and complex lesion subsets were investigated in the institutional registry based studies such as the BVS STEMI and BVS Expand. The BVS STEMI registry is a single centre prospective observational registry looking at the acute and long term outcomes of patients presenting with ST-segment elevation myocardial infarction and treated with Absorb BVS® at the Thoraxcenter, Erasmus MC in Rotterdam. The BVS Expand registry is a single center prospective observational registry conducted at Thoraxcentre, Erasmus Medical Centre that evaluates the long term safety and performance of the Absorb BVS® coronary device in routine clinical practice post market registration. The "real world" lesions are more complex including bifurcations and calcified lesions. From the registry based data, we present a series of studies that evaluated the clinical results and challenges of the Absorb BVS® by reporting on the outcomes of the scaffold in under-studied subpopulations which tend not to be studied in initial clinical trials. In so doing, this helps us to bridge the gap between device performance in early clinical trials and their use in routine practice over time.

References

1. 2014 ESC/EACTS Guidelines on Myocardial Revascularisation. Eur Heart J. 2014 Oct 1;35: 2541-619.
2. Paul Terstein. Matthew J. Price. State of the Art Paper Left Main Percutaneous Coronary Intervention. J Am Coll Cardiol 2012; 60: 1605–135.
3. Stettler C, Wandel S, Allemann S, Kastrati A, Morice MC, Schomig A, Pfisterer ME, Stone GW, Leon MB, de Lezo JS, Goy JJ, Park SJ, Sabate M, Suttorp MJ, Kelbaek H, Spaulding C, Menichelli M, Vermeersch P, Dirksen MT, Cervinka P, Petronio AS, Nordmann AJ, Diem P, Meier B, Zwahlen M, Reichenbach S, Trelle S, Windecker S, Juni P. Outcomes associated with drug-eluting and bare-metal stents: a collaborative network meta-analysis. Lancet 2007; 370: 937–48.
4. Stone GW, Moses JW, Ellis SG, Schofer J, Dawkins KD, Morice MC, Colombo A, Schampaert E, Grube E, Kirtane AJ, Cutlip DE, Fahy M, Pocock SJ, Mehran R, Leon MB.. Safety and efficacy of sirolimus- and paclitaxel-eluting coronary stents. N Engl J Med 2007; 356: 998–1008.
5. Raber L, Magro M, Stefanini GG, Kalesan B, van Domburg RT, Onuma Y, Wenaweser P, Daemen J, Meier B, Juni P, Serruys PW, Windecker S. Very late coronary stent thrombosis of a newer-generation everolimus-eluting stent compared with early-generation drug-eluting stents: a prospective cohort study. Circulation 2012;125: 1110–21.
6. Kereiakes DJ, Meredith IT, Windecker S, Lee Jobe R, Mehta SR, Sarembock IJ, Feldman RL, Stein B, Dubois C, Grady T, Saito S, Kimura T, Christen T, Allocco DJ, Dawkins KD. Efficacy and safety of a novel bioabsorbable polymer-coated, everolimus-eluting coronary stent: the EVOLVE II Randomized Trial. Circ

Cardiovasc Interv. 2015 Apr;8(4). pii: e002372. doi: 10.1161/CIRCINTERVENTIONS.114.002372.

7. Serruys PW, Silber S, Garg S, van Geuns RJ, Richardt G, Buszman PE, Kelbaek H, van Boven AJ, Hofma SH, Linke A, Klauss V, Wijns W, Macaya C, Garot P, DiMario C, Manoharan G, Kornowski R, Ischinger T, Bartorelli A, Ronden J, Bressers M, Gobbens P, Negoita M, van Leeuwen F, Windecker S. Comparison of zotarolimus-eluting and everolimus-eluting coronary stents. N Engl J Med. 2010 Jul 8;363(2):136-46. doi: 10.1056/NEJMoa1004130. Epub 2010 Jun 16.
8. Iqbal J, Serruys PW, Silber S, Kelbaek H, Richardt G, Morel MA, Negoita M, Buszman PE, Windecker S. Comparison of zotarolimus- and everolimus-eluting coronary stents: final 5-year report of the RESOLUTE all-comers trial. Circ Cardiovasc Interv. 2015 Jun;8(6):e002230. doi: 10.1161/CIRCINTERVENTIONS.114.002230.
9. Serruys PW, Ormiston JA, Onuma Y, Regar E, Gonzalo N, Garcia-Garcia HM, Nieman K, Bruining N, Dorange C, Miquel-Hebert K and others. A bioabsorbable everolimus-eluting coronary stent system (ABSORB): 2-year outcomes and results from multiple imaging methods. Lancet 2009;373(9667):897-910.
10. Diletti R, Onuma Y, Farooq V, Gomez-Lara J, Brugaletta S, van Geuns RJ, Regar E, de Bruyne B, Dudek D, Thuesen L and others. 6-month clinical outcomes following implantation of the bioresorbable everolimus-eluting vascular scaffold in vessels smaller or larger than 2.5 mm. J Am Coll Cardiol 2011;58(3):258-64.

I

PART

OPTICAL COHERENCE TOMOGRAPHY (OCT) FOR EVALUATION OF NEW THERAPIES AND IN CLINICAL PRACTICE

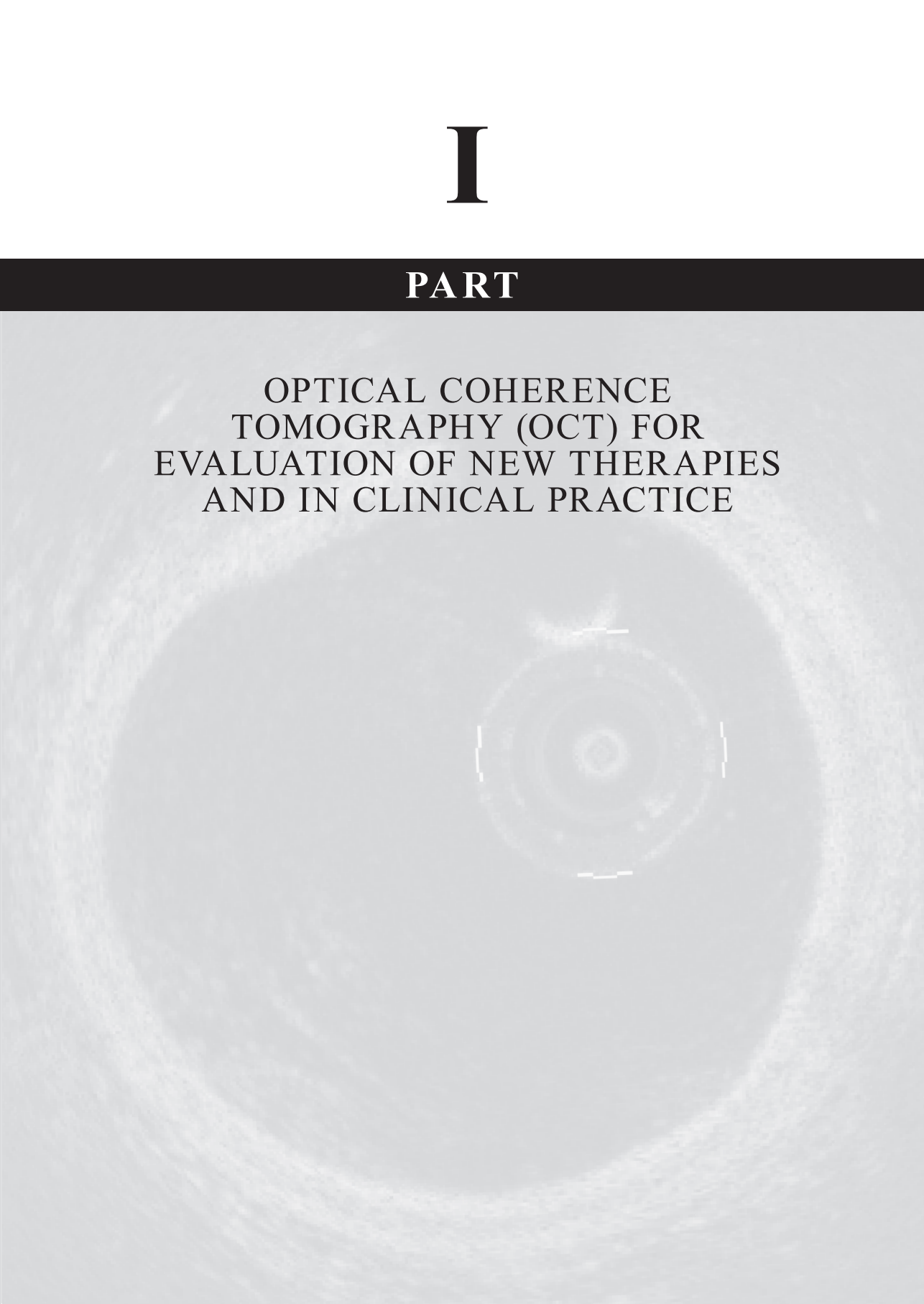

2

CHAPTER

SAFETY OF OPTICAL COHERENCE TOMOGRAPHY IN DAILY PRACTICE: A COMPARISON WITH INTRAVASCULAR ULTRASOUND

van der Sijde JN, Karanasos A, van Ditzhuijzen NS, Okamura T, van Geuns RJ, Valgimigli M, Ligthart JM, Witberg KT, Wemelsfelder S, **Fam JM**, Zhang B, Diletti R, de Jaegere PP , van Mieghem NM , van Soest G, Zijlstra F, van Domburg RT, Regar E.

Eur Heart J Cardiovasc Imaging. 2017 Apr 1; 18(4):467-474.

Safety of optical coherence tomography in daily practice: a comparison with intravascular ultrasound

Johannes N. van der Sijde[1], Antonios Karanasos[1], Nienke S. van Ditzhuijzen[1], Takayuki Okamura[2], Robert-Jan van Geuns[1], Marco Valgimigli[1], Jurgen M.R. Ligthart[1], Karen T. Witberg[1], Saskia Wemelsfelder[1], Jiang Ming Fam[1,3], BuChun Zhang[1,4], Roberto Diletti[1], Peter P. de Jaegere[1], Nicolas M. van Mieghem[1], Gijs van Soest[1], Felix Zijlstra[1], Ron T. van Domburg[1], and Evelyn Regar[1]*

[1]Thoraxcenter, Erasmus MC, Bd 585, 's-Gravendijkwal 230, 3015-CE Rotterdam, The Netherlands; [2]Department of Medicine and Clinical Science, Yamaguchi University Graduate School of Medicine, Yamaguchi, Japan; [3]National Heart Centre Singapore, Singapore; and [4]Department of Cardiology, The Affiliated Hospital of Xuzhou Medical College, Jiangsu, China

Received 2 December 2015; accepted after revision 22 January 2016

Aims Previous studies have reported the safety and feasibility of both time-domain optical coherence tomography (TD-OCT) and Fourier-domain OCT (FD-OCT) in highly selected patients and clinical settings. However, the generalizability of these data is limited, and data in unselected patient populations reflecting a routine cathlab practice are lacking. We compared safety of intracoronary FD-OCT imaging to intravascular ultrasound (IVUS) imaging in a large real-world series of consecutive patients who underwent invasive imaging during coronary catheterization in our centre.

Methods and results This is a prospective, single-centre registry of patients scheduled for coronary angiography or intervention undergoing intracoronary imaging with FD-OCT or IVUS between April 2008 and December 2013. Intra-procedural and major in-hospital adverse events that could be possibly related to invasive imaging were registered routinely by the operator as part of our clinical report and prospectively recorded in our database. These events were retrospectively individually adjudicated by an independent safety committee. Between April 2008 and December 2013, 13 418 diagnostic or interventional coronary catheterization procedures were performed. Of these, 1142 procedures used OCT and 2476 procedures used IVUS. Invasive imaging-related complications were rare, did not differ between the two imaging methods (OCT: $n = 7$, 0.6%; IVUS: $n = 12$, 0.5%; $P = 0.6$), and were self-limiting after retrieval of the imaging catheter or easily treatable in the catheterization laboratory. No major adverse events, prolongation of hospital stay, or permanent patient harm was observed.

Conclusion FD-OCT is safe in an unselected and heterogeneous group of patients with varying clinical settings.

Keywords Optical coherence tomography • Intravascular ultrasound • Safety • Adverse events

Introduction

Intracoronary optical coherence tomography (OCT) is increasingly used in the catheterization laboratory. Various clinical applications have been proposed, including assessment of plaque morphology in angiographic ambiguous lesions, guidance of stent placement during percutaneous coronary interventions (PCI), and follow-up stent assessment.[1,2] In the early days of the first generation, time-domain OCT (TD-OCT), intracoronary application was hampered by the need for proximal balloon occlusion to limit antegrade blood flow in combination with distal delivery of a translucent flush solution in order to create a blood-free environment during OCT data acquisition.[3] The currently commercially available and widespread used second-generation intracoronary Fourier-domain OCT (FD-OCT) was developed to overcome these limitations, allowing for a simplification of the image acquisition procedure. Importantly, the imaging device was redesigned to a monorail OCT imaging catheter that could be introduced into the coronary artery over any PCI

* Corresponding author. Tel: +31 10 70 35729; Fax: +31 10 70 32357. Email: e.regar@erasmusmc.nl

guide wire of choice, which substantially facilitated instrumentation. Further, the data acquisition speed was increased by using frequency domain techniques that are capable of acquiring images at high speed (up to 180 frames/s) and with fast pullback (up to 40 mm/s), alleviating the need for proximal balloon occlusion during imaging and the risk of creating ischaemia during imaging.[4] Previous smaller studies[5–10] have reported the safety and feasibility of both TD-OCT and FD-OCT in highly selected patients and clinical settings. However, the generalizability of these data is limited, and data in unselected patient populations reflecting a routine cathlab practice are lacking.

We report safety of intracoronary FD-OCT imaging in a large real-world series of consecutive patients who underwent OCT during coronary catheterization in our centre since the introduction of FD-OCT imaging in 2008 and compare the results with our intravascular ultrasound (IVUS) safety data from the same time period.

Methods

Study population

This is a single-centre study, prospectively evaluating the safety of FD-OCT. Consecutive patients who underwent FD-OCT examination during cardiac catheterization between April 2008 and December 2013 were included. These data were then compared with the cohort of patients who underwent IVUS within the same time period. All consecutive patients who underwent intracoronary OCT or IVUS during the study period were included. Additionally, to assess generalizability of our data, the indications for catheterization and patient baseline characteristics were also compared with the cohort that, at the discretion of the operators, did not undergo any form of invasive imaging during the same time period. Both OCT and IVUS were performed either as part of various clinical trial protocols or at the discretion of the operators. In the latter case, the exclusion criteria were acute, life-threatening haemodynamic instability and coronary anatomy not deemed suitable for introduction of an imaging catheter, such as extensive tortuosity or calcification or a lumen diameter >5 mm, beyond the penetration depth of OCT and lesions considered too tight to allow crossing of a device of $\sim$3F. In acute settings, restoration of antegrade flow always was the main priority and had to be secured before introduction of an imaging catheter.

Invasive imaging procedure

Invasive imaging was performed via radial or femoral access according to routine clinical standard in our centre using 6F (range 5–7F) guide catheters. Patients received weight-adjusted intravenous heparin in order to maintain the activated clotting time of >300 s and intracoronary administration of 0.2 mg nitroglycerine, as standard prior to invasive imaging. Imaging catheters were advanced distally to a region of interest over 0.014-inch conventional angioplasty guide wires, chosen at the discretion of the operators. All the imaging systems have dedicated pullback devices and consoles that allow data processing and storage.

IVUS image acquisition

IVUS images were acquired with different systems (Galaxy I, Galaxy II and iLab: Boston Scientific, Marlborough, MA, USA; In-Vision Gold and S5 imaging system: Volcano Corporation, San Diego, CA, USA). Different types of catheters (range 20–45 MHz, 3.2–3.5F) were used with a default motorized pullback speed of 0.5 mm/s.

OCT image acquisition

OCT imaging was performed with commercially available FD-OCT systems (Lightlab C7XR, Ilumien and Ilumien Optis: St Jude Medical, St Paul, MN, USA; Terumo Lunawave: Terumo, Tokyo, Japan) and in a limited number of patients with several different OCT prototypes (Lightlab M4: St Jude Medical, St Paul, MN, USA; MGH OCT system: The Wellman Center for Photomedicine, Boston, MA, USA; Volcano OCT system: Volcano Corporation, San Diego, CA, USA).

OCT imaging probes had a short monorail design with a fibre-optic imaging core integrated into a catheter. The catheter profile ranged from 2.4 to 2.7F. During OCT image acquisition, the optic imaging core rotated at a rate of 100–180 revolutions/s. OCT pullbacks were performed automated at the pullback speed of generally 20 mm/s (range 10–40 mm/s) during simultaneous flushing of viscous iso-osmolar contrast (Iodixanol 320, Visipaque^{TM}, GE Health Care, Cork, Ireland at 37°C) through the guiding catheter by use of an automated power injector (Medrad Inc., Warrendale, PA, USA) with a flow rate of 3 mL/s as standard setting, or in selected cases by manual injection.

Safety assessment

Both major in-hospital and intra-procedural adverse events were recorded and considered as potential imaging-related complications. Major in-hospital adverse events were defined as cerebrovascular event, emergency revascularization, and death. Intra-procedural events were defined as the occurrence of clinical symptoms (new or worsened chest pain or shortness of breath), adverse angiographic outcomes (dissection, perforation, vasospasm, thrombus formation, and no-reflow), or electrocardiographic changes (ST-segment elevation, severe bradycardia, and ventricular arrhythmias) requiring interruption of the imaging procedure during intracoronary imaging and were routinely registered by the operator as a standard item being part of our clinical PCI report and collected in our PCI database. In addition, all free text comments in the PCI database/reporting system were screened for 'OCT' or 'IVUS'. Comments containing these keywords were individually reviewed for any possible association with an adverse event. Major peri-procedural adverse events were also recorded and defined as cerebrovascular event, emergency revascularization, and death.

Adjudication

Complications were individually adjudicated by an independent safety committee by thorough review of the patient files, procedural notes, angiogram, and intracoronary images. A complication was considered related to the imaging procedure if it would not have occurred if the invasive imaging would not have been performed. 'Definitely related' was used for complications that were with great certainty caused by the invasive imaging. If the relation between invasive imaging procedure and registered event was less clear, but could not be completely ruled out, the event was defined as 'possibly related'. Possible and definite invasive imaging-related events were categorized as self-limiting after withdrawal of the imaging catheter, requiring action or major adverse events. The safety committee consisted of two teams that reviewed the events independently. In case of disagreement, the case was re-evaluated and discussed between both teams until consensus was reached. Each team consisted of a senior invasive cardiologist not directly involved in clinical or research coronary imaging projects and an invasive imaging expert (R.J.G. and J.M.R.L.; M.V. and K.T.W.).

Statistical analysis

Continuous data were expressed as mean values $\pm$ SD. An independent-samples *t*-test was used to analyse continuous data between two groups and ANOVA for more than two groups. Significance

of associations of categorical variables were assessed using the χ^2 test or Fisher's exact test, as appropriate. Univariate analyses to identify predictors of an adverse event during image acquisition were performed using a logistic regression model. A *P*-value of <0.05 was considered significant.

Results

Patient population

Between April 2008 and December 2013, 13 418 diagnostic or interventional coronary catheterization procedures were performed in our centre. During 1142 procedures (984 patients with 3045 pullbacks) FD-OCT was used, and during 2476 procedures (2054 patients with 5148 pullbacks) IVUS was used. A combination of OCT and IVUS images were acquired during 307 procedures. Invasive imaging was performed by 13 different senior operators, of whom 11 had >5 years of experience and the other two between 1 and 5 years of experience as senior operator in a catheterization laboratory. Baseline demographic characteristics of all patients who underwent OCT or IVUS are displayed in *Table 1*. Invasive imaging was used in a variety of clinical settings. Patients undergoing OCT had less renal failure (5.3 vs. 9.1%, $P < 0.001$) when compared with IVUS. OCT imaging was performed more often in patients with ST-elevation myocardial infarction (24.7 vs. 14.5, $P < 0.001$). Procedural characteristics are given in *Table 2*. The mean number of pullbacks per procedure was significantly higher in the OCT group compared with IVUS (2.66 vs. 2.07, $P < 0.001$), which might be explained in part by the shorter artery segment, which can be visualized in one pullback (typically 50 mm OCT vs. 100 mm IVUS). Imaged vessels and lesion types were roughly equal. Clearing of the coronary from blood during OCT imaging was performed with a contrast flush rate of 3 mL/s in 78% and 4 mL/s in 21% of the pullbacks.

Generalizability of invasive imaging cohorts

Table 3 shows the comparison of baseline characteristics of the OCT and IVUS cohorts to the population that did not undergo invasive imaging within the same time window. The most pronounced differences were the higher incidence of renal failure (12.7 vs. 5.3 vs. 9.1%, $P < 0.001$) in the non-imaging group, the lower incidence of patients with a prior PCI (26.9 vs. 46.4 vs. 42.7%), and the larger number of type C lesions (35.9 vs. 25.2 vs. 24.1%, $P < 0.001$) when compared with OCT and IVUS, respectively. *Figure 1* illustrates three examples of clinical settings that are typically considered difficult for invasive imaging acquisition. OCT images were successfully acquired in all of these cases without complications.

Safety assessment

After adjudication, 7 (0.6%) complications that occurred during image acquisition were possibly or definitely related to OCT and 12 (0.5%) to IVUS imaging ($P = 0.6$) (*Figure 2*). *Table 4* further specifies the complications as adjudicated. Transient ST-elevation requiring withdrawal of the imaging catheter was seen in 0.26 vs. 0.08% ($P = 0.2$), hypotension during image acquisition in 0.18 vs. 0.04% ($P = 0.2$), coronary spasm requiring infusion of additional intracoronary nitroglycerin in 0.09 vs. 0.04% ($P = 0.6$), thrombus formation in 0.09 vs. 0.16% ($P = 0.6$), dissection of the imaged vessel in 0.00 vs. 0.12% ($P = 0.2$), and stent deformation in 0.00 vs. 0.04% ($P = 0.5$) during OCT and IVUS imaging, respectively. The event rate per

Table 1 Characteristics of all consecutive patients undergoing invasive imaging in our centre between 2008 and 2013

Procedures	OCT[a]	IVUS[a]	*P*-value
n	1142	2476	
Age, years	61.9 ± 11.1	62.6 ± 11.2	0.112
Male	853 (74.7)	1852 (74.8)	0.967
Risk factors			
Hypertension	589 (53.9)	1465 (62.0)	<0.001
Diabetes	206 (18.1)	500 (20.5)	0.105
Dyslipidaemia	600 (55.3)	1413 (60.4)	0.006
Current smokers	299 (26.3)	576 (23.5)	0.073
Family history	471 (44.0)	1025 (44.2)	0.911
History			
Prior myocardial infarction	344 (30.1)	776 (31.3)	0.462
Prior CABG	50 (4.4)	136 (5.5)	0.169
Prior PCI	529 (46.3)	1058 (42.7)	0.047
Renal Failure	60 (5.3)	224 (9.1)	<0.001
Indications for catheterization			<0.001
Stable angina	433 (37.9)	1114 (45.0)	<0.001
Unstable angina	180 (15.7)	466 (18.8)	0.028
Non-STEMI	97 (8.5)	233 (9.4)	0.385
STEMI	282 (24.7)	360 (14.5)	<0.001
Other	150 (13.1)	303 (12.2)	0.45

[a]A combination of OCT and IVUS images were acquired during 307 procedures.
Age: mean ± standard deviation; other values: *n* (%).

Table 2 Invasive imaging procedure details

Procedures	OCT	IVUS	*P*-value
n	1142	2476	
Mean number of pullbacks	2.66 ± 1.54	2.07 ± 1.32	<0.001
Mean number of imaged vessels	1.18 ± 0.42	1.28 ± 0.51	<0.001
Total pullbacks, *n*	3042	5135	
Pullback distribution among vessels			<0.001
LAD	1484 (48.8)	2459 (47.9)	0.436
LCX	577 (19.0)	1136 (22.1)	0.001
RCA	846 (27.8)	1266 (24.7)	0.002
Other	135 (4.4)	274 (5.3)	0.074
Lesion type, *n*	946	1927	0.584
A	115 (12.2)	214 (11.1)	0.418
B1	235 (24.8)	519 (26.9)	0.241
B2	358 (37.8)	729 (37.8)	1.000
C	238 (25.2)	465 (24.1)	0.549

Values in *n* (%) or mean (±standard deviation).

Table 3 Comparison between invasive imaging cohorts and non-imaging population

	OCT	IVUS	Non-imaging	*P*-value
N	1142	2476	10 107	
Age, years	61.9 ± 11.1	62.6 ± 11.2	63.7 ± 12.8	<0.001
Male	853 (74.7)	1852 (74.8)	6992 (69.2)	<0.001
Risk factors				
Hypertension	589 (53.9)	1465 (62.0)	5037 (54.6)	<0.001
Diabetes	206 (18.1)	500 (20.5)	1981 (20.3)	0.210
Dyslipidaemia	600 (55.3)	1413 (60.4)	4347 (48.0)	<0.001
Current smokers	299 (26.3)	576 (23.5)	2345 (24.1)	0.180
Family history	471 (44.0)	1025 (44.2)	3248 (36.6)	<0.001
History				
Prior myocardial infarction	344 (30.1)	776 (31.3)	2324 (23.4)	<0.001
Prior CABG	50 (4.4)	136 (5.5)	1002 (10.1)	<0.001
Prior PCI	529 (46.3)	1058 (42.7)	2682 (26.9)	<0.001
Renal Failure	60 (5.3)	224 (9.1)	1260 (12.7)	<0.001
Indications for catheterization				<0.001
Stable angina	433 (37.9)	1114 (45.0)	2768 (27.4)	<0.001
Unstable angina	180 (15.7)	466 (18.8)	1552 (15.4)	<0.001
Non-STEMI	97 (8.5)	233 (9.4)	1271 (12.6)	<0.001
STEMI	282 (24.7)	360 (14.5)	2787 (27.6)	<0.001
Other	150 (13.1)	303 (12.2)	1729 (17.1)	<0.001
Lesion type, *n*	946	1927	7263	<0.001
A	115 (12.2)	214 (11.1)	571 (7.9)	<0.001
B1	235 (24.8)	519 (26.9)	1690 (23.3)	0.003
B2	358 (37.8)	729 (37.8)	2398 (33.0)	<0.001
C	238 (25.2)	465 (24.1)	2604 (35.9)	<0.001

pullback was the same for both modalities (0.23%). *Figure 3* shows an example of a typical angiographic and OCT image of coronary spasm occurring during image acquisition. A more detailed description of all the complications that were encountered can be found in the Supplementary data online.

Risk factors for adverse event

All baseline characteristics and indications for catheterization were tested in univariate analyses for the risk of invasive imaging events (see Supplementary data online, *Table S1*). The use of both modalities, the total number of pullbacks, and the total number of invasively imaged main vessels were also tested. No predictor of adverse events was identified in the individual OCT and IVUS cohorts, nor in the combined invasive imaging cohort. Additionally, the impact of the interventional cardiologist's experience with the use of invasive imaging on the risk of an adverse events was evaluated. When compared with the most experienced operator, there was no significant increase in risk for every individual senior operator.

Discussion

The present study demonstrates that intracoronary OCT and IVUS imaging is comparably safe in an unselected and heterogeneous group of patients with varying clinical settings, reflecting daily routine catheterization laboratory practice in a tertiary care centre. Imaging-related events were scarce, with a similar incidence for OCT and IVUS imaging and most importantly, self-limiting after withdrawal of the imaging catheter or easily treatable in the catheterization laboratory. No major adverse events, prolongation of hospital stay, or permanent patient harm was observed.

Comparison between the OCT and IVUS cohorts

During the study period, the frequency in the use of OCT and IVUS has changed in our centre. In 2008, OCT was not yet CE marked and, thus, infrequently used. In 2013, however, the use of OCT and IVUS has balanced out (*Figure 4*). While IVUS was more often performed in patients with stable angina, OCT was used more often in ST-segment elevation myocardial infarction (STEMI) patients. OCT has a higher sensitivity in visualizing thrombus and plaque ruptures, often present in STEMI patients.

OCT and IVUS were used in a heterogeneous population and in several clinical settings. Although most non-imaging variables in *Table 3* differ significantly from the OCT and IVUS cohorts, most differences can be explained by the features that are inextricably linked to both modalities. For example, in patients with renal failure, X-ray

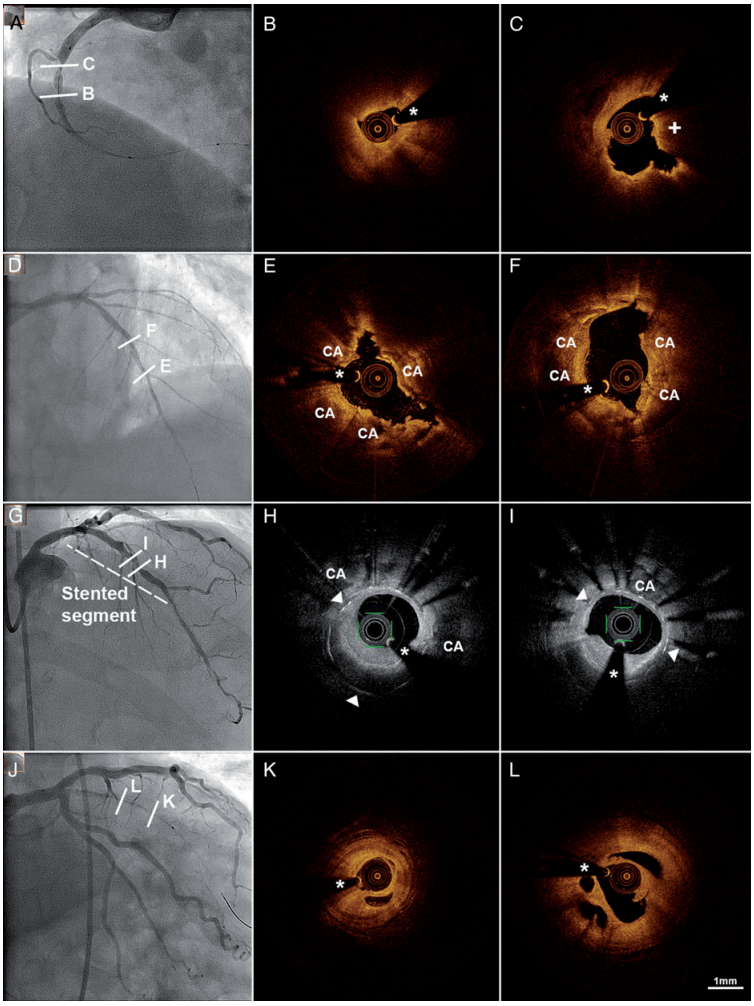

Figure 1 Examples of the use of OCT in different clinical settings. Angiogram (*A*) of a STEMI patient with corresponding OCT cross-sectional images (*B* and *C*) with the presence of thrombus (+). Angiogram (*D*) of a severely calcified vessel, which is clearly appreciated (CA) on the OCT images (*E* and *F*) after lesion preparation with a cutting balloon and rotablator. Angiogram (*G*) of a patient with in-stent restenosis. The OCT images reveal a lesion with neoatherosclerosis within the stent (*H* and *I*). Angiographic (*J*) and OCT image acquisition (*K* and *L*) in a recanalized chronic total occlusion. *Guide wire artefact.

contrast exposure has to be kept to a minimum. This explains the smaller numbers of patients with renal impairment in the OCT and, in lesser extent, the IVUS group. In patients with a chronic total occlusion (lesion type C), operators are less inclined to use invasive imaging, while additional imaging can be of great help in complex lesions (type B2), such as bifurcations. We believe that our data reflect the diversity in the use of invasive imaging and its many possible applications.

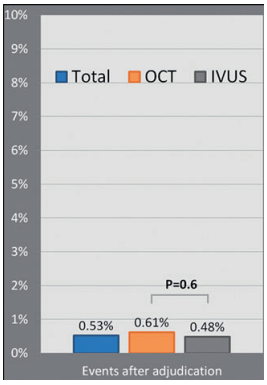

Figure 2 Event rates of IVUS and OCT after adjudication.

Table 4 Invasive imaging complications after adjudication

	OCT	IVUS	*P*-value
Transient ST-elevation	3 (0.26)	2 (0.08)	0.2
Bradycardia	2 (0.18)	1 (0.04)	0.2
Coronary spasm	1 (0.09)	1 (0.04)	0.6
Thrombus formation	1 (0.09)	4 (0.16)	0.6
Dissection	0 (0.00)	3 (0.12)	0.2
Stent deformation	0 (0.00)	1 (0.04)	0.5
Major adverse events	0 (0.00)	0 (0.00)	NA

Values in *n* (%).

Previous studies demonstrating the safety of OCT

OCT's need of clearance of blood from the vessel during image acquisition was perceived as the Achilles heel in the early days of intracoronary OCT imaging with time-domain technology, limiting its clinical application to a few expert centres. Today, this problem is largely solved by the introduction of FD-OCT technology. With FD-OCT, the need to clear the artery temporarily from blood does not appear as a major drawback anymore. The first studies that reported the safety of OCT[10,11] used the currently abandoned TD-OCT systems. At that time, OCT image acquisition was relatively slow (frame rate 15 frames/s and pullback speed of 1 mm/s) and thus requiring longer pullback times with temporary occlusion of the proximal vessel segment using a dedicated occlusion balloon. Prati *et al.* [5] were the first to perform OCT with a pullback speed of 3 mm/s and a non-occlusive technique demonstrating improved feasibility and reduced complication risk. This was then confirmed in a larger multicentre registry[6] comparing the occlusive balloon technique ($n = 256$) to the non-occlusive TD-OCT ($n = 212$) technique. No major adverse cardiac events (MACE) were observed during or in the 24 h period following OCT imaging.

The first study to report the safety and feasibility of FD-OCT was published by Imola *et al.* [7] in a group of 90 patients with unstable or stable coronary artery disease. In this population, one case of coronary spasm was recorded, but no MACE were observed. Likewise, two other studies[8,9] reported FD-OCT safety in small, selected groups. Our study presents safety of OCT in a high-volume centre, over several years. The findings corroborate the results of the prior, smaller studies with complication rates of 0–2%. The few complications that were encountered were all resolved before the patient left the catheterization laboratory. These complications were also in line with individual case reports that described rare adverse events during OCT imaging.[12–15] Importantly, our large-scale, systematic registry can demonstrate that these complications occur very rarely (all <0.2%) in a tertiary, high-volume centre and seem to happen randomly.

Comparison with IVUS

Although IVUS image acquisition shows many similarities to that of OCT, there are some distinct differences, most importantly IVUS's lack of need for a temporarily blood-free environment. Despite the differences, complications are seen very rarely for both modalities and do not significantly differ. In our study, we report 12 (0.5%) adverse events during IVUS image acquisition.

Large IVUS safety trials have been performed,[16,17] reporting 1–3% complications, a number that may be partially driven by a larger catheter size. The most recent large-scale study implementing IVUS, the PROSPECT[18] study, reported 11 patients (1.6%) with complications that were attributed to IVUS procedures. In contrast to our findings, all events were caused by mechanical damage (10 dissections and 1 perforation) to the vessel wall. The reasons for this difference is unclear. The mean number of vessels that were imaged with IVUS in our cohort is 1.28 per procedure, in contrast to the three vessels that were imaged as part of the protocol in the PROSPECT study. Furthermore, in the PROSPECT study, images were acquired within a shorter time window and in multiple centres.

Risk factors for adverse event

We did not find any patient characteristics, nor any procedural-related characteristics that increase the chance of occurrence of an imaging-related event in the light of our very low event rate. The absence of risk factors most likely demonstrates that adverse events occur infrequently and randomly, implicating that OCT and IVUS can both be used in a large variety of patients and in different clinical settings. We additionally explored if the amount of adverse events declined with increasing experience; however, an association between the operator's experience and the number of imaging procedures was not identified, tracking with previous reports.[9]

Limitations

A limitation of this study is its design. Collection of data has been recorded over several years as part of our clinical routine catheterization database. This could possibly cause inconsistency and create bias. Furthermore, reproduction of the procedures associated with adverse events that occurred during coronary catheterizations that were performed years ago can be complex. However, the

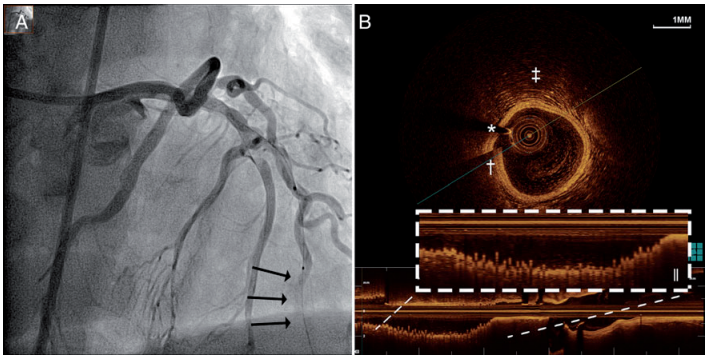

Figure 3 Coronary spasm during OCT pullback. Angiogram (*A*) and OCT image (*B*) of a diagonal branch with coronary spasm. Vasospasm can potentially mimic streaming effect due to poor contrast injection or dissection on the coronary angiogram. The seam-line (†) and non-uniform rotational distortion artefact (‡) on the cross-sectional and the 'sawtooth' appearance (||) on the longitudinal image, together with poor clearing of the artery from blood (arrows) despite good guide catheter position, suggest that coronary spasm could be present. *Guide wire artefact.

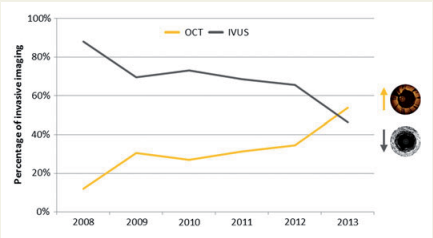

Figure 4 Change of invasive imaging policy during the study period. The use of IVUS and OCT has balanced out over time.

registration of events is done by experienced operators in a standardized way and for a long period of time. We included every patient undergoing FD-OCT and IVUS within the selected time window and used all available procedural data to reproduce the procedures with two independent adjudication committees. Therefore, we feel that the reported results represent clinical practice. The fact that imaging was acquired at the discretion of very experienced operators could create selection bias. Moreover, the high level of experience in this single-centre study does not mean that reported results can be translated to less experienced centres. Furthermore, it is of note that it is possible that the differences in clinical characteristics between OCT, IVUS, and non-imaging groups as presented in *Table 3* were mainly driven by its use in predefined research protocols in specific clinical settings. However, we intentionally included all imaging procedures that have taken place within the specified time window to assure that the presented data represent a modern, real-world catheterization laboratory population. Success rates of individual pullbacks were not routinely recorded in our databases. Therefore, we were unable to report on the feasibility of OCT image acquisition in daily clinical practice.

Another limitation of this study is that we were not able to report the incidence of peri-procedural myocardial infarctions and contrast-induced nephropathy, as the majority of our patients are being transferred to the referring hospital within 6 h after the procedure or dismissed after an uneventful procedure.

Conclusion

FD-OCT is safe in an unselected and heterogeneous group of patients with varying clinical settings. Adverse events that occur during image acquisition are rare, and similar to the event rates occurring during IVUS image acquisition.

Supplementary data

Supplementary data are available at *European Heart Journal – Cardiovascular Imaging* online.

Conflict of interest: None declared.

Funding

J.N.S. and A.K. received a research grant from St Jude Medical.

References

1. Tearney GJ, Regar E, Akasaka T, Adriaenssens T, Barlis P, Bezerra HG *et al.* Consensus standards for acquisition, measurement, and reporting of intravascular optical coherence tomography studies: a report from the International Working Group for Intravascular Optical Coherence Tomography Standardization and Validation. *J Am Coll Cardiol* 2012;**59**:1058–72.
2. Karanasos A, Ligthart J, Witberg K, van Soest G, Bruining N, Regar E. Optical coherence tomography: potential clinical applications. *Curr Cardiovasc Imaging Rep* 2012;**5**:206–20.
3. Prati F, Guagliumi G, Mintz GS, Costa M, Regar E, Akasaka T *et al.* Expert review document part 2: methodology, terminology and clinical applications of optical

coherence tomography for the assessment of interventional procedures. *Eur Heart J* 2012;**33**:2513–20.
4. Yun SH, Tearney GJ, Vakoc BJ, Shishkov M, Oh WY, Desjardins AE *et al.* Comprehensive volumetric optical microscopy in vivo. *Nat Med* 2006;**12**:1429–33.
5. Prati F, Cera M, Ramazzotti V, Imola F, Giudice R, Albertucci M. Safety and feasibility of a new non-occlusive technique for facilitated intracoronary optical coherence tomography (OCT) acquisition in various clinical and anatomical scenarios. *EuroIntervention* 2007;**3**:365–70.
6. Barlis P, Gonzalo N, Di Mario C, Prati F, Buellesfeld L, Rieber J *et al.* A multicentre evaluation of the safety of intracoronary optical coherence tomography. *EuroIntervention* 2009;**5**:90–5.
7. Imola F, Mallus MT, Ramazzotti V, Manzoli A, Pappalardo A, Di Giorgio A *et al.* Safety and feasibility of frequency domain optical coherence tomography to guide decision making in percutaneous coronary intervention. *EuroIntervention* 2010;**6**: 575–81.
8. Yoon JH, Di Vito L, Moses JW, Fearon WF, Yeung AC, Zhang S *et al.* Feasibility and safety of the second-generation, frequency domain optical coherence tomography (FD-OCT): a multicenter study. *J Invasive Cardiol* 2012;**24**:206–9.
9. Lehtinen T, Nammas W, Airaksinen JK, Karjalainen PP. Feasibility and safety of frequency-domain optical coherence tomography for coronary artery evaluation: a single-center study. *Int J Cardiovasc Imaging* 2013;**29**:997–1005.
10. Yamaguchi T, Terashima M, Akasaka T, Hayashi T, Mizuno K, Muramatsu T *et al.* Safety and feasibility of an intravascular optical coherence tomography image wire system in the clinical setting. *Am J Cardiol* 2008;**101**:562–7.
11. Tanigawa J, Barlis P, Di Mario C. Intravascular optical coherence tomography: optimisation of image acquisition and quantitative assessment of stent strut apposition. *EuroIntervention* 2007;**3**:128–36.
12. Koyama K, Yoneyama K, Mitarai T, Kobayashi Y, Saito M, Oono T *et al.* Periprocedural myocardial injury and right bundle branch block during coronary optical coherence tomography in an acute coronary syndrome patient with severe coronary ectasia. *Int J Cardiol* 2014;**177**:1113–5.
13. Dobarro D, Jiménez-Valero S, Moreno R. Severe coronary spasm induced by OCT wire. There are no innocuous procedures. *J Invasive Cardiol* 2010;**22**:385.
14. Sato K, Panoulas VF, Naganuma T, Miyazaki T, Latib A, Colombo A. Bioresorbable vascular scaffold strut disruption after crossing with an optical coherence tomography imaging catheter. *Int J Cardiol* 2014;**174**:e116–9.
15. Smith DK, Bourenane H, Strange JW, Baumbach A, Johnson TW. Catheter-induced coronary dissection during optical coherence tomography investigation. *EuroIntervention* 2012;**7**:1124–5.
16. Hausmann D, Erbel R, Alibelli-Chemarin MJ, Boksch W, Caracciolo E, Cohn JM *et al.* The safety of intracoronary ultrasound. A multicenter survey of 2207 examinations. *Circulation* 1995;**91**:623–30.
17. Batkoff BW, Linker DT. Safety of intracoronary ultrasound: data from a Multicenter European Registry. *Cathet Cardiovasc Diagn* 1996;**38**:238–41.
18. Stone GW, Maehara A, Lansky AJ, de Bruyne B, Cristea E, Mintz GS *et al.* A prospective natural-history study of coronary atherosclerosis. *N Engl J Med* 2011;**364**: 226–35.

3

CHAPTER

OPTICAL COHERENCE TOMOGRAPHY IS THE WAY TO GO

Jiang Ming Fam, Nienke Simone van Ditzhuijzen, Jors van der Sjide, Antonis Karanasos, Robert-Jan van Geuns, Evelyn Regar.

Textbook on Bioresorbable Scaffolds: from basic concept to clinical application, Edited by Yoshinobu Onuma and Patrick W. Serruys Chapter 5.7 pages 177-187. (Textbook chapter)

OCT is the way to go

JIANG MING FAM, NIENKE SIMONE VAN DITZHUIJZEN, JORS VAN DER SIJDE, BU-CHUN ZHANG, ANTONIOS KARANASOS, ROBERT-JAN M. VAN GEUNS, AND EVELYN REGAR

Introduction—Current Challenges Facing Bioresorbable Vascular Scaffolds in Percutaneous Coronary Intervention 193
Limitations of angiography to address These challenges 194
Why preprocedural sizing on OCT is mandatory *194*
OCT provides accurate luminal measurements *195*
OCT has the ability to assess plaque morphology and characteristics *195*
OCT findings can be used to optimize scaffold expansion postdeployment *197*
OCT is safe *198*
OCT imaging has the potential to improve outcomes *198*
Use of Optical Coherence Tomography in Special Situations 198
Bifurcation stenting *198*
Limitations of OCT 199
Dimensional measurements evaluated on OCT *199*
Lumen measurements *199*
Scaffold Measurements *199*
How to Perform Online OCT in the Catherization Lab 199
Proper technique is essential *199*
Online analysis *200*
Conclusion 200
References 200

INTRODUCTION—CURRENT CHALLENGES FACING BIORESORBABLE VASCULAR SCAFFOLDS IN PERCUTANEOUS CORONARY INTERVENTION

Bioresorbable vascular scaffolds (BRS) represent a new treatment for coronary artery disease. While imaging sightings have shown a favorable healing response after scaffold implantation with complete strut resorption and recovery of vasomotor function [1] and clinical studies have demonstrated similar clinical outcome of BRS compared to best-in-class drug eluting metallic platform stents (MPS) [2–4] in highly selected, simple lesions, there are still limitations facing the use of BRS in percutaneous coronary intervention (PCI). Compared to MPS, BRS have a limited range of expansion, limiting their use in cases of vessel tapering. While small malapposition may be correctable by postdilatation and resolve at follow-up, large malapposition can be uncorrectable and persist at follow-up until resorption occurs. Attempts to correct large malapposition by overexpansion with a large balloon can lead to acute disruption of the scaffold (Figure 5.7.1). Therefore, exact sizing and device matching of lumen dimension is crucial. As BRS are relatively bulky and have thicker struts (approximately 150 μm), it becomes even more important to achieve close matching of scaffold edges with minimal regions of overlap. Long regions of scaffold overlap should preferably be avoided as it increases the risk of scaffold thrombosis and also increases the risk of side branch occlusion. In addition, polymers are invisible under X-ray and thus suffer from poor visualization by coronary angiography. Most of the BRS such as the Absorb BVS are equipped with radiopaque markers on both ends of the scaffold (Figure 5.7.2) or on both ends of the delivery balloon [2,5,6] whereas in the REVA bioresorbable scaffold a proprietary iodinated material is added to the polymer that allows visualization of the entire scaffold under X-ray [7] (Figure 5.7.3). Therefore, acute placement of the scaffold can be challenging especially in regions of significant overlap or foreshortening. Finally, the paucity of visualization of the scaffold under direct angiography also makes it difficult to assess expansion of the scaffold post implantation and the need for further scaffold optimization.

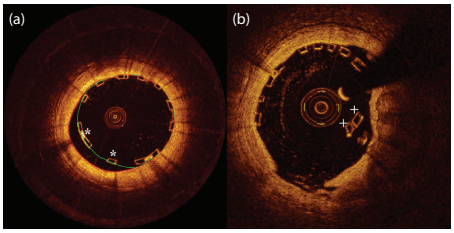

Figure 5.7.1 Panel **a** showing malapposed struts (marked *). Attempts to correct large malapposition by overexpansion with a large balloon can lead to acute disruption of the scaffold (Panel **b**: disrupted struts marked +).

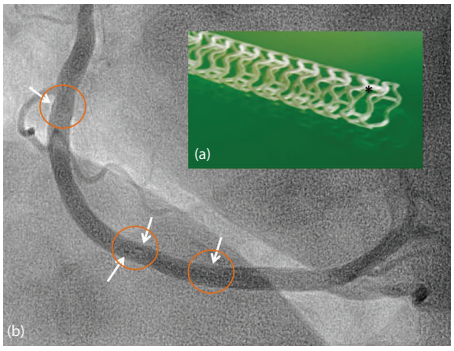

Figure 5.7.2 The Absorb BVS# seen on closeup with the platinum radiopaque marker (*) at one end (Panel **a**) and in the right coronary artery (RCA) after implantation (Panel **b**). The arrows indicate the radio-opaque markers of two scaffolds deployed in an overlapping manner in the RCA. (Reproduced with permission from Abbott Vascular.)

LIMITATIONS OF ANGIOGRAPHY TO ADDRESS THESE CHALLENGES

While angiography-based imaging remains the mainstay of assessment for the vast majority of cases in PCI, it is not able to provide detailed information regarding the true anatomic extent of disease and the procedural result of the scaffold postimplantation in certain situations. Even with the use of 3D quantitative coronary analysis (QCA), angiography offers a limited longitudinal assessment particularly in vessels with eccentric luminal lesions and when there are foreshortened or overlap angiographic images [8,9]. As a result, areas of overlap segments are difficult to assess using angiography as well. If scaffold length is either too short or too long leading to inadequate lesion coverage or excessive overlap segments, these can also potentially lead to adverse clinical outcomes. Last, angiography cannot reveal the true extent of plaque composition (such as lipid core plaque and calcium distribution) affecting the diseased coronary vessel, which has been shown to be associated with clinical and procedural outcomes such as target lesion revascularization rate [10] and periprocedural myocardial infarct [11]. Thus, angiographic assessment alone provides limited information to facilitate optimal lesion coverage and the need for further lesion preparation such as the potential need for cutting balloon dilation or the use of rotational artherectomy. Failure to fully appreciate the underlying plaque composition of the disease vessel may lead to inadequate lesion coverage or suboptimal lesion preparation thus potentially affecting scaffold expansion.

Why preprocedural sizing on OCT is mandatory

The application of OCT, a light-based intravascular imaging technology [12] has enabled us to address the challenges

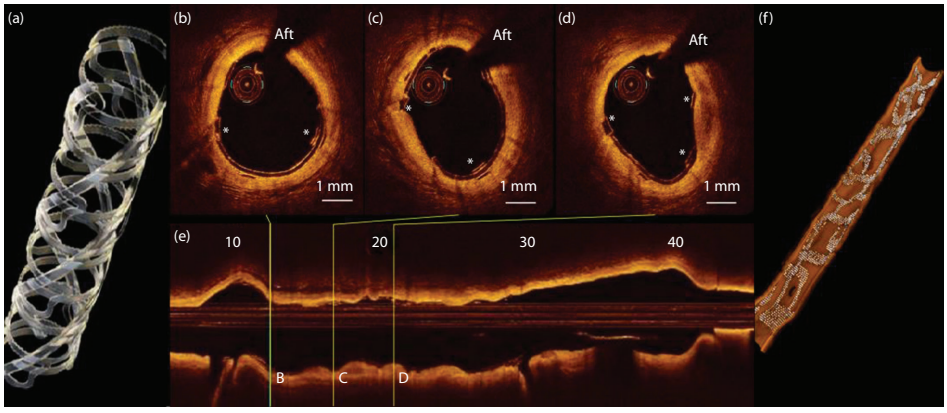

Figure 5.7.3 The REVA is designed with a unique slide-and-lock design, as can be visualized in the cartoon **(a)**, and the OCT cross-sections (* in **b**, **c**, **d**) that correspond to the letters b, c and d in the longitudinal view **(e)** of the OCT-pullback. Panel f shows the REVA implanted in the coronary vessel after 3-dimensional rendering. Aft: guidewire artifact.

facing the use of BRS and overcome the limitations of angiography in assessing the significance of coronary stenosis and results of PCI in a clinical setting [13,14]. There are clear advantages of using OCT in the deployment of BRS [15]. The advantages include the capability to provide accurate luminal measurements, and optimal detection of scaffold malapposition and fracture, which cannot be detected reliably on plain angiography. Last, 3-dimensional rendering and coregistration capabilities can provide additional information which can potentially improve procedural outcomes in more complex cases such as in bifurcation stenting. New OCT probes are of low profile (2.6–2.7 French), flexible, coated with a hydrophilic layer, and the acquisition speed is at least 10 times higher compared with intravascular ultrasound (IVUS). OCT catheters thus have a low delivery profile and can pass almost every lesion with few anatomical or patient exclusion criteria. The OCT imaging procedure is safe [16] and fast, providing all necessary information in just seconds. Radial access can also be used for OCT imaging, although a slight trend toward less optimal image quality and more artifacts has been observed [17]. Indeed, the latest European Society of Cardiology guidelines on myocardial revascularization has already recommended OCT as a tool in selected patients to optimize stent implantation (Class II b, level C) [18].

OCT provides accurate luminal measurements

OCT can reliably assess luminal dimensions accurately and provide quantitative indices of stent expansion in order to evaluate procedural outcomes. OCT can generate a clear and complete assessment of long coronary artery segments within a few seconds and allow for easier image interpretation compared with angiography. OCT offers a representation of the true lumen diameter over the length of the entire pullback with no projection-related error, foreshortening, or geometric distortion, which are limitations of angiographic assessment. Importantly, the information is reliable and instantaneously available making online analysis in the cath lab possible. Before the implantation of the BRS, luminal measurements are frequently taken to determine the severity of stenosis and the size of the "normal" reference segment. These measurements are critical as they are used to guide implantation of stent placement and sizing of the device to be implanted. OCT is especially important to make sure that the lumen diameter does not exceed the scaffold diameter by 0.5 mm to avoid incorrectable scaffold malapposition. OCT is the most accurate method in terms of comparison to phantom measurements [9] (Figure 5.7.4), has low interstudy, intraobserver, and interobserver variability, both in corelab [19] and in clinical setting [20–24], and is the best to measure scaffold length when compared with IVUS and QCA [25]. The location of minimal lumen area in relation to the diseased vessel can also be visualized clearly using the lumen profile (Figure 5.7.5), making it possible to determine the length of lesion to be treated allowing for highly accurate assessment of scaffold length required for optimal lesion coverage. Thus by accurately determining lumen dimensions, OCT can play a potentially important role in guiding treatment strategy, in terms of the selection of an appropriate balloon and optimal scaffold diameter and length, thus avoiding unnecessary overlap segments at sidebranch ostia or inadequate lesion coverage (Figure 5.7.6).

OCT has the ability to assess plaque morphology and characteristics

The high resolution of intracoronary OCT proffers advantages for the assessment of atherosclerotic plaque. OCT can reliably assess and quantify atherosclerotic plaque

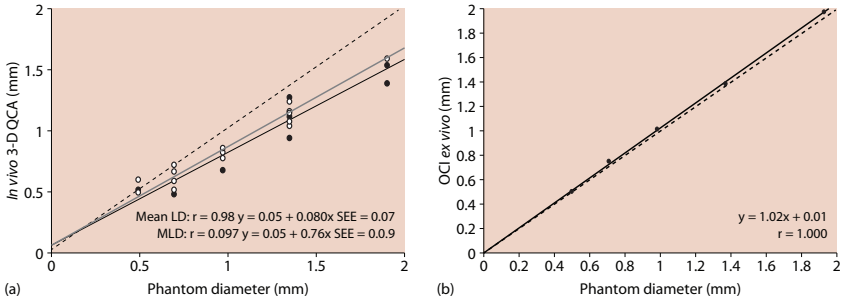

Figure 5.7.4 Panel **a** shows 3-dimensional QCA assessment of minimum (continuous black lines) and mean luminal diameter (continuous gray lines) with catheter calibration. The dashed lines indicate the line of identity. Panel **b** shows linear regression analysis of the phantom lumen diameter versus the cross-sectional luminal diameter measured with OCT. (Reproduced with permission from Tsuchida K, van der Giessen WJ, Patterson M, Tanimoto S, García-García HM, Regar E, Ligthart JMR et al. *EuroIntervention* 2007;3:100–108.)

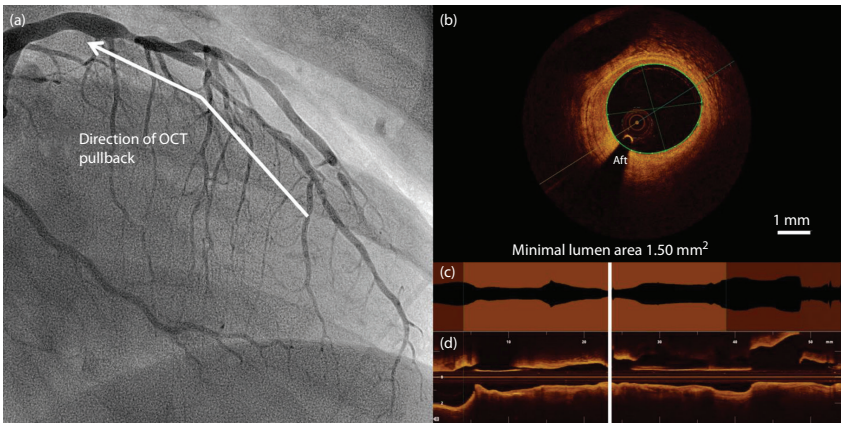

Figure 5.7.5 Coronary angiogram (Panel **a**) and OCT pullback (Panel **b**) of the left anterior descending (LAD) artery prior to percutaneous coronary intervention (PCI). The LAD as shown with the minimal lumen area seen on the lumen (Panel **c**) and longitudinal profile (Panel **d**) in relation to the length of the diseased vessel. Aft: guidewire artifact.

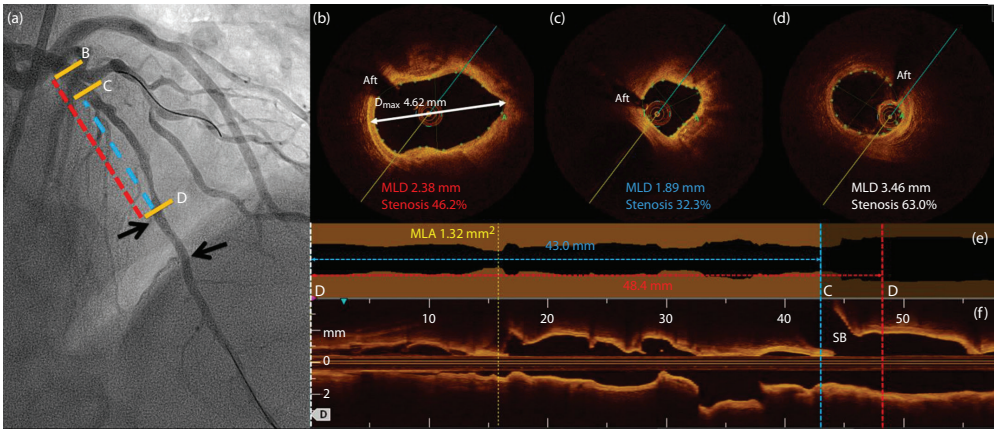

Figure 5.7.6 Panel **a**: Angiogram of a diffusely diseased left anterior descending artery (LAD). Arrows indicating markers of a distal 2.5 × 12 mm BVS Absorb scaffold already implanted. OCT images of the LAD at two choice landing zones before (Panel **b**) and after (Panel **c**) the bifurcation as well as the distal landing zone (Panel **d**). The landing zone before the bifurcation was not chosen in view of its large D_{max} diameter of 4.62 mm (Panel **b**). Two Absorb BVS (3.0 × 28 mm and 3.0 × 18 mm scaffolds) were deployed from c to d in an overlapping manner. The lumen profile (Panel **e**) and longitudinal or "L" profile (Panel f) show the location of the choice proximal landing zones, minimal lumen area (MLA) in relation to the distal landing zone with the required scaffold length, respectively, for optimal lesion coverage. Aft: guidewire artifact; MLD: mean lumen diameter; SB: side branch.

characteristics (thin fibrous cap, lipid core, and calcific plaques) (Figure 5.7.7). The implantation of struts into the necrotic cores of ruptured thin cap fibroatheromas has been associated with delayed healing in MPS (both BMS and DES) and increased risk of periprocedural myocardial infarct [11,26–28]. By identifying and avoiding landing sites containing lipid-rich plaque or thin cap fibroatheroma, OCT can precisely identify the optimal segment for stent deployment, the so-called "landing zone."

The BRS has potentially less deliverability in calcified lesions where focal areas of calcification limit expansion of the BRS more compared to MPS [29]. Hence, adequate

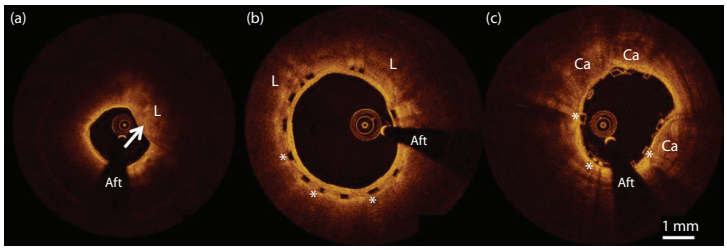

Figure 5.7.7 Different plaque characteristics that can be seen on OCT showing fibrous cap (arrow) covering a necrotic lipid core (Panel **a**) and lipid core plaque in a previously scaffolded vessel (struts marked * in Panel **b**). Panel c shows calcific plaques (marked Ca) in a previously scaffolded vessel (struts marked *). Aft: guidewire artifact.

lesion preparation is crucial, e.g., by predilation or lesion modification by scoring balloon angioplasty or even rotational artherectomy. OCT can provide information about the location of the calcium within the vessel wall (superficial vs. deep) and extent of involvement—calcium arc tapering, plaque type, and distribution both in the lesion and proximal to the lesion. Thus, the need for lesion preparation and postdilation may be realized upfront [30,31].

Therefore by understanding the true extent and nature of the underlying plaque in the diseased vessel wall, OCT can be used preprocedurally to guide BRS implantation by facilitating the selection of optimal landing zones (i.e., region with largest lumen and least plaque or normal vessel segment), in so doing ensuring optimal lesion coverage and facilitate the decision making process on overall stent implantation strategy [32–36]. With online analysis in the catheterization lab, "virtual PCI planning" involving the selection of optimal landing zone (Figure 5.7.8), planning of regions of scaffold overlap (e.g., with respect to side branch ostia), and estimation of required stent length can be performed.

OCT findings can be used to optimize scaffold expansion postdeployment

OCT demonstrated consistently high accuracy and reproducibility for the assessment of coronary stents and scaffolds, irrespective of the analysis method or software used

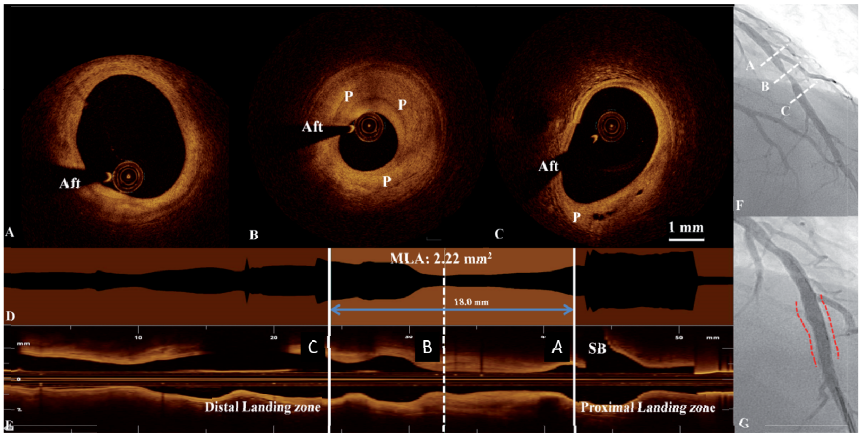

Figure 5.7.8 "Virtual PCI" planning. OCT images of the left anterior descending artery prior to scaffold implantation showing the proximal landing zone (Panel **a**), minimal lumen area (Panel **b**) and distal landing zone (Panel **c**). OCT can assess lumen dimensions accurately, assess underlying plaque composition (P), and show the location of the minimal lumen area in relation to the treated vessel on the lumen profile (Panel **d**). In this way, OCT can guide scaffold implantation strategy by assessing the scaffold length (18.0 mm in this example) required for optimal lesion coverage and avoiding side branch (SB) ostia. The side branch is seen on the longitudinal profile (Panel **e**). Panels **f** and **g** show the LAD before and after implantation of a 3.0 × 18.00 mm Absorb BVS scaffold (dashed line). Aft: guide wire artifact.

[37]. The major concern in inadequate scaffold expansion and incomplete strut apposition is that it can cause nonlaminar and turbulent blood flow that can trigger platelet activation, thrombosis, or restenosis [38]. Intracoronary OCT also enables high-resolution, *in-vivo*, serial imaging of the scaffold and vessel microarchitecture enabling investigators and clinicians to assess the effect of vascular injury caused by the implantation procedure and mechanical integrity of the scaffold over time [14,39,40]. In complex interventional settings that involve a high risk of complications such as in scaffold thrombosis, OCT can provide critical decision making by assessing for mechanistic causes such as malapposition. In CLI-OPCI, additional post-OCT interventions were performed in 34.7% of the patients undergoing OCT assessment. Notable findings that led to additional intervention post-OCT included edge dissection, scaffold underexpansion, and malapposition not previously detected on angiography alone [36]. In another study studying the utility of OCT in BRS implantation, 28% of patients [41] with optimal angiographic results underwent further intervention to optimize BRS scaffold placement following intravascular imaging. The reasons for further BRS optimization included scaffold malapposition and scaffold underexpansion. Additional intervention in OCT-guided PCI may influence clinical outcomes as stent expansion, tissue protrusion, and dissection have been associated with early stent thrombosis [42,43] and inadequate stent expansion has been implicated in restenosis [43]. However, further prospective studies would need to be conducted.

OCT is safe

In clinical studies [16,41,44,45], it has been shown that it is feasible to perform OCT safely during PCI. Current commercial systems use frequency domain detection (FD-OCT) that does not require vessel occlusion. As with any intracoronary instrumentation, there is a theoretical risk of intimal injury or dissection. Although particular care should be taken in patients with renal insufficiency, hemodynamic instability, and severely impaired ejection fraction contractility, the use of FD-OCT was not associated with any major complications including arterial dissection or life-threatening arrhythmias and worsening of postprocedural renal function [36].

OCT imaging has the potential to improve outcomes

Improvement in clinical and angiographic outcomes with intracoronary imaging guided PCI was first shown in the use of IVUS in the implantation of DES [46–50]. In a meta analysis involving DES involving 19,619 patients, IVUS-guided DES deployment compared with standard angiographic guidance was associated with a reduced incidence of death (hazard ratio [HR]: 0.59, 95% confidence interval [CI]: 0.48–0.73, $p < 0.001$), major adverse cardiac events (HR: 0.87, 95% CI: 0.78–0.96, $p = 0.008$), and stent thrombosis (HR: 0.58, 95% CI: 0.44–0.77, $p < 0.001$) [48]. The incidence of myocardial infarction and target vessel revascularization was comparable between the angiography and IVUS-guided arms.

The advantages of imaging guidance observed by IVUS may also apply to OCT. This was supported by findings from an observational study in that angiographic plus OCT guidance was associated with a significantly lower risk of cardiac death or MI, even after multivariate adjustment for baseline and procedural differences between the groups (OR = 0.49 [0.25–0.96], $p = 0.037$) or propensity-score adjusted analyses [36]. Though there is limited proven prognostic value of OCT in BRS, preliminary observations suggest a potentially beneficial role in improving outcomes [38].

USE OF OPTICAL COHERENCE TOMOGRAPHY IN SPECIAL SITUATIONS

As the clinical indications for BRS expands beyond simpler lesions, the need for procedural OCT to predetermine sizing becomes even more critical. The 3-dimensional rendering and co-registration capabilities of OCT facilitate the planning of PCI involving more complex anatomical subsets such as bifurcation and left main stenting. There have been positive studies that suggest that intracoronary imaging with IVUS can be of benefit in various subgroups such as small vessels [51], long lesions [50], bifurcation, and left main lesions [52,53]. Cases of BRS use have been reported in CTOs and bifurcations as well [54,55]. Potentially, OCT can be of benefit in these subgroups.

Bifurcation stenting

In appropriately selected patients, BRS potentially may be a good therapeutic option in bifurcation lesions [56]. Bifurcation lesion stenting is a potential application of OCT guidance. The unique ability of OCT to reconstruct 3-dimensional (3D) images allows better visualization of the scaffold surface and can provide additive information on luminal and lesion measurements, particularly in complex lesions such as bifurcations [57,58]. The application of 3D OCT within the coronary bifurcation seems promising, as the visualization of the complex anatomy of the bifurcation and the effects of intervention are difficult and not always reliable with 2-dimensional imaging. 3D-OCT can also produce images that indicate the relative position of the main vessel and the side-branch and help select a suitable strategy [57–59] and help identify the point of recrossing of a guidewire in a side branch through the cells of a stent implanted in the main vessel, and evaluate possible presence of struts at the ostia of the side branches following kissing balloon dilation [60]. Furthermore, in the case of BRS, OCT could help in one-scaffold strategies by identifying change in ostium dimensions after scaffold implantation [61,62], or by assessing strut protrusion into the main vessel in side-branch ostial scaffold implantation [63].

LIMITATIONS OF OCT

There are still limitations facing the use of OCT in certain situations. In severe cases of atherosclerosis marked by profound vessel remodeling, the extent of the disease process contributed by remodeling cannot be well assessed due to the limited penetration of OCT. OCT systems still require clearance of blood before the vessel can be imaged which is usually performed with injections of saline flushes with power injector systems limiting their use in large (>5 mm) and ostial, tortuous vessels and in patients unable to tolerate additional contrast and volume load such as patients with congestive cardiac failure or renal impairment.

Dimensional measurements evaluated on OCT

Dimensional measurements are well defined and have been published recently [64,65]. Important and commonly used measurements are described below. Other measurements such as plaque area and strut apposition are discussed elsewhere.

The following are important measurements at the cross-sectional level that are commonly reported with OCT.

LUMEN MEASUREMENTS

- Minimum lumen diameter: The shortest diameter through the center of mass of the lumen.
- Maximum lumen diameter: The longest diameter through the center of mass of the lumen.
- Residual area stenosis: Percentage residual area stenosis (%RAS) was calculated as: [1 – (minimal lumen area/reference lumen area] × 100.

SCAFFOLD MEASUREMENTS

- Minimum scaffold diameter: The shortest diameter through the center of mass of the scaffold.
- Maximum scaffold diameter: The longest diameter through the center of mass of the scaffold.
- Eccentricity index: (maximum scaffold diameter – minimum stent diameter)/maximum scaffold diameter, i.e., the lower the eccentricity index the higher the difference (Figure 5.7.9).
- Symmetry index: (maximal scaffold diameter – minimal scaffold diameter)/(maximal scaffold diameter).
- Minimum scaffold area: The area bounded by the scaffold border.

HOW TO PERFORM ONLINE OCT IN THE CATHERIZATION LAB

Proper technique is essential

OCT analysis can be performed online using the dedicated imaging consoles. A proper technique is essential since a proper image is a prerequisite for online OCT analysis. A key challenge especially for initial users is to acquire optimal imaging of the full scaffold length especially for long and complex lesions such as CTO. Currently, commercially

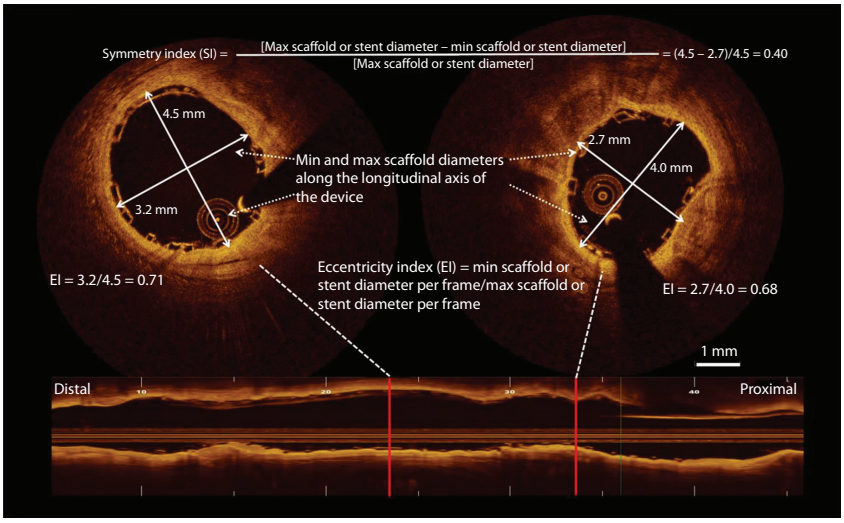

Figure 5.7.9 OCT measurements used to assess expansion of the bioresorbable vascular scaffold (BRS). Both the maximum (max) and minimum (min) scaffold/stent diameters were used to calculate the eccentricity index (EI) and the symmetry index (SI) as shown. EI is defined as the ratio between min and max scaffold/stent diameter in each analyzed frame. The SI was defined as: (max stent/scaffold diameter – min stent/scaffold diameter)/(max stent/scaffold diameter).

available systems include the Illumien™ and Illumiem Optis™ systems with the Dragonfly™ and Dragonfly Duo™ imaging catheters (LightLab/St. Jude Medical, St. Paul, MN) and the Terumo Lunawave™ with the dedicated Fastview™ imaging catheter. Both are compatible with a 6 Fr guide that can acquire frames with a pullback speed of up to 40 mm/s covering 54–150 mm within a single pullback. In contrast to IVUS, in OCT the coronary vessel needs to be cleared of blood. This is because red blood cells are opaque to light, which will lead to the light beam being scattered, resulting in severe signal attenuation. In our practice, the examined artery is cleared of blood by means of iso-osmolar X-ray or low molecular weight dextran contrast injected by power injector at rates 3–4 ml/s (total volume 10–30 ml). Multiple pullbacks or higher imaged length might be needed to cover long lesions with multiple stents.

Online analysis

For the analysis of the images, before the performance of any measurement, calibration of the Z-offset must be performed, in order to ensure accurate sizing of vessels [66,67]. The identification of the endoluminal border and measurement of vessel diameters/area as described earlier are automatically performed by the imaging system. The whole OCT run should be replayed on the imaging console while the procedure is "live" or ongoing. Manual adjustment of the auto-detected endoluminal border is performed when required especially in regions where blood clearance is inadequate or at regions of bifurcation. Online analysis also allows the image acquired to be displaced in "L-mode" or a lumen profile view where a longitudinal restitution of the study segment or the length of interest can be further selected to guide coronary intervention (Fig5.7.6). Most available OCT systems record cross-sectional images in great detail, but these are not easily matched to their geographical position on the angiogram, especially when clear anatomical landmarks are missing. Important data that are acquired by OCT are therefore not always translated into clinical use. Fortunately, several systems such as Medis System, Optis I System, and Termo System Co-registration Systems have been introduced that allow for quick and easy online co-registration of angiographic and OCT images. This integration of OCT and angiographic information enables immediate utilization of such information by the operator. Optimal landing zones for optimal scaffold deployment can be chosen based on the images acquired and specific scaffold dimensions chosen. Minimum scaffold areas are calculated and further postdilation recommended if necessary. The entire pullback should also be assessed for vascular trauma such as edge dissection which sometimes is not clearly visualized angiographically (Figure 5.7.10). Such information can guide further deployment of scaffolds to treat the edge dissection in severe cases especially if there is lumen reduction, occurring over long segments or compromise of TIMI flow. If there is severe incomplete strut apposition occurring over long segments, further postdilation can be required and further pullbacks performed to check for procedural efficacy.

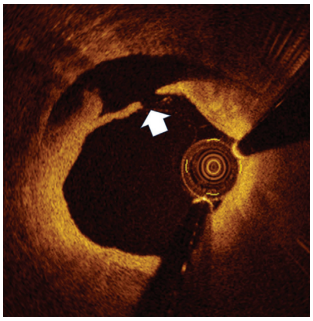

Figure 5.7.10 Edge dissection seen after predilation prior to scaffold implantation (white arrow: dissection flap).

CONCLUSION

The use of OCT for preprocedural guidance of BRS implantation can provide accurate estimation of lumen dimensions and lesion length, which can help in scaffold sizing and optimal lesion coverage, which can help achieve an optimal implantation result. Moreover, use of OCT during the procedure can help identify complications and suboptimal implantation, leading to additional intervention in order to optimize scaffold expansion and apposition and achieve optimal lesion coverage. This approach shows promise for use in more complex patient and lesion subsets and could translate to improved procedural and clinical outcomes.

REFERENCES

1. Karanasos A, Simsek C, Gnanadesigan M, van Ditzhuijzen NS, Freire R, Dijkstra J, Tu S et al. OCT assessment of the long-term vascular healing response 5 years after everolimus-eluting bioresorbable vascular scaffold. *J Am Coll Cardiol.* 2014 Dec 9;64 (22):2343–56.
2. Ormiston JA, Serruys PW, Regar E, Dudek D, Thuesen L, Webster MW et al. A bioabsorbable everolimus-eluting coronary stent system for patients with single de-novo coronary artery lesions (ABSORB): A prospective open-label trial. *Lancet.* 2008;371(9616):899–907.
3. Serruys PW, Onuma Y, Ormiston JA, de Bruyne B, Regar E, Dudek D, Thuesen L et al. Evaluation of the second generation of a bioresorbable everolimus drug-eluting vascular scaffold for treatment of de novo coronary artery stenosis: Six-month clinical and imaging outcomes. *Circulation.* 2010 Nov 30;122(22):2301-12. doi: 10.1161/CIRCULATIONAHA.110.970772. Epub 2010 Nov 15.

4. Serruys PW, Chevalier B, Dudek D, Cequier A, Carrié D, Iniguez A, Dominici M et al. A bioresorbable everolimus-eluting scaffold versus a metallic everolimus-eluting stent for ischaemic heart disease caused by de-novo native coronary artery lesions (ABSORB II): An interim 1-year analysis of clinical and procedural secondary outcomes from a randomised controlled trial. *Lancet*. 2015 Jan 3;385(9962):43-54. doi: 10.1016 /S0140-6736(14)61455-0. Epub 2014 Sep 14.
5. Tamai H, Igaki K, Kyo E, Kosuga K, Kawashima A, Matsui S et al. Initial and 6-month results of biodegradable poly-l-lactic acid coronary stents in humans. *Circulation*. 2000;102(4):399-404.
6. Verheye S, Ormiston JA, Stewart J, Webster M, Sanidas E, Costa R et al. A next-generation bioresorbable coronary scaffold system: From bench to first clinical evaluation: 6- and 12-month clinical and multimodality imaging results. *JACC Cardiovasc Interv*. 2014;7(1):89–99.
7. Pollman MJ. Engineering a bioresorbable stent: REVA programme update. *EuroIntervention*. 2009;5 Suppl F:F54–7.
8. Tu S, Xu L, Ligthart J, Xu B, Witberg K, Sun Z, Koning G et al. In vivo comparison of arterial lumen dimensions assessed by co-registered three-dimensional (3D) quantitative coronary angiography, intravascular ultrasound and optical coherence tomography. *Int J Cardiovasc Imaging*. 2012 Aug; 28(6): 1315–1327.
9. Tsuchida K, van der Giessen WJ, Patterson M, Tanimoto S, García-García HM, Regar E et al. In vivo validation of a novel three-dimensional quantitative coronary angiography system (CardiOp-B™): Comparison with a conventional two-dimensional system (CAAS II™) and with special reference to optical coherence tomography. *EuroIntervention* 2007;3:100–108.
10. Onuma Y, Tanimoto S, Ruygrok P, Neuzner J, Piek JJ, Seth A, Schofer JJ et al. Efficacy of everolimus eluting stent implantation in patients with calcified coronary culprit lesions: Two-year angiographic and three-year clinical results from the SPIRIT II study. *Catheter Cardiovasc Interv*. 2010 Nov 1;76(5):634–42. doi: 10.1002/ccd.22541.
11. Lee T, Yonetsu T, Koura K, Hishikari K, Murai T, Iwai T, Takagi T et al. Impact of coronary plaque morphology assessed by optical coherence tomography on cardiac troponin elevation in patients with elective stent implantation. *Circ Cardiovasc Interv*. 2011 Aug;4(4):378–86. doi: 10.1161/ CIRCINTERVENTIONS.111.962506. Epub 2011 Jul 26.
12. Lowe HC, Narula J, Fujimoto JG, Jang IK. Intracoronary optical diagnostics current status, limitations, and potential. *JACC Cardiovasc Interv*. 2011;4:1257–70.
13. Prati F, Cera M, Ramazzotti V, Imola F, Giudice R, Giudice M, Propris SD et al. From bench to bedside: A novel technique of acquiring OCT images. *Circ J*. 2008;72:839–43.
14. Prati F, Regar E, Mintz GS, Arbustini E, Di Mario C, Jang IK, Akasaka T et al. Expert's OCT review document. Expert review document on methodology, terminology, and clinical applications of optical coherence tomography: Physical principles, methodology of image acquisition, and clinical application for assessment of coronary arteries and atherosclerosis. *Eur Heart J*. 2010;31:401–15.
15. Nammas W, Ligthart JM, Karanasos A, Witberg KT, Regar E. Optical coherence tomography for evaluation of coronary stents in vivo. *Expert Rev Cardiovasc Ther*. 2013 May;11(5):577–88. doi: 10.1586/erc.13.37.
16. van der Sijde J, Karanasos A, van Soest G, Van Mieghem NM, De Jaegere P, Van Geuns RJ, Diletti R et al. TCT-382 safety and feasibility of optical coherence tomography: A single center experience. *Journal of the American College of Cardiology* 2014;64(11, Supplement):B112.
17. Lehtinen T, Nammas W, Airaksinen JK, Karjalainen PP. Feasibility and safety of frequency-domain optical coherence tomography for coronary artery evaluation: A single-center study. *Int J Cardiovasc Imaging*. 2013 Jun;29(5):997–1005. doi: 10.1007 /s10554-013-0196-8. Epub 2013 Feb 17.
18. Windecker S, Kolh P, Alfonso F, Collet JP, Cremer J, Falk V, Filippatos G et al. 2014 ESC/EACTS Guidelines on myocardial revascularization. *Eur Heart J*. 2014 Dec 7;35(46):3235-6. doi: 10.1093 /eurheartj/ehu422.
19. Kubo T, Akasaka T, Shite J, Suzuki T, Uemura S, Yu B, Kozuma K et al. OCT compared with IVUS in a coronary lesion assessment: The OPUS-CLASS study. *JACC Cardiovasc Imaging*. 2013 Oct;6(10):1095–104. doi: 10.1016/j.jcmg.2013.04.014. Epub 2013 Sep 4.
20. Gonzalo N, Serruys PW, García-García HM, van Soest G, Okamura T, Ligthart J, Knaapen M et al. Quantitative ex vivo and in vivo comparison of lumen dimensions measured by optical coherence tomography and intravascular ultrasound in human coronary arteries. *Rev Esp Cardiol*. 2009 Jun;62(6):615–24.
21. Gonzalo N, Escaned J, Alfonso F, Nolte C, Rodriguez V, Jimenez-Quevedo P, Bañuelos C et al. Morphometric assessment of coronary stenosis relevance with optical coherence tomography: A comparison with fractional flow reserve and intravascular ultrasound. *J Am Coll Cardiol*. 2012 Mar 20;59(12):1080–9. doi: 10.1016/j.jacc.2011.09.078.
22. Ramesh S, Papayannis A, Abdel-karim AR, Banerjee S, Brilakis E. In vivo comparison of Fourier-domain optical coherence tomography and intravascular ultrasonography. *J Invasive Cardiol*. 2012 Mar;24(3):111–5.
23. Jamil Z, Tearney G, Bruining N, Sihan K, van Soest G, Ligthart J, van Domburg R et al. Interstudy reproducibility of the second generation, Fourier domain optical coherence tomography in patients with

coronary artery disease and comparison with intravascular ultrasound: A study applying automated contour detection. *Int J Cardiovasc Imaging*. 2013 Jan; 29(1): 39–51. Published online 2012 May 26. doi: 10.1007/s10554-012-0067-8.

24. Tanimoto S, Rodriguez-Granillo G, Barlis P, de Winter S, Bruining N, Hamers R, Knappen M et al. A novel approach for quantitative analysis of intracoronary optical coherence tomography: High inter-observer agreement with computer-assisted contour detection. *Catheter Cardiovasc Interv*. 2008 Aug 1;72(2):228–35. doi: 10.1002/ccd.21482.
25. Gutiérrez-Chico JL, Serruys PW, Girasis C, Garg S, Onuma Y, Brugaletta S, García-García H et al. Quantitative multi-modality imaging analysis of a fully bioresorbable stent: A head-to-head comparison between QCA, IVUS and OCT. Quantitative multi-modality imaging analysis of a fully bioresorbable stent: A head-to-head comparison between QCA, IVUS and OCT. Int J Cv Imaging. 2012; 467-78
26. Farb A, Sangiorgi G, Carter AJ, Walley VM, Edwards WD, Schwartz RS, Virmani R. Pathology of acute and chronic coronary stenting in humans. *Circulation*. 1999 Jan 5–12;99(1):44–52.
27. Finn AV, Nakazawa G, Ladich E, Kolodgie FD, Virmani R. Does underlying plaque morphology play a role in vessel healing after drug-eluting stent implantation? *JACC Cardiovasc Imaging*. 2008 Jul;1(4):485–8. doi: 10.1016/j.jcmg.2008.04.007.
28. Imola F, Occhipinti M, Biondi-Zoccai G, Di Vito L, Ramazzotti V, Manzoli A, Pappalardo A et al. Association between proximal stent edge positioning on atherosclerotic plaques containing lipid pools and postprocedural myocardial infarction (from the CLI-POOL Study). *Am J Cardiol*. 2013 Feb 15;111(4):526–31. doi: 10.1016/j.amjcard.2012.10.033. Epub 2012 Dec 1.
29. Tanimoto S, Serruys PW, Thuesen L, Dudek D, de Bruyne B, Chevalier B, Ormiston JA. Comparison of in vivo acute stent recoil between the bioabsorbable everolimus-eluting coronary stent and the everolimus-eluting cobalt chromium coronary stent: Insights from the absorb and spirit trials. *Catheter Cardiovasc Interv* 2007;70:515–523.
30. Shaw E, Allahwala UK, Cockburn JA, Hansen TCE, Mazhar J, Figtree GA, Hansen PS et al. The effect of coronary artery plaque composition, morphology and burden on Absorb bioresorbable vascular scaffold expansion and eccentricity—A detailed analysis with optical coherence tomography. *International Journal of Cardiology* 184 (2015) 230–236.
31. Gonzalo N, Serruys PW, Okamura T, Shen ZJ, Garcia-Garcia HM, Onuma Y et al. Relation between plaque type and dissections at the edges after stent implantation: An optical coherence tomography study. *Int J Cardiol*. 2011;150(2):151–5.
32. Reiber JH, Serruys PW, Kooijman CJ, Wijns W, Slager CJ, Gerbrands JJ, Schuurbiers JC et al. Assessment of short-, medium-, and long-term variations in arterial dimensions from computer-assisted quantitation of coronary cineangiograms. *Circulation*. 1985;71:1–8.
33. Di Mario C, Haase J, den Boer A, Reiber JH, Serruys PW. Edge detection versus densitometry in the quantitative assessment of stenosis phantoms: An in vivo comparison in porcine coronary arteries. *Am Heart J*. 1992;124:1181–9.
34. Serruys PW, Booman F, Troost GJ, Reiber JHC, Gerbrands JJ, van de Brand M, Cherrier F et al. Computerized Quantitative coronary angiography applied to percutaneous transluminal coronary angioplasty: Advantages and limitations. In: Kaltenbach M, Gruentzig A, Rentrop K, Bussman WD, Eds. *Transluminal Coronary Angioplasty and Intracoronary Thrombolysis*. Berlin: Springer-Verlag; 1982:110–124.
35. Dvir D, Marom H, Guetta V, Kornowski R. Three-dimensional coronary reconstruction from routine single-plane coronary Angiograms: In vivo quantitative validation. *Int J Cardiovasc Intervent*. 2005;7:141–5.
36. Prati F, Di Vito L, Biondi-Zocca G, Occhipinti M, Alessio La Manna, Tamburino C, Burzotta F et al. Angiography alone versus angiography plus optical coherence tomography to guide decision-making during percutaneous coronary intervention: The Centro per la Lotta contro l'Infarto-Optimisation of Percutaneous Coronary Intervention (CLI-OPCI) study. *EuroIntervention* 2012:823–829.
37. Okamura T, Onuma Y, Garcia-Garcia HM, van Geuns RJ, Wykrzykowska JJ, Schultz C, van der Giessen WJ et al. First-in-man evaluation of intravascular optical frequency domain imaging (OFDI) of Terumo: A comparison with intravascular ultrasound and quantitative coronary angiography. *EuroIntervention*. 2011 Apr;6(9):1037–45. doi: 10.4244/EIJV6I9A182.
38. Karanasos A, Van Mieghem NM, van Ditzhuijzen N, Felix C, Daemen J, Autar A, Onuma Y et al. Angiographic and optical coherence tomography insights into bioresorbable scaffold thrombosis. A single-center experience. *Circ Intv* (in press).
39. Takarada S, Imanishi T, Liu Y, Ikejima H, Tsujioka H, Kuroi A, Ishibashi K et al. Advantage of next-generation frequency-domain optical coherence tomography compared with conventional time-domain system in the assessment of coronary lesion. *Catheter Cardiovasc Interv*. 2010;75:202–6.
40. Fujino Y, Bezerra HG, Attizzani GF, Wang W, Yamamoto H, Chamie D, Kanaya T et al. Frequency-domain optical coherence tomography assessment of unprotected left main coronary artery disease—A comparison with intravascular ultrasound. *Catheter Cardiovasc Interv*. 2013;82:E173–83.

41. Allahwala UK, Cockburn JA, Shaw E, Figtree GA, Hansen PS, Bhindi R. Clinical utility of optical coherence tomography (OCT) in the optimisation of Absorb bioresorbable vascular scaffold deployment during percutaneous coronary intervention. *EuroIntervention*. 2015 Feb;10(10):1154–9. doi: 10.4244/EIJV10I10A190.
42. Choi SY, Witzenbichler B, Maehara A, Lansky AJ, Guagliumi G, Brodie B, Kellett MA Jr et al. Intravascular ultrasound findings of early stent thrombosis after primary percutaneous intervention in acute myocardial infarction: A harmonizing outcomes with revascularization and stents in acute myocardial infarction (HORIZONS-AMI) substudy. *Circ Cardiovasc Interv*. 2011 Jun;4(3):239–47. doi: 10.1161/CIRCINTERVENTIONS.110.959791. Epub 2011 May 17.
43. Liu X, Doi H, Maehara A, Mintz GS, de Ribamar Costa Jr J, Sano K et al. Avolumetric intravascular ultrasound comparison of early drug-eluting stent thrombosis versus restenosis. *JACC Cardiovasc Interv*. 2009;2(5):428–34.
44. Imola F, Mallus MT, Ramazzotti V, Manzoli A, Pappalardo A, Di Giorgio A, Albertucci M et al. Safety and feasibility of frequency domain optical coherence tomography to guide decision making in percutaneous coronary intervention. *EuroIntervention*. 2010;6:575–81.
45. Viceconte N, Chan PH, Alegria-Barrero E, Ghilencea L, Lindsay A, Foin N, Di Mario C. Frequency domain optical coherence tomography for guidance of coronary stenting. *Int J Cardiol* 2011 Dec 30.
46. Parise H, Maehara A, Stone GW et al. Metanalysis of randomized studies comparing intravascular ultrasound versus angiographic guidance of percutaneous coronary intervention in pre drug eluting era. *Am J Cardiol*. 2011; 107 (3): 374–382.
47. Keane D, Haase J, Slager CJ, Montauban van Swijndregt E, Lehmann KG, Ozaki Y, di Mario C et al. Comparative validation of quantitative coronary angiography systems. Results and implications from a multicenter study using a standardized approach. *Circulation*. 1995;91:2174–83.
48. Zhang Y, Farooq V, Garcia-Garcia HM, Bourantas CV, Tian N, Dong S, Li M et al. Comparison of intravascular ultrasound versus angiography-guided drug-eluting stent implantation: A meta-analysis of one randomised trial and ten observational studies involving 19,619 patients. *EuroIntervention* 2012;8:855–865.
49. Fitzgerald PJ, Oshima A, Hayase M, Metz JA, Bailey SR, Baim DS, Cleman MW et al. Final results of the can routine ultrasound influence stent expansion (cruise) study. *Circulation*. 2000;102:523–530.
50. Oemrawsingh PV, Mintz GS, Schalij MJ, Zwinderman AH, Jukema JW, and van der Wall EE. Intravascular ultrasound guidance improves angiographic and clinical outcome of stent implantation for long coronary artery stenoses: Final results of a randomized comparison with angiographic guidance (TULIP study). *Circulation*. 2003;107:62– 67.
51. Park SW, Lee CW, Hong MK et al. Randomized comparison of coronary stenting with optimal balloon angioplasty for treatment of lesions in small coronary arteries. *Eur Heart J*. 2000;21:1785–1789.
52. Kim JS, Hong MK, Ko YG et al. Impact of intravascular ultrasound guidance on long term clinical outcomes in patients treated with drug eluting stent for bifurcational lesions: Data from a Korean multicentre bifurcation registry. *Am. Heart J*. 2011; 161 (1): 180–187.
53. Park SJ, Kim YH, Park DW et al. Impact of ultrasound guidance on long term mortality in stenting for unprotected left main coronary artery stenosis. *Circ Cardiovvascular Interv*. 2009;2: 167–177.
54. Vaquerizo B, Barros A, Pujadas S, Bajo E, Estrada D, Miranda-Guardiola F, Rigla J et al. Bioresorbable everolimus-eluting vascular scaffold for the treatment of chronic total occlusions: CTO-ABSORB pilot study.EuroIntervention. 2015 Sep; 11 (5): 555-63.
55. Jaguszewski M, Ghadri JR, Zipponi M, Bataiosu DR, Diekmann J, Geyer V, Neumann CA et al. Feasibility of second-generation bioresorbable vascular scaffold implantation in complex anatomical and clinical scenarios. *Clin Res Cardiol*. 2015 Feb;104(2):124-35. doi: 10.1007/s00392-014-0757-4. Epub 2014 Aug 31.
56. Everaert B, Felix C, Koolen J, den Heijer P, Henriques J, Wykrzykowska JJ, van der Schaaf R et al. Appropriate use of bioresorbable vascular scaffolds in percutaneous coronary interventions: A recommendation from experienced users: A position statement on the use of bioresorbable vascular scaffolds in the Netherlands. *Neth Heart J*. 2015 Mar;23(3):161–5. doi: 10.1007/s12471-015-0651-3.
57. Farooq V, Serruys PW, Heo JH, Gogas BD, Okamura T, Gomez-Lara J et al. New insights into the coronary artery bifurcation hypothesisgenerating concepts utilizing 3-dimensional optical frequency domain imaging. *JACC Cardiovasc Interv*. 2011;4(8):921–31.
58. Di Mario C, Iakovou I, van der Giessen WJ, Foin N, Adrianssens T, Tyczynski P, Ghilencea L et al. Optical coherence tomography for guidance in bifurcation lesion treatment. *EuroIntervention*. 2010;6:J99–106.
59. Okamura T, Serruys PW, and Regar E. The fate of bioresorbable struts located at a side branch ostium: Serial three-dimensional optical coherence tomography assessment. *European Heart Journal* May 2010: 2179.
60. Okamura T, Yamada J, Nao T, Suetomi T, Maeda T, Shiraishi K et al. Three-dimensional optical coherence tomography assessment of coronary wire re-crossing position during bifurcation stenting. *EuroIntervention*. 2011;7 (7):886–7.

61. Karanasos A, Tu S, van der Heide E, Reiber JH, and Regar E. Carina shift as a mechanism for side-branch compromise following main vessel intervention: Insights from three-dimensional optical coherence tomography. *Cardiovasc Diagn Ther.* 2012 Jun;2(2):173–7. doi: 10.3978/j.issn.2223-3652.2012.04.01.
62. Karanasos A, Tu S, van Ditzhuijzen NS, Ligthart JM, Witberg K, Van Mieghem N, van Geuns RJ et al. A novel method to assess coronary artery bifurcations by OCT: Cut-plane analysis for side-branch ostial assessment from a main-vessel pullback. *Eur Heart J Cardiovasc Imaging*. 2015 Feb;16(2):177-89. doi: 10.1093/ehjci/jeu176. Epub 2014 Sep 16.
63. Karanasos A, Li Y, Tu S, Wentzel JJ, Reiber JH, van Geuns RJ, Regar E. Is it safe to implant bioresorbable scaffolds in ostial side-branch lesions? Impact of "neo-carina" formation on main-branch flow pattern. Longitudinal clinical observations. *Atherosclerosis*. 2015 Jan;238(1):22–5. doi: 10.1016/j.atherosclerosis.2014.11.013. Epub 2014 Nov 18.
64. Tearney GJ, Regar E, Akasaka T et al. Consensus standards for acquisition, measurement, and reporting of intravascular optical coherence tomography studies: A report from the International Working Group for Intravascular Optical Coherence Tomography Standardization and Validation. *J Am Coll Cardiol* 2012;59:1058–72.
65. Garcia-Garcia HM, Serruys PW, Stone GW et al. Assessing bioresorbable coronary devices: Methods and parameters. *JACC Cardiovasc Imaging*. 2014 Nov;7(11):1130–48.
66. Bezerra HG et al Intracoronary optical coherence tomography: A comprehensive review clinical and research applications. *JACC Cardiovasc Interv* 2009;2(11):1035–1046.
67. Mehanna EA, Attizzani GF, Kyono H, Hake M, and Bezerra HG. Assessment of coronary stent by optical coherence tomography, methodology and definitions. *Int J Cardiovasc Imaging*. 2011 Feb;27(2):259–69.

4

CHAPTER

COMPARISON OF ACUTE EXPANSION OF BIORESORBABLE VASCULAR SCAFFOLDS VERSUS METALLIC DRUG-ELUTING STENTS IN DIFFERENT DEGREES OF CALCIFICATION - AN OPTICAL COHERENCE TOMOGRAPHY STUDY

Jiang Ming Fam, Jors N van Der Sjide, Antonis Karanasos, Roberto Dilleti, Nicolas van Mieghem, Marco Valgimigli, Floris Kauer, Peter de Jaegere, Felix Zijlstra, Robert Jan van Geuns, Evelyn Regar.

Catheter Cardiovasc Interv. 2017 Apr; 89 (5):798-810.

Comparison of Acute Expansion of Bioresorbable Vascular Scaffolds Versus Metallic Drug-Eluting Stents in Different Degrees of Calcification: An Optical Coherence Tomography Study

Jiang Ming Fam,[1,2] Johannes N van Der Sijde,[1] Antonios Karanasos,[1] Cordula Felix,[1] Roberto Diletti,[1] Nicolas van Mieghem,[1] Peter de Jaegere,[1] Felix Zijlstra,[1] Robert Jan van Geuns,[1] and Evelyn Regar[1]*

Objectives: The acute expansion of bioresorbable vascular scaffolds (BRS) and drug-eluting stents (DES) in lesions with different extent of calcification was compared by Optical Coherence Tomography (OCT). **Background:** The acute mechanical performance of polymeric BRS in calcified lesions is poorly understood. **Methods:** Acute device performance in lesions treated with either BRS($N = 50$) or DES ($N = 50$) was compared using Optical Coherence Tomography (OCT). According to angiographic degree of calcification the lesions were divided in three groups: no/mild, moderate and heavy calcification. Device performance was assessed with the following parameters by OCT: mean scaffold area, eccentricity index (EI), symmetry index (SI) and percentage incomplete strut apposition (ISA). **Results:** One hundred lesions from 85 patients (BRS/DES; 37/48) were analyzed. Scaffold area and SI were similar between BRS and DES groups in the three calcification subgroups. Compared to DES, EI in BRS was marginally lower in the no/mild calcification group (0.86 ± 0.03 versus 0.88 ± 0.03, $p = 0.018$) but was similar in the moderate and heavy calcification groups. Compared to DES, percentage ISA struts in BRS was similar in the no/mild calcification group and was significantly lower in the moderate and heavy calcification groups (2.96 ± 2.36 versus $6.78 \pm 4.61\%$, $p = 0.002$ and 1.82 ± 2.40 versus $8.89 \pm 8.25\%$, $p = 0.025$ respectively). **Conclusions:** With adequate lesion preparation, implantation of BRS in a population reflective of clinical practice, resulted in a similar luminal gain compared to DES as measured by OCT, regardless of the degree of angiographic calcification, while acute malapposition is lower with BRS in moderately and heavily calcified lesions. The clinical significance of our findings warrants further evaluation in future studies.

Key words: bioresorbable vascular scaffolds; angiographic calcification; drug-eluting stents; optical coherence tomography; percutaneous coronary intervention

Additional Supporting Information may be found in the online version of this article.

[1]Thorax Centre, Erasmus University Medical Centre, Rotterdam, Netherlands
[2]National Heart Centre Singapore

Contract grant sponsor: Abbott Vascular.

*Correspondence to: Evelyn Regar, Department of Cardiology, Thoraxcentre, Room Ba-585, Erasmus University Medical Centre, 's-Gravendijkwal 230,. 3015 GE Rotterdam, The Netherlands. E-mail: e.regar@erasmusmc.nl

Received 2 March 2016; Revision accepted 3 July 2016

DOI: 10.1002/ccd.26676
Published online 00 Month 2016 in Wiley Online Library (wileyonlinelibrary.com)

INTRODUCTION

Advances in tools and techniques of percutaneous coronary intervention (PCI) have led to PCI being increasingly accepted as a suitable mode of revascularisation in patients with coronary artery disease [1,2]. However, there are lesion subsets that still remain a major challenge. One such lesion subset is fibrocalcific atheromatous plaques, which account for 17 – 35% of patients undergoing PCI [3,4]. The presence of calcification can affect the interventional procedure in many ways such as during lesion crossing with a guide wire, lesion preparation, device delivery, and deployment. As a result, lesion calcification is associated with increased PCI complexity with worse procedural outcomes reported compared to noncalcified lesions [5]. Stent expansion may also be affected by the acute plaque recoil frequently encountered in calcific lesions which have been associated with adverse clinical and angiographic outcomes in metallic drug-eluting stents (DES) [6,7].

The everolimus-eluting bioresorbable vascular scaffold (BRS) (Absorb BVS, Abbott Vascular, Santa Clara, CA) is a new treatment for coronary artery disease. Besides the ability to have complete strut resorption at 36 months, there are several potential benefits of BRS including late lumen enlargement, restoration of vasoreactivity, no trigger for thrombosis or neoatherosclerosis and no late device fracture after resorption [8,9], while clinical studies has demonstrated similar clinical outcome of BRS compared to best-in-class DES [10] in highly selected, simple lesions. However, the acute mechanical performance of polymeric BRS compared with DES in calcified lesions is poorly understood. Contrary to the DES, the BRS is made of polymeric poly-L-lactic acid (PLLA). Due to the unique material composition, BRS have been reported to have lower radial strength and deliverability compared to DES [11] and whether this would lead to differences in acute scaffold performance in calcified lesions is still unknown.

Advances in intracoronary imaging through the use of intravascular ultrasound (IVUS) and optical coherence tomography (OCT) have allowed to investigate post procedural results of stent deployment. We thus compared the acute expansion of BRS (ABSORB, Abbott Vascular, Santa Clara, CA) compared with DES in noncalcified and calcified coronary artery lesions by optical coherence tomography (OCT) applying established imaging parameters to assess acute stent performance [6].

METHODS

Study Procedure

All moderately to severe calcified lesions from the BVS Expand registry with OCT imaging available post device implantation were studied. A group of selected non/mild calcified lesions matched for device dimensions, angiographic degree of calcification and treated vessel were also analyzed. Lesions treated with drug-eluting DES (Xience family stents, Abbott Vascular, Santa Clara, CA; BioMime™, Meril Life Sciences, Vapi, India; Nevo II™, Cordis, Bridgewater, NJ) with available postprocedural OCT pullback from our institution's OCT imaging database were then matched with the BRS group for device dimensions, angiographic degree of calcification and treated vessel in a 1:1 ratio. OCT analysis was performed offline and differences in markers of stent/scaffold expansion were assessed between the groups.

Study Population

The BVS Expand registry is a single center prospective observational registry conducted at Thoraxcentre, Erasmus Medical Centre that evaluates the long term safety and performance of the BRS-Absorb coronary device in routine clinical practice post market registration. The "real world" lesions are more complex including bifurcations and calcified lesions. Demographic and clinical characteristics were collected, retrospectively. All selected patients have provided informed consent for participation in the study, and all patients have consented for the use of their imaging data.

Treatment Procedure

The BRS was implanted at a pressure not exceeding the rated burst pressure (16atm). Pre- and post-dilation was performed at the discretion of the operator. In cases where further intervention was performed after post-implantation OCT, a final OCT study was performed and used for the study analysis. Procedural characteristics were analyzed. Pre and post balloon-to-artery ratios were calculated as ratio of largest pre- or post- balloon diameter used to the RVD of the treated vessel based on Quantitative Coronary Angiography (QCA).

Angiographic Assessment of Lesion Calcification

Calcification was identified as readily apparent radio-opacities within the vascular wall at the site of the treated lesion. Calcification was classified as either none/mild or moderate if the radio-opacities were noted only during the cardiac cycle before contrast injection, Severe calcification was defined as having multiple persisting (that are noted even without cardiac motion) opacifications of the coronary wall and visible in more than one projection, surrounding the complete lumen of the coronary artery at the site of the lesion) as per under the SYNTAX definition (www.syntaxscore.com).

Angiographic assessment of calcification was conducted independently by 2 cardiologists (Supporting Information Fig. 1, Online Video 1 and 2). In cases of disagreement, a third independent cardiologist reviewed the films and provided a final diagnosis.

Quantitative Coronary Angiography Analysis and Lesion Characterization

QCA was performed using a computer-based system (CAAS 5.10 system, Pie Medical Imaging BV, Maastricht, the Netherlands). Angiographic views with minimal foreshortening of the lesion and limited overlap with other vessels were used. For each lesion, the following QCA parameters were measured in diastole: minimal lumen diameter (MLD), reference vessel diameter (RVD), percentage of area stenosis, and lesion obstruction length.

OCT Image Acquisition

OCT was used for preprocedural sizing and optimization of scaffold/stent deployment at the sole discretion of the operator. The C7 system or the Ilumien Optis system and the corresponding DragonFly or DragonFly Duo imaging catheters (St. Jude Medical, St Paul, Minneapolis, Minnesota) were used for image acquisition. The OCT catheter was advanced distal to the treated segment, and an automated pullback was performed at 20 mm/s with simultaneous contrast injection at a rate of $3-4$ ml/s using a power injector. Two sequential pullbacks were performed to enable assessment of the entire scaffolded/stented segment when required.

OCT Offline Analysis

The OCT measurements were performed offline using the QCU-CMS software, (Medis Medical Imaging Systems, Leiden, The Netherlands). Only the final OCT pullbacks were used for analysis. Analysis was performed at 1-mm intervals within the entire scaffolded/stented segment and proximal and distal edge segments. Lumen and stent/scaffold area and diameter measurements were performed in the region of interest, as appropriate, using standard methodology for the analysis of metal stents and bioresorbable scaffolds [12–15].

QUANTITATIVE MEASUREMENTS

Indices of Device Expansion

Two previously described indexes of expansion, the eccentricity index (EI) and the symmetry index (SI) were used [16]. The EI was defined as the ratio between minimal and maximal diameter in each analyzed frame, i.e. the lower the eccentricity index the higher the difference. The SI was defined as: (maximal stent/scaffold diameter- minimal stent/scaffold diameter)/(maximal stent/scaffold diameter). For each device, both the mean EI and SI were computed (Fig. 1).

Stent and Scaffold Area

Traditionally, the scaffold/stent contour is traced using the *abluminal* contour in BRS and the *adluminal* contour in DES. In order to provide an unbiased comparison of morphometric measurements, we applied an additional modification in the analysis of DES by tracing the stent contour at the point corresponding to the abluminal strut surface. This was calculated automatically by shifting the stent contour towards the abluminal side for a value equal to the nominal strut thickness (Fig. 2). Comparisons of OCT measurements of the stent and scaffold areas based on both the abluminal and adluminal contours were done. This additional step ensured that results are not affected by methodological bias.

Reference Lumen Area

Reference lumen area (RLA) was calculated as the average of the mean proximal and distal reference areas, defined as 5 mm proximal and distal to the BRS/**DES** edge. In ostial lesions or in the presence of a large side branch at the stent edge, a meaningful proximal or distal edge segment may not be present. In such cases, only a proximal or distal reference cross section was used to calculate the RLA. Percentage Residual area stenosis (%RAS) was calculated as: [1 – (minimal lumen area/reference lumen area] x 100.

Incomplete Strut Apposition (ISA)

ISA was defined as presence of struts separated from the underlying vessel wall in BRS [11] and if the axial distance between the strut's surface and the luminal surface was greater than the strut thickness in DES [17]. The following quantitative parameters for each scaffold/stent were also assessed: percentage of struts with ISA, ISA area and prolapse area. ISA subanalysis at the scaffold/stent edge (defined as 5 mm at either proximal or distal scaffolded/stented segments) was also performed. Tissue prolapse was defined as protrusion of tissue between struts extending into the vessel lumen (Fig. 2).

Qualitative Measurements

Edge dissection was defined as a disruption of the intimal continuity at the edges of the stent/scaffold

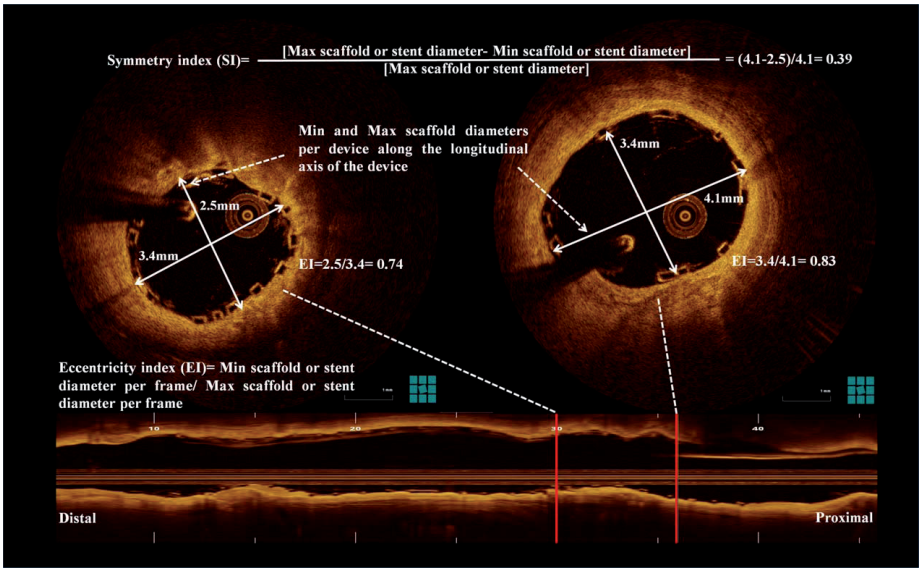

Fig. 1. OCT measurements used to assess expansion of the Bioresorbable vascular scaffold (BRS). OCT measurements in a sample case in the Bioresorbable vascular scaffold (BRS). Both the maximum (max) and minimum (min) scaffold/stent diameters were used to calculate the eccentricity index (EI) and the symmetry index (SI) as shown. EI is defined as the ratio between min and max scaffold/stent diameter in each analyzed frame. The SI was defined as: (max stent/scaffold diameter- min stent/scaffold diameter)/(max stent/scaffold diameter). The abluminal contours were used in the main analysis in comparison with the drug eluting stent (DES) for consistency.

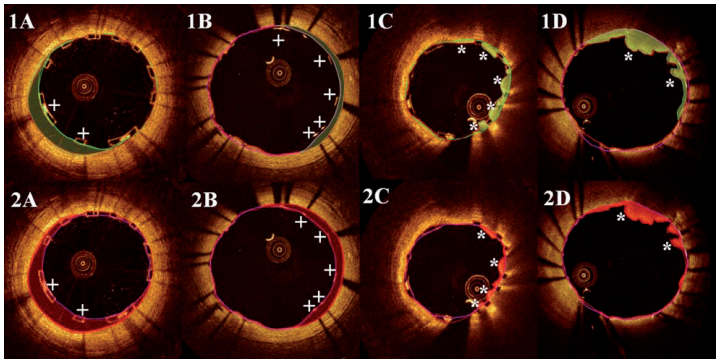

Fig. 2. Optical coherence tomography assessment of incomplete strut apposition (ISA) and tissue prolapse. Panels 1A to 1D shows segments with incomplete strut apposition (ISA) (Panels 1A and 1B; BRS versus DES) and tissue prolapse (Panels 1C and 1D; BRS versus DES) if the abluminal scaffold/stent contours are used (shaded green). Malapposed struts in Panels 1A and 1B (marked by +) are seen which are used to indicate the ISA area. Tissue prolapse areas seen in Panels 1C and 1D are defined as protrusion of tissue (marked by *) between struts extending into the vessel lumen. Panels 2A to 2D show the identical segments used for analysis if adluminal scaffold/stent contours are used (shaded red). BRS- Bioresorbable vascular scaffold DES- Drug Eluting Stent.

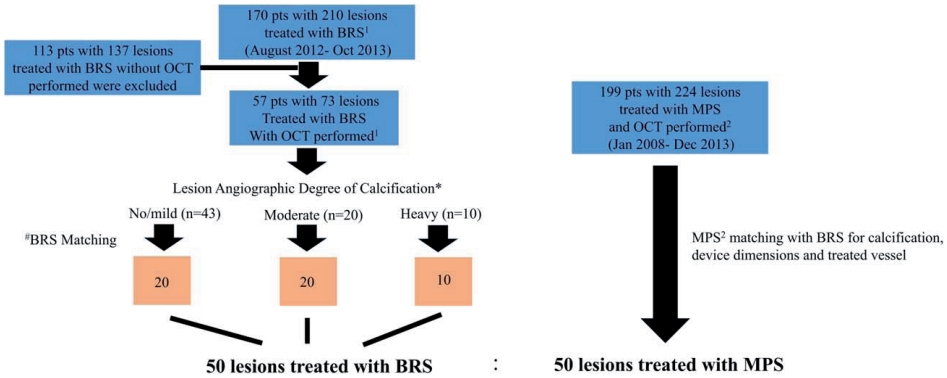

Fig. 3. Study Population. Angiographic Assessment of Lesion Calcification was performed as per under the SYNTAX definition (www.syntaxscore.com). 1- BVS Expand 2- Erasmus MC OCT Imaging Database # BRS matching for Device dimensions and Treated vessel.

with visible flap or cavities. Device fracture was suspected in the presence of isolated struts lying in the lumen with no connection or overridden by the adjacent device struts.

STATISTICAL ANALYSIS

The statistical analysis was performed using the SPSS statistical software package version 21.0 (SPSS Inc., Chicago, Illinois, USA). Continuous variables are reported as mean ± SD or estimated means (95% confidence intervals) and nominal variables as counts and percentages. Normality was assessed using the Kolmogorov-Smirnov test. Comparison for continuous variables was performed by Student's t test or the Mann-Whitney U test, as appropriate. Categorical variables were compared using the chi-square test or the Fisher exact test, as appropriate. Differences in incomplete strut apposition incidence and distance was assessed using a multilevel logistic or linear regression model respectively, with within-patient, within-lesion, and within-frame intercepts as random effects. A p value <0.05 was required to reject the null hypothesis.

RESULTS

Study Population

In the period August 2012- October 2013, 170 pts with 210 lesions were treated with BRS and enrolled into the BVS EXPAND registry. Of these, 57 patients with 73 lesions that were treated with BRS had available OCT imaging data for offline analysis. Of these 73 lesions, there were 43 no/mildly calcified, 20 moderately and 10 severely calcified lesions identified with available OCT imaging data post device implantation (Fig. 3-Study Flow Diagram). All moderately and severely calcified lesions were recruited into this study. 20 no/mildly calcified cases treated with BRS were matched with the moderately and heavily calcified lesions based on treated vessel and scaffold nominal dimensions making up a total of 50 lesions treated in the BRS group. 50 lesions treated with DES were then matched with the BRS group as described earlier. In summary, 50 BRS devices were implanted in 37 patients and 50 DES were implanted in 48 patients. The baseline demographics and lesion characteristics are shown in Tables I and II, respectively. Baseline demographics were similar between the two groups. Pre-treatment, the minimal luminal diameter (MLD) was significantly lower in the BRS group compared to DES group (0.93 ± 0.45 versus 1.21 ± 0.54mm, $p = 0.011$), while the diameter stenosis in the BRS group was significantly higher compared to the DES group (64.05 ± 16.82 versus $54.93 \pm 16.96\%$, $p = 0.012$). Pre-treatment lesion length and reference vessel diameter were similar in the 2 groups.

Procedural Characteristics

Procedural characteristics are as shown in Table III. As expected based on the instructions for use, predilation was more frequently performed in the BRS group (96.0% versus 58.0%, $p < 0.001$). Predilation with a balloon to artery ratio of 1:1 was performed in 43.6% of BRS and 37.9% of DES ($p = 0.804$). Device sizes used were similar in both groups with no significant difference in scaffold/stent diameter to preprocedural RVD ratio. Postdilation was performed equally in both

TABLE I. Baseline Clinical Variables of Patients in Both Groups

	BRS ($N=37$)	DES ($N=48$)	P value
Age (yrs)	63.15 ± 9.75	63.13 ± 8.93	0.993
Men	28 (75.7%)	31 (64.6%)	0.345
Hypertension	21 (56.8%)	25 (52.1%)	0.826
Hypercholesterolemia	23 (62.2%)	33 (68.8%)	0.645
Diabetes mellitus	7 (18.9%)	12 (25.0%)	0.604
Smoker (Active)	12 (32.4%)	6 (12.5%)	0.078
Family History	15 (40.5%)	26 (54.2%)	0.275
Previous CVA	4 (10.8%)	8 (16.7%)	0.539
Previous AMI	7 (18.9%)	16 (33.3%)	0.151
Previous PCI	2 (5.4%)	20 (41.7%)	<0.001
Previous CABG	0	2 (4.2%)	0.503
Clinical presentation			0.506
Stable or silent angina	21 (56.8%)	31 (64.6%)	
Acute coronary syndromes	16 (43.2%)	17 (35.4%)	

AMI, acute myocardial infarct; BRS, bioresorbable vascular scaffold; CABG, coronary artery bypass graft; CVA, cerebrovascular accident; DES, drug eluting stent; PCI, percutaneous coronary intervention.

groups. Importantly the maximal post dilation balloon diameter used was significantly larger in DES (BRS versus DES: 3.18 ± 0.39 versus 3.54 ± 0.68 mm, p = 0.023).

OCT Findings

OCT measurements based on abluminal contours are tabulated in Table IV, whereas morphometric stent/scaffold measurements based on the *adluminal* contours are shown in Supporting Information Table I. The minimal and mean scaffold/stent area was similar in the BRS group compared with DES. EI was marginally lower in BRS compared with DES (EI: BRS versus DES: 0.85 ± 0.04 versus 0.87 ± 0.02, $p = 0.002$), whereas EI at MSA and SI were similar in the 2 groups. Prolapse area was smaller in BRS compared to DES (BRS versus DES: 0.35 ± 0.17 versus 0.70 ± 0.38 mm^2, $p < 0.001$). There was one case with device fracture that was treated with additional scaffold implantation.

Edge Dissection and Incomplete Strut Apposition (ISA)

Edge dissection occurred to a similar extent in both device groups. A total of 28,900 struts (14, 432 struts in BRS and 14,468 struts in DES) were analysed. Compared with DES, the percentage of ISA struts was lower in BRS (2.57 ± 2.78 versus 5.97 ± 5.53%, $p < 0.001$), and the proportion of devices with equal or higher than 5% ISA was also lower for BRS (22.0% versus 52.0%; $p = 0.003$). There were no significant differences in ISA at scaffold/stent edge between the 2 device groups. However, the mean ISA area was higher

TABLE II. Angiographic and QCA Lesion Characteristics (N = 100)

	BRS ($N=50$)	DES ($N=50$)	P Value
Target vessel			1.000
LAD	25 (50.0%)	24 (48.0%)	
LCX	11 (22.0%)	13 (26.0%)	
RCA	14 (28.0%)	13 (26.0%)	
AHA/ACC lesion classification			
A	6 (12.0%)	4 (8.0%)	0.741
B1	13 (26.0%)	13 (26.0%)	1.000
B2	19 (38.0%)	27 (54.0%)	0.160
C	12 (24.0%)	6 (12.0%)	0.192
Degree of calcification			
No/mild	20	20	
Moderate	20	20	
Severe	10	10	
Extent of disease involvement			
SVD	20 (40.0%)	26 (52.0%)	0.228
DVD	25 (50.0%)	16 (32.0%)	0.103
TVD	5 (10.0%)	8 (16.0%)	0.554
Chronic Total occlusion	3 (6.0%)	2 (4.0%)	1.000
QCA Analysis			
Pre-treatment			
RVD (mm)	2.65 ± 0.38	2.71 ± 0.54	0.553
MLD (mm)	0.93 ± 0.45	1.21 ± 0.54	0.011
Diameter stenosis(%)	64.05 ± 16.82	54.93 ± 16.96	0.012
Pre-treatment lesion length (mm)	29.54 ± 16.01	25.18 ± 9.02	0.111
Post-treatment			
RVD (mm)	2.80 ± 0.41	2.86 ± 0.58	0.526
MLD (mm)	2.32 ± 0.45	2.43 ± 0.50	0.276
Diameter stenosis(%)	17.14 ± 9.12	14.34 ± 8.77	0.121

BRS, bioresorbable vascular scaffold; DES, drug eluting stent; DVD, double vessel disease; MLD, minimal lumen diameter; RVD, reference vessel diameter; SVD, single vessel disease; TVD, triple vessel disease. Values are expressed as numbers (percentages) when appropriate.

in the BRS group which trended towards significance (0.09 ± 0.11 versus 0.05 ± 0.06 mm^2, $p = 0.082$). Further strut level analysis showed that the ISA distance was greater in the BRS group compared with DES [BRS versus DES; 260 (218 − 303) versus 93 (66 − 120) μm, $p < 0.001$].

Comparison across Calcification Groups

Comparisons between BRS and DES for each calcification subgroup are presented in Table V. In each calcification subgroup, there were no significant differences in minimal stent/scaffold area, mean stent/scaffold area and % RAS between BRS and DES. BRS had a marginally lower EI than DES in the no/mild calcification group (0.86 ± 0.03 versus 0.88 ± 0.03, $p = 0.018$) but there were no significant differences in the moderate and heavy calcification subgroups (Fig. 4). BRS had a significantly lower percentage of ISA struts than DES in the moderate and severe calcification subgroups (BRS versus DES: moderate; 2.96 ± 2.36 versus 6.78 ± 4.61%, $p = 0.002$ and heavy; 1.82 ± 2.40 versus 8.89 ± 8.25%,

TABLE III. Procedural Characteristics (N = 100).

	BRS ($N = 50$)	DES ($N = 50$)	P value
Predilation performed	48 (96.0%)	29 (58.0%)	<0.001
Predilation balloon size: artery greater or equal to 1	17 (43.6%)	11 (37.9%)	0.804
Maximal diameter balloon predilation, mm	2.54 ± 0.36	2.38 ± 0.46	0.094
Maximal predilation balloon inflation, atm	12.79 ± 2.46	14.64 ± 4.29	0.052
Predilation Balloon/artery ratio	1.01 ± 0.32	0.94 ± 0.27	0.299
Cutting balloon	1 (2.0%)	0	1.000
Mean scaffold/stent diameter, mm	3.08 ± 0.35	3.01 ± 0.47	0.359
Scaffold/stent diameter: PreRVD	1.24 ± 0.38	1.17 ± 0.31	0.328
Mean total nominal scaffold/stent length	33.04 ± 20.93	30.46 ± 14.48	0.475
Number of scaffolds/stents per treated lesion			0.698
1	32 (64.0%)	34 (68.0)%	
2	13 (26.0%)	14(28.0%)	
3	2(4.0%)	1 (2.0%)	
4	3(6.0%)	1(2.0%)	
Overlapping Devices	20 (40.0%)	16 (32.0%)	0.532
Postdilation performed	25 (50.0%)	28 (56.0%)	0.689
Postdilation balloon size: artery greater or equal to 1	20 (90.9%)	24 (92.3%)	1.000
Postdilation balloon greater than device size	11 (44.0%)	16 (52.2%)	0.586
Maximal post dilation balloon diameter, mm	3.18 ± 0.39	3.54 ± 0.68	0.023
Maximal post- dilation balloon inflation, atm	14.33 ± 4.08	17.30 ± 3.29	0.071

BRS, bioresrobable vascular scaffold; DES, drug eluting stent; RVD, reference vessel diameter.

TABLE IV. Optical Coherence Tomography Measurements[a] (*N* = 100)

	BRS ($N = 50$)	DES ($N = 50$)	P value
Analyzed length/mm	29.88 ± 14.69	28.85 ± 11.79	0.700
Reference lumen area/mm^2	6.87 ± 1.91	6.65 ± 2.99	0.656
Minimum lumen area/mm^2	5.83 ± 1.75	5.70 ± 2.19	0.737
Mean lumen area/mm^2	7.82 ± 1.77	7.77 ± 2.71	0.919
Lumen volume/mm^3	226.15 ± 120.08	218.31 ± 110.38	0.734
Maximum scaffold/stent diameter/mm	3.85 ± 0.48	3.84 ± 0.68	0.939
Minimum scaffold/stent diameter/mm	2.43 ± 0.40	2.51 ± 0.54	0.400
Minimal scaffold/stent area/mm^2	6.26 ± 1.77	6.45± 2.69	0.665
Mean scaffold/stent area/mm^2	7.96 ± 1.84	8.38 ± 2.99	0.399
Scaffold/stent volume/mm^3	216.76 ± 120.12	229.62 ± 118.25	0.591
RAS/%	12.77 ± 20.78	12.34 ± 23.19	0.923
Device with 20% RAS or higher/%(n)	34.0 (17)	38.0 (19)	0.835
EI	0.85 ± 0.04	0.87 ± 0.02	0.002
EI at MSA	0.80 ± 0.10	0.83 ± 0.08	0.125
SI	0.37 ± 0.09	0.35 ± 0.09	0.250
Device with ISA detected			
Overall/%(n)	72.0 (36)	94.0 (47)	0.006
ISA distal edge/%(n)	32.0 (16)	46.0 (23)	0.218
ISA proximal edge/%(n)	52.0 (26)	68.0 (34)	0.153
ISA (Overall)/%	2.57 ± 2.78	5.97 ± 5.53	<0.001
Device with equal or higher than 5%ISA/%(n)	22.0 (11)	52.0 (26)	0.003
Mean ISA area/mm^2	0.09 ± 0.11	0.05 ± 0.06	0.082
ISA Distance/μm	260.33 (217.95-302.72)	93.19 (66.02-120.35)	<0.001
Prolapse area/mm^2	0.35 ± 0.17	0.70 ± 0.38	< 0.001
Edge Dissection (Proximal/Distal)/% (n)[a]	46.9 (23)	56.0 (28)	0.424

[a]Comparison between scaffold and stent abluminal contours.
BRS- Bioresorbable vascular scaffold.
EI- Eccentricity Index.
DES- Drug Eluting Stent.
ISA- Incomplete Strut Apposition.
MSA- Minimal scaffold/stent area.
RAS- Residual Area Stenosis.
SI-Symmetry Index.

TABLE V. Comparison of Optical Coherence Tomography Measurements across Calcification Groups[a].

	None/Mild calcification			Moderate calcification			Heavy calcification		
	BRS (N=20)	DES (N=20)	p value	BRS (N=20)	DES (N=20)	p value	BRS (N=10)	DES (N=10)	p value
Analyzed length/mm	26.06 ± 10.95	28.20 ± 13.47	0.585	30.87 ± 16.44	28.13 ± 10.77	0.536	35.54 ± 16.77	31.60 ± 10.86	0.542
Reference lumen area/mm^2	7.25 ± 1.59	7.53 ± 3.83	0.763	6.59 ± 1.87	6.06 ± 1.93	0.389	6.68 ± 2.58	6.04 ± 2.65	0.592
Minimum lumen area/mm^2	6.08 ± 1.61	5.92 ± 2.89	0.831	5.64 ± 1.67	5.57 ± 1.76	0.903	5.72 ± 2.26	5.50 ± 1.30	0.796
Mean lumen area/mm^2	7.84 ± 1.73	8.12 ± 3.46	0.764	7.79 ± 1.77	7.60 ± 2.30	0.770	7.79 ± 2.00	7.42 ± 1.78	0.661
Lumen volume/mm^3	198.01 ± 99.91	218.51 ± 125.65	0.571	235.04 ± 137.54	212.79 ± 109.12	0.574	264.67 ± 117.94	228.93 ± 87.61	0.452
Maximum scaffold/stent diameter/mm	3.82 ± 0.48	3.88 ± 0.79	0.774	3.83 ± 0.51	3.84 ± 0.64	0.930	3.97 ± 0.44	3.77 ± 0.55	0.388
Minimum scaffold/stent diameter/mm	2.52 ± 0.37	2.56 ± 0.68	0.804	2.38 ± 0.35	2.52 ± 0.48	0.298	2.37 ± 0.56	2.40 ± 0.34	0.868
Minimal scaffold/stent area (MSA)/mm^2	6.47 ± 1.71	6.79 ± 3.58	0.725	6.11 ± 1.53	6.31 ± 2.13	0.736	6.12 ± 2.41	6.08 ± 1.51	0.966
Mean scaffold/stent area/mm^2	7.99 ± 1.86	8.80 ± 3.84	0.394	7.91 ± 1.81	8.18 ± 2.43	0.690	8.00 ± 2.06	7.90 ± 2.04	0.918
Scaffold/stent volume/mm^3	196.57 ± 102.12	230.87 ± 135.75	0.372	229.17 ± 132.36	224.15 ± 115.77	0.899	232.33 ± 134.32	238.06 ± 93.75	0.913
RAS/%	15.37 ± 15.81	17.06 ± 25.11	0.801	10.95 ± 25.81	4.47 ± 24.34	0.420	11.19 ± 19.78	19.34 ± 7.59	0.263
Device with 20% RAS or higher/%(*n*)	35.0 (7)	50.0 (10)	0.523	40.0 (8)	20.0 (4)	0.301	20.0 (2)	50.0 (5)	0.350
EI	0.86 ± 0.03	0.88 ± 0.03	0.018	0.85 ± 0.05	0.87 ± 0.02	0.096	0.83 ± 0.04	0.85 ± 0.02	0.104
EI at MSA	0.83 ± 0.07	0.83 ± 0.08	0.797	0.80 ± 0.11	0.85 ± 0.07	0.094	0.78 ± 0.11	0.80 ± 0.09	0.629
SI	0.34 ± 0.07	0.34 ± 0.10	0.915	0.38 ± 0.08	0.34 ± 0.09	0.216	0.40 ± 0.13	0.36 ± 0.07	0.374
Device with ISA detected/%(*n*)	70.0 (14)	85.0 (17)	0.451	75.0 (15)	100.0 (20)	0.047	70.0 (7)	100.0 (10)	0.211
ISA/%	2.56 ± 3.33	3.70 ± 3.83	0.322	2.96 ± 2.36	6.78 ± 4.61	0.002	1.82 ± 2.40	8.89 ± 8.25	0.025
ISA (Distal edge)	4 (20.0)	8(40.0)	0.301	9 (45.0)	13 (65.0)	0.341	3 (30.0)	2 (20.0)	1.000
ISA (Proximal edge)	7 (35.0)	11 (55.0)	0.341	15 (75.0)	14 (70.0)	1.000	4 (40.0)	9 (90.0)	0.057
Device with equal or higher than 5% ISA/%(*n*)	20.0 (4)	35.0 (7)	0.480	30.0 (6)	65.0 (13)	0.056	10.0 (1)	60.0 (6)	0.057
Mean ISA area/mm^2	0.08 ± 0.14	0.04 ± 0.04	0.168	0.11 ± 0.10	0.06 ± 0.07	0.084	0.05 ± 0.08	0.08 ± 0.08	0.451
ISA Distance/μm	307.93 (216.84-399.03)	86.29 (27.11-145.46)	<0.001	234.16 (153.23-315.08)	90.84 (22.68-159.00)	<0.001	313.40 (211.46-415.33)	96.60 (41.24-151.95)	<0.001
Prolapse area/mm^2	0.33 ± 0.17	0.77 ± 0.49	0.001	0.35 ± 0.17	0.66 ± 0.23	<0.001	0.39 ± 0.17	0.63 ± 0.38	0.086
Edge Dissection (Proximal/Distal)/% (*n*)	50.0 (10)	55.0 (11)	1.000	42.1 (8)	50.0 (10)	0.751	50.0 (5)	70.0 (7)	0.650

[a]Cases without available edge segments for analysis were excluded. BRS, bioresorbable vascular scaffold; DES, drug eluting stent; EI, eccentricity index; ISA, incomplete strut apposition; MSA, minimal scaffold/stent area; RAS, residual area stenosis; SI, symmetry index.

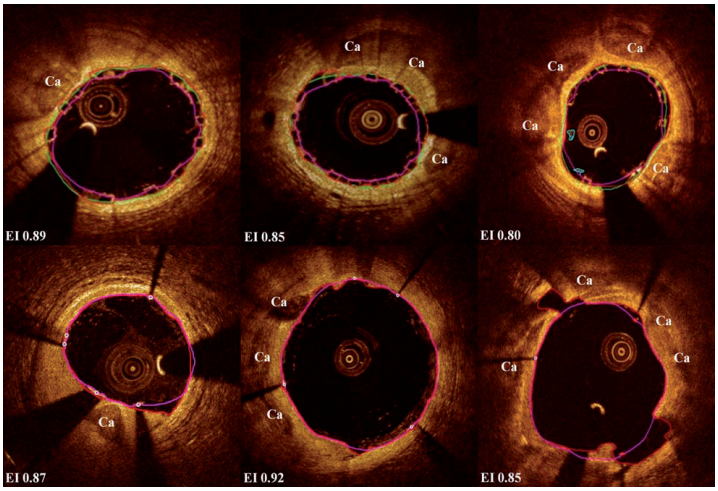

Fig. 4. Optical Coherence Tomography (OCT) measurements of the segments following device implantation. Case Examples of OCT images from patients in the calcification subgroups. Panels A to C: Scaffolded segments on OCT. Panels D to F: Stented segments on OCT. EI- Eccentricity Index Ca-calcification *Intraluminal material OCT- Optical coherence Tomography. Figure 5 Optical coherence tomography findings of the Bioresorbable vascular scaffold (BRS) versus the Drug Eluting Stent (DES) by degree of calcification. The figure shows similar mean scaffold/stent areas and percentage residual area stenosis (%RAS) between bioresorbable vascular scaffold (BRS) and drug eluting stent (DES) across the degrees of calcification. Eccentricity index (EI) was marginally lower in the BRS compared with DES in the mildly calcified group. % Incomplete strut apposition was significantly higher in DES compared with BRS in the moderate and heavily calcified groups. NS- non significant.

$p = 0.025$), but there was no significant difference in the no/mild calcification subgroup (Fig. 5).

Procedural and Clinical Outcomes

Procedural outcomes are available in all cases. In the BRS group, 9 cases encountered challenging device deliverability requiring the use of buddy wires or daughter catheters. All scaffolds eventually were deployed successfully. There were 2 and 1 BRS cases which were noted to have significant dissection and scaffold disruption respectively requiring further bail-out by scaffolds. 2 BRS cases encountered significant noflow requiring adenosine which resolved subsequently. 3 of the DES cases had significant dissection of which 2 requiring further bailout by metallic stents, among which 1 case developed concurrent significant no reflow.

1 year clinical outcomes are available in 29 of the BRS cases and 48 of the DES cases. There were 2 deaths at 1 year in the BRS group. One of the deaths was due to possible late scaffold thrombosis. 1 other case underwent target vessel revascularization (TVR) at 218 days after the procedure. There was 1 death and 1 myocardial infarction at 88 days and 360 days post procedure respectively in the DES group. 1 DES case had to undergo repeat target vessel revascularization 24 hr after implantation due to stent thrombosis. No episodes of thrombosis was reported in the DES group.

DISCUSSION

The main findings of this study were: (1) the expansion of BRS was similar to that of DES (in terms of scaffold/stent area, lumen area and percentage RAS) but with higher eccentricity; (2) these findings were consistent across the calcification subgroups; (3) tissue prolapse was significantly higher in the DES compared to BRS; and (4) ISA was lower in the BRS group compared to DES, a difference observed mainly in moderately and heavily calcified lesions.

BRS offers several unique potential advantages over DES but have been reported to have lower deliverabilty and radial strength compared to current second generation DES [11]. Concerns have been raised as to whether the structural differences attributed to the underlying material composition may produce less favourable stent performance compared with DES such

as expansion. Such a difference can be particularly more pronounced in calcified lesions where focal areas of calcification limit expansion of the BRS more compared to DES [11]. This is potentially important as inadequate expansion of stent has been identified as a predictor of metallic stent failure [18] and observations of inadequate scaffold expansion has been in reported case series with BRS failure [19,20]. In our study, the key finding was that the mean scaffold/stent areas, lumen areas and percentage RAS were similar in the BRS compared to the DES group regardless of the calcification group. This is a noteworthy finding since traditionally the degree of relative area stenosis has been included in several IVUS criteria of DES expansion and shown in previous trials to have a positive relationship with clinical outcomes [21,22]. We believe a key strength of this study was that despite reported weaknesses in deliverability and radial strength in BRS compared to second generation DES [11], the stent performance of BRS was still comparable to second generation DES in calcified lesions as assessed by OCT.

Comparison of acute stent performance between BRS and DES was previously studied using IVUS [16]. This is the first study looking at differences in scaffold/stent deployment parameters between BRS and DES in calcified lesions using OCT. In addition, we employed a novel methodology for a meaningful comparison of morphometric indexes of expansion comparing the abluminal contours in both types of devices. In contrast to previously applied methods that compared the abluminal contour of the BRS and the adluminal contour of DES, this adjustment allowed us to ensure that are results are not biased by methodological bias. In order to ensure the consistency of our findings, we repeated the analysis using adluminal contours, again in both devices, and the results were similar with the exception of minimum scaffold/stent diameter and mean scaffold area that tended to be lower in the BRS group (Supporting Information Table I). However, such a difference appears to be rather artificial and attributed to the difference in strut thickness (with BRS being around 60 μm thicker than DES) [12]. Lumen area, a more clinically relevant index remained unaffected and similar in the two groups.

In our study, BRS were associated with a lower EI (implying more eccentric expansion) than DES, and a similar trend was evident across the calcification subgroups. These findings appear consistent with IVUS observations of a lower EI in BRS compared to DES implanted in non-complex lesions[16]. One of the possible explanations that the higher EI is seen in the BRS group may be secondary to the higher conformability of the BRS compared to DES [23]. Difference in overall implantation strategy may also have an impact on the OCT findings. Though scaffold expansion was similar to metallic stents in calcified lesions in this study, more aggressive predilation was employed in the BRS compared to DES, yet larger balloons were employed for postdilation in DES. Importantly, the OCT findings were consistent across the calcification subgroups. Inadequate device expansion can increase the risk of stent thrombosis and in stent restenosis [24]. Therefore, in these lesions adequate lesion preparation is of outmost importance in order to ensure optimal device expansion.

Patients enrolled in the BVS Expand registry are in general younger with less comorbidities but with longer lesion length, as well as complex lesions such as chronic total occlusions (CTOs) and bifurcations, reflecting lesions encountered in routine clinical practice, compared to Absorb II [25] or Absorb III [26] trials. The relatively higher use of intracoronary imaging was part of the strategy when BRS was introduced for clinical use in our institution. We believe this reflects a wide variety of both simple and complex lesions encountered in real life clinical practice and since treatment was performed at the operator's discretion according to clinical judgement, we consider the type of lesions encountered and resultant outcomes seen on OCT in this study to be reflective of what happens in "real life". To the authors' knowledge, this is the first study that sought to address a real world clinical case scenario when procedurists may face the dilemma of choosing between BRS and DES in significantly calcified lesions. Our findings suggest that regardless of the degree of angiographic calcification, BRS can achieve a similar expansion as DES, in the context of an imaging-guided strategy with adequate lesion preparation while potentially offering the advantages unique to BRS. Our findings are also consistent with recent data [27] addressing the feasibility of BRS in calcified lesions. In a single device arm study conducted by Panoulas et al, expansion of BRS as measured in terms of lumen gain on QCA and intravascular ultrasound (IVUS) was similar between calcified and non-calcified lesions. However a greater degree of lesion preparation in calcified lesions was also required. OCT was not used and a comparison of the expansion of BRS compared with DES was not performed.

ISA was significantly lower in the BRS group compared with DES. The incidence of ISA in BRS in our study was 2.57%, which was lower than to the malapposition rate of $2.9-3.5\%$ of previous studies including either simple [28] or more complex lesions [29–31]. Of note, patients in our study cohort came from a real-world clinical registry with high lesion and scaffold length and high lesion complexity. The lower incidence of ISA in the BRS group is potentially due

to the higher extent of predilation supporting the notion that adequate lesion preparation and predilation using adequate sized balloons may play a key role in reducing ISA. Further studies would help to support this hypothesis. Data on the effect of ISA on clinical outcome are still inconclusive [32], and despite a high incidence of ISA in patients with events [33,34], this has not been validated prospectively. Interestingly, despite a lower percentage ISA struts in the BRS group, the ISA area and distance was higher in the BRS group. This discrepancy suggests that though ISA occurred less frequently in BRS, when ISA does occur, the extent in BRS is greater compared to DES. Further studies are required to further evaluate this finding. While prolapse might be affected by the extent of predilation-related tissue dissection, we think that the thicker strut thickness of the BRS also allowed a greater extent of the prolapse material to be accommodated between the struts compared to DES which can account for the lower mean prolapse area seen in the BRS group. Despite the differences in the prolapse area between the 2 groups, there were no significant differences in lumen areas and %RAS.

Though postdilation rates were comparable between the 2 device groups, postdilation rate was relatively lower in this study compared to what had been reported previously [35]. While the current scaffold implantation strategy recommends incorporating postdilation with high pressure, this study showed that it was potentially possible to achieve optimal acute device outcomes despite the lower use of postdilation in the context of adequate guidance from OCT.

STUDY LIMITATIONS

We acknowledge the following limitations. This is a single center retrospective nonrandomized study with its inherent limitations, including a possible selection bias. In addition, calcification assessment was based on angiographic classification alone which was inherent to our study question in mind, aiming to reflect widespread clinical practice if angiography only is used to plan PCI strategy. Data were obtained from a relatively small number of patients and our results should be confirmed in larger study population. As this study aimed to provide pilot observations regarding the expansion of BRS compared to DES, power calculations were not performed and a formal sample size was not defined.

Although this study showed that BRS may achieve a similar degree of expansion compared to DES, the precise impact of OCT guidance in influencing the decision for further optimization such as postdilation could not be studied in detail as other clinical or procedural factors may have influenced the operator's decision regarding further optimization. Postdilation was not performed routinely in both groups and only at operator's discretion which may affect comparisons between postdeployment measurements, while the use of imaging guidance both in DES and BRS might have contributed to our results. The current study population was too small to further evaluate the effect of predilation/postdilation in each group. As our study was underpowered to detect differences in clinical outcomes between the two devices, larger prospective studies would be able to address these issues in the future.

CONCLUSION

With adequate lesion preparation, implantation of BRS in a population reflective of clinical practice, resulted in a similar luminal gain compared to DES as measured by OCT, regardless of the degree of angiographic calcification, while acute malapposition is lower with BRS in moderately and heavily calcified lesions. The clinical significance of our findings warrants further evaluation in future studies.

REFERENCES

1. Windecker S, Kolh P, Alfonso F, Collet JP, Cremer J, Falk V, Filippatos G, Hamm C, Head SJ, Jüni P, Kappetein AP, Kastrati A, Knuuti J, Landmesser U, Laufer G, Neumann FJ, Richter DJ, Schauerte P, Sousa Uva M, Stefanini GG, Taggart DP, Torracca L, Valgimigli M, Wijns W, Witkowski A. 2014 ESC/EACTS guidelines on myocardial revascularisation. Eur Heart J 2014;35: 2541–2619.
2. Levine GN, Bates ER, Blankenship JC, Bailey SR, Bittl JA, Cercek B, Chambers CE, Ellis SG, Guyton RA, Hollenberg SM, Khot UN, Lange RA, Mauri L, Mehran R, Moussa ID, Mukherjee D, Nallamothu BK, Ting HH. American College of Cardiology Foundation; American Heart Association Task Force on Practice Guidelines; Society for Cardiovascular Angiography and Interventions. 2011 ACCF/AHA/SCAI Guideline for Percutaneous Coronary Intervention A Report of the American College of Cardiology Foundation/American Heart Association Task Force on Practice Guidelines and the Society for Cardiovascular Angiography and Interventions. J Am Coll Cardiol 2011;58:e44–e122. Dec 6;
3. Kawaguchi R, Tsurugaya H, Hoshizaki H, Toyama T, Oshima S, Taniguchi K. Impact of lesion calcification on clinical and angiographic outcome after sirolimus-eluting stent implantation in real-world patients. Cardiovasc Revasc Med 2008;9:2–8.
4. Moussa I, Ellis SG, Jones M, Kereiakes DJ, McMartin D, Rutherford B, Mehran R, Collins M, Leon MB, Popma JJ, Russell ME, Stone GW. Impact of coronary culprit lesion calcium in patients undergoing paclitaxel-eluting stent implantation (a TAXUS-IV sub study). Am J Cardiol 2005;96:1242–1247.
5. Bourantas CV, Zhang YJ, Garg S, Iqbal J, Valgimigli M, Windecker S, Mohr FW, Silber S, Vries Td Onuma Y, Garcia-Garcia HM, Morel MA Serruys PW. Prognostic implications of coronary calcification in patients with obstructive coronary artery disease treated by percutaneous coronary intervention: a patient-level pooled analysis of 7 contemporary stent trials. Heart 2014;100:1158–1164. Aug;

6. de Jaegere P, Mudra H, Figulla H, Almagor Y, Doucet S, Penn I, Colombo A, Hamm C, Bartorelli A, Rothman M, Nobuyoshi M, Yamaguchi T, Voudris V, DiMario C, Makovski S, Hausmann D, Rowe S, Rabinovich S, Sunamura M, van Es GA. Intravascular ultrasound-guided optimized stent deployment. Immediate and 6 months clinical and angiographic results from the multicenter ultrasound stenting in coronaries study (MUSIC Study). Eur Heart J 1998;19:1214–1223.
7. Otake H, Shite J, Ako J, Shinke T, Tanino Y, Ogasawara D, Sawada T, Miyoshi N, Kato H, Koo BK, Honda Y, Fitzgerald PJ, Hirata K. Local determinants of thrombus formation following sirolimus-eluting stent implantation assessed by optical coherence tomography. J Am Coll Cardiol Intv 2009;2:459–466.
8. Simsek C, Karanasos A, Magro M, Garcia-Garcia HM, Onuma Y, Regar E, Boersma E, Serruys PW, van Geuns RJ. Long-term invasive follow-up of the everolimus-eluting bioresorbable vascular scaffold: Five-year results of multiple invasive imaging modalities. EuroIntervention 2014;Oct 28. doi: 10.4244/EIJY14M10_12. [Epub ahead of print]
9. Karanasos A, Simsek C, Gnanadesigan M, van Ditzhuijzen NS, Freire R, Dijkstra J, Tu S, Van Mieghem N, van Soest G, de Jaegere P, Serruys PW, Zijlstra F, van Geuns RJ, Regar E. OCT assessment of the long-term vascular healing response 5 years after everolimus-eluting bioresorbable vascular scaffold. J Am Coll Cardiol 2014;64:2343–2356. Dec 9;
10. Serruys PW, Ormiston JA, Onuma Y, Regar E, Gonzalo N, Garcia-Garcia HM, Nieman K, Bruining N, Dorange C, Miquel-Hébert K, Veldhof S, Webster M, Thuesen L, Dudek D. A bioabsorbable everolimus-eluting coronary stent system (ABSORB): 2-year outcomes and results from multiple imaging methods. Lancet 2009;373:897–910.
11. Tanimoto S, Serruys PW, Thuesen L, Dudek D, de Bruyne B, Chevalier B, Ormiston JA. Comparison of in vivo acute stent recoil between the bioabsorbable everolimus-eluting coronary stent and the everolimus-eluting cobalt chromium coronary stent: Insights from the ABSORB and SPIRIT trials. Catheter Cardiovasc Interv 2007;70:515–523.
12. Tearney GJ, Regar E, Akasaka T, Adriaenssens T, Barlis P, Bezerra HG, Bouma B, Bruining N, Cho JM, Chowdhary S, Costa MA, de Silva R, Dijkstra J, Di Mario C, Dudek D, Falk E, Feldman MD, Fitzgerald P, Garcia-Garcia HM, Gonzalo N, Granada JF, Guagliumi G, Holm NR, Honda Y, Ikeno F, Kawasaki M, Kochman J, Koltowski L, Kubo T, Kume T, Kyono H, Lam CC, Lamouche G, Lee DP, Leon MB, Maehara A, Manfrini O, Mintz GS, Mizuno K, Morel MA, Nadkarni S, Okura H, Otake H, Pietrasik A, Prati F, Räber L, Radu MD, Rieber J, Riga M, Rollins A, Rosenberg M, Sirbu V, Serruys PW, Shimada K, Shinke T, Shite J, Siegel E, Sonoda S, Suter M, Takarada S, Tanaka A, Terashima M, Uemura TT, Ughi S, van Beusekom GJ, van der Steen HM, van Es AF, van Soest GA, Virmani G, Waxman R, Weissman S, Weisz NJ, International Working Group for Intravascular Optical Coherence Tomography G (, IVOCT IWG.). Consensus standards for acquisition, measurement, and reporting of intravascular optical coherence tomography studies: A report from the International Working Group for Intravascular Optical Coherence Tomography Standardization and Validation. J Am Coll Cardiol 2012;59:1058–1072.
13. Diletti R, Karanasos A, Muramatsu T, Nakatani S, Van Mieghem NM, Onuma Y, Nauta ST, Ishibashi Y, Lenzen MJ, Ligthart J, Schultz C, Regar E, de Jaegere PP, Serruys PW, Zijlstra F, van Geuns RJ. Everolimus-eluting bioresorbable vascular scaffolds for treatment of patients presenting with ST-segment elevation myocardial infarction: BVS STEMI first study. Eur Heart J 2014;35:777–786. Mar;
14. Serruys PW, Onuma Y, Ormiston JA, de Bruyne B, Regar E, Dudek D, Thuesen L, Smits PC, Chevalier B, McClean D, Koolen J, Windecker S, Whitbourn R, Meredith I, Dorange C, Veldhof S, Miquel-Hebert K, Rapoza R, García-García HM. Evaluation of the second generation of a bioresorbable everolimus drug-eluting vascular scaffold for treatment of de novo coronary artery stenosis: Six-month clinical and imaging outcomes. Circulation 2010;122:2301–2312. Nov 30;
15. Garcia-Garcia HM, Serruys PW, Campos CM, Muramatsu T, Nakatani S, Zhang YJ, Onuma Y, Stone GW. Assessing bioresorbable coronary devices: Methods and parameters. JACC Cardiovasc Imaging 2014;7:1130–1148. Nov;
16. Brugaletta S, Gomez-Lara J, Diletti R, Farooq V, van Geuns RJ, de Bruyne B, Dudek D, Garcia-Garcia HM, Ormiston JA, Serruys PW. Comparison of in vivo eccentricity and symmetry indices between metallic stents and bioresorbable vascular scaffolds: Insights from the ABSORB and SPIRIT trials. Catheter Cardiovasc Interv 2012;79:219–228.
17. Barlis P, Dimopoulos K, Tanigawa J, Dzielicka E, Ferrante G, Del Furia F, Di Mario C. Quantitative analysis of intracoronary optical coherence tomography measurements of stent strut apposition and tissue coverage. Int J Cardiol 2010;141:151–156.
18. Choi SY, Witzenbichler B, Maehara A, Lansky AJ, Guagliumi G, Brodie B, Kellett MA Jr, Dressler O, Parise H, Mehran R, Dangas GD, Mintz GS, Stone GW. Intravascular ultrasound findings of early stent thrombosis after primary percutaneous intervention in acute myocardial infarction: A Harmonizing Outcomes with Revascularization and Stents in Acute Myocardial Infarction (HORIZONS-AMI) substudy. Circ Cardiovasc Interv 2011;4:239–247. Jun;;
19. Karanasos A, Van Mieghem N, van Ditzhuijzen N, Felix C, Daemen J, Autar A, Onuma Y, Kurata M, Diletti R, Valgimigli M, Kauer F, van Beusekom H, de Jaegere P, Zijlstra F, van Geuns RJ, Regar E. Angiographic and optical coherence tomography insights into bioresorbable scaffold thrombosis. A single-center experience. Circ Cardiovasc Interv. 2015 May;8(5). pii: e002369. doi: 10.1161/CIRCINTERVENTIONS.114.002369.
20. Longo G, Granata F, Capodanno D, Ohno Y, Tamburino CI, Capranzano P, La Manna A, Francaviglia B, Gargiulo G, Tamburino C. Anatomical features and management of bioresorbable vascular scaffolds failure: A case series from the GHOST registry. Catheter Cardiovasc Interv 2015;Jan 8. doi: 10.1002/ccd.25819. [Epub ahead of print]
21. Fujii K, Carlier SG, Mintz GS, Yang YM, Moussa I, Weisz G, Dangas G, Mehran R, Lansky AJ, Kreps EM, Collins M, Stone GW, Moses JW, Leon MB. Stent underexpansion and residual reference segment stenosis are related to stent thrombosis after sirolimus- eluting stent implantation: An intravascular ultrasound study. J Am Coll Cardiol 2005;45:995–998.
22. Doi H, Maehara A, Mintz GS, Yu A, Wang H, Mandinov L, Popma JJ, Ellis SG, Grube E, Dawkins KD, Weissman NJ, Turco MA, Ormiston JA, Stone GW. Impact of post-intervention minimal stent area on 9-month follow-up patency of paclitaxel eluting stents: An integrated intravascular ultrasound analysis from the TAXUS IV, V, and VI and TAXUS ATLAS Workhorse, Long Lesion, and Direct Stent Trials. J Am Coll Cardiol Intv 2009;2:1269–1275.
23. Gomez-Lara J, Garcia-Garcia HM, Onuma Y, Garg S, Regar E, De Bruyne B, Windecker S, McClean D, Thuesen L, Dudek D, Koolen J, Whitbourn R, Smits PC, Chevalier B, Dorange C, Veldhof S, Morel MA, de Vries T, Ormiston JA, Serruys PW. A comparison of the conformability of everolimus-eluting bioresorbable vascular scaffolds to metal platform coronary stents. JACC Cardiovasc Interv 2010;3:1190–1198. Nov;;

24. Moses JW, Carlier S, Moussa I. Lesion preparation prior to stenting. Rev Cardiovasc Med 2004;5:S16–S21.
25. Diletti R, Serruys PW, Farooq V, Sudhir K, Dorange C, Miquel-Hebert K, Veldhof S, Rapoza R, Onuma Y, Garcia-Garcia HM, Chevalier B. ABSORB II randomized controlled trial: A clinical evaluation to compare the safety, efficacy, and performance of the Absorb everolimus-eluting bioresorbable vascular scaffold system against the XIENCE everolimus-eluting coronary stent system in the treatment of subjects with ischemic heart disease caused by de novo native coronary artery lesions: rationale and study design. Am Heart J 2012;164:654–663. Nov; doi: 10.1016/j.ahj.2012.08.010.
26. Kereiakes DJ, Ellis SG, Popma JJ, Fitzgerald PJ, Samady H, Jones-McMeans J, Zhang Z, Cheong WF, Su X, Ben-Yehuda O, Stone GW. Evaluation of a fully bioresorbable vascular scaffold in patients with coronary artery disease: Design of and rationale for the ABSORB III randomized trial. Am Heart J 2015;170:641–651.e3. Oct; doi: 10.1016/j.ahj.2015.07.013. Epub 2015 Jul 26.
27. Panoulas VF, Miyazaki T, Sato K, Naganuma T, Sticchi A, Kawamoto H, Figini F, Chieffo A, Carlino M, Montorfano M, Latib A, Colombo A. Procedural outcomes of patients treated with bioresorbable vascular scaffolds in calcified lesions. EuroIntervention 2015;10: Mar 30; pii: 20141121-01. doi: 10.4244/EIJY15M03_11. [Epub ahead of print].
28. Gomez-Lara J, Radu M, Brugaletta S, Farooq V, Diletti R, Onuma Y, Windecker S, Thuesen L, McClean D, Koolen J, Whitbourn R, Dudek D, Smits PC, Regar E, Veldhof S, Rapoza R, Ormiston JA, Garcia-Garcia HM, Serruys PW. Serial analysis of the malapposed and uncovered struts of the new generation of everolimus-eluting bioresorbable scaffold with optical coherence tomography. JACC Cardiovasc Interv 2011;4:992–1001.
29. Jaguszewski M, Ghadri JR, Zipponi M, Bataiosu DR, Diekmann J, Geyer V, Neumann CA, Huber MA, Hagl C, Erne P, Lüscher TF, Templin C. Feasibility of second-generation bioresorbable vascular scaffold implantation in complex anatomical and clinical scenarios. Clin Res Cardiol 2015;104:124–135. Feb;:
30. Mattesini A, Secco GG, Dall'Ara G, Ghione M, Rama-Merchan JC, Lupi A, Viceconte N, Lindsay AC, De Silva R, Foin N, Naganuma T, Valente S, Colombo A, Di Mario C. ABSORB biodegradable stents versus second-generation metal stents. A comparison study of 100 complex lesions treated under OCT guidance. J Am Coll Cardiol Intv 2014;7:741–750.
31. Brown AJ, McCormick LM, Braganza DM, Bennett MR, Hoole SP, West NE. Expansion and malapposition characteristics after bioresorbable vascular scaffold implantation. Catheter Cardiovasc Interv 2014;84:37–45. Jul 1;
32. Karanasos A, Regar E. Standing on solid ground? Reassessing the role of incomplete strut apposition in drug-eluting stents. Circ Cardiovasc Interv 2014;7:6–8. Feb;:
33. Guagliumi G, Sirbu V, Musumeci G, Gerber R, Biondi-Zoccai G, Ikejima H, Ladich E, Lortkipanidze N, Matiashvili A, Valsecchi O, Virmani R, Stone GW. Examination of the in vivo mechanisms of late drug-eluting stent thrombosis: Findings from optical coherence tomography and intravascular ultrasound imaging. JACC Cardiovasc Interv 2012;5:12 Jan;: 20
34. Cook S, Eshtehardi P, Kalesan B, Räber L, Wenaweser P, Togni M, Moschovitis A, Vogel R, Seiler C, Eberli FR, Lüscher T, Meier B, Jüni P, Windecker S. Impact of incomplete stent apposition on long-term clinical outcome after drug-eluting stent implantation. Eur Heart J 2012;33:1334–1343.
35. Capodanno D, Gori T, Nef H, Latib A, Mehilli J, Lesiak M, Caramanno G, Naber C, Di Mario C, Colombo A, Capranzano P, Wiebe J, Araszkiewicz A, Geraci S, Pyxaras S, Mattesini A, Naganuma T, Münzel T, Tamburino C. Percutaneous coronary intervention with everolimus-eluting bioresorbable vascular scaffolds in routine clinical practice: Early and midterm outcomes from the European multicentre GHOST-EU registry. EuroIntervention 2015; 10(10:1144–1153. Feb;):-. doi: 10.4244/EIJY14M07_11.

Comparison of Acute Expansion of Bioresorbable Vascular Scaffolds Versus Metallic Drug-Eluting Stents in Different Degrees of Calcification: An Optical Coherence Tomography Study. DOI: 10.1002/ccd.26676

Jiang Ming Fam, Johannes N. van Der Sijde, Antonios Karanasos, Cordula Felix, Roberto Diletti, Nicolas van Mieghem, Peter de Jaegere, Felix Zijlstra, Robert Jan van Geuns, and Evelyn Regar

Figure 5 was omitted from the paper listed above. Figure 5 along with the corresponding caption is listed below. The journal regrets any confusion caused by the error.

DOI: 10.1002/ccd.27327

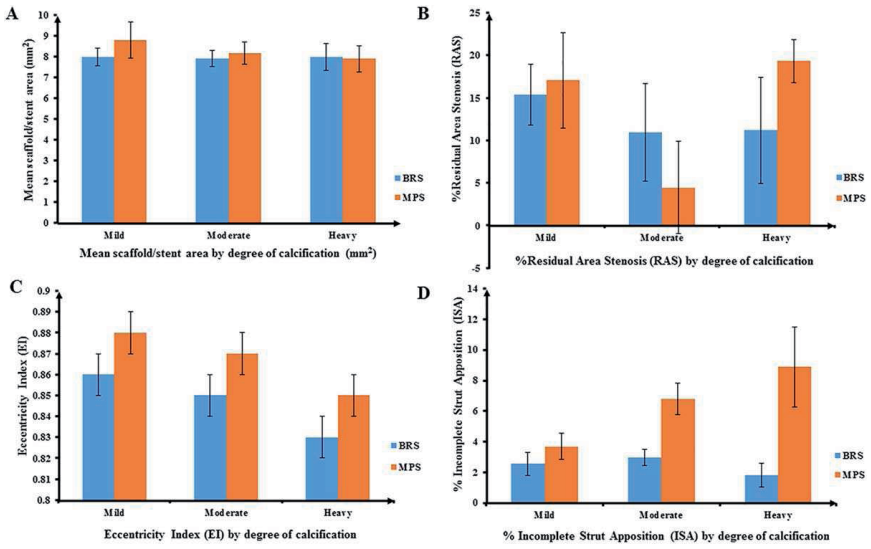

FIGURE 5 Optical coherence tomography findings of the Bioresorbable vascular scaffold (BRS) versus the Drug Eluting Stent (DES) by degree of calcification.The figure shows similar mean scaffold/ stent areas and percentage residual area stenosis (%RAS) between bioresorbable vascular scaffold (BRS) and drug eluting stent (DES)across the degrees of calcification. Eccentricity index (EI) was marginally lower in the BRS compared with DESin the mildly calcified group. % Incomplete strut apposition was significantly higher in DEScompared with BRS in the moderate and heavily calcified groups. NS- non significant. [Color figure can be viewed at wileyonlinelibrary.com]

5

CHAPTER

DIFFERENTIAL THROMBOTIC PROLAPSE BURDEN IN EITHER BIORESORBABLE VASCULAR SCAFFOLDS OR METALLIC STENTS IMPLANTED DURING ACUTE MYOCARDIAL INFARCTION: THE SNOWSHOE EFFECT: INSIGHTS FROM THE MAXIMAL FOOTPRINT ANALYSIS

Diletti R, van der Sijde J, Karanasos A, **Fam JM**, Felix C, van Mieghem NM, Regar E, Rapoza R, Zijlstra F, van Geuns RJ.

Int J Cardiol. 2016 Oct 1; 220: 802-8.

Differential thrombotic prolapse burden in either bioresorbable vascular scaffolds or metallic stents implanted during acute myocardial infarction The snowshoe effect: Insights from the maximal footprint analysis

Roberto Diletti [a,*], Jors van der Sijde [a], Antonios Karanasos [a], Jiang Ming Fam [a,b], Cordula Felix [a], Nicolas M. van Mieghem [a], Evelyn Regar [a], Richard Rapoza [c], Felix Zijlstra [a], Robert Jan van Geuns [a]

[a] Department of Interventional Cardiology, Thoraxcenter, Erasmus MC, Rotterdam, The Netherlands
[b] National Heart Centre Singapore, Singapore
[c] Abbott Vascular, Santa Clara, CA, United States

ARTICLE INFO

Article history:
Received 16 April 2016
Received in revised form 16 May 2016
Accepted 21 June 2016
Available online 23 June 2016

Keywords:
Bioresorbable vascular scaffolds
ST-segment elevation myocardial infarction
Maximal footprint
Snowshoe effect

ABSTRACT

Background: The hypothesized increased thrombus entrapment during bioresorbable vascular scaffold implantation in acute myocardial infarction, the so-called "snowshoe effect" has never been demonstrated.
Methods: Patients enrolled in the BVS STEMI FIRST study matched with STEMI patients implanted with everolimus-eluting metal stents (EES) and undergoing optical coherence tomography (OCT) at the index procedure were compared. Quantitative coronary angiography analysis and optical coherence tomography data for evaluation of thrombotic prolapse were reported. Percentage maximal footprint (%MFP) analysis as an indicator of the snowshoe effect was performed.
Results: A total of 302 patients were analyzed (151 with BVS and 151 with EES). Of those patients 30 implanted with BVS and 17 implanted with EES were imaged at the index procedure with OCT. Baseline clinical characteristics, TIMI-flow and thrombus burden were similar between groups. Aspiration thrombectomy was similarly performed in the two groups (BVS 83.3% vs 94.1% EES, $p = 0.405$). At the end of the procedure, final TIMI 3 flow was achieved in 93.3% and 82.4% of BVS and EES patients respectively ($p = 0.296$). The %MFP was significantly higher in the BVS treated patients ($36.59 \pm 5.65\%$ vs 17.61 ± 4.30, $p < 0.001$). The results of the OCT analysis showed a mean prolapse area (0.61 ± 0.26 mm^2 vs 0.90 ± 0.31 mm^2, $p = 0.001$) and a percentage prolapse area (7.11 ± 2.98 mm^2 vs 9.98 ± 2.90 mm^2, $p = 0.002$) significantly higher in the EES group.
Conclusions: Scaffold structural characteristics such as strut width may play a role in terms of thrombus dislodgment patterns and acute prolapsing material.

1. Introduction

Bioresorbable vascular scaffolds (BVS) have been recently introduced as a novel approach for treatment of coronary artery disease, providing transient vascular support and drug delivery potentially restoring the vascular physiology after device bioresorption [1–4].

The theoretical advantages of this novel technology such as late lumen enlargement restoration of coronary vasomotion and plaque sealing could be particularly appealing in patients with acute soft lesions [5–7]. However, limited data are currently available on the use of this novel device in patients presenting with acute myocardial infarction [8–10], especially in terms of angiographic and intravascular imaging comparisons with current generation drug eluting metal stents.

In addition, the larger BVS strut width and overall footprint on the vessel wall have been hypothesized to enable an increased retention of thrombus between BVS struts and the vessel wall with the so-called "snowshoe effect" [8]. Such effect could potentially result into a reduced amount of prolapsing thrombotic material and a decreased distal embolization [8]. On the other hand, although theoretically valid this "snowshoe effect" has never been demonstrated.

Given this background, we analyzed patients presenting with ST-elevation myocardial infarction treated with BVS and we compared angiographic and short-term clinical results with a matched population implanted with everolimus eluting stents (EES). The present investigation is a sub-analysis of the BVS STEMI FIRST Study [8], focusing on patients with optical coherence tomography (OCT) imaging at baseline. We introduced the concept of percentage maximal footprint (%MFP), representing an estimation of the maximal amount of paving provided

* Corresponding author at: Department of Cardiology, Thoraxcentre, room Ba-581, Erasmus University Medical Centre, 's-Gravendijkwal 230, 3015 GE Rotterdam, The Netherlands.
E-mail address: r.diletti@erasmusmc.nl (R. Diletti).

http://dx.doi.org/10.1016/j.ijcard.2016.06.077
0167-5273/

to the arterial wall by the device and its possible clinical implications when considering acute thrombotic lesions.

2. Methods

The present report is a sub-analysis of BVS STEMI FIRST Study focusing on patients who underwent OCT imaging at post BVS implantation during index procedure. The BVS STEMI FIRST Study has been previously described [8]. Briefly, patients presenting with ST-segment elevation myocardial infarction and treated with BVS at the Thoraxcenter, Erasmus MC in Rotterdam between 1 November 2012 and 31 December 2014, were evaluated. Subjects included were patients ≥18-years old admitted with ST-segment elevation myocardial infarction (STEMI). Culprit lesions were located in vessels within the upper limit of 3.8 mm and the lower limit of 2.0 mm by online quantitative coronary angiography (QCA). The BVS was implanted according to the manufacturer's indication for target-vessel diameter ranges and BVS diameters to be used. The BVS with a nominal diameter of 2.5 mm was implanted in vessels ≥2.0 and ≤3.0 mm by online QCA; the 3.0 mm BVS was implanted in vessels ≥2.5 and ≤3.3 mm by online QCA; the 3.5 mm BVS was implanted in vessels ≥3.0 and ≤3.8 mm. For each nominal diameter a further expansion of 0.5 mm was allowed. All patients were treated with unfractionated heparin at the dose of 70–100 UI/kg and dual antiplatelet therapy after treatment was planned to have a duration of 12 months. Exclusion criteria comprised pregnancy, known intolerance to contrast medium, uncertain neurological outcome after cardiopulmonary resuscitation, previous percutaneous coronary intervention with the implantation of a metal stent, left main (LM) disease, previous coronary artery bypass grafting (CABG), and participation in another investigational drug or device study before reaching the primary endpoints. Propensity score was applied to match each STEMI patient treated with BVS to a comparable patient treated with everolimus-eluting stent (EES) at the same institution. Baseline and post-scaffold/stent implantation quantitative coronary angiographic analysis, optical coherence tomography (when available) analyses at post-scaffold/stent implantation were performed.

2.1. Study device

The second-generation BVS (Absorb BVS, Abbott Vascular, Santa Clara, CA) is a balloon-expandable scaffold consisting of a polymer backbone of poly-L-lactide (PLLA) coated with a thin layer of a 1:1 mixture of an amorphous matrix of poly-D, L-lactide (PDLLA) polymer and 100 μg/cm^2 of the antiproliferative drug everolimus. Two platinum markers located at each BVS edge allow for accurate visualization of the radiolucent BVS during angiography or other imaging modalities. The PDLLA controls the release of everolimus, 80% of the drug is eluted within the first 30 days. Both PLLA and PDLLA are fully bioresorbable. The polymers are degraded via hydrolysis of the ester bonds, and the resulting lactate and its oligomers are transformed to pyruvate and metabolized in the Krebs cycle. Small particles, less than 2 μm in diameter, have also been shown to be phagocytized and degraded by macrophages. According to preclinical studies, [11] complete bioresorption of the polymer backbone occurs from 2 to 3 years after implantation [12].

2.2. Control device

The everolimus eluting coronary stent system is a balloon-expandable metallic platform stent manufactured from a flexible cobalt chromium alloy with a multicellular design and coated with a thin non-adhesive, durable, biocompatible acrylic, and fluorinated everolimus-releasing copolymer.

2.3. Quantitative coronary angiographic analysis

Angiographic views with minimal foreshortening of the lesion and limited overlap with other vessels were used whenever possible for all phases of the treatment. Comparison between pre and post treatment, was performed in matched angiographic views. In case of thrombotic total occlusion, pre-procedure quantitative coronary angiographic analysis was performed as proximally as possible from the occlusion (in case of a side branch distally to the most proximal take off of the side branch), as already reported [8]. Intracoronary thrombus was angiographically identified and scored in five grades as previously described [13,14]. Thrombus grade was assessed before procedure and after thrombectomy. The two-dimensional angiograms were analyzed with the CASS 5.10 analysis system (Pie Medical BV, Maastricht, The Netherlands). In each patient, the treated region and the peri-treated regions (defined as 5 mm proximal and distal to the device edge) were analyzed. The QCA measurements included reference vessel diameter (RVD), percentage diameter stenosis, minimal lumen diameter (MLD), and maximal lumen diameter (Dmax). Acute gain was defined as post-procedural MLD minus pre-procedural MLD (MLD value equal to zero was applied when culprit vessel was occluded pre-procedurally).

2.4. Maximal footprint (MFP) analysis

The larger strut width of the BVS imparts the scaffold with a higher footprint on the vessel segment. This has been recently hypothesized to be a favorable factor when treating thrombotic lesions, given a possible intrinsic enhanced thrombus retention between the scaffold and the vessel wall [8]. So far this theoretical advantage has never been proved. To objectivize such effect, we evaluated the percentage of vessel wall paved by either BVS or metal stents at its maximal point (the minimum lumen diameter), using the concept of percentage "maximal footprint" (%MFP). The %MFP represents a quantification of the device's paving of thrombotic material assessed at the level of the post-implantation minimal lumen diameter (where theoretically the maximal amount of trapped thrombus resides). The % MFP is dependent on device nominal diameter, scaffold/stent pattern and final MLD and is calculated as follows:

$$\%\mathrm{MFP} = 100 * \frac{SA}{\mathrm{VA}} = \frac{100 * SA}{\pi * MLD * L} = \left(\frac{100 * SA}{\pi * L}\right) * 1/\mathrm{MLD}$$

Where SA represents the Scaffold abluminal area in contact with the vessel, VA represents the vessel area and L is the scaffolded or stented length. The percentage maximal footprint was evaluated in both groups (Fig. 1).

2.5. Optical coherence tomography analysis

Optical coherence tomography (OCT) imaging after the BVS implantation was encouraged in all patients but was not mandatory, subordinate to device availability and left at the operator's discretion. Therefore, OCT imaging of the culprit lesion after treatment was performed in a subset of the population. The C7 system or the Ilumien Optis system and DragonFly or DragonFly Duo imaging catheters (St. Jude Medical, St Paul, Minneapolis, Minnesota) were used for image acquisition. The OCT catheter was advanced distal to the treated segment, and an automated pullback was performed at 20 mm/s with simultaneous contrast injection at a rate of 3 to 4 ml/s using a power injector. Two sequential pullbacks were performed to enable assessment of the entire scaffolded/ stented segment when required. The OCT measurements were performed offline using the QCU-CMS software, (Medis Medical Imaging Systems, Leiden, The Netherlands). Analysis was performed at 1-mm intervals within the entire scaffolded/stented segment.

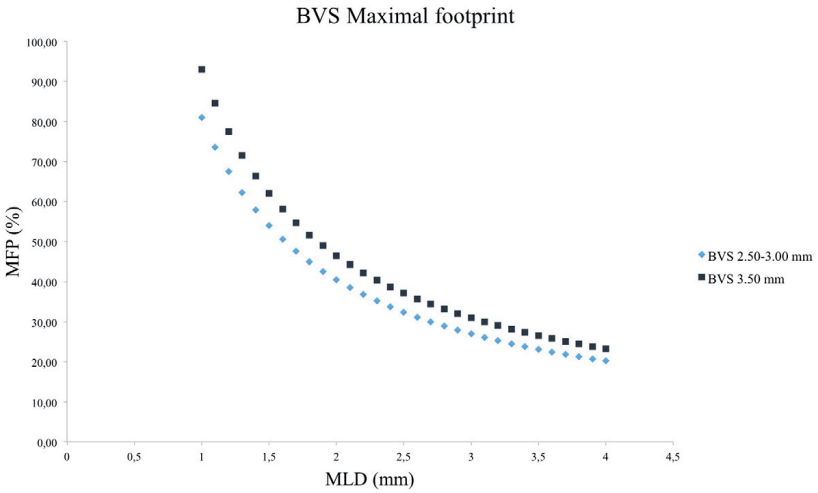

Fig. 1. Percentage Maximal footprint for different BVS sizes. The design of the two BVS sizes has an impact on %MFP, for a similar final MLD the amount of BVS footprint will be higher with the 3.50 mm device compared with the 2.50–3.00 device, on the other hand a high %MFP will be reached with the 2.50–3.00 device at lower MLD.

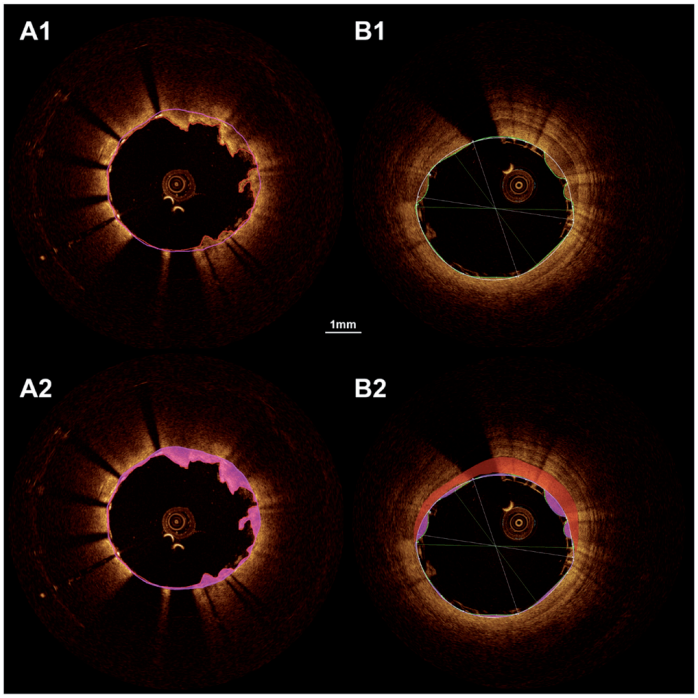

Fig. 2. Thrombotic lesions treated with EES left panel (A1 and A2) and with BVS right panel (B1 and B2). In the lower panels highlighted (pink) the prolapsing atherothrombotic material after EES implantation (A2) and BVS implantation (B2). In the lower right panel highlighted (red) possible atherothrombotic material trapped behind the BVS struts.

Lumen and stent/scaffold area and diameter measurements were performed using standard methodology for the analysis of metal stents and bioresorbable scaffolds [2,8,15,16].

Traditionally, the scaffold/stent contours are traced using the abluminal contour in BVS and the adluminal contour in EES. In order to provide an unbiased comparison of morphometric measurements, we applied an additional modification in the analysis of EES by tracing the stent contour at the point corresponding to the abluminal strut surface. This was calculated automatically by shifting the stent contour towards the abluminal side for a value equal to the nominal strut thickness. Incomplete stent apposition (ISA) was defined as presence of struts separated from the underlying vessel wall for BVS and if the axial distance between the strut's surface and the luminal surface was greater than the strut thickness (80–90 μm) for EES [17].

ISA area is traced in the case of malapposed struts as the area delineated between the lumen and scaffold contours. A scaffold strut is defined as incompletely apposed when there is no contact between the abluminal border of the strut and the vessel wall. This does not include struts located in front of side branches or their ostium (polygon of confluence region), which are defined as side branch-related struts. Intraluminal struts that are part of adjacent clusters of apposed struts in overlapping scaffolds are also not considered malapposed. Percentage of struts with ISA (Number of struts with incomplete apposition/Total Number of struts analyzed × 100%) was also assessed. Tissue prolapse was defined as protrusion of tissue between struts extending into the vessel lumen (Fig. 2). Prolapse area was defined as protrusion of tissue between struts extending into the vessel lumen using abluminal scaffold/stent contours. Tissue prolapse area was quantified as the difference between the scaffold and the lumen area. Device fracture was suspected in the presence of isolated struts lying in the lumen with no connection or overridden by the adjacent device struts.

3. Statistical analysis

A propensity score matching was performed using a proprietary macro developed and tested for SPSS version 22.0 (SPSS Inc., Chicago, Illinois). First, the program performed a logistic regression to score all patients according to the treatment (BVS vs. EES), using as covariates clinical and procedural parameters: age (years), sex (male/female), cardiogenic shock (yes/no), hypertension (yes/no), hypercholesterolemia (yes/no), smoking (yes/no), diabetes mellitus (yes/no), pre-procedure TIMI-flow, culprit vessel. Second, the macro searched and selected the best match case of the EES group for every BVS case according to the absolute value of the difference between the propensity score of BVS and EES cases under consideration. Patients in the 2 groups were matched through a Greedy algorithm based on local optimization [18]. The control selected for a particular case was the one closest to the case in terms of distance. Analyses were then performed on the 2 matched groups (BVS vs. EES), stratified by pairs to account for propensity score matching. For the study, individual data were pooled on a patient-level basis. Continuous variables are expressed as mean ± standard deviation (SD), and categorical variables are presented as absolute number and proportion (%). Overall comparisons between non-matched groups were performed by the t-test for continuous variables and by chi-square or Fisher exact test when appropriate. A 2-sided p value <0.05 was considered statistically significant. All statistical analyses were performed using SPSS version 22.0.

4. Results

A total of 1306 patients presenting with acute ST-segment elevation myocardial infarction were evaluated for the present analysis (161 patients implanted with BVS and 1145 patients implanted with EES). After matching, 302 patients treated with either BVS or EES (151 patients treated with BVS matched with 151 patients treated with EES) were analyzed. Of those patients 30 implanted with BVS and 17 implanted with EES were imaged at the index procedure with OCT.

Table 1
Baseline clinical characteristics.

	BRS (N = 30)	EES (N = 17)	P value
Age, years	59.67 ± 10.77	53.40 ± 9.93	0.055
Male	21/30 (70.0)	11/17 (64.7)	0.708
Active smoker	15/30 (50.0)	6/17 (35.3)	0.375
Diabetes mellitus	5/30 (16.7)	1/17 (5.9)	0.396
Dyslipidemia	11/30 (36.7)	4/17 (23.5)	0.517
Hypertension	12/30 (40.0)	3/17 (17.6)	0.193
Chronic kidney disease	0	0	–
Family history	8/30 (26.7)	7/17 (41.2)	0.344

Data are expressed as count and proportion (%) or mean ± standard deviation.

Baseline clinical characteristics were balanced between groups as shown in Table 1, with a trend towards a higher age in patients implanted with BVS. Aspiration thrombectomy was similarly performed in the two groups (BVS 83.3% vs 94.1% EES, p = 0.405). Predilatation was performed numerically more frequently in the BVS group (56.7% vs 35.3%, $p < 0.227$) with a similar balloon/artery ratio (1.06 ± 0.28 vs 0.96 ± 0.16, p = 0.414) and postdilatation rate (30.0% vs 41.2%, $p < 0.528$). Device success was achieved in all patients (Table 2). Baseline culprit vessels, vessel dimensions, percentage of stenosis, TIMI flow and thrombotic burden were similar between patients treated with BVS and those treated with EES (Table 3). At the end of the procedure, there were no cases of TIMI flow 0, and final TIMI 3 flow was achieved in 93.3% and 82.4% of BVS and EES group respectively (p = 0.296) with similar minimal lumen diameter and percentage stenosis. The percentage maximal footprint was significantly higher in the BVS treated patients (36.59 ± 5.65% vs 17.61 ± 4.30, $p < 0.001$) (Table 3) (Fig. 3). The results of the OCT analysis are reported in Table 4. No differences were observed in terms of mean lumen area (8.20 ± 1.77 mm^2 vs 9.12 ± 2.85 mm^2, p = 0.241), minimum lumen area 6.14 ± 1.46 mm^2 vs 7.07 ± 2.56 mm^2, p = 0.182), mean scaffold/stent (8.73 ± 1.82 mm^2 vs 9.92 ± 3.06 mm^2, p = 0.156) or minimum scaffold/stent areas (6.91 ± 1.80 mm^2 vs 7.86 ± 2.73 mm^2, p = 0.155) and mean ISA area (0.08 ± 0.14 mm^2 vs 0.05 ± 0.06 mm^2, p = 0.443). On the

Table 2
Procedural characteristics.

	BRS (N = 30)	EES (N = 17)	P value
Aspiration thrombectomy	25/30 (83.3)	16/17 (94.1)	0.405
Predilatation performed	17/30 (56.7)	6/17 (35.3)	0.227
Predilatation balloon/artery ratio	1.06 ± 0.28	0.96 ± 0.16	0.414
Maximal diameter balloon predilatation, mm	2.82 ± 0.56	2.67 ± 0.75	0.594
Supportive wire used	6/30 (20.0)	2/17 (11.8)	0.685
Device failure	0	0	–
Device success	30/30 (100)	17/17 (100)	–
Procedure success	30/30 (100)	17/17 (100)	–
Mean scaffold diameter, mm	3.23 ± 0.32	3.21 ± 0.47	0.882
Mean total nominal scaffold length, mm	28.80 ± 14.91	28.94 ± 18.93	0.978
Number of scaffolds deployed per treated vessel	1.28 ± 0.61	1.39 ± 0.73	0.148
1	21/30 (70.0)	14/17 (82.4)	
2	7/30(23.3)	2/17(11.8)	
3	1/30 (3.3)	0	
4	1/30 (3.3)	1/17 (5.9)	
Procedures with overlapping scaffolds, n (%)	8/30 (26.7)	3/17 (17.6)	0.722
Postdilatation performed	9/30 (30.0)	7/17 (41.2)	0.528
Complications occurring anytime during the procedure			
Any dissection	2/30 (6.7)	0	0.528
Thrombosis	0	0	
Perforation	0	0	

Data are expressed as count and proportion (%) or mean ± standard deviation.

Table 3
Angiographic characteristics.

	BRS (N = 30)	EES (N = 17)	P value
Target vessel			0.581
LAD	15/30 (50.0)	10/17 (58.8)	
LCX	4/30 (13.3)	3/17 (17.7)	
RCA	10/30 (33.3)	4/17 (23.5)	
Diagonal	1/30 (3.3)	0	
Ramus intermedius	0	0	
Left main	0	0	
SVG	0	0	
Pre-procedure			
TIMI flow			0.862
0	16/30 (53.3)	8/17 (47.1)	
1	5/30 (16.7)	2/17 (11.8)	
2	7/30 (23.3)	5/17 (29.4)	
3	2/30 (6.7)	2/17 (11.8)	
Thrombus burden			0.648
1	2/30 (6.7)	3/17 (17.6)	
2	7/30 (23.3)	4/17 (23.5)	
3	2/30 (6.7)	0/17 (0)	
4	3/30 (10.0)	2/17 (11.8)	
5	16/30 (53.3)	8/17 (47.1)	
Total thrombotic occlusion			
RVD (mm)	2.86 ± 0.56	2.73 ± 0.48	0.593
Non-total thrombotic occlusion			
RVD (mm)	2.57 ± 0.59	2.93 ± 0.59	0.163
MLD (mm)	0.31 ± 0.41	0.63 ± 0.93	0.108
Diameter stenosis (%)	87.50 ± 17.00	80.18 ± 26.37	0.253
Post-procedure			
TIMI flow			0.296
0	0	0	
1	0	0	
2	2/30 (6.7)	3/17 (17.6)	
3	28/30 (93.3)	14/17 (82.4)	
RVD (mm)	2.86 ± 0.49	3.02 ± 0.47	0.311
MLD (mm)	2.44 ± 0.47	2.69 ± 0.49	0.103
Diameter stenosis (%)	14.63 ± 7.72	11.88 ± 9.64	0.296
Acute lumen gain	2.14 ± 0.64	2.10 ± 0.88	0.876
% Maximum footprint	36.59 ± 5.65	17.61 ± 4.30	<0.001

Data are expressed as count and percentages or mean ± standard deviation.

Table 4
Optical coherence tomography analysis post scaffold/stent deployment.

	BVS (n = 30)	EES (n = 17)	P-value
Analyzed length (mm)	27.53 ± 13.16	29.64 ± 15.48	0.624
Mean lumen area (mm^2)	8.20 ± 1.77	9.12 ± 2.85	0.241
Minimum lumen area (mm^2)	6.14 ± 1.46	7.07 ± 2.56	0.182
Mean stent/scaffold area (mm^2)	8.73 ± 1.82	9.92 ± 3.06	0.156
Minimum stent/scaffold area (mm^2)	6.91 ± 1.80	7.86 ± 2.73	0.155
Mean prolapse area (mm^2)	0.61 ± 0.26	0.90 ± 0.31	0.001
Maximum prolapse area (mm^2)	1.59 ± 0.57	1.94 ± 0.81	0.089
% Prolapse area	7.11 ± 2.98	9.98 ± 2.90	0.002
Mean ISA area (mm^2)	0.08 ± 0.14	0.05 ± 0.06	0.443
Max ISA area (mm^2)	0.83 ± 1.95	0.60 ± 0.81	0.645
% ISA area	0.27 ± 0.62	0.58 ± 0.81	0.183
Percentage of malapposed struts	2.71 ± 4.01	3.74 ± 3.87	0.397
>5% malapposed struts n.	7 (23.3)	5 (29.4)	0.733

Data are expressed as count and percentages or mean ± standard deviation.
ISA: Incomplete stent/scaffold apposition.

other hand mean prolapse area (0.61 ± 0.26 mm^2 vs 0.90 ± 0.31 mm^2, p = 0.001) and % prolapse area (7.11 ± 2.98 mm^2 vs 9.98 ± 2.90 mm^2, p = 0.002) were significantly higher in the EES group (Table 4) (Fig. 4), with a moderate negative correlation between %MFP and mean prolapse area (beta coefficient - 0.49, p < 0.001).

5. Discussion

The feasibility of BVS implantation in patients presenting with acute myocardial infarction has been recently reported with preliminary information on mid-term clinical outcomes [8–10,19].

However, data comparing the performance of the bioresorbable technology with the current generation metal DES in this specific subset are limited.

The present study represents an early investigation evaluating the use of the second-generation BVS for the treatment of patients presenting with STEMI in comparison with everolimus eluting metal stents in terms of angiographic results intravascular imaging results.

Bioresorbable vascular scaffolds have been hypothesized to be particularly suitable for acute thrombotic lesion, which are frequently soft necrotic core rich plaques with a ruptured thin fibrotic cap [20]. Vessels with such lesions, associated frequently with acute phase vasoconstriction, could benefit the most from a treatment with bioresorbable devices leading to the so-called restoration therapy, represented by late lumen enlargement and re-acquisition of coronary vasomotion [21,22].

In addition, polymer bioresorption and concomitant formation of a neointimal layer given by connective tissue and smooth muscle cells could stabilize the plaque creating a neo-thick fibrous cap, without the long-term permanence of metallic material in the vessel wall [5].

On the other hand, a possible drawback of the usage of BVS in acute patients could be represented by the procedural characteristics of bioresorbable devices implantation, namely frequent good lesion preparation with balloon predilatation and appropriate postdilatation to ensure optimal scaffold expansion and apposition. These maneuvers, if performed in thrombotic lesions may lead to an enhanced thrombus dislodgement and distal embolization compared with a simple direct metal stenting.

In the present investigation we compared STEMI patients with similar percentage diameter stenosis, TIMI flow and thrombus burden, treated with either BVS or EES.

In previous studies, it was hypothesized that the larger BVS footprint, via a mechanism termed the "snowshoe effect", [8] could potentially increase the entrapment of thrombotic material between the scaffold struts and the vessel wall. We evaluated the amount of vessel wall area paved by the scaffold/stent with the introduction/calculation

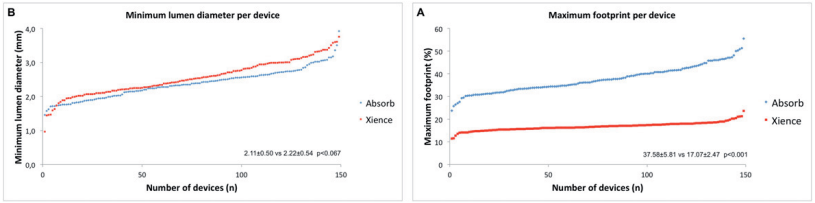

Fig. 3. Maximal footprint and Final Minimal lumen diameter. The final minimal lumen diameter is similar between the two devices (A), conversely the percentage maximal footprint of the BVS was higher compared to the EES (B).

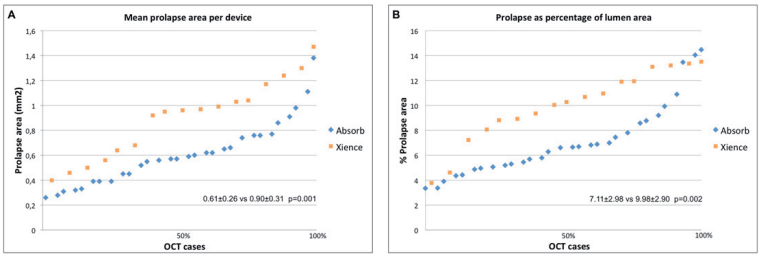

Fig. 4. Prolapse area and percentage prolapse area. The amount of mean prolapse area and percentage prolapse area was consistently lower in the BVS group compared to the EES group (A and B).

of the percentage maximal footprint, a measurement that is providing an estimation of the snowshoe effect for each patient taking into account the vessel coverage at the site of post implantation minimal lumen diameter where theoretically the higher amount of thrombotic material is located.

Our results showed that the percentage of artery covered by the device was definitively higher when implanting BVS as compared to EES at the site of thrombotic lesion by a factor of approximately two. As a possible theoretical consequence the amount of prolapsing and possibly embolizing atherothrombotic material in patients implanted with BVS could be reduced, mitigating the effect of additional predilatations and postdilatations.

In our analysis we observed a reduction of mean prolapse area and percentage area prolapse in the BVS group compared with EES and maximal footprint and prolapse area showed an inverse correlation. Such data reinforce the concept of a possible beneficial "snowshoe" effect when implanting bioresorbable scaffolds in acute patients.

From a clinical perspective, distal embolization has been showed to be associated with worse outcomes, lower myocardial blush grade, impaired ST-segment resolution, and higher enzyme realize [23].

Several devices comprising mesh covered metal stents were developed in the attempt to reduce such phenomenon. Promising acute results such as improved complete ST-segment resolution [24] were achieved at the cost of a higher rate of target lesion revascularizations at long-term [25].

Given this background the implantation of bioresorbable devices could offer the opportunity of reducing the distal embolization without the long-term limitation of metallic devices.

On the other hand a large amount of thrombotic material entrapped behind the struts could theoretically favor the occurrence of scaffold malapposition after thrombus resolution or have an impact on bioresorption kinetics. In addition a higher maximal footprint also translates into an increased amount of polymer per mm^2 of vessel surface and this could have an impact on the risk of scaffold thrombosis [26].

Such hypothesis is consistent with very recent data showing a possibly relevant impact of a high %MFP on the risk of scaffold thrombosis [26].

In conclusion, it could be hypothesized that a higher %MFP compared to metal stents could increase thrombus entrapment reducing prolapse and distal embolization, thus being beneficial up to certain level; on the other hand a very high %MFP could also increase the risk of scaffold thrombosis. Taking into account that the operator could vary the amount of %MFP by acting on the final MLD, the clarification of the correct balance between the risk and benefits of this factor could help in improving implantation strategies for bioresorbable technologies.

6. Limitations

The number of subject evaluated in the present study is limited and data should be considered descriptive and hypothesis generating. The two study groups were not randomized, despite the use of propensity matching, unadjusted confounders might remain, possibly having an impact on results.

The evaluation of the clinical outcomes of patients implanted with BVS during acute myocardial infarction goes beyond the purpose of the present study, larger patient population and longer follow-up would be needed to adequately compare this novel technology with current generation metal DES.

7. Conclusion

Implantation of bioresorbable vascular scaffold is feasible during acute myocardial infarction and could represent an effective reperfusion strategy as compared with second-generation metal drug eluting stents. Scaffold structural characteristics such as strut width and overall footprint may play a role in terms of thrombus dislodgment patterns.

Conflict of interest

R.J. van Geuns received speakers fees from Abbott Vascular. A. Karanasos received funding support from the Hellenic Heart Foundation and St Jude Medical.

References

[1] P.W. Serruys, J.A. Ormiston, Y. Onuma, E. Regar, N. Gonzalo, H.M. Garcia-Garcia, et al., A bioabsorbable everolimus-eluting coronary stent system (ABSORB): 2-year outcomes and results from multiple imaging methods, Lancet 373 (2009) 897–910.
[2] P.W. Serruys, Y. Onuma, J.A. Ormiston, B. de Bruyne, E. Regar, D. Dudek, et al., Evaluation of the second generation of a bioresorbable everolimus drug-eluting vascular scaffold for treatment of de novo coronary artery stenosis: six-month clinical and imaging outcomes, Circulation 122 (2010) 2301–2312.
[3] R. Diletti, Y. Onuma, V. Farooq, J. Gomez-Lara, S. Brugaletta, R.J. van Geuns, et al., 6-month clinical outcomes following implantation of the bioresorbable everolimus-eluting vascular scaffold in vessels smaller or larger than 2.5 mm, J. Am. Coll. Cardiol. 58 (2011) 258–264.
[4] P.W. Serruys, B. Chevalier, D. Dudek, A. Cequier, D. Carrie, A. Iniguez, et al., A bioresorbable everolimus-eluting scaffold versus a metallic everolimus-eluting stent for ischaemic heart disease caused by de-novo native coronary artery lesions (ABSORB II): an interim 1-year analysis of clinical and procedural secondary outcomes from a randomised controlled trial, Lancet 385 (2015) 43–54.
[5] S. Brugaletta, M.D. Radu, H.M. Garcia-Garcia, J.H. Heo, V. Farooq, C. Girasis, et al., Circumferential evaluation of the neointima by optical coherence tomography after ABSORB bioresorbable vascular scaffold implantation: can the scaffold cap the plaque? Atherosclerosis 221 (2012) 106–112.
[6] C.V. Bourantas, P.W. Serruys, S. Nakatani, Y.J. Zhang, V. Farooq, R. Diletti, et al., Bioresorbable vascular scaffold treatment induces the formation of neointimal cap that seals the underlying plaque without compromising the luminal dimensions: a concept based on serial optical coherence tomography data, EuroIntervention 11 (7) (2015) 746–756.

[7] R. Diletti, T. Yetgin, O.C. Manintveld, J.M. Ligthart, C. Zivelonghi, F. Zijlstra, et al., Percutaneous coronary interventions during ST-segment elevation myocardial infarction: current status and future perspectives, EuroIntervention 10 (Suppl. T) (2014) T13–T22.
[8] R. Diletti, A. Karanasos, T. Muramatsu, S. Nakatani, N.M. Van Mieghem, Y. Onuma, et al., Everolimus-eluting bioresorbable vascular scaffolds for treatment of patients presenting with ST-segment elevation myocardial infarction: BVS STEMI first study, Eur. Heart J. 35 (2014) 777–786.
[9] V. Kocka, M. Maly, P. Tousek, T. Budesinsky, L. Lisa, P. Prodanov, et al., Bioresorbable vascular scaffolds in acute ST-segment elevation myocardial infarction: a prospective multicentre study 'Prague 19', Eur. Heart J. 35 (2014) 787–794.
[10] S. Brugaletta, T. Gori, A.F. Low, P. Tousek, E. Pinar, J. Gomez-Lara, et al., Absorb bioresorbable vascular scaffold versus everolimus-eluting metallic stent in ST-segment elevation myocardial infarction: 1-year results of a propensity score matching comparison: the BVS-EXAMINATION study (bioresorbable vascular scaffold-a clinical evaluation of everolimus eluting coronary stents in the treatment of patients with ST-segment elevation myocardial infarction), JACC Cardiovasc. Interv. 8 (2015) 189–197.
[11] Y. Onuma, P.W. Serruys, Bioresorbable scaffold: the advent of a new era in percutaneous coronary and peripheral revascularization? Circulation 123 (2011) 779–797.
[12] Y. Onuma, P.W. Serruys, L.E. Perkins, T. Okamura, N. Gonzalo, H.M. Garcia-Garcia, et al., Intracoronary optical coherence tomography and histology at 1 month and 2, 3, and 4 years after implantation of everolimus-eluting bioresorbable vascular scaffolds in a porcine coronary artery model: an attempt to decipher the human optical coherence tomography images in the ABSORB trial, Circulation 122 (2010) 2288–2300.
[13] G. Sianos, M.I. Papafaklis, J. Daemen, S. Vaina, C.A. van Mieghem, R.T. van Domburg, et al., Angiographic stent thrombosis after routine use of drug-eluting stents in ST-segment elevation myocardial infarction: the importance of thrombus burden, J. Am. Coll. Cardiol. 50 (2007) 573–583.
[14] C.M. Gibson, J.A. de Lemos, S.A. Murphy, S.J. Marble, C.H. McCabe, C.P. Cannon, et al., Combination therapy with abciximab reduces angiographically evident thrombus in acute myocardial infarction: a TIMI 14 substudy, Circulation 103 (2001) 2550–2554.
[15] G.J. Tearney, E. Regar, T. Akasaka, T. Adriaenssens, P. Barlis, H.G. Bezerra, et al., Consensus standards for acquisition, measurement, and reporting of intravascular optical coherence tomography studies: a report from the International Working Group for Intravascular Optical Coherence Tomography Standardization and Validation, J. Am. Coll. Cardiol. 59 (2012) 1058–1072.
[16] H.M. Garcia-Garcia, P.W. Serruys, C.M. Campos, T. Muramatsu, S. Nakatani, Y.J. Zhang, et al., Assessing bioresorbable coronary devices: methods and parameters, JACC Cardiovasc. Imaging 7 (2014) 1130–1148.
[17] A. Menendez-Pelaez, C. Rodriguez, P. Dominguez, 5-Aminolevulinate synthase mRNA levels in the Harderian gland of Syrian hamsters: correlation with porphyrin concentrations and regulation by androgens and melatonin, Mol. Cell. Endocrinol. 80 (1991) 177–182.
[18] P.C. Austin, M.M. Mamdani, A comparison of propensity score methods: a case-study estimating the effectiveness of post-AMI statin use, Stat. Med. 25 (2006) 2084–2106.
[19] J.M. Fam, C. Felix, R.J. van Geuns, Y. Onuma, N.M. Van Mieghem, A. Karanasos, et al., Initial experience with everolimus-eluting bioresorbable vascular scaffolds for treatment of patients presenting with acute myocardial infarction: a propensity-matched comparison to metallic drug eluting stents 18-month follow-up of the BVS STEMI first study, EuroIntervention 12 (2016) 30–37.
[20] A. Farb, A.P. Burke, A.L. Tang, T.Y. Liang, P. Mannan, J. Smialek, et al., Coronary plaque erosion without rupture into a lipid core. A frequent cause of coronary thrombosis in sudden coronary death, Circulation 93 (1996) 1354–1363.
[21] R. Diletti, V. Farooq, C. Girasis, C. Bourantas, Y. Onuma, J.H. Heo, et al., Clinical and intravascular imaging outcomes at 1 and 2 years after implantation of absorb everolimus eluting bioresorbable vascular scaffolds in small vessels. Late lumen enlargement: does bioresorption matter with small vessel size? Insight from the ABSORB cohort B trial, Heart 99 (2013) 98–105.
[22] P.W. Serruys, Y. Onuma, D. Dudek, P.C. Smits, J. Koolen, B. Chevalier, et al., Evaluation of the second generation of a bioresorbable everolimus-eluting vascular scaffold for the treatment of de novo coronary artery stenosis: 12-month clinical and imaging outcomes, J. Am. Coll. Cardiol. 58 (2011) 1578–1588.
[23] M.L. Fokkema, P.J. Vlaar, T. Svilaas, M. Vogelzang, D. Amo, G.F. Diercks, et al., Incidence and clinical consequences of distal embolization on the coronary angiogram after percutaneous coronary intervention for ST-elevation myocardial infarction, Eur. Heart J. 30 (2009) 908–915.
[24] G.W. Stone, A. Abizaid, S. Silber, J.M. Dizon, B. Merkely, R.A. Costa, et al., Prospective, randomized, multicenter evaluation of a polyethylene terephthalate Micronet mesh-covered stent (MGuard) in ST-segment elevation myocardial infarction: the MASTER trial, J. Am. Coll. Cardiol. 60 (2012) 1975–1984.
[25] D. Dudek, A. Dziewierz, S.J. Brener, A. Abizaid, B. Merkely, R.A. Costa, et al., Mesh-covered embolic protection stent implantation in ST-segment-elevation myocardial infarction: final 1-year clinical and angiographic results from the MGUARD for acute ST elevation reperfusion trial, Circ. Cardiovasc. Interv. 8 (2015), e001484.
[26] T. Gori, Lessons learned from registry data, EuroPCR 2015 (2015).

6

CHAPTER

OCT ASSESSMENT OF THE MID-TERM VASCULAR HEALING AFTER EVEROLIMUS-ELUTING BIORESORBABLE SCAFFOLD IMPLANTATION IN STEMI (BVS-STEMI FIRST) A COMPARISON WITH METALLIC DRUG-ELUTING STENTS

Antonis Karanasos, Nicolas M. Van Mieghem, Hector Garcia-Garcia, Roberto Diletti, Cordula Felix, Jors N. van der Sijde, Yuki Ishibashi, **Jiang Ming Fam**, Peter De Jaegere, Patrick W. Serruys, Yoshinobu Onuma, Felix Zijlstra, Evelyn Regar, Robert J van Geuns.

Submitted for publication.

OCT assessment of the mid-term vascular healing after everolimus-eluting bioresorbable scaffold implantation in STEMI (BVS-STEMI-FIRST). A comparison with metallic drug-eluting stents.

Antonios Karanasos[1], Nicolas Van Mieghem[1], Roberto Diletti[1], Hector M. Garcia-Garcia[1], Cordula Felix[1], Johannes N. van der Sijde[1], Yuki Ishibashi[1], Jiang-Ming Fam[1], Peter de Jaegere[1], Martin van der Ent[2], Niels R. Holm[3], Patrick W. Serruys[4], Yoshinobu Onuma[1], Felix Zijlstra[1], Evelyn Regar[1], Robert-Jan van Geuns[1]

1. Department of Cardiology, Erasmus Medical Center, Rotterdam, the Netherlands
2. Maastad Ziekenhuis, Rotterdam, the Netherlands
3. Department of Cardiology, Aarhus University Hospital, Aarhus, Denmark
4. International Centre for Circulatory Health, Imperial College London, London, UK

Corresponding author: R.J. van Geuns

Department of Cardiology, Thoraxcenter, Room Ba585, Erasmus Medical Center. Molewaterplein 40, 3015 RD, Rotterdam, the Netherlands. Tel. No.: +31104635260. Fax. No: +31104369154. E-mail: r.vangeuns@erasmusmc.nl

Brief title: BVS healing in STEMI

Word count: 5100

Disclosures. The BVS-STEMI-first OCT study was supported by a grant from Abbott Vascular. The TROFI study was sponsored by Terumo. AK has received research support from St. Jude. NRH has received institutional research grants from Abbott, Terumo and St. Jude Medical and speakers fees from St. Jude Medical and Terumo. No conflicts of interest to declare for the rest of the authors.

Abstract

Background. Data regarding the vascular healing response, including coverage and apposition of BVS in thrombotic lesions of STEMI are scarce, while evidence regarding the natural history of ISA in such lesions is conflicting.

Objectives. We assessed the vascular healing response by optical coherence tomography (OCT) 6 months after bioresorbable vascular scaffold (BVS) implantation in patients with ST-elevation myocardial infarction (STEMI), and compared it to the healing response of a metallic drug-eluting stent (DES) with biodegradable polymer.

Methods. The BVS-STEMI–FIRST is a single-centre, investigator-driven, pilot cohort study. A total of 39 consecutive patients treated with BVS for STEMI underwent invasive follow-up at 6 months by angiography and OCT. The OCT findings were compared to a historical cohort of 49 patients treated with metallic DES for STEMI and undergoing 6-month follow-up OCT.

Results. No binary restenosis was observed for BVS and in-scaffold late lumen loss was 0.13±0.28mm. The mean and minimal lumen area were non-significantly lower in BVS (mean: 6.78±1.86mm² versus 7.36±2.23mm², p=0.20; minimal: 5.16±1.87mm² versus 5.83±2.11mm², p=0.12). There was no significant difference in malapposed struts (0.64% versus 0.38%, p=0.59), while the percentage of uncovered struts was significantly lower in BVS (0.65% versus 6.28%, p<0.001), in the absence of a significant difference in the coverage thickness. In 20 patients with BVS and serial baseline and follow-up OCT examinations, there were 3 patients (15%) with persistent incomplete scaffold apposition (ISA), 11 patients (55%) with resolved ISA, and 6 patients (30%) with late-acquired ISA.

Conclusions. The healing response after BVS implantation in STEMI is comparable to the healing response of a metallic DES with biodegradable polymer, demonstrating absence of lumen compromise or scaffold recoil, a low rate of malapposed struts in both groups and more complete strut coverage compared to metallic DES.

Keywords: Optical Coherence Tomography, Bioresorbable Vascular Scaffold, Primary Percutaneous Coronary Intervention, Strut Coverage, ST-elevation myocardial infarction

Abbreviations

BVS: Bioresorbable vascular scaffold

DES: Drug-eluting stent

DS%: Percent diameter stenosis

IQR: Interquartile range

ISA: Incomplete scaffold/stent apposition

LLL: Late lumen loss

MLD: Minimal lumen diameter

OCT: Optical coherence tomography

PCI: percutaneous coronary intervention

RVD: Reference vessel diameter

STEMI: ST-elevation acute myocardial infarction

Introduction

Implantation of metallic drug-eluting stents (DES) during primary percutaneous coronary intervention (PCI) for ST-elevation myocardial infarction (STEMI) has been associated with lower strut coverage and higher incomplete stent apposition (ISA) at follow-up compared to stable angina[1].

Bioresorbable vascular scaffolds (BVS) are a new treatment for obstructive coronary lesions, promising to restore physiological function of the treated vessels[2]. Initial observations in stable patients have shown a favourable healing response of an everolimus-eluting BVS (ABSORB BVS 1.1; Abbott Vascular; Santa Clara; CA; USA) with low rates of uncovered and malapposed struts at mid-term follow-up[3-5] and restoration of the vascular phenotype at long-term[6,7]. Recent angiographic and OCT studies of BVS in STEMI have demonstrated good procedural results with adequate expansion, and apposition rates comparable to metallic DES[8,9]. Nonetheless, data regarding coverage and apposition of BVS in thrombotic lesions of STEMI are scarce[10,11]. Concurrently, evidence regarding the natural history of ISA in such lesions is limited and conflicting.

We aimed to investigate the six-month healing response, including strut coverage and apposition, after BVS implantation for STEMI. We further compared our findings to a historical control group of patients treated for STEMI with a metallic DES with abluminal biodegradable polymer, and evaluated the natural history of ISA after BVS implantation in STEMI.

Methods

Study protocol. The BVS-STEMI–FIRST is a single-centre, investigator-driven, pilot cohort study. Consecutive patients admitted with STEMI and treated with BVS at the index

procedure that consented to undergo invasive follow-up by angiography and OCT at 6 months, were included. The primary study endpoint was the mid-term healing process of the implanted BVS, assessed by strut coverage and apposition by OCT at 6-month follow-up. The study was approved by the institutional ethics committee and conforms to the declaration of Helsinki.

OCT results were compared to a historical cohort of 49 patients treated with a metallic DES with biodegradable polymer (Nobori, Terumo Corporation, Tokyo, Japan) for STEMI and undergoing 6-month follow-up OCT (**Figure 1**).

Study population. As of 1/9/2012, ABSORB BVS has been utilized in our centre for the treatment of coronary artery disease, including STEMI. Patients with STEMI that had undergone BVS implantation during primary PCI for the treatment of a de-novo lesion of a native vessel were asked to participate in the follow-up study. Exclusion criteria were age <18 years, pregnancy, intolerance to contrast medium, and known thrombocytopenia. In the interval between 1/11/2012 and 31/10/2013, 72 patients fitted these criteria, and were asked to participate. Thirty nine accepted, provided written informed consent and were included (**Figure 1**).

Control group. The 6-month angiographic and OCT findings were compared to a historical control group from the TROFI study (Randomized Study to Assess the Effect of ThRombus Aspiration on Flow Area in STEMI Patients, NCT01271361)[12,13]. The TROFI study enrolled STEMI patients with a de novo lesion in a native coronary vessel and randomized them to primary PCI with thrombectomy versus primary PCI without thrombectomy, with subsequent implantation of Nobori DES in both groups. Detailed inclusion and exclusion criteria were described previously[13]. Forty-nine patients from this study, enrolled in three centres (Erasmus

Medical Centre, Maastad Ziekenhuis, Aarhus University Hospital) underwent 6-month follow-up OCT and were used as controls[12].

Procedure. In BVS, implantation technique was not pre-specified by protocol and implantation was performed at operator's discretion, according to clinical recommendations[14]. Details of baseline implantation for the control group have been published[13]. As the TROFI study randomized patients to primary PCI with thrombectomy using the Eliminate catheter (Terumo corp) versus primary PCI without thrombectomy, thrombectomy was performed in approximately 50% of the control group.

Angiographic analysis. See online supplement.

OCT image acquisition. See online supplement.

OCT analysis. OCT analysis for BVS was performed offline by dedicated software (QCU-CMS, LKEB, Leiden, the Netherlands) throughout the scaffolded segment and 5mm-long edge segments at 1mm intervals, using previously described methodology[3,5,8,15]. Evaluated parameters included strut coverage and apposition, coverage thickness and malapposition distance, healing score, morphometric measurements, apposition patterns, and incidence of persistent, resolved and late-acquired ISA.

OCT analysis in the control group was performed per 1mm throughout the stented segment at an independent imaging core laboratory (Cardialysis) using QCU-CMS, as previously described[13].

Coverage and apposition. In metallic stents, only the reflection of the adluminal strut surface is visualized by OCT. Therefore, coverage is assessed by visual confirmation of a tissue layer overlying the reflecting strut surfaces, while the distance from the centre of the adluminal surface of strut blooming to lumen contour for each strut represents coverage

thickness[16]. Malapposition is defined when this measurement has a negative value that exceeds the thickness of the strut and polymer, also adjusting for axial resolution of OCT.

Although in BVS the entire strut can be visualized post-implantation, at follow-up the light-scattering frame cannot be distinguished from surrounding tissue and is delineated by its black core area. Consequently, coverage in BVS was assessed by measuring the distance from the midpoint of the adluminal black core edge to the lumen contour and subtracting 30μm corresponding to the thickness of the light-scattering frame. If this distance was higher than 30μm the strut was considered covered[5]. Strut malapposition in BVS was defined by the absence of contact between abluminal strut border and vessel wall, with the exception of struts located in front of side branches or their ostium, which were defined as side branch-related struts. This definition includes struts connected to the vascular wall through tissue bridges, but without connection of the abluminal strut border with the vessel wall. Malapposition distance was assessed by measuring the distance from the midpoint of the abluminal black core edge to the lumen contour and subtracting 30μm corresponding to the thickness of the light-scattering frame (**Figure 2**). Methodology and results of an alternative methodology for strut coverage assessment in BVS are included in the online supplement.

Healing score. The OCT healing score was calculated for both cohorts as previously described (online supplement)[12].

Morphometric measurements. Morphometric measurements included lumen area, stent/scaffold area, neointimal area, and ISA area. As stent area is defined in metallic stents by joining points corresponding to adluminal strut surfaces, while in BVS by joining points corresponding to abluminal strut surfaces, scaffold area and neointimal area are overestimated in BVS compared to metallic stents, while ISA area is underestimated. Therefore, scaffold area was additionally delineated by using the adluminal strut surfaces of

BVS struts (**Figure 2**). Scaffold discontinuity in BVS was defined as overhanging struts at the same angular sector, with or without malapposition, or isolated struts at the luminal centre without obvious connection to other surrounding struts[3].

Patterns of apposition. In BVS, we observed several different apposition patterns, which resembled previously described patterns for metallic stents[17]. We introduced a new, detailed system for a systematic frame-level analysis (**Figure 3**). According to this score, frame-level ISA is categorized in 5 grades using a hierarchical classification:

- ISA grade 4: malapposed struts with ***no obvious connection*** to the adjacent vessel wall.
- ISA grade 3: malapposed struts ***partially*** connected to the nearby vessel wall by tissue bridges
- ISA grade 2: malapposed struts ***completely*** connected to the adjacent vessel wall by tissue bridges
- ISA grade 1: apposed struts but with ***outward vessel bulges***[18] between them with a total area >0.10mm²
- ISA grade 0: complete scaffold apposition

Serial OCT analysis. Twenty patients in the BVS group had undergone OCT post implantation per operator's discretion. In this subgroup, serial changes in OCT parameters from baseline to follow-up were evaluated.

Serial apposition analysis. In BVS with serial OCT imaging, all malapposed struts were identified on a frame-level basis (0.2mm interval) for both post-implantation and follow-up, and plotted in spread-out maps[7,19]. Protruding apposed struts adjacent to outward vessel bulges were also denoted, and so were platinum scaffold markers and side-branch struts for ensuring spatial co-registration. The presence of persistent, resolved, and late-acquired ISA

was estimated on a scaffold level, by visual assessment of these maps and simultaneous inspection of synchronized pullbacks (QCU-CMS). *Persistent* ISA was defined as presence of malapposed struts at baseline that remained malapposed at follow-up, *resolved* as presence of malapposed struts at baseline that were apposed at follow-up, while *late-acquired* as new occurrence of malapposed struts at follow-up, that were apposed at baseline (**Figure 4**).

Statistical analysis. All analyses were performed with SPSS 20.0 (IBM, Chicago, IL). Continuous variables are presented as mean±SD or median [interquartile range; IQR], while categorical variables as count and percentages. The Kolmogorov-Smirnov test assessed normality of distribution. Differences in continuous normally-distributed patient-level variables were assessed with t-test and in non-normally-distributed with Mann-Whitney, while in categorical variables with chi-square or Fisher's exact test. Differences from baseline to follow-up were assessed with paired t-test (normally-distributed variables) or Wilcoxon paired (non-normally-distributed variables). As struts are clustered within each frame within each patient, strut-level variables were compared by mixed model regression using within-frame and within-patient intercepts as random effects. All p-values are two-sided with a value <0.05 indicating significance.

Results

Baseline characteristics. Baseline characteristics are presented in **Table 1**. The follow-up interval was significantly higher for BVS (7.2months [6.2-9.2months] versus 6.0months[5.9-6.2months], p<0.001). There were no significant differences between BVS and metallic DES in diameter (3.0mm[3.0-3.5mm] versus 3.0mm[2.75-3.5mm]; p=0.41), length (18mm[18-28mm] versus 24mm[14-28mm]; p=0.63), or treated vessel (p=0.49). Patients in BVS-STEMI-FIRST had undergone thrombus aspiration more often (82% versus 51%, p<0.01).

Angiographic analysis. Angiographic analysis is summarized in **Table 2**. There were no significant differences in baseline QCA between BVS and control group. At follow-up, there was no binary restenosis in BVS, while in-stent and in-segment LLL were 0.13±0.28 and 0.09±0.38, respectively (**Figure 5**).

OCT analysis. There was no significant difference in percentage of malapposed struts (0.64% versus 0.38%, p=0.59), however malapposition distance was higher in BVS (647μm[416-1084μm] versus 221μm[58-438μm], p<0.002; **Table 3; Central illustration**). The percentage of uncovered struts was significantly lower in BVS (0.65% versus 6.28%, p<0.001), in the absence of difference in coverage thickness (67μm[45-105μm] versus 68μm[42-115μm], p=0.44). The healing score was significantly lower in the BVS group (1.2[0.1-3.6] versus 9.7[2.6-20.2], p<0.001), Two examples of BVS follow-up are illustrated in **Figures 6 and 7**. There were 12 BVS cases with scaffold discontinuity, however in the majority it was small-scale (observed in 1-2 frames), and associated with late-acquired ISA only in one case.

The mean and minimal lumen area were non-significantly lower in BVS (mean: 6.78±1.86mm² versus 7.36±2.23mm², p=0.20; minimal: 5.16±1.87mm² versus 5.83±2.11mm², p=0.12). Although conventional comparison of scaffold area did not show any difference between the groups, use of the adluminal scaffold contour revealed a lower minimal scaffold/stent area in the BVS group (5.75±1.75mm² versus 6.78±2.15mm², p=0.018).

Patterns of apposition. In the majority of frames at follow-up (96.4%), all struts were apposed: 813 (87.3%) with ISA grade 0, and 85 (9.1%) with ISA grade 1. Out of the 33 frames with malapposed struts (3.6%), 7 (0.8%) had ISA grade 2, 8 (0.9%) had ISA grade 3 and 18 (1.9%) had ISA grade 4.

Serial OCT analysis. In serial OCT analysis of BVS, both mean and minimal lumen area were reduced at follow-up compared to post implantation (p<0.001; **Supplementary Table 1**). There was no significant difference of reference lumen or scaffold area from post-implantation to follow-up. Post-implantation dissections in 8 proximal and 5 distal edges had completely healed by follow-up in all cases but one. Malapposed struts were non-significantly reduced from baseline to follow-up (1.44% versus 0.82%, p=0.16). Malapposition distance increased from baseline to follow-up (210[130-400] versus 818[518-1238], p<0.001), however there was no significant difference in mean ISA area between the two intervals (p=0.48).

The spread-out maps illustrating strut apposition post-implantation and at follow-up are presented in **Figure 8**. Overall, 3 patients (15%) had persistent ISA, 11 patients (55%) had resolved ISA, and 6 patients (30%) had late-acquired ISA.

Discussion

In our study, we documented the mid-term healing response after BVS implantation in STEMI, and compared it to the healing response of a second-generation metallic DES, with excellent clinical results[20,21]. Moreover, we describe in detail the observed apposition patterns at this mid-term BVS follow-up, and document the natural history of ISA after BVS implantation in STEMI. Our main findings are that at the mid-term follow-up of BVS in STEMI: 1) strut coverage after BVS implantation is more complete than the coverage of a metallic biolimus-eluting stent with biodegradable polymer; 2) there are no significant differences between these two devices in ISA incidence; 3) several apposition patterns are observed in BVS, however in the vast majority of frames all struts are apposed; and 4) in most patients acute ISA is resolved, but may persist in a minority of cases, while the incidence of late-acquired ISA is non-negligible.

More complete strut coverage in BVS. Strut coverage has been considered an important component of vascular healing, with incomplete coverage linked to late thrombotic events in pathologic and OCT studies[22,23]. Experimental studies have demonstrated the absence of difference in early (<1 month) coverage by immunohistochemistry between BVS and other metallic DES[24]. In our study, BVS was associated with higher 6-month coverage compared to a second-generation metallic DES. This is notable, as the healing response of the comparator biolimus-eluting stent compares favourably to first-generation DES with higher rates of coverage, while not significantly different from other contemporary DES[25-27]. By individual analysis of a large number of struts, using a methodology that allows meaningful comparison of coverage thickness, we demonstrated that although uncovered struts were less in BVS, coverage thickness over individual struts was identical in the two groups and at the low range of 70μm. Moreover, despite a seemingly higher neointimal coverage area for BVS, comparison with an adjusted methodology circumventing methodological differences in the OCT assessment of these devices, we did not find any differences in neointimal area. This finding implies that this improved coverage is not at the cost of increased neointimal proliferation as in BMS[27], a finding further corroborated by the finding of low in-stent and in-segment LLL in BVS.

Low incidence of ISA. ISA has also been implicated in impaired stent healing and associated with vascular toxicity in first-generation DES[28]. Despite a lack of prospective association of acute ISA with late events[29], late-acquired ISA has been linked to adverse very long-term outcome[30]. Importantly, also in BVS, high prevalence of large-scale ISA has been reported in BVS thrombosis[31]. Collectively, these findings indicate a need to better document the incidence and natural history of ISA in BVS. In our study, 6-month ISA incidence in STEMI did not differ significantly between BVS and metallic DES, being at the range of previous reports in acute coronary syndrome patients[32]. However, ISA distance was higher in BVS. A

closer look at serial imaging results reveals an increase of ISA distance, with mean ISA area not significantly changing. This supports the notion that this observed increase is rather the result of ISA resolution in struts with low ISA distance, tracking with observations in metallic DES where ISA with distance <270μm resolved in all cases[17]. Indeed, partial or complete resolution of acute ISA was observed in 55% of cases in our study, while persistence of malapposed struts was observed in only 15% and was mainly associated with struts with higher ISA distance.

Apposition patterns in BVS. Despite this low incidence of ISA, several apposition patterns were observed, related to a differential growth of neointimal tissue connecting the struts to the vessel wall. These patterns resemble previously described responses to acute ISA in metallic stents[17], although visualization by OCT of the entire BVS strut surface might give the visual impression of cavities and flap-like tissue rims within the coronaries. These findings could appear worrisome, as it could be speculated that such flaps might compromise flow after significant scaffold mass loss due to bioresorption. However, three-dimensional renderings (**Figure 7**) demonstrate that these tissue rims are fixed bilaterally to the vessel wall, thus implying limited mobility, similar to the 'neo-carina' finding, described in side-branch jailing of by BVS[7,33]. Similarly, strut connection to the vessel wall only through their abluminal surface creates the appearance of outward vessel bulges, also dubbed 'crenellated appearance' or 'evaginations'[17,18]. This pattern in metallic DES has been described as a vascular response to acute ISA[17], while it has also been associated with positive vessel remodelling[18]. In our STEMI series, thrombus degradation and vascular tone recovery are equally plausible explanations. It is unclear what are the implications of this morphology for BVS healing, however the close clustering with malapposed struts, and morphological resemblance with other ISA patterns suggests that it is part of the ISA spectrum.

Natural history of ISA in BVS in STEMI. STEMI comprises a setting with a potentially higher risk of late-acquired ISA, due to possibility of suboptimal sizing caused by increased thrombus burden and enhanced vascular tone[34]. Evidence regarding late-acquired ISA after BVS implantation in STEMI is limited, with previous series showing conflicting results, ranging from absence of late-acquired ISA[10] to increase of malapposed struts due to the presence of late-acquired ISA[11]. In our study, we observed 6 cases with late-acquired ISA (30%). In one case, late-acquired ISA was the result of scaffold discontinuity, resembling first observations of late-acquired ISA in first-in-man studies[7,19]. Although thrombus resolution and vasorelaxation are the most likely explanation for the remaining cases, vigilance is warranted as an impaired healing response cannot be excluded.

Clinical implications. Our study findings indicate an overall favourable mid-term healing response for BVS in STEMI. Although the association of healing response with long-term outcome has not been prospectively documented, we consider the finding of low rates of incomplete coverage and ISA favourable. These positive signs in terms of vascular healing, need validation by large randomized trials comparing BVS with current state-of-the-art metallic DES in order to prove a potential benefit for BVS in the long-term. Moreover, the significance of the observed apposition patterns and late ISA needs to be better clarified in terms of pathomechanism and potential clinical sequences.

Limitations. This is a single-centre study with small number of patients. As the control group was historical, direct randomization that could allow accounting for potential confounders was not performed. Nevertheless, there were no significant differences in baseline characteristics between the two cohorts, with the exception of thrombectomy that was lower in TROFI, due to the study design. However, the absence of significant differences in follow-up OCT findings between thrombectomy and no thrombectomy demonstrated in the TROFI study[13], implies that differences in thrombectomy use are unlikely to affect our results.

Moreover, although follow-up interval was intended to be the same, it was longer in the BVS-STEMI-FIRST study. Nonetheless, comparison after excluding longer follow-up intervals did not change our findings (**Supplementary Table 2**).

Conclusions

The mid-term healing response after BVS implantation in STEMI is comparable to the healing response of a metallic DES with biodegradable polymer, demonstrating absence of lumen compromise or scaffold recoil, a low rate of malapposed struts in both groups and more complete strut coverage compared to metallic DES. The observed apposition patterns and the observation of late ISA in a non-negligible percentage of BVS are findings warranting further investigation.

Perspectives

Competency in medical knowledge. There is a favourable mid-term healing response of an everolimus-eluting bioresorbable vascular scaffold in STEMI with low rates of incomplete strut coverage and incomplete scaffold apposition, comparable to the healing response of a contemporary metallic DES with biodegradable polymer.

Translational outlook 1. These positive signs in terms of vascular healing, need to be validated by large randomized trials comparing BVS with current state-of-the-art metallic DES in order to prove a potential benefit for BVS in the long-term.

Translational outlook 2. The significance of the observed apposition patterns and late incomplete scaffold apposition needs to be better documented in terms of pathomechanism and potential clinical sequences.

Acknowledgements

The authors would like to thank Jouke Dijkstra of LUMC for his support with the QCU-CMS software, and Dragica Paunovic and Vladimir Borovicanin of Terumo Europe for their role in the TROFI study.

References

1. Gonzalo N, Barlis P, Serruys PW et al. Incomplete stent apposition and delayed tissue coverage are more frequent in drug-eluting stents implanted during primary percutaneous coronary intervention for ST-segment elevation myocardial infarction than in drug-eluting stents implanted for stable/unstable angina: insights from optical coherence tomography. JACC Cardiovasc Interv 2009;2:445-52.

2. Simsek C, Karanasos A, Magro M et al. Long-term invasive follow-up of the everolimus-eluting bioresorbable vascular scaffold: five-year results of multiple invasive imaging modalities. EuroIntervention 2014.

3. Serruys PW, Onuma Y, Ormiston JA et al. Evaluation of the second generation of a bioresorbable everolimus drug-eluting vascular scaffold for treatment of de novo coronary artery stenosis: six-month clinical and imaging outcomes. Circulation 2010;122:2301-12.

4. Serruys PW, Ormiston JA, Onuma Y et al. A bioabsorbable everolimus-eluting coronary stent system (ABSORB): 2-year outcomes and results from multiple imaging methods. Lancet 2009;373:897-910.

5. Serruys PW, Onuma Y, Garcia-Garcia HM et al. Dynamics of vessel wall changes following the implantation of the absorb everolimus-eluting bioresorbable vascular scaffold: a multi-imaging modality study at 6, 12, 24 and 36 months. EuroIntervention 2014;9:1271-84.

6. Karanasos A, Schuurbiers JC, Garcia-Garcia HM et al. Association of wall shear stress with long-term vascular healing response following bioresorbable vascular scaffold implantation. Int J Cardiol 2015;191:279-83.

7. Karanasos A, Simsek C, Gnanadesigan M et al. OCT assessment of the long-term vascular healing response 5 years after everolimus-eluting bioresorbable vascular scaffold. J Am Coll Cardiol 2014;64:2343-56.

8. Diletti R, Karanasos A, Muramatsu T et al. Everolimus-eluting bioresorbable vascular scaffolds for treatment of patients presenting with ST-segment elevation myocardial infarction: BVS STEMI first study. Eur Heart J 2014;35:777-86.

9. Kocka V, Maly M, Tousek P et al. Bioresorbable vascular scaffolds in acute ST-segment elevation myocardial infarction: a prospective multicentre study 'Prague 19'. Eur Heart J 2014;35:787-94.

10. Kochman J, Tomaniak M, Koltowski L et al. A 12-month angiographic and optical coherence tomography follow-up after bioresorbable vascular scaffold implantation in patients with ST-segment elevation myocardial infarction. Catheter Cardiovasc Interv 2015.

11. Tousek P, Kocka V, Maly M, Lisa L, Budesinsky T, Widimsky P. Neointimal coverage and late apposition of everolimus-eluting bioresorbable scaffolds implanted in the acute phase of myocardial infarction: OCT data from the PRAGUE-19 study. Heart Vessels 2015.

12. Garcia-Garcia HM, Muramatsu T, Nakatani S et al. Serial optical frequency domain imaging in STEMI patients: the follow-up report of TROFI study. Eur Heart J Cardiovasc Imaging 2014;15:987-95.

13. Onuma Y, Thuesen L, van Geuns R-J et al. Randomized study to assess the effect of thrombus aspiration on flow area in patients with ST-elevation myocardial infarction: an optical frequency domain imaging study—TROFI trial. Eur Heart J 2013;34:1050-1060.

14. Windecker S, Kolh P, Alfonso F et al. 2014 ESC/EACTS Guidelines on myocardial revascularization: The Task Force on Myocardial Revascularization of the European Society of Cardiology (ESC) and the European Association for Cardio-Thoracic Surgery (EACTS)Developed with the special contribution of the European Association of Percutaneous Cardiovascular Interventions (EAPCI). Eur Heart J 2014;35:2541-619.

15. Garcia-Garcia HM, Serruys PW, Campos CM et al. Assessing bioresorbable coronary devices: methods and parameters. JACC Cardiovasc Imaging 2014;7:1130-48.

16. Gutiérrez-Chico JL, Regar E, Nüesch E et al. Delayed Coverage in Malapposed and Side-Branch Struts With Respect to Well-Apposed Struts in Drug-Eluting Stents In Vivo Assessment With Optical Coherence Tomography. Circulation 2011;124:612-623.

17. Gutierrez-Chico JL, Wykrzykowska J, Nuesch E et al. Vascular tissue reaction to acute malapposition in human coronary arteries: sequential assessment with optical coherence tomography. Circ Cardiovasc Interv 2012;5:20-9, S1-8.

18. Radu MD, Raber L, Kalesan B et al. Coronary evaginations are associated with positive vessel remodelling and are nearly absent following implantation of newer-generation drug-eluting stents: an optical coherence tomography and intravascular ultrasound study. Eur Heart J 2014;35:795-807.

19. Gomez-Lara J, Radu M, Brugaletta S et al. Serial Analysis of the Malapposed and Uncovered Struts of the New Generation of Everolimus-Eluting Bioresorbable Scaffold With Optical Coherence Tomography. JACC Cardiovasc Interv 2011;4:992-1001.

20. Smits PC, Hofma S, Togni M et al. Abluminal biodegradable polymer biolimus-eluting stent versus durable polymer everolimus-eluting stent (COMPARE II): a randomised, controlled, non-inferiority trial. Lancet 2013;381:651-60.

21. Raber L, Kelbaek H, Taniwaki M et al. Biolimus-eluting stents with biodegradable polymer versus bare-metal stents in acute myocardial infarction: two-year clinical results of the COMFORTABLE AMI trial. Circ Cardiovasc Interv 2014;7:355-64.

22. Finn AV, Nakazawa G, Joner M et al. Vascular responses to drug eluting stents: importance of delayed healing. Arterioscler Thromb Vasc Biol 2007;27:1500-10.

23. Guagliumi G, Sirbu V, Musumeci G et al. Examination of the in vivo mechanisms of late drug-eluting stent thrombosis: findings from optical coherence tomography and intravascular ultrasound imaging. JACC Cardiovasc Interv 2012;5:12-20.

24. Koppara T, Cheng Q, Yahagi K et al. Thrombogenicity and early vascular healing response in metallic biodegradable polymer-based and fully bioabsorbable drug-eluting stents. Circ Cardiovasc Interv 2015;8:e002427.

25. Adriaenssens T, Ughi GJ, Dubois C et al. STACCATO (Assessment of Stent sTrut Apposition and Coverage in Coronary ArTeries with Optical coherence tomography in patients with STEMI, NSTEMI and stable/unstable angina undergoing everolimus vs. biolimus A9-eluting stent implantation): a randomised controlled trial. EuroIntervention 2014.

26. Barlis P, Regar E, Serruys PW et al. An optical coherence tomography study of a biodegradable vs. durable polymer-coated limus-eluting stent: a LEADERS trial sub-study. Eur Heart J 2010;31:165-76.

27. Kuramitsu S, Sonoda S, Yokoi H et al. Long-term coronary arterial response to biodegradable polymer biolimus-eluting stents in comparison with durable polymer sirolimus-eluting stents and bare-metal stents: five-year follow-up optical coherence tomography study. Atherosclerosis 2014;237:23-9.

28. Nakazawa G, Finn AV, Vorpahl M, Ladich ER, Kolodgie FD, Virmani R. Coronary responses and differential mechanisms of late stent thrombosis attributed to first-generation sirolimus- and paclitaxel-eluting stents. J Am Coll Cardiol 2011;57:390-8.

29. Karanasos A, Regar E. Standing on solid ground?: Reassessing the role of incomplete strut apposition in drug-eluting stents. Circ Cardiovasc Interv 2014;7:6-8.

30. Cook S, Eshtehardi P, Kalesan B et al. Impact of incomplete stent apposition on long-term clinical outcome after drug-eluting stent implantation. Eur Heart J 2012;33:1334-43.

31. Karanasos A, Van Mieghem N, van Ditzhuijzen N et al. Angiographic and optical coherence tomography insights into bioresorbable scaffold thrombosis: single-center experience. Circ Cardiovasc Interv 2015;8.

32. Gori T, Schulz E, Hink U et al. Clinical, Angiographic, Functional, and Imaging Outcomes 12 Months After Implantation of Drug-Eluting Bioresorbable Vascular Scaffolds in Acute Coronary Syndromes. JACC Cardiovasc Interv 2015;8:770-7.

33. Karanasos A, Li Y, Tu S et al. Is it safe to implant bioresorbable scaffolds in ostial side-branch lesions? Impact of 'neo-carina' formation on main-branch flow pattern. Longitudinal clinical observations. Atherosclerosis 2015;238:22-5.

34. van Geuns RJ, Tamburino C, Fajadet J et al. Self-expanding versus balloon-expandable stents in acute myocardial infarction: results from the APPOSITION II study: self-expanding stents in ST-segment elevation myocardial infarction. JACC Cardiovasc Interv 2012;5:1209-19.

Tables

Table 1. Baseline and procedural characteristics.

	BVS-STEMI-FIRST (n=39)	TROFI (n=49)	p-value
Age, (years)	56.4±9.6	58.5±11.2	0.37
Male, n(%)	32(82.1)	38(77.6)	0.79
Follow-up interval, months	7.2[6.2-9.2]	6.0[5.9-6.2]	<0.001
Hypertension, n(%)	16(41.0)	16(32.7)	0.51
Dyslipidemia, n(%)	13(33.3)	15(30.6)	0.82
Diabetes, n(%)	6(15.4)	4(8.2)	0.33
Smoking, n(%)	20(51.3)	26(53.1)	0.99
Prior myocardial infarction, n(%)	1(2.6)	2(4.1)	0.99
Prior PCI, n(%)	0(0)	1(2.0)	0.99
Prior CABG, n(%)	0(0)	0(0)	
Culprit vessel, n(%)			0.49
LAD	20(51.3)	20(40.8)	
LCX	6(15.4)	12(24.5)	
RCA	13(33.3)	17(34.7)	
Procedural characteristics			
Thrombectomy, n(%)	32(82.1)	25(51.0)	0.003
Average scaffold/stent diameter, mm	3.0[3.0-3.5]	3.0[2.75-3.5]	0.53
Total scaffold/stent length, mm	18[18-28]	24[14-28]	0.63

Values presented as mean±SD, median [IQR], or n(%)

Table 2. Quantitative angiographic analysis.

	BVS-STEMI-FIRST (n=39)	TROFI (n=49)	p-value
Post-procedure			
In-device RVD, mm	2.79±0.53	2.83±0.47	0.73
In-device MLD, mm	2.38±0.41	2.51±0.47	0.18
In-device DS%	14.5±8.3	11.5±7.6	0.09
In-segment RVD, mm	2.68±0.59	2.72±0.51	0.70
In-segment MLD, mm	2.15±0.48	2.22±0.51	0.51
In-segment DS%	21.1±12.1	18.9±9.5	0.36
Follow-up			
In-scaffold RVD, mm	2.65±0.54		
In-scaffold MLD, mm	2.25±0.42		
In-scaffold DS%	13.8±8.8		
In-scaffold LLL, mm	0.13±0.28		
In-scaffold binary restenosis, n(%)	0(0)		
In-segment RVD, mm	2.60±0.66		
In-segment MLD, mm	2.05±0.47		
In-segment DS%	19.8±10.3		
In-segment LLL, mm	0.09±0.38		
In-segment binary restenosis, n(%)	0(0)		

Values presented as n(%) or mean±SD. RVD=reference vessel diameter, MLD=minimal lumen diameter, DS%=percent diameter stenosis, LLL=late lumen loss.

Table 3. OCT analysis.

	BVS-STEMI-FIRST (n=39)	TROFI (n=49)	p-value
Mean lumen area, mm²	6.78±1.86	7.36±2.23	0.20
Minimal lumen area, mm²	5.16±1.87	5.83±2.11	0.12
Mean reference area, mm²	6.91±2.99	6.80±2.70	0.86
Mean scaffold/stent area, mm²	8.32±1.92*	8.01±2.33	0.50
Minimal scaffold/stent area, mm²	6.79±1.91*	6.78±2.15	0.97
Mean neointimal area, mm²	1.38±0.34*	0.74±0.45	<0.001
Mean ISA area, mm²	0[0-0.036]*	0[0-0.016]	0.45
Comparison using adluminal measurements for BVS scaffold contour			
Mean scaffold/stent area, mm²	7.14±1.78	8.01±2.33	0.059
Minimal scaffold/stent area, mm²	5.75±1.75	6.78±2.15	0.018
Mean neointimal area, mm²	0.61±0.23	0.74±0.45	0.08
Mean ISA area, mm²	0[0-0.053]	0[0-0.016]	0.36
Patient-level healing parameters			
Scaffold/stent-level ISA (any), n(%)	14(35.9)	15(30.6)	0.65
Scaffold/stent-level ISA (>5%), n(%)	1(2.6%)	0(0)	0.44

Scaffolds/stents with all struts covered n(%)	16(41.0)	5(10.2)	0.001
Healing score‡	1.2[0.1-3.6]	9.7[2.6-20.2]	<0.001
Strut-level analysis			
Struts analysed	8,930	10,656	
Malapposed struts, n(%)	57(0.64)	41(0.38)	0.59†
Malapposition distance, μm	647[416-1084]	221[58-438]	0.002†
Uncovered struts n(%)	58(0.65)	669(6.28)	<0.001†
Coverage thickness, μm	67[45-105]	68[42-115]	0.44†

Values presented as mean±SD, median [IQR], or n(%).

*The abluminal strut surface was used for segmentation of the scaffold contour

†Calculated with mixed model regression using within-patient and within-frame intercepts as random coefficients

‡Lower values imply better healing

Figures

Figure 1. Study flow-chart.

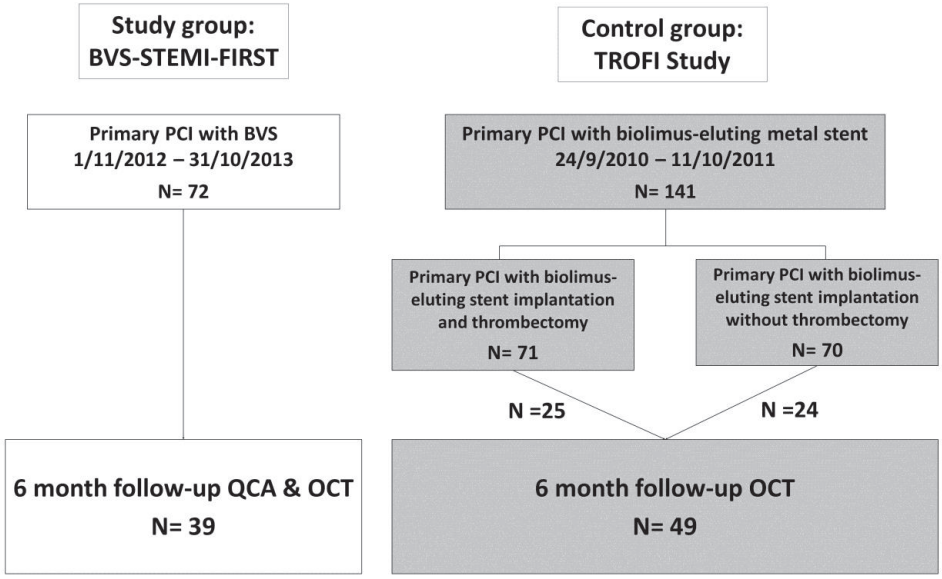

Figure 2. OCT analysis in BVS and metallic DES.

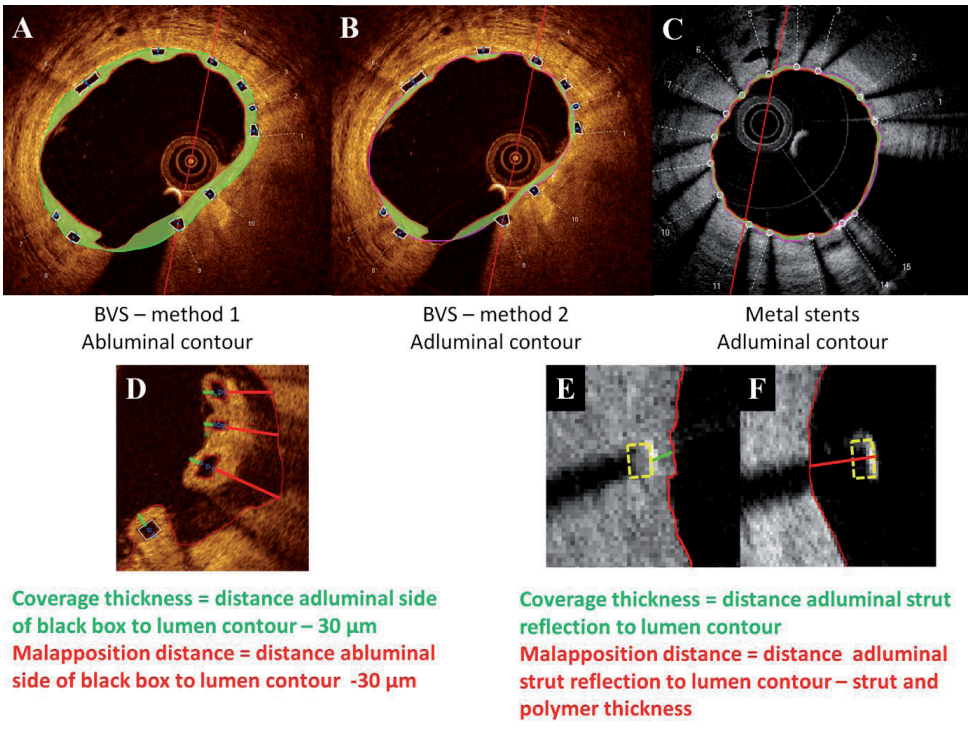

A-C. Scaffold contour segmentation A. in BVS using the abluminal strut surface or the B. adluminal strut surface, and C. in metallic stents. Green area corresponds to neointimal area.

D-F. Methodology for measurement of coverage thickness (green line) and malapposition distance (red line) in D. BVS and E-F. metallic DES. Striped yellow box indicates the position of the metallic strut

Figure 3. Apposition patterns at BVS follow-up.

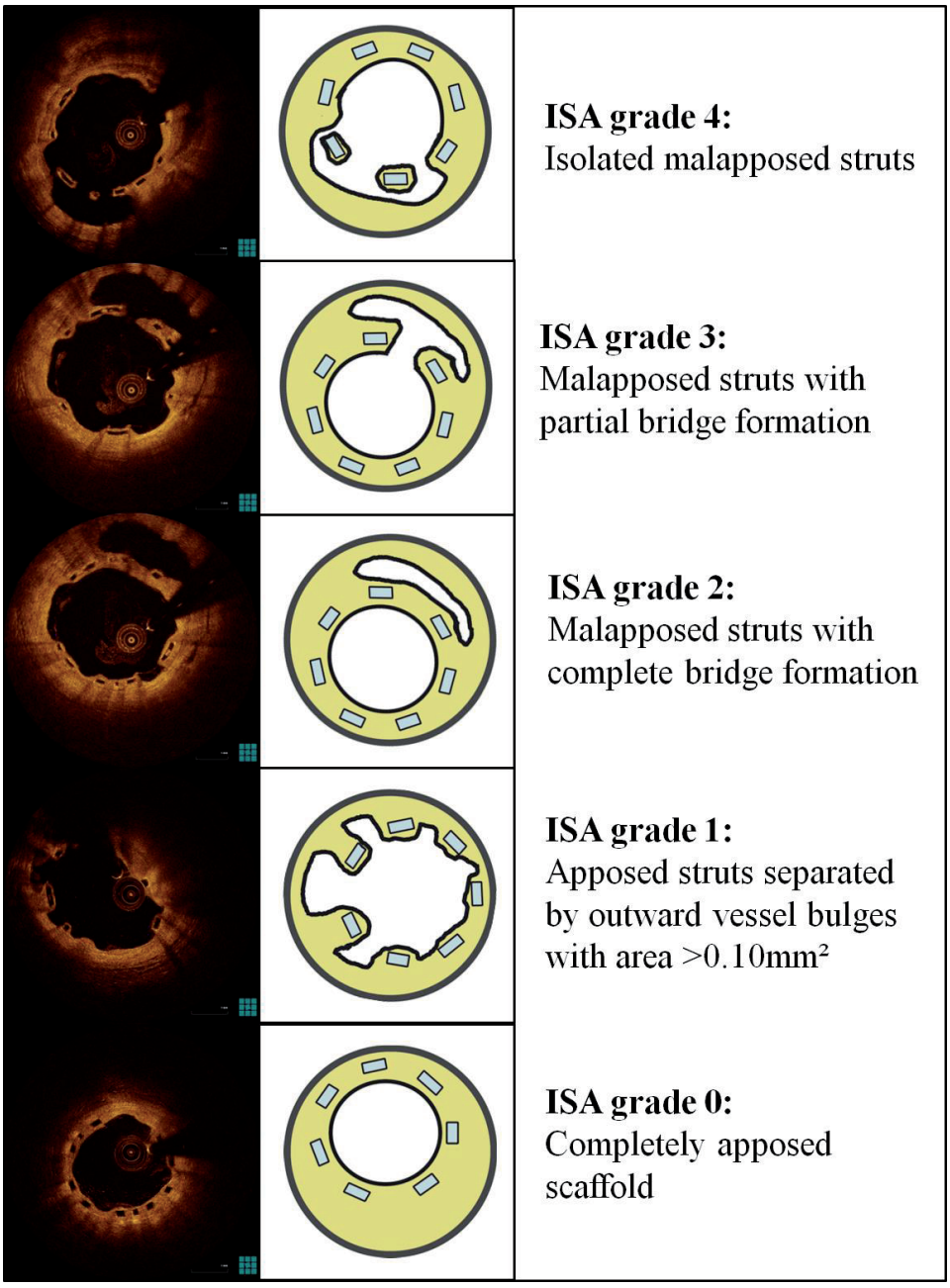

Figure 4. Examples of A. resolved, B. persistent, and C. late ISA.

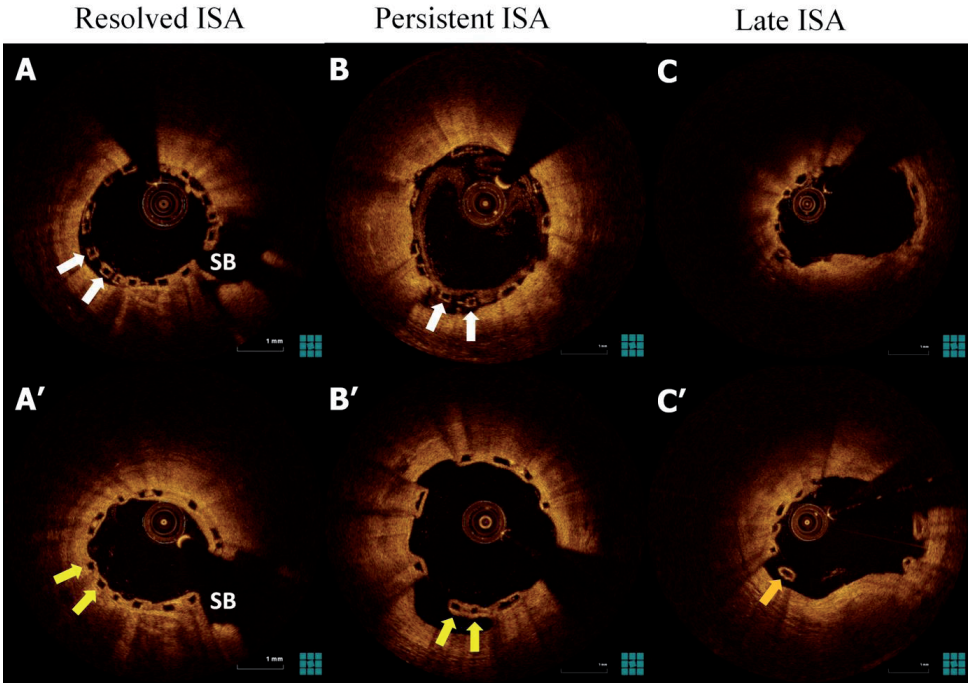

White arrows indicate malapposed struts at baseline, green arrows struts with resolved ISA, yellow arrows struts with persistent ISA, and orange arrows struts with late-acquired ISA. SB=side-branch

Figure 5. Cumulative distribution curves of A. in-scaffold and B. in-segment LLL in bioresorbable scaffolds.

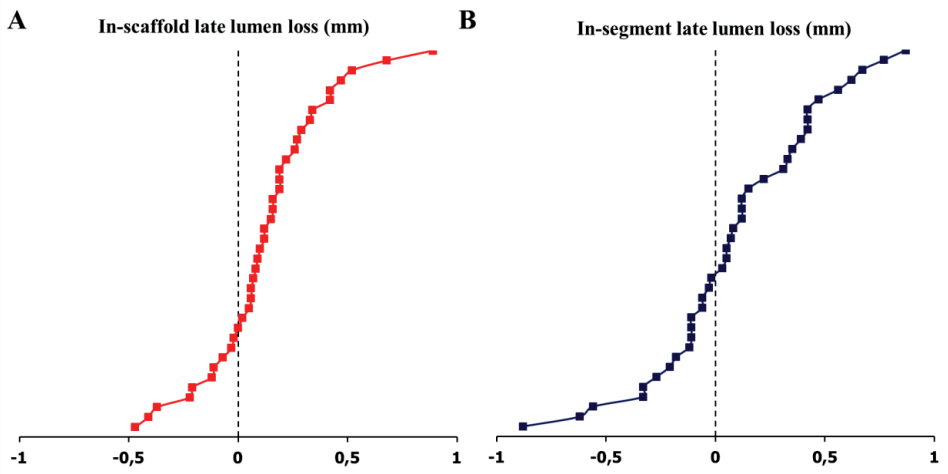

Central illustration. Healing response in BVS and metallic DES.

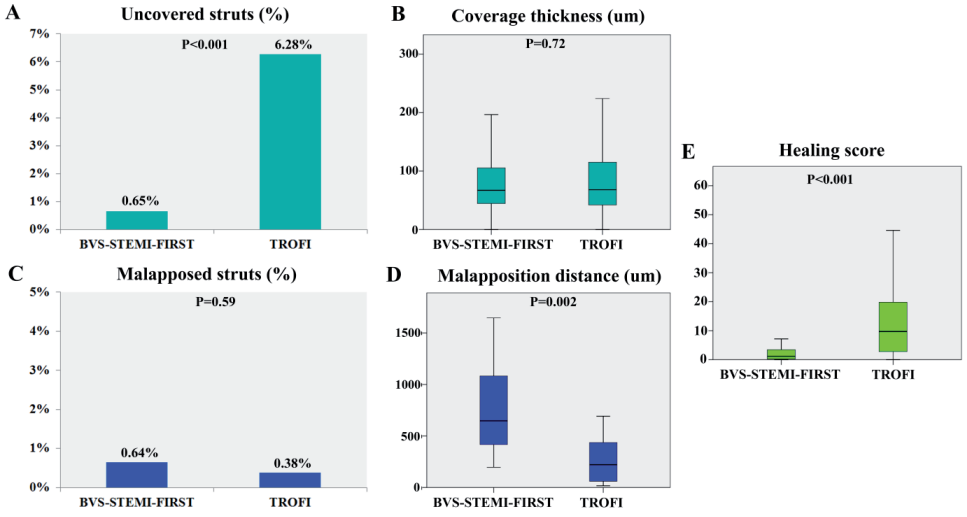

The incidence of uncovered struts was lower in BVS compared to metallic DES (A), without differences in coverage thickness (B). There was no difference in the incidence of malapposed struts (C), however malapposition distance was higher in BVS (D). The healing score was lower in the BVS (E).

Figure 6. Favourable healing response.

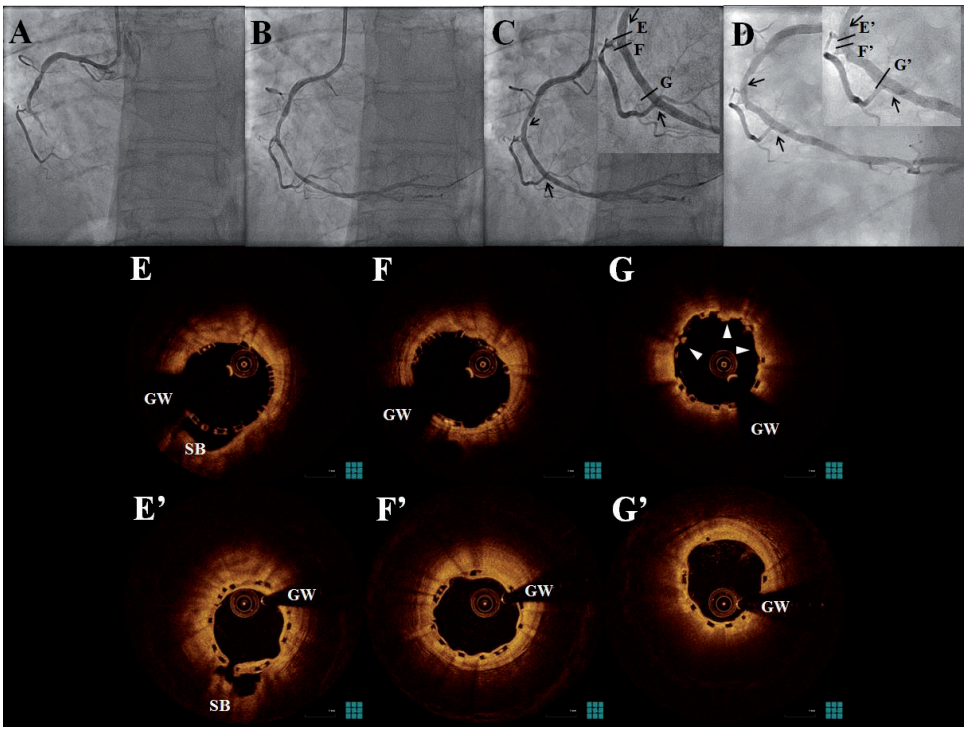

A-D. Culprit lesion angiography (A) at presentation, (B) after thrombus aspiration, (C) post BVS implantation, and (D) at 6-month follow-up. Arrows indicate scaffold markers and lines the sites corresponding to OCT. **E-G'.** OCT images (E-G) post BVS implantation demonstrate mild intra-scaffold thrombus/plaque prolapse (arrowheads). Follow-up images (E'-G') demonstrate thrombus resolution, good coverage and apposition, and partial tissue bridge formation in front of a side-branch (SB) (E-E'). GW=guidewire

Figure 7. Persistent and late-acquired ISA with bridge formation.

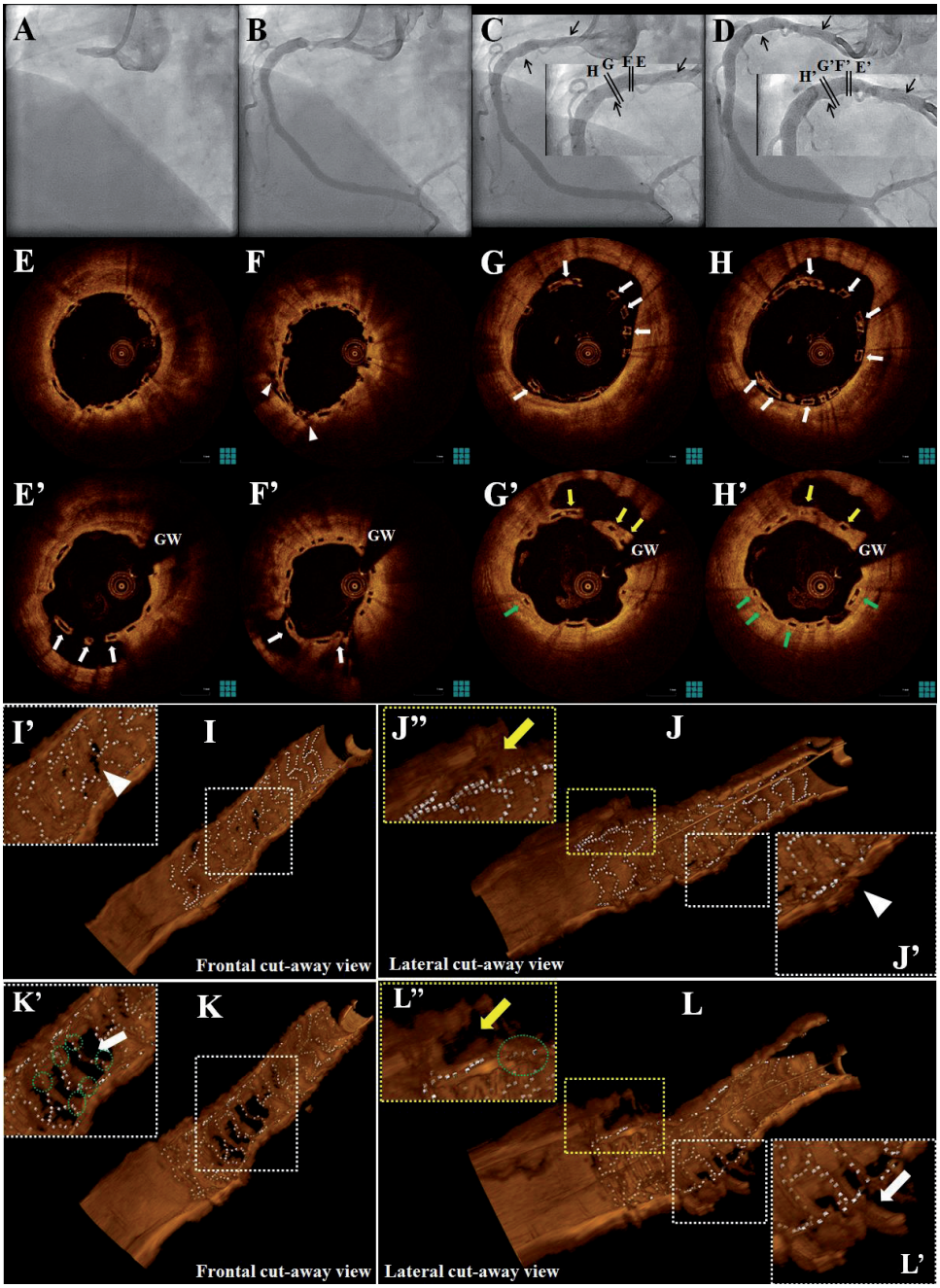

A-D. Culprit lesion angiography (A) at presentation, (B) after thrombus aspiration, (C) post BVS implantation, and (D) at 6-month follow-up. Arrows indicate scaffold markers and lines the sites corresponding to OCT. **E-H'.** OCT images (E-H) post BVS implantation and (E'-H') at follow-up. Late-acquired ISA (white arrows) is developed (E'-F') at a site with mild intra-scaffold dissection post-implantation (white arrowheads in E-F). Panels G'-H' demonstrate persistent (yellow arrows) and resolved (green arrows) ISA, as response to acute ISA (white arrows in G-H). **I-L.** 3D-OCT cut-away views (QAngioOCT, Medis specials bv, Leiden, NL) of the scaffolded segment. White boxes (I'-L') demonstrate the development of late ISA (white arrow) in the site of a mild intra-scaffold dissection post implantation (white arrowheads). Note the formation of cavity-like structures, not corresponding to side-branches, covered by tissue bridges over malapposed struts that are bilaterally connected to the adjacent vessel wall (green circles). Yellow boxes (J''-L'') show persistent ISA (yellow arrows), with tissue growth over malapposed struts. GW=guidewire

Figure 8. Individual patient maps showing the distribution of malapposed struts at baseline and follow-up in a serial population.

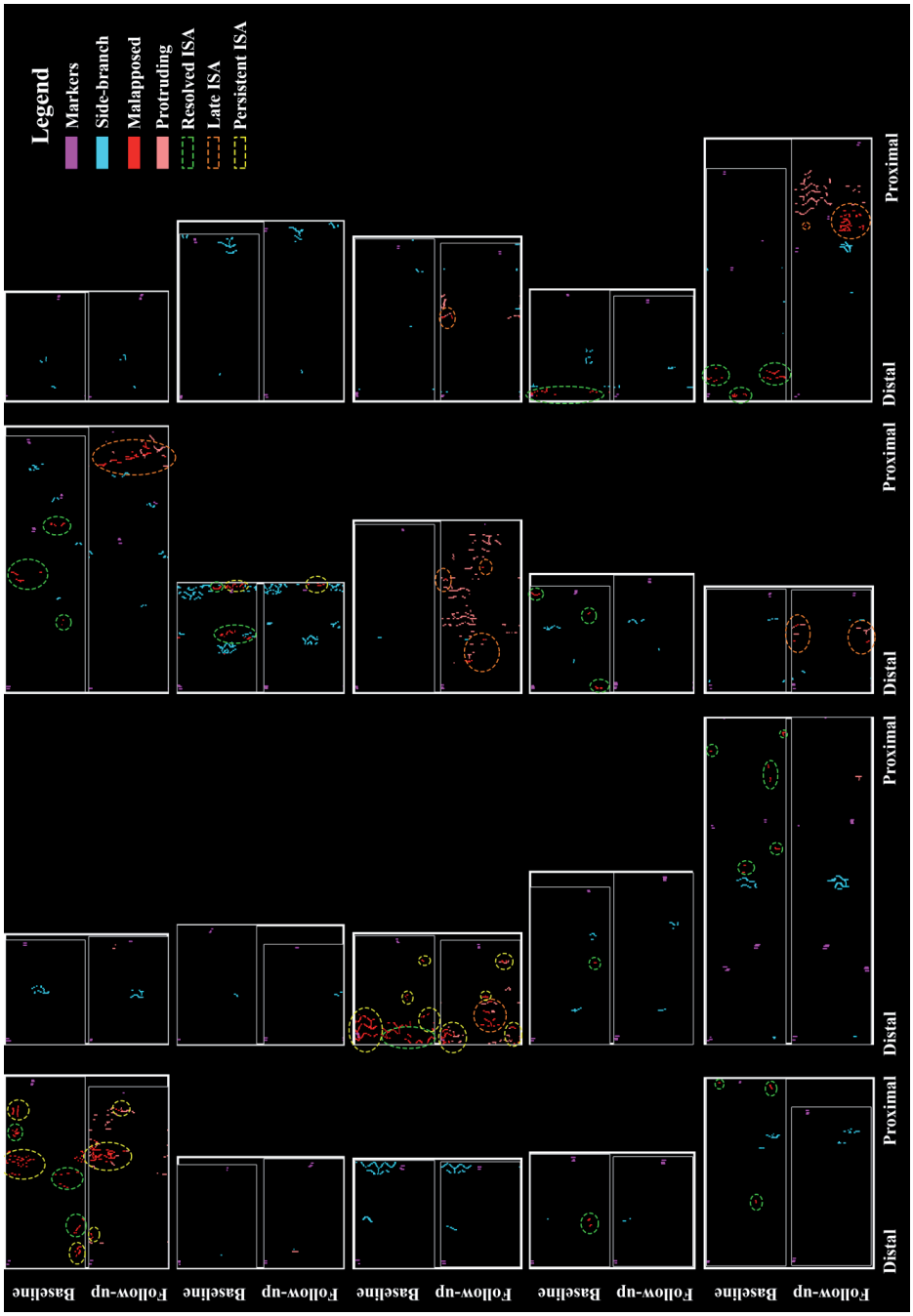

SUPPLEMENTARY MATERIAL

Study devices.

The second-generation everolimus-eluting bioresorbable vascular scaffold (BVS) is a balloon expandable device consisting of a polymer backbone of Poly-L lactide Acid (PLLA) coated with a thin layer of amorphous matrix of Poly-D and -L lactide acid (PDLLA) polymer (strut thickness 150μm). The PDLLA controls the release of the anti-proliferative drug everolimus (100 micrograms/cm2), 80% of which is eluted within the first 30-days. Both PLLA and PDLLA are fully bioresorbable. The polymers are degraded via hydrolysis of the ester bonds and the resulting lactate and its oligomers are metabolized within 2 years via the Krebs cycle[1].

The Nobori drug eluting stent system (Terumo Corporation, Tokyo, Japan) comprises three components: the stainless steel S-stent and its delivery catheter, a drug carrier, poly-lactic acid (PLA), and an anti-proliferative substance, Biolimus A9 (Biosensors International). PLA has been used in a variety of medical applications and the final products of its degradation are carbon dioxide and water. The Nobori DES is coated only abluminally with a matrix containing Biolimus A9 and PLA (15.6 μg each per millimeter of stent length)[2].

Angiographic analysis.

Quantitative coronary angiography was performed offline by dedicated software (CAAS, Pie-Medical, Maastricht, the Netherlands) after baseline implantation and at 6-month follow-up[1]. Angiographic endpoints included in-segment and in-scaffold reference vessel diameter (RVD), minimal lumen diameter (MLD), percent diameter stenosis (DS%), and late lumen loss (LLL) and binary restenosis.

Post-implantation angiographic analysis for the control group was performed offline using CAAS II (Pie-Medical) at an independent imaging corelab (Cardialysis, Rotterdam, the Netherlands), as previously described[3].

OCT image acquisition.

OCT imaging in our study was performed using the Illumien/Illumien Optis imaging systems, with the Dragonfly or Dragonfly Duo imaging catheters (all St. Jude/Lightlab, St. Paul, MN, USA), or the Lunawave system with the Fastview catheter (Terumo Corp), as previously described[1].

Image acquisition in the control group was performed using the Terumo optical frequency domain imaging prototype system with the Fastview catheter (Terumo Corp)[3].

Healing score.

The OCT healing score is a device-level weighted index that combines the following parameters:

- ***in-stent intraluminal material*** (%IL) is assigned a weight of '4';
- presence of both ***malapposed and uncovered struts*** (%MU) is assigned a weight of '3';
- presence of ***uncovered struts alone*** (%U) is assigned a weight of '2';
- and finally, presence of ***malapposition alone*** (%M) is assigned a weight of '1'.

Neointimal healing score = (%IL×4) + (%MU×3) + (%U×2) + (%M×1).

Coverage assessment (complementary analysis).

An additional sensitivity analysis was performed for the assessment of coverage in BVS using an alternative methodology, potentially underestimating coverage thickness and thus potentially overestimating the percentage of uncovered struts[4,5]. According to this method, coverage thickness is measured in every strut between the abluminal border of the strut core and the lumen. As the nominal strut thickness is 150μm, the strut is considered covered whenever the thickness of the coverage is above this threshold value, and coverage thickness is calculated by subtracting 150μm from the measurement. Using this alternative methodology for the assessment of coverage in BVS, our results remained similar, as the percentage of uncovered struts in BVS was 1.25% versus 6.28% in metallic DES ($p<0.001$), while the coverage thickness in BVS was 80μm [53-121μm] versus 68μm [42-115μm] in metallic DES ($p=0.66$).

Analysis in patients with follow-up interval <9 months.

As the time interval from implantation to follow-up was higher in the BVS-STEMI-FIRST study compared to TROFI implantation, with several cases undergoing follow-up in an interval >9 months, we performed an additional comparison, including patients with follow-up interval <9 months (BVS-STEMI-FIRST: n=27; TROFI: n=49). Our main findings remained the same even after this adjustment (Supplementary table 2).

Variability analysis.

Variability data from our group concerning the OCT analysis of BVS in STEMI post-implantation has previously been reported, with intra-observer biases and 95% confidence

intervals being 0.01 mm^2 (−0.12 to 0.15mm^2) for lumen area and −0.01 mm^2 (−0.20 to 0.17mm^2) for scaffold area, while the inter-observer biases and 95% confidence intervals were −0.01 mm^2 (−0.30 to 0.28mm^2) for lumen area and −0.22 mm^2 (−0.68 to 0.24 mm^2) for scaffold area[1].

Variability in the follow-up OCT assessment was assessed by reanalysis of a random sample of 8 patients by the same analyst >1 month after the initial analysis for intra-observer variability, and by a second analyst for inter-observer variability. Type A intraclass correlation coefficients (ICCs) for absolute agreement were used for assessing intra- and inter-observer agreement, while measurement error and 95% limits of agreement were assessed by Bland–Altman analysis. The ICCs were computed with a two-way mixed effects model (single measures).

For evaluating variability in assessing ISA grade, reanalysis was performed in all analyzed frames in the selected patients and Cohen's kappa was calculated.

Both intra- and inter-observer variability were low and are summarized in **Supplementary Table 2**. Cohen's kappa for ISA grade was 0.90 for intra-observer and 0.74 for inter-observer agreement.

Supplementary References.

1. Diletti R, Karanasos A, Muramatsu T et al. Everolimus-eluting bioresorbable vascular scaffolds for treatment of patients presenting with ST-segment elevation myocardial infarction: BVS STEMI first study. Eur Heart J 2014;35:777-86.

2. Chevalier B, Serruys PW, Silber S et al. Randomised comparison of Nobori, biolimus A9-eluting coronary stent with a Taxus(R), paclitaxel-eluting coronary stent in patients with stenosis in native coronary arteries: the Nobori 1 trial. EuroIntervention 2007;2:426-34.

3. Onuma Y, Thuesen L, van Geuns R-J et al. Randomized study to assess the effect of thrombus aspiration on flow area in patients with ST-elevation myocardial infarction: an optical frequency domain imaging study—TROFI trial. Eur Heart J 2013;34:1050-1060.

4. Garcia-Garcia HM, Serruys PW, Campos CM et al. Assessing bioresorbable coronary devices: methods and parameters. JACC Cardiovasc Imaging 2014;7:1130-48.

5. Serruys PW, Onuma Y, Ormiston JA et al. Evaluation of the second generation of a bioresorbable everolimus drug-eluting vascular scaffold for treatment of de novo coronary artery stenosis: six-month clinical and imaging outcomes. Circulation 2010;122:2301-12.

Supplementary Table 1. Serial OCT analysis in BVS (n=20).

	Post-implantation	Follow-up	p-value
Mean lumen area(mm²)	7.54±1.72	6.77±1.98	<0.001
Minimal lumen area(mm²)	5.81±1.49	4.89±1.92	<0.001
Proximal reference area(mm²)	7.30±2.08	6.69±2.52	0.10
Distal reference area(mm²)	6.41±3.22	6.59±2.98	0.32
Mean scaffold/stent area(mm²)	8.01±1.78	8.27±1.98	0.17
Minimal scaffold/stent area(mm²)	6.58±1.89	6.48±1.97	0.66
Mean ISA area(mm²)	0[0-0.027]	0[0-0.034]	0.48
Scaffold/stent-level ISA (>5%) n(%)	3(15.0)	1(5.0)	0.33*
Strut-level analysis			
Struts analyzed	4521	5227	
Malapposed struts	65(1.44)	43(0.82)	0.16†
Malapposition distance(μm)	210[130-400]	818[518-1238]	<0.001†

Values presented as mean±SD, median [IQR], or n(%). ISA=incomplete scaffold/stent apposition

*Calculated with mixed model regression for repeated measurements

†Calculated with mixed model regression using within-patient and within-frame intercepts as random coefficients

Supplementary Table 2. OCT analysis limited to patients with follow-up <9 months.

	BVS-STEMI-FIRST (n=27)	TROFI (n=49)	p-value
Mean lumen area (mm²)	6.80±2.01	7.36±2.23	0.28
Minimal lumen area (mm²)	5.21±2.12	5.83±2.11	0.23
Mean reference area (mm²)	7.14±3.47	6.80±2.70	0.65
Mean scaffold/stent area (mm²)	8.29±2.06*	8.01±2.33	0.60
Minimal scaffold/stent area (mm²)	6.77±2.08*	6.78±2.15	0.99
Mean neointimal area (mm²)	1.34±0.31*	0.74±0.45	<0.001
Mean ISA area (mm²)	0 [0-0.036]*	0 [0-0.016]	0.32
Comparison using adluminal measurements for BVS scaffold contour			
Mean scaffold/stent area (mm²)	7.12±1.91	8.01±2.33	0.10
Minimal scaffold/stent area (mm²)	5.76±1.95	6.78±2.15	0.044
Mean neointimal area (mm²)	0.58±0.20	0.74±0.45	0.039
Mean ISA area (mm²)	0 [0-0.053]	0 [0-0.016]	0.25
Patient-level healing parameters			
Scaffold/stent-level ISA (any) n(%)	11 (40.7)	15 (30.6)	0.45
Scaffold/stent-level ISA (>5%) n(%)	1 (3.7)	0 (0)	0.36

Scaffolds/stents with all struts covered n(%)	13 (48.1)	5 (10.2)	<0.001
Healing score	1.1[0-3.3]	9.7[2.6-20.2]	<0.001
Strut-level analysis			
Struts analyzed	6,282	10,656	
Malapposed struts n(%)	40 (0.63)	41 (0.38)	0.64†
Malapposition distance (μm)	541 [376-814]	221 [58-438]	0.008†
Uncovered struts n(%)	35 (0.55)	669 (6.28)	<0.001†
Coverage thickness (μm)	67 [45-102]	68 [42-115]	0.34†

Values presented as mean±SD, median [IQR], or n(%). ISA=incomplete scaffold/stent apposition

*The abluminal strut surface was used for segmentation of the scaffold contour

†Calculated with mixed model regression using within-patient and within-frame intercepts as random coefficients

Supplementary Table 3. Intra- and inter-observer variability of OCT analysis.

	Mean lumen area (mm²)	Mean scaffold area (mm²)	Mean neointimal area (mm²)	Mean ISA area (mm²)	Malapposed struts per scaffold (%)
			Intra-observer variability		
ICC	0.998	0.991	0.926	0.902	0.978
Bias	0.17	0.04	−0.12	−0.02	0.1
95% limits of agreement	−0.22 to 0.55	−0.40 to 0.48	−0.46 to 0.22	−0.09 to 0.06	−0.7 to 1.0
			Inter-observer variability		
ICC	0.999	0.997	0.901	0.923	0.964
Bias	0.07	0.19	0.13	0.02	0.2
95% limits of agreement	−0.11 to 0.24	−0.13 to 0.51	−0.12 to 0.38	−0.06 to 0.09	−0.9 to 1.3

Abbreviations: ISA=incomplete scaffold apposition; ICC=intraclass correlation coefficient

7

CHAPTER

BIORESORBABLE VASCULAR SCAFFOLD FOR ST ELEVATION MYOCARDIAL INFARCTION: OPTICAL COHERENCE TOMOGRAPHY OBSERVATIONS AT THE 2-YEAR FOLLOW-UP

Jiang Ming Fam, Antonis Karanasos, Evelyn Regar, Robert-Jan van Geuns.

Coron Artery Dis. 2015 Sep; 26 (6): 545-7.

Bioresorbable vascular scaffold for ST elevation myocardial infarction: optical coherence tomography observations at the 2-year follow-up

Jiang Ming Fam[a,b], Antonios Karanasos[a], Evelyn Regar[a] and Robert-Jan van Geuns[a], [a]Department of Cardiology, Thoraxcentre, Erasmus Medical Centre, Rotterdam, The Netherlands and [b]National Heart Centre Singapore, Singapore

Correspondence to Jiang Ming Fam, MBBS (Singapore), MRCP (UK), MMED (Singapore), Department of Cardiology, Thoraxcentre, Room Ba-585, Erasmus University Medical Centre, 's-Gravendijkwal 230, 3015 GE Rotterdam, The Netherlands
Tel: +31 0 10 703 33 48; fax: +31 0 10 703 52 54; e-mail: j.fam@erasmusmc.nl

Received 13 March 2015 **Revised** 27 March 2015 **Accepted** 31 March 2015

Case description

A 51-year-old man was treated at our institution in March 2013 for inferior ST elevation myocardial infarction (STEMI). His cardiovascular risk factors included smoking, hyperlipidaemia and hypertension. A primary percutaneous coronary intervention was performed with two nonoverlapping bioresorbable vascular scaffolds (BRS; Absorb BVS 3.5 × 18 mm and 3.0 × 18 mm; Abbott Vascular, Santa Clara, California, USA) deployed in the proximal and the mid right coronary artery, respectively (Fig. 1) (Video 1, Supplemental digital content 1, *http://links.lww.com/MCA/A44*).

The patient was treated successfully and discharged. In January 2015, he underwent a nontarget vessel

Fig. 1

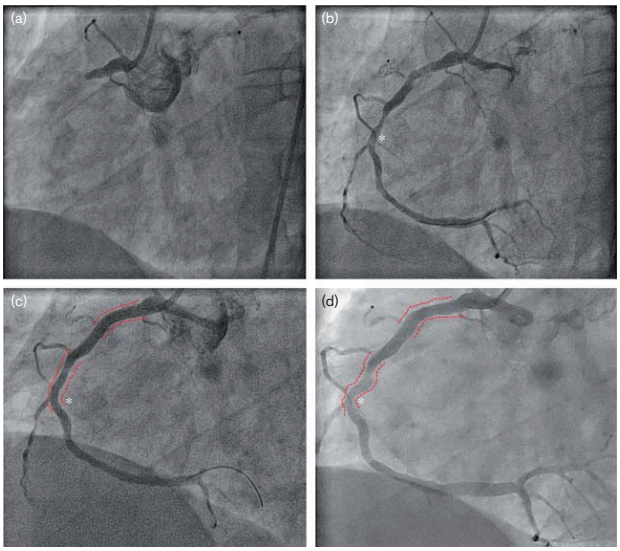

Angiograms of the right coronary artery (RCA). (a) The preprocedural angiogram showed the culprit with TIMI 0 flow. (b) Aspiration thrombectomy was performed with successful restoration of antegrade flow. (c) Two bioresorbable vascular scaffolds (BRS; 3.5 × 18 mm and 3.0 × 18 mm) were deployed in the proximal and mid-RCA, respectively (red lines). Postdilation was performed with a Sprinter 3.0 × 12 mm balloon at 16 atm. (d) Follow-up angiogram performed 24 months later showed that the RCA remained patent with no in-stent restenosis. *From baseline (b), there was minimal change in the curvature of the treated segment immediately after implantation (c) and a restoration of the curvature towards baseline seen on follow-up 2 years later (d).

Supplemental digital content is available for this article. Direct URL citations appear in the printed text and are provided in the HTML and PDF versions of this article on the journal's website (*www.coronary-artery.com*).

DOI: 10.1097/MCA.0000000000000256

Fig. 2

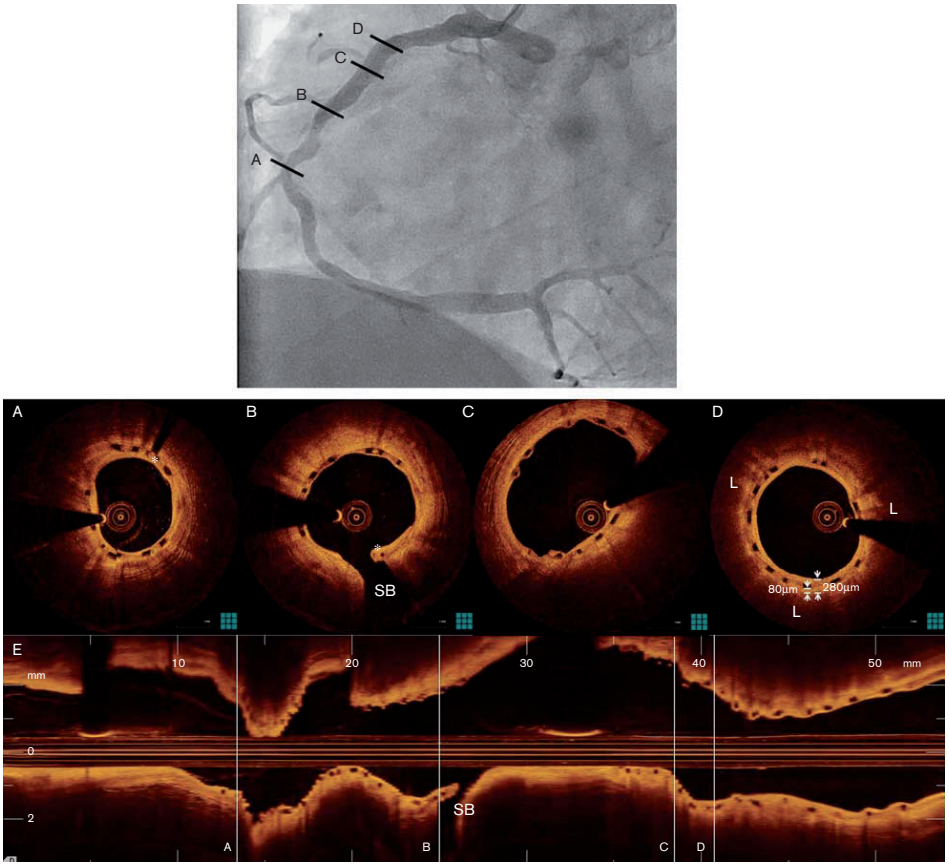

The right coronary artery (RCA) at follow-up with OCT 2 years after the index procedure. (A–D) Cross-sectional images of the scaffolded vessel, showing coverage of the struts in the mid and proximal RCA with a signal-rich layer of tissue covering a lipid-rich plaque (marked 'L'). (b) The patency of the side branch (marked SB), despite the presence of a BRS strut. Different patterns of neointimal coverage are observed, ranging from mild tissue coverage over individual struts in (C) to complete coverage of the interstrut regions in (D). In (D), the BRS strut, originally implanted 80 µm over the fibrous cap covering a lipid pool, is now embedded in an intimal layer of 280 µm. The L-mode illustration (E) shows the corresponding cross-sectional images in a longitudinal axis view. The platinum markers of the distal scaffolds are indicated by an asterisk in (A,B). BRS, bioresorbable scaffold; OCT, optical coherence tomography.

revascularization of the left circumflex artery at our institution because of stable angina. During the same procedure, coronary angiography indicated the patency of the BRS in the right coronary artery and absence of restenosis (Video 2, Supplemental digital content 2, *http://links.lww.com/MCA/A45*). Vessel curvature was minimally altered after the index procedure and restoration of vascular geometry in terms of vessel curvature was noted during the follow-up procedure, which has been reported in previous studies (Fig. 1) [1,2]. Optical coherence tomography showed a good healing response with lumen patency, good scaffold apposition and the presence of strut coverage with side-branch patency and absence of overt neointimal proliferation (Video 3, Supplemental digital content 3, *http://links.lww.com/MCA/A46*). Different patterns of neointimal coverage were observed, with the majority of the scaffolds also having coverage within the interstrut regions, whereas in several sites, tissue coverage was restricted to individual struts (Fig. 2) (Video 4, Supplemental digital content 4, *http://links.lww.com/MCA/A47*).

The use of BRS as part of the acute revascularization option in STEMI does not hamper utilization of any future revascularization procedures, if required [3]. BRS have been used in STEMI, with acute device success rates above 97% [4]. However, limited information is available on the mid-term and long-term healing response after BRS implantation in STEMI. We present optical coherence tomography imaging observations in a patient treated with BRS for STEMI 2 years after the initial treatment. We observed lumen and side-branch patency, optimal scaffold apposition and a layer of signal-rich, low-attenuating tissue covering the struts. We consider that these findings mirror previous long-term observations in a small cohort of the ABSORB Cohort A study [5], showing long-term lumen enlargement. Although the vessel's ability for vascular remodelling and subsequent plaque regression is limited by the vessel being permanently 'caged' in the case of metallic stents, the vessel with BRS implantation maintains the potential for vascular remodelling after the healing process. Despite concerns in terms of the long-term patency of side branches potentially blocked or partially blocked by BRS because of the high strut width (~150 μm), the side branch remained patent even after coverage of the overlying struts. This is the first case showing the 24-month result after STEMI of a BRS used in our institution. Our images suggest a favourable mid-term to long-term healing response after BRS implantation in STEMI, similar to previous reports in stable patients.

Acknowledgements

Conflicts of interest

Professor Van Geuns received speaker fees from Abbott Vascular. For the remaining authors there are no conflicts of interest.

References

1 Gomez-Lara J, Garcia-Garcia HM, Onuma Y, Garg S, Regar E, de Bruyne B, *et al.* A comparison of the conformability of everolimus-eluting bioresorbable vascular scaffolds to metal platform coronary stents. *JACC Cardiovasc Interv* 2010; **3**:1190–1198.

2 Gomez-Lara J, Brugaletta S, Farooq V, van Geuns RJ, de Bruyne B, Windecker S, *et al.* Angiographic geometric changes of the lumen arterial wall after bioresorbable vascular scaffolds and metallic platform stents at 1-year follow-up. *JACC Cardiovasc Interv* 2011; **4**:789–799.

3 Onuma Y, Serruys PW. Bioresorbable scaffold: the advent of a new era in percutaneous coronary and peripheral revascularization? *Circulation* 2011; **123**:779–797.

4 Diletti R, Karanasos A, Muramatsu T, Nakatani S, van Mieghem NM, Onuma Y, *et al.* Everolimus-eluting bioresorbable vascular scaffolds for treatment of patients presenting with ST-segment elevation myocardial infarction: BVS STEMI first study. *Eur Heart J* 2014; **35**:777–786.

5 Karanasos A, Simsek C, Gnanadesigan M, van Ditzhuijzen NS, Freire R, Dijkstra J, *et al.* OCT assessment of the long-term vascular healing response 5 years after everolimus-eluting bioresorbable vascular scaffold. *J Am Coll Cardiol* 2014; **64**:2343–2356.

8

CHAPTER

USE OF INTRACORONARY IMAGING IN ST ELEVATION MYOCARDIAL INFARCTION WITH CORONARY ARTERY ANEURYSM AND VERY LATE STENT THROMBOSIS

Jiang Ming Fam, Jors N van der Sijde, Antonis Karanasos, Buchun Zhang, Robert-Jan van Geuns, Evelyn Regar.

Int J Cardiol. 2015 Oct 15; 197: 296-9.

Letter to the Editor

Use of intracoronary imaging in ST Elevation Myocardial Infarction with coronary artery aneurysm and very late stent thrombosis

Jiang Ming Fam [a,b,*], Jors N. van der Sijde [a], Antonios Karanasos [a], Buchun Zhang [a,c], Robert-Jan van Geuns [a], Evelyn Regar [a]

[a] Thoraxcentre, Erasmus Medical Centre, Rotterdam, The Netherlands
[b] National Heart Centre Singapore, Singapore
[c] The Affiliated Hospital of Xuzhou Medical College, Jiangsu, China

ARTICLE INFO

Article history:
Received 12 May 2015
Accepted 14 May 2015
Available online 15 May 2015

Keywords:
Optical Coherence Tomography
Coronary aneurysm
Stent thrombosis

The use of Optical Coherence Tomography (OCT)-guided percutaneous coronary intervention (PCI) has been described in ST-Elevation Myocardial Infarction (STEMI) involving relatively simple culprit lesions [1]. Coronary artery aneurysms have a reported incidence of up to 4.9% among coronary angiograms performed and may present clinically as STEMI either from thrombus formation or embolic phenomena [2]. There has been limited experience described regarding the use of OCT in STEMI with an aneurysm in the infarct related artery (IRA). We present a case which illustrates the use of OCT in a STEMI case due to very late stent thrombosis (VLST) occurring in the IRA with a preexisting aneurysm.

A 46-year old gentleman with significant cardiovascular risk factors of diabetes mellitus, hyperlipidemia and family history of ischaemic heart disease had prior revascularization with a 5.0 × 12 mm drug eluting stent (DES) (Taxus Liberte™ stent; Boston Scientific, MA, USA) in the mid-right coronary artery (RCA) for a non-STEMI 13 months prior to presentation. He presented to our institution with inferior STEMI and an emergency coronary angiogram was performed which showed that the IRA was the RCA. The previously stented segment of the RCA was completely occluded up to the aneurysmal segment with TIMI 0 flow (Fig. 1A–C). A large amount of thrombus was present and aspiration thrombectomy using Thrombuster™ (Kaneka Medix Corporation, Osaka, Japan) and Angiojet™ (Boston Scientific, MA, USA) was performed (Fig. 1D–E). On-line OCT analysis involving preprocedural sizing and device landing zone assessment was performed. Residual thrombus was seen and there was a disruption of the intimal layer suggestive of neointimal plaque rupture within and extending proximal to the stented segment. Features of atherosclerosis such as fibroatheroma were seen in the vessel just distal to the aneurysmal segment (Fig. 2A–D). There was minimal presence of thrombus in the aneurysmal segment itself. Predilation was performed with a 3.0 × 15 mm balloon. A 4.0 × 33 mm Xience Prime™ (Abbott Vascular, Santa Clara, CA, USA) and a 4.0 × 23 mm Xience V™ were deployed in an overlapping manner with good angiographic result (Fig. 1F). OCT performed post-stent deployment showed that both the proximal and distal stents were well expanded and well apposed with no vascular injury (Fig. 2E–H). The proximal stent was well implanted at the transition zone between the aneurysm and normal sized vessel as seen in a 3-dimensional reconstruction (QAngioOCT software; Medis specials, Leiden, The Netherlands) (Fig. 2I).

An aneurysm of the coronary artery is a localized dilatation of the vessel that is larger than the diameter of adjacent normal segments by 50%. Atherosclerosis is the commonest cause. Other causes include infection and connective tissue disorders. The RCA is the most frequently affected vessel [2]. They may be asymptomatic or produce symptoms such as angina, myocardial infarction, sudden rupture or congestive cardiac failure as a result of fistula formation.

VLST, defined by Academic Research Consortium as occurring more than 1 year after stent implantation, can cause either partial or complete occlusion of the stented segment and associated with myocardial infarct [3]. It is a rare but potentially life threatening complication after coronary stent implantation [4]. First-generation paclitaxel eluting DES such as the Taxus Liberte™ was among the main devices associated with this complication, with an annual incidence rate of late and VLST of 0.2–0.6% [5,6]. Multiple factors may predispose to VLST. In this case, patient and device factors such as diabetes mellitus [7] and polymer present in paclitaxel eluting stents [4, 8] may have contributed to the cause. In addition, part of the healing process after stent implantation — the neoatherosclerotic process within the previously stented segment with subsequent plaque rupture may be a contributory factor [9]. Possible findings seen on OCT included intraluminal thrombus, neointimal disruption suggestive of plaque rupture, dissection flaps and cavities.

* Corresponding author at: Department of Cardiology, Thoraxcentre, Room Ba-585, Erasmus University Medical Centre, 's-Gravendijkwal 230, 3015 GE Rotterdam, The Netherlands.
E-mail address: e.regar@erasmusmc.nl (E. Regar).

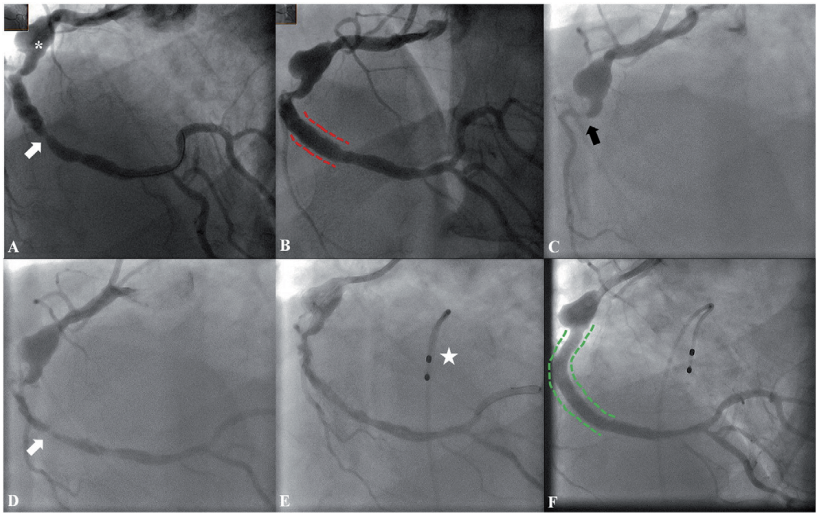

Fig. 1. Angiogram of the right coronary artery (RCA). Panel A. Baseline angiogram showing the RCA aneurysm (*) on initial presentation with a stenotic lesion affecting the mid-segment (white arrow). Panel B. Baseline angiogram showing the RCA after the 5.0 × 12 mm Taxus Liberte™ (dashed line) was deployed. Panel C. Angiogram showing a total thrombotic occlusion of the stented segment of the RCA 13 months after implantation for a NSTEMI. Panel D. Angiogram following recanalization of the vessel after wiring of the vessel with the thrombosed segment still visible as a haziness within the stented region (white arrow). Panel E. Angiogram following the culprit vessel after successful mechanical thrombectomy and predilation using Thrombuster™, Angiojet™ and 3.5 mm balloon respectively. The patient developed ventricular tachycardia likely secondary to successful reperfusion. As he became unstable, overdrive pacing was performed via a temporary transvenous pacing wire placed in the right ventricle (white star). Panel F. Angiogram post procedure with a 4.0 × 33 mm Xience Prime™ and a 4.0 × 23 mm Xience V™ stents deployed in overlapping manner (dashed line) in the RCA with good angiographic result. RCA — right coronary artery. NSTEMI — Non-ST Elevation Myocardial Infarct.

Basic tenets in the management of VLST include rapid restoration of blood flow by removing thrombotic material usually with the aid of mechanical devices, dilating the thrombosed segment and correction of any predisposing mechanical factors such as stent underexpansion. Gp IIb/IIIa inhibitors may be indicated if there is a large amount of thrombus present. Though the additional benefit of aspiration thrombectomy has been recently questioned with recent data [10], there may still remain a role in cases with large thrombotic burden. Adequate clearance of thrombus enables restoration of antegrade flow, facilitates intraprocedural imaging and may improve myocardial perfusion [1].

Online OCT analysis facilitates preprocedural sizing of the lumen prior to stent placement. In this case, angiographic assessment alone may be inaccurate due to the presence of an aneurysm proximal to the occlusion. Intracoronary imaging allows for more accurate and reliable intraluminal measurements such as lumen size, tapering and lesion length. Images acquired with the superior resolution of OCT can also help to clarify the cause of VLST in this case. One might also consider embolization from the aneurysm into the DES as a cause or progression of a lesion in-between the aneurysm and the DES. The differential amount of thrombus detected in the stented segment relative to the aneurysmal segment would support the hypothesis of VLST rather than embolization from the aneurysm into the DES per se. Intracoronary imaging such as intravascular ultrasound (IVUS) and OCT can also provide information about the likely patho-mechanism of the event which may include causes such as stent underexpansion, late acquired malapposition due to positive remodeling and neoatherosclerotic changes within stented segments (such as fibroatheromas and plaque rupture). Post-deployment, OCT may further guide PCI by assessing stent expansion and apposition highlighting the need for further intervention if required. Therefore, an approach based on the use of multimodal imaging technologies may be used in the setting of VLST. To our knowledge, this is the first reported case which illustrates how OCT can improve diagnosis and procedural outcomes in a case of STEMI due to VLST occurring in an IRA that has a preexisting aneurysm.

Conflict of interest

The authors report no relationships that could be construed as a conflict of interest.

Acknowledgments

The authors thank Dr. Shengxian Tu for providing the QAngioOCT software used for the 3-dimensional rendering.

References

[1] M. Magro, E. Regar, J.L. Gutiérrez-Chico, H. Garcia-Garcia, C. Simsek, C. Schultz, F. Zijlstra, P.W. Serruys, R.J. van Geuns, Residual atherothrombotic material after stenting in acute myocardial infarction—an optical coherence tomographic evaluation, Int. J. Cardiol. 167 (3) (Aug 10 2013) 656–663.
[2] W.O. Myers, E.H. Blackstone, K. Davis, E.D. Foster, G.C. Kaiser, CASS Registry long term surgical survival. Coronary Artery Surgery Study, J. Am. Coll. Cardiol. 33 (1999) 488–498.
[3] L. Mauri, W.H. Hsieh, J.M. Massaro, K.K. Ho, R. D'Agostino, D.E. Cutlip, Stent thrombosis in randomized clinical trials of drug-eluting stents, N. Engl. J. Med. 356 (10) (Mar 8 2007) 1020–1029.
[4] C. Spaulding, J. Daemen, E. Boersma, D.E. Cutlip, P.W. Serruys, A pooled analysis of data comparing sirolimus-eluting stents with bare-metal stents, N. Engl. J. Med. 356 (10) (Mar 8 2007) 989–997.

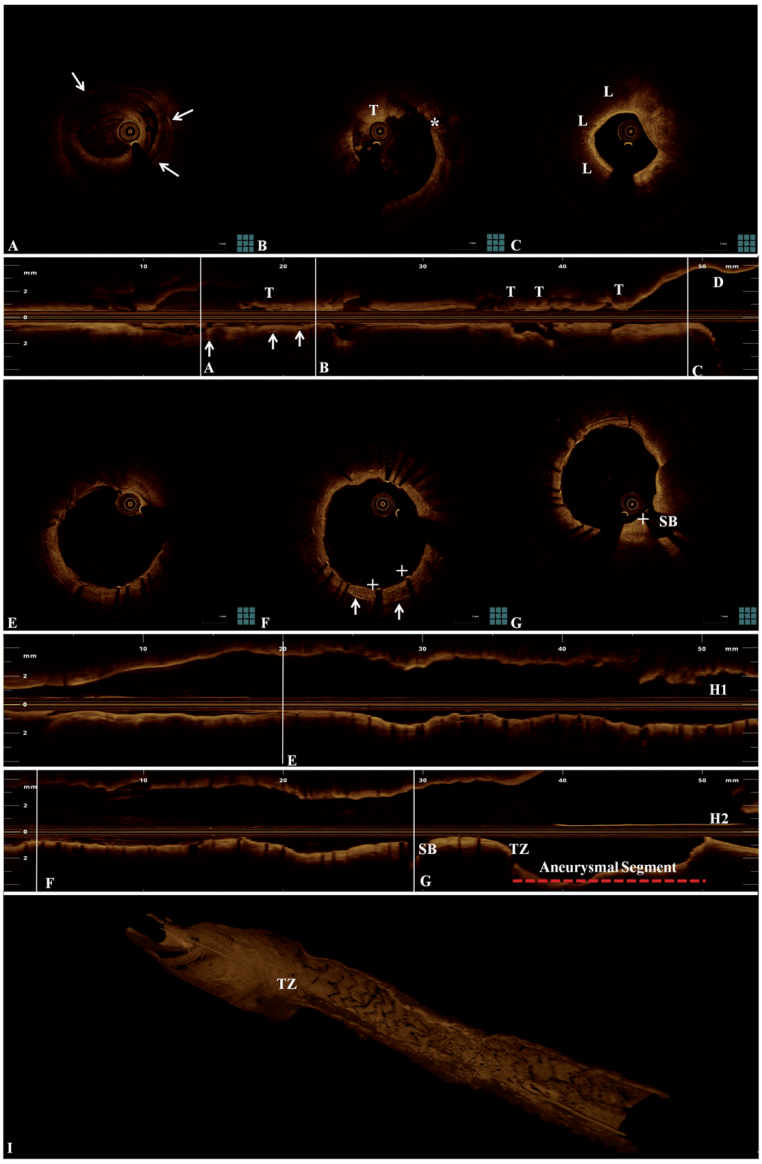
A
B
C
T
*
L
L
L
mm
10
20
30
40
50
T
T
T
T
D
A
B
C
E
F
G
SB
H1
H2
SB
TZ
Aneurysmal Segment
TZ
I

[5] L. Räber, M. Magro, S. Windecker, et al., Very late coronary stent thrombosis of a newer-generation everolimus-eluting stent compared with early-generation drug-eluting stents: a prospective cohort study, Circulation 125 (2012) 1110–1121.
[6] Edoardo Camenzind, William Wijns, Ph. Gabriel Steg, for the PROTECT Steering Committee and Investigators, et al., Stent thrombosis and major clinical events at 3 years after zotarolimus-eluting or sirolimus-eluting coronary stent implantation: a randomised, multicentre, open-label, controlled trial, Lancet 380 (2012) 1396–1405.
[7] N. Beohar, C.J. Davidson, D.O. Williams, et al., Outcomes and complications associated with off-label and untested use of drug-eluting stents, JAMA 297 (18) (May 9 2007) 1992–2000.
[8] G.W. Stone, J.W. Moses, M.B. Leon, et al., Safety and efficacy of sirolimus- and paclitaxel-eluting coronary stents, N. Engl. J. Med. 356 (10) (Mar 8 2007) 998–1008.
[9] Soo-Jin Kang, Gary S. Mintz, Seung-Jung Park, et al., Optical coherence tomographic analysis of in-stent neoatherosclerosis after drug-eluting stent implantation, Circulation 123 (2011) 2954–2963.
[10] B. Lagerqvist, O. Fröbert, S.K. James, et al., Outcomes 1 year after thrombus aspiration for myocardial infarction, N. Engl. J. Med. 371 (12) (Sep 18 2014) 1111–1120.

Fig. 2. Procedural guidance in ST Elevation Myocardial Infarction (STEMI) using Optical Coherence Tomography (OCT). Panel A. Image showing the distal segment after mechanical thrombectomy. There is a cavity in the neointimal layer after rupture. Despite the limited penetration of OCT, struts from the previous stent (white arrows) can still be seen within a layer of neointimal tissue. Panel B. Image showing the region near the previously stented region after successful mechanical thrombectomy. An irregular large intraluminal mass composed of signal poor tissue and high light attenuation that is suggestive of red thrombus ('T') is seen. There is a disruption of the neointimal layer suggestive of plaque disruption (*). Panel C. Image showing the proximal reference segment adjacent to the aneurysmal segment. There is a circumferential signal-intense layer, suggestive of a fibrous cap which overlies a relatively diffusely demarcated signal-poor region with a high light attenuation, suggestive of a lipid pool/necrotic core (L). The OCT findings suggest the presence of a fibroatheroma in the proximal reference segment, a characteristic feature commonly seen in atherosclerosis. The majority of coronary aneurysms are atherosclerotic in nature. Panel D. Longitudinal or 'L' mode of the OCT pullback done after thrombectomy and predilation. The most prominent finding is that of a large area of signal-poor tissue showing high light attenuation, suggestive of red thrombus. Prior struts with shadow artifacts can be seen embedded in a layer of neotimal tissue. Panel E. Image showing the distal stent after implantation. The stent appears well expanded and well apposed with no intrastent dissection. Panel F. Image showing a region of the new stent overlapping with the old stent. The new struts ('+') are seen here well apposed to the neotimal layer which had the old struts embedded within (white arrows). Panel G. Image showing a region of the proximal stent after implantation which appeared well expanded and well apposed. The side branch (SB) remained patent with an overlying strut ('+'). Panel H. 'L' mode of the OCT pullback of the RCA after stent deployment. Panel H1 shows the pullback of the distal stent. Panel H2 shows the proximal stent with the transition zone (TZ) between the stented segment and aneurysmal segment. Panel I. 3-Dimensional reconstruction of the RCA showing the transition zone between the aneurysm and the proximal stent edge.

9

CHAPTER

AN UNUSUAL CASE OF STENT- IN-STENT THROMBOSIS

Jiang Ming Fam, W. den Dekker, Paul de Graaf, Evelyn Regar.

JACC Cardiovasc Interv. 2015 Dec 28; 8 (15):e261-e262.

An Unusual Case of Stent-in-Stent Thrombosis

Jiang Ming Fam, MBBS,*† W. den Dekker, MD,* Paul de Graaf, BsC,* Evelyn Regar, MD, PhD*

A 71-year-old man was admitted for acute coronary syndrome. Six weeks earlier, he had a Promus Premier 3.0 × 12-mm (Boston Scientific, Natick, Massachusetts) drug-eluting stent (DES) implanted in the obtuse marginal (OM) artery for unstable angina. On repeat coronary angiography, haziness (**Figure 1A**, Online Video 1) in the ostial stented region was observed; however Thrombolysis In Myocardial Infarction flow grade was good. Optical coherence tomography (OCT) revealed a nonexpanded stent (star with struts marked with +) within and protruding out of the deployed stent. The deployed stent appeared well expanded and apposed to the vessel wall (deployed stent with struts marked with asterisk [**Figures 1C and 1D**, Online Video 2]). There was lumen compromise secondary to a large amount of thrombus formation seen around the nonexpanded stent struts together with incomplete lesion coverage proximally. Attempts to rewire or retrieve the nonexpanded stent were unsuccessful. On the basis of the OCT findings, the decision was made to crush the nonexpanded stent and to deploy a Promus Premier 3.5 × 12-mm DES proximally with good results (angiography shown in **Figure 1B**, Online Video 3). Multiple layers of struts (OCT) (white arrows in **Figure 1**, D-3; Online Video 4) from the 2 overlapping deployed stents as well as the previously nonexpanded stent can be seen in **Figures 1D and 1E**. **Figure 1F** shows the 3-dimensional reconstruction (QAngioOCT software, Medis Specials, Leiden, the Netherlands) of the vessel pre- and post-procedure showing the crushed stent in stent.

We describe a rare cause of stent thrombosis, emphasizing that mechanical stent-related causes should always be ruled out, especially if stent thrombosis occurs soon after implantation. In our case, a nonexpanded stent formed the nidus of thrombus formation. The nonexpanded stent was likely due to loss or embolization during attempts at device delivery in a challenging procedure due to significant calcification, severe tortuosity, and suboptimal guide catheter backup. Of note, this complication was previously undetected on angiography. This is a rare case of stent-in-stent thrombosis in which OCT demonstrates the potential to improve clinical diagnosis and procedural outcome.

ACKNOWLEDGMENT The authors thank Dr. Shengxian Tu for providing the QAngioOCT software used for the 3-dimensional rendering.

REPRINT REQUESTS AND CORRESPONDENCE: Dr. Jiang Ming Fam, Department of Cardiology, Thoraxcentre, Room Ba-585, Erasmus University Medical Center, 's-Gravendijkwal 230, 3015 GE Rotterdam, the Netherlands. E-mail: j.fam@erasmusmc.nl.

KEY WORDS optical coherence tomography, stent thrombosis

APPENDIX For supplemental videos, please see the online version of this article.

From the *Thoraxcentre, Erasmus Medical Centre, Rotterdam, the Netherlands; and the †National Heart Centre Singapore, Singapore. The authors have reported that they have no relationships relevant to the contents of this paper to disclose.

Manuscript received July 20, 2015; accepted July 31, 2015.

FIGURE 1 **Angiographic and OCT Images of the OM Artery With Stent-in-Stent Thrombosis**

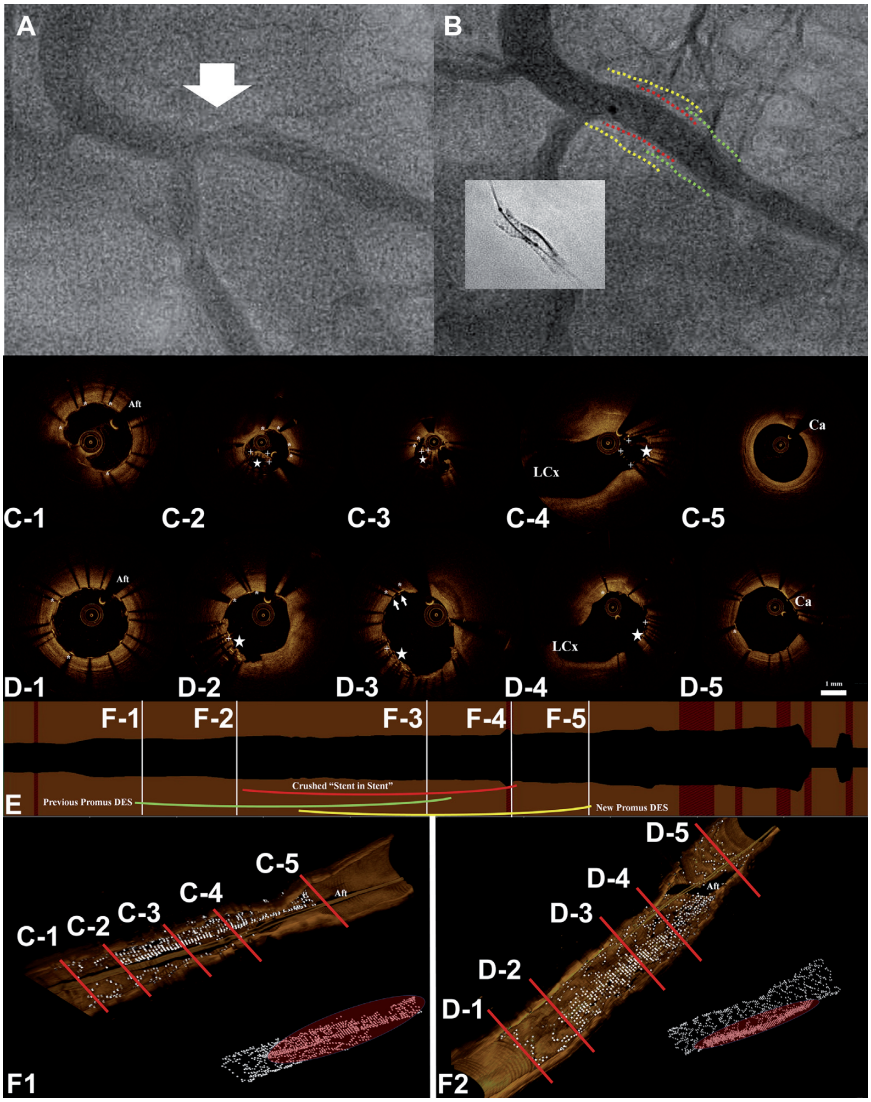

(A) Angiographic haziness **(white arrow**, Online Video 1**)** seen in the ostial segment of the OM artery that was stented (Promus Premier 3.0 × 12 mm, Boston Scientific) 6 weeks earlier. **(B)** Angiogram (Online Video 3) after deployment of a new stent (Promus Premier 3.5 × 12 mm). **(Inset)** Fluoroscopic image of the overlapping stents. **(C)** OCT of the OM/LCx arteries before Promus Premier 3.5 × 12-mm stent deployment. The previously deployed Promus Premier 3.0 × 12-mm stent (**C-1–C-3**; struts marked with **asterisks**, Online Video 2**)** appeared well expanded and apposed to the vessel wall. A nonexpanded stent (**C-2–C-4**; **star** with struts marked with +) could be seen within the deployed stent. There was lumen compromise secondary to a large amount of thrombus formation seen around the nonexpanded stent struts **(C-3)**. The nonexpanded stent protruded out of the deployed stent and could be seen at the bifurcation **(C-4)** of the OM and the LCx **(C-5)** arteries. **(D)** Corresponding OCT done post-deployment of new Promus 3.5 × 12 mm DES Multiple layers of struts (**D-3**, **white arrows**, Online Video 4) from the 2 overlapping deployed stents as well as the previously unexpanded stent **(star)** can be seen. **(E)** The lumen profile of the OM artery as seen by OCT after deployment of the Promus Premier 3.5 × 12-mm stent showing the relationship between the nonexpanded and deployed stents. **(F)** The 3-dimensional reconstruction (QAngioOCT software; Medis Specials, Leiden, the Netherlands) of the vessel pre- **(F1)** and post- **(F2)** procedure showing the crushed stent in stent. Aft = artifact caused by guidewire; Ca = calcium; DES = drug-eluting stent(s); LCx = left circumflex artery; OCT = optical coherence tomography; OM = obtuse marginal.

10

CHAPTER

OPTICAL COHERENCE TOMOGRAPHY IN GRAFTS

AL-Qezweny M.N.A., van der Sijde J.N., **Fam J.M.**, Karanasos A.,
Zhang B., Regar E.

Optical Coherence Tomography in Grafts. (2016) In: Ţintoiu I., Underwood M., Cook S., Kitabata H., Abbas A. (eds) Coronary Graft Failure. Springer, Cham pp 539-554. (Textbook chapter)

Optical Coherence Tomography in Grafts

Mustafa N.A. AL-Qezweny, Johannes N. van der Sijde, Jiang Ming Fam, Antonios Karanasos, BuChun Zhang, and Evelyn Regar

Abstract

Coronary artery bypass graft (CABG) is a commonly used surgery to treat patients with complex artery disease. Long-term outcome of specifically saphenous vein grafts (SVG) is considered unfavorable, while it is the most commonly used conduit. The SVG is prone to occlude and half of the patients will develop vein graft failure (VGF) within 10 years. VGF is the result of the accelerated atherosclerosis that differs from what is seen in native coronaries. Revascularization of SVGs is considered challenging, due to their challenging anatomy and embolic nature. Optical coherence tomography (OCT) imaging is an invasive imaging technique that can be used to get a visual assessment of the development of this process. It is able to generate high-resolution cross-sectional images of the vessel. Ultimately, this could lead to a better understanding of VGF and possibly a better way of anticipating and treating complications. This chapter will discuss the challenges of OCT in SVG and the feasibility, findings, and potential clinical applications of OCT in saphenous vein grafts.

Keywords

Optical coherence tomography • Vein graft failure • Atherosclerosis • Percutaneous coronary intervention • Restenosis

Introduction

Coronary artery bypass grafting (CABG) is one of the most widely used surgical procedures and is used to treat coronary artery disease [1]. The short-term clinical outcome varies. Patency of arterial grafts is known to be higher when compared to venous grafts [2], but the saphenous vein graft (SVG) still remains the most commonly used conduit. Occlusion of an SVG within 30 days after CABG occurs in approximately 10 % of the grafts [3]. Technical failure of the operation, suboptimal anatomical features of the vein, and a poor distal runoff can contribute to stasis in the graft leading to thrombosis and, ultimately, occlusion. Vein graft failure at 12–18 months occurs in 25 % of the grafts [4] and approximately 50 % of the grafts are occluded at 10 years [3, 5]. Late VGF differs from the early occlusion and is often a result of intimal hyperplasia, accelerated atherosclerosis, and thrombosis [3]. VGF leads to repeat CABG or percutaneous coronary interventions (PCI) of the graft. This poses a challenge because revascularization of SVG patients is associated with high mortality and morbidity [6–9].

Development of atherosclerosis in venous grafts is considered different than the development in native coronary

M.N.A. AL-Qezweny, MSc • J.N. van der Sijde, MD
J.M. Fam, MD • A. Karanasos, MD
Department of Cardiology, Thoraxcenter, Erasmus MC, Rotterdam, Zuid-Holland, The Netherlands
e-mail: m.alqezweny@erasmusmc.nl; j.vandersijde@erasmusmc.nl; jiangmingf@gmail.com; akaranasos@outlook.com

B. Zhang, MD, PhD
Department of Cardiology, The Affiliated Hospital of Xuzhou Medical College, Xuzhou, Jiangsu Province, China
e-mail: zhangbc138@sina.com.cn

E. Regar, MD, PhD (✉)
Thoraxcenter, Erasmus MC, Bd 585, 's-Gravendijkwal 230, Jiang3015CE, Rotterdam, The Netherlands
e-mail: e.regar@erasmusmc.nl

vessels. It has a faster progression and is more severe in nature than what can be seen in arteries. Important contributors to this fast progression are chronic endothelial cell injury and dysfunction. This begins as early as in the surgical harvesting of the saphenous vein. The surgical harvesting results in a loss of the vasa vasorum—a microvessel complex that provides nutrition and oxygen and removes waste products. The results of these changes are hypoxemia of the vein and the formation of free radicals, which are predispositions of vein graft disease [3]. Histologically, there are also factors contributing to the fast progression of atherosclerosis, such as the presence of more foam cells and inflammatory cells. The handling of lipid in vein grafts promotes atherosclerosis as there is slower lipolysis, more active lipid synthesis, and higher lipid uptake in comparison to native coronaries [10].

Because of the different pathophysiology and challenging treatment of the SVG compared to native vessels, it would be of great interest to learn more about the pathophysiological changes that develop over time and use that knowledge in the treatment of graft failure.

Optical Coherence Tomography

Optical coherence tomography (OCT) imaging is an invasive imaging technique that can be used to get a visual assessment of the development of this process. Ultimately, this could lead to a better understanding of VGF and possibly a better way of anticipating and treating complications. OCT is a technique based on near infrared light (1310 nm) and is able to generate high-resolution cross-sectional images of the vessel. The underlying concept of OCT is similar to that of ultrasound: by measuring the delay time of optical echoes reflected or backscattered from subsurface structures in biological tissues, structural information as a function of depth within the tissue can be obtained [11]. OCT has a high resolution of approximately 10–15 μ(mu)m and can create cross-sectional images of the vessel wall with great detail. These images can provide valuable information about lesion characteristics and stent implantation that could potentially be missed on angiography alone. Various clinical applications have been proposed (Table 47.1) [12]. In a diagnostic setting it can be used to evaluate a culprit lesion, assess plaque morphology in angiographic ambiguous lesions (Fig. 47.1), or to investigate reasons for stent or graft failure. OCT can also be used in a therapeutic setting to guide stent or scaffold placement during PCI by planning the lesion preparation and selecting an optimal stent length. Unlike intravascular ultrasound (IVUS), OCT requires clearance of the blood from the vessel during image acquisition, because the light is unable to penetrate blood. In the currently commercially available and widespread use of second-generation intracoronary Fourier domain OCT, this is achieved by simultaneous flushing with contrast agent.

Thoraxcenter OCT Imaging Protocol

Image acquisition is done following a set protocol. Patients are on chronic aspirin therapy and receive weight-adjusted

Table 47.1 Potential clinical applications of OCT

Setting	Application
Lesion evaluation	Assessment of culprit lesion in acute coronary syndromes: evaluation for plaque rupture and/or thrombus in patients without angiographically evident culprit lesion
	Evaluation of lesions with angiographic haziness: differential diagnosis between thrombus, dissection, heavy calcification
	Determination about presence or absence of plaque (e.g., in coronary spasm)
Pre-procedural assessment	Luminal measurements for selection of balloon and stent dimensions
	Assessment of plaque morphology in order to guide therapeutic strategy and device selection (rotablation, cutting balloon, etc.)
	Evaluation of the optimal location in the vessel for implantation of a coronary stent
	Use for tracking the exact guidewire position (i.e., in chronic total occlusion or in bifurcation stenting)
	Use in bifurcation intervention (assessment of carina, ostia of side branches, stent cell geometry)
Post-procedural assessment	Assessment of stent expansion (detection of underexpansion, residual stenosis, incomplete stent apposition)
	Assessment of vascular injury: detection of edge dissections, tissue protrusion, intra-stent thrombus
	Assessment of intervention by adjunctive devices: measurement of luminal enlargement after cutting balloon angioplasty, assessment of the reduction of calcification after rotablation
	Assessment of adjunctive therapies in acute coronary syndromes: evaluation of residual thrombus burden after thrombectomy or selective administration of IIb/IIIa antagonists
Follow-up stent assessment	Mid-term and long-term assessment of stent safety and efficacy: evaluation of stent restenosis (quantitative and qualitative), stent thrombosis, and stent coverage as a surrogate for vessel healing
	Monitoring of the bioresorption and the healing response after implantation of bioresorbable scaffolds

Modified from Karanasos et al. [12]

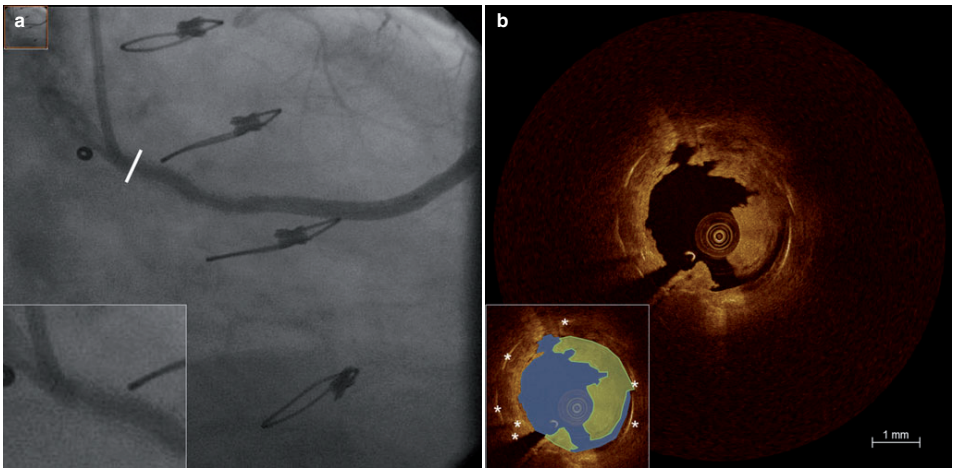

Fig. 47.1 Angiography ambiguity. Angiogram with haziness in the proximal saphenous vein graft, suggesting possible presence of thrombus panel (**a**). Inlayed panel left: enlarged angiogram with haziness in the graft. Although the angiogram can be ambiguous, the cross-sectional OCT image panel (**b**) clearly confirms the presence of severe thrombus formation in a stented segment of the graft with neoatherosclerosis covering the stent struts (*). Inlayed panel right: lumen in *blue* and thrombus in *green*

intravenous heparin in order to maintain the activated clotting time >300 s and nitroglycerin to prevent catheter-induced vasospasm, unless contraindicated. The OCT catheter is advanced distally of a region of interest via a standard angioplasty guide wire. Pullbacks are usually performed at a pullback speed of 20–40 mm/s during simultaneous flushing of viscous iso-osmolar contrast through the guiding catheter (6F or larger, no sideholes) by use of an automated power injector with a flow rate of generally 3 ml/s (with a maximum pressure limit of 300 psi). In vessels with a very large diameter, the flush rate can be increased, but flush rates higher than 4 ml/s are rarely required. Flushing of the vessels is done with viscous iso-osmolar contrast at 37 °C and should be performed with caution in patients who have impaired renal function, a single remaining vessel, severely impaired left ventricular function, and hemodynamic compromise [11].

OCT Image Acquisition in Vein Grafts

There are a few, but distinct, differences that make OCT image acquisition in grafts potentially more difficult than in coronary arteries. These factors are mainly related to the larger vessel size, different anatomy [13], and their higher propensity for thrombosis [7–9]. The larger vessel size of the SVG could compromise adequate flushing and thus reduce the quality of the OCT image. Grafts can be tortuous and long, which might impede blood clearance or require two pullbacks to image the complete length of the graft. Furthermore, a non-coaxial position [14] of the OCT catheter in a large vessel would mean that furthest lumen wall cannot be visualized due to a so-called "out-of-view" artefact, thereby averting the circumferential interpretation of the vessel wall. Accessibility of the vessel can be a challenge posed by the anatomy of the graft. The proximal, aortic anastomosis of a venous graft has a disadvantageous position within the coronary system, which may render access to the vessel with good support from the guide catheter more challenging. In theory, also the potential presence of thrombus in graft lesions could be of concern. It is, however, important to realize that OCT imaging is regularly performed in patients with thrombotic lesions such as in acute coronary syndrome (ACS) and ST segment elevation myocardial infarction (STEMI) [15, 16] with no signs of increased risk for adverse events during OCT imaging.

Tips and Tricks

- Always administer intracoronary nitroglycerin before the introduction of the OCT catheter.
- Optimal, co-axial guide catheter position with good intubation of the ostium is a key prerequisite to achieve optimal blood clearance during flush agent delivery.
- In case of suboptimal guide catheter engagement, consider the use of mother-and-child guide catheter technology.
- In case of large graft (>4.0 mm diameter), consider a flush rate at 4.0 ml/s. When using mother-and-child guide

catheter approach, however, flush flow rate should be set at 3.0 ml/s as the pressure required to deliver higher flow rate might exceed the pre-chosen pressure limit (we use 300 psi) and as a result the injector pump will reduce flow.
- In case of distal lesion position, consider OCT catheter with short monorail tip (Fig. 47.2) to avoid spasm of the native vessel or dissection by the catheter tip.
- Wait for good blood clearance with optimal image quality before starting the pullback.

Literature About the Use of OCT in Vein Grafts

As OCT image acquisition in vein grafts has not been intensively investigated, studies describing the safety, feasibility, and clinical use of OCT imaging in grafts are scarce (Table 47.2) [13, 17–19]. The first study [17] that investigated the use of OCT in grafts demonstrated the feasibility of OCT in arterial and venous grafts in-situ prior to harvest and ex-vivo after harvest with the first-generation OCT devices.

Another study [18] has evaluated culprit SVG lesions with OCT in patients with acute coronary syndromes. Twenty-eight grafts with presumably culprit atherosclerotic lesions were investigated for their OCT characteristics. In most of the studied SVGs, a distinct layer of tissue in discontinuity with the vein wall, loosely attached to the latter, was identified. This fragmented and loosely adherent tissue without a distinct cavity and without a fibrous cap fragment was correlated with areas of severe angiographic degeneration, and was speculated to represent degenerated fragmented graft atheroma. This tissue was labeled "friable tissue." Such OCT features of friability were present in 67.9 % of the SVGs. Culprit lesions demonstrated fibrofatty composition, relatively thin fibrous cap, plaque rupture, and thrombus, which correlate with the clinical spectrum of acute coronary syndromes. This suggests that similar mechanisms contribute to acute coronary syndromes in SVG as in native coronaries. A small imaging study [19] has described OCT characteristics of saphenous vein atherosclerosis in 16 patients. Fifty-five percent of SVGs were occluded. In the remaining patent grafts, 6 of the 16 SVGs demonstrated findings consistent with thin-cap fibroatheroma and luminal adherent thrombus in 4 of 16 SVGs. The authors concluded that their findings suggest that high-resolution imaging techniques such as OCT may begin to allow us insights into the causes of vein graft failure.

Although evidence is limited, we believe that, if used with caution and under adequate antithrombotic therapy and vasodilation, OCT images can be used to retrieve additional important information that can be used for both procedural and research applications.

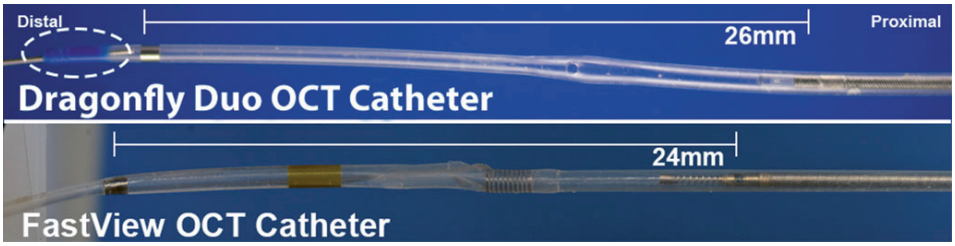

Fig. 47.2 Dragonfly Duo and Fastview OCT catheters. The two commercially available OCT catheters. Note that the distance from the distal marker to the optical lens is slightly shorter of the Terumo Fastview™ catheter (24 mm) than of the Dragonfly™ Duo from St Jude Medical (26 mm), but the latter also has a longer "nose" (dashed circle)

Table 47.2 Overview of available literature describing the use of OCT in grafts [13, 17–19]

Author (year)	N	OCT method	Publication type	Main findings
Brown (2007) [17]	60	Time domain OCT	Original research	OCT imaging of bypass conduits showed unique imaging characteristics based on the respective compositions of their vasculature walls.
Gonzalo (2009) [13]	–	–	Review	OCT can provide unique information about the characteristics of stent restenosis in grafts.
Davlouros (2011) [18]	28	Fourier domain OCT	Original research	Culprit lesions of old SVGs in patients with ACS demonstrated similar characteristics as in native vessels' atherosclerosis.
Adlam (2011) [19]	16 (OCT)	Not stated	Imaging vignette	OCT identified clear features of atherosclerosis in grafts and may allow us to gain insights into the causes of vein graft failure.

Quality and Feasibility Assessment of OCT Imaging in Venous Grafts

To get a better understanding of the feasibility of OCT, we retrospectively retrieved all consecutive cases that underwent diagnostic or therapeutic coronary catheterization of a coronary graft with OCT imaging between 2008 and 2014 in our center. We found 25 procedures in which 59 pullbacks were acquired. In all of these pullbacks, the quality of the pullbacks was assessed by reviewing the angiographic and OCT images. Since there is no general consensus on the quality criteria of OCT images, we defined the quality criteria based on experience and one available study on OCT quality in native coronaries [20]. The number of visible wall quadrants and sufficient clearing of the lumen with flushing agent were assessed to determine image quality. Optimal image quality was defined as visibility of at least 3 quadrants with optimal lumen transparency in more than 75 % of all visualized frames. If the lumen transparency was considered suboptimal due to insufficient lumen clearance with still more than 3 quadrants visible in 75 % of the frames, the image quality was deemed good. Both optimal and good quality were considered suitable for quantitative analysis, while the remaining poor quality group has too much loss of visibility to give reliable measurements.

During retrospective reviewing of our pullbacks in grafts, the image quality was deemed as optimal or good in 85 % of the pullbacks throughout the complete pullback of generally 54 mm. The remaining 15 % was considered poor quality, which was related to a combination of insufficient blood clearance and non-coaxial [14] position of the OCT catheter, causing "out of view artefacts." The average flush rate of pullbacks with an optimal quality was 3.4 and 4.0 ml/s for the poor quality, suggesting that clearance of the lumen was harder to achieve in the latter group.

OCT Features of Venous Grafts

Normal Appearance of a Venous Graft

Like a healthy coronary artery, a normal saphenous vein consists of three layers: the tunica intima, media, and adventitia. The intima has high backscattering (signal-rich); the media has low backscattering (signal poor); and the adventitia has heterogeneous backscattering, which is frequently high (Fig. 47.3a). Changes in backscattering and signal strength can be attributed to different kinds of plaques such as fibrous plaques, fibrocalcific plaques, and necrotic core but also more intricate characteristics such as macrophages, cholesterol crystals, and intimal vasculature [11]. The tunica media of a vein, consisting of smooth muscle cells, is generally thin and cannot easily be appreciated on OCT images. Vein grafts usually appear, therefore, as what seems to be a 2-layered vessel (Fig. 47.3b).

While vein grafts that have just been implanted appear as 2-layered vessels, they typically undergo morphological changes overtime, called arterialization. This includes intimal fibrous thickening, medial hypertrophy, and lipid deposition [21], thereby mimicking the 3-layered appearance of a healthy coronary (Fig. 47.3c, d). This change in appearance is probably a physiological adaption of the vein to the different environment. To normalize tangential wall stress from the increased pressure (100 mmHg vs 10 mmHg), the graft intima becomes hyperplastic and forms a neointima. The neointima resembles a combined intima media layer of a normal artery and is predominantly formed by vascular smooth muscle cells [3].

A distinct difference between arteries and veins is that the latter contains valves to stimulate blood flow in the direction of the heart. OCT has the capability to detect these valves, although they are easily missed. They appear as a high signaling structure that crosses the lumen area [17].

Atherosclerosis in Venous Grafts

Angiographically, severe atherosclerosis is often appreciated by an irregular and crooked appearance of the venous graft (Fig. 47.4). OCT images typically reveal narrowing of the lumen of the graft with intimal hyperplasia or lipid rich plaques (Fig. 47.5), much like diseased coronary arteries. Available studies on OCT findings in grafts purely describe typical findings seen in grafts and often report thrombus, plaque ruptures, tissue protrusion, and arterialization [13, 18, 19].

A typical aspect of atherosclerosis in venous grafts that we witnessed during reviewing of our graft population was the appearance of a peel-like morphology in the vessel wall, which appeared as a heterogeneous, low-attenuating and sharply delineated structure, very much consistent with the appearance of calcifications (Fig. 47.6). The extensiveness of these peels varied in arc, ranging from 1 quadrant to fully circumferential. A circumferential appearance shows similarities with the previously described sign of arterialization, but the latter is less heterogeneous and has a more smooth curvature. This "calcium peel" was seen in 72 % of the pullbacks that we investigated. This phenomenon shows similarities in appearance as well as incidence with the previously described "friable" tissue [18]. It is, however, not clear if this in indeed similar tissue and histologic studies are needed to provide insights into this entity.

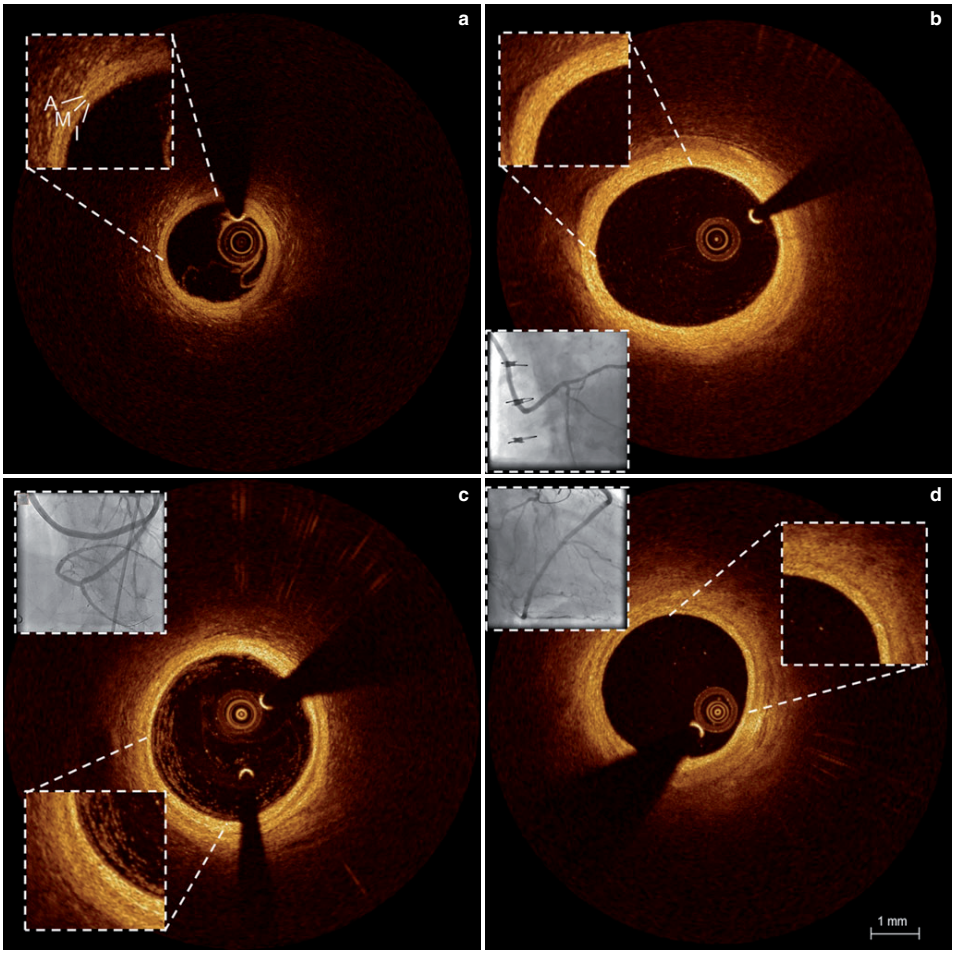

Fig. 47.3 Arterialization of venous grafts. (**a**) Typical 3-layered appearance in a healthy, native coronary artery. The intima (*I* bright, high reflective structure), media (*M* dark, low reflective structure) and adventitia (*A* bright, high reflective structure) are very well distinguished. (**b**) Typical image of the vessel wall of a venous graft. The 3-layered appearance is less distinct. (**c**, **d**) Arterialization of the venous graft, with mimicking of the three layers

Tissue Protrusion

A known problem of vein grafts is the presence of intraluminary debris. This is one of the factors that could contribute to no-reflow and be a mediator for the worse outcome after graft intervention with increased restenosis [22]. Interestingly, pre-interventional OCT images seldom reveal this debris or thrombotic material. However, OCT cross-sectional images acquired directly after stent implantation show tissue protrusion in the vast majority (94 %) of our pullbacks (Fig. 47.7). This percentage is comparable to the incidence (81–95 %) of tissue protrusion after stent implantation in native coronaries [23–25]. While the incidence of tissue protrusion is comparable, grafts appear to have more severe tissue protrusion compared to native coronaries based on the findings in our reviewed cases. Unfortunately, quantitative measurements have not

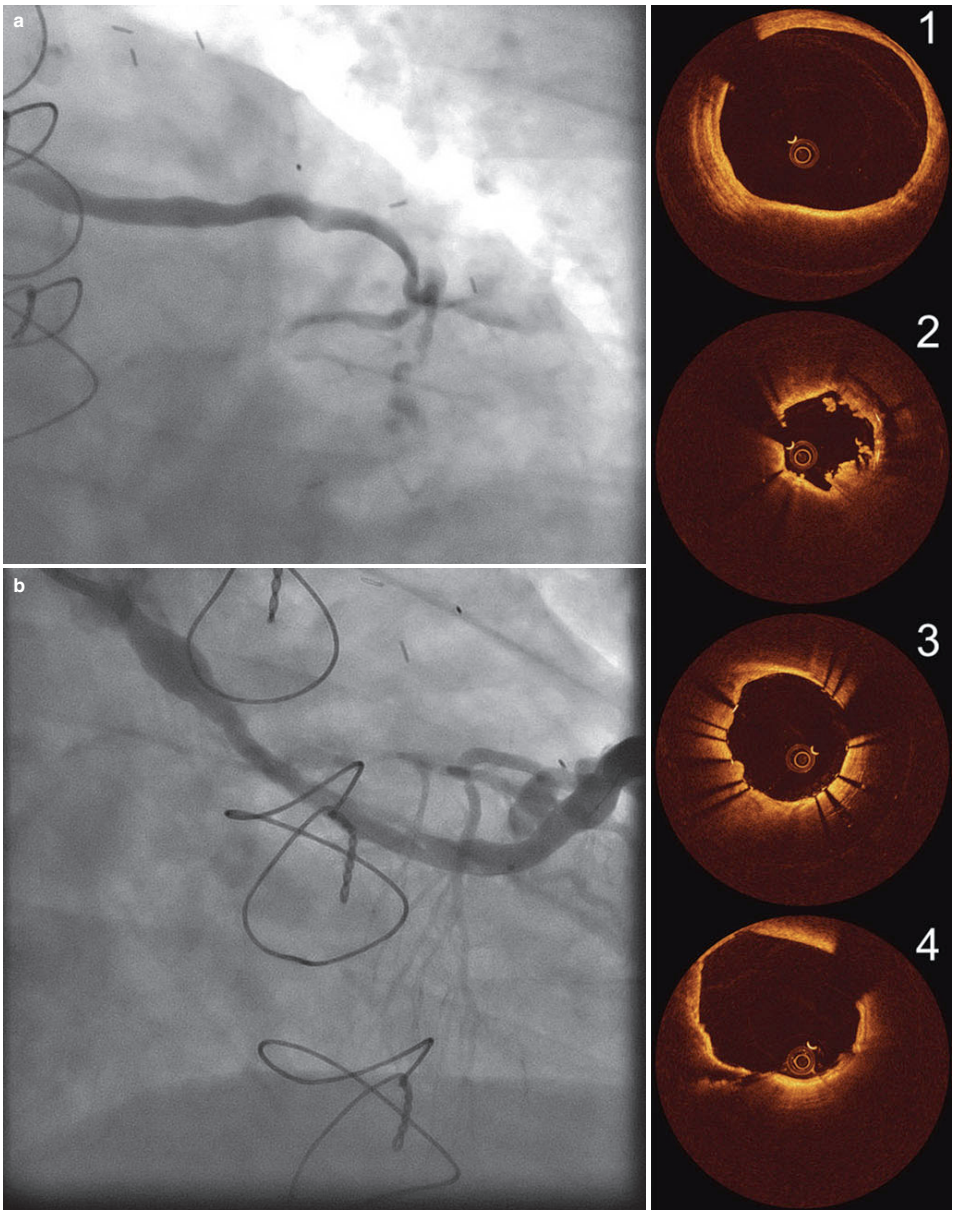

Fig. 47.4 Crooked and irregular appearance of venous graft. Signs of severely diseased venous graft as seen on angiogram. The shape of the graft is irregular, with narrowing of the lumen and haziness throughout the entire graft. Flow distally of the first anastomosis is severely impaired, but clear angiographic visualization is challenging due to overlap and distortion (**a**). After stenting flow has improved, but the extensive disease is pronounced (**b**). Post-stent cross-sectional OCT images reveal severe atherosclerosis from throughout the entire graft (*panels 1–4*, from proximally to distally)

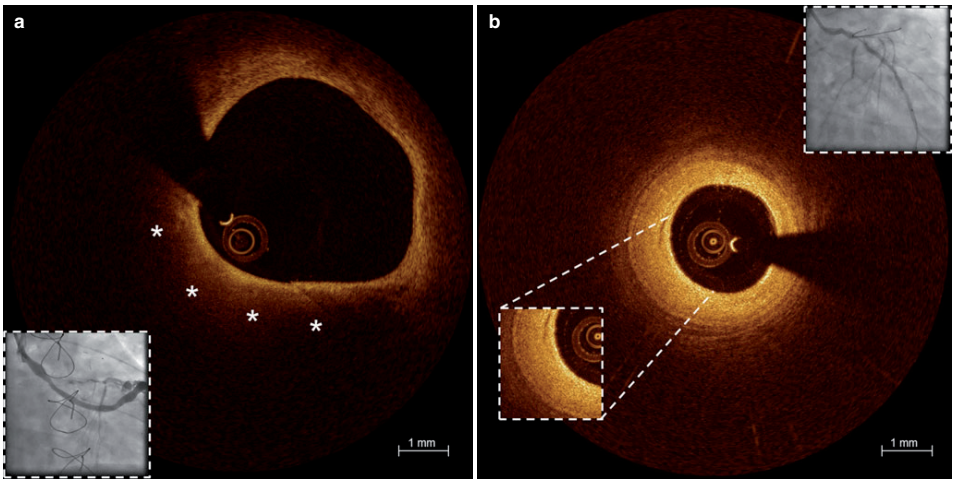

Fig. 47.5 Atherosclerosis of venous grafts. (**a**) The low-intensity signal (*) beneath the intima strongly suggests fibroatheroma with a lipid rich/necrotic core-rich plaque. (**b**) Mild lumen narrowing caused by marked, concentric intimal thickening

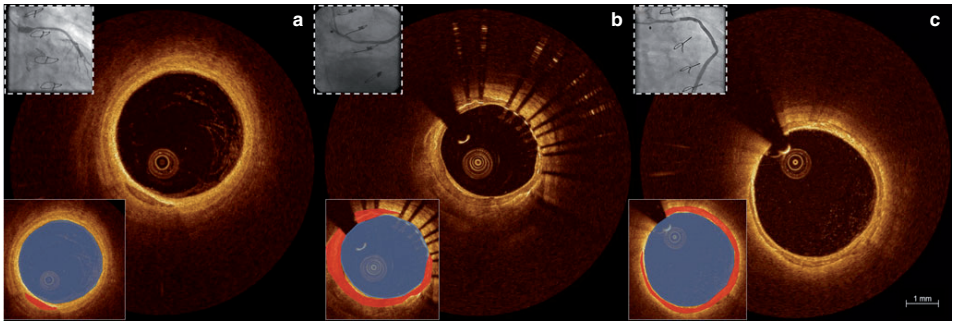

Fig. 47.6 Presence of calcium-like peels. Panel (**a**) Heterogeneous, calcium-like peel (low-attenuating, dark, sharply delineated structure, inlayed panels: *red*) in one quadrant of the vessel wall. In panel (**b**) and (**c**) this peel extends up to three and four quadrants, respectively

been made yet and should be considered in future studies. At this time, there are, however, also no studies that could prove a prognostic impact of tissue protrusion [24].

OCT Guidance of Percutaneous Coronary Intervention

Guidance in Native Vessels

From extensive studies of OCT in native coronaries [11], it is known that OCT can provide high quality images of the lumen, with semi-automatic lumen area measurements in some devices. Variables such as the minimum lumen area, fibrous cap thickness, stent dimensions, or malapposition distance can be retrieved with relative ease. This data can be used to assess stenosis severity, coronary atherosclerosis, and stent implantation with high reproducibility [26]. OCT could therefore find application in the guidance of percutaneous coronary intervention (PCI), allowing a thorough pre-procedural lesion assessment, which enables accurate device sizing, selection of the vessel segment requiring treatment, and the proper selection of an implantation strategy [12]. It has been demonstrated that

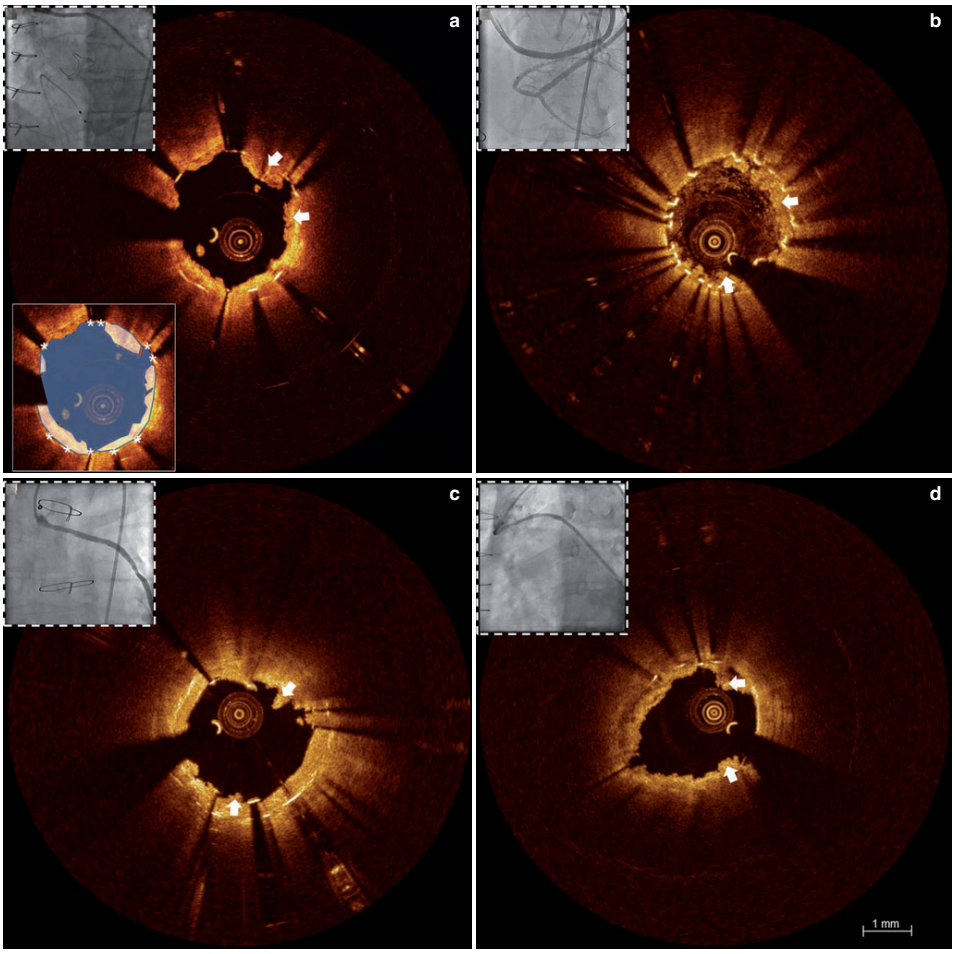

Fig. 47.7 Tissue protrusion after acute stent implantation. Tissue protrusion (*white arrows*, inlayed panel: *white*) direct after stent (stent struts labelled with *) implantation in a Xience™ V stent panel (**a**), Stentys™ bare metal stent panel (**b**) and Trendymed™ Over-and-Under Pericardium covered stent panel (**c**) and (**d**)

angiography alone underestimates plaque burden, severity of stenosis [27], and lumen dimensions [28], while OCT gives the true, accurate lumen dimensions. Moreover, it can be used in the assessment of the acute procedural result, allowing the estimation of stent expansion and vessel injury. Consequently, intravascular imaging can in this way assist in the optimization of the acute implantation result, the significance of which is underscored by observations of an association between suboptimal implantation and stent failure [29]. Importantly, several studies and meta-analyses have shown that the use of imaging guidance might improve outcome [30–32].

Overall, in our practice, OCT is being frequently used in the pre-procedural lesion assessment, providing accurate measurements for stent or scaffold sizing, aiding in the choice of the interventional strategy, and in the delineation of a suitable landing zone. According to our experience, the use of OCT often facilitates decision making in a way that is

readily and easily available, without obstructing the workflow of the laboratory.

Guidance in Grafts

PCI in grafts is considered challenging, due to the difficult assessment by angiography and the high incidence of distal embolization [7] and no-reflow [8], which may be contributed to by the disruption of atherosclerotic plaques and adherent thrombus. This leads to higher rates of periprocedural myocardial infarction, restenosis (Fig. 47.8), in-hospital mortality, and occlusion compared to PCI of the native coronaries [33].

The relatively large vessel size of a venous graft makes correct angiographic assessment, due to geometric distortion, difficult. In addition, the tortuous course of a graft makes selection of an optimal angiographic projection strenuous, hampering measurements of the true lumen dimensions at the site of the distal anastomosis. The difficulty to achieve adequate visualization also makes assessment of the extent of disease and lesion length laborious. These factors make adequate stent sizing challenging, which is specifically important because of the often fragile location. A too small stent can result in early failure, while a too large stent may exaggerate trauma to the vessel wall and increase the risk for distal embolization and no reflow, or in case of lesions at the anastomosis site, might cause damage to the surgical suture. OCT can help to reliably determine the previously mentioned characteristics to select both the optimal stent diameter and length. With the ability to identify lesion composition and least diseased "landing zones," a stent can be placed more accurately. One could speculate that this could avoid implantation of a stent's edge on a necrotic core, thereby possibly avoiding abundant thrombus formation, embolization, and no-reflow. Transition from the graft to the native vessel can cause severe tapering of the vessel, which is another asset that can be clearly visualized by OCT. When seen, a post-dilation immediately after stent implantation can be planned in order to avoid proximal inadequate stent expansion or malapposition without the need of extra fluoroscopy in between.

Figure 47.9 demonstrates the clinical use of OCT in a 78-year-old male presenting with non-ST elevated myocardial infarction (NSTEMI) caused by late stent thrombosis in a 12-year-old venous graft. The angiogram revealed a hazy spot distally in the graft at the site of the anastomosis with the first marginal branch of the circumflex artery, which was identified as the culprit lesion. The quality of the initial OCT pullback was poor due to inadequate flushing of the lumen. This was averted with the use of a Guidezilla™ guide extension catheter (5 Fr in 6 Fr). With the additional backup, adequate clearance of the lumen could be achieved, resulting in better quality OCT images. These images were used to

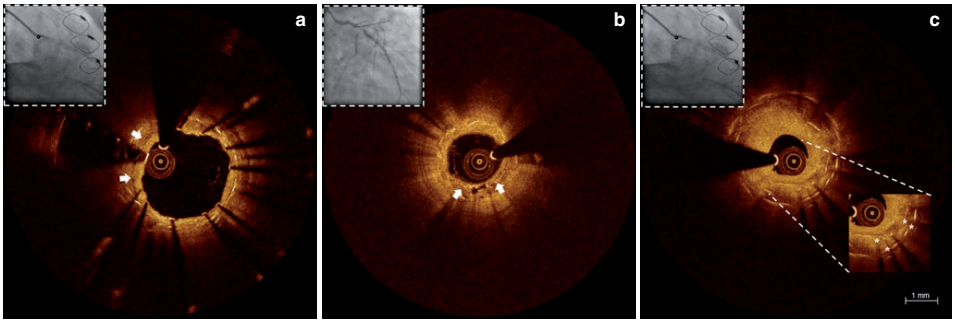

Fig. 47.8 Different patterns of neointimal coverage in venous grafts. Calcium-rich (*arrow*) neo-atherosclerosis in a stented vein graft (**a**). Fibrous tissue with a heterogeneous (*arrow*) (**b**) and a homogeneous appearance (**c**) causing restenosis in two overlapping stents (*) within a saphenous vein graft

Fig. 47.9 OCT-guided PCI of a venous graft. Angiogram of a lesion in a 12-year-old venous graft at the site of anastomosis with the marginal branch (**a**). Initial OCT cross-sectional image with poor quality due to inadequate flushing (*panel 1*). The use of a Guidezilla™ (*arrow*) (**b**) improved the quality of the OCT images, which revealed late stent thrombosis (*arrow*, *panel 2*, struts labelled with *) as cause of the myocardial infarction. A proximal (*panel 3*) landing zone was selected, with a distal landing zone after the anastomosis with the marginal branch (*MO*) (*panel 4*). Final angiogram showed an adequately revasularized graft (**c**) and good stent apposition at the site of the thrombus (*panel 5*)

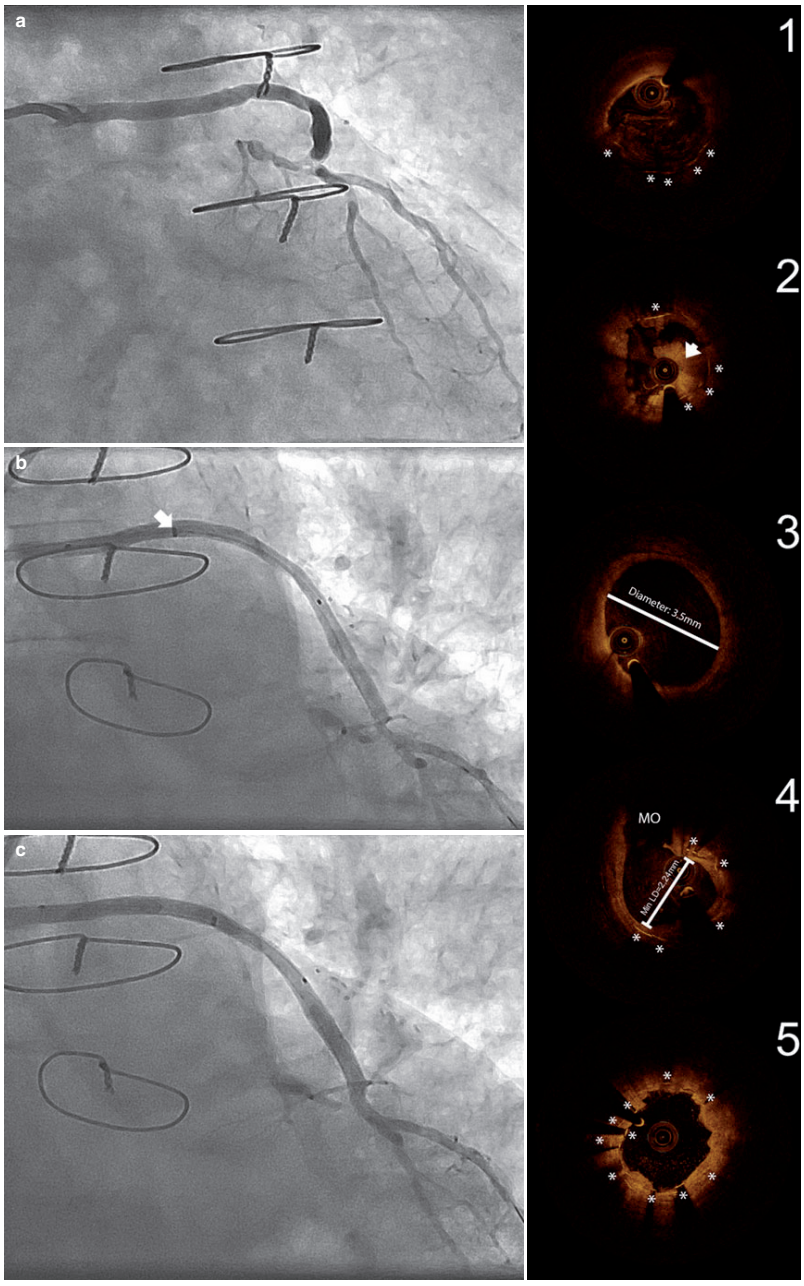
a
b
c
1
2
3
Diameter: 3.5mm
4
MO
Min LD=2.4mm
5

assess the culprit lesion and to determine optimal landing zones with their corresponding lumen diameters. Distal minimal lumen diameter was 2.24 mm, so a Promus™ 2.25×16 mm drug-eluting stent was chosen to treat the lesion. Proximally, the lumen diameter increased up to 3.5 mm, so proximal post-dilation with a Sprinter™ 3.5×10 mm was planned directly after stent implantation. The first post-stent pullback showed malapposition proximally, which was treated with additional dilation with a larger balloon (Sprinter™ 4.0×10 mm). The final OCT pullback demonstrated a nicely expanded stent, with a minimum lumen area of 5.26 mm^2 and only some mild remaining malapposition at the proximal stent edge.

Co-registration of Angiography and OCT

OCT guidance of a PCI in general can be difficult in daily clinical practice, despite these several potential advantages. Most available OCT systems record cross-sectional images in great detail, but these are not easily matched to their geographical position on the angiogram, especially when clear anatomical landmarks are missing. Important data that is acquired by OCT is therefore not always translated into clinical use. Fortunately, several systems have been introduced that allow for quick and easy online co-registration of angiographic and OCT images. The use of a system able to provide online a spatial co-registration of the high-resolution intravascular imaging findings with the angiographic image could improve decision making in the catheterization lab. This integration of OCT information on an angiographic roadmap enables the easy and immediate utilization of such information by the operator. This could find broad application in the treatment of diffuse disease in segments without clear angiographic landmarks (such as grafts), where spatial orientation might be challenging, requiring continuous fluoroscopy and multiple views in order to correctly localize the segment that needs to be treated.

Another important field where OCT can provide useful guidance in clinical practice is in the management of stent failure, where the recent European Society of Cardiology guidelines have given OCT a class IIa recommendation (level of evidence: C) [34]. In acute and subacute stent thrombosis, mechanical factors, such as incomplete expansion and vessel trauma, are playing a pivotal role [30]. It is important to recognize these mechanical complications in order to provide the appropriate treatment (e.g., post-dilation in incomplete expansion or additional stent implantation in edge injury). The knowledge of the precise anatomical location can facilitate local treatment, especially in long stents or stents with asymmetric expansion, where the exact localization of the site with mechanical issue might be poorly visualized by angiography. Also, in late stent failure, the distinction of restenosis with thrombosis might be unclear by angiography [35], while use of OCT can help discriminate between these two mechanisms, and guide the choice between local or systematic antithrombotic therapy, balloon post-dilation, or additional stent implantation. Again, the localization of the stent pathology is important, as the severity and extent of restenotic tissue and/or thrombus could vary, while the visualization by the angiography remains poor. In such cases, co-registered OCT could allow treatment that is focused on treating the proper segment within the stent.

Figure 47.10 shows the clinical use of this co-registered technique in a 68-year old lady, who underwent a PCI of the right coronary artery (RCA) 2 weeks earlier with implantation of an Ultimaster™ 2.5×18 mm for an acute inferior infarction. She presented with recurrent inferior ST-elevation myocardial infarction. The angiogram revealed an occlusion of the RCA proximally to the previously implanted stent. A co-registered OCT was performed to investigate the pathomechanism of the stent failure. Cross-sectional OCT images revealed the presence of an underexpanded and malapposed stent with thrombotic material at the site of the most severe underexpansion. Moreover, OCT showed the presence of extensive disease distally to the stent, that had not been treated at the baseline procedure (Fig. 47.11). Several stenotic lesions, mainly eccentric, were observed in the OCT pullback, despite not being clearly visible on angiography. A landing zone was selected based on the lumen profile view, aiming to cover the entire diseased segment. Based on OCT measurements, a Promus™ 3.0×32 mm (Boston Scientific, Natick, MA, US) was selected, with the intention to distal overlap the pre-existing stent. Immediately post implantation, after considering the lumen area at the site of the malapposition (2.67 mm) and a distal reference area of 2.82 mm, the balloon of the stent (3.0 mm diameter) was used for post-dilation of the entire stented region, including the underexpanded and malapposed Ultimaster™ stent. This resulted in a well-expanded stent, landing in a relatively healthy segment and with a short segment of strut overlap. The lumen area within the previous stent was also improved, as were apposition and expansion of this stent.

Future Directions

Although OCT has seen many technical improvements over the last 10 years, it is still a technique that is undergoing a lot of developments. The pullback speed is among the features that has seen that biggest advancements. Currently commercially available systems allow for pullback speeds up to 40 mm/s, but an ultrafast, "heartbeat" OCT [36] has recently been presented. With an increased pullback speed of 100 mm/s it is possible to acquire the entire pullback within one cardiac cycle, thereby overcoming the motion artifacts that occur caused by beating of the heart.

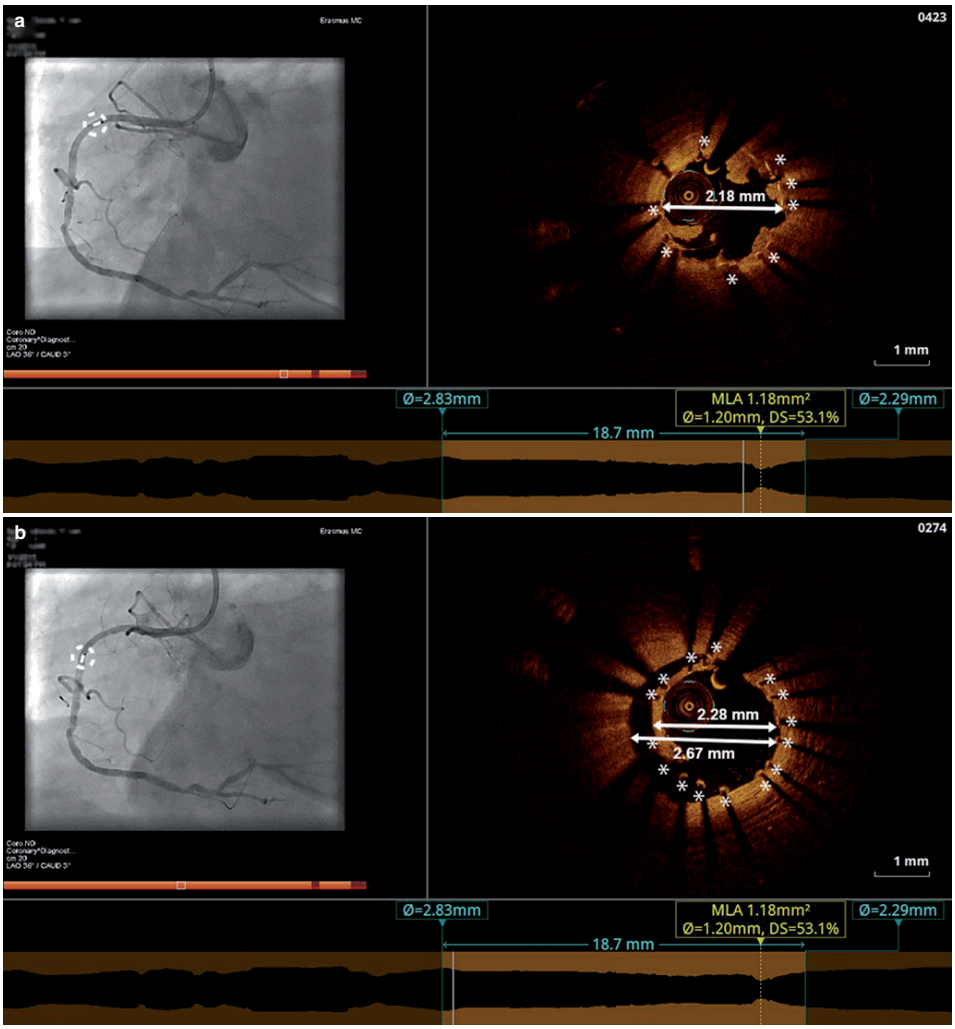

Fig. 47.10 Co-registration of angiography and OCT in stent failure. OCT demonstrates (**a**) underexpansion of the implanted Ultimaster™ 2.5×18 mm stent (*) with a minimum stent diameter of 2.18 mm, also accompanied by (**b**) malapposition at the distal segment. The corresponding angiographic positions are shown left of the cross-sectional OCT images (*dashed circles*). The schematic directly below the angiogram/OCT image represents a reconstruction of the true, undistorted lumen dimensions and can be used in a similar way as the angiogram

Another field of research is tissue characterization by OCT, which can still be challenging in certain scenarios. A potential promising technique, which could improve tissue characterization based on merely "traditional" intensity OCT images, is polarization sensitive imaging [37]. This technique further exploits specific features of light that can further help to differentiate between the various types of tissue that can be found within the coronary vessel wall. Together with tissue characterization, comes quantification—a process that, if done manually, can be cumbersome

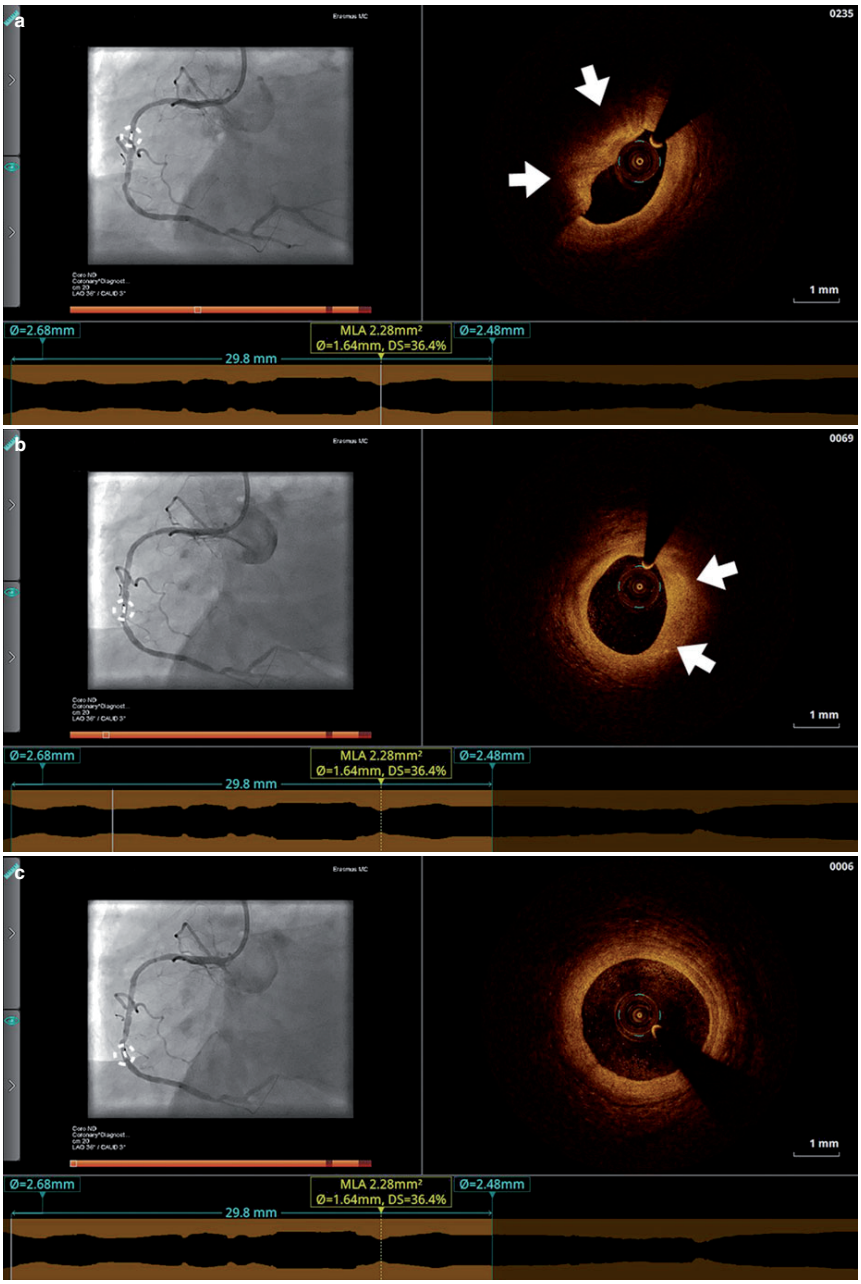
a
0235
1 mm
Ø=2.68mm
MLA 2.28mm²
Ø=1.64mm, DS=36.4%
Ø=2.48mm
29.8 mm
b
0069
1 mm
Ø=2.68mm
MLA 2.28mm²
Ø=1.64mm, DS=36.4%
Ø=2.48mm
29.8 mm
c
0006
1 mm
Ø=2.68mm
MLA 2.28mm²
Ø=1.64mm, DS=36.4%
Ø=2.48mm
29.8 mm

Fig. 47.11 Co-registered OCT images downstream of the stented segment demonstrating extensive disease. Just distally of the stent, an eccentric stenotic lesion panel (**a**) can be appreciated on the cross-sectional OCT images caused by a thick cap fibroatheroma (*arrows*). Further distally, several stenoses are observed with the most distal (arrows) being more than 25 mm distally to the previously implanted stent panel (**b**). Therefore, a healthy landing zone with a three-layered appearance panel (**c**) was selected at approximately 30 mm distal of the underexpanded stent to entirely cover this diseased segment. The corresponding angiographic positions are shown left of the cross-sectional OCT images (*dashed circles*)

and time-consuming. Software that can semi-automatically detect lumen contours or stent struts have been available for quite some time. However, fully automated fibrous cap thickness measurement [38] is currently under development and could further help to implement decision-making based on OCT images in the catheterization laboratory workflow.

The previously mentioned developments are just a few examples of projects currently being worked on. This list is far from complete; there are many more promising projects currently under development. Which of these will eventually make it to clinical practice, does yet need to be seen, but it shows the potential that OCT has in further improving coronary interventions in the future.

Conclusion

Optical coherence tomography has distinct features that could potentially unravel some of the mysteries that are still connected to the rapid formation of atherosclerosis in grafts. Its unmatched resolution allows for visualization of even the smallest structures in the vessel wall. Although OCT imaging of grafts is generally considered challenging, we believe that with the correct preparation it is feasible to acquire good quality images in the majority of the grafts.

References

1. Yusuf S, Zucker D, Peduzzi P, Fisher LD, Takaro T, Kennedy JW, et al. Effect of coronary artery bypass graft surgery on survival: overview of 10-year results from randomised trials by the Coronary Artery Bypass Graft Surgery Trialists Collaboration. Lancet. 1994;344(8922):563–70.
2. Goldman S, Zadina K, Moritz T, Ovitt T, Sethi G, Copeland JG, et al. Long-term patency of saphenous vein and left internal mammary artery grafts after coronary artery bypass surgery: results from a department of veterans affairs cooperative study. J Am Coll Cardiol. 2004;44(11):2149–56.
3. Harskamp RE, Lopes RD, Baisden CE, de Winter RJ, Alexander JH. Saphenous vein graft failure after coronary artery bypass surgery pathophysiology, management, and future directions. Ann Surg. 2013;257(5):824–33.
4. Hess CN, Lopes RD, Gibson CM, Hager R, Wojdyla DM, Englum BR, et al. Saphenous vein graft failure after coronary artery bypass surgery: insights from PREVENT IV. Circulation. 2014;130(17):1445–51.
5. Campeau L, Enjalbert M, Lesperance J, Bourassa MG, Kwiterovich Jr P, Wacholder S, et al. The relation of risk factors to the development of atherosclerosis in saphenous-vein bypass grafts and the progression of disease in the native circulation. A study 10 years after aortocoronary bypass surgery. N Engl J Med. 1984;311(21):1329–32.
6. Coolong A, Baim DS, Kuntz RE, O'Malley AJ, Marulkar S, Cutlip DE, et al. Saphenous vein graft stenting and major adverse cardiac events: a predictive model derived from a pooled analysis of 3958 patients. Circulation. 2008;117(6):790–7.
7. Trono R, Sutton C, Hollman J, Suit P, Ratliff NB. Multiple myocardial infarctions associated with atheromatous emboli after PTCA of saphenous-vein grafts – a clinicopathologic correlation. Cleve Clin J Med. 1989;56(6):581–4.
8. Kaplan BM, Benzuly KH, Kinn JW, Bowers TR, Tilli FV, Grines CL, et al. Treatment of no-reflow in degenerated saphenous vein graft interventions: comparison of intracoronary verapamil and nitroglycerin. Cathet Cardiovasc Diagn. 1996;39(2):113–8.
9. Piana RN, Paik GY, Moscucci M, Cohen DJ, Gibson CM, Kugelmass AD, et al. Incidence and treatment of no-reflow after percutaneous coronary intervention. Circulation. 1994;89(6):2514–8.
10. Motwani JG, Topol EJ. Aortocoronary saphenous vein graft disease – pathogenesis, predisposition, and prevention. Circulation. 1998;97(9):916–31.
11. Tearney GJ, Regar E, Akasaka T, Adriaenssens T, Barlis P, Bezerra HG, et al. Consensus standards for acquisition, measurement, and reporting of intravascular optical coherence tomography studies: a report from the international working group for intravascular optical coherence tomography standardization and validation. J Am Coll Cardiol. 2012;59(12):1058–72.
12. Karanasos A, Ligthart J, Witberg K, van Soest G, Bruining N, Regar E. Optical coherence tomography: potential clinical applications. Curr Cardiovasc Imaging Rep. 2012;5(4):206–20.
13. Gonzalo N, Serruys PW, Piazza N, Regar E. Optical coherence tomography (OCT) in secondary revascularisation: stent and graft assessment. EuroIntervention. 2009;5 Suppl D:D93–100.
14. Karanasos A, Tu S, Van Ditzhuijzen N, Ligthart J, Van Mieghem N, Van Geuns RJ, et al. A novel method to assess coronary artery bifurcations by OCT: Cut-plane analysis for side-branch ostial assessment from a main vessel pullback. Eur Heart J Cardiovasc Imaging. 2015;16(2):177–89.
15. Onuma Y, Thuesen L, van Geuns RJ, van der Ent M, Desch S, Fajadet J, et al. Randomized study to assess the effect of thrombus aspiration on flow area in patients with st-elevation myocardial infarction: an optical frequency domain imaging study – TROFI trial. Eur Heart J. 2013;34(14):1050–60.
16. Magro M, Regar E, Gutiérrez-Chico JL, Garcia-Garcia H, Simsek C, Schultz C, et al. Residual atherothrombotic material after stenting in acute myocardial infarction – an optical coherence tomographic evaluation. Int J Cardiol. 2013;167(3):656–63.
17. Brown EN, Burris NS, Gu J, Kon ZN, Laird P, Kallam S, et al. Thinking inside the graft: applications of optical coherence tomography in coronary artery bypass grafting. J Biomed Opt. 2007;12(5):051704.
18. Davlouros P, Damelou A, Karantalis V, Xanthopoulou I, Mavronasiou E, Tsigkas G, et al. Evaluation of culprit saphenous vein graft lesions with optical coherence tomography in patients with acute coronary syndromes. JACC Cardiovasc Interv. 2011;4(6):683–93.

19. Adlam D, Antoniades C, Lee R, Diesch J, Shirodaria C, Taggart D, et al. Oct characteristics of saphenous vein graft atherosclerosis. JACC Cardiovasc Imaging. 2011;4(7):807–9.
20. Motreff P, Levesque S, Souteyrand G, Sarry L, Ouchchane L, Citron B, et al. High-resolution coronary imaging by optical coherence tomography: feasibility, pitfalls and artefact analysis. Arch Cardiovasc Dis. 2010;103(4):215–26.
21. Mintz GS, Nissen SE, Anderson WD, Bailey SR, Erbel R, Fitzgerald PJ, et al. American college of cardiology clinical expert consensus document on standards for acquisition, measurement and reporting of intravascular ultrasound studies (IVUS). A report of the american college of cardiology task force on clinical expert consensus documents. J Am Coll Cardiol. 2001;37(5):1478–92.
22. Webb JG, Carere RG, Virmani R, Baim D, Teirstein PS, Whitlow P, et al. Retrieval and analysis of particulate debris after saphenous vein graft intervention. J Am Coll Cardiol. 1999;34(2):468–75.
23. Kawamori H, Shite J, Shinke T, Otake H, Matsumoto D, Nakagawa M, et al. Natural consequence of post-intervention stent malapposition, thrombus, tissue prolapse, and dissection assessed by optical coherence tomography at mid-term follow-up. Eur Heart J Cardiovasc Imaging. 2013;14(9):865–75.
24. Bonnet B, Plastaras P, Huang JF, Seronde MF, Chopard R, Schiele F, et al. Prognostic impact of tissue protrusion after stenting in patients with acute coronary syndrome: an optical coherence tomography study. Eur Heart J. 2014;35:1143.
25. Sugiyama T, Kimura S, Akiyama D, Hishikari K, Kawaguchi N, Kamiishi T, et al. Quantitative assessment of tissue prolapse on optical coherence tomography and its relation to underlying plaque morphologies and clinical outcome in patients with elective stent implantation. Int J Cardiol. 2014;176(1):182–90.
26. Di Mario C, Iakovou I, van der Giessen WJ, Foin N, Adrianssens T, Tyczynski P, et al. Optical coherence tomography for guidance in bifurcation lesion treatment. EuroIntervention. 2010;6 Suppl J:J99–106.
27. Mintz GS, Painter JA, Pichard AD, Kent KM, Satler LF, Popma JJ, et al. Atherosclerosis in angiographically "normal" coronary artery reference segments: an intravascular ultrasound study with clinical correlations. J Am Coll Cardiol. 1995;25(7):1479–85.
28. Okamura T, Onuma Y, Garcia-Garcia HM, van Geuns RJ, Wykrzykowska JJ, Schultz C, et al. First-in-man evaluation of intravascular optical frequency domain imaging (OFDI) of Terumo: a comparison with intravascular ultrasound and quantitative coronary angiography. EuroIntervention. 2011;6(9):1037–45.
29. Choi SY, Witzenbichler B, Maehara A, Lansky AJ, Guagliumi G, Brodie B, et al. Intravascular ultrasound findings of early stent thrombosis after primary percutaneous intervention in acute myocardial infarction: a harmonizing outcomes with revascularization and stents in acute myocardial infarction (HORIZONS-AMI) substudy. Circ Cardiovasc Interv. 2011;4(3):239–47.
30. Witzenbichler B, Maehara A, Weisz G, Neumann FJ, Rinaldi MJ, Metzger DC, et al. Relationship between intravascular ultrasound guidance and clinical outcomes after drug-eluting stents: the assessment of dual antiplatelet therapy with drug-eluting stents (ADAPT-DES) study. Circulation. 2014;129(4):463–70.
31. Prati F, Di Vito L, Biondi-Zoccai G, Occhipinti M, La Manna A, Tamburino C, et al. Angiography alone versus angiography plus optical coherence tomography to guide decision-making during percutaneous coronary intervention: the centro per la lotta contro l'infarto-optimisation of percutaneous coronary intervention (CLI-OPCI) study. EuroIntervention. 2012;8(7):823–9.
32. Zhang Y, Farooq V, Garcia-Garcia HM, Bourantas CV, Tian N, Dong S, et al. Comparison of intravascular ultrasound versus angiography-guided drug-eluting stent implantation: a meta-analysis of one randomised trial and ten observational studies involving 19,619 patients. EuroIntervention [Metaanal]. 2012;8(7):855–65.
33. Lee MS, Park SJ, Kandzari DE, Kirtane AJ, Fearon WF, Brilakis ES, et al. Saphenous vein graft intervention. JACC Cardiovasc Interv. 2011;4(8):831–43.
34. Windecker S, Kolh P, Alfonso F, Collet JP, Cremer J, Falk V, et al. 2014 ESC/EACTS guidelines on myocardial revascularization: the Task Force on Myocardial Revascularization of the European Society of Cardiology (ESC) and the European Association for Cardio-Thoracic Surgery (EACTS) developed with the special contribution of the European Association of Percutaneous Cardiovascular Interventions (EAPCI). Eur Heart J. 2014;35(37):2541–619.
35. Karanasos A, Ligthart J, Witberg K, Toutouzas K, Daemen J, van Soest G, et al., editors. Association of neointimal morphology by optical coherence tomography with rupture of neoatherosclerotic plaque very late after coronary stent implantation. Proc. SPIE 8565, Photonic Therapeutics and Diagnostics IX, 856542. 2013.
36. Wang T, Wieser W, Springeling G, Beurskens R, Lancee CT, Pfeiffer T, et al. Intravascular optical coherence tomography imaging at 3200 frames per second. Opt Lett. 2013;38(10):1715–7.
37. Villiger M, Zhang EZ, Nadkarni SK, Oh WY, Vakoc BJ, Bouma BE. Spectral binning for mitigation of polarization mode dispersion artifacts in catheter-based optical frequency domain imaging. Opt Express. 2013;21(14):16353–69.
38. Zahnd G, Karanasos A, van Soest G, Regar E, Niessen W, Gijsen F, et al. Quantification of fibrous cap thickness in intracoronary optical coherence tomography with a contour segmentation method based on dynamic programming. Int J Comput Assist Radiol Surg. 2015;10(9):1383–94.

II

PART

PERFORMANCE AND OUTCOMES OF NOVEL METALLIC STENTS FOR LEFT MAIN STENTING

11

CHAPTER

OVER-EXPANSION CAPACITY AND STENT DESIGN MODEL: AN UPDATE WITH CONTEMPORARY DES PLATFORMS

Ng J, Foin N, Ang HY, **Fam JM**, Sen S, Nijjer S, Petraco R, Di Mario C, Davies J, Wong P.

Int J Cardiol. 2016 Oct 15; 221: 171-9.

Over-expansion capacity and stent design model: An update with contemporary DES platforms

Jaryl Ng [a,1], Nicolas Foin [a,*,1], Hui Ying Ang [a], Jiang Ming Fam [a], Sayan Sen [b], Sukhjinder Nijjer [b], Ricardo Petraco [b], Carlo Di Mario [c], Justin Davies [b], Philip Wong [a]

[a] National Heart Research Institute Singapore, National Heart Centre Singapore, Singapore
[b] International Centre for Circulatory Health, NHLI, Imperial College London, UK
[c] Biomedical Research Unit, Royal Brompton & Harefield NHS Trust, London, UK

ARTICLE INFO

Article history:
Received 5 February 2016
Received in revised form 23 May 2016
Accepted 21 June 2016
Available online 24 June 2016

Keywords:
DES
Stent
Left main
Expansion

ABSTRACT

Background: Previously, we examined the difference in stent designs across different sizes for six widely used Drug Eluting Stents (DESs).
Although stent post-dilatation to larger diameter is commonly done, typically in the setting of long tapering segment or left-main PCI, there is an increasing recognition that information with regard to the different stent model designs has a critical impact on overexpansion results.
This study aims to provide an update on stent model designs for contemporary DES platforms as well as test overexpansion results under with oversized post-dilatation.
Methods and results: We studied 6 different contemporary commercially available DES platforms: *Synergy, Xience Xpedition, Ultimaster, Orsiro, Resolute Onyx* and *Biomatrix Alpha*. We investigated for each platform the difference in stent designs across different sizes and results obtained after post-expansion with larger balloon sizes. The stents were deployed at nominal diameter and subsequently over expanded using increasingly large post dilatation balloon sizes (4.0, 5.0 and 6.0 mm at 14ATM). Light microscopy was used to measure the changes in stent geometry and lumen diameter after over-expansion.
For each respective DES platform, the MLD observed after overexpansion of the largest stent size available with a 6.0 mm balloon was 5.7 mm for *Synergy*, 5.6 mm for *Xience*, 5.2 mm for *Orsiro*, 5.8 mm for *Ultimaster*, 5.5 mm for 4 mm *Onyx* (5.9 mm for the 5 mm XL size) and 5.8 mm for BioMatrix *Chroma*.
Conclusion: This update presents valuable novel insights that may be helpful for careful selection of stent size for contemporary DES based on model designs. Such information is especially critical in left main bifurcation stenosis treatment where overexpansion to larger oversized diameter may be required to ensure full stent apposition.

1. Introduction

DESs are nowadays commonly used in PCI for treatment of left-main and long bifurcated segments. Due to the difference in lumen diameter between the vessel and the stent size in some coronary arteries, proximal post-expansion of the stent is normally necessary to match proximal reference diameter and optimize stent apposition.

As stent post-dilatation is commonly performed, typically with large over-expansion in the setting of long tapering vessel segment, there is an increasing recognition that information with regard to the different stent model designs can have a critical impact on overexpansion results.

Incomplete stent apposition has been associated with increased risk of in stent restenosis (ISR) and stent thrombosis (1). Previously, we examined the difference in stent designs across different sizes for 6 widely used Drug Eluting Stents (DESs) (2).

We tested overexpansion capacity of each stent design with post-dilatation using balloon diameters up to 6 mm and showed how, in absence of this critically important information, stents implanted in segments with major changes in vessel diameter have the potential to become grossly overstretched and to remain incompletely apposed (2–4).

This study aims to provide an update on stent model designs for contemporary DES platforms as well as test overexpansion results under with oversized post-dilatation.

* Corresponding author: National Heart Centre Singapore, 5 Hospital Drive, 169609, Singapore.
E-mail address: Nicolas.foin@gmail.com (N. Foin).
[1] Authors contributed equally

2. Method

2.1. Stent design nomenclature

By convention, for DES platforms with only two designs, these were named here as *small vessel* and *large vessel* model designs. For the *Synergy* platform which has three designs, these were termed *small, medium/workhorse* and *large vessel* designs. It has to be noted that this terminology was used for a uniform presentation in this manuscript and manufacturers may use a different nomenclature. A *Crown* or *Peak* is defined as 2 adjacent struts forming an angle. A complete *stent Ring* is formed by a number of adjacent crowns which give the stent its expansion capacity from a crimping state. Rings are connected to each other longitudinally by *Connectors* and a *stent Cell* is defined as the area enclosed by a pair of connectors and crowns (2).

3. DES overexpansion experiments

Six commercially available drug-eluting stents (DESs) were analysed: the everolimus-eluting PtCr SYNERGY™ (Boston Scientific, Natick, MA, USA), everolimus-eluting Cobalt Chromium (CoCr) XIENCE PRIME/XPEDITION™ (Abbott Vascular, Santa Clara, *CA*, USA), the ULTIMASTER® - Drug eluting stent (Terumo Corporation, Shibuya-ku, Tokyo, Japan), the ORSIRO Sirolimus Eluting Stent (BIOTRONIK AG, Berlin, Germany), the Resolute ONYX™ Zotarolimus-Eluting Stent (Medtronic, *CA*, US) and the BioMatrix Alpha/Chroma CoCr Stent Platform (Biosensors Interventional Technologies, Singapore) (Fig. 2). Samples of different stent sizes/models were deployed *in vitro* at nominal pressure (NP). Subsequently, over-expansion results for each design was tested with successive post-dilations using a 4.0 × 12 and a 5.0 × 12 non-compliant balloons (Expected Diameter at 14 ATM = 5.02 mm) (NC Quantum Apex; Boston Scientific, Natick, MA, USA) inflated at 14 ATM; for the largest designs, we used first a 5.0 × 12 non-compliant balloon followed by a 6.0 × 15 mm semi-compliant balloon (Maverick XL; Boston Scientific, Natick, MA, USA) with a pressure of 14ATM (Expected Diameter at 14 ATM = 6.46 mm). Post-dilation was performed on the proximal segment of the stent with a stent length equivalent to length of the post-dilatation balloon. Final dilations were repeated on the samples a second time to ensure an optimal expansion of the stent struts. For each individual stent diameter, two samples were deployed.

4. Microscope analysis

Stent samples were mounted and analysed using light microscopy (Leica MZ16 FA, Meyer Instruments, Houston, TX, USA). The magnified images of the stents were saved and used for quantitative measurement and analysis of the deformation. Longitudinal and transverse sections of the overexpanded stent at different reference in the proximal and distal sections of the stents were compared to assess the differences after overexpansion of the stents. Fig. 1 shows what parameters were measured from each of the images.

5. MLD and MSA

Cross-Sectional minimal lumen diameter was defined as the minimal lumen diameter (MLD) measured on the cross-sectional images of the stent from one strut edge to the opposite strut edge. The minimal stent area (MSA) was defined to be the cross-sectional inner lumen stent area excluding the stent struts. Lumen diameters were also derived from the measured MSA to compare with the MLD values measured from the cross sectional images.

On the proximal (over expanded) side, the lumen diameter was measured both at the proximal edge of the stent as well as 5 mm distally from the proximal edge. Lumen diameter was also measured using the side-view. Each measurement of MLD and MSA was repeated twice. The result provided was an average of measures on two samples with standard deviation.

6. Cell opening

The change in cell opening was estimated for each stent design after being deployed at nominal pressure (NP) as well as after overexpansion. Cell opening was measured using the longitudinal view and was estimated using a circle with its circumference fitted within the stent cell struts.

For a stent that has been ideally deployed in a vessel, the radius of the circle fitted within the cell represents the maximal distance between the arterial tissue and a neighbouring stent strut. An average of three measures was taken at NP and at maximal dilation (over expanded). The maximal cell opening at maximal dilation was also noted down and this occurs at the transition between the over expanded stent portion and the stent portion at NP. To ensure that the maximal dilation at the transition was measured, the stent was reoriented to be able to view the stent cells in the transition region.

7. Crown angle analysis

To study the effects of over expansion on strut deformation, the longitudinal view was used to measure the angle between 2 adjacent struts within a crown, avoiding crowns attached to a connector. Crown Angle was measured at NP and at over. An average of 3 measures was taken at NP and at post dilation (over expanded).

8. Results

8.1. Stent platforms and model designs

Of the six DES platforms investigated, four of them: *Xience, Orsiro, Ultimaster* and *BioMatrix A/Chroma* had two designs to cover the entire range of their diameter while *Synergy* has three designs and *Onyx* has four designs. For *Synergy,* we tested stents with nominal diameters of *2.75, 3.0* and 4.0 mm. For *Xience* and *BioMatrix A/Chroma*, stents with nominal diameters of 3.0 (SV Model) and 3.5 mm (LV Model) were tested. For *Orsiro* and *Ultimaster* we tested stents with nominal diameters of 3.0 and 4.0 mm. For *Onyx*, stents with nominal diameters of 2.5, 3.0, 4.0 and 5.0 mm were tested. Details of each DES design can be found in Table 1.

8.2. Maximal expansion capacity

Table 2 shows the obtained measurements of lumen diameter from both the cross-sectional and longitudinal images. Most stents were able to expand well above their labelled maximal stent diameter using larger post-dilatation balloons. Achieved MLD (considering minimal inner lumen obtained, excluding struts) after overexpansion was between 25% and 78% higher than the nominal stent diameter and average increase was 56%.

MLD observed after overexpansion of small-vessel workhorse (below 2.5 mm size) was 3.6 mm for *Synergy* and 3.3 mm for *Onyx* after post-expansion with a maximal non-compliant balloon of 4.0 mm at 14 atm. For medium-vessel workhorse (3 mm diameter stents), the MLD observed after overexpansion with a maximal non-complaint 5.0 mm balloon at 14ATM was 4.2 mm for *Synergy*, 4.0 mm for *Xience*, 4.0 mm for *Orsiro*, 4.3 mm for *Ultimaster*, 4.3 mm for *Onyx* and 4.1 mm for *Chroma.* For large-vessel workhorse (4.0 mm diameter stents, 3.5 mm for *Chroma*), the MLD observed after overexpansion with a 6.0 mm semi compliant balloon at 14ATM was 5.7 mm for *Synergy*, 5.6 mm for *Xience*, 5.2 mm for *Orsiro*, 5.8 mm for *Ultimaster*, 5.5 mm for *Onyx* and 5.8 mm for *Chroma*. Additionally, we tested the *Onyx* extra-large design which is available up to 5.0 mm size and MLD after overexpansion with 6.0 mm semi compliant balloon at 14ATM was 5.9 mm.

The LD derived from MSA also showed very good agreement with direct LD measurement, with the maximum difference being 0.2 mm (Table 2).

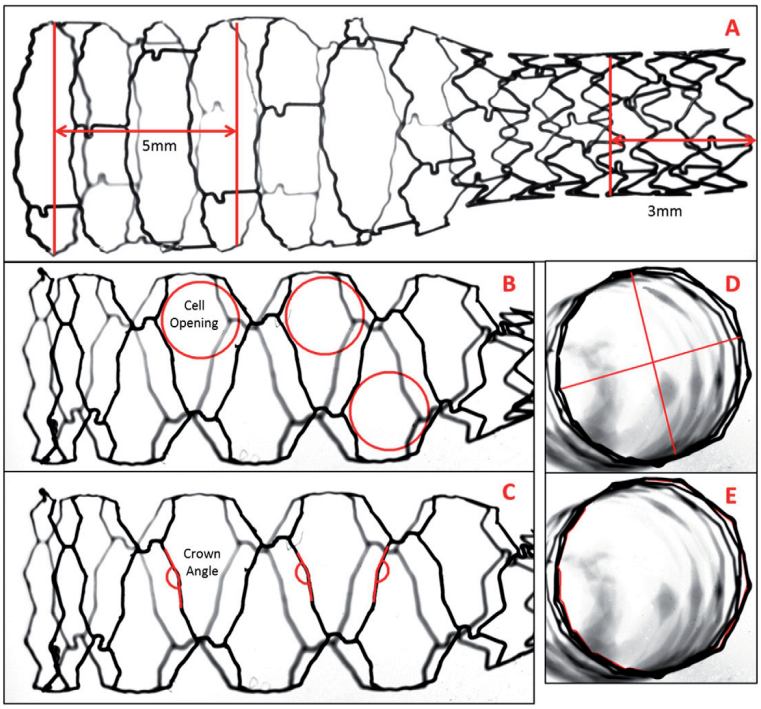

Fig. 1. Methods of Measurements: Minimal Lumen Diameter (MLD) is measured from the side view at the edge and 5 mm distal from the overexpanded edge (A). Cell opening diameter, including a cell opening diameter at the stent transition (B) and crown angle (C) are also measured from the side view. From the cross-sectional view, the Stent Luminal Diameter on 2 perpendicular axis (D) and the minimal stent lumen Area (E) are also measured.

8.3. Cell opening

Over expansion of stents are characterized by important strut distortion and large cell enlargements depending on the stent structure designs. Larger average distances between adjacent struts indicate large gaps in strut scaffolding which increases the risk of plaque prolapsing between struts, reducing drug delivery efficacy per unit wall surface area.

Diameter cell opening was assessed for each design and compared between maximal expansion and nominal pressure deployment. For the different platform, cell opening varied based on model design and largely increased after over expansion (Table 3 and Fig. 3).

For cell opening diameter at nominal pressure, the cell openings for *Synergy* were 0.6, 0.8 and 0.8 mm for the small, medium and large designs respectively, for *Xience* the cell openings were 1.1 and 0.9 mm for the medium and large designs respectively, for *Orsiro* the cell openings were 0.6 and 0.8 mm for the small and mid-large designs respectively, for *Ultimaster*, the cell openings were 0.7 and 1.0 mm for the small and mid-large designs respectively, for *Onyx*, the cell openings were 0.9 mm for all diameters and for *Chroma*, the cell openings were 1.1 and 1.0 mm for the medium and large designs respectively.

Cell opening diameter increased by an average of 114% between nominal pressure deployment and over expansion. The percentage increase for *Synergy* was 150, 131 and 145% for the small, medium and large designs respectively, for *Xience* it was 48 and 83% for the medium and large designs respectively, for *Orsiro* it was 164 and 145% for the small and mid-large designs respectively, for *Ultimaster* it was 119 and 123% for the small and mid-large designs respectively, for *Onyx* it was 90, 107, 104 and 89% for the small, medium, large and extra-large designs respectively and for *Chroma* it was 70 and 147% for the medium and large designs respectively.

The largest cell opening diameter was generally observed in the mid-section of the stent at the transition. For *Synergy* it was 1.5, 1.8 and 1.9 mm for the small, medium and large designs respectively, for *Xience* it was 1.6 and 1.7 mm for the medium and large designs respectively, for *Orsiro* it was 1.5 and 2.0 mm for the small and mid-large designs respectively, for *Ultimaster* it was 1.6 and 2.2 mm for the small and mid-large designs respectively, for *Onyx* it was 1.7, 1.8, 1.8 and 1.7 mm for the small, medium, large and extra-large designs respectively and for *Chroma* it was 1.8 and 2.5 mm for the medium and large designs respectively.

8.4. Crown deformations

Increasing the post-dilatation diameter causes the stent struts to progressively straighten with some stent rings becoming almost circular in the post-dilated segment as they approach their stretching limit (Table 3 and Fig. 4).

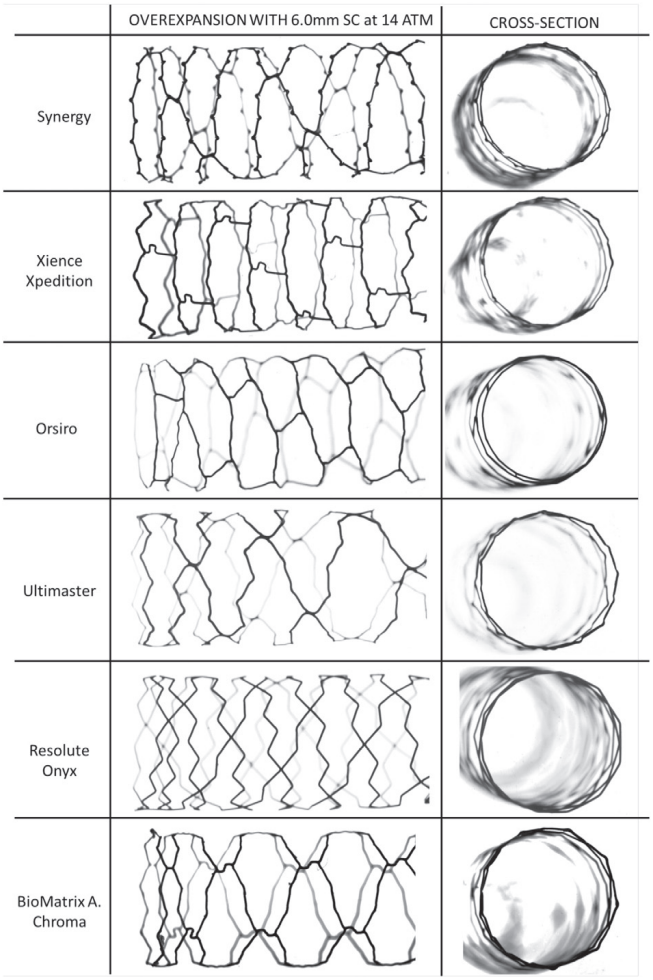

Fig. 2. Largest workhorse designs for each stent platform: Each of the picture shows the longitudinal image as well as the cross sectional image of the largest workhorse design of each platform after over expansion to 6.0 mm.

Over expansion caused noticeable straightening of the stent crown angle from an average crown angle of 77 $\pm$ 8° across all stents at nominal pressure deployment to 146 $\pm$ 15° after over expansion.

For the largest workhorse designs of all the platforms, *Chroma* showed the largest percentage increase in crown angle at 151% while *Onyx* on the other hand showed the smallest percentage increase in crown angle at 50%.

9. Discussion

In this study, we tested the overexpansion capabilities from six contemporary DES platforms, testing each design of each platform using increasing balloon sizes. Light microscopy was used to assess the morphological changes from nominal deployment to overexpansion. The main findings show that:

- Newer DES designs have similar cut-off diameter between small and large vessel size, and are able to expand largely beyond their nominal diameter.
- Overexpansion not only increases the MLD and MSA, but also increases the cell size and also the straightening of the struts.
- The morphological change in stent varies between stent platforms as well as stent size (model design) for a given platform.

Although normally comprised between 4.5 and 5.0 mm, the average diameter of a left main artery may reach over 5.5 mm in some patients according to some recent imaging studies (5,6), which means most of

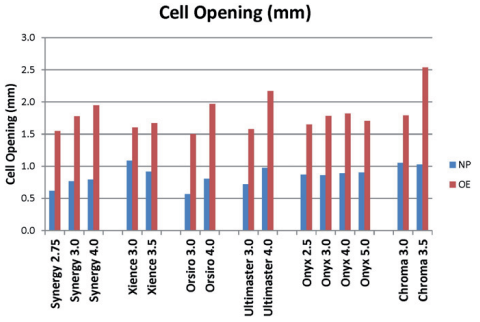

Fig. 3. Cell opening measurements at nominal pressure (NP) deployment and at over expansion (OE): Cell opening values are the average values across 6 measurements. Comparable cell opening values between the platforms and designs are observed at nominal diameter. Overexpansion increased cell opening by more than two folds, which is likely to affect scaffolding and drug delivery.

the current DES platforms are not provided in suitable sizes for those anatomies (currently, only the Taxus and the Resolute Onyx XL are provided in size above 4.5 mm). Other platforms will require post dilatation of at least 0.5 mm beyond their nominal diameter to ensure the optimal apposition of the stent in these anatomies (2,6,7).

We should note the fact that these DESs can be oversized does not imply that it is safe to do so. Indeed approaching physical limit of the stent induces changes in mechanical stiffness and drug delivery, therefore the performance of the device can be completely altered.

To our knowledge, in the main stream DES platforms, only the large size design of the Synergy (4.0 size), Promus Element (4.0 size), Resolute Onyx XL (4.5 and 5.0 size) and Taxus (4.5 and 5.0 size, Boston Scientific) have been labelled for post-expansion beyond 5.0 mm.

Malapposition of stents due to lack of incomplete stent expansion has been known to be a predicator of adverse outcomes (8–10). Although there is a need for overexpansion to treat left main stenosis, data regarding overexpansion beyond labelled recommendation are rarely provided by the manufacturers.

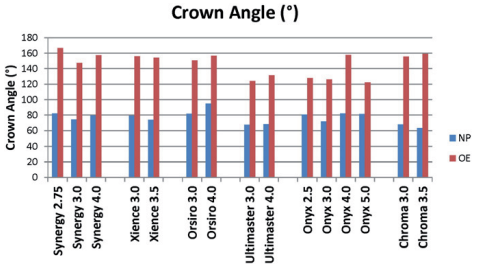

Fig. 4. Crown Angle measurements at Nominal Pressure (NP) deployment and at Over Expansion (OE): The crown angles are measured between adjacent struts that do not have a connector between them. Although at nominal diameter crown angles usually ranged from 63 to 95°, this was increased after overexpansion to over 122°, indicative of how much straightening was present in the crowns after overexpansion.

There have been previous studies done on stent over expansion. A previous study from our group on overexpansion looked at six stent platforms and their morphological changes after overexpansion (2).

This study aimed at applying a similar methodology to look at contemporary DES platforms.

Kissing balloon technique was not investigated in this study. Several experiments showed that Kissing balloon technique, which is commonly employed in bifurcation cases, may lead to severe elliptical stent distortion and even malapposition in some case if used to optimize apposition of the entire proximal stent segment (11–14). A more circular stent cross section is expected after Proximal Optimization Technique (POT). Therefore POT is nowadays recommended not only to optimize the stent before but also as a final step if Simultaneous Kissing Balloon is performed to correct the potential stent distortion caused by the overlap of the 2 balloons (4,11–13,15).

10. Lumen diameter and minimal stent area

In this study, we can see that all stent designs were able to expand well beyond nominal diameter. From the longitudinal measurements, most stents show similar diameters between the proximal over expanded edge and 5 mm distal from the proximal edge, indicating that the stent expanded evenly length-wise. Cross sectional LD measurements show that the MLD is within 0.1 mm of the average LD measured from side-view. This indicates that the overexpansion was even and the stent expanded uniformly.

The general consensus is that the stents should be sized based on the distal diameter of the vessel, especially for bifurcations, using POT for optimal apposition of the proximal side of the vessel (4). Although in an ideal scenario, the stents should be able to achieve a MLD equal to the diameter of the balloon, we see here that this is often not the case, which is in accordance with other reports (1,2,6,16,17). For our study, all large stent designs were post dilated using a 6.0 mm semi-compliant Maverick balloon (Expected Diameter at 14 ATM = 6.46 mm) but the MLD obtained on the stents only ranged from 5.3 mm to 6.0 mm.

As the strut straightens, the hoop force that the balloon has to provide to induce plastic deformation of the stent and limit elastic stent recoil increases. An *in-vivo* study by Berrocal et al. observed more stent recoil in overexpanded stents (18). Minimizing stent recoil is important as it leads to lowered risk of restenosis (19). Another study by Carrozza et al. suggested that an overexpansion of 10–20% above the reference vessel diameter is necessary as a solution to compensate the difference with compliance chart and optimize stent-to-artery ratio (16).

Post-dilatation balloon applied to stents tend to achieve lesser diameter enlargement than indicated by their post dilatation balloon compliance chart. Nevertheless, all stent platforms here could achieve with their largest design a MSA ranging from 22.2mm^2 to 28.4 mm^2 and a MLD ranging from 5.3 mm to 6.0 mm, which can accommodate most left main anatomies.

It can also be observed that stent platforms with only two designs are able to generally expand as much as stents with more designs, indicating that only 2 stent designs does not necessary hinder the stent's overexpansion capabilities.

11. Crown angle

It can be observed that overexpansion of the stents leads to a large discrepancy in crown angles, with increase ranging from 50% up to a 151% increase in crown angles. Large crown angle >150° indicates that the stent crowns are almost completely straightened and the stent is reaching its physical limit. Overexpansion and straightening of crowns is expected to be associated with increased radial force and stiffness. Although increase in radial force is good, an increase in stiffness can reduce the stent durability and get it more prone to fatigue and stent

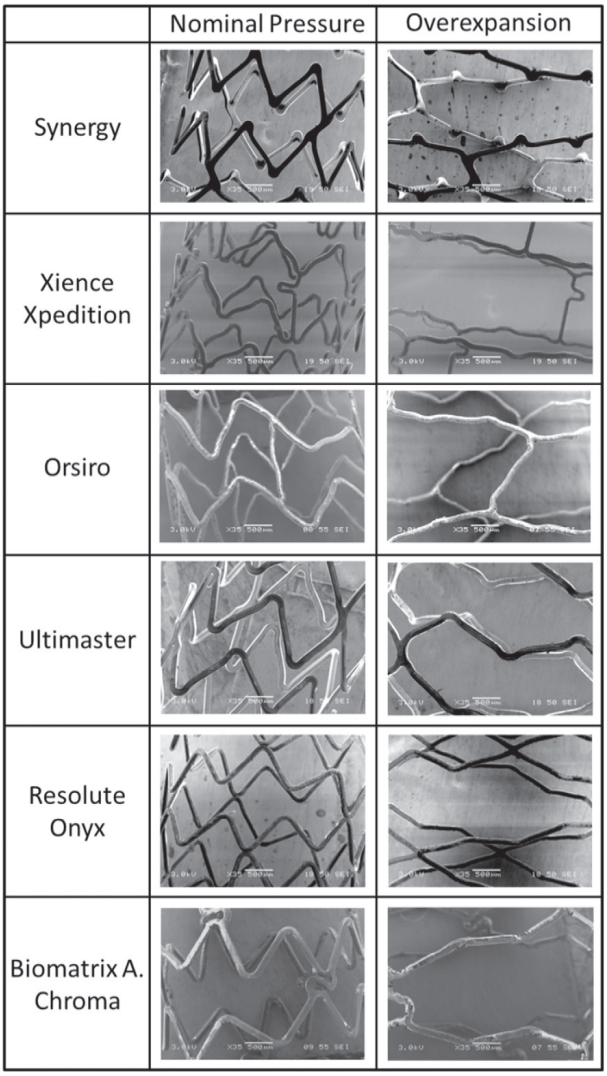

Fig. 5. SEM analysis of DESs after nominal pressure (left) deployment and overexpansion (right): Stents shown in the table are the largest workhorse design for each platform. All stents were first post dilated using a 5 mm NC balloon followed by overexpansion with a 6.0 mm SC balloon. Overexpansion causes visible straightening of the stent struts. Most coating resisted well despite oversizing with only minor cracks on the coating appearing in the crowns when deformation was the most severe.

fracture (2). Recent bench studies have shown the impact of stent designs and connectors on mechanical response, such as longitudinal strength and bending fracture (20,21).

12. Cell opening diameter

Cell opening diameter increase during overexpansion also varies largely depending on stent design: we observed a range up to 164% increase in cell opening diameter. This indicates an increase in cell size during overexpansion and the distance between strut scaffolds, hence increasing the risk of underlying plaque prolapse in between the struts. The increased gap between strut scaffolding can also negatively affect the drug eluting properties of the stent, potentially causing reduction in drug elution in overexpanded regions and chance of neointimal proliferation. A study done previously by Basalus et al. showed how cell area of a partly overexpanded stents varied based on the location

Table 1
DES workhorse and model designs: This table shows the designs of stents for each platform and also the sizes covered for each design. Most DESs only use 2 designs to cover the entire range of diameters, with the exception of *Synergy* and *Resolute Onyx*.

New DES workhorse and model designs

	Synergy	Xpedition	Res. Onyx	Ultimaster	BioMatrix A	Orsiro
2.25	Small vessel (8 crowns, 2-4 connectors)	Small vessel (6 crowns, 3 connectors)	Small vessel (6.5 crowns, 2 connectors)	Small vessel (8 crowns, 2 connectors)	Small vessel (6 crowns, 2 connectors)	Small vessel (6 crowns, 3 connectors)
2.50						
2.75			Medium vessel (8.5 crowns, 2 connectors)			
3.00	Workhorse(8 crowns, 2-4 connectors)					
3.50		Large vessel (9 crowns, 3 connectors)	Large vessel (9.5 crowns, 2.5 connectors)	Large vessel (8 crowns, 2 connectors)	Large vessel (9 crowns, 3 connectors)	Large vessel (6 crowns, 3 connectors)
4.00	Large vessel (10 crowns, 2-5 connectors)					
4.50			Extra-Large vessel (10.5 crowns, 2.5 connectors)			
5.00						

of the cell and the larger cell opening was shown to be at the transition region between the oversized and nominal segment (17). Although the relationship between struts scaffolding and drug distribution per unit area and the onset of restenosis is not known, careful stent selection based on design model is important to minimize stent deformations and risk of prolapse.

13. Drug coating integrity

Damage on the drug coating was not specifically looked at in this study. Overexpansion subjects the stent strut and the coating to extreme forces and deformation (14), increasing the risk of polymer coating damage. Other studies have addressed previously this point (14) and it is important to realize that the drug coating can be affected during severe over-expansion or Kissing Balloon technique. Drug coating damages or detachment of debris may expose patients to potential risks of thrombosis and inflammation with neointimal reactions (22,23). In Fig. 5, scanning electron microscope (SEM) images of each stent design at nominal pressure deployment as well as after overexpansion show that, although some minor coating defects may start to appear at the crowns which undergo the most severe deformation, stent coating resisted overall well for all the DESs during oversizing.

Table 2
Measured values of MSA and LD from cross-sectional and longitudinal images: The measurements are the minimal lumen diameter within the boundaries of the stent (not including the strut). Values obtained are the average of the measurement from 2 oversized samples for each stent design. Percentage change was calculated using the measurement values obtained using the longitudinal axis of the stent. All 4.0 mm DESs could be expanded to at least 5.3 mm with a 6.0 mm semi-compliant balloon at 14ATM.

Stent	Model design	Largest stent size NP (mm)	Max expansion balloon (mm)	Cross-sectional				Longitudinal		% Increase in LD after overexpansion
				LD		MSA		LD Edge	LD 5 mm	
				Minimum	Average	Average	SD			
Synergy	SV	2.75	5.0	3.6	3.6	11.4	0.4	3.7	3.7	53
	WH	3.5	5.0	4.2	4.2	14.4	0.5	4.1	4.2	57
	LV	4.0	6.0	5.7	5.7	27.5	0.3	5.8	5.8	56
Xience	SV	3.0	5.0	4.0	4.1	13.6	0.4	4.2	4.2	48
	LV	4.0	6.0	5.6	5.6	26.1	1.3	5.6	5.5	67
Orsiro	SV	3.0	5.0	4.0	4.0	13.0	0.2	4.0	4.3	60
	LV	4.0	6.0	5.2	5.3	22.2	0.5	5.3	5.5	58
Ultimaster	SV	3.0	5.0	4.3	4.3	15.1	0.0	4.3	4.4	69
	LV	4.0	6.0	5.8	5.8	27.5	0.3	5.7	5.8	63
Resolute Onyx	SV	2.5	4.0	3.3	3.3	9.1	0.0	3.4	3.6	43
	MV	3.0	5.0	4.3	4.4	15.5	0.1	4.3	4.5	60
	LV	4.0	6.0	5.5	5.6	24.6	0.1	5.5	5.2	39
	XL	5.0	6.0	5.9	6.0	28.4	0.3	6.0	6.0	25
BioMatrixA/Chroma	SV	3.0	5.0	4.1	4.1	14.0	0.1	4.3	4.3	61
	LV	4.0	6.0	5.8	5.9	27.7	0.1	5.9	5.8	78

Table 3
Measured and derived cell opening and crown angle values and percentages: The percentage change in crown angle and cell opening varies based on the design used. Cell opening diameters at the segment of the stent transition from the nominal deployment to the over expanded segment showed the largest cell opening diameters and are noted down as the maximal transitional cell opening. The cell opening and crown angle values are obtained from the average of 6 measurements, 3 different locations per sample and 2 samples per stent design.

Stent	Model design	Largest stent size NP (mm)	Max expansion balloon (mm)	Crown angle (°)			Cell opening (mm)			
				NP	OE	% Increase	NP	OE	% Increase	Maximal transition OE
Synergy	SV	2.75	5.0	82	167	103	0.6	1.5	150	1.7
	WH	3.5	5.0	74	147	98	0.8	1.8	131	2.0
	LV	4.0	6.0	80	157	97	0.8	1.9	145	2.2
Xience	SV	3.0	5.0	79	156	97	1.1	1.6	48	1.8
	LV	4.0	6.0	74	154	108	0.9	1.7	83	1.9
Orsiro	SV	3.0	5.0	82	151	85	0.6	1.5	164	1.7
	LV	4.0	6.0	95	157	65	0.8	2.0	145	2.2
Ultimaster	SV	3.0	5.0	68	124	83	0.7	1.6	119	2.1
	LV	4.0	6.0	68	131	93	1.0	2.2	123	3.0
Resolute Onyx	SV	2.5	4.0	81	128	59	0.9	1.7	90	1.8
	MV	3.0	5.0	72	126	76	0.9	1.8	107	2.1
	LV	4.0	6.0	82	158	92	0.9	1.8	104	2.1
	XL	5.0	6.0	81	122	50	0.9	1.7	89	1.8
BioMatrixA/Chroma	SV	3.0	5.0	68	155	129	1.1	1.8	70	1.9
	LV	4.0	6.0	63	159	151	1.0	2.5	147	2.6

14. Radial strength

As stent crowns straighten, the resulting radial force of the stent is also expected to increase. Although not specifically looked at in this study, overexpansion also increases stent stiffness due to the straightening of the crown close to the stent physical limit (2,24). This may increase risk of strut fracture due to metal fatigue on the stent. Mechanical response and durability data on stents overexpanded close to maximal expansion capacity are still lacking and need to be evaluated further.

15. Limitations of study

- Measurements obtained from this study should be carefully interpreted as the stents were deployed *in vitro* without the presence of a constraining arterial wall to limit the expansion of the stent. Hence, the results obtain are only an approximation of the actual *in vivo* behaviour of the stent-artery response during overstretching (25). Also, the hoop force the balloon has to overcome to induce further stent deformation would be much higher *in vivo* due to the presence of stiff fibrotic plaque.
- In some design, increasing the diameter of the balloon used may further straighten the struts and further expand the stents. The largest maximal balloon diameter used in this study was 6.0 mm and the dilatation pressure was limited to the Rated Burst Pressure (14 ATM), equivalent to a maximal balloon diameter of 6.46 mm. The Inner MLD achieved on the stent large designs was inferior to this balloon size by at least 0.5 mm.
- Both the radial strength and drug kinetics of stents were not sufficiently investigated in this study. As such, the key information on the importance of stent oversizing alone does not allow for a complete assessment of which stent is preferable.

16. Conclusion

Knowledge of the cut-off diameters between different stent models has been previously shown to help in selecting the most suitable stent size and hence help in the treatment of large bifurcation and left main PCI. Careful selection of size according to contemporary DES model designs may help to avoid implanting stent sizes with too limited expansion capacity which could result in malapposition and severe overstretching of the stent.

Conflict of interest

The authors report no relationships that could be construed as a conflict of interest.

Acknowledgements

This study was independently initiated and conducted by the authors. No industry sponsor was received for the study and only the test samples were provided in kinds by the manufacturers for the experiments. The authors would like to thank the manufacturers for accepting to provide test samples for this study.

References

[1] R.L. Noad, C.G. Hanratty, S.J. Walsh, Clinical impact of stent design, Interv. Cardiol. Rev. 9 (2014) 89–93.
[2] N. Foin, S. Sen, E. Allegria, et al., Maximal expansion capacity with current DES platforms: a critical factor for stent selection in the treatment of left main bifurcations? EuroIntervention 8 (2013) 1315–1325.
[3] N. Foin, E. Alegria, S. Sen, et al., Importance of knowing stent design threshold diameters and post-dilatation capacities to optimise stent selection and prevent stent overexpansion/incomplete apposition during PCI, Int. J. Cardiol. 166 (2013) 755–758.
[4] J.F. Lassen, N.R. Holm, G. Stankovic, et al., Percutaneous coronary intervention for coronary bifurcation disease: consensus from the first 10 years of the European bifurcation Club meetings, EuroIntervention 10 (2014) 545–560.
[5] J. Dodge, B.G. Brown, E.L. Bolson, H.T. Dodge, Lumen diameter of normal human coronary arteries. Influence of age, sex, anatomic variation, and left ventricular hypertrophy or dilation, Circulation 86 (1992) 232–246.
[6] J.A. Shand, D. Sharma, C. Hanratty, et al., A prospective intravascular ultrasound investigation of the necessity for and efficacy of postdilation beyond nominal diameter of 3 current generation DES platforms for the percutaneous treatment of the left main coronary artery, Catheter. Cardiovasc. Interv. 84 (2014) 351–358.
[7] E. Romagnoli, G.M. Sangiorgi, J. Cosgrave, E. Guillet, A. Colombo, Drug-eluting stenting: the case for post-dilation, J. Am. Coll. Cardiol. Intv. 1 (2008) 22–31.
[8] S. Cook, P. Wenaweser, M. Togni, et al., Incomplete stent apposition and very late stent thrombosis after drug-eluting stent implantation, Circulation 115 (2007) 2426–2434.
[9] N.G. Uren, S.P. Schwarzacher, J.A. Metz, et al., Predictors and outcomes of stent thrombosis. An intravascular ultrasound registry, Eur. Heart J. 23 (2002) 124–132.
[10] K. Fujii, S.G. Carlier, G.S. Mintz, et al., Stent underexpansion and residual reference segment stenosis are related to stent thrombosis after sirolimus-eluting stent implantation. An intravascular ultrasound study, J. Am. Coll. Cardiol. 45 (2005) 995–998.
[11] N. Foin, R. Torii, P. Mortier, et al., Kissing balloon or sequential dilation of the side branch and main vessel for provisional stenting of bifurcations: lessons from micro-computed tomography and computational simulations, J. Am. Coll. Cardiol. Intv. 5 (2012) 47–56.
[12] Y. Murasato, G. Finet, N. Foin, Final kissing balloon inflation: the whole story, EuroIntervention 11 (Suppl V) (2015) (V81-5).

[13] N. Foin, G.G. Secco, L. Ghilencea, R. Krams, C. Di Mario, Final proximal post-dilatation is necessary after kissing balloon in bifurcation stenting, EuroIntervention 7 (2011) 597–604.
[14] P. Guérin, P. Pilet, G. Finet, et al., Drug-eluting stents in bifurcations/CLINICAL PERSPECTIVE, Circ. Cardiovasc. Interv. 3 (2010) 120–126.
[15] G. Finet, F. Derimay, P. Motreff, et al., Comparative analysis of sequential proximal optimizing technique versus kissing balloon inflation technique in provisional bifurcation stenting: fractal coronary bifurcation bench test, J. Am. Coll. Cardiol. Intv. 8 (2015) 1308–1317.
[16] J.P. Carrozza, S.E. Hosley, M.D. DJC, D.S. Baim, In vivo assessment of stent expansion and recoil in normal porcine coronary arteries : differential outcome by stent design, Circulation 100 (1999) 756–760.
[17] M.W.Z. Basalus, K.G. van Houwelingen, M.J.K. Ankone, J. Feijen, C. von Birgelen, Micro-computed tomographic assessment following extremely oversized partial postdilatation of drug-eluting stents, EuroIntervention 6 (2010) 141–148.
[18] D.H. Berrocal, G.E. Gonzalez, A. Fernandez, et al., Effects of overexpansion on stents' recoil, symmetry/asymmetry, and neointimal hyperplasia in aortas of hypercholesterolemic rabbits, Cardiovasc. Pathol. 17 (2008) 289–296.
[19] P. Barragan, R. Rieu, V. Garitey, et al., Elastic recoil of coronary stents: a comparative analysis, Catheter. Cardiovasc. Interv. 50 (2000) 112–119.
[20] J.A. Ormiston, B. Webber, M.W.I. Webster, Stent longitudinal integrity: bench insights into a clinical problem, J. Am. Coll. Cardiol. Intv. 4 (2011) 1310–1317.
[21] J.A. Ormiston, B. Webber, B. Ubod, J. White, M.W. Webster, Coronary stent durability and fracture: an independent bench comparison of six contemporary designs using a repetitive bend test, EuroIntervention 10 (2015) 1449–1455.
[22] Y. Otsuka, N.A. Chronos, R.P. Apkarian, K.A. Robinson, Scanning electron microscopic analysis of defects in polymer coatings of three commercially available stents: comparison of BiodivYsio, Taxus and Cypher stents, J. Invasive Cardiol. 19 (2007) 71–76.
[23] M. Joner, G. Nakazawa, A.V. Finn, et al., Endothelial cell recovery between comparator polymer-based drug-eluting stents, J. Am. Coll. Cardiol. 52 (2008) 333–342.
[24] N. Foin, R. Lee, A. Mattesini, et al., Bioabsorbable vascular scaffold overexpansion: insights from in vitro post-expansion experiments, EuroIntervention 11 (2016) 1389–1399.
[25] C.J. de Ribamar, G.S. Mintz, S.G. Carlier, et al., Intravascular ultrasonic assessment of stent diameters derived from manufacturer's compliance charts, Am. J. Cardiol. 96 (2005) 74–78.

12

CHAPTER

DEFINING OPTIMAL STENT OVEREXPANSION STRATEGIES FOR LEFT MAIN STENTING: INSIGHTS FROM BENCH TESTING

Jiang Ming Fam, Peter Mortier, Matthieu De Beule, Tim Dezutter, Nicolas van Mieghem, Roberto Diletti, Bert Everaert , Soo Teik Lim, Felix Zijlstra, Robert-Jan van Geuns.

AsiaIntervention 2017; 3: 111-120.

Defining optimal stent overexpansion strategies for left main stenting: insights from bench testing

Jiang Ming Fam[1,2*], MBBS; Peter Mortier[3,4], PhD; Matthieu De Beule[3,4], MS, PhD; Tim Dezutter[3,4], MS; Nicolas Van Mieghem[1], MD, PhD; Roberto Diletti[1], MD, PhD; Bert Everaert[1,5], MD, PhD; Soo Teik Lim[2], MBBS; Felix Zijlstra[1], MD, PhD; Robert-Jan van Geuns[1], MD, PhD

1. Thoraxcenter, Erasmus University Medical Center, Rotterdam, the Netherlands; 2. National Heart Centre Singapore, Singapore; 3. IBiTech-bioMMeda, iMinds Medical IT, Ghent University, Ghent, Belgium; 4. FEops, Ghent, Belgium; 5. AZ Monica Hospital, Antwerp, Belgium

This paper also includes supplementary data published online at: www.asiaintervention.org

KEYWORDS

- bifurcation
- drug-eluting stent
- left main

Abstract

Aims: Left main stenting frequently requires overexpansion of stents which can be performed by proximal optimisation technique (POT) or final kissing balloon dilation (FKBD). Yet, there are limited data concerning the effect of post-dilation of metallic stents beyond the overexpansion limit. The objectives of this study were to evaluate stent performance after overexpansion using POT or FKBD.

Methods and results: We deployed 4.00 mm drug-eluting platinum-chromium stents in silicone models of 6.00 mm diameter. We compared stent expansion and apposition using: 1) POT with 6.00 mm balloons using low, standard and high pressures (LP, SP and HP, respectively), and 2) final kissing balloon dilation (FKBD) using undersized (US) balloons at SP and optimally sized (OS) balloons at LP and SP. The platinum-chromium 4.00 mm stent can be expanded to an outer diameter of 5.10 mm by POT using a 6.00 mm balloon at LP. Further post-dilatation at higher pressures (SP, HP) resulted in an outer diameter of 6.00 mm. FKBD with US balloons resulted in a high ellipticity index and malapposition; with OS balloons, stent area improved but ellipticity and malapposition were still higher compared to POT. After overexpansion, the radial strength of metallic stents was maintained.

Conclusions: In PCI involving relatively larger vessel diameters such as left main stenting, POT but not FKBD can safely expand the platinum-chromium 4.00 mm stent beyond the overexpansion limit to 6.00 mm with optimal stent apposition and performance. POT may be the technique of first choice to achieve optimal stent expansion in left main stenting but requires higher pressures.

**Corresponding author: Department of Cardiology, National Heart Centre Singapore, 5 Hospital Drive, Singapore 169609, Singapore. E-mail: fam.jiang.ming@singhealth.com.sg*

Abbreviations

DES drug-eluting stent
EI ellipticity index
FKBD final kissing balloon dilation
FKBD-US final kissing balloon dilation undersized
FKBD-OS/LP final kissing balloon dilation - optimally sized low pressure
FKBD-OS-SP final kissing balloon dilation - optimally sized standard pressure
ID inner diameter
MA malapposition area
NC non-compliant
OD outer diameter
PCI percutaneous coronary intervention
POT proximal optimisation technique
POT-LP proximal optimisation technique low pressure
POT-SP proximal optimisation technique standard pressure
SAR surface to artery ratio
SC semi-compliant

Introduction

With improved percutaneous coronary intervention (PCI) techniques, PCI has emerged as a safe option for revascularisation in selected patients with unprotected left main coronary artery disease with good long-term outcomes[1,2]. However, left main PCI has remained a technically challenging procedure with several key considerations. The left coronary artery is of larger diameter, frequently above 5 mm. In an intravascular ultrasound (IVUS) study on the use of drug-eluting stents (DES) in left main PCI, the maximal diameter of the distal left main was 5.7±0.7 mm on average[3]. Left main stenting often involves bifurcation treatment and deployment of a single stent across vessels with marked disparity in diameters[4]. Thus, key procedural challenges to achieve adequate stent expansion while maintaining minimal malapposition still remain.

In left main stenting using current metallic stents, overexpansion using either proximal optimisation technique (POT) or final kissing balloon dilation (FKBD) is widely performed to minimise stent malapposition. The phenomenon of malapposition is of particular importance for two reasons: one is the acute risk during the procedure where subsequent vessel rewiring and balloon dilatations might engage the malapposed space immediately deforming stent integrity, and the second, in the longer term, is increasing the risk of stent thrombosis[5-7]. For bifurcation lesions, FKBD has traditionally been the method to reach maximal expansion[8,9]. However, clinically, this is limited by side branch diameters and will result in undesired elliptical deformation. POT is another commonly used bifurcation technique that was devised later by Darremont[10] to achieve overexpansion at the carina using short, larger balloons. Although earlier studies have been performed to evaluate the results of stent oversizing and the impact of post-dilation on strut geometry in bench testing situations[9,11-14], there is still a paucity of data concerning the feasibility of aggressive post-dilation of metallic stent platforms within large left main coronary phantoms performed by either FKBD or POT to achieve adequate expansion with optimal apposition[3] and concerning the impact on mechanical stent performance such as radial strength[4]. The objectives of this study were to compare expansion and apposition of stents overexpanded by POT and FKBD from the nominal diameter of 4.00 mm beyond the recommended expansion limit to 6.00 mm in a bench testing scenario and to investigate the mechanical stent performance of overexpanded stents.

Methods

In vivo bench testing of thin-strut (81 µm) platinum-chromium DES (SYNERGY™ II; Boston Scientific, Marlborough, MA, USA) was conducted. All experiments were performed in the Boston Scientific Research and Development Facility at Maple Grove, MN, USA, between July and September 2014. **Table 1** shows the models we used in our bench testing. In brief, we performed the following bench tests using the SYNERGY II drug-eluting stent (DES) in silicone phantom models with a diameter of 6.00 mm:

– To measure the effect of overexpansion on the stent performance of a 4.00 mm SYNERGY stent with 6.00 mm balloons

Table 1. Summary of post-dilation methods performed for the stent proximal ends.

			Stent deployment			First post-dilation			Second post-dilation		
Post-dilation method	Group number	Sample size	Stent	Size (mm)	Deployment pressure (atm)	Post-deployment balloon	Size (mm)	Pressure (atm)	Post-deployment balloon	Size (mm)	Pressure (atm)
POT-SC/LP	1	3	SYNERGY	4.0×28	16	Apex	5.0×15	9	Maverick XL	6.0×15	6
POT-SC/SP	2	10	SYNERGY	4.0×28	16	Apex	5.0×15	12	Maverick XL	6.0×15	14
POT-NC/HP	3	3	SYNERGY	4.0×28	16	NC Quantum	5.0×15	16	NC Emerge	6.0×15	24
FKBD-US/SP	4	3	SYNERGY	4.0×28	16	Apex	5.0×15	12	Apex	3.5×15+ 4.0×15	12
FKBD-OS/LP	5	3	SYNERGY	4.0×28	16	Apex	5.0×15	12	Apex	4.0×15+ 5.0×15	4
FKBD-OS/SP	6	3	SYNERGY	4.0×28	16	Apex	5.0×15	12	Apex	4.0×15+ 5.0×15	12

FKBD: final kissing balloon dilation; HP: high pressure; LP: low pressure; NC: non-compliant; OS: optimally sized; POT: proximal optimisation technique; SC: semi-compliant; SP: standard pressure; US: undersized

(semi-compliant [SC] Maverick™ XL or non-compliant [NC] Emerge™; both Boston Scientific) using:
- POT at low pressure (LP) of 6 atm (Group 1 POT-SC/LP),
- POT at standard pressure (SP) of 14 atm (Group 2 POT-SC/SP),
- POT at high pressure (HP) of 24 atm (Group 3 POT-NC/HP).

– To evaluate the effect of common clinical FKBD methods using:
- The relatively undersized (US), but commonly used, 3.50 mm and 4.00 mm (Apex™; Boston Scientific) balloons at standard pressure (SP) of 12 atm (Group 4 FKBD-US/SP)
- The optimally (according to Finet's law) sized (OS) 4.00 mm and 5.00 mm (Apex) balloons at LP of 4 atm (Group 5 FKBD-OS/LP) and at SP of 12 atm (Group 6 FKBD-OS/SP).

– To evaluate the effect of overexpansion on mechanical stent performance by overexpanding the stent beyond the overexpansion limit to 6.00 mm.

The 3.5 and 4.0 mm balloons were used for FKBD as this was the largest combination for kissing balloons used in the clinical setting of our hospital. The inflation pressures needed for full overexpansion of the balloons to the intended diameters were chosen.

Comparison of stent expansion and malapposition among the six models was achieved by measuring the dimensions and mechanical characteristics of the stents after overexpansion **(Table 1)**. Detailed information regarding the methodology is provided in the **Supplementary Appendix**. The malapposition area (MA/mm^2) of each stent was the difference of tube inner diameter (ID) area and stent outer diameter (OD) area. The ellipticity index (EI) is the ratio of maximum stent ID to minimum stent ID. The mechanical performance of the stents was evaluated at various sizes from 4.00 mm (baseline) to 6.00 mm (overexpansion as measured by average maximum compression resistance [hoop force/length: N/mm]). Mechanical characteristics evaluated included radial strength, stent length, elastic recoil and percentage surface to artery ratio (SAR). Forty stents (10 stents per group, at 4.00 mm, 5.00 mm, 5.75 mm and 6.00 mm) were used to collect the radial strength data since this is a destructive test. Stent length was also captured from these stents as it is an input factor in the radial strength calculation (force/length). The average length values from these groups were also used to calculate vessel area at each diameter in the SAR calculation. The recoil was measured sequentially from the same 10 stents deployed to 4 mm, then post-dilated to 5 mm, 5.75 mm and 6.00 mm.

STATISTICAL ANALYSIS

Descriptive statistical analysis was performed with continuous variables expressed as averages (standard deviation) and with categorical variables presented as counts (percentage). The ANOVA test was used for comparison between groups. All statistical tests were carried out at the 5% level of significance in SPSS, Version 21 (IBM Corp., Armonk, NY, USA).

Results

STENT OUTER DIAMETER AND STENT OUTER AREA

A total of 25 stents were subject to bench testing in the following models: POT-SC/LP (n=3), POT-SC/SP (n=10), POT-NC/HP (n=3), FKBD-US/SP (n=3), FKBD-OS/LP (n=3) and FKBD-OS/SP (n=3). Representative phantoms of the respective models post dilation are shown in **Figure 1**. Detailed results of the stent measurements in the various models are tabulated in **Table 2**. Additional data regarding stent measurements are shown in **Supplementary Table 1** in the **Supplementary Appendix**. Using the POT-SC/LP model, the 4.00 mm stent reached a maximum stent outer diameter of 5.10 mm using a 6.00 mm SC balloon at 6 atm. In POT-SC/SP and POT-NC/HP, further post-dilatation with higher pressures of 14 atm and 24 atm, respectively, resulted in the maximum stent outer diameter reaching 6.00 mm and 6.22 mm, respectively, with a stent outer area of 30.30 mm^2 and 28.60 mm^2 as the final result. These were the only models in which the stent outer area reached the target stent outer area of 28.30 mm^2 (based on a stent outer diameter of 6.00 mm). The POT-SC/SP model was repeated 10 times without any fractures on visual inspection, demonstrating a safety margin above the designated expansion limit, and with minimal malapposition in a 6.00 mm vessel. We achieved the highest stent outer diameters

Table 2. Actual stent measurements after overexpansion.

Group number	Post-dilation method	Sample size	Stent ID				Stent OD			Tube ID max			
			Stent ID max (mm)	Stent ID min (mm)	EI_{ID}	Stent ID area (mm^2)	Stent OD max (mm)	Stent OD min (mm)	Stent OD area (mm^2)	Tube ID max (mm)	Tube ID min (mm)	Tube ID area (mm^2)	Malapposed area (ID_{Tube}-OD_{Stent}) (mm^2)
1	POT-SC/LP	3	5.00	5.00	1.0	19.60	5.10	5.10	20.80	6.40	5.90	29.20	8.40
2	POT-SC/SP	10	5.90	5.90	1.0	27.20	6.00	6.00	28.60	6.20	6.20	29.70	1.10
3	POT-NC/HP	3	6.07	6.07	1.0	28.77	6.22	6.22	30.30	6.22	6.22	30.30	0
4	FKBD-US/SP	3	6.30	4.10	1.5	21.40	6.50	4.30	22.80	6.70	5.60	29.00	6.20
5	FKBD-OS/LP	3	5.50	4.60	1.2	19.70	5.70	4.80	20.90	6.50	5.80	29.10	8.20
6	FKBD-OS/SP	3	6.70	4.70	1.4	25.70	6.90	4.90	27.20	6.90	5.30	29.00	1.80

EI: ellipticity index; FKBD: final kissing balloon dilation; ID: inner diameter; HP: high pressure; LP: low pressure; NC: non-compliant; OD: outer diameter; OS: optimally sized; POT: proximal optimisation technique; SC: semi-compliant; SP: standard pressure; US: undersized

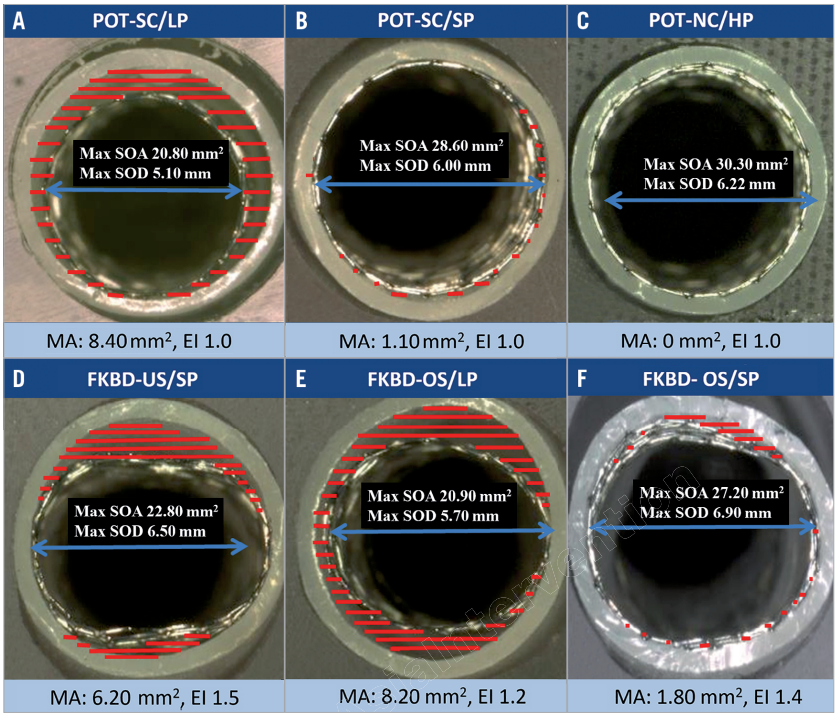

Figure 1. *Cross-sections of stents (proximal edge) post dilation in bench testing. A) & B) Cross-sections of the proximal edge of the stents after post-dilation by POT using 6.00 mm balloons (semi-compliant [SC] Maverick XL) at low pressure (LP) of 6 atm (POT-SC/LP) and standard pressure (SP) of 14 atm (POT-SC/SP), respectively. Optimal ellipticity index (EI) was seen in the POT models. C) The SYNERGY stent was post-dilated to 6 mm using the new NC Emerge 6 mm balloon at very high pressures of 24 atm (POT-NC/HP). D) - F) Cross-sections of the proximal edge of the stents after post-dilation by FKBD using Apex balloons: i) the relatively undersized (US), but commonly used, 3.50 mm and 4.00 mm balloons at standard pressure (SP) of 12 atm (Panel D - FKBD-US/SP), ii) optimally sized (OS) 4.00 mm and 5.00 mm balloons at LP of 4 atm (Panel E - FKBD-OS/LP), and iii) at SP of 12 atm (Panel F - FKBD-OS/SP), correspondingly. FKBD resulted in an elliptical shape of the proximal edge of the stents. Higher pressures will result in larger diameters and stent areas but also in increased ovalisation and malapposition. FKBD: final kissing balloon dilation; LP: low pressure; MA: malapposed area; POT: proximal optimisation technique; RBP: rated burst pressure; SOD: stent outer diameter; US: undersized*

of 6.90 mm in the FKBD-OS/SP model. However, the stent outer area of 27.20 mm² in FKBD-OS/SP was still significantly lower compared to that of POT-SC/SP and POT-NC/HP. **Figure 2A** and **Figure 2B** show the significant differences in the stent outer diameters and stent outer areas following expansion among the six models. We further investigated the relation of stent diameters to pressures as they are gradually overexpanded by 6.00 mm balloons, showing that the largest outer stent diameter is possible with an NC balloon **(Figure 3)**.

ELLIPTICITY INDEX (EI)

Among the five models, we found that POT-SC/SP and POT-NC/HP resulted in the most optimal EI. With POT, the EI was 1.0 whereas all FKBD models resulted in elliptical stents (with the EI ranging from 1.2 to 1.5) with significant potential for malapposition, in particular with the use of US balloons. Under the FKBD-US/SP model where balloon diameters are frequently used in the clinical setting, the 3.50 mm and 4.00 mm balloons resulted in the highest EI of 1.5. **Figure 2C** shows the significant differences in EI among the different models.

MALAPPOSED AREA (MA)

Among the five models, the POT-NC/HP resulted in the least amount of MA **(Table 2, Figure 2D)**. Of note, among the POT models, the POT-LP model also exhibited a high MA (8.40 mm²) which only improved with higher pressures employed in the

POT-SC/SP or NC/HP models. Importantly, with FKBD, MA was higher in the FKBD- US/SP, OS/LP and OS/SP models (MA was 6.20, 8.20 and 1.80 mm^2, respectively).

STENT MECHANICAL PERFORMANCE AT OVEREXPANSION LIMITS

Figure 4 shows the impact of overexpansion on stent mechanical performance. Additional data regarding stent performance measurements are shown in **Supplementary Table 2** in the **Supplementary Appendix**. The radial strength of the stent was similar among the control, 5.00 mm and 5.75 mm groups; however, it significantly increased at 6.00 mm diameter (0.26±0.01; 0.27±0.02; 0.28±0.04; 0.38±0.04 N/mm, respectively, p<0.001). Stent recoil significantly decreased from 2.9% to 1.4% at larger sized diameters (p<0.01). There was a significant change in measured average stent length from 16.1±0.2 mm at 4.0 mm to 17.5±0.5 mm and 16.8±0.6 mm at 5.0 and 5.75 mm, respectively (p<0.01). Percentage stent surface to artery ratio calculated on the manufacturer-provided data decreased from 14.2% at 4.0 mm to 9.4% at 6.00 mm **(Supplementary Table 3)**.

Discussion

In this study, we investigated whether a 4.00 mm SYNERGY stent could be overexpanded beyond the recommended expansion limit to 6.00 mm. We subsequently compared different expansion techniques to achieve optimal stent apposition in a 6.00 mm phantom model. In addition, we evaluated the impact of overexpansion on the mechanical characteristics of the stent.

The main findings were that:

– The 4.00 mm thin-strut platinum-chromium stent can be expanded to a 6.00 mm outer stent diameter using high-pressure SC and NC coronary balloons. Of note, if low pressures were used, a maximal stent diameter of only 5.10 mm could be obtained using correctly sized balloons in the POT-SC/LP model.
– POT-SC/SP and POT-NC/HP resulted in more optimal EI and minimal MA while achieving adequate overexpansion compared to FKBD.
– FKBD also requires high-pressure inflation to achieve significant overexpansion, resulting in stent eccentricity and focal malapposition.
– Radial strength was still maintained despite stent overexpansion. Stent recoil and % surface to artery ratio decreased as stents were overexpanded.

Studies have shown that clinical outcomes after PCI are linked to the ability of metallic stents to reach adequate stent expansion and maintain elastic recoil, without compromising on radial strength, thereby achieving a large final lumen. Incomplete stent expansion is considered a predictor of stent thrombosis, and high-pressure post-dilation has generally been recommended to avoid incomplete stent apposition and to reduce the risk of adverse outcomes[16]. A consensus statement from the European Bifurcation Club recommended the use of POT to restore stent geometry and

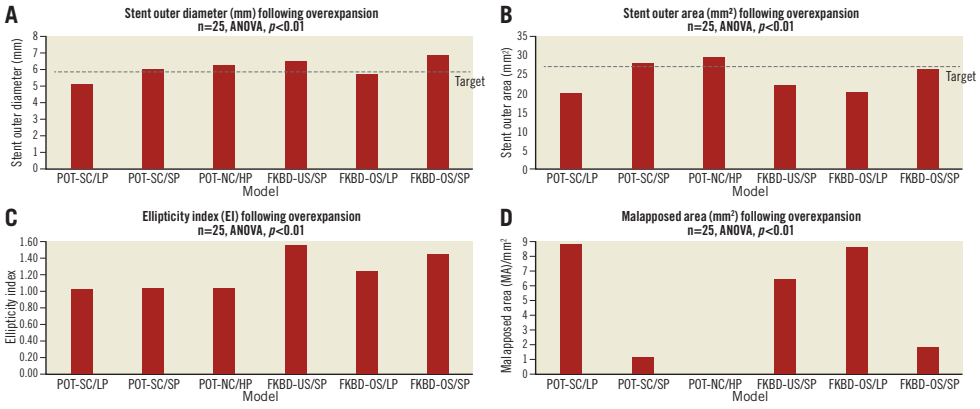

Figure 2. *Comparison of stent measurements among the models. A) Stent outer diameter (mm) following overexpansion. Stent outer diameter could reach a target of 6.0 mm in three of the six models as shown. B) Stent outer area (mm^2) following overexpansion. The stent outer area could reach the target of 28.3 mm^2 in only the POT-SC/SP and NC/HP models. The target area is based on a 6.0 mm circular stent diameter. C) Ellipticity index following overexpansion. An ideal ellipticity index of 1.0 was achieved in the POT models but not in the FKBD models. D) Malapposed area (mm^2) following overexpansion. Among the models tested, POT-NC/HP resulted in the least amount of MA. The POT-SC/LP model also exhibited a high MA (8.40 mm^2) which only improved with higher pressures employed in the POT-SC/SP and POT-NC/HP models. FKBD: final kissing balloon dilation; HP: high pressure; LP: low pressure; NC: non-compliant; OS: optimally sized; POT: proximal optimisation technique; SC: semi-compliant; SP: standard pressure; US: undersized*

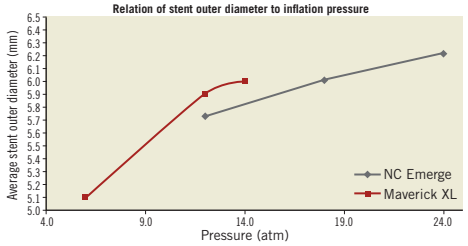

Figure 3. *The relation of the change in stent diameters to pressure used for stent expansion using 6.00 mm balloons (SC Maverick and NC Emerge). Very high pressures were required to overexpand the stents at 5.5 to 6.0 mm diameters. The preserved radial strength of the SYNERGY allows it to be post-dilated with a 6 mm balloon to RBP without fractures. Note: Maverick XL RBP=14 atm; NC Emerge RBP=18 atm.*

minimise malapposition in large vessels and proximal to the carina in bifurcation lesions[10]. It is especially useful in the presence of large side branches as it allows the operator to match the proximal segment of the main branch stent with the main branch diameter by means of a short balloon adapted to the proximal segment. This study added information on the high pressures needed to reach maximum overexpansion typically necessary in left main PCI. However, such adequately sized balloons may not always be available and FKBD is still frequently the final step in left main PCI.

Numerous studies have documented that more complete stent expansion is associated with a reduction in late restenosis[17]. The MUSIC trial showed how the use of intravascular ultrasound (IVUS) criteria (such as the EI) may improve acute and six-month clinical and angiographic outcomes[18]. In a study by Kang et al[19], the minimal stent area was an important factor in predicting angiographic restenosis. This was found to be 5.0 mm^2 for the left circumflex artery ostium, 6.3 mm^2 for the left anterior descending artery ostium, 7.2 mm^2 for the polygon of confluence, and 8.2 mm^2 for the proximal left main above the polygon of confluence.

The recommended stent overexpansion is generally between 0.5 mm and 0.75 mm above the largest nominal diameter. Previous studies have reported results of DES overexpansion experiments in bench testing[20] and with the use of computer modelling[21]. In an earlier study by Basalus et al, bench testing on the impact of large partial post-dilation for overexpanded DES on micro-CT assessment showed differences in strut dimensions which varied in relation to position and type of stent platform tested[11]. However, to the best of

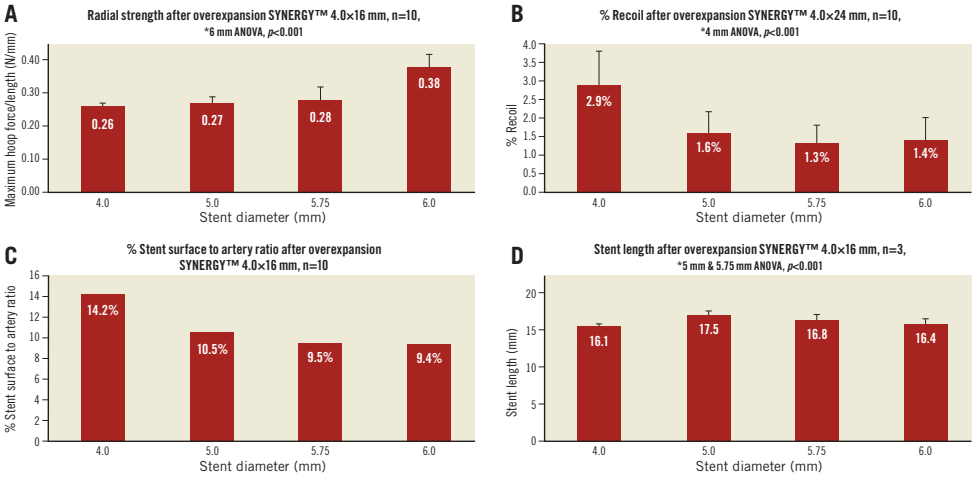

Figure 4. *Impact of overexpansion on stent mechanical performance. A) Radial strength is still maintained even at the overexpansion limit. Radial strength was not affected in overexpanded stents. There were no significant differences in the radial strength; it actually showed an increasing trend as measured by average maximum compression resistance (hoop force/length: N/mm) among the 4.00 mm, 5.00 mm, 5.75 mm and 6.00 mm groups (p=0.20). B) Stent recoil shows a decreasing trend when the stent reaches the overexpansion limit. Stent recoil was significantly decreased as the stent size increased (p<0.01). C) Percentage surface to artery ratio change in relation to stent diameter. Percentage stent surface to artery ratio (calculated as a ratio of stent outer surface area and outer vessel area multiplied by 100) decreases as the diameter of the stent increases from 4.00 mm to 6.00 mm. D) Stent length changes as the stent approaches the overexpansion limit. There was a significant change in measured average stent length when the stents were expanded from a diameter of 4.00 mm to 6.00 mm (p<0.01). Detailed measurements are provided in online Supplementary Table 2.*

our knowledge, neither has a comparison of the different post-dilation strategies such as POT and kissing balloon dilation been carried out nor has the mechanical response of overexpanded stents been evaluated. In our bench test model, the FKBD technique resulted in more elliptical stent geometry with higher malapposition compared with POT, regardless of the size of balloon or pressures used.

In a clinical study conducted by Shand et al[3], the use of DES in left main stenting was evaluated with IVUS. The BioMatrix Flex™ (Biosensors, Bülach, Switzerland) (3.5 and 4.0 mm stents), PROMUS Element™ (Boston Scientific) (3.5 and 4.0 mm stents) as well as the Resolute Integrity® (Medtronic, Minneapolis, MN, USA) (3.5 mm stent) were implanted followed by post-dilation with 5.5 or 6.0 mm balloons. In a subgroup of 31 patients who had undergone left main PCI with post-stent IVUS images available for analysis, the mean maximal stent area (at the proximal left main) and mean maximal stent diameter achieved were 19.7±3.7 mm^2 and 5.5 (4.7-6.4) mm for the BioMatrix Flex 4.0 mm stent and 20.6±2.8 mm^2 and 5.3 (4.3-6.3) mm for the PROMUS Element 4.0 mm stent. The results appear comparable with the stent measurements achieved in our study. Our study showed that overexpansion of a 4.0 mm metallic stent platform can be achieved beyond the recommended overexpansion limit with minimal malapposition and optimal ellipticity, which holds potential for favourable clinical outcomes. We believe that our study set-up represented a frequent clinical situation where the diameter of the left main artery is larger than that of clinically available (and approved) stents. Most coronary stents are only available up to 4 mm, whereas previous IVUS studies[3] showed that the diameter of most left main arteries ranges from 5-6 mm in diameter. For these vessels, the risk of coronary artery rupture will be minimal. The use of IVUS in left main stenting as recommended in European guidelines[1] will also confer additional safety against adverse procedural outcomes such as coronary artery rupture by providing additional information about the vessel dimensions. This, however, should be further studied in clinical trials using intravascular imaging. This would be particularly relevant if we were to evaluate the suitability of current-generation DES for the treatment of left main stenosis in which vessel diameters routinely extend beyond 5.00 mm.

In the present study, stent diameters were measured directly rather than calculated from geometric assumptions and different imaging modalities. In the silicone phantoms used in our study, the stent diameters were significantly smaller than the diameters indicated on the manufacturers' compliance charts of the post-dilatation balloons **(Supplementary Table 4)**. This illustrates the serious constrainment of overexpanded metallic stents on the post-dilatation balloons. This may be of clinical significance since the inability of the stent balloon to reach its target size during deployment of the stent and subsequent elastic recoil are two important contributory factors towards stent underdeployment[22]. The findings support the recommendation that adequately sized balloons and pressures are necessary to facilitate adequate expansion.

The results of the mechanical performance of overexpanded stents as the stent diameter increases in size from 4.00 mm to 6.00 mm provide interesting insights. The effect on the mechanical response in overexpanded stents is still unknown and may be difficult to predict[5]. It has been shown previously that extremely oversized post-dilation, for example caused by kissing post-dilation, considerably modifies the strut configuration[11]. There are concerns that distortion of the stent crowns may occur with stent overexpansion with several potential risks – a change in the mechanical response of the stent, a decrease in the stent resistance to fatigue, and damage to polymer coating[9]. The graphical data in **Figure 4A** suggest that, despite overexpansion, the radial strength would not be affected, as the stent size increased after overexpansion and in fact increases when the diameter reaches 6.00 mm.

This is potentially advantageous, as radial strength is a key component towards eliminating acute elastic recoil post stenting. The higher radial strength may be attributed to a change in the geometrical arrangement of the stent struts. The struts exhibit a "column-like" effect as the circumferential struts straighten out and lose their curved interlinked architecture, resulting in an increased resistance to radial forces. Such a finding was demonstrated in a crown deformation analysis of the stent struts after post-dilation by Foin et al[4]. At 6 mm, the stent segments would have been stretched outwards to their limits and nearly straightened out. This extreme state may contribute to an increase in radial strength. Another explanation for the increase in radial strength can be attributed to the decrease in stent length as stents approach their expansion limit. The radial strength values are normalised to stent length (N/mm) so stent length impacts on these values.

There was a decrease in the stent recoil as the stent expanded from 4.00 mm towards 6.00 mm. This finding may be expected, as mechanically the more "column-like" structure of the struts at larger sizes is less likely to recoil than a "spring-like" shape of a "v" at smaller sizes. Stent length change can be unpredictable, as it is a complex function that is dependent on many variables such as the method of deployment, type of balloon used, manner of dilation and final stent diameter.

To our knowledge, this is the first time that bench testing has compared the two post-dilation strategies in an overexpansion model and evaluated the mechanical performance of DES overexpansion. In addition, we have performed advanced finite element computer simulations of the complete stenting procedures. These simulations were based on predetermined pressures and diameters of balloons and stents used in a virtual stent model for every step during the deployment sequence and with assessment of the final stent outcomes **(Figure 5A)**. The results confirmed the experimental findings and provided insights during the balloon inflation during FKBD and additional information on the resulting forces exerted on the stent by the vascular wall. In summary, these simulations revealed that the use of POT results in a highly uniform distribution of these contactile forces in contrast to the FKBD **(Figure 5B, Figure 5C)**.

Limitations

The limitations of our study are inherent to bench testing. Firstly, our data refer to *in vitro* stent deployments performed in standard

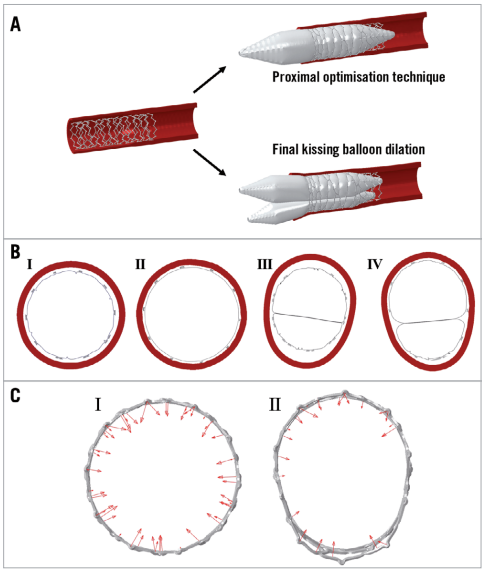

Figure 5. *Computer simulations of the stenting procedures. A) Different models used for overexpansion. This figure illustrates the two types of overexpansion strategy, namely the proximal optimisation technique (POT) and final kissing balloon dilation (FKBD), studied in both the bench testing and modelling process. B) Cross-section of stents (proximal edge) post dilation in virtual testing. Left to right: I) POT-SC/LP with some malapposition, II) POT-SC/SP with full apposition, III) FKBD-OS/LP with ellipticity and some malapposition, IV) FKBD-OS/SP with ellipticity and some malapposition. FKBD: final kissing balloon dilation; LP: low pressure; OS: optimally sized; POT: proximal optimisation technique; SC: semi-compliant; SP: standard pressure C) Distribution of contactile forces on stents after virtual implantation. The cross-section of a computer simulation post POT (I). The arrows indicate the uniform distribution of the contact forces seen during the computer modelling. The right image (II) shows the cross-section of a computer simulation post FKBD. The arrows indicate a non-uniform distribution of the contact forces seen during the computer modelling.*

laboratory environments in silicone phantom models. *In vivo* behaviour and stent artery response during stent deployment of different sizes in diseased arterial walls constraining the stents in a real-world clinical setting may be different. Other vascular characteristics including vascular wall stiffness, calcification, plaque characteristics and distortion, as well as more complex procedures involving bifurcation and overlapping stents, may affect the resultant expansion of stents deployed in a real-world setting. Secondly, assessment of the side branch in the bifurcation lesion was not available. This is because the effect of kissing balloon dilation in improving blood flow to the side branch during bifurcation stenting has been previously studied[8,21,23,24]. However, in left main stenting, the effect of POT for overexpansion has not been widely studied as it is not routinely carried out, since most operators would consider kissing balloon dilation adequate to achieve optimal stent apposition in the main branch. The main aim of this study was to evaluate the impact of different approaches, namely POT and FKBD, in achieving full apposition in large left main vessels and to compare the impact of POT and FKBD on the main vessel. This is especially important as the left main diameter is generally underestimated and the maximum overexpansion diameters of the stents commonly used in the catheterisation laboratory are unknown to operators. Thirdly, our sample size is relatively small. One stent design and size was tested and no claim on overexpansion of other sizes and designs can be made. Further studies are indicated to perform similar investigations for other stent designs and diameters and to assess long-term structural integrity. Lastly, we have studied POT as a separate entity from FKBD though in reality POT is also frequently performed with FKBD. In our bench testing scenario, while we assume that single use of POT is equivalent to the use of POT with intermediate FKBD, the results still support the recommendation that POT should be the final step regardless of whether FKBD is performed in cases of stent overexpansion.

Conclusions

In conclusion, our study shows that POT but not FKBD can expand the platinum-chromium 4.00 mm stent beyond the overexpansion limit of 5.75 mm with optimal stent apposition and performance in bench testing. In PCI involving relatively larger vessel diameters, such as left main stenting, POT may be the technique of first choice to achieve optimal stent expansion but requires adequately sized balloons with high pressures. The impact on the mechanical performance of the stents after overexpansion would merit further evaluation.

Impact on daily practice

For left main percutaneous coronary intervention (PCI) which is sometimes up to 6 mm in diameter, full pressure (16 atm) large size non-compliant balloons are necessary during the proximal optimisation technique (POT) to achieve a predicted stent diameter of 6 mm and avoid malapposition seen in different final kissing balloon post-dilatation approaches. Platinium-chromium stents maintain their mechanical characteristics at these diameters.

Funding

This research was supported by a research grant from Boston Scientific.

Conflict of interest statement

R.J. van Geuns has received speakers fees from Boston Scientific. The other authors have no conflicts of interest to declare.

References

1. Authors/Task Force members, Windecker S, Kolh P, Alfonso F, Collet JP, Cremer J, Falk V, Filippatos G, Hamm C, Head SJ, Jüni P, Kappetein AP, Kastrati A, Knuuti J, Landmesser U, Laufer G, Neumann FJ, Richter DJ, Schauerte P, Sousa Uva M, Stefanini GG, Taggart DP, Torracca L, Valgimigli M, Wijns W, Witkowski A. 2014 ESC/EACTS Guidelines on myocardial revascularization: The Task Force on Myocardial Revascularization of the European Society of Cardiology (ESC) and the European Association for Cardio-Thoracic Surgery (EACTS)Developed with the special contribution of the European Association of Percutaneous Cardiovascular Interventions (EAPCI). *Eur Heart J.* 2014;35:2541-619.

2. Teirstein PS, Price MJ. Left main percutaneous coronary intervention. *J Am Coll Cardiol.* 2012;60:1605-13.

3. Shand JA, Sharma D, Hanratty C, McClelland A, Menown IB, Spence MS, Richardson G, Herity NA, Walsh SJ. A prospective intravascular ultrasound investigation of the necessity for and efficacy of postdilation beyond nominal diameter of 3 current generation DES platforms for the percutaneous treatment of the left main coronary artery. *Catheter Cardiovasc Interv.* 2014;84:351-8.

4. Foin N, Sen S, Allegria E, Petraco R, Nijjer S, Francis DP, Di Mario C, Davies JE. Maximal expansion capacity with current DES platforms: a critical factor for stent selection in the treatment of left main bifurcations? *EuroIntervention.* 2013;8:1315-25.

5. Cook S, Wenaweser P, Togni M, Billinger M, Morger C, Seiler C, Vogel R, Hess O, Meier B, Windecker S. Incomplete stent apposition and very late stent thrombosis after drug-eluting stent implantation. *Circulation.* 2007;115:2426-34.

6. Alfonso F, Suárez A, Angiolillo DJ, Sabaté M, Escaned J, Moreno R, Hernández R, Bañuelos C, Macaya C. Findings of intravascular ultrasound during acute stent thrombosis. *Heart.* 2004; 90:1455-9.

7. Cheneau E, Leborgne L, Mintz GS, Kotani J, Pichard AD, Satler LF, Canos D, Castagna M, Weissman NJ, Waksman R. Predictors of subacute stent thrombosis: results of a systematic intravascular ultrasound study. *Circulation.* 2003;108:43-7.

8. Murasato Y, Iwasaki K, Yamamoto T, Yagi T, Hikichi Y, Suematsu Y, Yamamoto T. Optimal kissing balloon inflation after single-stent deployment in a coronary bifurcation model. *EuroIntervention.* 2014;10:934-41.

9. Guérin P, Pilet P, Finet G, Gouëffic Y, N'Guyen JM, Crochet D, Tijou I, Pacaud P, Loirand G. Drug-eluting stents in bifurcations: bench study of strut deformation and coating lesions. *Circ Cardiovasc Interv.* 2010;3:120-6.

10. Hildick-Smith D, Lassen JF, Albiero R, Lefevre T, Darremont O, Pan M, Ferenc M, Stankovic G, Louvard Y; European Bifurcation Club. Consensus from the 5th European Bifurcation Club meeting. *EuroIntervention.* 2010;6:34-8.

11. Basalus MW, van Houwelingen KG, Ankone MJ, Feijen J, von Birgelen C. Micro-computed tomographic assessment following extremely oversized partial postdilatation of drug-eluting stents. *EuroIntervention.* 2010;6:141-8.

12. Foin N, Secco GG, Ghilencea L, Krams R, Di Mario C. Final proximal post-dilatation is necessary after kissing balloon in bifurcation stenting. *EuroIntervention.* 2011;7:597-604.

13. Ormiston JA, Webster MW, El Jack S, Ruygrok PN, Stewart JT, Scott D, Currie E, Panther MJ, Shaw B, O'Shaughnessy B. Drug-eluting stents for coronary bifurcations: bench testing of provisional side-branch strategies. *Catheter Cardiovasc Interv.* 2006;67:49-55.

14. Mortier P, Van Loo D, De Beule M, Segers P, Taeymans Y, Verdonck P, Verhegghe B. Comparison of drug-eluting stent cell size using micro-CT: important data for bifurcation stent selection. *EuroIntervention.* 2008;4:391-6.

15. Ormiston JA, Webster MW, Ruygrok PN, Stewart JT, White HD, Scott DS. Stent deformation following simulated side-branch dilatation: a comparison of five stent designs. *Catheter Cardiovasc Interv.* 1999;47:258-64.

16. Romagnoli E, Sangiorgi GM, Cosgrave J, Guillet E, Colombo A. Drug-eluting stenting: the case for post-dilation. *JACC Cardiovasc Interv.* 2008;1:22-31.

17. Serruys PW, de Jaegere P, Kiemeneij F, Macaya C, Rutsch W, Heyndrickx G, Emanuelsson H, Marco J, Legrand V, Materne P, et al. A comparison of balloon-expandable-stent implantation with balloon angioplasty in patients with coronary artery disease. Benestent Study Group. *N Engl J Med.* 1994;331:489-95.

18. de Jaegere P, Mudra H, Figulla H, Almagor Y, Doucet S, Penn I, Colombo A, Hamm C, Bartorelli A, Rothman M, Nobuyoshi M, Yamaguchi T, Voudris V, DiMario C, Makovski S, Hausmann D, Rowe S, Rabinovich S, Sunamura M, van Es GA. Intravascular ultrasound-guided optimized stent deployment. Immediate and 6 months clinical and angiographic results from the Multicenter Ultrasound Stenting in Coronaries Study (MUSIC Study). *Eur Heart J.* 1998;19:1214-23.

19. Kang SJ, Ahn JM, Song H, Kim WJ, Lee JY, Park DW, Yun SC, Lee SW, Kim YH, Lee CW, Mintz GS, Park SW, Park SJ. Comprehensive intravascular ultrasound assessment of stent area and its impact on restenosis and adverse cardiac events in 403 patients with unprotected left main disease. *Circ Cardiovasc Interv.* 2011;4:562-9.

20. Foin N, Torii R, Mortier P, De Beule M, Viceconte N, Chan PH, Davies JE, Xu XY, Krams R, Di Mario C. Kissing balloon or sequential dilation of the side branch and main vessel for provisional stenting of bifurcations: lessons from micro-computed tomography and computational simulations. *JACC Cardiovasc Interv.* 2012;5:47-56.

21. Mortier P, Hikichi Y, Foin N, De Santis G, Segers P, Verhegghe B, De Beule M. Provisional stenting of coronary bifurcations: insights into final kissing balloon post-dilation and stent design by computational modeling. *JACC Cardiovasc Interv.* 2014;7:325-33.

22. Bermejo J, Botas J, García E, Elízaga J, Osende J, Soriano J, Abeytua M, Delcán JL. Mechanisms of residual lumen stenosis after high-pressure stent implantation: a quantitative coronary angiography and intravascular ultrasound study. *Circulation.* 1998;98:112-8.

23. Gao Z, Xu B, Yang YJ, Qiao SB, Wu YJ, Chen T, Xu L, Yuan JQ, Chen J, Qin XW, Yao M, Liu HB, You SJ, Zhao YL, Yan HB, Chen JL, Gao RL. Effect of final kissing balloon dilatation after one-stent technique at left-main bifurcation: a single center data. *Chin Med J (Engl)*. 2015;128:733-9.

24. Peighambari M, Sanati H, Hadjikarimi M, Zahedmehr A, Shakerian F, Firouzi A, Kiani R, Sadeghipour P, Kzaemi Asl S. The Effects of Side Branch Predilation During Provisional Stenting of Coronary Bifurcation Lesions: A Double-Blind Randomized Controlled Trial. *Res Cardiovasc Med.* 2016;5:e31378.

25. Instructions For Use Guide for Synergy II Stent (Boston Scientific, MN, USA). https://www.bostonscientific.com/content/dam/Manuals/us/current-rev-en/50417779-01A_Synergy_eDFU_en-US_s.pdf

26. Finet G, Gilard M, Perrenot B, Rioufol G, Motreff P, Gavit L, Prost R. Fractal geometry of coronary bifurcations: a quantitative coronary angiography and intravascular ultrasound analysis. *EuroIntervention.* 2008;3:490-8.

27. Yoshihiro M, Yamamoto H, Mitsudo K, Nagaoka M, Takeuchi H, Okamoto N, Kozuma K, Matsuzaki A, Tanabe K, Hara K, Tanabe T, Ikari Y. Functional formula to determine adequate balloon diameter of simultaneous kissing balloon technique for treatment of bifurcated coronary lesions: clinical validation by volumetric intravascular ultrasound analysis. *Circ J.* 2008;72:886-92.

Supplementary data

Supplementary Appendix. Methodology.

Supplementary Table 1. Stent measurements groups 1-6.

Supplementary Table 2. Stent performance measurements.

Supplementary Table 3. Stent performance at overexpansion limits - surface to artery ratio.

Supplementary Table 4. Compliance table of stents/balloons used.

Supplementary Figure 1. Illustration of the bench testing methods performed.

The supplementary data are published online at: www.asiaintervention.org

Supplementary data

Supplementary Appendix. Methodology

The 4.00 mm SYNERGY II stent was used in this study. The SYNERGY II 4.00 mm stent was used based on its unique large vessel design with an increased number of cells and peaks. This results in a labelled post-dilation limit of 5.75 mm which is within the range of most diameters of the left main coronary artery [25]. For FKBD, the 4.00 mm and 5.00 mm balloons were used to achieve a final diameter of 6.00 mm in accordance to Finet's law which states that the diameter of the main branch is related to the two distal branches: diameter of main branch=2/3 (diameter of main distal branch+diameter of side branch) [26]. However, these balloon sizes are not frequently employed; therefore, we also included a model using FKBD with more usual (but undersized) balloon sizes (3.50 and 4.00 mm). FKBD has been studied in the expansion of large calibre proximal vessels without overdilating smaller vessels distal to the bifurcation site [27].

All stents were deployed in an aqueous bath at standard temperature of 37+/-1 degrees Celsius. Stent strut apposition and expansion were evaluated by implanting the stents in silicone tube phantom models. The phantoms had elastic properties that allowed stretching of the material beyond the nominal diameter. Each stent was distally fixated in a 5.00 mm silicone tube. Both the stent and 5.00 mm silicone tube are housed in an outer 6.00 mm silicone tube to accommodate expansion of the proximal stents. Each stent was first deployed using the stent delivery system catheter at rated burst pressure (16 atm) **(Supplementary Figure 1A)**. The distal and proximal stent was then post-dilated in a sequential manner using the semi-compliant (SC) Apex 5.00 mm

balloon at rated burst pressure of 12 atm **(Supplementary Figure 1B, Supplementary Figure 1C)**. Finally, different approaches were used for proximal post-dilation in a 6.00 mm tube **(Supplementary Figure 1D, Supplementary Figure 1E)**.

Supplementary Figure 1. Illustration of the bench testing methods performed.

A) Initial deployment of the stents. The SYNERGY 4.0x28 mm stents were first deployed using the stent delivery system catheter at rated burst pressure (16 atm). Each stent was distally fixated in a 5.00 mm silicone tube. Both the stent and 5.00 mm silicone tube are housed in an outer 6.00 mm silicone tube to accommodate expansion of the proximal stents.

B) Post-dilation of distal end of SYNERGY II stent.

The distal end of the stent was post-dilated with an Apex 5.0x15 mm semi-compliant balloon at rated burst pressure (12 atm) to ensure that the stent was well apposed to the 5 mm tubing. During the post-dilation of the distal end, the proximal end was not in contact with the tubing.

C) Post-dilation of proximal end of SYNERGY II stent.

The proximal end of the stent was post-dilated such that the proximal end of the stent was aligned with the proximal end of the 6 mm tube. An Apex 5.0x15 mm semi-compliant balloon at rated burst pressure of 12 atm was used.

D) Proximal optimisation technique (POT).

POT using the 6.0x15 mm Maverick XL or NC Emerge at rated burst pressure of 14 atm was one of the post-dilation methods used.

E) Final kissing balloon dilation (FBKD).

Final kissing balloon dilation with 5.0x15 mm and 4.0x15 mm balloons (low pressure [LP] of 4 atm and standard pressure [SP] of 12 atm were used separately). A combination of 4.0x15 mm and 3.5x15 mm balloons was also used in an “undersized” model.

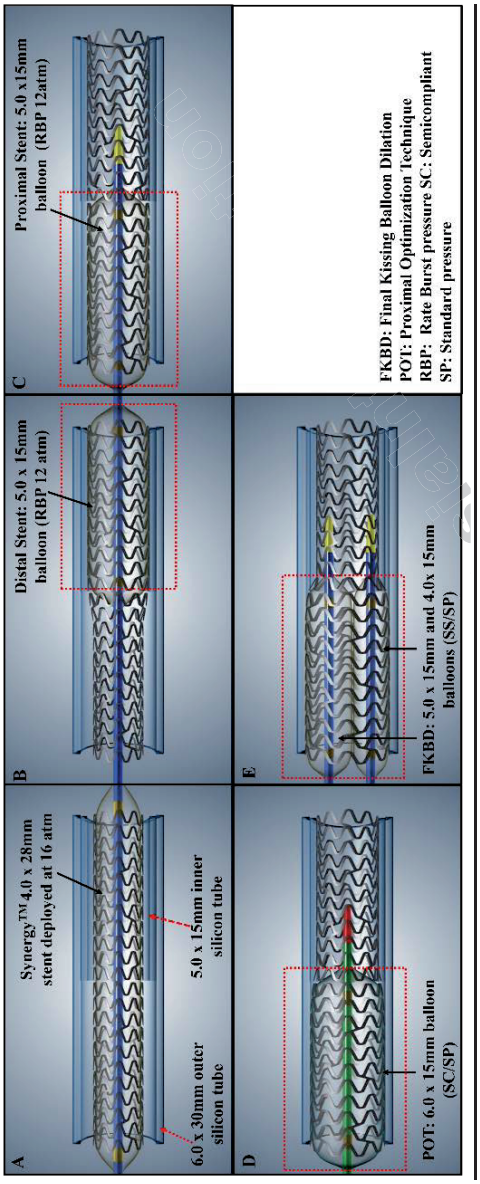
A
Synergy™ 4.0 x 28mm stent deployed at 16 atm
6.0 x 30mm outer silicon tube
5.0 x 15mm inner silicon tube
B
Distal Stent: 5.0 x 15mm balloon (RBP 12 atm)
C
Proximal Stent: 5.0 x15mm balloon (RBP 12atm)
D
POT: 6.0 x 15mm balloon (SC/SP)
E
FKBD: 5.0 x 15mm and 4.0x 15mm balloons (SS/SP)
FKBD: Final Kissing Balloon Dilation
POT: Proximal Optimization Technique
RBP: Rate Burst pressure SC: Semicompliant
SP: Standard pressure

Stent measurements

A precalibrated Keyence VHX 100 Measurement Scope (Keyence Corporation, Osaka, Japan) was used to obtain the following stent measurements at the proximal stent end after final dilation: 1) stent inner diameter (ID) and outer diameter (OD) with maximum and minimum values for oval stents, 2) stent inner and outer area (calculated based on the dimensions of the stent ID, stent OD, 3) tube inner diameter and area with corresponding maximum and minimum values for oval stents, 4) malapposition area (MA/mm^2)=tube ID area–stent OD area, 5) ellipticity index (EI)=maximum stent inner diameter/minimum stent inner diameter. The circular and oval stents were measured using a 3-point and 2 reference point interpolation method, respectively, for stent maximum and minimum diameters. The stent area was calculated by tracing for oval stents and a 3-point method was used for circular stents.

Mechanical stent performance

Forty 4.0x16 mm stent samples were tested in four groups for radial strength and stent length at 4.0 mm diameter (control group) and at 5.00 mm, 5.75 mm and 6.00 mm diameters (overexpanded groups). Stent length was also captured from these stents as it is an input factor in the radial strength calculation (force/length). The average length values from these groups were also used to calculate vessel area at each diameter in the SAR calculation. The recoil was measured sequentially from the same 10 stents deployed to 4.00 mm, then post-dilated to 5.00 mm, 5.75 mm, and finally to 6.00 mm.

The radial strength or maximum compression resistance of the stent was evaluated by the RX750 Radial Compression Tester (Machine Solutions Inc., Flagstaff, AZ, USA), and the radial strength (N/mm) was calculated by a ratio of peak hoop strength (N) to stent length (mm). Measurements for the length and elastic recoil for each stent after final dilation were quantified using a 3D optical contactless machine (SmartScope® MVP; OGP, Rochester, NY, USA). The amount of elastic recoil was calculated by comparing the stent inner diameters after expanding the stent to a target outer diameter and then deflating the stent (% recoil=(inflated ID- final ID)/inflated ID) * 100). Percentage surface to artery ratio (% SAR) was calculated as a ratio of stent outer surface area to vessel area (outer diameter d * π * stent length) multiplied by 100.

Supplementary Table 1. Stent measurements groups 1-6.

A. Group 1 - proximal optimisation technique - semi-compliant/low pressure (POT-SC/LP).

	Stent ID			Stent OD			Tube ID max			Malapposed area	
Stent sample	Stent ID max (mm)	Stent ID min (mm)	Stent ID area (mm²)	Stent OD max (mm)	Stent OD min (mm)	Stent OD area (mm²)	Tube ID max (mm)	Tube ID min (mm)	Tube ID area (mm²)	Malapposed area ID/ID (mm²)	Malapposed area OD/ID (mm²)
44	4.95	4.95	19.06	5.07	5.07	20.20	6.38	5.93	29.17	10.11	8.97
45	5.05	5.05	19.94	5.17	5.17	21.11	6.55	5.66	28.85	8.91	7.74
46	5.05	5.05	19.82	5.19	5.19	21.11	6.16	6.16	29.60	9.78	8.49
Average	5.02	5.02	19.61	5.14	5.14	20.81	6.36	5.92	29.21	9.60	8.40
SD	0.06	0.06	0.48	0.06	0.06	0.53	0.20	0.25	0.38	0.62	0.62

B. Group 2 - proximal optimisation technique - semi-compliant/standard pressure (POT-SC/SP).

	Stent ID			Stent OD			Tube ID max			Malapposed area	
Stent sample	Stent ID max (mm)	Stent ID min (mm)	Stent ID area (mm^2)	Stent OD max (mm)	Stent OD min (mm)	Stent OD area (mm^2)	Tube ID max (mm)	Tube ID min (mm)	Tube ID area (mm^2)	Malapposed area ID/ID (mm^2)	Malapposed area OD/ID (mm^2)
24	5.96	5.96	27.78	6.09	6.09	29.00	6.23	6.23	29.41	1.63	0.41
25	5.86	5.86	26.89	6.03	6.03	28.54	6.20	6.20	29.95	3.06	1.41
26	5.86	5.86	26.89	6.03	6.03	28.69	6.18	6.18	29.95	3.06	1.26
47	5.85	5.85	26.82	5.95	5.95	28.02	6.16	6.16	29.73	2.91	1.71
48	5.86	5.86	26.97	5.99	5.99	28.17	6.13	6.13	29.26	2.29	1.09
49	5.89	5.89	26.97	5.98	5.98	28.32	6.22	6.00	29.06	2.09	0.74
50	5.84	5.84	26.58	5.99	5.99	28.17	6.12	6.12	29.16	2.58	0.99
51	5.95	5.95	27.72	6.07	6.07	28.78	6.21	6.21	29.94	2.22	1.16
52	5.98	5.98	27.87	6.13	6.13	29.40	6.21	6.21	30.20	2.33	0.80
53	5.93	5.93	27.42	6.09	6.09	29.09	6.23	6.23	30.20	2.78	1.11
Average	5.90	5.90	27.19	6.04	6.04	28.62	6.19	6.17	29.69	2.50	1.07
SD	0.05	0.05	0.46	0.06	0.06	0.46	0.04	0.07	0.43	0.47	0.36

C. Group 3 - proximal optimisation technique - non-compliant/high pressure (POT-NC/HP).

	Stent ID			**Stent OD**			**Tube ID max**			**Malapposed area**	
Stent sample	**Stent ID max (mm)**	**Stent ID min (mm)**	**Stent ID area (mm²)**	**Stent OD max (mm)**	**Stent OD min (mm)**	**Stent OD area (mm²)**	**Tube ID max (mm)**	**Tube ID min (mm)**	**Tube ID area (mm²)**	**Malapposed area ID/ID (mm²)**	**Malapposed area OD/ID (mm²)**
P10	6.07	6.07	28.72	6.19	6.19	29.98	6.19	6.19	29.98	1.26	0.00
P11	6.13	6.13	29.34	6.29	6.29	31.09	6.29	6.29	31.09	1.75	0.00
P12	6.01	6.01	28.26	6.17	6.17	29.82	6.17	6.17	29.82	1.56	0.00
Average	**6.07**	**6.07**	**28.77**	**6.22**	**6.22**	**30.30**	**6.22**	**6.22**	**30.30**	**1.52**	**0.00**
SD	0.06	0.06	0.54	0.06	0.06	0.69	0.06	0.06	0.69	0.25	0.00

D. Group 4 - final kissing balloon dilation - undersized/standard pressure (FKBD-US/SP).

	Stent ID			Stent OD			Tube ID max			Malapposed area	
Stent number	Stent ID max (mm)	Stent ID min (mm)	Stent ID area (mm^2)	Stent OD max (mm)	Stent OD min (mm)	Stent OD area (mm^2)	Tube ID max (mm)	Tube ID min (mm)	Tube ID area (mm^2)	Malapposed area ID/ID (mm^2)	Malapposed area OD/ID (mm^2)
18	6.36	4.15	21.90	6.52	4.40	23.50	6.90	5.42	28.68	6.78	5.18
19	6.37	4.09	21.61	6.62	4.30	22.96	6.62	5.64	29.10	7.49	6.14
20	6.15	4.06	20.63	6.38	4.26	21.88	6.58	5.73	29.15	8.52	7.27
Average	6.29	4.10	21.38	6.51	4.32	22.78	6.70	5.60	28.98	7.60	6.20
SD	0.12	0.05	0.67	0.12	0.07	0.82	0.17	0.16	0.26	0.87	1.05

E. Group 5 - final kissing balloon dilation - optimally sized/low pressure (FKBD-OS/LP).

	Stent ID			Stent OD			Tube ID max			Malapposed area	
Stent number	Stent ID max (mm)	Stent ID min (mm)	Stent ID area (mm²)	Stent OD max (mm)	Stent OD min (mm)	Stent OD area (mm²)	Tube ID max (mm)	Tube ID min (mm)	Tube ID area (mm²)	Malapposed area ID/ID (mm²)	Malapposed area OD/ID (mm²)
15	5.45	4.64	19.81	5.66	4.85	20.94	6.47	5.90	29.25	9.44	8.31
16	5.36	4.63	19.48	5.52	4.82	20.64	6.54	5.78	28.97	9.49	8.33
17	5.61	4.61	19.68	5.84	4.81	21.02	6.49	5.84	29.09	9.41	8.07
Average	5.47	4.63	19.66	5.67	4.83	20.87	6.50	5.84	29.10	9.45	8.24
SD	0.13	0.02	0.17	0.16	0.02	0.20	0.04	0.06	0.14	0.04	0.14

F. Group 6 - final kissing balloon dilation - optimally sized/standard pressure (FKBD-OS/SP).

	Stent ID			Stent OD			Tube ID max			Malapposed area	
Stent sample number	Stent ID max (mm)	Stent ID min (mm)	Stent ID area (mm^2)	Stent OD max (mm)	Stent OD min (mm)	Stent OD area (mm^2)	Tube ID max (mm)	Tube ID min (mm)	Tube ID area (mm^2)	Malapposed area ID/ID (mm^2)	Malapposed area OD/ID (mm^2)
2	6.60	4.72	25.53	6.87	4.89	26.74	6.87	5.24	28.54	3.01	1.80
3	6.57	4.68	25.33	6.77	4.98	27.05	6.77	5.42	29.29	3.96	2.24
4	6.82	4.69	26.24	7.03	4.89	27.88	7.03	5.10	29.10	2.86	1.22
Average	6.66	4.70	25.70	6.89	4.92	27.22	6.89	5.25	28.98	3.28	1.75
SD	0.14	0.02	0.48	0.13	0.05	0.59	0.13	0.16	0.39	0.60	0.51

Supplementary Table 2. Stent performance measurements.

A. SYNERGY 4x16 mm radial strength, as measured by average maximum compression resistance (hoop force/length: N/mm).

Sample	4 mm maximum compression resistance (N/mm)	5 mm maximum compression resistance (N/mm)	5.75 mm maximum compression resistance (N/mm)	6 mm maximum compression resistance (N/mm)
1.00	0.26	0.27	0.26	0.36
2.00	0.24	0.28	0.30	0.38
3.00	0.25	0.30	0.24	0.37
4.00	0.26	0.28	0.28	0.42
5.00	0.24	0.26	0.29	0.36
6.00	0.28	0.25	0.30	0.31
7.00	0.25	0.26	0.38	0.44
8.00	0.28	0.26	0.26	0.43
9.00	0.28	0.25	0.23	0.37
10.00	0.25	0.30	0.27	0.34
Average	**0.26**	**0.27**	**0.28**	**0.38**
SD	**0.01**	**0.02**	**0.04**	**0.04**

B. SYNERGY 4.0x16 mm recoil.

	% ID recoil			
unit #	**4.0 mm % recoil**	**5.0 mm % recoil**	**5.75 mm % recoil**	**6.0 mm % recoil**
1	3.5%	0.4%	0.3%	1.8%
2	2.7%	2.0%	1.2%	1.2%
3	2.2%	1.6%	1.2%	1.7%
4	4.4%	1.8%	2.2%	2.0%
5	3.0%	1.6%	1.7%	2.0%
6	2.2%	1.8%	0.9%	0.8%
7	1.7%	2.0%	1.5%	0.7%
8	2.0%	1.0%	1.2%	0.5%
9	3.2%	1.4%	1.4%	2.0%
10	3.7%	2.6%	1.2%	1.2%
Average % recoil	**2.9%**	**1.6%**	**1.3%**	**1.4%**
SD	**0.9%**	**0.6%**	**0.5%**	**0.6%**

C. SYNERGY 4.0x16 mm SAR calculation (%).

Stent ID (mm)	**Stent OD (mm)**	**Stent length (mm)**	**Vessel area (mm^2)**	**SAR %**
4.0	4.17	16.1	210	14.2%
5.0	5.17	17.5	284	10.5%
5.75	5.92	16.8	313	9.5%
6.0	6.17	16.4	317	9.4%

D. SYNERGY 4.0x16 mm length (mm).

Sample	4.0 mm length (mm)	5.0 mm length (mm)	5.75 mm length (mm)	6.0 mm length (mm)
1.00	16.10	16.82	17.35	16.20
2.00	15.80	17.24	17.10	16.32
3.00	16.03	16.61	17.45	16.30
4.00	16.21	17.24	16.67	16.55
5.00	15.90	17.70	16.30	16.03
6.00	16.18	18.05	16.05	16.95
7.00	16.28	17.77	16.29	16.02
8.00	16.03	17.78	16.63	16.35
9.00	16.19	17.96	17.67	16.38
10.00	15.82	17.45	16.93	16.58
Average	**16.05**	**17.46**	**16.84**	**16.37**
SD	**0.17**	**0.48**	**0.55**	**0.28**

Supplementary Table 3. Stent performance at overexpansion limits - surface to artery ratio.

			Stent length (mm)		Radial strength (maximum hoop force / length [N/mm])		% Surface to artery ratio		% Stent recoil	
Stent model	Sample size	Stent diameter (mm)	Average	Standard deviation	Average	Standard deviation	Vessel area (mm^2)	SAR %	Average	Standard deviation
SYNERGY II 4.0x16 mm	10	4.0	16.1	0.2	0.26	0.01	210	14.2%	2.9	0.9
SYNERGY II 4.0x16 mm	10	5.0	17.5	0.5	0.27	0.02	283	10.5%	1.6	0.6
SYNERGY II 4.0x16 mm	10	5.75	16.8	0.6	0.28	0.04	313	9.5%	1.3	0.5
SYNERGY II 4.0x16 mm	10	6.0	16.4	0.3	0.38	0.04	317	9.4%	1.4	0.6

Supplementary Table 4. Compliance table of stents/balloons used*.

Stent/balloon size		Pressure		Stent/balloon dimensions	
		(atm)	(kPa)	(mm)	
SYNERGY II 4.0 mm	Nominal	11.0	1,117	ID 4.06	OD 4.24
	RBP	16.0	1,620	ID 4.30	OD 4.48
NC Quantum Apex 5.0 mm	Nominal	12.0	1,216	4.95	
	RBP	18.0	1,824	5.15	
Apex 4.0 mm	Low	4.0	405	3.80	
	Nominal	6.0	608	3.96	
	RBP	12.0	1,216	4.25	
Apex 5.0 mm	Low	4.0	405	4.79	
	Nominal	6.0	608	4.99	
	RBP	12.0	1216	5.30	
Maverick XL 6.0 mm	Nominal	6.0	608	6.00	
	RBP	14.0	1,419	6.46	
NC Emerge 6.0 mm	Nominal	6.0	608	6.09	
	RBP	14.0	1,419	6.28	

*Source: Boston Scientific, Maple Grove, MN, USA.

ID: inner diameter; OD: outer diameter; RBP: rated burst pressure

13

CHAPTER

LEFT MAIN STEM BIFURCATION TREATMENT WITH THE TRYTON SIDE-BRANCH STENT: A PROSPECTIVE STUDY WITH INVASIVE IMAGING FOLLOW-UP

Jiang Ming Fam, Pieter Stella, Joanna Wykrzykowska, Antonio L. Bartorelli, Guiseppe Tarantini, Eulogio Garcia, Indulis Kumsars, Michael Magro, Peter O'Kane, Robert-Jan van Geuns.

Submitted for publication.

Left main stem bifurcation treatment with the Tryton side-branch stent:

A prospective study with invasive imaging follow-up

Jiang Ming Fam [1,10], Pieter Stella[2], Joanna Wykrzykowska[3], Antonio L. Bartorelli [4], Guiseppe Tarantini [5], Eulogio Garcia[6], Indulis Kumsars[7], Michael Magro[1,8], Peter O'Kane[9], Robert-Jan van Geuns[1]

[1]Thoraxcenter, Erasmus MC, Rotterdam, The Netherlands; [2]UMCU, Utrecht, The Netherlands; [3]AMC, Amsterdam, The Netherlands; [4]Centro Cardiologico Monzino, Milan, University of Milan, Italy; [5]Padova University Hospital, Padova, Italy; [6]Hospital Universitario "Gregorio Marañón", Madrid, Spain; [7]Paula Stradins Clinical University, Riga, Lativa; [8]ETZ (Elisabeth-Tweesteden Ziekenhuis), Tilburg, The Netherlands; [9]Royal Bournemouth Hospital, United Kingdom; [10]National Heart Centre Singapore, Singapore

Running Title: Tryton Left Main FIM trial

Keywords: Left main stem bifurcation; Tryton stent; intravascular ultrasound

Corresponding Author and Address:

Prof. dr. R.J van Geuns, MD, PhD
Thoraxcenter, Ba-585
Dr. Molewaterplein 40,
3015 RD Rotterdam,
The Netherlands.
Tel: +31-10-4635260 (33348)
Fax: +31-10-4369154
E-mail: r.vangeuns@erasmusmc.nl

Word Count: 5591 (Abstract, Main Text, Figure Legends, References)

ABSTRACT

Aims: While acute angiographic success and safety of the Tryton stent for left main (LM) bifurcation treatment has been established, further analysis on factors that may determine the long-term efficacy of this technique is needed.

Methods: We enrolled thirty patients with LM bifurcation disease who were treated with the Tryton stent in a multicenter prospective study. Baseline and 6-month angiographic and intravascular ultrasound (IVUS) analysis were performed and 9-month clinical outcome data were obtained.

Results: Twenty seven percent of patients presented with an acute coronary syndrome**.** The mean SYNTAX score was 28±8 and a Medina 1,1,1 LM lesion was present in 73%. Post-procedure, one patient had a residual stenosis of >30% in the side branch (SB). At follow-up, angiographic late loss was highest in the SB compared to the main vessel (MV) (SB: 0.65±0.46; proximal MV: 0.28±0.41; distal MV: 0.17±0.37mm). Neointimal hyperplasia was highest in the distal SB portion of the Tryton stent (proximal MV 1.11mm^2; distal SB 1.36mm^2), particularly at the ostium (1.42mm^2). At 9 months, target lesion revascularization occurred in five (17%) patients, of whom four (13%) had SB restenosis. Myocardial infarction was reported in four (13%) patients, (2 peri-procedural). MACE rate was 23%. No cases of death or stent thrombosis occurred.

Conclusion: At 6 months, angiographic and IVUS analysis showed excellent MV outcome with low late loss and neointimal growth, while late loss at the SB site (that was covered by the distal portion of the Tryton) was that expected for a bare metal stent.

Keywords: Left main stem bifurcation; Tryton stent; intravascular ultrasound

INTRODUCTION

Distal left main (LM) coronary stenting is a revascularization option in patients with disease in this important part of the coronary tree [1]. Elderly age at presentation and co-morbidities increase the surgical risk of treating this patient population and with improved percutaneous coronary intervention (PCI) techniques, distal LM coronary stenting has emerged as a viable alternative in selected patients with good long term outcomes.

Although a significant proportion of LM lesions involving the bifurcation can be treated effectively with a provisional one-stent technique, true bifurcation lesions present a major challenge for this conventional approach. In such cases, the one-stent technique often results in suboptimal results with residual stenosis in the side branch (SB). The dedicated bifurcation Tryton stent in combination with a conventional drug-eluting stent (DES) has been shown to provide good angiographic results in such lesions [2-4]. The Tryton stent is implanted with a 'reverse culotte' technique and provides adequate scaffolding of all bifurcation segments. There are two advantages of this technique firstly being able to secure the SB at the beginning of the procedure, and secondly being able to provide good coverage at the level of the carina while leaving minimal metal in the main vessel (MV) thus facilitating the deployment of a standard DES in the proximal to distal MV [2]. Securing the SB first is of major importance in the setting of LM stenting where the side branch is nearly always of important caliber and therefore significance. This strategy has been investigated in the retrospective Tryton left main registry [4]. In this study, while the safety profile was clearly acceptable, there were concerns raised regarding the long-term efficacy of this stenting strategy. Of note, 12% of patients treated in the registry required repeat revascularization at 6 months and in all cases the restenosis involved the SB. For the registry the distal portion of the side branch stent was available in 2.5mm size only, which resulted in a patient population with relatively small side

branches, a factor associated with a higher risk of stent failure. [5]Apart from the important role of SB size, factors such as depth of implantation of the Tryton stent and change in bifurcation angle after stenting did not appear to predict stent failure. In-depth analysis of baseline and follow-up angiographic and intravascular imaging is therefore required to examine this issue further.

To this end, the Tryton LM FIM prospective serial invasive imaging study was designed. The aims of the study are 1. To prospectively assess the qualitative and quantitative angiographic acute outcomes of patients treated with the Tryton LM bifurcation stenting technique; 2. To assess acute stent results by intravascular ultrasound (IVUS) in an attempt to identify markers of short- and long-term stent failure; 3. To assess stent result angiographically and by IVUS at 6 months and finally 4. To determine the 9-month safety and efficacy profile of this stenting technique for LM disease.

METHODS

Patient Population

Eligible patients were those with angiographic evidence of LM bifurcation lesions in whom PCI was considered as a reasonable or the only option. Further, patients could be enrolled if the LM length was >12mm and the diameter was <5mm, while the proximal left circumflex coronary artery needed to be ≤ 4 mm in diameter and a TIMI III flow in both vessels was required. Key exclusion criteria included hemodynamically unstable patients, those with a left ventricular ejection fraction of <30% and patients with contraindications to antiplatelet therapy.

Study Device and PCI strategy

The Tryton Side-Branch Stent is a slotted tube, balloon-expandable cobalt chromium bare-metal stent (BMS) with three zones: a distal side branch zone, a central transition zone and a proximal main vessel zone. The distal zone has a standard slotted tube workhorse stent design, the central transition zone consists of three panels while the proximal MV (PMV) zone is composed of three fronds that terminate proximally in two circumferential bands. The stent is mounted either on a balloon with uniform diameter (straight type) or on a stepped balloon (tapered type). For the purpose of this Tryton LM study, large diameter stents (3.5-3.0 and 4.0-3.5) were also available. The stent delivery system has four markers, two of which delineate the proximal and distal end of the stent and the other two the proximal and distal part of the transition zone. Further details of the stent design as well as the standard technique for implantation have been published [4]. In short, the procedure is typically performed via a 6Fr guiding catheter; after wiring of both MV and SB for pre-dilation, the Tryton stent is advanced over the wire into the SB and, using the two middle markers on the delivery system, the stent is positioned till these markers straddle the carina. Deployment of the stent is followed by retraction of the guidewire from the SB that is repositioned through the fronds of the transition zone into the distal MV (DMV). A standard DES is then advanced and positioned in MV jailing the stented SB ostium. Once the MV stent is deployed, re-crossing into the SB and final kissing balloon inflation are performed.

Procedure

Patients were pre-treated with aspirin (300-500mg) and clopidogrel (300mg or 600mg) or prasugrel (60mg) or ticagrelor (180mg) unless they were already taking these antiplatelet agents. Intravenous heparin was administered to maintain an activated clotting time of >250 seconds. Glyoprotein IIb/IIIa inhibitor use was left to the treating interventional cardiologist's discretion, as was the use of other additional devices such as thrombectomy and rotablator.

The need for additional overlapping stents to cover the whole lesion, additional ballooning and procedural angiographic and clinical complications were noted. Aspirin was continued indefinitely and clopidogrel/prasugrel/ticagrelor was continued for a minimum of 12 months after the index procedure.

Intravascular Ultrasound (IVUS)

For the purposes of the study two final IVUS pullbacks were required; one from the SB and the other from the MB into the LM. Use of additional IVUS pullbacks during PCI including pre-stenting was allowed and supported by all operators who followed the class IIa recommendation for LM PCI by the ESC guidelines [1] . IVUS was acquired with the Atlantis SR Pro 40-MHz catheter and iLab system (Boston Scientific, Natick, MA, USA) at a frame rate of 30 frames/s and a pullback speed of 0.5mm/s, according to international standards.

Cardiac enzymes and ECG

Serial cardiac enzymes including creatinine kinase (CK)-MB mass, troponin-T, or troponin-I were measured after the procedure. Pre-procedure biomarkers were assessed in all patients with an acute coronary syndrome. These patients were included in the biomarker analysis only if the pre-procedure markers were normal. A 12-lead ECG was obtained before and after the procedure as part of routine institutional practices.

Angiographic and IVUS follow-up

Angiographic follow-up was performed at 6 months as per local hospital protocol for distal LM PCI using matched angiographic views from baseline films. Matched IVUS pullbacks from the left anterior descending and the left circumflex coronary arteries were also performed. For the serial investigations, the same imaging systems were used at baseline and follow-up. Unscheduled coronary angiography/IVUS study within the 6-month period was

considered a follow-up study either if a target lesion intervention was required or if it occurred within 8 weeks of the scheduled follow-up investigation. A clinical example of a patient treated and followed-up for LM bifurcation stenting with the Tryton stent is presented in Figure 1.

Core-lab Analysis

All imaging data analyses were performed by an independent core-lab (Cardialysis BV, Rotterdam, the Netherlands).

Quantitative Coronary Angiography (QCA)

Angiographic films were analyzed with dedicated bifurcation software (CAAS 5.10, Maastricht, PIE Medical software, The Netherlands) [6-7]. Reference vessel diameter, minimal luminal diameter (MLD) and percentage diameter stenosis (DS%) were obtained for the proximal MV (PMV), distal MV (DMV) and SB in the pre-procedural angiographic film. Matched views of immediate post-procedural films were then selected for determination of the same parameters. Acute gain was determined from the difference between MLD in each of the three segments (PMV, DMV and SB). Matched follow-up views were assessed in the same way, obtaining the parameters at 6 months. The late loss was calculated as the difference in MLD between post-procedure and follow-up values.

Intravascular Ultrasound

Intravascular ultrasound pullbacks were analyzed off-line using the QCU-CMS software (Medis, Leiden, the Netherlands) at standard 1-mm intervals. The lumen, stent and external elastic membrane area (vessel area) were measured. The minimal lumen area (MLA) and the mean lumen area were identified for each of the target regions (5mm proximal to the bifurcation region), bifurcation region (all images with visible side branches) and distal region

(5 mm distal to carina) for each of the MV-LM and SB-LM pullbacks. The ostial region of the side branch was defined as the first 3 mm distal to the carina. Neointimal hyperplasia area (stent area-lumen area) was also derived.

Clinical follow-up

Clinical follow-up was obtained by clinical visits during which data on possible adverse cardiovascular events was obtained. Events were adjudicated by the local cardiologists and verified by the principle investigator according to criteria defined below.

Definitions

Procedural success is a composite end point defined as (1) successful implantation of the Tryton stent and MV stent; (2) angiographic success, that is, TIMI III flow post-procedure and <30% stenosis in the LM-LAD/LCx bifurcation; and (3) absence of in-hospital MACE; cardiac death, myocardial infarction (MI) (Q-wave and non-Q wave) and clinically driven target lesion revascularization (TLR). MACE were defined as a composite of cardiac or non-cardiac death, Q-wave or non-Q-wave MI and ischemia driven TLR. Non-Q wave MI was defined as clinical signs of MI associated with a CK-MB mass or troponin –T/troponin-I increase ≥3 times the upper limit of normal in the absence of Q waves and not related to an interventional procedure. Q-wave MI occurred when there was chest pain or symptoms consistent with myocardial ischemia and new pathological Q waves in two or more contiguous electrocardiograph leads. TLR was defined as any PCI of the index lesion and including the 5 mm peri-stent segments in either MV or SB. Target vessel revascularization (TVR) was defined as revascularization of any part of the index coronary artery. Stent thrombosis was defined according to the Academic Research Consortium (ARC) [8]. The study design is depicted in the flow chart (Figure 2).

Statistical analysis

Continuous data are expressed as mean ± SD or as median (interquartile ranges), whereas dichotomous data are summarized as frequencies. The paired t-test was used for comparisons of quantitative parameters pre- and post-procedure and at 6-month follow-up. Statistical analysis was performed using SPSS software version 20.0 (SPSS, Chicago, USA)

Results

Thirty consecutive patients in 8 European hospitals were treated according to the study protocol, provided informed consent and formed the study cohort. The baseline clinical characteristics of the cohort are detailed in Table I. The mean age of the patients was 68 ±9 years. Twenty seven percent of patients presented with an acute coronary syndrome (Table II)**.** Nearly half of the patients had a history of previous revascularization; PCI in twelve (40%) and CABG in two (7%). The average Euroscore was 0.74±1.1, whereas the SYNTAX score averaged 28 ± 8. A Medina 1,1,1 LM bifurcation lesion was seen in 73% (n=22) of the cases (Table III). The great majority (93%) of the LM bifurcations had an angle >30 degrees. Severe calcification was present in 47% of patients.

Procedural details are listed in Table IV. Pre-dilatation of the bifurcation lesion was performed in 80% (n=24). Importantly, 83% (n=25) of Tryton stents implanted were of the larger sizes (3.5-3.0 and 4.0-3.5 mm). In 90 % (n=27) of cases, the Tryton stent was post-dilated after implantation. The MB stent had a mean diameter of 3.5 (3.5-4.0). In 70% (n=21) of cases, additional stents had to be implanted in an overlapping manner with the stents implanted in the bifurcation were required in 53% (n=16) of cases, 37% (n=11) and 17% (n=5) in the MV and in the SB respectively. Final kissing balloon dilation was performed in all cases. Procedural success was 90% (n=27). Of the three patients without procedural

success, one had a residual stenosis due to heavy calcification in the SB and two had peri-procedural cardiac enzyme elevation in the range of an MI (non-Q wave).

Quantitative angiographic analysis (QCA)

Baseline pre- and post-angiographic analysis was available in all cases. Nineteen matched pairs of post-procedure and follow-up angiographies were found suitable by the Core Lab for analysis. Two of the nineteen patients had binary restenosis at the SB ostium. Baseline pre-procedural, post-procedural and 6-month follow-up QCA data are listed in Table V. Angiographic late loss was highest in the SB (SB: 0.65±0.46; PMV: 0.28±0.41; DMV: 0.17±0.37mm).

Intravascular ultrasound analysis

Baseline post-procedural IVUS pullbacks of sufficient quality from the SB and MV were available in twenty patients. The MLA in the PMV was 11.75 ± 2.9 mm^2. The MLA in the DMV was 8.46 ± 1.90 mm^2 where one patient showed a MLA below 6.3 mm^2. The MLA in the side branch stent was smaller compared to the distal main branch: 7.12 ± 2.45 mm^2 and four out of twenty patients showed a MLA below the target of 5.0 mm^2.

Sixteen follow-up IVUS pullbacks were of sufficient quality for comparative analysis. Values for minimal lumen area, mean lumen area at the proximal, bifurcation, distal regions and neointima area at follow-up of the MV are shown in Table VI. Neointimal hyperplasia was highest in the SB region, (the segment covered by the distal portion of the Tryton stent), with the ostium showing the greatest involvement (1.42 mm^2). Using IVUS, minimal lumen area in the proximal left main vessel was stable (11.08 ± 1.97 mm^2 and 11.59 ± 2.48 mm^2 at baseline and at 6 months respectively, p= 0.697). Minimal and mean lumen area in the side-branch decreased significantly (Minimal lumen area: 6.68±1.80 mm^2 and 5.10±2.01 mm^2 at baseline and at 6 months respectively, p =0.004; Mean lumen area: 7.79±2.15 mm^2 and 6.53±2.31

mm^2 at baseline and at 6 months respectively, p=0.002) respectively as a result of 1.59±0.77 mm^2 neointimal area.

Clinical Outcome

The in-hospital, 6-month and 9-month clinical outcomes are summarized in Table VII. All treated patients were alive 9 months after the procedure. Twenty three percent of patients had an adverse cardiac event during or after the procedure. Myocardial infarction occurred in four (13%) patients, half of whom presented peri-procedurally, while the other two occurred during the 9-month follow-up period. Clinically indicated TLR at 9 months occurred in five (17%) patients, with 80% (n=4) and 20% (n=1) occurring in the SB (TLR-SB) and MB (TLR-MB) respectively. Hierarchical MACE rate was 23%. No cases of death or stent thrombosis occurred.

Baseline Minimal Lumen Area and clinical outcome

From available IVUS analysis, the single TLR in the distal main branch occurred in the patient with the smallest MLA of 4.35 mm^2 post-procedure (Figure 3A). All the other patients had an MLA of more than 6.3 mm^2 in the MV and had no revascularization events at follow-up. For the distal side branch TLR was more frequent in the patients with a MLA below 5.0 mm^2 (1 out of 4 or 25%) versus patients with a MLA above 5.0mm^2, (3 out of 16 or 19%). The mean MLA for patients with TLR in the SB, although numerically smaller (5.94 [5.09-7.28] mm^2) was not statistically different from the MLA of patients free of TLR in the SB. (6.76 [5.07-8.56] mm^2) (Figure 3C).

Discussion

The Tryton Left Main bifurcation study was designed to prospectively evaluate the effect of percutaneous interventions of left main bifurcation lesions using a dedicated sidebranch stent technology. Our main findings for LM bifurcation lesions treated with the Tryton dedicated

side-branch stent were: 1. Very low procedural complication rates during LM PCI; 2. Satisfactory acute angiographic and IVUS results; 3. Low main branch neointimal formation, but inadequate sidebranch neointimal hyperplasia suppression during follow-up, and subsequently 4. Significant sidebranch re-intervention rates.

The very low procedural complication rate during this complex distal LM bifurcation stenting, in which 73% of the lesions were Medina 1,1,1 supports the concept of the Tryton bifurcation stent, where the SB is treated first and the full bifurcation area supported by the 'culotte' approach. Although the single stent provisional approach is favored for most distal LM lesions, two stents are frequently deemed necessary by the operators. In the Syntax Left main group, two stents were implanted in 38.4% of the patients [9]. In the PRECOMBAT-2 trial bifurcation lesions were present in 71.9% while 2 stents were used in 26% of all patients and 37% of the bifurcation lesions [10]. In the ASAM-Left Main series of 1124 patients treated with PCI the prevalence of LM bifurcation disease in the PCI cohort increased from 46.5% to 67% in the 2007-2010 cohort. In this population two stents were used in 25.1% of all patients [11]. The lesions requiring two stents had a much higher revascularisation rate compared to single stent procedures. Additionally two-stents techniques require more time and greater operator experience. Innovations in dedicated stent design are therefore specifically driven by the need to simplify and improve true bifurcation stenting procedures. A better understanding of stent failure at follow-up despite an adequate acute angiographic result and clinical outcome is the key aim of this study. In addition, IVUS is more accurate in assessment of post-stenting luminal area when compared to angiography. In the current study, IVUS allowed for further investigation of the seemingly good angiographic result obtained with this stenting technique. Kang et al. [12] reported post-stenting IVUS derived MLA cut-off values

of 5.0 mm^2 for left circumflex coronary artery and 6.3 mm^2 for the left anterior descending coronary artery for prediction of in-stent restenosis.

The angiographic and IVUS results of the Tryton study were consistent with previous similar studies. In the two-stent LM group of the J-Cypher registry MLD in the main branch was 3.01 mm with a final DS% 10.5%. In the SB, the effect was good with a MLD of 2.61 mm and DS% of 11.7% [13]. Unfortunately for this two stent (DES) strategy late lumen loss was still 0.75mm in the side branch, even worse compared to the 0.65mm for the bare metal stented SB segment of the Tryton strategy. For IVUS standards, our results are best compared to the IVUS analysis in the ASAN-MAIN series [12]. The average MLA of the distal bifurcation main branch segment of 8.46mm^2 was well above the cut-off value of Kang et al [12]. However if we examine cases individually, while the single TLR of the main branch occurred in a patient with an MLA below 6.3mm^2 (Figure 3A), 4 of our patients did not reach the 5 mm^2 'cut-off' for the SB and 1 (25%) of them had a subsequent TLR (Figure 3B). 3 of the remaining patients who underwent TLR in the side branch had achieved MLA above the cut off of 5.0mm^2 suggesting that an implantation strategy focused on lesion preparation and postdilation was not sufficient in all patients and that other factors (eg clinical and drug factors) may be influential in affecting clinical outcomes such as TLR. This has to be evaluated in further studies.

Therefore baseline target MLA were equally achieved in both main vessel and side branch, and although below target MLAs increase the risk of re-stenosis, the fact that 80% (Table VII) of repeat interventions occurred in the SB may not be explained by failure to achieve target MLA alone. The higher incidence of SB failure suggests that a possible cause is a difference in the type of stent in the MV and SB, namely the lack of drug-elution of the Tryton stent. A drug-eluting version is therefore recommended to improve the clinical outcome of LM

stenting with this technique. Still these results compare favorably to the three year results of the J-Cypher LM registry where TLR for the two-drug eluting stent group reached 30.9% [14]. In the Italian registry a two-stent strategy resulted in a TLR of 20% at one year and reaching 25% at two year [15]. Best results currently are reported using the Double Kissing Crush technique with a TLR of 2.3% at 12 months [16]. In our previous exploratory registry [4] we noticed a MACE rate of 22% with a target lesion revascularization rate of 12 % at 6 months which is much higher than the average reported in all published series of 5.5% in non-LM setting [3]. A plausible explanation for this might be the bifurcation angle which is much higher in LM bifurcations vs non-LM bifurcations. In the DKCRUSH-III study, Culotte was especially ineffective if the bifurcation was ≥70° [16], also Freixa et al showed an impact of bifurcation angle on clinical outcome [17]. Another potential explanation is that the proximal circumflex supplied a larger myocardial territory than other bifurcations and stenosis in this area results in a larger ischaemic burden. As a result, patients present with symptoms more often, resulting in more repeat interventions. Another reasonable cause of SB restenosis may be the lack of scaffolding due to the incorrect placement of the Tryton stent at the carina site. In this series, the majority of SB restenosis occurred within the SB ostium. The variant of the Tryton stent utilized for this study is provided with two markers delineating the 4-mm transition zone that are used to precisely position this zone at the SB ostium. In addition, the MV portion of the stent may be longer than the length of some LM often requiring more distal Tryton deployment. This can result in the Tryton side branch stent being placed too distally within the LM bifurcation resulting in insufficient scaffolding specifically within the SB ostium. In angiographic analysis we could not relate the positioning to cases of re-stenosis and therefore this mechanism remains hypothetical. Future studies with 3 dimensional Tryton stent reconstruction post deployment and/or at follow-up may help evaluate this theory.

In summary although acute outcome was good and comparable to many other two stent LM bifurcation studies, clinical outcome still needs improvement. These data suggest that the result of this approach could improve if a drug-eluting version is developed. More studies looking at further optimization during implantation and anti-proliferative drug elution in the sidebranch to inhibit neointima proliferation may improve procedural and clinical results.

Study Limitations

This study gives insights over the possible mechanisms of the Tryton stent performance and stent failure. However it has significant limitations. The number of studied patients is small, the patients were selected and therefore the observations noted cannot be extrapolated to a broader patient population. However, this was not the prime objective of the study. Unfortunately, the lack of availability of good quality baseline and follow-up matched angiographic and IVUS images has significantly compromised the analysis.

There is no comparative arm, in which culotte technique in conjunction with conventional DES or other bifurcation stenting techniques were used. The finding of greater neointimal hyperplasia in the BMS portion of the Tryton stent, although highly suggestive, can be correctly attributed to the lack of drug elution only if prevention of exuberant hyperplasia will be demonstrated by a randomized study comparing a drug-eluting version vs. a conventional Tryton stent.

Conclusions

At 6 months, angiographic and IVUS analyses showed excellent MV outcome with low late loss and neointimal growth, while late loss at the SB covered only by the distal portion of the Tryton stent showed rates expected for a BMS.

References

1. Kolh, P., Kolh P, Windecker S, Alfonso F, Collet JP, Cremer J, Falk V, Filippatos G, Hamm C, Head SJ, Jüni P, Kappetein AP, Kastrati A, Knuuti J, Landmesser U, Laufer G, Neumann FJ, Richter DJ, Schauerte P, Sousa Uva M, Stefanini GG, Taggart DP, Torracca L, Valgimigli M, Wijns W, Witkowski A; European Society of Cardiology Committee for Practice Guidelines, Zamorano JL, Achenbach S, Baumgartner H, Bax JJ, Bueno H, Dean V, Deaton C, Erol Ç, Fagard R, Ferrari R, Hasdai D, Hoes AW, Kirchhof P, Knuuti J, Kolh P, Lancellotti P, Linhart A, Nihoyannopoulos P, Piepoli MF, Ponikowski P, Sirnes PA, Tamargo JL, Tendera M, Torbicki A, Wijns W, Windecker S; EACTS Clinical Guidelines Committee, Sousa Uva M, Achenbach S, Pepper J, Anyanwu A, Badimon L, Bauersachs J, Baumbach A, Beygui F, Bonaros N, De Carlo M, Deaton C, Dobrev D, Dunning J, Eeckhout E, Gielen S, Hasdai D, Kirchhof P, Luckraz H, Mahrholdt H, Montalescot G, Paparella D, Rastan AJ, Sanmartin M, Sergeant P, Silber S, Tamargo J, ten Berg J, Thiele H, van Geuns RJ, Wagner HO, Wassmann S, Wendler O, Zamorano JL; Task Force on Myocardial Revascularization of the European Society of Cardiology and the European Association for Cardio-Thoracic Surgery; European Association of Percutaneous Cardiovascular Interventions. et al., *2014 ESC/EACTS Guidelines on myocardial revascularization: the Task Force on Myocardial Revascularization of the European Society of Cardiology (ESC) and the European Association for Cardio-Thoracic Surgery (EACTS). Developed with the special contribution of the European Association of Percutaneous Cardiovascular Interventions (EAPCI).* Eur J Cardiothorac Surg, 2014. 46(4): p. 517-92.

2. Onuma, Y., Müller R, Ramcharitar S, van Geuns RJ, Louvard Y, Morel MA, Morice MC, Davis R, Kaplan AV, Lefèvre T, Grube E, Serruys PW. *Tryton I, First-In-Man (FIM) study: six month clinical and angiographic outcome, analysis with new quantitative coronary angiography dedicated for bifurcation lesions.* EuroIntervention, 2008. 3(5): p. 546-52.

3. Genereux, P., Kumsars I, Lesiak M, Kini A, Fontos G, Slagboom T, Ungi I, Metzger DC, Wykrzykowska JJ, Stella PR, Bartorelli AL, Fearon WF, Lefèvre T, Feldman RL, LaSalle L, Francese DP, Onuma Y, Grundeken MJ, Garcia-Garcia HM, Laak LL, Cutlip DE, Kaplan AV, Serruys PW, Leon MB. *A randomized trial of a dedicated bifurcation stent versus provisional stenting in the treatment of coronary bifurcation lesions.* J Am Coll Cardiol, 2015. 65(6): p. 533-43.

4. Magro, M., Girasis C, Bartorelli AL, Tarantini G, Russo F, Trabattoni D, D'Amico G, Galli M, Gómez Juame A, de Sousa Almeida M, Simsek C, Foley D, Sonck J, Lesiak M, Kayaert P, Serruys PW, van Geuns RJ. *Acute procedural and six-month clinical outcome in patients treated with a dedicated bifurcation stent for left main stem disease: the TRYTON LM multicentre registry.* EuroIntervention, 2013. 8(11): p. 1259-69.

5. Grundeken, M.J., Asgedom S, Damman P, Lesiak M, Norell MS, Garcia E, Bethencourt A, Woudstra P, Koch KT, Vis MM, Henriques JP, Onuma Y, Foley DP, Bartorelli AL, Stella PR, Tijssen JG, de Winter RJ, Wykrzykowska JJ. *Six-month and one-year clinical outcomes after placement of a dedicated coronary bifurcation stent: a patient-level pooled analysis of eight registry studies.* EuroIntervention, 2013. 9(2): p. 195-203.

6. Girasis, C., Schuurbiers JC, Onuma Y, Aben JP, Weijers B, Boersma E, Wentzel JJ, Serruys PW. *Two-dimensional quantitative coronary angiographic models for*

bifurcation segmental analysis: in vitro validation of CAAS against precision manufactured plexiglas phantoms. Catheter Cardiovasc Interv, 2011. 77(6): p. 830-9.

7. Girasis, C., Schuurbiers JC, Onuma Y, Aben JP, Weijers B, Morel MA, Wentzel JJ, Serruys PW. *Advances in two-dimensional quantitative coronary angiographic assessment of bifurcation lesions: improved small lumen diameter detection and automatic reference vessel diameter derivation.* EuroIntervention, 2012. 7(11): p. 1326-35.
8. Cutlip, D.E., Windecker S, Mehran R, Boam A, Cohen DJ, van Es GA, Steg PG, Morel MA, Mauri L, Vranckx P, McFadden E, Lansky A, Hamon M, Krucoff MW, Serruys PW; Academic Research Consortium. *Clinical end points in coronary stent trials: a case for standardized definitions.* Circulation, 2007. 115(17): p. 2344-51.
9. Morice, M.C., Serruys PW, Kappetein AP, Feldman TE, Ståhle E, Colombo A, Mack MJ, Holmes DR, Torracca L, van Es GA, Leadley K, Dawkins KD, Mohr F. *Outcomes in patients with de novo left main disease treated with either percutaneous coronary intervention using paclitaxel-eluting stents or coronary artery bypass graft treatment in the Synergy Between Percutaneous Coronary Intervention with TAXUS and Cardiac Surgery (SYNTAX) trial.* Circulation, 2010. 121(24): p. 2645-53.
10. Kim, Y.H., Park DW, Ahn JM, Yun SC, Song HG, Lee JY, Kim WJ, Kang SJ, Lee SW, Lee CW, Park SW, Jang Y, Jeong MH, Kim HS, Hur SH, Rha SW, Lim DS, Her SH, Seung KB, Seong IW, Park SJ; PRECOMBAT-2 Investigators. *Everolimus-eluting stent implantation for unprotected left main coronary artery stenosis. The PRECOMBAT-2 (Premier of Randomized Comparison of Bypass Surgery versus Angioplasty Using Sirolimus-Eluting Stent in Patients with Left Main Coronary Artery Disease) study.* JACC Cardiovasc Interv, 2012. 5(7): p. 708-17.

11. Park, S.J., Ahn JM, Kim YH, Park DW, Yun SC, Yoon SH, Park HW, Chang M, Lee JY, Kang SJ, Lee SW, Lee CW, Park SW. *Temporal trends in revascularization strategy and outcomes in left main coronary artery stenosis: data from the ASAN Medical Center-Left MAIN Revascularization registry.* Circ Cardiovasc Interv, 2015. 8(3): p. e001846.

12. Kang, S.J., Ahn JM, Song H, Kim WJ, Lee JY, Park DW, Yun SC, Lee SW, Kim YH, Lee CW, Mintz GS, Park SW, Park SJ. *Comprehensive intravascular ultrasound assessment of stent area and its impact on restenosis and adverse cardiac events in 403 patients with unprotected left main disease.* Circ Cardiovasc Interv, 2011. 4(6): p. 562-9.

13. Toyofuku, M., Kimura T, Morimoto T, Hayashi Y, Shiode N, Okimoto T, Otsuka M, Tamekiyo H, Tamura T, Kadota K, Inoue K, Mitsudo K; j-Cypher Registry investigators. *Comparison of target-lesion revascularisation between left main coronary artery bifurcations and left anterior descending coronary artery bifurcations using the one and two stent approach with sirolimus-eluting stents.* EuroIntervention, 2011. 7(7): p. 796-804.

14. Toyofuku, M., Kimura T, Morimoto T, Hayashi Y, Ueda H, Kawai K, Nozaki Y, Hiramatsu S, Miura A, Yokoi Y, Toyoshima S, Nakashima H, Haze K, Tanaka M, Take S, Saito S, Isshiki T, Mitsudo K; j-Cypher Registry Investigators. *Three-year outcomes after sirolimus-eluting stent implantation for unprotected left main coronary artery disease: insights from the j-Cypher registry.* Circulation, 2009. 120(19): p. 1866-74.

15. Palmerini, T., Sangiorgi D, Marzocchi A, Tamburino C, Sheiban I, Margheri M, Vecchi G, Sangiorgi G, Ruffini M, Bartorelli AL, Briguori C, Vignali L, Di Pede F, Ramondo A, Inglese L, De Carlo M, Bolognese L, Benassi A, Palmieri C, Filippone

V, Barlocco F, Lauria G, De Servi S. *Ostial and midshaft lesions vs. bifurcation lesions in 1111 patients with unprotected left main coronary artery stenosis treated with drug-eluting stents: results of the survey from the Italian Society of Invasive Cardiology.* Eur Heart J, 2009. 30(17): p. 2087-94.

16. Chen, S.L, Xu B, Han YL, Sheiban I, Zhang JJ, Ye F, Kwan TW, Paiboon C, Zhou YJ, Lv SZ, Dangas GD, Xu YW, Wen SY, Hong L, Zhang RY, Wang HC, Jiang TM, Wang Y, Chen F, Yuan ZY, Li WM, Leon MB. *Comparison of double kissing crush versus Culotte stenting for unprotected distal left main bifurcation lesions: results from a multicenter, randomized, prospective DKCRUSH-III study.* J Am Coll Cardiol, 2013. 61(14): p. 1482-8.

17. Freixa, X. Almasood AA, Asif N, Bui S, Ivanov J, Osten MD, Ing D, Overgaard CB, Horlick E, Seidelin PH, Džavík V. *Long-term outcomes using a two-stent technique for the treatment of coronary bifurcations.* Int J Cardiol, 2013. 168(1): p. 446-51.

Figures

Figure 1

A 84 year old patient known with HT and DM presented with stable angina due to important left main and proximal LAD lesion (Upper left). A heart team discussion concluded that PCI was preferred over CABG. IVUS guidance during the procedure demonstrated involvement of the proximal MV and both distal branches (Upper row right A-C: cross sectional images a different locations). Middle row right: After predilation with a 3.0x15 mm SC balloon a Tryton 4.0x3.5x18mm side branch stent was implanted. After rewiring and predilation a Promus DES stent 3.5 x20mm was implanted in the LAD. After proximal optimization with a 4.0 balloon, a final kissing balloon dilation completed the procedure with excellent angiographic result (Lower left) and lumen area as seen on final IVUS (Lower right A'-C') (CABG- Coronary artery bypass graft; DM- Diabetes mellitus; HT-Hypertension; IVUS- Intravascular Ultrasound; LAD- Left Anterior Descending artery; MV- Main Vessel; PCI- percutaneous coronary intervention; SB- Side Branch

Figure 2

Flow chart of study. f/u- Follow up; IVUS- Intravascular Ultrasound; PCI- percutaneous coronary intervention; Quantitative Coronary Angiography (QCA).

Figure 3

Baseline Minimal Luminal Area (MLA) of the Main Branch (MB) (Panel 3A) and the Side branch (SB) (Panel 3B) in patients treated with the Tryton Stenting technique in the left main (LM) bifurcation according to the eventuality of revascularization at 9 month follow-up. The difference in the MLA of the SB was not statistically significant in patients with versus patients without eventual target lesion revascularization (TLR) (Panel 3C).

Table I Baseline clinical characteristics of the study cohort

Baseline Characteristics	**N =30**	
Age, years	68 ± 9	
Male	26	87%
Diabetes	9	30%
Smoker	15	50%
Hypertension	20	67%
Hyercholesterolaemia	22	73%
Previous MI	8	27%
Previous PCI	12	40%
Previous CABG	2	7%
Congestive Heart Failure	2	7%
Renal Dysfunction	2	7%

CABG- Coronary Artery Bypass Surgery

MI- Myocardial Infarct

PCI- Percutaneous Coronary Intervention

Table II Clinical presentation of the study cohort

Clinical Presentation	**N=30**	
Stable Angina	12	40%
Silent ischaemia	8	27%
Unstable Angina	2	7%
Acute Coronary Syndrome	8	27%
NSTEMI	2	7%
STEMI	6	20%

NSTEMI- Non ST-Elevation myocardial infarct

STEMI- ST elevation myocardial infarct

Table III Angiographic characteristics of the treated lesions

Angiographic Characteristics (N=30)		
Medina class		
1,1,1	22	73%
1,1,0	4	13%
1,0,1	2	7%
0,1,1	1	3%
1,0,0	0	0%
0,1,0	0	0%
0,0,1	1	3%
Thrombus	0	0%
Calcification	14	47%
Lesion angle/°		
<30	2	7%
30-79	21	70%
>79	7	23%

Table IV Procedural Characteristics

Stenting Procedure (N=30)	
Pre-dilatation	24 (80%)
Post-dilatation of Tryton stent	27 (90%)
Final kissing balloon	30 (100%)
Tryton stent	-
2.5 - 2.5	2 (7%)
3.0 – 2.5	3 (10%)
3.5 - 2.5	9 (30%)
3.5 - 3.0	16 (53%)
4.0 - 3.5	0
Main Vessel Stent Diameter	3.5 (3.5-4.0)
Length	22 (18-26)
Additional stents	21 (70%)
prox MV	11 (37%)
prox SB	5 (17%)

MV- Main Vessel; SB- Side Branch

Table V Quantitative Angiographic Analysis (QCA) at baseline pre-procedural, post-procedural and 6-month follow-up

N=19	Pre-MLD /mm	Post-MLD /mm	Acute gain /mm	F/u-MLD /mm	Late Loss /mm
Proximal Main Vessel	2.41±0.53	3.82±0.47	1.41±0.62	3.54±0.54	0.28±0.41
Distal Main Vessel	1.61±0.68	2.68±0.50	1.07±0.50	2.51±0.44	0.17±0.37
Side Branch	1.37±0.44	2.43±0.39	1.06±0.38	1.78±0.49	0.65±0.46

MLD- Minimal Lumen Diameter; F/u - Follow up

Table VI Intravascular Ultrasound (IVUS) Analysis of the Main Vessel at baseline and follow up at 6 months

Vessel (N=16)	Minimal Lumen Area /mm^2			Mean Lumen area /mm^2			Neo intimal Plaque area
	Baseline	6 months	p value	Baseline	6 months	p value	6 months
Proximal target region	11.08±1.97	11.59±2.48	0.697	12.31±1.98	12.93±2.75	0.832	0.01±0.56
Bifurcation region	13.80±4.39	13.51±4.33	0.610	14.81±4.31	14.72±4.56	0.908	0.31±0.45
Distal main branch	8.00±1.99	7.42±2.41	0.222	9.40±2.64	9.00±3.25	0.352	0.32±0.75
Distal side branch	6.68±1.80	5.10±2.01	0.004	7.79±2.15	6.53±2.31	0.002	1.59±0.77

Table VII. Clinical Outcome of the Study Cohort (N=30)

In-Hospital Outcome		
Death	0	0%
Myocardial infarction	3	10%
Peri-procedural	2	7%
Target Lesion Revascularization	1	3%
Main Vessel	0	0%
Side Branch	1	3%
6-month Outcome		
Death	0	0%
Myocardial Infarction	4	13%
Peri-procedural	2	7%
Target Lesion Revascularization	4	13%
Main Vessel	0	0%
Side Branch	4	13%

9 Month Outcome		
Death	0	0%
Myocardial infarction	4	13%
Peri-procedural	2	7%
Target Lesion Revascularization	5	17%
Main Vessel	1	3%
Side Branch	4	13%
MACE*	7	23%

***** Defined as a composite of cardiac or non-cardiac death, Q-wave or non-Q-wave MI and ischemia driven target lesion revascularization (TLR).

Figures

Figure 1

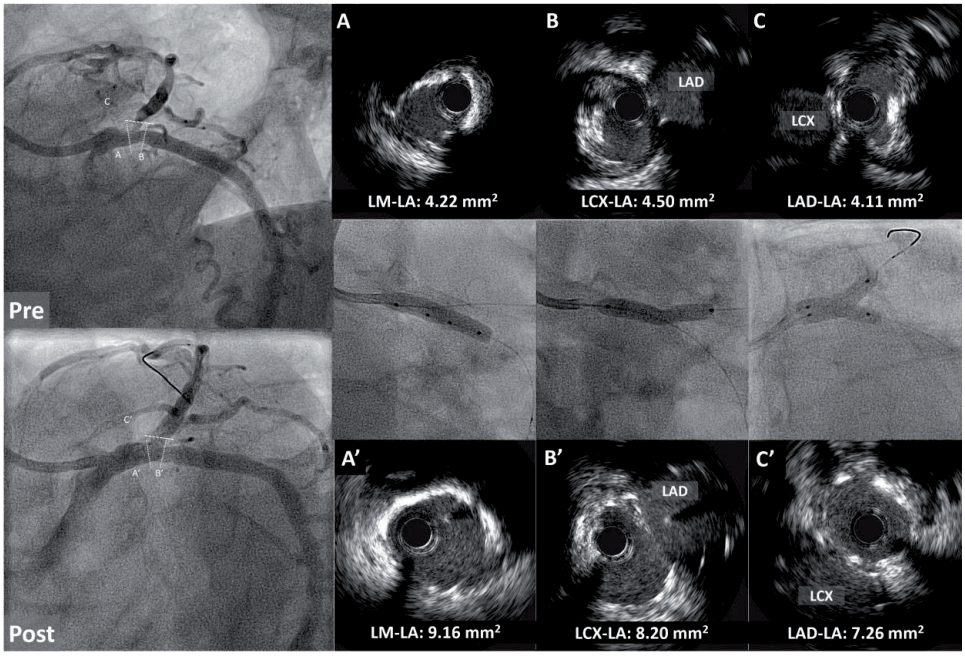

Figure 2

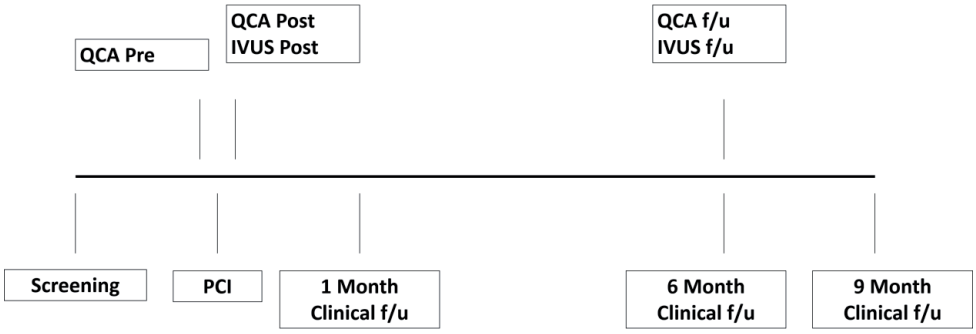
QCA Pre
QCA Post
IVUS Post
QCA f/u
IVUS f/u
Screening
PCI
1 Month
Clinical f/u
6 Month
Clinical f/u
9 Month
Clinical f/u

Figure 3A

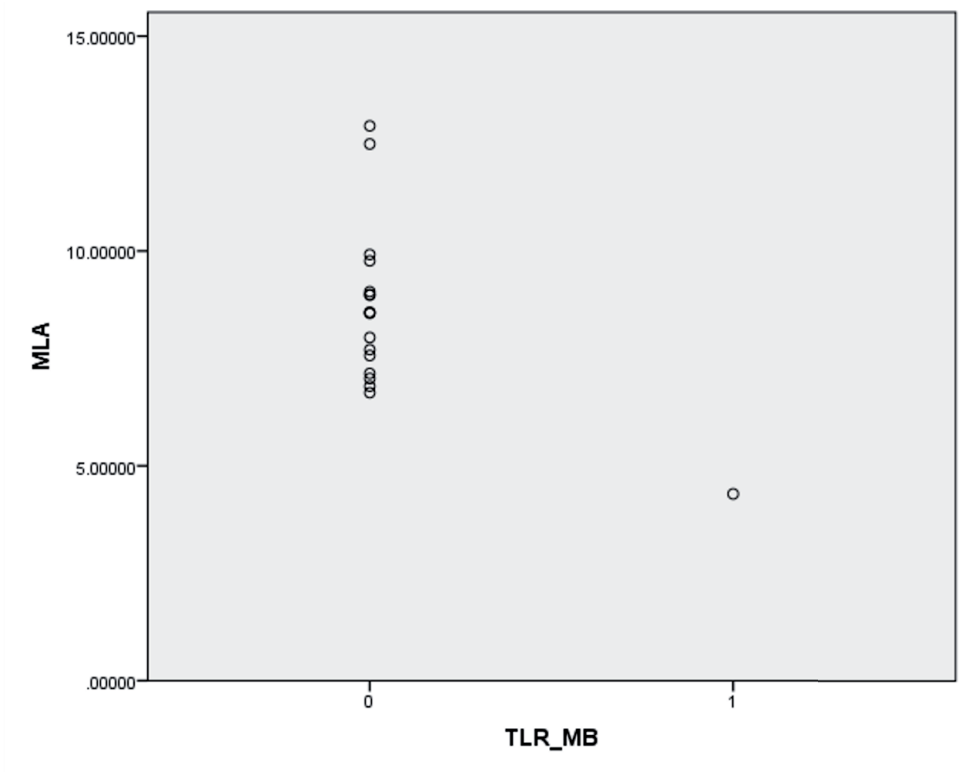

Figure 3B

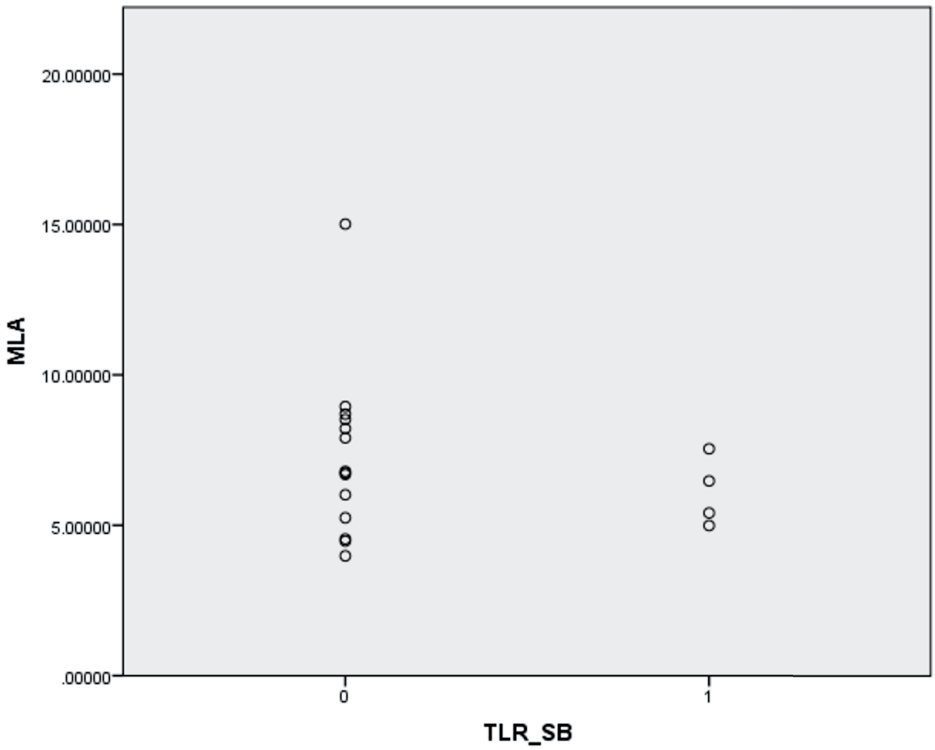

Figure 3C

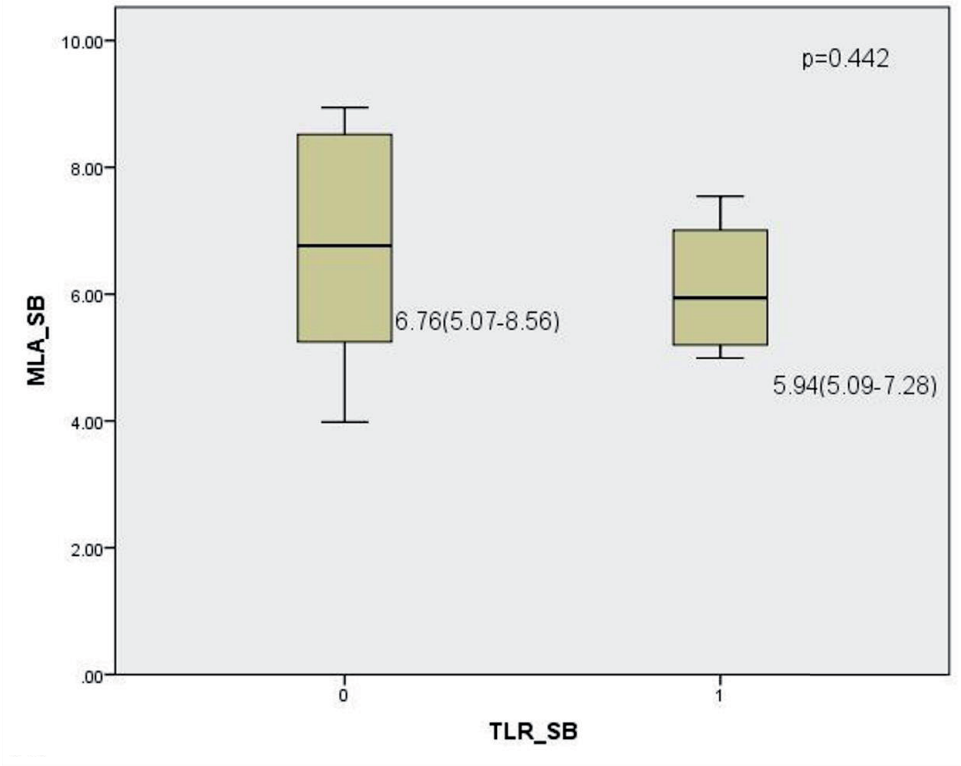
p=0.442
6.76(5.07-8.56)
5.94(5.09-7.28)
MLA_SB
TLR_SB
10.00
8.00
6.00
4.00
2.00
.00
0
1

III

PART

IMPLANTATION TECHNIQUE OF BIORESORBABLE VASCULAR SCAFFOLDS

14

CHAPTER

IMPLANTATION TECHNIQUE FOR BIORESORBABLE SCAFFOLDS

Jiang Ming Fam, Robert-Jan van Geuns.

Cardiac Interventions Today January 2017.

Implantation Technique for Bioresorbable Scaffolds

Device description and patient/lesion selection with the Absorb BVS.

BY JIANG MING FAM, MD, MBBS, AND ROBERT-JAN VAN GEUNS, MD, PHD, FESC, FACC

The need for mechanical support for dilated vessels is temporary; beyond the first few months, there are potential disadvantages to the use of a permanent metallic prosthesis.[1,2] Bioresorbable scaffolds (BRSs) were recently developed as an alternative to metallic stents. BRSs demonstrated complete bioresorption after approximately 3 years, accomplished by vessel lumen enlargement, a reduction of the plaque-to-media ratio, and restoration of vasomotion,[3,4] essentially overcoming the limitations of metallic drug-eluting stents (DESs). The Absorb bioresorbable vascular scaffold (BVS; Abbott Vascular) is the most widely available commercial BRS and has demonstrated in early studies to be safe and efficacious when implanted in simple coronary lesions.[5] Early studies have also suggested that implantation of the Absorb BVS is noninferior to second-generation DESs in terms of clinical outcomes, although these outcomes vary.[6-8]

These varying clinical outcomes have also been attributed to the lack of a standardized protocol in the implementation of a BRS-specific protocol, especially in light of a new device that is structurally different from the newer-generation DESs currently used. The Absorb BVS is constructed of a poly-L-lactide (PLLA) polymer backbone in a semicrystalline composition. To achieve sufficient radial strength, the current strut thickness is 156 µm, almost twice that of current metallic DESs. Even more, overexpansion of these semicrystalline scaffolds is limited to 0.5 mm to avoid rupture of the device during implantation.

Recently, there have been concerns regarding the risk of scaffold thrombosis (ST).[9] Main pathomechanisms include factors pertaining to incomplete lesion coverage, underexpansion of the scaffold, and malapposition. The reported findings of a slightly higher thrombosis rate—early ST in particular—seem to be related to procedural factors such as the implantation technique necessary to compensate for the relative thick struts, similar to first-generation metallic bare-metal stents and DESs, and are therefore potentially preventable.[10,11] The importance of a dedicated implantation protocol for BRSs, including preimplantation plaque modification, routine high-pressure scaffold postdilatation with noncompliant balloons, and the liberal use of intracoronary imaging, such as optical coherence tomography (OCT) to evaluate scaffold apposition and coverage, was highlighted in a recent study that showed that BRS thrombotic rates can be reduced by approximately 70% using a specific implantation technique.[11] In this article, we discuss the standard implantation technique of the Absorb BVS and its potential use in more complex and challenging lesions.

DEVICE DESCRIPTION

The Absorb BVS is composed of a bioresorbable PLLA polymer backbone coated with a thin bioabsorbable poly-D,L-lactide, which allows everolimus to be eluted in a manner identical to that of the Xience V stent (Abbott Vascular). The scaffold is balloon-expandable, and other than two platinum radiopaque markers at each end of the scaffold, the rest of the scaffold is radiolucent, facilitating clear visualization on angiography and other imaging modalities such as cardiac CT. The scaffold edges on each end start within 1 mm of the balloon markers. The radiopaque scaffold markers are not located at the edges of the scaffold, but are placed approximately 1 mm from the proximal edge and 0.3 mm from the distal edge of the scaffold, which is worth noting, especially when implanting overlapping scaffolds.

The first generation of the Absorb BVS (revision 1.0; average strut thickness, 150 µm; crossing profile, 1.4 mm; circumferential out-of-phase zigzag hoops linked together by three longitudinal struts between each hoop) was tested in ABSORB Cohort A.[5] This version unfortunately showed significant angiographic late loss and strut area reduction at 6 months, suggesting loss of radial support before vascular healing was completed.[5] At 2-year follow-up, the concept of bioresorbable technology was finally demonstrated with resorption of the device, late lumen enlargement, restoration of vasomotion, and endothelial function.[12,13] The second-generation Absorb BVS (revision 1.1) underwent modification in the strut design (in-phase zigzag hoops linked by bridges) and polymer manufacturing process. The metabolic process is slower in the second version, thus it provided more lasting mechanical support with reduced recoil. The polymeric scaffold maintains its radial strength for approximately 6 months after implantation and then undergoes a gradual metabolic process through the Krebs cycle into CO_2 and H_2O over the course of 2 to 4 years.[14,15]

GENERAL TECHNICAL CONSIDERATIONS

Technical considerations behind the successful implantation of the Absorb BVS are largely related to mechanical and structural properties of the polymeric scaffold structure. The current scaffold has relatively thick struts (156 µm) to maintain its radial strength. After the crimping process, the crossing profile (1.4 mm) is significantly larger than a contemporary metallic DES.[16] This has implications on device delivery and trackability, creation of flow disturbances, and delays in scaffold re-endothelialization, possibly accounting for the differences seen in procedure duration, device success rates, and event rates in myocardial infarction (MI) and ST at 12 months.[17-19] Table 1 summarizes the limitations and their impact on percutaneous coronary intervention (PCI).[20] The situation is exacerbated by operators' varying experience with Absorb BVS implantation, inconsistencies in device sizing, lesion preparation, routine high-pressure postdilation, and guidance with intracoronary imaging. Only 66.2% of patients treated with Absorb in four randomized trials had postdilation, and 23.9% underwent intracoronary imaging.[21]

A BRS-specific implantation protocol is based on following the five simple rules:

- Prepare the lesion
- Properly size the vessel
- Pay attention to the expansion limits of the scaffold
- Postdilate the BRS with a properly sized noncompliant balloon
- Pay attention to dual antiplatelet therapy and patient compliance

PATIENT AND LESION SELECTION

In general, patients who may benefit from BRS implantation are younger and have longer lesions, as long metallic stents are associated with an increased risk of stent failure.[22] Lesions that cannot be adequately predilated, such as when the predilation balloon cannot fully expand or when residual stenosis exceeds 40%, may not be considered for a BRS because the BRS with relatively thick struts would be underexpanded, increasing the potential risk of ST.[11] Other factors to be considered include lesions that may pose potential deliverability issues, such as vessel tortuosity (vessels with extreme angulation of the segment proximal to the lesion) or heavily calcified lesions, and should be avoided. In such lesions, the thick polymeric struts of the scaffold with a large crossing profile may cause a buildup of friction between the device and lesion/catheter, increasing the risk of scaffold dislodgement during forceful movement in delivering the scaffold,

TABLE 1. LIMITATIONS AND ASSOCIATED IMPACT OF ABSORB BVS ON PCI

Technical Considerations	Effect on Procedural Technique and Outcomes
Thicker struts	• Higher crossing profile leading to reduced deliverability, particularly in calcified lesions • Predisposed to increased turbulence • Increased risk of malapposition or scaffold underexpansion • Potential increased risk of coronary dissections, side branch occlusion, and periprocedural myocardial infarct
Strongly recommended lesion preparation such as 1:1 predilation	• Particularly in lesions that are calcified • Potentially requires more elaborate lesion debulking techniques such as the use of cutting balloons or rotational atherectomy
Limited scaffold lengths and diameters	• Need for longer or overlapping stents
Limited compatibility with guide extension catheter	• Limited
Expansion limits restricts "upsizing" due to risk of scaffold fracture associated with overdilatation	• Require accurate preprocedural sizing • Increased use of intravascular imaging or assessment leading to longer procedure times

especially when used by relatively inexperienced operators.[21] Ideally, new operators of BRSs should start with stable, simpler lesions in stable patients and build up their expertise gradually before attempting implantation of the BRS in more complex lesions.

Rule 1: Prepare the Lesion

It is highly recommended to achieve adequate lesion preparation by using semi- or noncompliant balloons with a diameter equal or just undersized compared to the reference diameter of the BRS device selected (1:1 predilation). Sometimes, short, high-pressure balloons may be used to treat isolated segments of underexpansion.

Rule 2: Properly Size the Vessel

Exact vessel sizing and compliance to manufacturers' guidelines on scaffold matching of lumen dimension are crucial. An analysis of the nominal BVS scaffold size to quantitative coronary angiography (QCA) maximum reference vessel diameter and to clinical outcomes was reported in a pooled patient-level analysis involving > 1,200 patients from three ABSORB studies.[23] Subjects in the "scaffold oversize" group (defined as subjects with both proximal and distal maximum reference vessel diameters smaller than nominal scaffold size) experienced higher rates of major cardiovascular events and target vessel MI than those in the "scaffold non-oversize" group (defined as those in whom the proximal or distal maximum reference vessel diameter was larger than that of the scaffold). In ABSORB III, if vessels < 2.25 mm were excluded from the analysis, the incidence of ST was equivalent to the Xience EES.[6] Compliance to vessel sizing guidelines may further improve target lesion failure by reducing the incidence of MI and ST. Thus, implanting BRSs in vessel sizes that are too small (mean reference vessel external elastic lamina diameter < 2.5 mm, which corresponds to a reference vessel diameter of 2.25 mm on QCA) should be avoided.

Because the Absorb BVSs have thicker struts, preferably, long regions of scaffold overlap should be avoided because it increases the risk of ST and side branch occlusion. In addition, polymers are invisible under x-ray, with the exception of two radiopaque edge markers. Therefore, placement of the scaffold can be difficult, especially in regions of significant overlap or foreshortening.

Rule 3: Pay Attention to the Expansion Limits of the Scaffold

Compared to DESs, BRSs have a limited range of expansion (ie, 0.5 mm more than the reference diameter) due to their polymeric composition, limiting their use in cases of vessel tapering (Table 2). Huge malapposition can be uncorrectable and persist at follow-up until resorption occurs, and attempts to correct large malapposition by overexpansion with a large balloon can lead to scaffold disruption (Figure 1).

TABLE 2. SIZING RECOMMENDATION FOR ABSORB BVS

Proximal and Distal Reference Diameters of Target Vessels (mm)	Recommended Diameter of the Absorb BVS Scaffold (mm)
> 2.5, < 2.75	2.5
> 2.75, < 3.25	3
> 3.25, < 3.75	3.5

Scaffold implantation. Delivery of the BRS requires the application of gentle constant pressure to the lesion through a 6 F or larger guiding system. The main difference from the metallic stents is that balloon inflation for scaffold deployment should be gradual (2 atm every 5 seconds), with a minimum inflation duration of 30 seconds. When difficulties are encountered during delivery of the BRS, active support with the guiding catheter in the form of deep-vessel intubation may alleviate this problem, but there is a risk of coronary dissection with potentially disastrous consequences. Other methods to overcome this problem include vessel straightening with a second buddy wire[24] or buddy balloon,[25] the use of an anchor balloon,[26] and the use of an extra back-up support guiding catheter or a guide extension.[27]

Rule 4: Postdilate the BVS With a Properly Sized Noncompliant Balloon

Operators should aim to achieve to cover ≥ 2 mm of the healthy vessel at either edge of the treated lesion using the BRS, with a result of < 10% residual stenosis

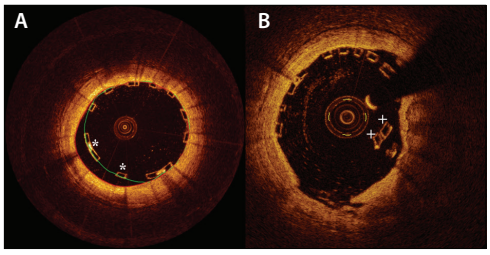

Figure 1. Malapposed struts (indicated by *) (A). Attempts to correct large malapposition by overexpansion with a large balloon can lead to acute disruption of the scaffold (disrupted struts indicated by +) (B).

after deployment of the BRS with optimal scaffold expansion and apposition.[1] Performing postdilation using high-pressure balloons (> 16 atm) for 10 to 30 seconds is frequently required, and an optimal result is confirmed using intravascular imaging.

Role of intravascular imaging. The application of IVUS and OCT, a light-based intravascular imaging technology,[28] has enabled us to address the challenges facing the use of BRSs and overcome the limitations of angiography in assessing the significance of coronary stenosis and the results of PCI in a clinical setting.[29] The advantages of using intracoronary imaging include the capability to provide accurate luminal measurements and optimal detection of scaffold malapposition and fracture, which cannot be reliably detected on a simple angiogram. One main advantage of IVUS is the high depth of penetration that allows direct and easy visualization of total vessel diameter and area, allowing operators to optimize scaffold size without increasing the risk of disruption with oversized balloons.[30]

There are also advantages to using OCT in the deployment of BRSs. OCT was one of the most useful techniques for the early evaluation of the Absorb BVS and its resorption process. New OCT probes are low-profile (2.6–2.7 F), flexible, coated with a hydrophilic layer, and the acquisition speed is at least 10 times higher when compared to IVUS. OCT catheters have a low delivery profile and can pass almost every lesion with few anatomical or patient exclusion criteria. The OCT imaging procedure is safe[30] and fast, providing all necessary information in just seconds (Figure 2).[31] The latest European Society of Cardiology guidelines on myocardial revascularization has already recommended OCT as a tool in selected patients to optimize stent implantation (level of evidence class II B, level C).[29]

An improvement in clinical and angiographic outcomes with intracoronary imaging-guided PCI was first shown in the use of IVUS.[32] In a meta-analysis, IVUS-guided DES deployment compared with standard angiographic guidance was associated with a reduced incidence of major adverse cardiac events.[33] The advantages of imaging guidance observed by IVUS may also apply to OCT, which was supported by findings of an observational study in which angiographic plus OCT guidance was associated with a significantly lower risk of cardiac mortality or MI, even after multivariate adjustment or propensity score-adjusted analyses.[34] Preliminary observations support a potentially beneficial role of OCT during BVS implantation in improving outcomes.[9]

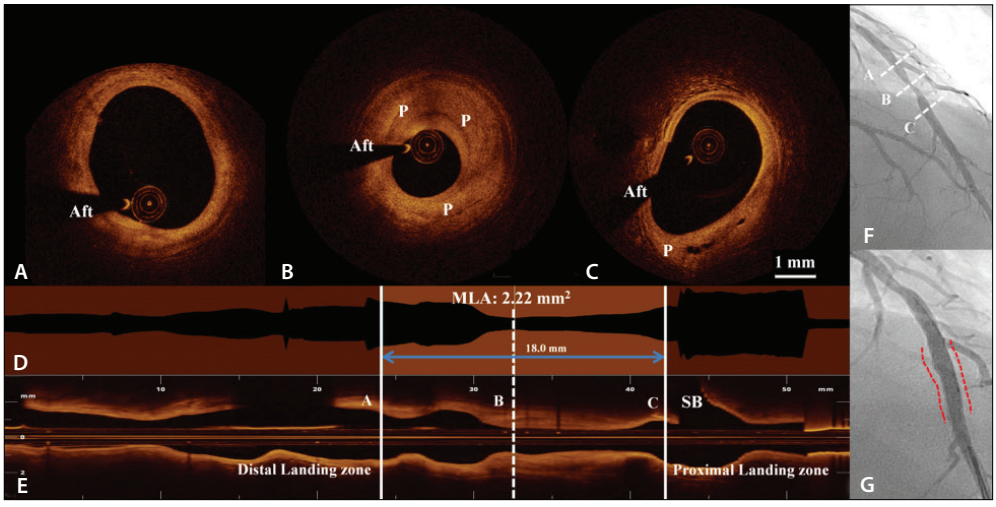

Figure 2. "Virtual PCI" planning. OCT images of the left anterior descending artery before scaffold implantation showing the distal landing zone (A), minimal lumen area (B), and proximal landing zone (C). OCT can assess lumen dimensions accurately, assess underlying plaque composition, and shows the location of the minimal lumen area in relation to the treated vessel on the lumen profile (D). In this way, OCT can guide scaffold implantation strategy by assessing the scaffold length (18 mm, in this example) required for optimal lesion coverage and avoiding SB ostia. The SB is seen on the longitudinal profile (E). The LAD is shown before (F) and after (G) implantation of a 3- X 18-mm Absorb BVS (dashed line). Aft, guidewire artifact.

Rule 5: Pay Attention to Dual Antiplatelet Therapy and Patient Compliance

A minimum duration of 12 months of dual antiplatelet therapy is suggested in both stable and acute patients treated with a BRS. However, an even longer duration of dual antiplatelet therapy (18–24 months) and/or more potent antiplatelet medications, such as ticagrelor or prasugrel, may be used depending on the risk-benefit balance between thrombotic/ischemic risk and bleeding risk.

CONCLUSION

Procedure- and lesion-related factors play an important role in acute procedural success, and various technical difficulties can be encountered in the implantation of the Absorb BVS. The impact of these factors may be mitigated by systematically applying the BRS implantation recommendations. The long-term success of BRSs relies on a combination of careful patient and lesion selection with proper implantation technique and optimization of procedural results in the clinical arena. By taking proactive steps to perform accurate patient/lesion selection and implement an optimal implantation technique, risks of adverse outcomes will be minimized, translating into improved clinical outcomes. ■

1. Tamburino C, Latib A, van Geuns RJ, et al. Contemporary practice and technical aspects in coronary intervention with bioresorbable scaffolds: a European perspective. EuroIntervention. 2015;11:45-52.
2. Stefanini GG, Holmes DR Jr. Drug-eluting coronary-artery stents. N Engl J Med. 2013;368:254-265.
3. Simsek C, Karanasos A, Magro M, et al. Long-term invasive follow-up of the everolimus-eluting bioresorbable vascular scaffold: five-year results of multiple invasive imaging modalities. EuroIntervention. 2016;11:996-1003.
4. Karanasos A, Simsek C, Gnanadesigan M, et al. OCT assessment of the long-term vascular healing response 5 years after everolimus-eluting bioresorbable vascular scaffold. J Am Coll Cardiol. 2014;64:2343-2356.
5. Ormiston JA, Serruys PW, Regar E, et al. A bioabsorbable everolimus-eluting coronary stent system for patients with single de-novo coronary artery lesions (ABSORB): a prospective open-label trial. Lancet. 2008;371:899-907.
6. Ellis SG, Kereiakes DJ, Metzger DC, et al. Everolimus-eluting bioresorbable scaffolds for coronary artery disease. N Engl J Med. 2015;373:1905-1915.
7. Gao R, Yang Y, Han Y, et al. Bioresorbable vascular scaffolds versus metallic stents in patients with coronary artery disease: ABSORB China trial. J Am Coll Cardiol. 2015;66:2298-2309.
8. Kimura T, Kozuma K, Tanabe K, et al. A randomized trial evaluating everolimus-eluting Absorb bioresorbable scaffolds vs. everolimus-eluting metallic stents in patients with coronary artery disease: ABSORB Japan. Eur Heart J. 2015;36:3332-3342.
9. Karanasos A, Van Mieghem N, van Ditzhuijzen N, et al. Angiographic and optical coherence tomography insights into bioresorbable scaffold thrombosis: single-center experience. Circ Cardiovasc Interv. 2015;8:pii:e002369.
10. Cassese S, Byrne RA, Ndrepepa G, et al. Everolimus-eluting bioresorbable vascular scaffolds versus everolimus-eluting metallic stents: a meta-analysis of randomised controlled trials. Lancet. 2016;387:537-544.
11. Puricel S, Cuculi F, Weissner M, et al. Bioresorbable coronary scaffold thrombosis: multicenter comprehensive analysis of clinical presentation, mechanisms, and predictors. J Am Coll Cardiol. 2016;67:921-931.
12. Serruys PW, Ormiston JA, Onuma Y, et al. A bioabsorbable everolimus-eluting coronary stent system (ABSORB): 2-year outcomes and results from multiple imaging methods. Lancet. 2009;373:897-910.
13. Onuma Y, Serruys PW, Gomez J, et al. Comparison of in vivo acute stent recoil between the bioresorbable everolimus-eluting coronary scaffolds (revision 1.0 and 1.1) and the metallic everolimus-eluting stent. Catheter Cardiovasc Interv. 2011;78:3-12.
14. Oberhauser JP, Hossainy S, Rapoza RJ. Design principles and performance of bioresorbable polymeric vascular scaffolds. EuroIntervention. 2009;5(suppl F):F15-F22.
15. Serruys PW, Onuma Y, Garcia-Garcia HM, et al. Dynamics of vessel wall changes following the implantation of the absorb everolimus-eluting bioresorbable vascular scaffold: a multi-imaging modality study at 6, 12, 24 and 36 months. EuroIntervention. 2014;9:1271-1284.
16. Iqbal J, Onuma Y, Ormiston J, et al. Bioresorbable scaffolds: rationale, current status, challenges, and future. Eur Heart J. 2014;35:765-776.
17. Stone GW, Gao R, Kimura T, et al. 1-year outcomes with the Absorb bioresorbable scaffold in patients with coronary artery disease: a patient-level, pooled meta-analysis. Lancet 2016;387:1277-1289.
18. Capodanno D, Gori T, Nef H, et al. Percutaneous coronary intervention with everolimus-eluting bioresorbable vascular scaffolds in routine clinical practice: early and midterm outcomes from the European multicentre GHOST-EU registry. EuroIntervention 2015;10:1144-53.
19. Panoulas VF, Miyazaki T, Sato K, et al. Procedural outcomes of patients with calcified lesions treated with bioresorbable vascular scaffolds. EuroIntervention. 2016;11:1355-1362.
20. Rizik DG, Hermiller JB, Kereiakes DJ. The ABSORB bioresorbable vascular scaffold: a novel, fully resorbable drug-eluting stent: current concepts and overview of clinical evidence. Catheter Cardiovasc Interv. 2015;86:664–677.
21. Ishibashi Y, Onuma Y, Muramatsu T, et al. Lessons learned from acute and late scaffold failures in the ABSORB EXTEND trial. EuroIntervention. 2014;10:449-457.
22. Kobayashi Y, De Gregorio J, Kobayashi N, et al. Stented segment length as an independent predictor of restenosis. J Am Coll Cardiol. 1999;34:651-659.
23. Ishibashi Y, Nakatani S, Sotomi Y, et al. Relation between bioresorbable scaffold sizing using QCA-Dmax and clinical outcomes at 1 year in 1,232 patients from 3 study cohorts (ABSORB Cohort B, ABSORB EXTEND, and ABSORB II). JACC Cardiovasc Interv. 2015;8:1715-1726.
24. Burzotta F, Trani C, Mazzari MA, et al. Use of a second buddy wire during percutaneous coronary interventions: A simple solution for some challenging situations. J Invasive Cardiol. 2005;17:171-174.
25. Li SS, Cheng CW. Coronary angioplasty on an impassable calcified stenosis using a buddy balloon technique. Catheter Cardiovasc Interv. 2004;62:35-37.
26. Fujita S, Tamai H, Kyo E, et al. New technique for superior guiding catheter support during advancement of a balloon in coronary angioplasty: the anchor technique. Catheter Cardiovasc Interv. 2003;59:482-488.
27. Rao U, Gorog DA, Szygula J, et al. The GuideLiner "child" catheter. EuroIntervention. 2010;6:277-279.
28. Lowe HC, Narula J, Fujimoto JG, Jang IK. Intracoronary optical diagnostics current status, limitations, and potential. JACC Cardiovasc Interv. 2011;4:1257-1270.
29. Kolh P, Windecker S. ESC/EACTS myocardial revascularization guidelines 2014. Eur Heart J. 2014;35:3235-3236.
30. Roy P, Steinberg DH, Sushinsky SJ, et al. The potential clinical utility of intravascular ultrasound guidance in patients undergoing percutaneous coronary intervention with drug-eluting stents. Eur Heart J. 2008;29:1851-1857.
31. van der Sijde JN, Karanasos A, van Ditzhuijzen NS. Safety of optical coherence tomography in daily practice: a comparison with intravascular ultrasound [published online March 18, 2016]. Eur Heart J Cardiovasc Imaging.
32. Foin N, Lee R, Mattesini A, et al. Bioabsorbable vascular scaffold overexpansion: insights from in vitro post-expansion experiments. EuroIntervention. 2016;11:1389-1399.
33. Shin DH, Hong SJ, Mintz GS, et al. Effects of intravascular ultrasound-guided versus angiography-guided new-generation drug-eluting stent implantation: meta-analysis with individual patient-level data from 2,345 randomized patients. JACC Cardiovasc Interv. 2016;9:2232-2239.
34. Prati F, Di Vito L, Biondi-Zocca G, et al. Angiography alone versus angiography plus optical coherence tomography to guide decision-making during percutaneous coronary intervention: the Centro per la Lotta contro l'Infarto-Optimisation of Percutaneous Coronary Intervention (CLI-OPCI) study. EuroIntervention 2012;8:823-829.

Jiang Ming Fam, MD, MBBS
Consultant
Department of Cardiology
National Heart Centre Singapore
Singapore
Disclosures: None.

Robert-Jan van Geuns, MD, PhD, FESC, FACC
Professor of Interventional Cardiology
Department of Cardiology
Thorax Centre
Erasmus Medical Centre
Rotterdam, The Netherlands
r.vangeuns@erasmusmc.nl
Disclosures: Research grants and speaker fees from Abbott Vascular.

15

CHAPTER

AVOIDING LATE ACQUIRED BIORESORBABLE SCAFFOLD MALAPPOSITION

Jiang Ming Fam; Antonis Karanasos, Robert-Jan van Geuns.

Submitted for publication.

AVOIDING LATE ACQUIRED BIORESORBABLE SCAFFOLD MALAPPOSITION

Jiang Ming, Fam, MBBS[1,2]; Antonios Karanasos; MD, PhD[1]; Robert-Jan van Geuns, MD, PHD[1]

1- Thoraxcentre, Erasmus MC, Rotterdam, Netherlands
2- National Heart Centre Singapore, Singapore

Address for correspondence:

Robert-Jan van Geuns

Department of Cardiology

Thoraxcentre

Erasmus University Medical Centre

‘s-Gravendijkwal 230

3015 GE Rotterdam, The Netherlands

Tel: +31 (0)10 703 33 48

Fax: +31 (0)10 703 52 54

E-mail: r.vangeuns@erasmusmc.nl

Word Count: 6737 (Abstract, Main Text, References, Tables and Figure Legends)

Abstract

Introduction: Scaffold malapposition (ScM) refers to the separation of at least one scaffold strut from the artery's intimal surface with evidence of blood behind the strut, in a segment without the presence of side branches. ScM has been linked to an increased risk of scaffold thrombosis, a potentially life threatening clinical complication which has significant negative impact on the therapeutic potential of bioresorbabe scaffolds (BRS). ScM can be classified as early (during the time of scaffold implantation), late persistent (i.e., already present after index procedure and persistent at follow-up assessment) or late acquired (i.e., not present after index procedure initially, but identified at follow-up assessment). Disintegration as part of the bioresorption of malapposed struts may create a local instability triggering thrombosis. A complex interaction of factors during the scaffold implantation and subsequent vascular healing process may drive some of the pathomechanisms behind late acquired ScM (LAScM). LAScM is more commonly seen when there is vessel- scaffold size mismatch, in certain clinical scenarios such as acute coronary syndromes and certain anatomic subsets such as CTOs and large calibre vessels. Knowledge of the risk factors and possible pathomechanisms behind LAScM may help mitigate the risks of LAScM and its predisposition to scaffold thrombosis.

Areas Covered: This review aims to describe the types of scaffold malapposition with a focus on LAScM, possible pathophysiology and risk factors, imaging findings, its impact in various clinical and anatomic subsets and ways to reduce LAScM.

Expert commentary: Late malapposition after bioresorbable scaffolds pose a significant problem in part due to the predisposition to scaffold thrombosis. Late malapposition can be the result of acute malapposition or acquired during plaque remodelling. Both can be

minimalized by the use of a proper and meticulous implantation technique using adequate predilation, proper sizing and postdilatation with adequate size balloons supported by the judicious use of intravascular imaging.

Introduction

Bioresorbable vascular scaffolds (BRS) are a new treatment for obstructive coronary lesions, with the ultimate aim to eradicate permanent metallic caging of the treated vessel, promising to restore physiological function of the treated vessels [1]. Initial observations in stable patients have shown a favourable healing response of an everolimus-eluting BVS (ABSORB BVS 1.1; Abbott Vascular; Santa Clara; CA; USA) with low rates of uncovered and malapposed struts at mid-term follow-up [2-3] and restoration of the vascular phenotype at long-term.[4]; While there is a theoretical value proposition associated with BRS due to the complete resorption process, current generation BRS faced several limitations such as thicker and wider struts, less radial strength and limited expansion. As a consequence clinical outcomes up to 3 years were inferior [5], in particular certain lesion subsets such as smaller vessels with the BRS compared with best in class DES, with the BRS showing either similar or increased risk of TLR and increased risks of scaffold thrombosis (ScT) compared to DES [6-9].

Scaffold malapposition (ScM), also referred to as incomplete scaffold apposition (ISA), is defined by the separation of at least one scaffold strut from the intimal surface of the arterial wall with evidence of blood behind the strut, as seen on intravascular imaging, in a segment without the presence of side branches [10]. Due to insufficient resolution, it is not possible to detect ScM on plain angiography. Detection of ScM requires the use of intravascular imaging modalities, namely either intravascular ultrasound (IVUS) or optical coherence tomography (OCT) [11]. It may be seen to occur during the time of scaffold implantation (early ScM) or during follow up (late ScM). Late scaffold malapposition can be further classified into 1) late persistent ScM (i.e., already present after index procedure and persistent at follow-up assessment); and 2) late acquired scaffold malapposition (LAScM) (i.e., not present after

index procedure initially, but identified at follow-up assessment) [**Figure 1**]. Late acquired scaffold malapposition (LAScM) is thus defined when it is documented at follow-up intravascular imaging despite appropriate apposition of the scaffold during the index procedure. In the absence of baseline imaging, ScM seen on intravascular imaging performed after an index procedure is classified as LAScM [12].

Not all patients who actually develop LAScM may be detected, since performing intracoronary imaging on follow-up after scaffold implantation is not done routinely. The reported incidence of stent malapposition has increased in the era of drug eluting stents (DES), involving up to 25% of the procedures where a stent is implanted [13-14]. Reports have suggested that late stent malapposition may be associated with very late stent thrombosis [15-16]. There is thus a need to further understand the significance of late ScM especially in light of findings that suggest that BRS may exhibit an increased risk of device thrombosis compared to DES [6-9], especially it may be a potentially preventable risk factor in ScT [17]. This review aims to describe the types of scaffold malapposition, possible pathophysiology and risk factors, imaging findings, its impact in various clinical and anatomic subsets and ways to reduce malapposition.

Pathophysiology of late acquired ScM

While late persistent ScM can be as a result of initial inadequate stent implantation either from a) marked mismatch between stent size selection and luminal dimensions (i.e., stent diameter smaller than reference lumen diameter), [18]; or b) stent underexpansion despite an adequate stent–artery ratio due to several different factors, such as inadequate pressure of implantation and/or plaque/ calcium-related factors; pathophysiological mechanisms involved in LAScM are different. Main mechanisms behind LAScM include positive arterial remodelling [19-21], and plaque volume reduction/thrombus dissolution [19, 22]. Other

postulated mechanisms include chronic stent recoil [23] and inadequate (i.e., insufficient and/or delayed) neointimal hyperplasia [24-25]; and localised hypersensitivity reactions and chronic inflammation [26]. Positive remodelling results from the increase of total vessel area [defined by the change in the cross sectional area of the external elastic membrane seen on either IVUS or optical coherence tomography (OCT)] out of proportion to the increase in persistent plaque and media area, such that the vessel pulls away from the stent [11, 13, 27]. Inflammatory reactions seen in the intima and media such as extensive vasculitis, apoptosis, eosinophil and lymphocyte infiltration, and necrosis (that have not been observed with BMS) have been observed in autopsy studies of specimens involving DES thrombosis [26]. Inflammatory changes that probably represent the local effect of the drug or the polymer in the DES may account for the increased incidence of late acquired stent malapposition seen in DES in comparison to BMS [11, 28].

Another pathophysiological mechanism of LAScM is related to plaque volume reduction. The most common case is related to thrombus dissolution, usually after scaffold deployment in acute myocardial infarction patients, that results in strut detachment from the vessel wall. Other factors include plaque volume reduction from the BRS implantation and possibly intensive statin therapy. Another reason why late ScM may be prevalent in BRS can be due to the postulated Glagovian effect of vessel expansive remodelling with late lumen gain [29].

Need for lesion selection and accurate lesion sizing

Further elucidation of the underlying mechanisms involved in LAScM is important as it identifies the causes or mechanisms which are potentially preventable and how procedural steps may be undertaken to mitigate the risks of LAScM and its adverse effects [10,]. Causes/ mechanisms for the development of LASM can be divided into two broad categories: clinical and periprocedural (lesion/procedure/materials used) parameters; they are summarised in

Table 1. A marked mismatch between scaffold size selection and luminal dimensions can result in undersizing of the scaffold and predispose to adverse events such as increased target lesion revascularisation [30]. Inappropriate scaffold size selection even in appropriate vessel sizes could result in oversizing or underexpansion of the scaffold which has been associated with increased scaffold thrombosis [31]. Implantation of a relatively 'large' scaffold in a relatively small vessel would result in an incomplete expansion of the BRS and a large scaffold footprint. As a result the scaffold remains crimped, exacerbated by a lower tensile strength and thicker strut thickness of the scaffold relative to other metallic DES, creating increased area of endothelial shear stress which may predispose to increased thrombosis. In addition, the oversized scaffold could create vessel dissection in a small target vessel [**Figure 2]**. Conversely, implantation of a relatively small scaffold in a relative larger vessel can result in incomplete apposition, predisposing to scaffold thrombosis particularly if DAPT is prematurely terminated [32].

Imaging findings of LAScM

Although LAScM was originally reported as an IVUS phenomenon, OCT has emerged to become an alternative light-based intravascular imaging tool used in the evaluation of device outcomes in view of its higher resolution [33]. In addition, OCT probes are of low profile, flexible, coated with a hydrophilic layer, and the acquisition speed is at least ten times higher compared with intravascular ultrasound (IVUS). These enabled procedurists to overcome the limitations of angiography in assessing the significance of coronary stenosis and results of PCI in a clinical setting [33]. The advantages of using OCT in the deployment of BRS include the capability to provide accurate luminal measurements, optimal detection of scaffold malapposition and fracture which cannot be detected reliably on plain angiography

[34]. Previous studies have also demonstrated the higher sensitivity of OCT compared with IVUS for the detection of malapposed stent struts [35].

OCT analysis for BVS can be performed offline by dedicated software (QCU-CMS, Leiden, the Netherlands) throughout the scaffolded segment and 5mm-long edge segments at 1mm intervals, using previously described methodology [36-37]. OCT analysis include strut coverage and apposition patterns, other evaluated parameters include coverage thickness and malapposition distance, healing score and morphometric measurements.

Apposition. In metallic stents, only the reflection of the adluminal strut surface is visualized by OCT. The evaluation of malapposition in PLLA based BRS is different from that of metallic stents [37]. The frequency of malapposed struts is potentially overestimated using the metallic methods compared to BRS methods. In metallic stents, diffuse high intensity signal artefacts ("blooming artefacts") are seen due to the attenuation of signal behind the metallic surface. Metallic struts are classified as malapposed if the distance from the midpoint of the bright leading edge to the interpolated lumen contour exceeds the strut thickness (including polymer, if present)[38, 39] . In this method, partially malapposed struts (a part of the strut is in contact with the vessel wall, which is invisible due to outer shadow) are counted as malapposed struts. In polymeric devices, the contact of struts with the vessel wall is directly visible [36-37]. Strut malapposition in PLLA based BRS was defined by the absence of contact between abluminal strut border and vessel wall, with the exception of struts located in front of side branches or their ostium, which were defined as side branch-related struts. (**Figure 3 panels J and N)**. For magnesium based BRS methodology is similar to permanent metallic stents. For BRS of other materials like Tyrosine, imaging characteristics may be different and thus methods may have to be adjusted.

There were initial concerns that rim-like tissue flaps might compromise flow after significant scaffold mass loss due to bioresorption. However, three-dimensional renderings demonstrate that these tissue rims are fixed bilaterally to the vessel wall, thus implying limited mobility, similar to the 'neo-carina' finding, described in side-branch jailing by BRS [40]. Similarly, strut connection to the vessel wall only through their abluminal surface creates the appearance of outward vessel bulges, also dubbed 'crenellated appearance' or 'evaginations' [25, 41-42]. These findings have been described in metallic DES and attributed to be either a form of vascular response to early ScM [25], or positive vessel remodelling [41]. Resolution of thrombus and improvement in vascular tone may account for the increase in LAScM in STEMI cases [43]. The exact clinical implications of this pattern for BRS healing remain unclear.

Significance of malapposition and risk of scaffold thrombosis

While stent malapposition seems to be benign after implantation of permanent metallic stents [13-14], scaffold malapposition was among the most frequent OCT findings in reported ScT cases. If the scaffold is not in contact with the vessel wall at the time of implantation, the tissue coverage required to integrate the scaffold into the vessel such that it does not collapse into the lumen during the scaffold resorption may be reduced. If the strut is not well covered by neointima and late discontinuity allow protrusion of the struts into the lumen hence exposing the thrombogenic provisional matrix into contact with blood, this form of late scaffold discontinuity may be a cause of thrombosis. Strut coverage has been considered an important component of vascular healing, with malapposition linked to late thrombotic events in pathologic and OCT studies [44, 45]. Though no prospective study has yet linked LAScM to late ScT, recent research have identified ScM as a significant predictor of ScT [46]. A series of ScT cases investigated by OCT has already been published. Sotomi et al have summarised all published cases of early (N=17), late (N=10) and very late (N=16) ScT that

underwent intracoronary imaging at the time point of thrombosis [46]. The most frequent findings associated with early ScT were malapposition (24%), incomplete lesion coverage (18%), and device underexpansion (12%). The degree of SM, in terms of extent of malapposition area as well as length and distance [33], seems to be proportionally related to the risk of clinical events. A shorter strut-vessel distance ≤ 270 μm was the best cut off value for predicting resolved strut malapposition in one study [25]. This could be due to the partial endothelisation of malapposed scaffold struts that predispose to fibrin deposition and ultimately ScT [14, 47]. As the resorption process of the malapposed struts in BRS may differ from that of metallic DES, clinical events that result may vary compared to DES.

Special considerations

While little data on LAScM rates were available, various studies have been done looking at late malapposition in DES. Predictors of late malapposition post DES implantation were total stent length, primary stenting in acute myocardial infarction, and chronic total occlusion lesions [27]. Late-stent malapposition after DES implantation was not associated with any major adverse cardiac events during a subsequent 10-month (mean) follow-up. In a meta-analysis involving 1,834 patients (972 DES, and 862 BMS) from 12 randomized trials that compared DES and BMS and included IVUS follow up, the risk of developing late-acquired incomplete stent apposition was 2.5 times higher after DES versus BMS implantation (6.5% vs. 2.6% in those allocated to BMS; OR 2.48, 95% CI 1.26 to 4.87; p = 0.008) [28].

Acute Coronary Syndromes

Implantation of metallic DES during STEMI has been associated with lower strut coverage and higher incomplete stent apposition at follow-up compared to stable angina [27]. In a detailed OCT analysis 3 days post primary PCI comparing the frequency and mechanisms of incomplete stent apposition in self expanding and balloon expandable stents, 14.8% of the

segments in balloon expandable stents showed newly acquired incomplete stent apposition. These may be due to tissue resorption, vasorelaxation and “early” recoil in balloon-expandable stents [43]. Other possible reasons include the increased thrombus burden and vasoconstriction in the setting of acute STEMI leading to underestimation of the actual size of the infarct-related artery, and the risk of the implantation of undersized stents [48]. This may, in turn, contribute to malapposition, restenosis or stent thrombosis [49]. While initial observations in stable patients have shown good procedural results with adequate expansion, apposition as well as a favourable healing response of an everolimus-eluting BRS (ABSORB BVS 1.1; Abbott Vascular; Santa Clara; CA; USA) with low rates of uncovered and malapposed struts at mid-term follow-up [50], evidence regarding LAScM after BRS implantation in STEMI is limited, with previous series showing conflicting results, ranging from absence of LAScM [51] to an increase in malapposed struts due to the presence of LAScM [52]. Recently, in the TROFI-II study, stenting of culprit lesions with Absorb BVS® in the setting of STEMI resulted in a nearly complete arterial healing which was comparable with that of metallic EES at 6 months. In addition, the frequency of malapposed struts and uncovered struts were lower in the Absorb BVS® group [53].

CTOs

An intravascular ultrasound study demonstrated that late-stent malapposition is found in more than a quarter of CTO lesions treated with DES [27]. Subintimal passage of the guidewire, creation of a false lumen and stenting of the false lumen were suggested mechanisms of injury to the adventitial layer during DES implantation of CTO lesions, contributing to late-stent malapposition. In the same study, late-stent malapposition was not associated with any major adverse cardiac event [27]. However, in a recent meta-analysis, the risk of late-stent malapposition was increased after DES implantation and late-stent malapposition appeared to be associated with very late ST [47].

Large calibre vessels

In large calibre vessels with long tapering lesions, there may be marked differences in vessel dimensions in the treated region. Implantation of a relatively small scaffold in a relative larger vessel (> 3.5mm or larger) can result in incomplete apposition, thus predisposing to LAScM and ScT. The use of balloons disproportionately larger than the nominal stent diameter during postdilation in large calibre vessels can cause scaffold deformation [54] leading to polymer damage [55] and create significant gaps between the scaffold struts, resulting in suboptimal antirestenotic drug delivery affecting vascular healing responses.

Ways/ Measures to prevent late scaffold malapposition

How to minimise the advent of positive vessel remodelling

LAScM may be caused by positive remodelling of the coronary arterial wall and is a marker of other underlying local sustained hypersensitivity/inflammatory reactions possibly to one of the scaffold components [16]. BRS and stents with bioresorbable polymer may reduce LAScM by reducing device component induced local hypersensitivity/inflammatory reactions at the vessel level. Several approaches involving the drug, the polymer and the stent platform, aiming to improve stent biocompatibility, are still under development.

Management of thrombotic lesions

It may be important to effectively remove the thrombotic material before stent implantation in the setting of primary percutaneous coronary intervention. This was initially emphasised in the TAPAS trial, where thrombus aspiration was associated with less re-infarction [56]. However recently the use of aspiration thrombectomy has been discouraged [57]. The introduction of self-expandable devices which can better accommodate early changes in the vessel wall (thrombus dissolution and vasodilatation) with better apposition due to its self-expandable properties may play a future role in reducing stent malapposition rates. Results from the randomised APPOSITION II trial [43] have shown that there is a tenfold reduction

in stent strut malapposition with the self-apposing stent compared with conventional balloon-expandable BMS, as measured by optical coherence tomography (OCT) at three days.

Optimal Implantation of BRS

Since late ScM also include late persistent ScM, when an inadequately apposed stent (during the initial intervention) remains incompletely apposed at follow-up; optimal implantation of BRS to reduce ScM during the initial intervention would potentially reduce LAScM. A BRS specific implantation protocol is based on following the five simple rules, summarized in the **five Ps**: 1) Prepare the lesion, 2) Properly size the vessel, 3) Pay attention to the expansions limits of the scaffold, 4) Postdilate the BRS with a properly sized noncompliant balloon, and 5) Pay attention to dual antiplatelet therapy and patient compliance. This has been supported by studies that show BRS specific implantation protocol may reduce ScT rates possibly by reducing the extent ScM [31]. In the implantation of Absorb BVS®, adopting a simple memomic **PSP** (**P**repare the vessel to be re-engineered, **S**ize the vessel appropriately, **P**ost-dilate to embed the scaffold struts into the vessel wall) may be of use. **Table 2** summarises the key procedural recommendations in BRS implantation.

Management of Late Acquired Scaffold Malapposition

Depending on the risk benefit balance between thrombotic/ischaemic and bleeding risk, even longer duration of dual antiplatelet therapy and/or more potent antiplatelet medications may be considered. However, the clear benefit in reducing thrombotic or ischaemic outcomes versus the continued risk of bleeding complications remains uncertain and should be discussed with the patient. Clear guidelines on the management of LAScM remain under discussion. It remains ambiguous whether there is a time threshold at which antiplatelet therapy could be discontinued with negligible event rates. A possible strategy would be to perform an IVUS/OCT follow-up at a single time point (between 9 and 12 months) in high

risk patients (eg, STEMI, diabetics, elderly) or in complex lesions (eg, calcified, high thrombotic load).

Conclusion

Late malapposition after PCI is a significant problem for metallic DES and probably even more for bioresorbable scaffolds. In the latter disintegration as part of the bioresorption of malapposed struts may create local areas of shear stress triggering thrombosis especially if DAPT is previously discontinued. Late malapposition can be the result of acute malapposition or acquired during plaque remodelling. Both can be minimalized by adherence to proper implantation technique comprising of proper sizing, adequate predilation and postdilatation with adequate size balloons supported by intravascular imaging where appropriate.

References

1. Simsek C, Karanasos A, Magro M et al. Long-term invasive follow-up of the everolimus-eluting bioresorbable vascular scaffold: five-year results of multiple invasive imaging modalities. EuroIntervention 2014.

2. Serruys PW, Ormiston JA, Onuma Y et al. A bioabsorbable everolimus-eluting coronary stent system (ABSORB): 2-year outcomes and results from multiple imaging methods. Lancet 2009; 373: 897-910.

3. Serruys PW, Onuma Y, Garcia-Garcia HM et al. Dynamics of vessel wall changes following the implantation of the absorb everolimus-eluting bioresorbable vascular scaffold: a multi-imaging modality study at 6, 12, 24 and 36 months. EuroIntervention 2014;9:1271-84.

4. Karanasos A, Simsek C, Gnanadesigan M et al. OCT assessment of the long-term vascular healing response 5 years after everolimus-eluting bioresorbable vascular scaffold. J Am Coll Cardiol 2014 ;64: 2343-56.

5. Serruys PW, Chevalier B, Sotomi Y, Cequier A, Carrié D, Piek JJ, Van Boven AJ, Dominici M, Dudek D, McClean D, Helqvist S, Haude M, Reith S, de Sousa Almeida M, Campo G, Iñiguez A, Sabaté M, Windecker S, Onuma Y. Comparison of an everolimus-eluting bioresorbable scaffold with an everolimus-eluting metallic stent for the treatment of coronary artery stenosis (ABSORB II): a 3 year, randomised, controlled, single-blind, multicentre clinical trial. Lancet. 2016 Nov 19;388(10059):2479-2491. doi: 10.1016/S0140-6736(16)32050-5. Epub 2016 Oct 30.

6. Stephen G. Ellis, M.D., Dean J. Kereiakes, M.D., D. Christopher Metzger, M.D., Ronald P. Caputo, M.D., David G. Rizik, M.D., Paul S. Teirstein, M.D., Marc R. Litt, M.D.,

Annapoorna Kini, M.D., Ameer Kabour, M.D., Steven O. Marx, M.D., Jeffrey J. Popma, M.D., Robert McGreevy, Ph.D., Zhen Zhang, Ph.D., Charles Simonton, M.D., and Gregg W. Stone, M.D., for the ABSORB III Investigators. Everolimus-Eluting Bioresorbable Scaffolds for Coronary Artery Disease. N Engl J Med 2015; 373:1905-1915November 12, 2015DOI: 10.1056/NEJMoa1509038.

7. Stone GW, Gao R, Kimura T, Kereiakes DJ, Ellis SG, Onuma Y, Cheong WF, Jones-McMeans J, Su X, Zhang Z, Serruys PW. 1-year outcomes with the Absorb bioresorbable scaffold in patients with coronary artery disease: a patient-level, pooled meta-analysis. Lancet. 2016 Mar 26;387(10025):1277-89. doi: 10.1016/S0140-6736(15)01039-9. Epub 2016 Jan 27.

8. Joanna J. Wykrzykowska, Robin P. Kraak, M.D.,Sjoerd H. Hofma, Rene J. van der Schaaf, E. Karin Arkenbout, Alexander J. IJsselmuiden, Joelle Elias, Ivo M. van Dongen, Ruben Y.G. Tijssen, Karel T. Koch, Jan Baan, Jr., , M. Marije Vis, Robbert J. de Winter,Jan J. Piek, Jan G.P. Tijssen,nd Jose P.S. Henriques for the AIDA Investigators. Bioresorbable Scaffolds versus Metallic Stents in Routine PCI.NEJM Mar 29th 2017. DOI: 10.1056/NEJMoa1614954.

9. Mahmoud AN, Barakat AF, Elgendy AY, Schneibel E, Mentias A, Abuzaid A, Elgendy IY. Long-Term Efficacy and Safety of Everolimus-Eluting Bioresorbable Vascular Scaffolds Versus Everolimus-Eluting Metallic Stents: A Meta-Analysis of Randomized Trials. Circ Cardiovasc Interv. 2017 May; 10(5). pii: e005286. doi: 10.1161/CIRCINTERVENTIONS.117.005286.

10. Ioannis Karalis, Tarek A H N Ahmed, J W Jukema. Late acquired stent malapposition: why, when and how to handle? Heart 2012; 98:1529e1536. doi:10.1136/heartjnl-2011-301220.

18. Kume T, Waseda K, Ako J, et al. Intravascular ultrasound assessment of postprocedural incomplete stent apposition. J Invasive Cardiol 2012; 24:13–6.

19. Guo N, Maehara A, Mintz GS, et al. Incidence, mechanisms, predictors, and clinical impact of acute and late stent malapposition after primary intervention in patients with acute myocardial infarction: an intravascular ultrasound substudy of the Harmonizing Outcomes with Revascularization and Stents in Acute Myocardial Infarction (HORIZONS- AMI) trial. Circulation 2010; 122:1077–84.

20. Ako J, Morino Y, Honda Y, et al. Late incomplete stent apposition after sirolimus-eluting stent implantation: a serial intravascular ultrasound analysis. J Am Coll Cardiol 2005; 46:1002–5.

21. Mintz GS, Shah VM, Weissman NJ. Regional remodeling as the cause of late stent malapposition. Circulation 2003; 107: 2660–3.

22. Mintz GS. What to do about late incomplete stent apposition? Circulation 2007; 115: 2379e81.

23. Fujino Y, Attizzani GF, Nakamura S, Costa MA, Bezerra HG. Frequency-domain optical coherence tomography assessment of stent constriction 9 months after sirolimus-eluting stent implantation in a highly calcified plaque. J Am Coll Cardiol Intv 2013; 6: 204–5.

24. Gutiérrez-Chico JL, Regar E, Nüesch E, et al. Delayed coverage in malapposed and side-branch struts with respect to well-apposed struts in drug-eluting stents: in vivo assessment with optical coherence tomography. Circulation 2011; 124:612–23.

25. Gutiérrez-Chico JL, Wykrzykowska J, Nüesch E, et al. Vascular tissue reaction to acute malapposition in human coronary arteries: sequential assessment with optical coherence tomography. Circ Cardiovasc Interv 2012; 5: 20–9.

26. Virmani R, Guagliumi G, Farb A, et al. Localized hypersensitivity and late coronary thrombosis secondary to a sirolimus-eluting stent: should we be cautious? Circulation 2004; 109: 701e5.

27. Hong MK, Mintz GS, Lee CW, Park DW, Park KM, Lee BK, Kim YH, Song JM, Han KH, Kang DH, Cheong SS, Song JK, Kim JJ, Park SW, Park SJ. Late stent malapposition after drug-eluting stent implantation: an intravascular ultrasound analysis with long-term follow-up. Circulation. 2006 Jan 24;113(3):414-9.

28. Angel Sanchez-Recalde, MD, Raul Moreno, MD, Laura Barreales, MD, Fernando Rivero, MD, Guillermo Galeote, MD, Santiago Jimenez-Valero, MD, Luis Calvo, MD, Esteban López de Sá, MD, José L. López-Sendón, MD. Risk of Late-Acquired Incomplete Stent Apposition after Drug-Eluting Stent versus Bare-Metal Stent. J Invasive Cardiology 2008; 20: 417–422.

29. Lane JP, Perkins LE, Sheehy AJ, Pacheco EJ, Frie MP, Lambert BJ, Rapoza RJ, Virmani R. Lumen gain and restoration of pulsatility after implantation of a bioresorbable vascular scaffold in porcine coronary arteries. JACC Cardiovasc Interv. 2014 Jun; 7(6): 688-95. doi: 10.1016/j.jcin.2013.11.024. Epub 2014 May 14.

30. Ishibashi Y, Nakatani S, Sotomi Y, Suwannasom P, Grundeken MJ, Garcia-Garcia HM, Bartorelli AL, Whitbourn R, Chevalier B, Abizaid A, Ormiston JA, Rapoza RJ, Veldhof S, Onuma Y, Serruys PW. Relation Between Bioresorbable Scaffold Sizing Using QCA-Dmax and Clinical Outcomes at 1 Year in 1,232 Patients From 3 Study Cohorts (ABSORB

Cohort B, ABSORB EXTEND, and ABSORB II). JACC Cardiovasc Interv. 2015 Nov;8(13):1715-26. doi: 10.1016/j.jcin.2015.07.026.

31. Puricel S, Cuculi F, Weissner M, Schmermund A, Jamshidi P, Nyffenegger T, Binder H, Eggebrecht H, Münzel T, Cook S, Gori T. Bioresorbable Coronary Scaffold Thrombosis: Multicenter Comprehensive Analysis of Clinical Presentation, Mechanisms, and Predictors. J Am Coll Cardiol. 2016 Mar 1;67(8):921-31. doi: 10.1016/j.jacc.2015.12.019.

32. Cordula M. Felix, Georgios J. Vlachojannis, Alexander J.J. IJsselmuiden, Jiang Ming Fam, Peter C. Smits, Wouter J. Lansink, Roberto Diletti, Felix Zijlstra, Evelyn S. Regar, Eric Boersma, Yoshinobu Onuma, Robert J.M. van Geuns. Potentially increased incidence of scaffold thrombosis in patients treated with Absorb BVS who terminated DAPT before 18 months. EuroIntervention. 2017 Jun 2; 13(2):e177-e184. doi: 10.4244/EIJ-D-17-00119.

33. Prati F, Regar E, Mintz GS, Arbustini E, Di Mario C, Jang IK, Akasaka T, Costa M, Guagliumi G, Grube E, Ozaki Y, Pinto F, Serruys PW; Expert's OCT Review Document. Expert review document on methodology, terminology, and clinical applications of optical coherence tomography: physical principles, methodology of image acquisition, and clinical application for assessment of coronary arteries and atherosclerosis. Eur Heart J. 2010;31:401-15.

34. Nammas W, Ligthart JM, Karanasos A, Witberg KT, Regar E. Optical coherence tomography for evaluation of coronary stents in vivo. Expert Rev Cardiovasc Ther. 2013 May;11(5):577-88. doi: 10.1586/erc.13.37.

35. Akiko Maehara, MD, Ori Ben-Yehuda, MD, Ziad Ali, MD, William Wijns, MD, PHD, Hiram G. Bezerra, MD, Junya Shite, MD, Philippe Généreux, MD, Melissa Nichols, MS, Paul Jenkins, PHD, Bernhard Witzenbichler, MD, Gary S. Mintz, MD, Gregg W. Stone, MD.

Comparison of Stent Expansion Guided by Optical Coherence Tomography Versus Intravascular Ultrasound The ILUMIEN II Study (Observational Study of Optical Coherence Tomography [OCT] in Patients Undergoing Fractional Flow Reserve [FFR] and Percutaneous Coronary Intervention). J Am Coll Cardiol Intv 2015;8:1704–14.

36. Garcia-Garcia HM, Serruys PW, Campos CM et al. Assessing bioresorbable coronary devices: methods and parameters. JACC Cardiovasc Imaging 2014;7:1130-48.

37. Nakatani S, Sotomi Y, Ishibashi Y, Grundeken MJ, Tateishi H, Tenekecioglu E, Zeng Y, Suwannasom P, Regar E, Radu MD, Räber L, Bezerra H, Costa MA, Fitzgerald P, Prati F, Costa RA, Dijkstra J, Kimura T, Kozuma K, Tanabe K, Akasaka T, Di Mario C, Serruys PW, Onuma Y. Comparative analysis method of permanent metallic stents (XIENCE) and bioresorbable poly-L-lactic (PLLA) scaffolds (Absorb) on optical coherence tomography at baseline and follow-up. EuroIntervention. 2016 Dec 20;12(12):1498-1509. doi: 10.4244/EIJY15M10_03.

38. Tearney GJ, Regar E, Akasaka T, Adriaenssens T, Barlis P, Bezerra HG, Bouma B, Bruining N, Cho JM, Chowdhary S, Costa MA, de Silva R, Dijkstra J, Di Mario C, Dudek D, Falk E, Feldman MD, Fitzgerald P, Garcia-Garcia HM, Gonzalo N, Granada JF, Guagliumi G, Holm NR, Honda Y, Ikeno F, Kawasaki M, Kochman J, Koltowski L, Kubo T, Kume T, Kyono H, Lam CC, Lamouche G, Lee DP, Leon MB, Maehara A, Manfrini O, Mintz GS, Mizuno K, Morel MA, Nadkarni S, Okura H, Otake H, Pietrasik A, Prati F, Raber L, Radu MD, Rieber J, Riga M, Rollins A, Rosenberg M, Sirbu V, Serruys PW, Shimada K, Shinke T, Shite J, Siegel E, Sonoda S, Suter M, Takarada S, Tanaka A, Terashima M, Thim T, Uemura S, Ughi GJ, van Beusekom HM, van der Steen AF, van Es GA, van Soest G, Virmani R, Waxman S, Weissman NJ, Weisz G; International Working Group for Intravascular Optical Coherence Tomography (IWG-IVOCT). Consensus standards for acquisition, measurement,

and reporting of intravascular optical coherence tomography studies: a report from the International Working Group for Intravascular Optical Coherence Tomography Standardization and Validation. J Am Coll Cardiol. 2012;59:1058-72.

39. Bruining N, Dudek D, Radu M, Erglis A, Motreff P, Alfonso F, Toutouzas K, Gonzalo N, Tamburino C, Adriaenssens T, Pinto F, Serruys PW, Di Mario C; Expert's OCT Review Document. Expert review document part 2: methodology, terminology and clinical applications of optical coherence tomography for the assessment of interventional procedures. Eur Heart J. 2012;33:2513-20.

40. Karanasos A, Simsek C, Gnanadesigan M et al. OCT assessment of the long-term vascular healing response 5 years after everolimus-eluting bioresorbable vascular scaffold. J Am Coll Cardiol 2014;64:2343-56.

41. Radu MD, Raber L, Kalesan B et al. Coronary evaginations are associated with positive vessel remodelling and are nearly absent following implantation of newer-generation drug-eluting stents: an optical coherence tomography and intravascular ultrasound study. Eur Heart J 2014;35:795-807.

42. Gori T, Jansen T, Weissner M, Foin N, Wenzel P, Schulz E, Cook S, Münzel T. Coronary evaginations and peri-scaffold aneurysms following implantation of bioresorbable scaffolds: incidence, outcome, and optical coherence tomography analysis of possible mechanisms. Eur Heart J. 2016 Jul 7;37(26):2040-9. doi: 10.1093/eurheartj/ehv581. Epub 2015 Nov 4.

43. Shimpei Nakatani, MD; Yoshinobu Onuma, MD, PhD; Yuki Ishibashi, MD, PhD; Antonios Karanasos, MD; Evelyn Regar, MD, PhD; Hector M. Garcia-Garcia, MD, PhD; Corrado Tamburino, MD, PhD; Jean Fajadet, MD; Mathias Vrolix, MD; Bernhard

Witzenbichler, MD; Eric Eeckhout, MD, PhD; Christian Spaulding, MD, PhD; Krzysztof Reczuch, MD, PhD; Alessio La Mann, MD; René Spaargaren, MD; Davide Capodanno, MD; Glenn Van Langenhove, MD, PhD; Stefan Verheye, MD, PhD; Patrick W. Serruys, MD, PhD; Robert-Jan van Geuns, MD, PhD. Incidence and potential mechanism of resolved, persistent and newly acquired malapposition three days after implantation of self-expanding or balloon-expandable stents in a STEMI population: insights from optical coherence tomography in the APPOSITION II study. EuroIntervention 2015; 11: 885-894 published online ahead of print November 2015.

44. Finn AV, Nakazawa G, Joner M et al. Vascular responses to drug eluting stents: importance of delayed healing. Arterioscler Thromb Vasc Biol 2007;27:1500-10.

45. Guagliumi G, Sirbu V, Musumeci G et al. Examination of the in vivo mechanisms of late drug-eluting stent thrombosis: findings from optical coherence tomography and intravascular ultrasound imaging. JACC Cardiovasc Interv 2012;5:12-20.

46. Sotomi Y, Suwannasom P, Serruys PW, Onuma Y. Possible mechanical causes of scaffold thrombosis: insights from case reports with intracoronary imaging. EuroIntervention. 2017;12:1747-56.

47. Hassan AK, Bergheanu SC, Stijnen T, et al. Late stent malapposition risk is higher after drug-eluting stent compared with bare-metal stent implantation and associates with late stent thrombosis. Eur Heart J 2010;31:1172e80.

48. van Geuns RJ, Tamburino C, Fajadet J et al. Self-expanding versus balloon-expandable stents in acute myocardial infarction: results from the APPOSITION II study: self-expanding stents in ST-segment elevation myocardial infarction. JACC Cardiovasc Interv 2012;5:1209-19.

49. Robert-Jan M. van Geuns, MD, PhD; Tuncay Yetgin, MD; Alessio La Manna, MD; Corrado Tamburino, MD, PhD; Géraud Souteyrand, MD; Pascal Motreff, MD, PhD; Karel T. Koch4, MD, PhD; Mathias Vrolix, MD; Alexander IJsselmuiden, MD, PhD; Giovanni Amoroso, MD, PhD; Jacques Berland, MD; Gilles Montalescot, MD, PhD; Emmanuel Teiger, MD, PhD; Evald H. Christiansen, MD, PhD; René Spaargaren, MD; William Wijns, MD, PhD. STENTYS Self-Apposing sirolimus-eluting stent in ST-segment elevation myocardial infarction: results from the randomised APPOSITION IV trial. EuroIntervention. 2016 Feb; 11(11):e1267-74. doi: 10.4244/EIJV11I11A248.

50. Serruys PW, Ormiston JA, Onuma Y et al. A bioabsorbable everolimus-eluting coronary stent system (ABSORB): 2-year outcomes and results from multiple imaging methods. Lancet 2009;373:897-910.

51. Kochman J, Tomaniak M, Koltowski L et al. A 12-month angiographic and optical coherence tomography follow-up after bioresorbable vascular scaffold implantation in patients with ST-segment elevation myocardial infarction. Catheter Cardiovasc Interv 2015.

52. Tousek P, Kocka V, Maly M, Lisa L, Budesinsky T, Widimsky P. Neointimal coverage and late apposition of everolimus-eluting bioresorbable scaffolds implanted in the acute phase of myocardial infarction: OCT data from the PRAGUE-19 study. Heart Vessels 2015.

53. Sabate M, Windecker S, In iguez A, Okkels-Jensen L, Cequier A, Brugaletta S, Hofma SH, Ra¨ber L, Christiansen EH, Suttorp M, Pilgrim T, Anne van Es G, Sotomi Y, Garcı´a-Garcı´a HM, Onuma Y, Serruys PW. Everolimus-eluting bioresorbable stent vs. durable polymer everolimus-eluting metallic stent in patients with ST segment elevation

myocardial infarction: results of the randomized ABSORB ST-segment elevation myocardial infarction—TROFI II trial. Eur Heart J 2016;37:229–240.

54. Basalus MW, van Houwelingen KG, Ankone MJ, Feijen J, von Birgelen C. Micro-computed tomographic assessment following extremely oversized partial postdilatation of drug-eluting stents. EuroIntervention 2010;6:141–8.

55. Guérin P, Pilet P, Finet G, et al. Drug-eluting stents in bifurcations: bench study of strut deformation and coating lesions. Circ Cardiovasc Interv 2010;3:120–6.

56. Svilaas T, Vlaar PJ, van der Horst IC, et al. Thrombus aspiration during primary percutaneous coronary intervention. N Engl J Med. 2008;358:557–67.

57. Levine GN, O'Gara PT, Bates ER, et al. 2015 ACC/AHA/SCAI Focused Update on Primary Percutaneous Coronary Intervention for Patients With ST-Elevation Myocardial Infarction: An Update of the 2011 ACCF/AHA/SCAI Guideline for Percutaneous Coronary Intervention and the 2013 ACCF/AHA Guideline for the Management of ST-Elevation Myocardial Infarction: A Report of the American College of Cardiology/American Heart Association Task Force on Clinical Practice Guidelines and the Society for Cardiovascular Angiography and Interventions. J Am Coll Cardiol. 2015 Oct 21; doi: 10.1016/j.jacc.2015.10.005. [Epub ahead of print].

Table 1 Risk factors associated with the development of late acquired scaffold malapposition (LAScM)

Clinical and lesion factors
Acute myocardial infarction
Chronic total occlusion
Vessel size (both ectatic and small calibre vessels)
Plaque characteristics eg calcified lesions
Marked mismatch between stent size selection and luminal dimensions (i.e. stent diameter smaller than reference lumen diameter)

Procedure related factors
Use of drug eluting stents especially first generation
Inadequate implantation pressure and postdilation resulting in stent underexpansion

Device factors
Longer stent length
Overlapping stents

Table 2 Summary of Key Recommendations in Bioresorbable vascular scaffolds (BRS) Implantation

1	Patient and lesion selection	a. Consider BRS in younger patients (55 years old or younger). b. Avoid BRS use in extremely angulated/ tortuous vessels, heavily calcified lesions or lesions that require overlap scaffolds such as lesions with size discrepancy.
2	Prepare the lesion*	a. Use semi/ non-compliant/ high pressure balloons to achieve balloon: vessel size dilation in a 1: 1 manner.
3	Properly size the vessel	a. Absorb BVS is indicated for vessels with a reference vessel diameter of ≥ 2.5 mm and ≤ 3.75 mm. b. Avoid implanting BRS in small vessels (less than 2.5mm). c. Consider the use of intravascular imaging such as IVUS or OCT to facilitate preprocedural sizing and planning.
4	Pay attention to the expansions limits of the scaffold	a. Consider the use of intravascular imaging such as IVUS or OCT to facilitate preprocedural sizing and planning.
5	Postdilate the BRS with a properly sized noncompliant balloon	a. Use high pressure balloons up to 0.5 mm above nominal scaffold diameter (>16 atm) for 10-30 seconds to achieve residual stenosis < 10%. b. Confirm optimal result using intravascular imaging such as IVUS or OCT.
6	Intravascular Imaging	a. Use of IVUS or OCT is highly recommended to aid preprocedural sizing and optimize implantation results.
7	Period of dual antiplatelets duration	a. A minimum duration of 1 years of dual antiplatelets is recommended till further data is available. b. Depending on the risk benefit balance between thrombotic/ischaemic and bleeding risk, even longer duration of dual antiplatelet therapy and/or more potent antiplatelet medications may be considered.

*The memomic **PSP** (**P**repare the vessel to be re-engineered, **S**ize the vessel appropriately, **P**ost-dilate to embed the scaffold struts into the vessel wall) may also be used for the implantation of Absorb BVS GTI^{R}.

IVUS- Intravascular Ultrasound; OCT- Optical Coherence Tomography

Figures

Figure 1 Examples of A. resolved, B. persistent, and C. late ISA.

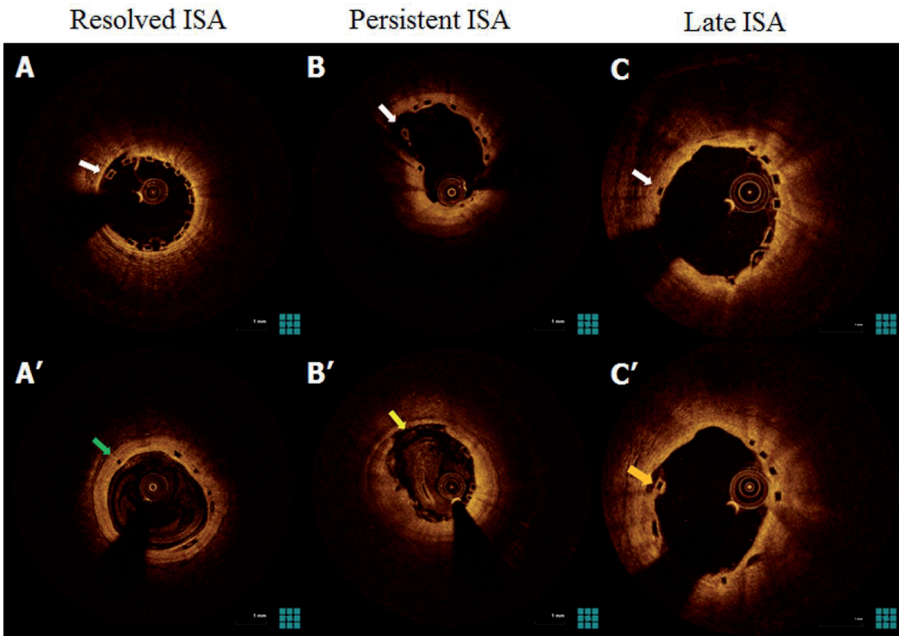

White arrows indicate malapposed struts at baseline, green arrows struts with resolved ISA, yellow arrows struts with persistent ISA, and orange arrows struts with late-acquired ISA. SB=side-branch. ISA- Incomplete Scaffold Apposition.

Figure 2 The Potential Consequences of a Device–Vessel Mismatch Implantation

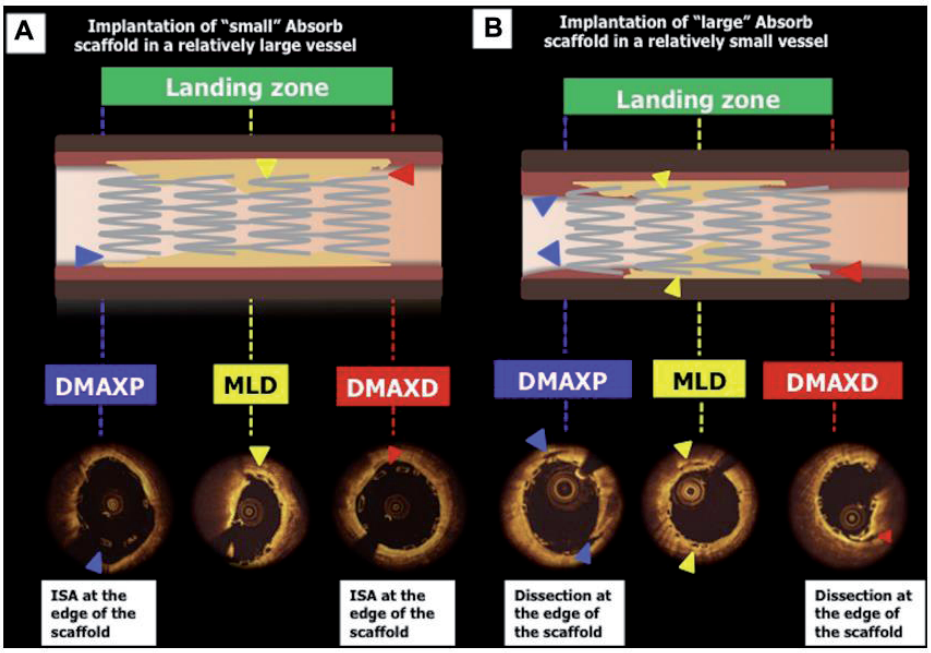

Implantation of a too "small" Absorb scaffold in a relatively large vessel can cause incomplete apposition of the device edges (A, top panel, blue and red arrowheads). Incomplete scaffold apposition (blue and red arrow heads) and scaffold under-expansion (yellow arrowhead) are visible in the OCT images (A, bottom panel). Implantation of a too "large" Absorb scaffold in a relatively small vessel can cause vessel injury (B, top panel, blue and red arrowheads). Edge dissections (blue and red arrowheads) are visible in the OCT images (B, bottom panel). ISA- incomplete scaffold apposition; OCT- optical coherence tomography. (Ishibashi et al [30])

Figure 3 Assessment of scaffold malapposition in BRS and DES

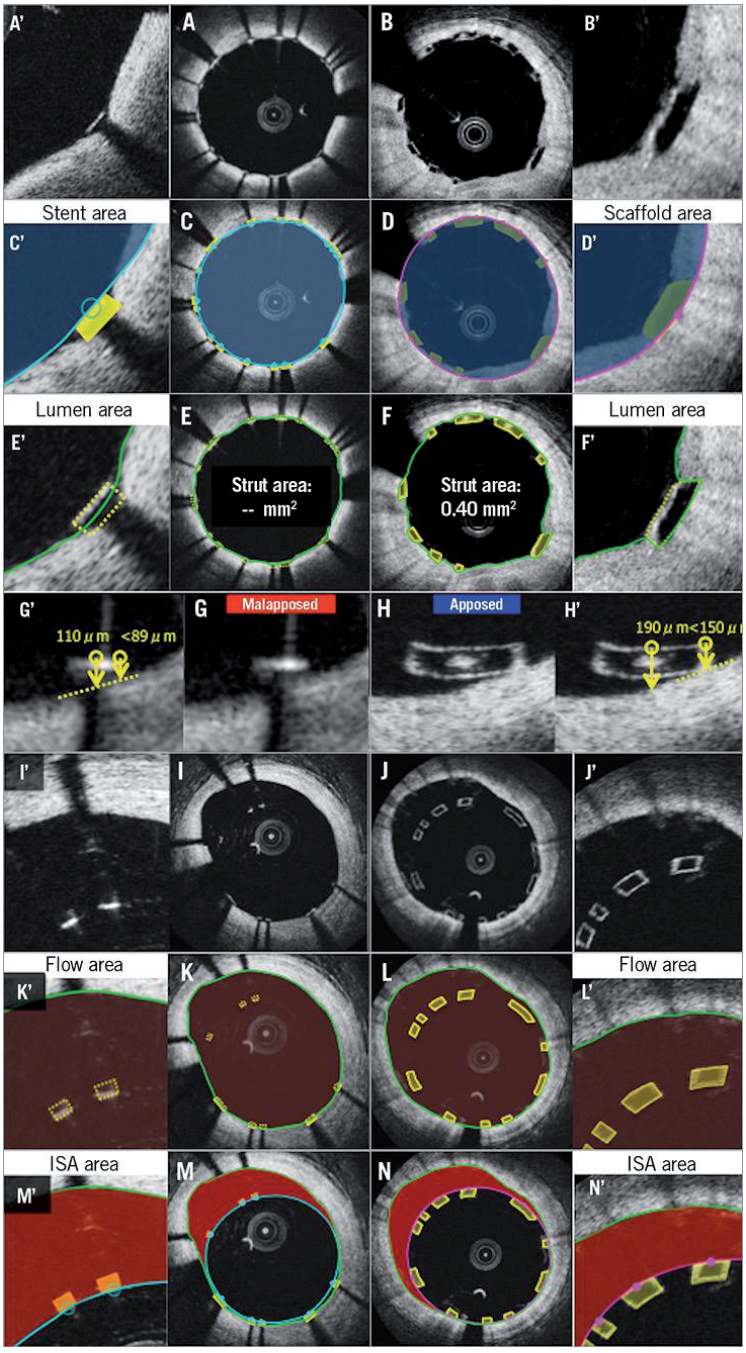

Potential biases caused by application of conventional methods post procedure. Representative cross-sections of apposed struts, stent/scaffold area measurement, lumen area measurement, apposition of struts, ISA, flow area measurement, and ISA area measurement are shown in A, C, E, G, I, K, M (metallic stents) and B, D, F, H, J, L, N (polymeric struts), respectively. A'-N' are magnified views of A-N. ISA- Incomplete stent apposition. (With permission from Nakatani et al [37])

16

CHAPTER

IMPACT OF POSTDILATION ON PROCEDURAL AND CLINICAL OUTCOMES IN COMPLEX LESIONS TREATED WITH BIORESORBABLE VASCULAR SCAFFOLDS- A PROSPECTIVE REGISTRY STUDY

Jiang Ming Fam, Cordula Felix, Yoshinobu Onuma, Roberto Diletti, Nicolas M Van Mieghem, Evelyn Regar, Peter De Jaegere, Felix Zijlstra, Robert J Van Geuns

Submitted for publication.

Impact of postdilation on procedural and clinical outcomes in complex lesions treated with bioresorbable vascular scaffolds- a prospective registry study

Jiang Ming Fam[1,2], Cordula Felix[1], Yuki Ishibashi [1], Yoshinobu Onuma[1], Roberto Diletti[1], Nicolas M Van Mieghem[1], Evelyn Regar[1], Peter De Jaegere[1], Felix Zijlstra[1], Robert J Van Geuns[1]

[1]Thoraxcenter, Erasmus MC, Rotterdam,

[2] National Heart Centre Singapore

Correspondence

Address for correspondence:

Robert J Van Geuns

Department of Cardiology

Thoraxcentre

Erasmus University Medical Centre

's-Gravendijkwal 230

3015 GE Rotterdam, The Netherlands

Tel: +31 (0)10 703 33 48

Fax: +31 (0)10 703 52 54

E-mail: r.vangeuns@erasmusmc.nl

Word Count: 4414 (Abstract, main text, references and figure legend)

Disclosure of relationship with industry: The authors acknowledged that BVS Expand is supported by research grants from Abbott Vascular. Prof van Geuns and Yoshinobu Onuma received speaker's fee from Abbott Vascular.

ABSTRACT

Background:

There is limited data on the impact of postdilation (PostDil) on acute procedural and late clinical outcomes in patients with complex lesions treated with bioresorbable vascular scaffolds (BRS). We sought to evaluate the effect of Postdil on procedural and clinical outcomes.

Methods:

We performed an analysis of patients who underwent BRS implantation. The effects of PostDil on quantitative coronary angiographic (QCA) results immediately after BRS implantation, after PostDil and major adverse cardiovascular events (MACE) were investigated.

Results:

294 patients treated with BRS (387 lesion, PostDil 54%) were studied. Baseline clinical characteristics were similar between both groups, with more complex lesion characteristics in the PostDil group. PostDil resulted in 6% increase in minimal lumen diameter (MLD; after BRS implantation 2.18±0.43mm vs Final 2.32±0.35mm; Δ 0.14 ± 0.32mm, $p<0.001$) and an increase in proportion of final MLD > 2.4mm (28.2% vs 41.9%, $p<0.001$). Still acute lumen gain (ALG) was significantly less in PostDil compared to non-PostDil (1.33±0.59 vs 1.53±0.63mm, p=0.002). ALG was significantly affected by PostDil high inflation pressure (>16mmHg) and the vessel size (pre RVD >2.25mm) but not size of PostDil balloon. At 2 years, there was no difference in MACE (9.9 vs 6.9% respectively, p=0. 402).

Conclusions:

In BRS treated lesions that underwent PostDil, PostDil resulted in a slight increase (6%) in MLD and rate of acceptable final (> 2.4mm) MLD. 2 year MACE were similar between PostDil and non-PostDil groups.

Word Count: 231 words

Keywords:

Bioresorbable vascular scaffolds

Percutaneous Coronary Intervention

Quantitative coronary angiography

Main Text

INTRODUCTION

Bioresorbable vascular scaffolds (BRS) were recently deemed an attractive therapeutic device to metallic stents as the need for mechanical support for the healing artery is temporary, and beyond the first few months there are potential disadvantages of a permanent metallic prosthesis. Imaging studies have also supported the novel attributes of bioresorbable scaffolds, with restoration of cyclic pulsatility at the device site 6 months after implantation, restored vasomotion by 12 months, and late lumen gain with plaque regression between 2 and 5 years, benefits that are not possible with permanent metallic stents. [1-5].

Due to intrinsic properties related to its design and composition, the deployment of BRS requires a more aggressive lesion preparation. While larger vessel size has been reported to predict greater minimal luminal diameter (MLD) at follow-up, in patients treated by directional atherectomy or stent implantation [6-7] and postdilation (PostDil) of metallic stents is widely performed without disruption risk, concerns of scaffold disruption have been raised over aggressive PostDil of the Absorb BVS® (Abbott Vascular, Santa Clara, CA, USA) which is polymeric based with lower radial and tensile strength with finite expansion compliance. It has been observed that systematic PostDil was implemented on average in less than 50% of previously published studies and it is still debatable if pursuing a systematic PostDil strategy will have an impact on long term results particularly the risk of scaffold thrombosis (VScT) [8]. The aim of the study was to evaluate the effect of PostDil on acute procedural angiographic and late clinical outcomes in a 'real world' population with complex lesions treated with the Absorb BVS®.

METHODS

Study population

This is an investigator-initiated, prospective, single-center, single-arm study performed in an experienced, tertiary PCI center evaluating the performance of the BRS in lesions representative of daily clinical practice, including calcified lesions, total occlusions, long lesions and small vessels [2]. Inclusion criteria for the BVS-EXPAND registry were patients presenting with NSTEMI, stable/ unstable angina, or silent ischemia caused by a *de novo* stenotic lesion in a native previously untreated coronary artery. Angiographic inclusion criteria included lesions with a Dmax (proximal and distal mean lumen diameter) within the upper limit of 3.8 mm and the lower limit of 2.0 mm by online quantitative coronary angiography (QCA). Exclusion criteria were patients with a history of a previously implanted metal DES in the intended target vessel, coronary bypass grafting (CABG), presentation with cardiogenic shock, allergy or contra-indications to antiplatelet therapy, patients with expected survival of less than one year.

Study Procedure

Predilation and PostDil were performed at the discretion of the operator. When performed, pre-dilatation with balloons shorter than the planned study device length were recommended. For PostDil, non-compliant balloons without overexpanding the scaffold beyond its limits of expansion (0.5mm > nominal diameter) were recommended. Patients were treated with unfractionated heparin and dual antiplatelets according to guideline recommendations.

Quantitative Coronary Analysis

The angiographic analysis was performed by three independent investigators. The 2-dimensional (2D) angiograms were analyzed with the CASS 5.10 analysis system (Pie Medical

BV, Maastricht, the Netherlands). Angiographic views with minimal foreshortening of the lesion and limited overlap with other vessels were used whenever possible for all phases of the treatment: preprocedural angiography, after BVS implantation and after obtaining final result if PostDil was performed [9]. In each patient, the treated region and the peri-treated regions (defined by 5 mm proximal and distal to the device edge) were analyzed. The computer defined QCA (Quantitative Coronary Analysis) measurements provided minimal luminal diameter (MLD), reference vessel diameter (RVD) obtained by an interpolated method, and percentage diameter stenosis (%DS) in the post procedure angiogram. The primary acute angiographical endpoint of Acute lumen gain (ALG) was defined as post-procedural MLD minus pre-procedural MLD (in an occluded vessel MLD value was zero by default). Adequate angiographic implantation was defined as a MLD of >2.4mm as this has been correlated with good clinical outcomes previously [10].

Follow-up.

Clinical demographic data of all patients were obtained from hospital records. Follow-up information specific for hospitalization and cardiovascular events was obtained through questionnaires, medical records or discharge letters from other hospitals. Survival status was checked additionally checked from municipal civil registries. Events were adjudicated by an independent clinical events committee (CEC). All information concerning baseline characteristics and follow-up was gathered in a clinical data management system. Only patients who had given written consent for follow up were included in the clinical outcome assessments.

Definitions

The primary clinical endpoint was MACE, defined as the composite endpoint of cardiac death, myocardial infarction (MI) and target lesion revascularization (TLR). The secondary endpoints were device oriented composite endpoints (DOCE: composite of cardiac death, target vessel myocardial infarct and clinically indicated target lesion revascularization) and patient oriented composite endpoints (POCE: composite of all-cause mortality, all-cause myocardial infarct and any revascularization). Deaths were considered cardiac unless a non-cardiac cause was definitely identified. TLR was described as any repeated revascularization of the target lesion. Target vessel revascularization (TVR) was defined as any repeat percutaneous intervention or surgical bypass of any segment of the target vessel. Target vessel myocardial infarct (TvMI) was defined as any repeat percutaneous intervention or surgical bypass of any segment of the target vessel which presented with myocardial infarct. Non-target vessel revascularization was described as any revascularization in a vessel other than the target lesion. Scaffold thrombosis (ST) and MI were classified according to the Academic Research Consortium (ARC) [11]. Clinical device success was defined as successful delivery and deployment of the first study scaffold/ stent at the intended target lesion and successful withdrawal of the delivery system with adequate angiographic result achieved.

Statistical analysis

Categorical variables are reported as counts and percentages, continuous variables as mean ± standard deviation. The cumulative incidence of adverse events was estimated according to the Kaplan-Meier method. Patients lost to follow-up were considered at risk until the date of last contact, at which point they were censored. All statistical tests were two-sided and the P value

of < 0.05 was considered statistically significant. The cumulative incidence of adverse events was estimated according to the Kaplan-Meier method. Patients lost to follow-up were considered at risk until the date of last contact, at which point they were censored. To investigate possible predictors for clinical outcomes MACE and ST, univariate analysis using a binary logistic regression model was used. For the cumulative event rates, Kaplan-Meier estimates were described and non-hierarchical counts were used. Statistical analyses were performed using SPSS, version 21 (IL, US).

RESULTS

Clinical and lesion characteristics are shown in **Tables I** and **IIA**. 294 patients with 387 lesions treated with 529 BRS were studied of which 164 patients with 211 lesions underwent PostDil (PostDil Balloon: Scaffold ratio: 1.06 ± 0.12; mean maximal PostDil pressure: 16.05 ± 4.24mmhg). Baseline clinical characteristics were similar between the PostDil and non-PostDil groups. The left anterior descending artery (47.8%) was the most commonly treated vessel. Lesion complexity and calcification were higher in the PostDil group (AHA B2/C lesion: 48.4% in PostDil vs 24.5% in non- PostDil, p < 0.001; Moderate/heavy calcification: 51.2% vs 29.6%, p<0.001). QCA data are as shown in **Table IIB**. Preprocedure RVD, MLD and %DS were similar between the two groups. Treatment length was significantly longer in PostDil compared to non- PostDil (25.31 ±14.53 vs 20.06 ±10.13, p<0.001). Procedural characteristics are as shown in **Table IIIA**. Lesion preparation (percentage predilation performed and predilation Balloon: Artery ratio) was similar between the PostDil and non-PostDil groups. In patients in whom scaffold overlapping was planned, post-dilation was more often performed (36.5% vs. 14.2%, p<0.001). The mean length of scaffolds implanted was longer in the PostDil group (32.50 ± 19.30mm vs 23.92 ± 13.45mm, p=0.001).

The effects of PostDil on angiographic outcome (MLD, RVD and %DS) were evaluated using appropriate views taken immediately after BRS implantation (before PostDil) and final procedure in 117 pairs with matched views [**Table IIIB**]. ALG was significantly less in PostDil compared to non- PostDil (1.33 ±0.59 vs 1.53 ±0.63mm, p= 0.002). From QCA, PostDil resulted in a significant 6.1% increase in RVD (0.16 ± 0.37mm, p< 0.001) as well as the MLD (0.14 ± 0.32mm, p < 0.001) and non-significant decrease in %DS (S- 0.03 ± 12.39%, p= 0.976) after BRS implantation. In the PostDil group, adequate MLD (2.4mm or greater) was achieved in only 28.2 % of the lesions immediately after implantation, which was increased to 41.9% after PostDil. The relation of ALG to vessel size and PostDil are shown in **Table IIIC**. ALG was higher in larger vessel compared to smaller vessels (small vessel as defined by pre RVD smaller than 2.25mm) regardless whether PostDil is performed. In larger vessels, ALG after PostDil was still less compared to the group where PostDil was not deemed necessary wheras in smaller vessels, there was no significant difference in ALG when PostDil was performed. In lesions where PostDil was performed, we found that ALG was related to PostDil balloon pressure and not by PostDil balloon size.

The device success rate was 99.5% [**Table IVA**]. Of note, bail out rates (bailout by scaffold: 2.8% vs 2.3%, p=0.541 and bailout by stent 1.4% vs 0.6%, p=0.601 and dissection were similar between the PostDil and non PostDil groups (5.7% vs 3.4%, p=0.582). Written consent for the follow up program was obtained in 226 patients (76.9%). Clinical outcomes were available in all (100%) of these patients with median FU of 772 days (IQR: 729 - 1099) (**Table IVB**). The primary clinical endpoint, MACE occurred in 8.0% (n=18) of the subjects available on follow up at 2 years. The secondary clinical endpoints, DOCE and POCE occurred in 6.6% (n= 15) and 9.3% (n=21) of the subjects available on follow up at 2 years respectively and were driven

by TvMI and revascularization events respectively. All-cause mortality and ST occurred in 5 (4.5%) and 3 (2.6%) of the patients on follow up respectively in which all 3 ST cases occurred in the PostDil group [**Table IVB**]. 2 year event rates were similar in patients treated with BRS with and without PostDil performed **(Figure 1A-D).** Further analysis did not show that there were significant differences in clinical events between the cases with pre RVD < 2.25mm and those with RVD ≥ 2.25mm as well as those with final in scaffold MLD < 2.4mm compared to those ≥ 2.4mm though there was a trend towards higher TLT, TvMI and Def ST in patients with final in scaffold MLD < 2.4mm [**Online Supplementary Table I**]. Using Cox regression, PostDil was not a significant predictor for adverse clinical outcome at 2 years follow up (See **online supplementary Table II**).

DISCUSSION

Recently, BRS specific implantation techniques such as PSP (Prepare the lesion; Size the vessel appropriately; Postdilate) have been recommended to improve post implantation clinical outcomes particularly late scaffold thrombosis [10]. To the authors' knowledge, this is the first study that looks at the effect of PostDil on improving scaffold performance in terms of final procedure MLD and RVD and its impact on 2 year clinical outcomes. A previous study by Foley et al [12] had determined that increasing coronary vessel size was independently predictive of decreasing late luminal loss and increasing follow-up MLD after successful balloon angioplasty. Our study showed that PostDil using high inflation pressure with a non-compliant balloon of at least 1:1 balloon to scaffold ratio in addition to standard lesion preparation and scaffold implantation protocols can improve final BRS MLD and RVD by 6% which may improve clinical outcomes as seen in DES [13-14]. While the number of lesions whose MLD was ≥2.4mm was increased after PostDil compared to immediately after BRS

implantation (41.9% vs 28.2%, p<0.001) (**Table IIIB**) and acute luminal gain were significantly affected by PostDil inflation pressure and the vessel size but not size of PostDil balloon (**Table IIIC**), the fact that ALG was greater when lower inflation pressures was used may be attributed by the fact that this group had softer and more expandable lesions.

The size of the final scaffold diameter is influenced by a combination of device factors [such as the scaffold nominal diameter and material composition], procedural factors [inflation balloon size and inflation pressure] as well as clinical and biological factors such as presence of diabetes and age [7; 21] all of which in combination may theoretically modify the influence of PostDil on final vessel size which merits further study. It had been shown in an earlier study [22] that as a result of the inherent polymer component, the Absorb BVS exhibits a slightly higher though non-statistically significant acute recoil rate with the Absorb BVS when compared to a contemporary metallic DES of a similar design (0.19±0.18 mm for the Absorb BVS vs. 0.13±0.21 mm for the cobalt-chromium EES, p=0.4). However, as the same BRS size was deployed in both groups of the present study, the lesion, vessel and procedural characteristics become the main factors affecting the acute expansion of the Absorb BVS. Our findings (from **Table IIIC**) which showed that acute lumen gain is higher in larger vessels compared to smaller vessels supports firstly the recommendation that BRS should be avoided in smaller vessels specifically RVD smaller than 2.25mm. Secondly if a mismatch between scaffold and vessel size occurs, one may not expect PostDil to be able to overcome or correct the mismatch particularly in smaller vessels, emphasizing the importance of accurate preprocedural sizing, supported by the use of intravascular imaging if necessary. In larger vessels, while PostDil may increase MLD, other characteristics like lesion calcification may limit its effect. In our study, while the proportion of DM was similar between the post-Dil and

non-PostDil groups, the PostDil group had a higher proportion of calcified lesion which may account for the reduction in acute lumen gain in the PostDil group.

While PostDil of metallic stents is widely if not routinely performed without disruption risk, concerns of scaffold disruption with an increase in MACE such as periprocedual MI have been raised over aggressive PostDil of the Absorb BVS which is polymeric-based with lower radial and tensile strength as well as finite expansion compliance. Our study sought to address a real world clinical case scenario when procedurists may face the dilemma of choosing to perform further PostDil of an implanted BRS and chose to do so based on operators' discretion or individual preference. A recent study by Costa et al [15] showed that similar final angiographic and clinical results may be attained with or without post-dilation in the treatment of low to moderately complex coronary lesions with BRS. In this study, a higher MACE rate was observed in the post-Dil compared to the non- PostDil which was driven by a marginally higher rate of periprocedural non Q wave MI in the PostDil group. In our study, there were no significant differences in procedural MI between the two groups. This is despite the longer scaffold length implanted as well as more overlapping scaffolds used in the PostDil group compared to non-PostDil group.

Previous studies have reported lower restenosis rates in larger vessels after balloon angioplasty [16], directional atherectomy and stent implantation [6] whereas others have found no relation between vessel size and incidence of restenosis [17-20]. In this study, we evaluated the impact of final MLD on clinical outcomes following the Absorb BVS implantation. Our subanalysis of clinical events based on preprocedure RVD and final MLD yield interesting insights. Though our analysis did not show any significant difference in clinical outcomes in lesions whose RVD are smaller than 2.25mm [**Supplementary Table IA**], further analysis of clinical events

showed that there was a trend towards higher Target lesion failure (TLF), target vessel myocardial infarct (TvMI) and definite scaffold thrombosis (Def ST) in the group with final in scaffold MLD that is less than 2.4mm [**Supplementary Table IB**]. Of note all 3 cases of definite scaffold thrombosis occurred in the group with final in scaffold MLD that is less than 2.4mm (**Supplementary Table IB**). Such a finding was also observed in the recently published ABSORB III [3] which showed that a larger final in scaffold MLD is associated with lower TLF, TvMI and Def ST rates. Such a finding can be explained by the resultant relatively higher scaffold footprint from a lower final MLD [10] that forms from a crimped scaffold thus creating more areas of wall shear stress leading to increased thrombogenicity and higher scaffold thrombosis rates. It also reinforces the importance of optimal nominal scaffold size in relation to accurate vessel sizing to reduce scaled residual stenosis [10].

We acknowledge the following limitations. This is a single centre retrospective non-randomised study with its inherent limitations, including a possible selection bias. Firstly, there is a possibility of selection bias since where the decision as to whether or not to post-dilate was based solely on the operator's discretion. Secondly, enrollment in BVS EXPAND was restricted to patients with in a non-acute setting. Our findings may not be necessarily applicable to patients who present acutely in STEMI. Thirdly, the study was underpowered to examine clinical events such as cardiac death and stent or scaffold thrombosis. Larger prospective randomised control trials are necessary to further confirm this trend and evaluate the impact of higher MLD or RVD on angiographic outcomes such as late lumen loss.

CONCLUSION

In our study, immediately post BRS implantation, an acceptable MLD above 2.40mm was seldom achieved which nevertheless improved after PostDil. PostDil of BRS resulted in a slight increase in minimal lumen diameter, not yet achieving similar acute gain and final MLD as in patient where PostDil was deemed not indicated by the operator. Yet PostDil importantly increased the rate of acceptable final MLD in these complex lesion and 2 year clinical outcomes was not affected by PostDil. Further studies are required to further the long term impact of post dilation in optimizing final MLD on clinical outcomes.

References

1. Diletti R, Karanasos A, Muramatsu T, Nakatani S, Van Mieghem NM, Onuma Y, Nauta ST, Ishibashi Y, Lenzen MJ, Ligthart J, Schultz C, Regar E, de Jaegere PP, Serruys PW, Zijlstra F, van Geuns RJ. Everolimus-eluting bioresorbable vascular scaffolds for treatment of patients presenting with ST-segment elevation myocardial infarction: BVS STEMI first study. Eur Heart J. 2014 Mar;35(12):777-86. doi: 10.1093/eurheartj/eht546. Epub 2014 Jan 6.

2. Felix CM, Fam JM, Diletti R, Ishibashi Y, Karanasos A, Everaert BR, van Mieghem NM, Daemen J, de Jaegere PP, Zijlstra F, Regar ES, Onuma Y, van Geuns R^2. Mid- to Long-Term Clinical Outcomes of Patients Treated With the Everolimus-Eluting Bioresorbable Vascular Scaffold: The BVS Expand Registry. JACC Cardiovasc Interv. 2016 Aug 22;9(16):1652-63. doi: 10.1016/j.jcin.2016.04.035. Epub 2016 Jul 27.

3. Ellis SG, Kereiakes DJ, Metzger DC, Caputo RP, Rizik DG, Teirstein PS, Litt MR, Kini A, Kabour A, Marx SO, Popma JJ, McGreevy R, Zhang Z, Simonton C, Stone GW; ABSORB III Investigators. Everolimus-Eluting Bioresorbable Scaffolds for Coronary Artery Disease.N Engl J Med. 2015 Nov 12;373(20):1905-15. doi: 10.1056/NEJMoa1509038. Epub 2015 Oct 12.

4. Gao R, Yang Y, Han Y, Huo Y, Chen J, Yu B, Su X, Li L, Kuo HC, Ying SW, Cheong WF, Zhang Y, Su X, Xu B, Popma JJ, Stone GW. ABSORB China Investigators. Bioresorbable Vascular Scaffolds Versus Metallic Stents in Patients With Coronary

Artery Disease: ABSORB China Trial. J Am Coll Cardiol. 2015 Dec 1;66(21):2298-309. doi: 10.1016/j.jacc.2015.09.054. Epub 2015 Oct 12.

5. Kimura T, Kozuma K, Tanabe K, Nakamura S, Yamane M, Muramatsu T, Saito S, Yajima J, Hagiwara N, Mitsudo K, Popma JJ, Serruys PW, Onuma Y, Ying S, Cao S, Staehr P, Cheong WF, Kusano H, Stone GW. ABSORB Japan Investigators. A randomized trial evaluating everolimus-eluting Absorb bioresorbable scaffolds vs. everolimus-eluting metallic stents in patients with coronary artery disease: ABSORB Japan. Eur Heart J. 2015 Dec 14;36(47):3332-42. doi: 10.1093/eurheartj/ehv435. Epub 2015 Sep 1.

6. Kuntz RE, Safian RD, Carroza JP, Fischman RF, Mansour M, Bairn DS. The importance of acute luminal diameter in determining restenosis after coronary atherectomy or stenting. Circulation. 1992;86;1827-1835.

7. Umans VA, Robert A, Foley D, Wijns W, Haine E, de Feyter PJ, Serruys PW. Clinical, histologic and quantitative angiographic predictors of restenosis following directional coronary atherectomy: a multivariate analysis of the renarrowing process and late outcome. JAm Coll Cardiol. 1994;23:49-58.

8. Yamaji K, Räber L, Windecker S. What determines long-term outcomes using fully bioresorbable scaffolds - the device, the operator or the lesion? EuroIntervention. 2017 Feb 20;12(14):1684-1687. doi: 10.4244/EIJV12I14A277.

9. Tanimoto S, Serruys PW, Thuesen L, et al. Comparison of in vivo acute stent recoil between the bioabsorbable everolimus-eluting coronary stent and the everolimus-eluting cobalt chromium coronary stent: insights from the ABSORB and SPIRIT trials. Catheter Cardiovasc Interv 2007;70:515–23.

10. Serban Puricel, Florim Cuculi, Melissa Weissner, MTA, Axel Schmermund, Peiman Jamshidi,Tobias Nyffenegger, Harald Binder, Holger Eggebrecht, Thomas Münzel, Stephane Cook, Tommaso Gori. Bioresorbable Coronary Scaffold Thrombosis Multicenter Comprehensive Analysis of Clinical Presentation, Mechanisms, and Predictors. J Am Coll Cardiol 2016;67: 921–31.

11. Cutlip DE, Windecker S, Mehran R, Boam A, Cohen DJ, van Es GA, et al. Clinical end points in coronary stent trials: a case for standardized definitions. Circulation. 2007;115:2344-51.

12. David P. Foley, MB BCh, MRCPI; Rein Melkert, MD; Patrick W. Serruys, MD, PhD, FACC,on behalf of the CARPORT, MERCATOR, MARCATOR, and PARK Investigators. Influence of Coronary Vessel Size on Renarrowing Process and Late Angiographic Outcome After Successful Balloon Angioplasty. Circulation. 1994;90:1239-1251.)

13. de Jaegere P, Mudra H, Figulla H, Almagor Y, Doucet S, Penn I, Colombo A, Hamm C, Bartorelli A, Rothman M, Nobuyoshi M, Yamaguchi T, Voudris V, DiMario C,

Makovski S, Hausmann D, Rowe S, Rabinovich S, Sunamura M, van Es GA. Intravascular ultrasound-guided optimized stent deployment. Immediate and 6 months clinical and angiographic results from the multicenter ultrasound stenting in coronaries study (MUSIC Study). Eur Heart J 1998;19:1214–1223

14. Otake H, Shite J, Ako J, Shinke T, Tanino Y, Ogasawara D, Sawada T, Miyoshi N, Kato H, Koo BK, Honda Y, Fitzgerald PJ, Hirata K. Local determinants of thrombus formation following sirolimus-eluting stent implantation assessed by optical coherence tomography. J Am Coll Cardiol Intv 2009;2: 459–66.

15. José De Ribamar Costa Jr, MD, PhD; Alexandre Abizaid, MD, PhD; Antonio L. Bartorelli, MD; Robert Whitbourn, MD; Robert Jan van Geuns, MD, PhD; Bernard Chevalier, MD; Marcos Perin, MD, PhD; Ashok Seth, MD; Roberto Botelho, MD, PhD; Patrick W. Serruys, MD, PhD; on behalf of the ABSORB EXTEND Investigators. Impact of post-dilation on the acute and one-year clinical outcomes of a large cohort of patients treated solely with the Absorb Bioresorbable Vascular Scaffold. EuroIntervention. 2015 Jun;11(2):141-8. doi: 10.4244/EIJY15M05_06.

16. Hirshfeld JW, Schwartz SS, Jugo R, Macdonald RG, Goldberg S, Savage MP, Bass TA, Vetrovec G, Cowley M, Taussig AS, Withworth HB, Margolis JR, Hill JA, Pepine CJ, and the M-Heart Investigators. Restenosis after coronary angioplasty: a multivariate statistical model to relate lesion and procedural variables to restenosis. JAm Coil CardioL 1991;18:647-656.

17. Serruys PW, Rensing BJ, Luijten HE, Hermans WR, Beatt KJ. Restenosis following coronary angioplasty. In: Meier B, ed. Interventional Cardiology. Toronto/Lewiston, NY/Bern/Gottingen/ Stuttgart: Hogrefe and Huber; 1990:79-115.

18. Bobbio M, Detrano R, Colombo A, Lehmann KG, Park JB. Restenosis rate after percutaneous transluminal coronary angioplasty: a literature overview. J Invas Cardiol. 1991;3:214-224.

19. Strauss BH, Serruys PW, de Scheerder IK, Tijssen JGP, Bertrand ME, Puel J, Meier B, Kaufmann U, Strauffer JC, Rickards AF, Sigwart U. A relative risk analysis of the angiographic predictors of restenosis within the coronary Wallstent. Circulation. 1991;84: 1636-1643.

20. de Jaegere P, Serruys PW, Bertrand M, Wiegand V, Marquis JF, Vrolicx M, Piessens J, Valeix B, Kober G, Bonnier H, Rutsch W, Uebis R. Angiographic predictors of recurrence of restenosis after Wiktor stent implantation in native coronary arteries. Am J Cardiol. 1993;72: 165-170.

21. Rensing BJ, Hermans WRM, Vos J, Thijssen JGP, Rutsch W, Danchin N, Heyndrickx GR, Mast EG, Wijns W, Serruys PW. Luminal narrowing after percutaneous transluminal coronary angioplasty: a study of clinical, procedural, and lesional factors related to long-term angiographic outcome. Circulation. 1993;88: 975-985.

22. Onuma Y, Serruys PW, Gomez J, de Bruyne B, Dudek D, Thuesen L, Smits P, Chevalier B, McClean D, Koolen J, Windecker S, Whitbourn R, Meredith I, Garcia-Garcia H, Ormiston JA; ABSORB Cohort A and B investigators. Comparison of in vivo acute stent recoil between the bioresorbable everolimus-eluting coronary scaffolds (revision 1.0 and 1.1) and the metallic everolimus-eluting stent. *Catheter Cardiovasc Interv.* 2011;78:3-12.

Figure Legends

Figure 1A-D. Kaplan-Meier curves showing no significant difference in MACE (A), ST (B), DOCE (C) and POCE (D) at 2 years in patients treated with bioresorbable vascular scaffolds with and without postdilation done. MACE- major adverse cardiovascular events; ST scaffold thrombosis; DOCE- device oriented composite endpoints; POCE- patient oriented composite endpoints.

Table I Demographic Characteristics

	BRS (N= 294)		
	PostDilation Performed (N= 164)	**PostDilation Not Performed(N=130)**	
Age	59.82 ±10.81	60.07 ±10.46	0.843
Male	124 (75.6)	99 (76.2)	1.000
Active smoker	53 (32.3)	53(40.8)	0.197
Diabetes mellitus	27 (16.5)	27 (20.8)	0.366
Dyslipidaemia	82 (50.3)	67 (51.9)	0.814
Hypertension	96 (58.9)	74 (56.9)	0.812
Family History	64 (39.0)	62 (47.7)	0.442
CVA/TIA	14 (8.5)	10 (7.7)	0.834
Prior MI	28 (17.1)	18 (13.8)	0.519
Prior PCI	15 (9.1)	12 (9.2)	1.000
Prior CABG	0	1 (0.8)	0.442
Kidney disease	11 (6.7)	7 (5.4)	0.807
Heart failure	5 (3.0)	9 (6.9)	0.168
Clinical presentation			0.352
Stable Angina	72 (43.9)	44 (33.8)	
Unstable Angina	22 (13.4)	23 (17.7)	
NSTEMI	69 (42.1)	62 (47.7)	
Congestive cardiac failure	1 (0.6)	1 (0.8)	
SVD/DVD/TVD	102(66.2)/47(28.7)/15(9.1)	91(70.0)/27(20.8)/12(9.2)	0.291

CVA- Cerebrovascular accident, TIA- Transient Ischaemic Attack; MI- Myocardial Infarct; PCI- percutaneous coronary intervention; CABG- Coronary artery bypass graft; NSTEMI- non ST elevation MI; SVD- Single vessel disease; DVD- double vessel disease; TVD- triple vessel disease

Values are expressed in numbers (percentages) or mean ± standard deviation when appropriate.

Table IIA Lesion Characteristics

	BRS (N= 294; L = 387)		
	PostDilation performed (N= 164; L= 211)	**PostDilation not performed N=130; L=176)**	**P value**
Target vessel			0.081
LAD	115 (54.5)	72 (40.9)	
LCX	33 (15.7)	49 (27.9)	
RCA	110 (23.7)	50 (28.4)	
Diagonal	10 (4.7)	5 (2.9)	
Ramus	1 (0.5)	0	
Left Main	2 (1.0)	0	
SVG	0	0	
Lesion AHA			<0.001
A	21(10.0)	42 (23.9)	
B1	87(41.6)	91 (51.7)	
B2	57(27.3)	33(18.8)	
C	44(21.1)	10(5.7)	
Bifurcation	97 (23.5)	22 (16.5)	0.116
Mod/Heavy calcification	108 (51.2)	52 (29.6)	<0.001
Chronic Total occlusions	12 (5.7)	5 (2.8)	0.050
TIMI			0.591
Preprocedure			
TIMI 0	19 (9.0)	21 (11.9)	
TIMI 1	3 (1.4)	4 (2.3)	
TIMI 2	24 (11.4)	24 (13.6)	
TIMI 3	164 (77.7)	127 (72.2)	
Postprocedure			0.070
TIMI 0	0	0	
TIMI 1	0	1 (0.6)	
TIMI 2	10 (4.7)	2 (1.1)	
TIMI 3	201 (95.3)	173 (98.3)	

Table IIB Comparison of Quantitative Coronary Analysis between the post dilation and non-postdilation groups

	BRS (N= 294; L = 387)		
	PostDilation performed (N= 164; L= 211)	**PostDilation not performed N=130; L=176)**	**P value**
QCA Analysis			
Pre-procedure			
Treatment length	25.31 ±14.53	20.06 ±10.13	<0.001
RVD (mm)	2.52 ±0.52	2.57 ±0.55	0.358
MLD (mm)	0.99 ±0.44	0.90 ± 0.41	0.054
Diameter stenosis (%)	60.81 ± 16.62	63.87 ±16.99	0.086
Post-procedure			
RVD (mm)	2.71 ±0.45	2.84 ±0.46	0.005
MLD (mm)	2.25 ± 0.39	2.38 ±0.44	0.002
Diameter stenosis (%)	16.77 ± 8.82	16.59 ± 8.93	0.840
Acute Lumen Gain	1.33 ±0.59	1.53 ±0.63	0.002

MLD: Minimal Lumen Diameter; RVD: Reference Vessel diameter; Values are expressed as numbers (percentages) or mean ± standard deviation when appropriate.

Table IIIA Procedural Characteristics

	BRS (N= 294; L = 387)		
	PostDilation performed (N= 164; L= 211)	**PostDilation not performed N=130; L=176)**	**P value**
Number of treated lesions per procedure	1.21 ±0.49	1.18 ±0.47	0.590
Aspiration thrombectomy	7 (3.3)	11 (6.3)	0.227
Rotablation	8 (3.8)	2 (1.1)	0.367
Scoring balloon	9 (4.3)	1 (0.6)	0.025
Intracoronary imaging			
IVUS	37 (17.6)	21 (11.9)	0.152
OCT	64 (30.3)	33 (18.8)	0.010
Predilation	191 (90.5)	156 (88.6)	0.616
Max predilation diameter	2.60 ± 0.37	2.59 ± 0.39	0.806
Predilation Balloon: artery ratio	1.05 ± 0.24	1.02 ± 0.24	0.225
Maximum predilation inflation pressure, atm	14.28 ± 3.09	13.47 ± 2.86	0.049
Buddy wire	22 (10.4)	5 (2.8)	0.004
Mean Number of scaffold	1.50 ± 0.75	1.20 ± 0.57	<0.001
Number of scaffolds (529)	317	212	<0.001
1	132 (62.6)	150 (85.2)	
2	58 (27.5)	20 (11.4)	
3	15 (7.1)	2 (1.1)	
4	6 (2.8)	4 (2.3)	
Scaffold diameter, mm	3.04 ± 0.35	3.13 ± 0.36	0.014
Scaffold length implanted, mm	32.50 ± 19.30	23.92 ± 13.45	<0.001
Overlapping scaffolds	77 (36.5)	25 (14.2)	<0.001
Maximum scaffold implantation pressure, atm	14.83 ± 1.93	15.38 ± 1.52	0.007
Postdilation balloon: mean scaffold diameter ratio	1.06 ± 0.12	-	-
Max postdilation balloon	3.26 ± 0.44	-	-
Maximum postdilation inflation pressure, atm	16.05 ± 4.24	-	-

Table IIIB Effect of postdilation on scaffold and vessel Diameters

N= 117 pairs	After BRS Implantation	Final	Difference (Final- After BRS)	P value
RVD, mm	2.64 ± 0.47	2.81 ± 0.43	0.16 ± 0.37 (+6.1%)	<0.001
MLD, mm	2.18±0.43	2.32±0.35	0.14 ± 0.32 (+6.1%)	<0.001
Number of lesions MLD 2.4 mm or greater	33/117 (28.2%)	49/117 (41.9%)		<0.001
Diameter Stenosis, %	17.02 ± 10.48	16.98 ± 9.23	(-) 0.03 ± 12.39	0.976

Table IIIC Acute luminal gain in relation to vessel size and postdilation characteristics (N= 117 pairs)*

Vessel size*	Pre RVD less than 2.25mm			Pre RVD 2.25mm or greater			P value
Acute luminal gain	1.16 ± 0.54			1.43 ± 0.55			<0.001
Vessel size*	Pre RVD less than 2.25mm			Pre RVD 2.25mm or greater			
	Postdilation (+)	Postdilation (-)	P value	Postdilation (+)	Postdilation (-)	P value	
Acute luminal gain	1.11± 0.51	1.24 ± 0.59	0.246	1.34 ± 0.56	1.53 ± 0.53	0.004	
Postdilation characteristics	Post dilation Inflation pressure 16mmhg or greater			Post dilation Inflation pressure less than 16mmhg			P value
Acute luminal gain	1.14 ± 0.63			1.41 ± 0.56			0.002
	Post dilation balloon: Scaffold ratio 1.1 or greater			Post dilation balloon: Scaffold ratio less than 1.1			
Acute luminal gain	1.39 ± 0.62			1.31 ± 0.57			0.353

*small vessel as defined by pre RVD smaller than 2.25mm

Table IVA Procedural Outcomes

	BRS (N= 294; L = 387)		
	PostDilation performed (N= 164; L= 211)	**PostDilation not performed N=130; L=176)**	**P value**
Procedural Outcomes			
Device Success	209 (99.1)	176 (100.0)	0.503
Bailout by scaffold	6 (2.8)	4 (2.3)	0.541
Bailout by metallic stent	3 (1.4)	1 (0.6)	0.601
Intraprocedural thrombosis	1 (0.5)	1(0.6)	1.000
Significant Dissection	12 (5.7)	6 (3.4)	0.582
Signifcant no reflow/ slow flow	8 (3.8)	7 (4.0)	0.622
Periprocedural MI (Definite)	1.6 (2)	0 (0.0)	0.19

Table IVB Clinical endpoints at 2 years

	Post-Dil (n=119)	No-Post-dil (n=107)	P value
MACE (%)	9.9 (11)	6.9 (7)	0.402
Device Oriented Composite Endpoint (DOCE)			
DOCE (%)	9.9 (11)	3.8 (4)	0.89
Cardiac death (%)	3.7 (4)	0.8 (1)	0.202
Target Vessel MI	6.3 (7)	3.1 (3)	0.241
Clinically indicated TLR (%)	5.5 (6)	2.9 (3)	0.360
Definite ST (%)	2.6 (3)	0	0.092
Early	0	0	-
Late	2.6 (3)	0.0	0.092
Very late	0	0	-
Patient Oriented Composite Endpoint (POCE)	**Post-Dil (n=119)**	**No-Post-dil (n=107)**	**P value**
POCE (%)	13.4 (14)	7.0 (7)	0.160
All-cause mortality (%)	3.7 (4)	0.8 (1)	0.202
Any revascularization	13.1 (14)	9.9 (10)	0.512
TVR (%)	6.3 (7)	3.8 (4)	0.427
Non-TVR (%)	7.3 (8)	7.0 (7)	0.893
All cause MI (%)	6.3 (7)	6.1 (6)	?0.844

DOCE: device oriented composite endpoints (Composite of cardiac death, target vessel myocardial infarct and clinically indicated target lesion revascularization); POCE: patient oriented composite endpoints (Composite of all- cause mortality, all cause myocardial infarct and any revascularization). (Number of composite endpoints does not add up as any patient may have multiple events.)

Online Supplement

Supplementary Table 1A

Cumulative event rates at two years, described as Kaplan-Meier estimates

	Pre-proc RVD < 2.25mm (n=51)	**Pre- proc RVD ≥ 2.25mm (n=159)**	**P value**
TLF	6.1 (3)	7.4 (11)	0.834
TLR	3.9 (3)	4.0 (6)	0.939
CI-TLR	3.9 (3)	4.0 (6)	0.939
TVR	7.8 (4)	4.0 (6)	0.216
MI	3.9 (2)	6.8 (10)	0.555
Tv-MI	3.9 (2)	4.8 (7)	0.899
Definite ST	2.0 (1)	0.6 (1)	0.393

Supplementary Table 1B

Cumulative event rates at two years, described as Kaplan-Meier estimates

	Final in-scaffold MLD < 2.4 mm (N=139)	**Final in-scaffold MLD ≥ 2.4 mm (N=87)**	**P value**
TLF	7.5 (10)	6.2 (5)	0.613
TLR	4.6 (6)	3.6 (3)	0.719
CI-TLR	4.6 (6)	3.6 (3)	0.719
TVR	6.0 (8)	3.6 (3)	0.414
MI	5.9 (8)	6.4 (5)	0.925
Tv MI	5.2 (7)	3.9 (3)	0.537
Definite ST	2.2 (3)	0	0.171

Supplementary Table 1C Impact of Postdilation on Clinical Events

	Pre-proc RVD < 2.25mm (n=51)				Pre- proc RVD ≥ 2.25mm (N=159)			
	Total (n=51)	PostDil (n=31)	No PostDil (n=20)	p	Total (n=159)	PostDil (n=78)	No PostDil (n=81)	**P**
TLR	3.9 (3)	6.5 (2)	0	0.252	4.0 (6)	4.3 (3)	3.8 (4) with P 0.960	0.939
TVR	7.8 (4)	9.7 (3)	5.0 (1)	0.569	4.0 (6)	4.7 (3)	3.8 (3) with P 0.960	0.216
Tv MI	3.9 (2)	6.5 (2)	0	0.252	4.8 (7)	5.6 (4)	4.1 (3) with P 0.646	0.899
Def ST	2.0 (1)	3.2 (1)	0	0.422	0.6 (1)	1.3 (1)	0.0 with P 0.302	0.393
TLF	6.1 (3)	10 (3)	0	0.157	7.4 (11)	9.3 (7)	5.2 (4) with P 0.297	0.834

PostDil- PostDilation; TLR- Target lesion revascularization; TVR- Target vessel revacsularisation; Tv MI- Target vessel myocardial infarct; Def ST- Definite scaffold thrombosis; TLF- Target lesion failure

Supplementary Table 1D Impact of Postdilation on Clinical Events in Final Minimal Luminal Diameter (MLD)

	Final in-scaffold MLD < 2.4 mm (n=139)				**Final in-scaffold MLD ≥ 2.4 mm (n=139)**			
	Total (N=139)	**Post-dil (n=80)**	**No post-dil (n=59)**	**P value**	**Total (n=87)**	**Post-dil (n=39)**	**No post-dil (n=48)**	**P value**
TLF	7.5 (10)	10.3 (8)	3.6 (2)	0.136	6.2 (5)	8.9 (I3)	4.3 (2)	0.414
TLR	4.6 (6)	6.6 (5)	2.0 (1)	0.192	3.6 (3)	3.0 (1)	4.2 (2)	0.718
TVR	6.0 (8)	6.3 (5)	3.7 (2)	0.434	3.6 (3)	3.0 (1)	4.2 (2)	0.718
Tv MI	5.2 (7)	6.3 (5)	3.7 (2)	0.434	3.9 (3)	5.8 (2)	2.4 (1)	0.402
Definite ST	2.2 (3)	3.8 (0)	0.0 (0)	0.129	0	0	0	-

Supplementary Table 2 Predictors for clinical outcomes at two years follow-up (using Cox regression), post-dil + vs post-dil -

	Unadjusted HR (95% CI)	p-value	Adjusted* HR (95% CI)	p value
All-cause death				
post-dil + vs post-dil -	3.732 (0.417 – 33.401)	0.239	2.967 (0.318 – 27.696)	0.340
Cardiac death				
post-dil + vs post-dil -	3.732 (0.417 – 33.401)	0.239	2.967 (0.318 – 27.696)	0.340
MACE				
post-dil + vs post-dil -	1.495 (0.579 – 3.857)	0.406	1.406 (0.535 – 3.696)	0.489
DOCE				
post-dil + vs post-dil -	2.602 (0.828 – 8.171)	0.102	2.352 (0.734 – 7.535)	0.150
POCE				
post-dil + vs post-dil -	1.895 (0.765 – 4.696)	0.467	1.755 (0.698 – 4.414)	0.232
MI				
post-dil + vs post-dil -	1.105 (0.371 – 3.287)	0.858	1.084 (0.357 – 3.287)	0.887
TLR				
post-dil + vs post-dil -	1.871 (0.468 – 7.483)	0.376	1.582 (0.383 -6.531)	0.526
TVR				
post-dil + vs post-dil -	1.620 (0.474 – 5.535)	0.441	1.395 (0.397 – 4.899)	0.604
Non-TVR				
post-dil + vs post-dil -	1.072 (0.389 – 2.958)	0.893	1.017 (0.362 – 2.855)	0.974
Definite ScT				
post-dil + vs post-dil -	61.394 (0.006 – 665429.200)	0.385		

*Adjusted with propensity score (using gender, age, presentation with ACS, pre-procedural RVD < 2.25mm and final in-scaffold MLD < 2.4mm)

Figures

Figure 1A

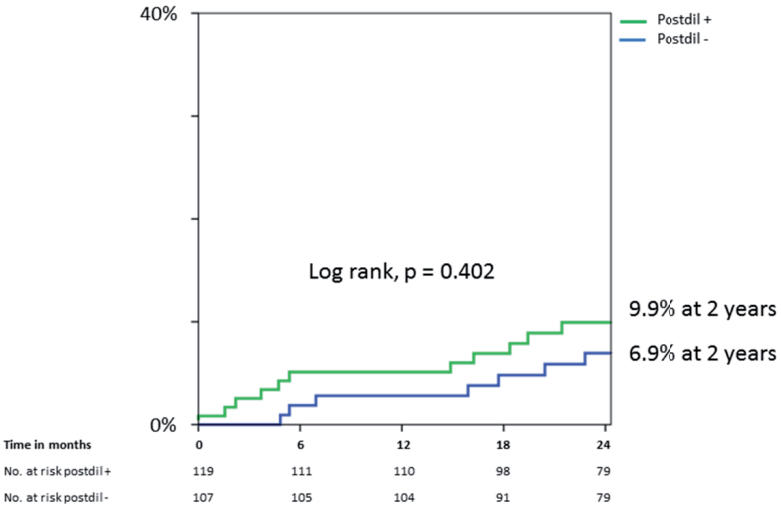

Figure 1B

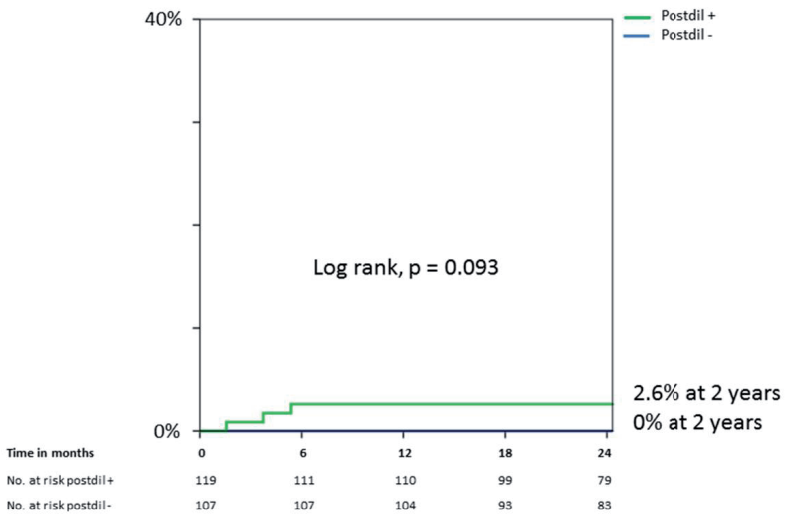
40%
0%
Postdil +
Postdil -
Log rank, p = 0.093
2.6% at 2 years
0% at 2 years
Time in months 0 6 12 18 24
No. at risk postdil + 119 111 110 99 79
No. at risk postdil - 107 107 104 93 83

Figure 1C

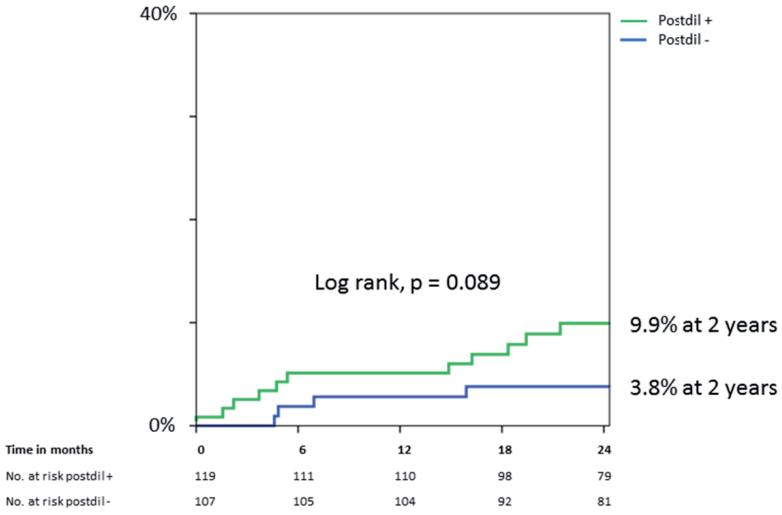
40%
0%
Postdil +
Postdil -
Log rank, p = 0.089
9.9% at 2 years
3.8% at 2 years
Time in months 0 6 12 18 24
No. at risk postdil+ 119 111 110 98 79
No. at risk postdil- 107 105 104 92 81

Figure 1D

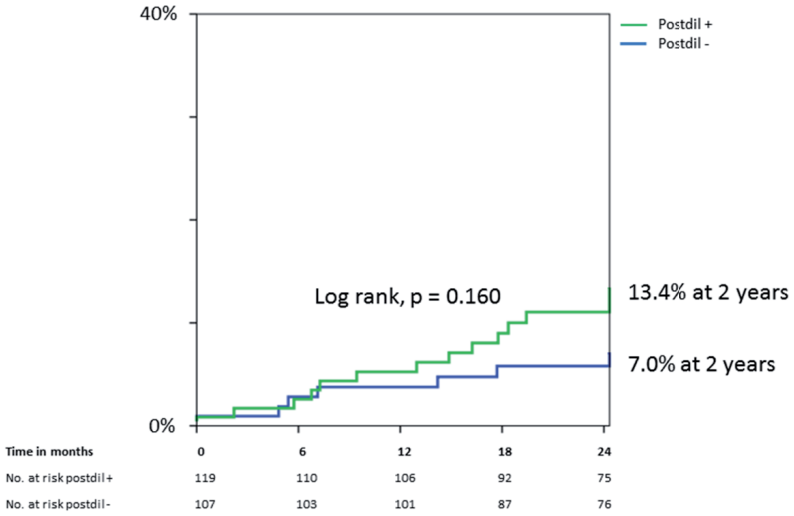
40%
0%
Postdil +
Postdil -
Log rank, p = 0.160
13.4% at 2 years
7.0% at 2 years
Time in months 0 6 12 18 24
No. at risk postdil+ 119 110 106 92 75
No. at risk postdil- 107 103 101 87 76

IV

PART

TREATMENT OF CORONARY ARTERY DISEASE WITH BIORESORBABLE VASCULAR SCAFFOLDS- OUTCOMES AND LIMITATIONS IN DIFFERENT CLINICAL AND LESION SUBSETS

17

CHAPTER

EXPANDED CLINICAL USE OF EVEROLIMUS ELUTING BIORESORBABLE VASCULAR SCAFFOLDS FOR TREATMENT OF CORONARY ARTERY DISEASE

Roberto Diletti, Yuki Ishibashi, Cordula Felix, Yoshinobu Onuma, Shimpei Nakatani, Nicolas M. van Mieghem, Eveliyn Regar, Marco Valgimigli, Peter P. de Jaegere, Nienke van Ditzhuijzen, **Jiang Ming Fam**, Jurgen M.R. Ligthart, Mattie J. Lenzen, Patrick W. Serruys, Felix Zijlstra, Robert Jan van Geuns.

Catheter Cardiovasc Interv. 2017 Jul; 90 (1):58-69.

Expanded Clinical Use of Everolimus Eluting Bioresorbable Vascular Scaffolds for Treatment of Coronary Artery Disease

Roberto Diletti,[1*] MD, PhD, Yuki Ishibashi,[1] MD, PhD, Cordula Felix,[1] MD, Yoshinobu Onuma,[1,2] MD, Shimpei Nakatani,[1] MD, Nicolas M. van Mieghem,[1] MD, PhD, Eveliyn Regar,[1] MD, PhD, Marco Valgimigli,[1] MD, PhD, Peter P. de Jaegere,[1] MD, PhD, Nienke van Ditzhuijzen,[1] MD, Jiang Ming Fam,[1] MBBS, MD, Jurgen M.R. Ligthart,[1] RT, Mattie J. Lenzen,[1] PhD, Patrick W. Serruys,[1] MD, PhD, Felix Zijlstra,[1] MD, PhD, and Robert Jan van Geuns,[1] MD, PhD

Background: Limited data are currently available on the performance of everolimus eluting bioresorbable vascular scaffold (BVS) for treatment of complex coronary lesions representative of daily practice. Methods: This is a prospective, mono-center, single-arm study, reporting data after BVS implantation in patients presenting with stable, unstable angina, or non-ST segment elevation myocardial infarction caused by *de novo* stenotic lesions in native coronary arteries. No restrictions were applied to lesion complexity. Procedural results and 12-month clinical outcomes were reported. Results: A total of 180 patients have been evaluated in the present study, with 249 treated coronary lesions. Device Success per lesion was 99.2%. A total of 119 calcified lesions were treated. Comparable results were observed among severe, moderate and noncalcified lesions in term of %diameter stenosis (%DS) (20.3 ± 10.5%, 17.8 ± 7.7%, 16.8 ± 8.6%; $P = 0.112$) and acute gain (1.36 ± 0.41 mm, 1.48 ± 0.44 mm, 1.56 ± 0.54 mm; $P = 0.109$). In bifurcations (54 lesions), side-branch ballooning after main vessel treatment was often performed (33.3%) with low rate of side-branch impairment (9.3%). A total of 29 cases with coronary total occlusions were treated. After BVS implantation %DS was not different from other lesion types (17.2 ± 9.4%, vs. 17.7 ± 8.6%; $P = 0.780$). At one year, all-cause mortality was reported in three cases. The rate of target lesion revascularization and target vessel revascularization was 3.3%. The rate of definite scaffold thrombosis was 2.6%. Conclusions: The implantation of the everolimus eluting bioresorbable vascular scaffold in an expanded range of coronary lesion types and clinical presentations was observed to be feasible with promising angiographic results and mid-term clinical outcomes.

Key words: bioabsorbable devices/polymers; coronary artery disease; interventional devices/innovation

INTRODUCTION

The everolimus eluting bioresorbable vascular scaffolds (BVS) represent a novel approach for treatment of coronary artery disease. Similarly to conventional metal stents the absorb BVS provide acute lumen gain, vessel scaffolding and drug elution to the vessel wall immediately after implantation [1]. However, at variance with standard stents, the polymeric structure of this device allows a gradual bioresorption of the implant over time [2]. Complete scaffold bioresorption is hypothesized to offer several advantages over permanent metal devices

Additional Supporting Information may be found in the online version of this article.

[1]Thoraxcenter Erasmus MC, Rotterdam, The Netherlands
[2]Cardialysis BV, Rotterdam, The Netherlands

Conflict of interest: Nothing to report

Contract grant sponsors: Abbott Vascular, Hellenic Heart Foundation, St Jude Medical..

*Correspondence to: Robert Jan van Geuns, MD, PhD, Erasmus MC, 's-Gravendijkwal 230, 3015 CE Rotterdam, the Netherlands. E-mail: r.vangeuns@erasmusmc.nl

Received 5 July 2015; Revision accepted 8 October 2016

DOI: 10.1002/ccd.26832
Published online 29 November 2016 in Wiley Online Library (wileyonlinelibrary.com)

comprising reacquirement of physiological vasomotion, late lumen enlargement, noninvasive imaging, and future treatment with bypass grafting [3–5]. In addition, the absence of a foreign body could avoid phenomena such as permanent side-branch jailing, late acquired malapposition and the occurrence of late and very late stent thrombosis [5].

The absorb BVS has been initially tested in humans in two cohort studies, both showing promising results in terms of surrogate and clinical endpoints [6–9]. However, being those studies an early evaluation of this technology, they were characterized by a patient population showing stable coronary artery disease and relatively simple lesions. The first randomized data in very selected patients (Absorb II, Absorb Japan) supported the further development of this technique.

At the current state of the art, very limited data are available on BVS performance in real-world patients, including those presenting with acute coronary syndromes and complex lesions. A lack of information is especially evident when considering important lesion subsets such as calcified plaques, long lesions, bifurcations, and total occlusions.

Given this background, the present study aims to report angiographic and clinical data after an expanded clinical use of the second generation BVS, implanted in patients admitted with different clinical presentations including acute coronary syndromes and having a broad range of coronary lesion types.

METHODS

This is an investigator initiated, prospective, single-center, single-arm post market study, aiming to evaluate the feasibility safety and performance of the absorb BVS for treatment of patients with coronary artery disease in routine clinical practice. Enrolled patients were subjects presenting with stable, unstable angina, or non-ST segment elevation myocardial infarction caused by *de novo* stenotic lesions in native coronary arteries. No restrictions were applied to lesion complexity. Because of the absorb BVS size availability, a D_{max} (proximal and distal mean lumen diameter) within the upper limit of 3.8 mm and the lower limit of 2.0 mm by online QCA was required. Exclusion criteria were minimal and comprised allergies or contraindications to antiplatelet medication, female patient with childbearing potential or currently breastfeeding, acute ST segment elevation myocardial infarction, and post CABG patients. As per hospital policy patients with a previously implanted metal DES in the intended target vessel were also excluded. Also, although old age was not an exclusion criterion, BVS were in general reserved for younger patients, and left to operator's interpretation of biological age. A hybrid approach combining BVS with small DES or large DES where necessary was also not recommended.

All patients were treated with DAPT according to current guidelines. DAPT was prescribed for one year after PCI. Prasugrel was standard therapy for ACS presenting patients while Clopidogrel was initiated for stable angina patients only.

To assess clinical outcomes, a questionnaire was sent to all living patients with specific queries on rehospitalization and cardiovascular events. For patients who suffered an adverse event at another center, medical records, or discharge letters from the other institutions were systematically reviewed. General practitioners and referring physicians were contacted for additional information if necessary.

Ethics

This is an observational study, performed according to the privacy policy of the Erasmus MC, and to the Erasmus MC regulations for the appropriate use of data in patient-oriented research, which are based on international regulations, including the declaration of Helsinki. The BVS received the CE mark for clinical use, indicated for improving coronary lumen diameter in patients with ischemic heart disease due to *de novo* native coronary artery lesions with no restriction in terms of clinical presentation. Therefore, the BVS can be currently used routinely in Europe in different settings without a specific written informed consent in addition to the standard informed consent prior to the procedure. Therefore, a waiver from the hospital Ethical Committee was obtained for written informed consent, as according to Dutch law written consent is not required, if patients are not subject to acts other than as part of their regular treatment. Specific written informed consent post procedure was asked for a detailed follow-up program which targets to include 300 patients in the full BVS-EXPAND study.

Study Device

The device used in the present study is the second generation Absorb BVS (Abbott Vascular, Santa Clara, CA); a balloon expandable scaffold with a polymer backbone of Poly-L lactide acid (PLLA) coated with a thin layer of a 1:1 mixture of an amorphous matrix of Poly-D and L-lactide acid (PDLLA) polymer, controlling the release of 100 $\mu g/cm^2$ of the antiproliferative drug everolimus. Two platinum markers located at each Absorb BVS edge allowing for accurate visualization of the radiolucent Absorb BVS during angiography or other imaging modalities. Approximately 80% of the drug is eluted within the first 30 days. Both PLLA and PDLLA are fully bioresorbable. The polymers are degraded mainly via hydrolysis resulting

oligomers of lactate metabolized by Krebs cycle. Small particles, less than 2 μm in diameter, have also been shown to be phagocytized and degraded by macrophages.

Definitions

Device success was defined as the attainment of <30% final in segment residual stenosis after absorb BVS implantation, by angiographic visual estimation. Procedure success was defined as device success and no major periprocedural complications (Emergent CABG, coronary perforation requiring pericardial drainage, residual dissection impairing vessel flow—TIMI-flow II or less -). Clinical success was defined as procedural success and no in-hospital major adverse cardiac events (MACE). All deaths were considered cardiac unless an undisputed noncardiac cause was identified. Myocardial infarction (MI) and scaffold thrombosis were defined according to the Academic Research Consortium (ARC) definition. Any Target lesion revascularization (TLR) was defined as clinically driven if at repeat angiography a diameter stenosis >70% was observed, or if a diameter stenosis >50% was present in association with recurrent angina pectoris; objective signs of ischaemia (ECG changes) at rest or during exercise test, likely to be related to the target vessel; abnormal results of any invasive functional diagnostic test.

Target lesion failure was defined as the composite of cardiac death, target vessel myocardial infarction, or ischemia driven target lesion revascularization. Major adverse cardiac events (MACE), defined as the composite of cardiac death, any reinfarction (Q or Non Q-Wave), emergent bypass surgery (CABG), or clinically driven target lesion revascularization (TLR). Target vessel failure (TVF) was defined as cardiac death, target vessel myocardial infarction (MI), or clinically driven target vessel revascularization (TVR). Delivery failure was defined as opening of scaffold from its cover and insertion into the guiding-catheter without final implantation.

All potential events were adjudicated by a local independent Clinical Events Committee (CEC).

Quantitative Coronary Angiography

Quantitative coronary angiography (QCA) analyses were performed using the Coronary Angiography Analysis System (Pie Medical Imaging, Maastricht, Netherlands).

The QCA measurements we performed pre and post BVS implantation. The 37 μm platinum radio-markers located at each end of the Absorb BVS aided in the localisation of the nonradio-opaque scaffold for QCA. Analysed parameters included reference vessel diameter (RVD)—calculated with interpolate method—percentage diameter stenosis (%DS) and minimal lumen diameter (MLD). Acute gain was defined as postprocedural MLD minus preprocedural MLD. The angiographic analysis were performed by three investigators (YI, YO, and RD) who where extensively trained in an experienced core-lab (Cardialysis BV, Rotterdam, The Netherlands).

A calcified coronary culprit lesion was defined as already reported [10] "readily apparent densities noted within the apparent vascular wall at the site of the stenosis." By qualitative assessment of the angiograms, target lesions were classified as severe ("radioopacities noted without cardiac motion prior to contrast injection generally involving both sides of the arterial wall"), moderate ("densities noted only during the cardiac cycle prior to contrast injection"), or none/mild (lesions other than severe and moderate calcified lesions). The inter- and intra-observer variability in the qualitative analysis of coronary calcium on coronary angiograms have been already reported [11].

To provide insights on the coronary bifurcation treatment with BVS we performed a full analysis of techniques and material used and we reported the occurrence of side-branch impairment, an end-point already reported in the literature as "side-branch trouble" [12] and defined as follow: at least 1 of the following procedural parameters: (1) Side-branch TIMI flow grade <3 after main vessel stenting; (2) need of guidewire(s) different from the workhorse wire to rewire side-branch after main vessel scaffolding; (3) failure to rewire the side-branch after main vessel scaffolding; or (4) failure to dilate the side-branch after main vessel scaffolding and side-branch rewiring.

Statistical Analysis

Categorical variables are reported as counts and percentages, continuous variables as mean ± standard deviation; *P*-values were calculated with Fisher's Exact test for binary variables, Wilcoxon's Rank Sum test for continuous variables. Comparisons among multiple means were performed with analysis of variance (One-way ANOVA). A *P*-value <0.05 was considered statistically significant. Statistical analyses were performed using SPSS, version 15.0 for windows (IL).

RESULTS

From September 2012 to July 2013 a total of 1,529 percutaneous coronary interventions were performed in our center. A total of 180 patients have been enrolled in this first cohort of the BVS-EXPAND study, with

TABLE I. Baseline Clinical and Lesion Characteristics

Clinical characteristics	$N = 180$
Age	60.6 ± 10.6
Male *n* (%)	134 (74.4%)
Hypertension *n* (%)	94 (52.2%)
Hypercholesterolemia *n* (%)	84 (46.7%)
Diabetes *n* (%)	32 (17.8%)
Smoke *n* (%)	99 (55.0%)
Peripheral vascular disease *n* (%)	19 (10.6%)
CVA *n* (%)	14 (7.8%)
Kidney disease *n* (%)	11 (6.1%)
Prior MI *n* (%)	30 (16.7%)
Prior PCI *n* (%)	17 (9.4%)
Prior CABG *n* (%)	0 (0.0%)
COPD *n* (%)	11 (6.1%)
History of heart failure *n* (%)	10 (5.6%)
Lesion characteristics	**L = 249**
One vessel disease	107/180 (59.4%)
Two vessel disease	61/180 (33.9%)
Three vessel disease	12/180 (6.7%)
Number of treated lesions per vessel (%)	
0 lesion	1/249 (0.4%)
1 lesion	189/249 (75.9%)
2 lesions	54/249 (21.7%)
3 lesions	4/249 (1.6%)
4 lesions	1/249 (0.4%)
Lesion Location (%)	
LAD	120/249 (48.2%)
LCX	55/249 (22.1%)
RCA	66/249 (26.5%)
DIAGONAL	7/249 (2.8%)
LMCA/Ramus	1/249 (0.4%)
AHA/ACC Lesion classification (%)	
A	38/249 (15.3%)
B1	103/249 (41.4%)
B2	63/249 (25.3%)
C	46/249 (18.5%)
Lesion length (mm)	25.86 ± 13.64
Range min, max (mm)	5.32 – 80.01
Bifurcation lesion n. (%)	54/249 (21.7%)
Total occlusion (%)	29/249 (11.6%)
Calcification lesion (%)	119/249 (47.8%)

CVA, cerebrovascular accident; PCI, percutaneous coronary intervention; CABG, coronary artery bypass graft; COPD, chronic obstructive pulmonary disease.

Data are expressed as mean ± standard deviation or number and proportion.

249 treated coronary lesions (Table I). A total of 1,157 patients were treated with standard second generation drug eluting stents. The remaining cases were treated with bare metal stents, dedicated bifurcation stents, balloon angioplasty only or thrombectomy only. Baseline clinical characteristics of the patients implanted with bioresorbable devices as compared with those of the patients implanted with second generation drug eluting metal stents are reported in the Supporting Information (Table IV). We observed that patients treated with bioresorbable devices were overall younger, more frequently smokers, and had a lower rate of prior myocardial infarction, PCI and CABG. Therefore, this patient population is slightly different from the general population treated with percutaneous coronary intervention in everyday practice. However, the observed differences are in line with the predefined exclusion criteria.

Seventy-three patients (40.6%) showed multivessel disease. A total of 109 lesions (43.8%) were classified as type B2 or C, mean lesion length was 25.86 mm, bifurcation lesions with side-branch ≥ 2 mm were 54, a total of 119 lesion were defined with severe or moderate calcification and in 29 case was present a total occlusion (Table I).

Lesion preparation was performed in a large part of the cases mainly through balloon predilatation (89.2%); rotational atherectomy was necessary in 4.8% of cases. Multiple scaffold implantation per lesion was allowed and often performed, (31.7%) up to the implantation of 5 scaffolds.

No scaffold dislodgment was reported.

Bailout with drug eluting metal stents was performed in only two cases. Balloon postdilatation was performed in a remarkable percentage of cases (45.0%) with often a balloon/scaffold ratio >1.0 (41.8%) (Table II).

The overall device, procedure and clinical success rates per lesion, were respectively 99.2%, 98.8%, and 98.8%.

QCA Analysis

The mean preprocedure reference vessel diameter (RVD) was 2.63 ± 0.43 mm, with a mean percentage diameter stenosis (%DS) of $64.8 \pm 14.5\%$ and a mean minimal lumen diameter (MLD) equal to 0.90 ± 0.35 mm. Postprocedure %DS was $17.60 \pm 8.65\%$ with a mean MLD equal to 2.41 ± 0.41 mm reflecting a mean acute gain of 1.51 ± 0.49 mm. TIMI 3 flow was observed in 99.2% of the final angiograms (Table II, Fig. 1).

Bifurcation Lesions

A total of 54 lesions were located at the site of a bifurcation with a side-branch ≥ 2.0 mm. In 51 cases a provisional side branch technique was used, in addition 1 T-stenting, 1 culotte, 1 T-stenting with small protrusion (TAP) techniques were performed. In 18 cases side-branch wire protection was used, predilatation and postdilatation of the main vessel was often performed. Side-branch dilatation post MV stenting was necessary in 18 lesions. A final TIMI flow <3 in the main vessels (MV) was observed in only one case, in the side-branch this was reported in three lesions. Failure to rewire the side-branch was never reported but in one case the operator was unable to recross the scaffold with a small balloon of 1.5 mm in diameter

TABLE II. Procedural Data Perlesion Analysis

Lesion characteristics	$L = 249$
Number of Scaffold or stent—per lesion (%)	
Average	1.41 ± 0.75
0 scaffold or stent	1/249 (0.4%)
1 scaffold or stent	169/249 (67.9%)
2 scaffolds or stents	61/249 (24.5%)
3 scaffolds or stents	10/249 (4.0%)
4 scaffolds or stents	7/249 (2.8%)
5 scaffolds or stents	1/249 (0.4%)
Overlapping	78
Overlapping BVS-BVS	76
Overlap scaffolds diameters 3.5–3.5 mm, *n* (%)	20 (26.3%)
Overlap scaffolds diameters 3.5–3.0 mm, *n* (%)	15 (19.7%)
Overlap scaffolds diameters 3.5–2.5 mm, *n* (%)	3 (3.9%)
Overlap scaffolds diameters 3.0–3.0 mm, *n* (%)	15 (19.7%)
Overlap scaffolds diameters 3.0–2.5 mm, *n* (%)	15 (19.7%)
Overlap scaffolds diameters 2.5–2.5 mm, *n* (%)	8 (10.5%)
Overlapping BVS-metal	2 (2.6%)
Bailout scaffold/stent (%)—per lesion	
With BVS	8/249 (3.2%)
With metallic stent	2/249 (0.8%)
Pre dilatation (%)	222/249 (89.2%)
Type of predilatation balloon[a]	
Noncompliant	16/203 (7.9%)
Semicompliant	187/203 (92.1%)
The usage of scoring (scoreflex or cutting)	9/219 (4.1%)
Average size of balloon	2.52 ± 0.36
Balloon/artery (pre RVD) Ratio < 1 (excluding total occlusion before procedure)	100/184 (54.3%)
Balloon/scaffold ratio ≤ 1	198/202 (98.0%)
Balloon 0.5 mm smaller $\leq$ scaffold size	172/202 (85.1%)
Max pressure	13.95 ± 2.86
Use of other devices for lesion preparation	
Rotational atherectomy	12/249 (4.8%)
Manual thrombectomy	11/249 (4.4%)
Daughter catheter	5/249 (2.0%)
Buddy wire	18/249 (7.2%)
Postdilatation (%)	112/249 (45.0%)
Type of postdilatation balloon[b]	
Compliant	32/110 (29.1%)
Noncompliant	78/110 (70.9%)
Average size of balloon	3.27 ± 0.46 mm
Max pressure	15.58 ± 3.46
Balloon/Artery < 1	25/110 (22.7%)
Balloon $>$ Scaffold size	46/110 (41.8%)
Balloon $>$ Scaffold size $+ 0.25$ mm	15/110 (13.6%)
Device success per lesion (%)	247/249 (99.2%)
Procedure success per lesion (%)	246/249 (98.8%)
Clinical success per lesion	246/249 (98.8%)
QCA preprocedure	
RVD (mm)	2.63 ± 0.43
MLD (mm)	0.90 ± 0.35
% DS (%)	64.8 ± 14.5
Proximal D_{max} (mm)	3.92 ± 8.28
Distal D_{max} (mm)	2.89 ± 2.31
QCA postprocedure in-scaffold	
RVD (mm)	2.89 ± 0.42
DS (%)	17.6 ± 8.65
MLD (mm)	2.41 ± 0.41
Scaffold length	29.44 ± 15.71
Acute gain (mm)	1.51 ± 0.49
TIMI grade 2	2/249 (0.8%)
TIMI grade 3	247/249 (99.2%)

[a]Type of predilatation balloon is reported in a subgroup of 203 patients.
[b]Type of posdilatation balloon is reported in a subgroup of 110 patients.
Data are expressed as mean $\pm$ standard deviation or number and proportion.

(Table V, Supporting Information). The overall rate of side-branch impairment was 9.3% (5/54).

Calcified Lesions

A total of 119 calcified lesions were treated with BVS, 33 with severe calcification, 86 with moderate calcification, (Fig. 2) and compared with noncalcified lesions. After treatment no differences were observed between calcified and noncalcified lesions in terms of MLD (Severe calcified 2.38 ± 0.38 mm, moderate calcified 2.41 ± 0.39 mm, noncalcified 2.42 ± 0.43 mm; $P = 0.889$), %DS (Severe calcified $20.3 \pm 10.5\%$, moderate calcified $17.8 \pm 7.7\%$, noncalcified $16.8 \pm 8.6\%$; $P = 0.112$) and acute gain (Severe calcified 1.36 ± 0.41 mm, moderate calcified 1.48 ± 0.44 mm, noncalcified 1.56 ± 0.54 mm; $P = 0.109$). These results were achieved with an overall higher use of buddy wires in calcified lesions (severe calcified 18.2%, moderate calcified 9.3%, noncalcified 3.0%; $P = 0.016$).

Lesion preparation was more aggressive in calcified lesions with a higher use of rotational atherectomy (Severe calcified 18.2%, moderate calcified 4.7%, noncalcified 1.5%; $P < 0.001$) and scoring balloons (Severe calcified 15 .2%, moderate calcified 3.5%, noncalcified 0.8%; $P = 0.001$). Success rates were high in calcified vessels showing no significant differences when compared to noncalcified ones. Device success in severe calcified lesions was 97.0%, in moderate calcified 100% and in noncalcified 99.2%; $P = 0.251$ (Table III).

Total Occlusions

Vessels showing a total occlusion were 29. After vessel recanalization, BVS implantation was performed achieving a final MLD and %DS not different from other lesion types (MLD: 2.51 ± 0.53 mm vs. 2.40 ± 0.39; $P = 0.163$; %DS: $17.2 \pm 9.4\%$ vs. $17.7 \pm 8.6\%$; $P = 0.780$), with a high rate of final device success (96.6% vs. 98.2%; $P = 0.465$) and procedure success (96.6% vs. 98.6%; $P = 0.393$). To reach those results supportive wires were used much more frequently in occluded vessels (54.2% vs. 2.1%; $P < 0.001$) (Table III, Fig. 2).

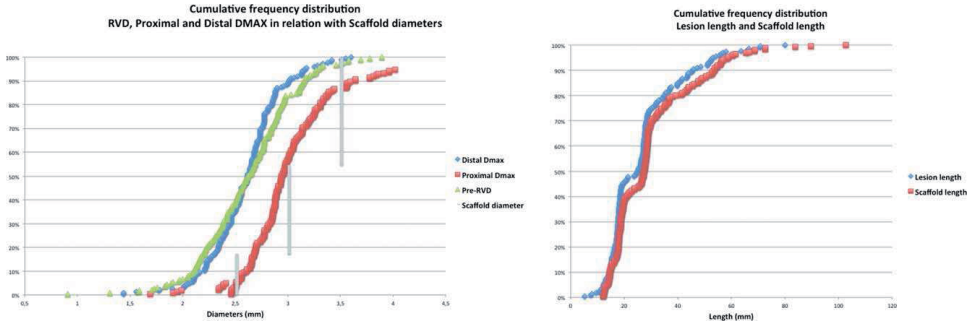

Fig. 1. Vessel and scaffold diameters and lengths. Left panel, Cumulative frequency distribution of the reference vessel diameter the proximal end distal diameter in relation with the nominal size of the implanted scaffolds. Right panel, Cumulative frequency distribution of the lesion length in relation with the length of the implanted scaffolds. [Color figure can be viewed at wileyonlinelibrary.com]

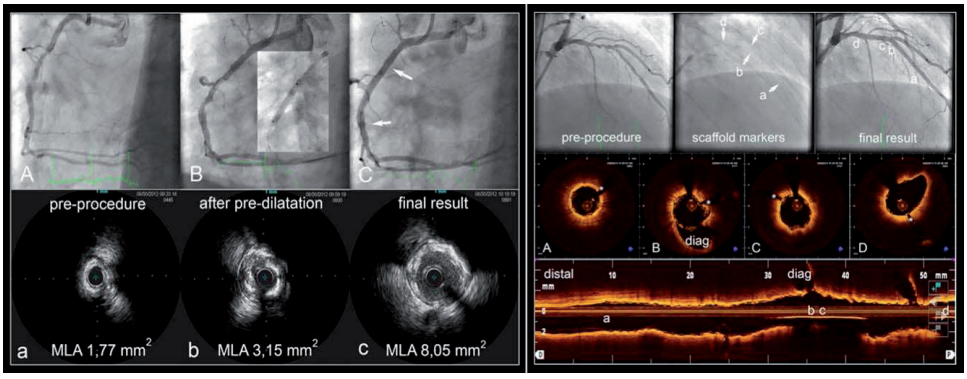

Fig. 2. Calcified lesion and long lesions. Right panel. Calcified lesions. Angiogram showing a long lesion in the RCA (panel A). IVUS preprocedure (Panel a) shows at the MLA more than 180° superficial calcium (*). Panel B shows the angiogram after predilatation (semicompliant balloon 3.0 × 20 mm^2). IVUS (panel b) shows clear "cracks" in the calcium (arrowheads), reducing the plaque resistance, thus sufficiently prepared for BVS implantation. Panels C and c show respectively the result on angiogram and on IVUS after implanting a BVS 3.5 × 28 mm^2. Left panel. Long lesions. The angiogram top left shows the long lesion in the LAD. The mid-panel shows the markers of the two overlapping scaffolds (a and c distal BVS 3.0 × 28 mm^2 and b and d proximal BVS 3.5 × 18 mm^2). The top right shows the final result with the OCT cross-section positions indicated by a–d). OCT (St. Jude Lightlab Dragonfly™) shows a well deployed scaffold. Panels B and C show the markers of respectively the proximal and distal scaffolds (*), indicating an overlap of ~1 mm.

Long Lesions

In a total of 79 lesions (31.7%) more than one device was implanted (Figs. 1 and 3). The mean lesion length treated with BVS was 25.86 ± 13.64 mm. The maximum lesion length covered by BVS was 80.01 mm. Overlapping of BVS with BVS was often performed with a total of 76 overlapping scaffolds. The great majority (96%, 73/76) were performed using scaffold of the same diameter or with a maximum of 0.5 mm difference in nominal diameter. In three cases a 3.5 mm scaffold was placed in overlap with a 2.5 mm device.

Clinical Outcomes

Survival data at 12 months after the procedure were available for 99.4% of patients and all cause-death was reported in three cases. Detailed clinical follow-up was available in 86% of the cases. The rate of target lesion

TABLE III. BVS Implantation in Calcified and Total Occluded Lesions

Calcified lesions	Severe calcification (L = 33)	Moderate calcification (L = 86)	No calcification (L = 130)	*P*-value
Lesion preparation				
Rotational atherectomy, % (n)	18.2% (6/33)	4.7% (4/86)	1.5% (2/130)	<0.001
Scoring balloon, % (n)	15.2% (5/33)	3.5% (3/86)	0.8% (1/130)	0.001
Daughter catheter, % (n)	3.0% (1/33)	2.3% (2/86)	1.5% (2/130)	0.886
Buddy wire,% (n)	18.2% (6/33)	9.3% (8/86)	3.0% (4/130)	0.016
Average size of balloon	2.48 ± 0.38	2.55 ± 0.35	2.52 ± 0.36	0.702
Non-compliant balloon, % (n)	13.3% (4/30)	9.5% (7/74)	5.1% (5/99)	0.276
QCA preprocedure				
RVD (mm)	2.51 ± 0.35	2.66 ± 0.43	2.64 ± 0.46	0.256
MLD (mm)	0.97 ± 0.40	0.92 ± 0.36	0.87 ± 0.34	0.358
% DS (%)	62.3 ± 13.5	65.0 ± 12.6	65.3 ± 15.7	0.592
Lesion length	36.11 ± 2.34	27.99 ± 1.54	22.11 ± 1.16	<0.001
QCA postprocedure				
RVD (mm)	2.97 ± 0.38	2.93 ± 0.39	2.85 ± 0.46	0.244
MLD (mm)	2.38 ± 0.38	2.41 ± 0.39	2.42 ± 0.43	0.889
% DS	20.3 ± 10.5	17.8 ± 7.7	16.8 ± 8.6	0.112
Acute gain (mm)	1.36 ± 0.41	1.48 ± 0.44	1.56 ± 0.54	0.109
Device success per lesion, % (n)	97.0% (32/33)	100% (86/86)	99.2% (129/130)	0.251
Procedure success per lesion, % (n)	97.0% (32/33)	98.8% (85/86)	99.2% (129/130)	0.571
Clinical success (per lesion), % (n)	97.0% (32/33)	98.8% (85/86)	99.2% (129/130)	0.571

Occluded vs. nonoccluded	Occluded (L = 29)	Nonoccluded (L = 220)	*P*-value
QCA postprocedure			
RVD (mm)	3.01 ± 0.47	2.88 ± 0.41	0.103
MLD (mm)	2.51 ± 0.53	2.40 ± 0.39	0.163
% DS (%)	17.2 ± 9.4	17.7 ± 8.6	0.780
Acute gain (mm)	–	1.51 ± 0.49	–
Procedural characteristics			
Daughter catheter, % (*n*)	3.4% (1/29)	1.8% (4/220)	0.465
Buddy wire, % (*n*)	10.3% (3/29)	6.8% (15/220)	0.449
Type of first wire (after recanalization)			
Supportive	54.2% (13/24)	2.1% (4/195)	<0.001
Nonsupportive	45.8% (11/24)	97.9% (191/195)	<0.001
Device success after recanalization, % (*n*)	100% (29/29)	99.1% (218/220)	1.0
Procedure success after recanalization, % (*n*)	100% (29/29)	98.6% (217/220)	1.0
Clinical success after recanalization, % (*n*)	100% (29/29)	98.6% (217/220)	1.0

Data are expressed as mean ± standard deviation or number and proportion.

revascularization and target vessel revascularization was 3.3% in this first cohort of the BVS-EXPAND study. The rate of definite scaffold thrombosis (ST) was 2.6% none of them was acute or sub-acute. Of note, one of those cases was meeting the ARC criteria for ST but no clear thrombus was observed by optical coherence tomography (OCT). In the remaining three cases, severe calcification, bifurcation lesion, and long overlap were observed but BVS underexpansion was the factor that was present in all of them.

DISCUSSION

The present investigation represents an evaluation of the feasibility of BVS implantation in everyday clinical practice reflected by in a wide range of coronary lesions subsets including bifurcations, calcified vessels, chronic total occlusions, and long lesion in patients with stable coronary artery disease and acute coronary syndromes. At variance of previous reports we also aimed to provide a detailed description of procedural data en techniques that were used to allow the use of this novel device in challenging subsets.

Bifurcation Lesions

A common concern regarding this technology is the fact that implantation of the BVS in bifurcation lesions might result in side-branch compromise because of the thick strut nature of this device. In keeping with this concept, a recent study performed by our group showed that BVS deployment could be associated with

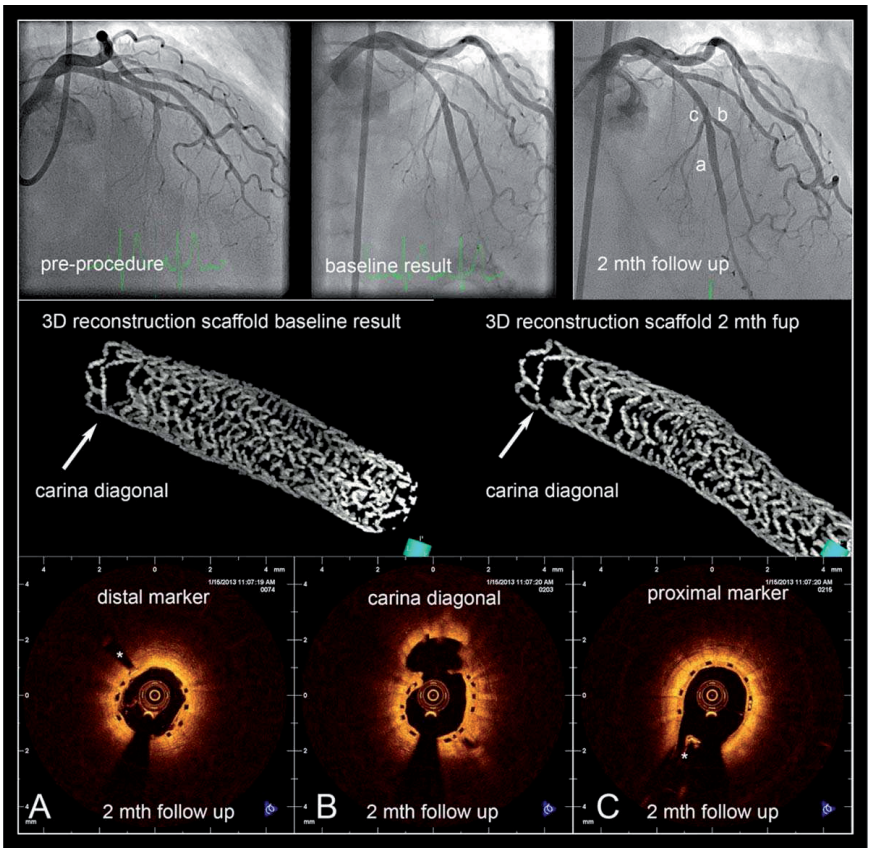

Fig. 3. Chronic total occlusion and bifurcation. Top panels show from left to right the angiograms preprocedure, after recanalization and scaffold implantation (BVS 3.0 × 28 mm^2 with the sequential postdilatation of the diagonal and the scaffold in the main branch) and 2-month follow-up with partial distal vessel positive remodeling. Characters a–c indicate the positions of the OCT cross-sections. OCT (St. Jude Lightlab Dragonfly^{TM}) postprocedure show distal a well deployed scaffold (Panel A), an well opened carina with the diagonal branch (Panel B*) and the overlap of the proximal marker with the septal branch (Panel C*). The 3D reconstruction (Intage realia^{TM}, Cybersystems, Tokyo, Japan) shows the opening of the struts at the carina with the diagonal branch (Arrowhead bottom panel).

an increased small (≤0.5 mm) side-branch occlusion and a consequent increase of enzymes release after procedure [13].

However, in the present report the effect of BVS implantation in what is commonly considered a bifurcation lesion (with a side branch ≥2 mm) was specifically investigated.

Rewiring of the side-branch in those cases and consequent ballooning (mainly with small balloon 1.5–2 mm in diameter) of the SB ostium is feasible as we already reported [13] and safe also in terms of scaffold geometry and fracture [14,15]. In the present study, side-branch ballooning was performed in one-third of the patients (33%, 18/54) with promising results. In majority of the cases this was done with sequential ballooning and proximal optimization technique (POT), kissing balloon only in three cases.

Taking into consideration the rates of TIMI flow <3 in the main vessel or in the side-branch, the rate of failure to rewire the side-branch and failure to dilate

the side-branch, the BVS performed at least as good as metallic if considering historical data [12].

In addition, the rate of the composite endpoint side-branch impairment (9.3%) was observed to be encouraging especially when compared with data recently reported by Burzotta et al. with rates of side-branch impairment in sirolimus and everolimus eluting stents 16% and 11%, respectively [12]. These data are supportive of the concept that BVS could be used safely in bifurcation lesions with side-branch $\geq$2.0 mm with a single scaffold approach and could provide results similar to metallic stents.

Calcified Lesions

A total of 119 calcified lesions with a considerable percentage of heavily calcified plaques, were treated with BVS. A large number of those lesions were located in diffusely diseased vessels with an overall mean treated lesion length of more than 36 mm (severe calcified group). QCA analysis showed a final MLD, %DS, acute gain and device, procedural and clinical success not different from noncalcified lesions. These results were obtained at the cost of a more aggressive lesion preparation with a considerable use of rotational atherectomy and scoring balloons.

Such approach is needed to facilitate the delivery of the scaffold given its slightly higher profile compared with second generation DES. In addition, appropriate lesion preparation could avoid scaffold under-expansion or need for aggressive postdilatation. This strategy could be relevant also when using metallic stents [16]. Our data might suggest feasibility of BVS implantation in calcified vessels with optimal results given an adequate lesion preparation.

Although, many of the advantages proposed for BVS, namely the restoration of the vasomotion and vessel physiology could be minimized in calcified artery, patients with diffused calcified vessels have often also a multivessel disease [17]; in such scenario a temporary implant would allow future surgical treatments.

Total Occlusions

Successful recanalization of total occlusions has been previously associated with a significant improvement in angina symptoms [18,19] and complete coronary revascularization was demonstrated to have an important impact on long-term clinical outcomes [20].

Vessels with total occlusions have peculiar characteristics in terms of vascular remodeling; this is a dynamic process involving regulation of vascular cell migration and mitosis and apoptosis rates in response to several factors comprising blood flow and pressure, shear stress, circumferential stretch, and wall tension [21]. Reduction or even more absence of blood flow in totally occluded vessels might promote negative remodeling and plaque growth; on the other hand restoration of flow could have an opposite effect.

Recently, Park et al. reported, at 6-month follow-up after successful total occlusion revascularization, a flow-dependent vascular remodeling process in human coronary arteries, associated with increases in lumen diameter, lumen area, and external elastic membrane area [22]. This process was observed in a large part of treated vessels (69%) with a mean lumen diameter increase of 0.40 ± 0.34 mm. IVUS analysis of those vessels revealed that the amount of incomplete stent apposition increased significantly during 6 months in patients with positive remodeling and lumen area increase but not in those without lumen area increase.

In this scenario choosing a metal stent based on the vessel diameter at the index procedure might lead to stent under-sizing.

Given this background a theoretical advantage of BVS implantation in patients with total occlusion is the fact that it might allow at mid-term follow-up, after the loss of scaffold mechanical integrity, late lumen enlargement without late acquired malapposition, as at that time the remnants of the bioresorbable implant can follow the vessel remodeling.

Long Lesions and Overlap

In the present series, several lesions were treated with more than one scaffold up to a maximum of 5 scaffolds for a maximum lesion length of 80 mm. Operators were advised to minimize the extension of overlapping segment using a marker-to-marker technique.

In the metal stent era, long segments treatment has been associated to an increased risk of stent thrombosis [23–25] and could results in prevention of future surgical revascularisations.

Both these issues could be overcome with the use of bioresorbable technologies and the introduction in the near future of bioresorbable scaffold with thinner struts could mitigate the effect of overlap on delayed vascular healing.

Clinical Outcomes

The mid-term clinical outcomes of this first BVS-EXPAND cohort revealed a relatively reassuring safety profile of the BVS when used in a large range of lesion type and in patients with either stable symptoms or acute coronary syndromes. The event rate in this study is only minimally higher compared to the results in noncomplex patients reported in the randomized Absorb II and Absorb Japan studies [26,27]. In other

European registries like GHOST-EU and AMC registries [28,29] reporting early experience with BVS, the event rate was in slightly higher as compared with more recent registries like the Milan registry [30] and ASSURE BVS [31] where more BVS specific implantation protocols where applied. Such observations suggest the relevance of a BVS dedicated implantation technique ensuring good lesion preparation and optimal scaffold deployment often facilitated by high pressure postdilatation.

Regarding the occurrence of scaffold thrombosis (ST), at variance with previous reports no acute or sub-acute STs were observed in the present investigation. These findings could be related to procedural characteristics including a meticulous lesion preparation pre-BVS implantation and a reasonably high rate of postdilatation.

The review of the cases with ST revealed that several factors might be associated with such events comprising severe lesion calcification, the presence of bifurcations, long overlap and antiplatelet therapy discontinuation. However, the factor that was particularly consistent was scaffold under-expansion. Previous investigations described stent underexpansion as an important predictor of ST with both bare metal stents and DES [32–36] with an impact on the occurrence of ST that was hypostasized to be superior to stent malapposition [37]. The mechanisms behind these findings could be the fact that stent underexpansion translates into an abnormal shear stress. In particular, increased radial transport of blood components and low wall shear stress, were described to promote platelet-dependent thrombosis [38]. In addition the impact of underexpansion on shear stress could be potentiated by the presence of the BVS thick struts [39].

Although, given the small number of patients and events reported in the present study it is not possible to reach firm conclusions, our findings suggest that optimal BVS expansion, with lesion preparation and appropriate scaffold postdilatation, should be pursued given the possible relevant clinical implications.

LIMITATIONS

The present report is a first report of an investigator initiated, single center, single arm study. The choice for BVS implantation was left to operator discretion, this could be source of selection bias. The absence of a comparator arm is limiting the interpretation of our data. The limited number of patients does not allow reaching firm conclusions on clinical outcomes. The mid-term follow-up is preventing the availability of information on long-term safety and efficacy.

CONCLUSION

The implantation of the everolimus eluting bioresorbable vascular scaffold in an expanded range of coronary lesion types and clinical presentations was observed to be viable with promising angiographic results and mid-term clinical outcomes. Larger studies with longer follow-up and a direct comparison with currently available metallic drug eluting stents are needed to fully evaluate the possible additional value of the bioresorbable technologies an all comers setting.

ACKNOWLEDGMENTS

The authors want to thank Isabella Kardys, Johannes Schaar, and Martijn Akkerhuis, for their contribution in the event adjudication.

REFERENCES

1. Serruys PW, Onuma Y, Ormiston JA, de Bruyne B, Regar E, et al.Evaluation of the second generation of a bioresorbable everolimus drug-eluting vascular scaffold for treatment of de novo coronary artery stenosis: six-month clinical and imaging outcomes. Circulation 2010;122:2301–2312.
2. Onuma Y, Serruys PW, Perkins LE, Okamura T, Gonzalo N, et al. Intracoronary optical coherence tomography and histology at 1 month and 2, 3, and 4 years after implantation of everolimus-eluting bioresorbable vascular scaffolds in a porcine coronary artery model: An attempt to decipher the human optical coherence tomography images in the ABSORB trial. Circulation 2010;122:2288–2300.
3. Onuma Y, Serruys PW. Bioresorbable scaffold: The advent of a new era in percutaneous coronary and peripheral revascularization? Circulation 2011;123:779–797.
4. Diletti R, Farooq V, Girasis C, Bourantas C, Onuma Y, et al. Clinical and intravascular imaging outcomes at 1 and 2 years after implantation of absorb everolimus eluting bioresorbable vascular scaffolds in small vessels. Late lumen enlargement: does bioresorption matter with small vessel size? Insight from the ABSORB cohort B trial. Heart 2013;99:98–105.
5. Serruys PW, Garcia-Garcia HM, Onuma Y. From metallic cages to transient bioresorbable scaffolds: Change in paradigm of coronary revascularization in the upcoming decade? Eur Heart J 2012;33:16–25b.
6. Serruys PW, Ormiston JA, Onuma Y, Regar E, Gonzalo N, et al. A bioabsorbable everolimus-eluting coronary stent system (ABSORB): 2-year outcomes and results from multiple imaging methods. Lancet 2009;373:897–910.
7. Onuma Y, Dudek D, Thuesen L, Webster M, Nieman K, Garcia-Garcia HM, Ormiston JA, Serruys PW. Five-year clinical and functional multislice computed tomography angiographic results after coronary implantation of the fully resorbable polymeric everolimus-eluting scaffold in patients with de novo coronary artery disease: The ABSORB cohort. Trial. JACC Cardiovasc Interv 2013;6:999–1009.
8. Serruys PW, Onuma Y, Garcia-Garcia HM, Muramatsu T, van Geuns RJ, et al. Dynamics of vessel wall changes following the implantation of the absorb everolimus-eluting bioresorbable vascular scaffold: A multi-imaging modality study at 6, 12, 24 and 36 months. EuroIntervention 2014;9:1271–1284.

9. Diletti R, Onuma Y, Farooq V, Gomez-Lara J, Brugaletta S, et al. 6-month clinical outcomes following implantation of the bioresorbable everolimus-eluting vascular scaffold in vessels smaller or larger than 2.5 mm. J Am Coll Cardiol 2011;58:258–264.
10. Onuma Y, Tanimoto S, Ruygrok P, Neuzner J, Piek JJ, et al. Efficacy of everolimus eluting stent implantation in patients with calcified coronary culprit lesions: Two-year angiographic and three-year clinical results from the SPIRIT II study. Catheter Cardiovasc Interv 2010;76:634–642.
11. Herrman JP, Azar A, Umans VA, Boersma E, von Es GA, Serruys PW. Inter- and intra-observer variability in the qualitative categorization of coronary angiograms. Int J Card Imaging 1996;12:21–30.
12. Burzotta F, Trani C, Todaro D, Mariani L, Talarico GP, et al. Prospective randomized comparison of sirolimus- or everolimus-eluting stent to treat bifurcated lesions by provisional approach. JACC Cardiovasc Interv 2011;4:327–335.
13. Muramatsu T, Onuma Y, Garcia-Garcia HM, Farooq V, Bourantas CV, et al. Incidence and short-term clinical outcomes of small side branch occlusion after implantation of an everolimus-eluting bioresorbable vascular scaffold: An interim report of 435 patients in the ABSORB-EXTEND single-arm trial in comparison with an everolimus-eluting metallic stent in the SPIRIT first and II trials. JACC Cardiovasc Interv 2013;6: 247–257.
14. Dzavik V, Colombo A. The absorb bioresorbable vascular scaffold in coronary bifurcations: Insights from bench testing. JACC Cardiovasc Interv 2014;7:81–88.
15. Ormiston JA, Webber B, Ubod B, Webster MW, White J. Absorb everolimus-eluting bioresorbable scaffolds in coronary bifurcations: A bench study of deployment, side branch dilatation and post-dilatation strategies. EuroIntervention 2015;10: 1169–1177.
16. Abdel-Wahab M, Baev R, Dieker P, Kassner G, Khattab AA, et al. Long-term clinical outcome of rotational atherectomy followed by drug-eluting stent implantation in complex calcified coronary lesions. Catheter Cardiovasc Interv 2013;81:285–291.
17. Genereux P, Madhavan MV, Mintz GS, Maehara A, Palmerini T, et al. Ischemic outcomes after coronary intervention of calcified vessels in acute coronary syndromes. Pooled analysis from the HORIZONS-AMI (Harmonizing Outcomes With Revascularization and Stents in Acute Myocardial Infarction) and ACUITY (Acute Catheterization and Urgent Intervention Triage Strategy) TRIALS. J Am Coll Cardiol 2014;63:1845–1854.
18. Stone GW, Kandzari DE, Mehran R, Colombo A, Schwartz RS, et al. Percutaneous recanalization of chronically occluded coronary arteries: a consensus document: Part I. Circulation 2005;112:2364–2372.
19. Stone GW, Reifart NJ, Moussa I, Hoye A, Cox DA, et al. Percutaneous recanalization of chronically occluded coronary arteries: a consensus document: Part II. Circulation 2005;112: 2530–2537.
20. Farooq V, Serruys PW, Garcia-Garcia HM, Zhang Y, Bourantas CV, et al. The negative impact of incomplete angiographic revascularization on clinical outcomes and its association with total occlusions: the SYNTAX (Synergy Between Percutaneous Coronary Intervention with Taxus and Cardiac Surgery) trial. J Am Coll Cardiol 2013;61:282–294.
21. Langille BL. Arterial remodeling: Relation to hemodynamics. Can J Physiol Pharmacol 1996;74:834–841.
22. Park JJ, Chae IH, Cho YS, Kim SW, Yang HM, et al. The recanalization of chronic total occlusion leads to lumen area increase in distal reference segments in selected patients: an intravascular ultrasound study. JACC Cardiovasc Interv 2012;5: 827–836.
23. Park DW, Park SW, Park KH, Lee BK, Kim YH, Lee CW, Hong MK, Kim JJ, Park SJ. Frequency of and risk factors for stent thrombosis after drug-eluting stent implantation during long-term follow-up. Am J Cardiol 2006;98:352–356.
24. Moreno R, Fernandez C, Hernandez R, Alfonso F, Angiolillo DJ, Sabate M, Escaned J, Banuelos C, Fernandez-Ortiz A, Macaya C. Drug-eluting stent thrombosis: Results from a pooled analysis including 10 randomized studies. J Am Coll Cardiol 2005;45:954–959.
25. Suh J, Park DW, Lee JY, Jung IH, Lee SW, et al. The relationship and threshold of stent length with regard to risk of stent thrombosis after drug-eluting stent implantation. JACC Cardiovasc Interv 2010;3:383–389.
26. Serruys PW, Chevalier B, Dudek D, Cequier A, Carrie D, et al. A bioresorbable everolimus-eluting scaffold versus a metallic everolimus-eluting stent for ischaemic heart disease caused by de-novo native coronary artery lesions (ABSORB II): An interim 1-year analysis of clinical and procedural secondary outcomes from a randomised controlled trial. Lancet 2015;385:43–54.
27. Kimura T, Kozuma K, Tanabe K, Nakamura S, Yamane M, et al. A randomized trial evaluating everolimus-eluting absorb bioresorbable scaffolds vs. everolimus-eluting metallic stents in patients with coronary artery disease: ABSORB Japan. Eur Heart J 2015;36:3332–3342.
28. Capodanno D, Gori T, Nef H, Latib A, Mehilli J, et al. Percutaneous coronary intervention with everolimus-eluting bioresorbable vascular scaffolds in routine clinical practice: Early and midterm outcomes from the European multicentre GHOST-EU registry. EuroIntervention 2015;10:1144–1153.
29. Kraak RP, Hassell ME, Grundeken MJ, Koch KT, Henriques JP, et al. Initial experience and clinical evaluation of the absorb bioresorbable vascular scaffold (BVS) in real-world practice: The AMC Single Centre Real World PCI Registry. EuroIntervention 2015;10:1160–1168.
30. Costopoulos C, Latib A, Naganuma T, Miyazaki T, Sato K, et al.Comparison of early clinical outcomes between ABSORB bioresorbable vascular scaffold and everolimus-eluting stent implantation in a real-world population. Catheter Cardiovasc Interv 2015;85:E10–E15.
31. Wohrle J, Naber C, Schmitz T, Schwencke C, Frey N, et al.Beyond the early stages: Insights from the ASSURE registry on bioresorbable vascular scaffolds. EuroIntervention 2015; 11:149–156.
32. Fujii K, Carlier SG, Mintz GS, Yang YM, Moussa I, et al. Stent underexpansion and residual reference segment stenosis are related to stent thrombosis after sirolimus-eluting stent implantation. An Intravascular Ultrasound Study. J Am Coll Cardiol 2005;45:995–998.
33. Cheneau E, Leborgne L, Mintz GS, Kotani J, Pichard AD, et al. Predictors of subacute stent thrombosis: Results of a systematic intravascular ultrasound study. Circulation 2003;108: 43–47.
34. Kasaoka S, Tobis JM, Akiyama T, Reimers B, Di Mario C, Wong ND, Colombo A. Angiographic and intravascular ultrasound predictors of in-stent restenosis. J Am Coll Cardiol 1998; 32:1630–1635.
35. Sonoda S, Morino Y, Ako J, Terashima M, Hassan AH, et al. Impact of final stent dimensions on long-term results following sirolimus-eluting stent implantation: Serial intravascular ultrasound analysis from. The Sirius Trial. J Am Coll Cardiol 2004; 43:1959–1963.

36. Uren NG, Schwarzacher SP, Metz JA, Lee DP, Honda Y, Yeung AC, Fitzgerald PJ, Yock PG, Investigators PR. Predictors and outcomes of stent thrombosis: An intravascular ultrasound registry. Eur Heart J 2002;23:124–132.
37. Liu X, Doi H, Maehara A, Mintz GS, Costa Jde R, Jr., et al. A volumetric intravascular ultrasound comparison of early drug-eluting stent thrombosis versus restenosis. JACC Cardiovasc Interv 2009;2:428–434.
38. Sukavaneshvar S, Rosa GM, Solen KA. Enhancement of stent-induced thromboembolism by residual stenoses: contribution of hemodynamics. Ann Biomed Eng 2000;28:182–193.
39. Bourantas CV, Papafaklis MI, Kotsia A, Farooq V, Muramatsu T, et al. Effect of the endothelial shear stress patterns on neointimal proliferation following drug-eluting bioresorbable vascular scaffold implantation: An optical coherence tomography study. JACC Cardiovasc Interv 2014;7:315–324.

18

CHAPTER

CORONARY STENT CURVATURE QUANTIFICATION IN X-RAY ANGIOGRAPHY AND COMPUTED TOMOGRAPHY ANGIOGRAPHY

Gerardo Dibildox, **Jiang Ming Fam**, Yoshinobu Onuma, Koen Nieman, Robert-Jan van Geuns, Theo van Walsum.

Submitted for publication.

Coronary Stent Curvature Quantification in X-ray Angiography and Computed Tomography Angiography

Gerardo Dibildox[1,2], MSc*; Jiang Ming Fam[3,4], MD; Yoshinobu Onuma[3], MD, PhD; Koen Nieman[2,3], MD, PhD; Robert-Jan van Geuns[2,3], MD, PhD; Theo van Walsum[1,2], PhD

1. Department of Medical Informatics; 2. Department of Radiology; 3 Department of Interventional Cardiology, Thoraxcenter, Erasmus MC, Rotterdam, The Netherlands; 4 Department of Cardiology, National Heart Centre Singapore

[Work was performed at Erasmus MC, Rotterdam, The Netherlands]

** Corresponding author: Na-26, Dr. Molewaterplein 40, 3015 RD Rotterdam, The Netherlands*

E-mail: g.dibildox@erasmusmc.nl Telephone: +31 107044131

Short Title: Quantifying Stent Curvature in CTA and XA

Indexing words: Imaging, stent conformability, quantitative coronary angiography

Total word count: 3650

Abstract

Objective: To quantify stent curvature in computed tomography angiography (CTA), in X-ray angiography (XA), and evaluate to what extent these quantifications can be compared.

Background: Geometric changes in coronary arteries post-stent implantation relate to clinical outcomes. Accurate assessment of stent curvature is therefore relevant.

Methods: This study quantifies stent curvature in 14 patients with bioresorbable absorb scaffolds (Abbott Vascular, Santa Clara, California). The quantifications are based on CTA and XA. Curvature quantifications are also performed on 2-dimensional (2D) projections of the stent extracted from the CTA, to investigate the effect of the viewing angle on the quantifications.

Results: The mean absolute difference in measured curvature angle using 2D projections of the 3D CTA centrelines with optimal imaging angles compared to the 3D CTA measurement was 0.6 degrees (SD: 1.1). The Bland-Altman analysis of the XA curvature angle measurements gives a mean bias (95% limit of agreement) of 1.6 (-9.3 to 12.4) degrees between observers. The Passing-Bablok regression and linearity tests ($P>0.1$) indicate agreement between the 2D projections of the 3D CTA centerline with actual imaging angles and the XA curvature angle quantifications. The sensitivity tests indicate a high dependence of the median curvature angle measured - up to 30 deg. - and the spread of the measurements on the optimal positioning of the system.

Conclusions: Suboptimal viewing angles may give inaccurate XA curvature quantifications. It is therefore important to quantify curvature in 3D or use optimal projection angles guided by a previously acquired CTA to perform XA measurements.

Introduction

Stent conformability is a measure of how well a stent can adapt to the shape of a vessel and is the main factor that determines vessel distortion post implantation as well as subsequent changes in vessel curvature. Low stent conformability has been proposed as a mechanism for stent fracture and has been associated to major adverse cardiac events (1, 2, 3, 4). It is therefore desirable to be able to quantify the curvature of a stent to evaluate stent conformability and to track curvature changes over time. Previous studies (5,6) have quantified curvature and changes in curvature by performing measurements on X-ray angiography (XA). XA is the imaging modality of choice for coronary interventions; however there are important limitations when used for curvature quantification. XA offers a 2-dimensional (2D) projection image of a 3-dimensional (3D) structure (7), and it comes with the inherent risks of an invasive procedure such as bleeding and vessel trauma. The use of computed tomography angiography (CTA) may provide the necessary imaging information for curvature quantification at a lower procedural risk to the patient. We therefore develop an algorithm to perform stent curvature measurements in 3D using CTA, simulate 2D XA curvatures and compare these to the XA measurements. Additionally, we investigate the sensitivity of XA measurements w.r.t. the chosen imaging angles of the XA system.

Materials and Methods

Study Device and Population

This is a non-randomized, retrospective study performed on 14 patients from the Absorb Cohort A study (8, 9) whom received an everolimus-eluting bioresorbable absorb scaffold (Absorb; Abbott Vascular, Santa Clara, California). The Absorb scaffold is a balloon-expandable radiolucent device with 2 platinum markers at the edges that are visible on XA and CTA.

As part of the protocol patients had CTA after 5 years for late non-invasive follow-up of the treated segment. In Rotterdam, a single centre addendum for additional invasive follow-up with angiography, intravascular ultrasound (IVUS) and optical coherence tomography (OCT) was initiated and approved by the medical ethics committee (10).

Data and Data Processing

Image Data

The image data consisted of a coronary CTA dataset and an XA image sequence for each patient (N=14) in our study population. For all patients ECG-synchronized contrast-enhanced CT angiography was performed on a Siemens Somatom Definition Flash scanner, using standard scan protocols. XA imaging was performed with a Siemens AXIOM-Artis system using standard scan protocols.

CTA centreline and marker extraction

The centreline of the coronary artery is extracted from CTA using a minimum cost path approach (11), followed by a two-step refinement to correct for calcifications (12), and a medialness filter that is used to position the centreline at the artery centre (13). A Gaussian smoothing (st. dev. = 1 mm) is applied to eliminate voxel -sized steps. The platinum markers of the Absorb scaffold show up as bright dots and are easy to annotate in CTA. An example of a CTA extracted centreline is shown in Figure 1.

XA centreline and marker annotation

Annotation of the XA image sequences is done in the diastolic phase as this is the phase used for CTA reconstruction. For the XA annotation we use an in-house build tool, based on MeVisLab (MeVis Medical Solutions AG, Bremen Germany), that allows to manually annotate the centreline of the vessel and the Absorb platinum markers.

Curvature Measurement

The curvature of a vessel centreline is defined as the infinitesimal rate of change in the tangent vector at each point of the centreline. We are interested in measuring the curvature of a particular segment of the vessel centreline, i.e. the stented/scaffolded segment. This stented segment is determined to be the vessel centreline segment between the annotated markers in our XA and CTA images. To this end, at the proximal (and distal) side of the stent, the centreline point closest to the stent marker is used as start (and end) point of the stent centreline. For the CTA stent curvature quantification, a principal component analysis is performed on the 3D stent centreline points to determine the plane that will give a planar stent centreline that best matches the 3D stent centreline. The curvature measurement is subsequently achieved by fitting a planar circle to the XA or CTA stent centreline segment. The curvature of the segment is then 1/radius of the fitted circle. We report the curvature angle as the angle of the circle segment fitted to the stented segment as shown in Figure 2. The curvature angle conveys the same information as the 1/radius curvature since the length of the stent is known.

The stent curvature algorithm was implemented in MeVisLab and used to perform the stent curvature measurements in five different ways:

1. We quantified stent curvature using the vessel centreline and platinum stent markers extracted from the CTA images for each patient. This CTA measurement served as a baseline for our analysis. [CTA3D]
2. We quantified the curvature on the XA images using the vessel centreline and platinum stent markers annotated by two observers. This yielded two sets of quantifications. [XAObs1 and XAObs2]
3. We projected the 3D CTA extracted vessel and markers to a 2D imaging plane that corresponds to the patient's XA system primary and secondary angles, assuming a supine patient position for

the CTA and the XA, and quantified the curvature using the projected CTA centrelines. See Figure 3. [CTA2DReal]

4. We repeated the previous quantification, but instead of using the projection angles that were used for the XA sequences, we used optimal projection angles that were computed from the 3D CTA vessel centreline. The optimal projection angles are chosen such that the projection is orthogonal to the centreline curve in 3D. [CTA2DOpt]
5. To investigate the sensitivity of the curvature quantification to changes in the projection angles of the C-arm system we repeated the quantifications 3 and 4, but we introduced deviations of 5, 10, 15 and 20 degrees to the projection angles of the C-arm system. These deviations are achieved by simulating rotation of the C-arm position 5, 10, 15 and 20 degrees away from the original position and quantifying 100 instances about a circle around the projection axis such that the deviations in all directions are measured.

Data analysis

We assessed the curvature measurements with a Bland-Altman analysis (14) and a Passing-Bablok non-parametric regression (15). The Bland-Altman analysis is the standard approach in comparing two sets of measurements and provides their limits of agreement. The Passing-Bablok non-parametric regression gives the slope and intercept of the regression line along with their 95% confidence interval and makes no special assumptions regarding the distribution of the samples and the measurement errors. A statistical test of linearity was also performed using the Cusum adapted method (Kolgomogrov-Smirnov) described by Passing and Bablok (15).

The curvature quantifications of the CTA projections to actual XA imaging planes (CTA2DReal) were compared to the curvature quantifications of the XA sequences with 2 observers (XAObs1 and XAObs2). This was done to gain insight into how similar the measurements are between the two different

modalities. The XA curvature quantifications were compared between the two observers as well to determine the inter-observer variability. The analysis was performed with R v3.1.1 (R Foundation for Statistical Computing, Vienna, Austria).

Results

CTA curvature measurements

The 3D CTA based curvature analysis showed a mean curvature angle of 23.4 degrees with a standard deviation of 13.5 degrees (Table 1). The inter-patient variability was large with a range of 5 to 61 degrees. The mean absolute difference in curvature using the 2D projections of the 3D centrelines with optimal imaging angles compared to the 3D CTA measurement was only 0.6 degrees (standard deviation: 1.1) with a range of 0 to 4 degrees difference. For the 2D projections at the angulations as actually used during XA, the mean curvature was slightly less than the 3D CTA mean at 20.8 degrees (standard deviation: 15.9), a -2.6 degrees difference compared to the 3D measurements, although in individual cases the difference was maximal 31 degrees.

Table 1 contains the results of the first four ways of measuring curvature.

Bland-Altman Analysis

The Bland-Altman analysis of the curvature quantifications of the CTA projections to actual XA imaging planes (CTA2DReal) compared to the curvature quantifications of the XA sequences with 2 observers, XAObs1 and XAObs2, gives a mean bias (95% limit of agreement) of -3.2 (-19.7 to 13.3) degrees and -1.7 (-17 to 13.7) degrees respectively. The mean bias (95% limit of agreement) between observers for the XA measurements was 1.6 (-9.3 to 12.4) degrees, this represents a standard deviation of 5.4 degrees in measured curvature angle differences between observers. See Figure 4 and 5 for the identity and Bland-Altman plots of these comparisons.

Passing-Bablok Regression

The Passing-Bablok regression on the curvature quantifications of the CTA projections to actual XA imaging planes and those of the XA sequences with 2 observers, XAObs1 and XAObs2, results in a a slope (95% CI) of 0.77 (0.59,1.30) and an intecept (95% CI) of 4.74 (-2.29,8.94) for CTA2DReal & XAObs1 and a slope (95% CI) of .83 (0.58,1.11)and an intercept (95% CI) of 4.08 (0.23,9.71) for CTA2DReal & XAObs2. For the Passing-Bablok regression on the XA measurements (XAObs1 and XAObs2) the slope (95% CI) of the regression line is 0.85 (0.67,1.16) and the intercept (95% CI) is 0.06 (-3.92,5.17). The Cusum tests show no significant deviation from linearity with $P > 0.1$ for all cases.

Impact of suboptimal positioning

Diverging from the optimal angle in our CT projections had increasing impact on the sensitivity of measured curvature with a maximum impact of over 30 degrees (Figure 6). At the optimal projection angles variation in curvature quantification caused by small deviations from the angulations is much lower (figure 7B) than for the actual suboptimal projections, which shows that the measurements under suboptimal projections are sensitive to small deviations (Figure 7A).

Figures 6 and 7 contain the overall results of the sensitivity to deviation test.

Discussion

We presented a method for measuring stent and vessel curvature and performed stent curvature measurements on a dataset of CTA and XA images of 14 patients. Furthermore we compared the measurements done on CTA with the XA measurements and quantified the impact of projection angles as determined by C-arm position and deviations of projection angles on XA measurements.

Table 1 shows the difference between performing 3D curvature measurements on CTA and 2D measurements on XA. By projecting the 3D CTA centrelines to the optimal imaging plane and measuring

the curvature on the 2D projection, the quantification in 3D can be reproduced in 2D. The Bland-Altman analysis also shows some inter-observer variability in the XA measurements, reflecting the non-trivial task of annotating XA images, with a standard deviation of 5.4 degrees in the differences of measured curvature between observers. Some of the discrepancies of the curvature measurements of the projected 3D CTA structures using actual XA system projection angles and the XA measurements may be explained by the observer variability in the XA annotations, the reported errors in the CTA centreline extraction (11), relative differences in patient positioning between the imaging modalities or actual changes in curvature. The sample size of 14 patients along with the CTA centreline extraction errors and possible actual changes in curvature between modalities are the main limitations of this study. However, the Passing-Bablok regression and linearity test shows the measurements for the projected 3D CTA using actual XA system projections angles and the XA measurements have no significant deviation from linearity ($P > 0.1$) indicating agreement.

Figure 6 shows how the median curvature can vary as a function of small deviations in the angulations, depending on whether or not the C-arm projection angles are optimal. It suggests, as can be expected, that for XA imaging projection angles that are further away from the optimal projection angles the tendency is to have a greater change in the measured curvature compared to the actual curvature (as measured in 3D). Figure 7(a) and 7(b) show how the spread of the measurements increases with larger deviations and for non-optimal projection angles. We also found that this decrease in measurement accuracy does not depend on the actual curvature (as determined by our 3D CTA measurement). This indicates that the effect of the projection angles can make a relatively straight or curved segment appear straighter or more curved than it actually is. In our dataset only one patient had an optimal C-arm position within 10 degrees of the actual position used (see Figure 6).

Given the uncertainty in patient positioning and the dependency of the quantifications on the projection angles, for the purposes of vessel or stent curvature measurements in XA, consideration should be given to the projection angles in order to reduce the measurement error. These optimal C-arm angles may be determined by a prior CT scan, whereby an analysis such as ours will indicate an optimal viewing angle. Alternatively, if a biplane system is available, the 3D quantification could be applied on a 3D reconstruction of the vessel of interest (16). A rotational scan with a monoplane system may provide another option. Follow-up measurements can be performed on XA as long as the projection angles are optimal or close to optimal and unchanged from previous measurements. These can now be interpreted with knowledge of the uncertainties inherent to the XA measurement. If the goal of a follow-up study is to measure the changes in curvature (i.e. assess the conformability of a stent) and no invasive modalities such as IVUS and OCT are planned then we recommend the use of CTA to assess curvature. Curvature measurement on CTA is view independent, less invasive than XA and with recent advances in CTA algorithms that reduce radiation dose exposure (17) of comparable radiation dose to XA.

Conclusion

In conclusion, stent curvature measurements can be performed with CTA and is preferred over XA measurements, especially for longitudinal studies. If other invasive follow-up is required then XA quantifications of stent or vessel curvature can be performed using the optimal projection angles. These can be obtained from a 3D coronary model via e.g., a previously acquired CTA.

References

1. Lee MS, Jurewitz D, Aragon J, Forrester J, Makkar RR, Kar S. Stent fracture associated with drug-eluting stents: Clinical characteristics and implications. Catheterization and Cardiovascular Interventions. 2007;69(3):387–94.

2. Canan T, Lee MS. Drug-eluting stent fracture: Incidence, contributing factors, and clinical implications. Catheterization and Cardiovascular Interventions. 2010;75(2):237–45.

3. Hecht HS, Polena S, Jelnin V, Jimenez M, Bhatti T, Parikh M, Panagopoulos G, Roubin G. Stent Gap by 64-Detector Computed Tomographic Angiography. Journal of the American College of Cardiology. 2009;54(21):1949–59.

4. Gyongyosi M, Yang P, Khorsand A, Glogar D. Longitudinal straightening effect of stents is an additional predictor for major adverse cardiac events. J. Am. Coll. Cardiol. 2000;35(6):1580-9.

5. Gomez-Lara J, Garcia-Garcia HM, Onuma Y, Garg S, Regar E, de Bruyne B, Windecker S, McClean D, Thuesen L, Dudek D, Koolen J, Whitbourn R, Smits PC, Chevalier B, Dorange C, Veldhof S, Morel MA, de Vries T, Ormiston JA, Serruys PW. A Comparison of the Conformability of Everolimus-Eluting Bioresorbable Vascular Scaffolds to Metal Platform Coronary Stents. JACC: Cardiovascular Interventions. 2010;3(11):1190–1198.

6. Garcia-Garcia HM, Serruys PW, Campos CM, Muramatsu T, Nakatani S, Zhang YJ, Onuma Y, Stone GW. Assessing Bioresorbable Coronary Devices: Methods and Parameters. JACC: Cardiovascular Imaging. 2014;7(11):1130–1148.

7. Liao R, Green N, James Chen SY, Messenger J, Hansgen A, Groves B, Carroll J. Three-Dimensional Analysis of in vivo Coronary Stent – Coronary Artery Interactions. The International Journal of Cardiovascular Imaging. 2004;20(4):305–313.

8. Nieman K, Serruys PW, Onuma Y, van Geuns RJ, Garcia-Garcia HM, de Bruyne B, Thuesen L, Smits PC, Koolen JJ, McClean D, Chevalier B, Meredith I, Ormiston J. Multislice computed tomography angiography for noninvasive assessment of the 18-month performance of a novel radiolucent bioresorbable vascular scaffolding device: the ABSORB trial (a clinical evaluation of the bioabsorbable everolimus eluting coronary stent system in the treatment of patients with de novo native coronary artery lesions). J Am Coll Cardiol. 2013;62(19):1813-4.

9. Onuma Y, Dudek D, Thuesen L, Webster M, Nieman K, Garcia-Garcia HM, Ormiston JA, Serruys PW. Five-year clinical and functional multislice computed tomography angiographic results after coronary implantation of the fully resorbable polymeric everolimus-eluting scaffold in patients with de novo coronary artery disease: the ABSORB cohort A trial. JACC Cardiovasc Interv. 2013;6(10):999-1009.

10. Simsek, C, Karanasos A, Magro M, Garcia-Garcia HM, Onuma Y, Regar E, Boersma E, Serruys PW, van Geuns RJ. Long-term invasive follow-up of the everolimus-eluting bioresorbable vascular scaffold: five-year results of multiple invasive imaging modalities. EuroIntervention. 2014;10:0724-03.

11. Metz CT, Schaap M, Weustink AC, Mollet NRA, van Walsum T, Niessen WJ. Coronary centerline extraction from CT coronary angiography images using a minimum cost path approach. Medical Physics. 2009;36:5568-5579.

12. Shahzad R, Kirisli H, Metz C, Tang H, Schaap M, Vliet L, Niessen WJ, van Walsum T. Automatic segmentation, detection and quantification of coronary artery stenoses on CTA. The International Journal of Cardiovascular Imaging. 2013;29:1847-1859.

13. Tang H, van Walsum T, van Onkelen RS, Hameeteman R, Klein S, Schaap M, Tori FL, van den Bouwhuijsen QJA, Witteman JCM, van der Lugt A, van Vliet LJ, Niessen WJ. Semiautomatic carotid lumen

segmentation for quantification of lumen geometry in multispectral MRI. Medical Image Analysis. 2012;16(6):1202-1215.

14. Martin Bland J., Altman D. Statistical methods for assessing agreement between two methods of clinical measurement. The Lancet. 1986;327(8476): 307–310.

15. Passing H, Bablok W. A new biometrical procedure for testing the equality of measurements from two different analytical methods. Application of linear regression procedures for method comparison studies in clinical chemistry, Part I. J. Clin. Chem. Clin. Biochem. 1983;21(11):709–20.

16. Zhu H, Warner JJ, Gehrig TR, Friedman MH. Comparison of coronary artery dynamics pre- and post-stenting. Journal of Biomechanics. 2003;36(5):689–697.

17. Stehli J, Fuchs TA, Bull S, Clerc OF, Possner M, Buechel RR, Gaemperli O, Kaufmann PA. Accuracy of Coronary CT Angiography Using a Submillisievert Fraction of Radiation Exposure: Comparison With Invasive Coronary Angiography. J Am Coll Cardiol. 2014;64(8):772-780.

Legends

Table I. Curvature Results – Angle of least squares circle fit (degrees). CTA3D – Quantification on 3D extracted centerline from CT, CTA2DOpt – Quantification on 2D projection of CT centerline using optimal XA system projection angles, CTA2DReal – Quantification on 2D projection of CT centerline using actual XA system projection angles, XAObs1 – Quantification on XA image by observer 1, XAObs2 – Quantification on XA image by observer 2.

Figure 1. Example of CTA centreline seeding (1A) and extracted centreline (1B) in red

Figure 2. Example of curvature measurement angle, red – vessel, blue – markers, green – fitted circle

Figure 3. Illustration of CTA centerline projections to two imaging planes. Note that one plane allows for a better quantification of curvature than the other. In our experiments the optimal XA geometry is determined by placing the C-arm such that vector orthogonal to the fitted circle in the 3D quantification intersects the detector center.

Figure 4. Identity Plots of Curvature Measurements. Dashed diagonal line is the identity line. CTA2DReal – Quantification on 2D projection of CT centerline using actual XA system projection angles, XAObs1 – Quantification on XA image by observer 1, XAObs2 – Quantification on XA image by observer 2.

Figure 5. Bland-Altman Plots of Curvature Measurements. Blue lines represent the 95% limit of agreement. CTA2DReal – Quantification on 2D projection of CT centerline using actual XA system projection angles, XAObs1 – Quantification on XA image by observer 1, XAObs2 – Quantification on XA image by observer 2.

Figure 6. Absolute changes in median curvature for deviations of 5, 10, 15 and 20 deg. from actual position compared to optimal position as a function of angle between the actual and optimal C-arm positions.

Figure 7. Curvature measurements spreads – maximum minus minimum curvature angle measured at the sensitivity angle in all directions – per patient for deviations about the Actual (7A) and Optimal (7B) XA projection angles. Note that Patient 11 is out of range in the Actual position plot.

Table I

Patients	CTA3D Curvature Angle (deg.)	CTA2DOpt Curvature Angle (deg.)	CTA2DReal Curvature Angle (deg.)	XAObs1 Curvature Angle (deg.)	XAObs2 Curvature Angle (deg.)
1	32	32	40	33	35
2	21	21	12	12	14
3	24	24	32	43	36
4	20	21	21	16	20
5	18	18	22	19	28
6	6	2	3	5	4
7	20	20	13	28	22
8	15	15	15	19	23
9	33	33	2	22	18
10	22	23	43	34	25
11	24	25	17	19	17
12	61	60	54	63	53
13	5	5	5	8	6
14	27	27	12	16	14

Figures

Figure 1A

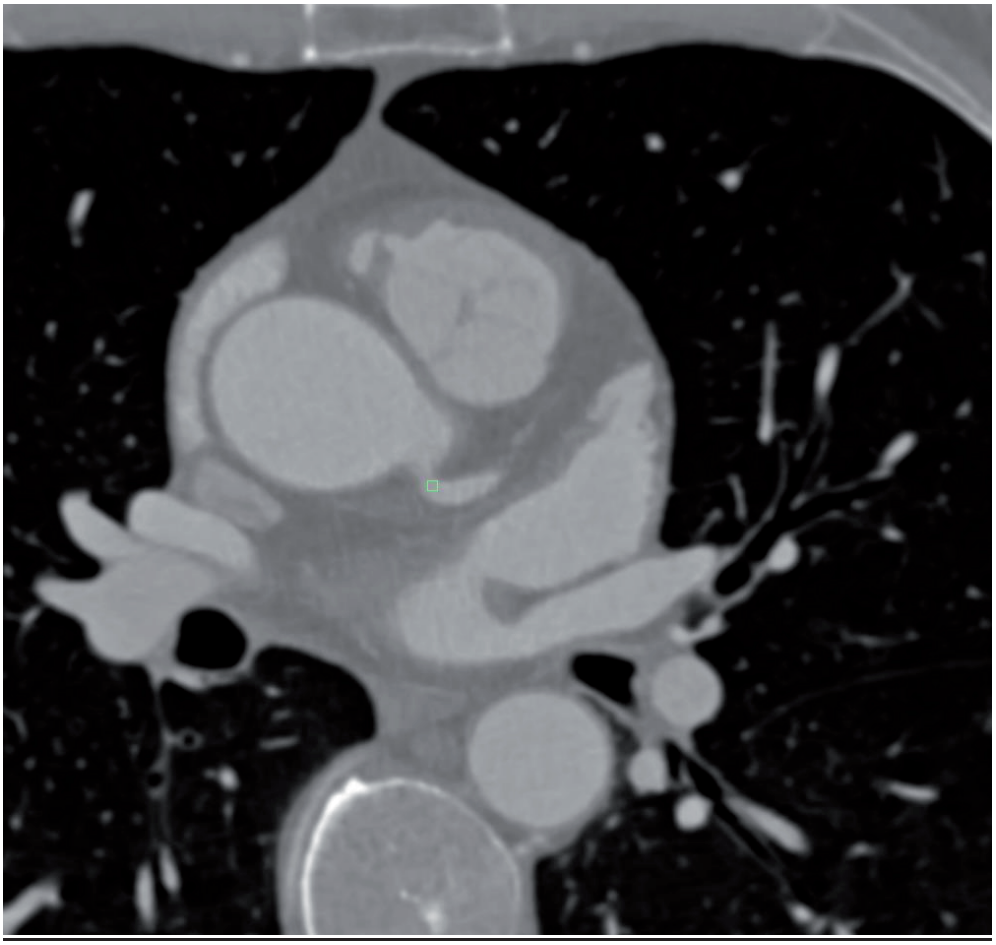

Figure 1B

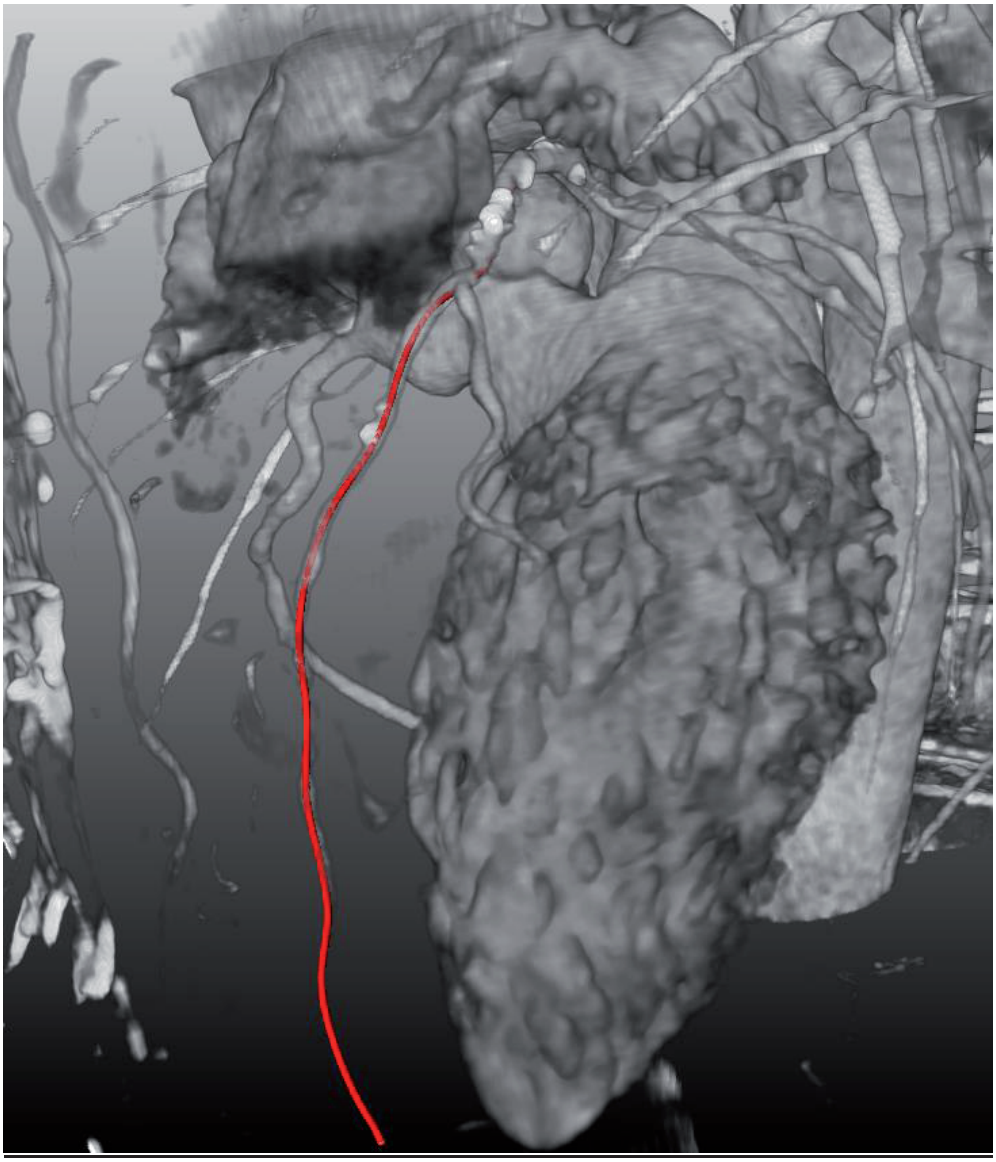

Figure 2

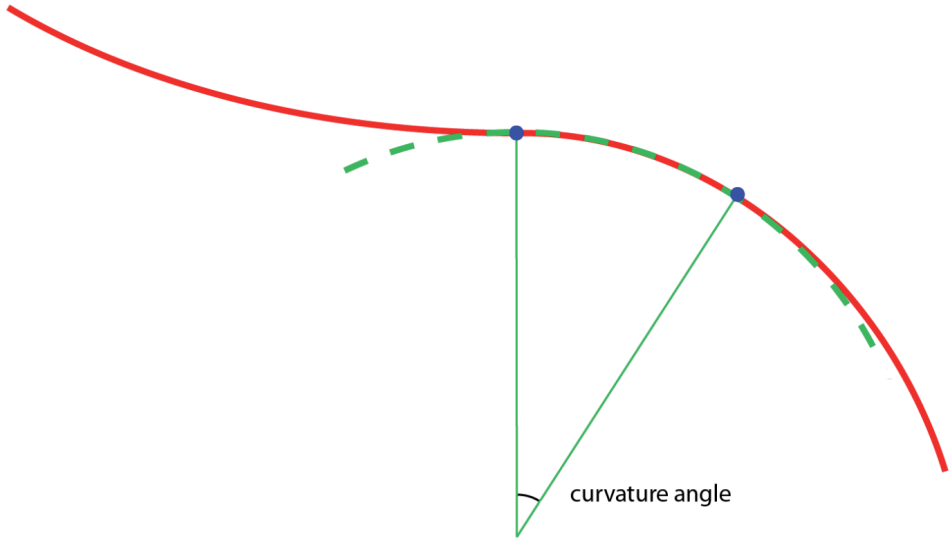

Figure 3

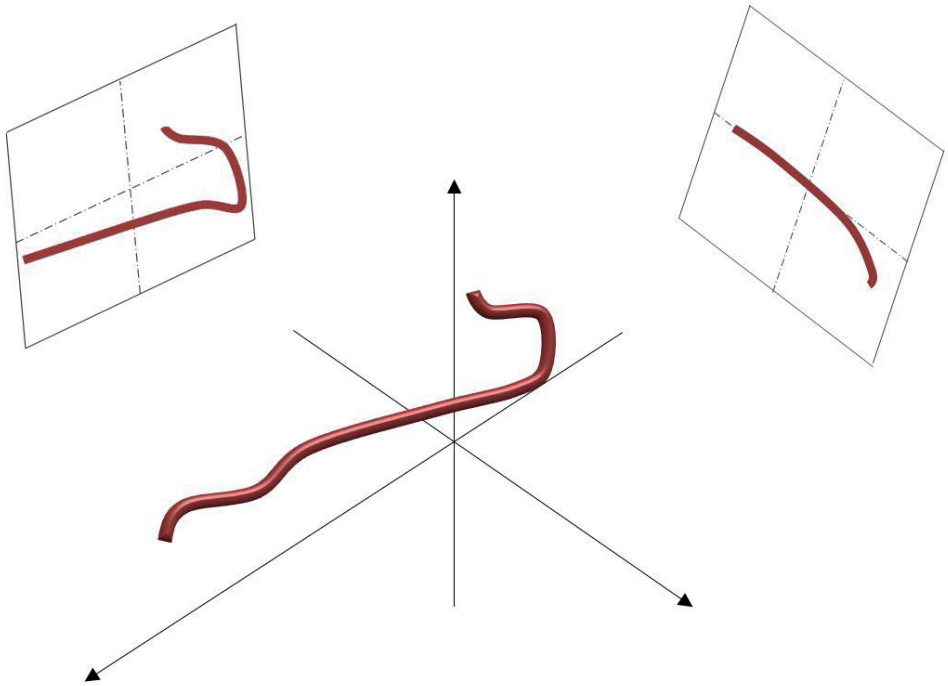

Figure 4

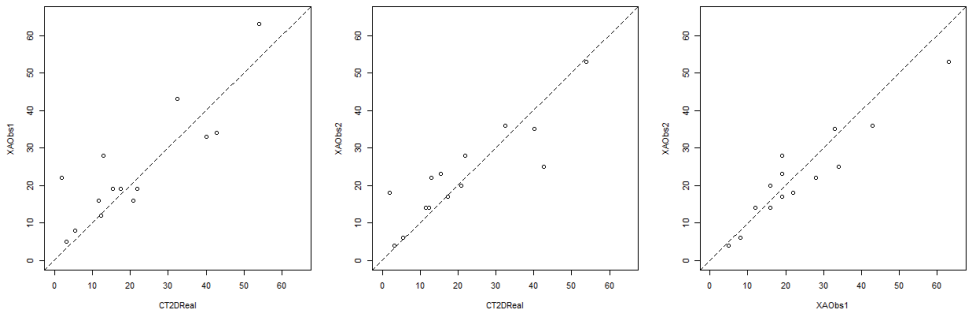

Figure 5

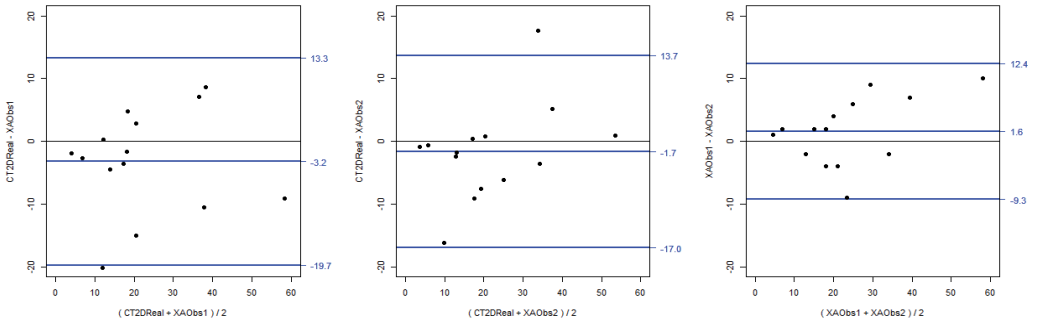

Figure 6

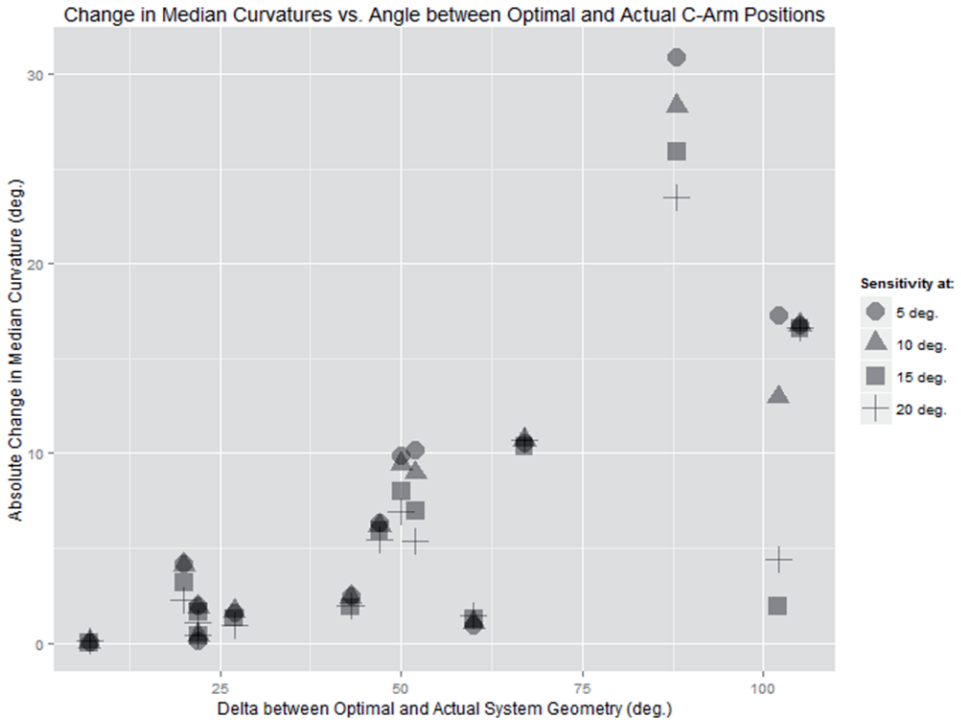
Change in Median Curvatures vs. Angle between Optimal and Actual C-Arm Positions
Absolute Change in Median Curvature (deg.)
30
20
10
0
25
50
75
100
Delta between Optimal and Actual System Geometry (deg.)
Sensitivity at:
5 deg.
10 deg.
15 deg.
20 deg.

Figure 7

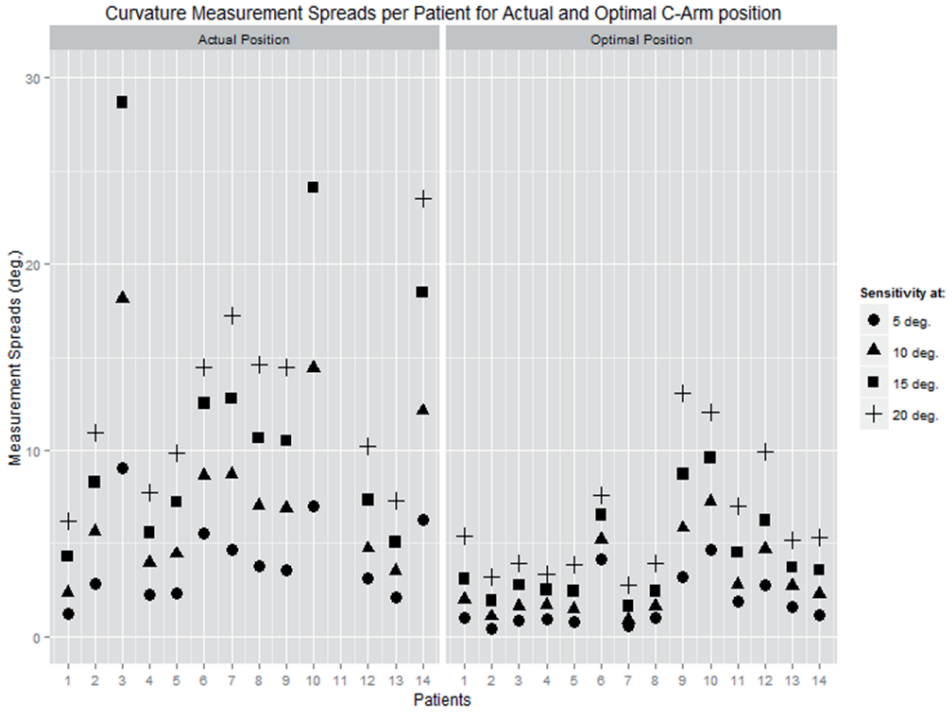
Curvature Measurement Spreads per Patient for Actual and Optimal C-Arm position
Actual Position
Optimal Position
Measurement Spreads (deg.)
30
20
10
0
1 2 3 4 5 6 7 8 9 10 11 12 13 14
1 2 3 4 5 6 7 8 9 10 11 12 13 14
Patients
Sensitivity at:
5 deg.
10 deg.
15 deg.
20 deg.

19

CHAPTER

CONFORMABILITY IN EVEROLIMUS-ELUTING BIORESORBABLE SCAFFOLDS COMPARED WITH METAL PLATFORM CORONARY STENTS IN LONG LESIONS

Jiang Ming Fam, Yuki Ishibashi, Cordula Felix, Bu Chun Zhang, Roberto Diletti, Nicolas van Mieghem, Evelyn Regar, Ron van Domburg, Yoshinobu Onuma, Robert- Jan van Geuns.

Int J Cardiovasc Imaging. 2017 Dec; 33(12):1863-1871.

Conformability in everolimus-eluting bioresorbable scaffolds compared with metal platform coronary stents in long lesions

Jiang Ming Fam[1,2] · Yuki Ishibashi[1] · Cordula Felix[1] · Bu Chun Zhang[1,3] · Roberto Diletti[1] · Nicolas van Mieghem[1] · Evelyn Regar[1] · Ron van Domburg[1] · Yoshinobu Onuma[1] · Robert-Jan van Geuns[1]

Received: 3 December 2016 / Accepted: 13 June 2017

Abstract The aim of this study was to determine if there are significant differences in curvature of the treated vessel after the deployment of a polymeric BRS or MPS in long lesions. The impact of long polymeric bioresorbable scaffolds (BRS) compared with metallic platform stents (MPS) on vessel curvature is unknown. This retrospective study compares 32 patients who received a single everolimus-eluting BRS with 32 patients treated with a single MPS of 28 mm. Quantitative coronary angiography (QCA) was used to evaluate curvature of the treatment and peri-treatment region before and after percutaneous coronary intervention (PCI). Baseline demographic and angiographic characteristics were similar between the BRS and MPS groups. Pretreatment lesion length was 22.19 versus 20.38 mm in the BRS and MPS groups respectively ($p=0.803$). After treatment, there was a decrease in median diastolic curvature in the MPS group (from 0.257 to 0.199 cm^{-1}, $p=0.001$). A similar trend was observed in the BRS group but did not reach statistical significance (median diastolic curvature from 0.305 to 0.283 cm^{-1}, $p=0.056$). Median Percentage relative change in diastolic curvature was lower in the BRS group compared with the MPS group (BRS vs. MPS: 7.48 vs. 29.4%, $p=0.013$). By univariate analysis, use of MPS was an independent predictor of change in diastolic curvature ($p=0.022$). In the deployment of long coronary scaffolds/stents (28 mm in length), BRS provides better conformability compared with MPS.

Keywords Bioresorbable scaffolds · Conformability · Drug eluting stents · Long coronary lesions · Metallic platform stents · Percutaneous coronary Intervention

Abbreviations

AMI	Acute myocardial infarct
BRS	Bioresorbable scaffolds (BRS)
CABG	Coronary artery bypass graft
CoCr- EES	Cobalt chromium- everolimus eluting stent
Cv	Curvature
CVA	Cerebrovascular accident
DES	Drug eluting stent
LAD	Left anterior descending artery
LCX	Left circumflex artery
MLD	Minimal luminal diameter
MPS	Metallic platform stent
PCI	Percutaneous coronary intervention
PLLA	Poly-L-lactic acid
QCA	Quantitative coronary angiography
RCA	Right coronary artery
RVD	Reference vessel diameter
STEMI	ST Elevation myocardial infarct

Introduction

The everolimus-eluting bioresorbable scaffolds (BRS) represented a novel change in the treatment of coronary artery lesions. The BRS is composed of a poly-L-lactic acid (PLLA)—based platform. Besides the ability to have complete strut resorption at 36 months, there are several

✉ Robert-Jan van Geuns
r.vangeuns@erasmusmc.nl

[1] Department of Cardiology, Thorax Centre, Room Ba-585, Erasmus University Medical Centre, 's-Gravendijkwal 230, 3015 GE Rotterdam, The Netherlands

[2] National Heart Centre, Singapore, Singapore

[3] The Affiliated Hospital of Xuzhou Medical College, Xuzhou, Jiangsu, China

potential benefits of BRS including no trigger for thrombosis after resorption and restoration of vasoreactivity [1]. Typically, implantation of hard metallic implants straightens the coronary artery and thus modifies its curvature. A previous computational study demonstrated that after implantation of a metallic implant in a coronary artery, the curvature of the stent edges alters significantly which correlate to the changes in shear stress distribution and potentially with the neointimal proliferation pattern [2]. As implantation of coronary stents/scaffolds can alter blood rheology especially at the inflow and outflow edge of the stents, the vessel distortion post device implantation may contribute to early and late stent failure such as pertaining to stent fracture. Geometric changes in the arteries post implantation are largely determined by the conformability of the stent [3]. The conformability of the stent has been described as the flexibility of a stent in its expanded state with adaptation to the natural shape of the vessel. A higher conformability of the stent is associated with less potential for vessel distortion and trauma [4].

Previous studies using BRS in short lesions demonstrate better conformability and favorable clinical outcomes compared to MPS in the acute setting [5, 6]. In the study by Gomez Lara et al., the acute change in curvature and angulation as quantified by quantitative coronary angiographic analysis was decreased in BRS compared to MPS [6] and was shown to recover on follow up [7]. This effect may be more pronounced and more relevant in a long lesion in either the coronary or peripheral arterial system. However, the acute effects of its implantation on vessel geometry in long coronary lesions are yet to be investigated. The aim of this study was to determine if there are any significant differences in terms of curvature of the treated vessel after the deployment of a polymeric scaffold device in long lesions and compare this to a MPS.

Methods

Study design, population, and treatment device

This is a non-randomized, 2-arm, retrospective study performed with patients from the BVS Expand and BVS STEMI First registries that received a everolimus eluting BRS (ABSORB-BVS, Abbott Vascular, Santa Clara, CA, USA) compared with a subset of historical controls from the same institutional registries (X-SEARCH) who received a cobalt chromium- everolimus eluting stent (CoCr-EES; XIENCE^R stent, Abbott Vascular, Santa Clara, CA, US).

In brief, the common inclusion criteria for this study are patients who had received a single BRS or CoCr EES that are 28 mm in length in long coronary lesions. The patients in the BRS group are selected from the BVS Expand [8] and BVS STEMI [9] registries which are single centre prospective observational registries conducted at Thorax Centre, Erasmus Medical Centre that evaluates the long term safety and performance of the BRS-absorb coronary stent in routine clinical practice post market registration. Informed, written consent was obtained from the patients before they undergo any procedure. The lesions are also more complex with more bifurcations and calcified lesions. From the X-SEARCH registry, patients with similar angiographic characteristics were selected for this study [10].

The BRS-Absorb vascular scaffold is a balloon-expandable device, consisting of a polymer backbone of PLLA coated with a thin layer of a 1:1 mixture of an amorphous matrix of PLLA polymer containing 100 μg/cm^2 of the antiproliferative drug everolimus. The implant is radiolucent but has two platinum markers at each edge that allow visualization on angiography and other imaging modalities. Physically the scaffold has struts with an approximate thickness of 150 μm, which are arranged as in-phase zigzag hoops linked together by three longitudinal links (Fig. 1a).

The metallic platform of the everolimus-eluting XIENCE^R family stent (EES) is composed of a cobalt chromium (CoCr) alloy. The platform has a design similar to the Absorb platform and consists of serpentine rings connected by links fabricated from a single piece (Fig. 1b). The metallic platforms of the CoCr EES are constructed by a strut thickness of 81 μm each [11].

Treatment procedure

Lesions treated with the BRS were implanted according to the procedural steps in line with the accepted recommendations at the time of the study. Predilation with either a semi-compliant or non-compliant balloon was highly encouraged. The BRS was implanted at a pressure not exceeding the rated burst pressure (16 atm). Post-dilation with either a semi-compliant or non-compliant balloon was performed at the discretion of the operator. Patients were prescribed with standard guideline recommended medical therapy including at least 12 months' duration of dual antiplatelet therapy and antianginal therapy when appropriate.

Quantitative coronary angiography (QCA) evaluation

Angiographic views with minimal foreshortening of the lesion and limited overlap with other vessels were used whenever possible for all phases of the treatment: preprocedural angiography, and after obtaining final result [12]. Comparison between pre and post treatment, were performed in matched angiographic views of 10° or less. The 2-dimensional (2D) angiograms were analyzed with the CASS 5.10 analysis system (Pie Medical BV, Maastricht, the Netherlands). In each patient, the treated region and the

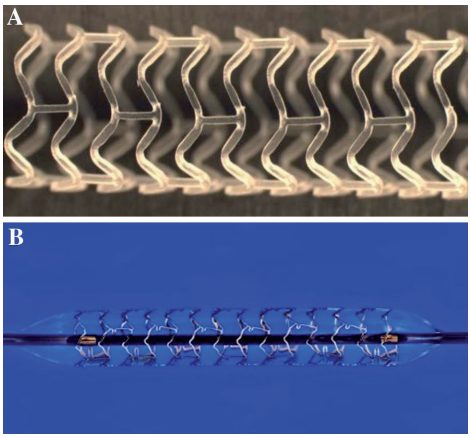

Fig. 1 **a** Bioresorbable scaffold: The second generation ABSORB-BVS (Abbott Vascular, Santa Clara, CA, USA) has a strut thickness of 150 μm, consisting of in-phase zigzag hoops linked by bridges. The device is radiolucent but has two radioopaque platinum markers at each proximal and distal edge that facilitate ease of visualization on angiography. **b** Cobalt chromium everolimus- eluting stent (CoCr EES- XIENCE^{R}, Abbott Vascular, Santa Clara, CA, US): The XIENCE^{R} are the metal platform stents and consist of a metallic platform made of cobalt chromium alloy. The struts are serpentine rings connected by links fabricated from a single piece. The XIENCE^{R} is covered by an everolimus coating

peri-treated regions (defined by 5 mm proximal and distal to the device edge) were analyzed. The computer defined minimal luminal diameter, reference diameter obtained by an interpolated method, and percentage diameter stenosis in the post procedure angiogram.

The definition of "Curvature" is the infinitesimal rate of change in the tangent vector at each point of the centerline. This measurement has a reciprocal relationship to the radius of the perfect circle defined by the curve at each point. The curvature of the vessel is calculated as 1/radius of the circle in cm^{-1}, with a research program installed in the QCA Analysis software (CASS 5.10, Pie Medical Imaging) [13]. The segment of interest was defined as the stented/scaffolded length. To enable analysis of curvature in the same anatomical region, the scaffold position was superimposed on the preprocedural angiogram (Fig. 2). The software automatically detects the lumen contours of the selected segment and configures the centerline. Three points are then defined according to the centerline: one at the proximal, one at the distal, and one at the center of the defined segment. Next, a perfect circle is drawn through these points, calculating the radius of the circle and the curvature value. Prior to and after the procedure, the curvature of the segment of interest was repeatedly measured both during systole and diastole. Percentage relative change in curvature (Cv) was calculated as % (postCv–preCv)/preCv in the respective cardiac phases. Cyclic changes in vessel curvature were estimated as differences between systole and diastole at both pre-treatment and post-treatment.

Statistical analysis

The Kolmogorov–Smirnov test was used to evaluate the normality assumptions of all continuous variables. Descriptive statistical analysis was performed with continuous variables expressed as median (interquartile range) and with categorical variables presented as counts (%). For comparison between groups, Mann–Whitney *U* test were used for the continuous variables. The Chi square test has been used to assess differences in categorical variables. Pre and post treatment comparisons within groups were assessed with Wilcoxon signed rank tests. Because the curvature, cyclic changes of curvature, and difference of curvature between pre- and post-treatment did not have a normal distribution, a log transformation was performed to achieve a normal distribution. A univariate analysis was performed between curvature and angulation changes with baseline demographic and angiographic variables. Variables that were found to be significant at the univariate level were tested with a multivariate linear regression model. (The thresholds for entry into and removal from the model were 0.1.) All statistical tests were carried out at the 5% level of significance. All analysis was performed by SPSS version 21 (SPSS, Inc., Chicago Illinois).

Results

The baseline clinical and angiographic characteristics are shown in Table 1. A total of 64 patients were involved in this study of which 32 were treated with the BRS and 32 with the MPS. A flow chart summarizing patient selection is shown in Fig. 3. There was no difference in median age (BRS vs. MPS: 59.6 vs. 64.9 years, $p=0.453$), gender or clinical presentation between the 2 device groups. There were no significant differences in the cardiovascular risk factors.

The left anterior descending artery was the most commonly treated vessel in the study population. Lesion calcification and complexity were similar between the two groups (Table 1). Procedural data are as shown in Table 1. Lesions treated with BRS were predilated more frequently and at higher pressures compared to the lesions treated with metallic stents. Postdilation rates were similar. The pre treatment region length was 21.38 mm (17.67–25.58) in the overall group. There were no significant differences in reference vessel diameter, minimal lumen diameter and

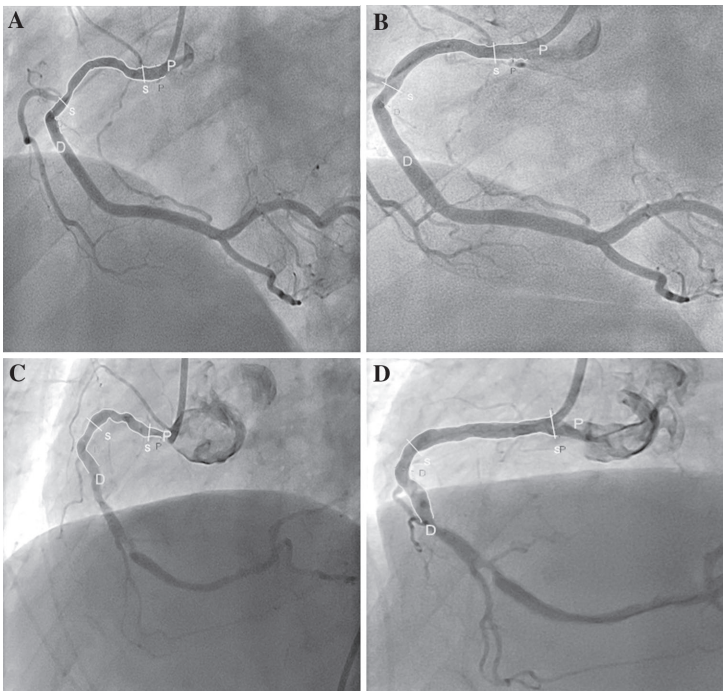

Fig. 2 Curvature Analysis of the BRS and MPS: curvature analysis before and after deployment of a BRS (Fig. 2a, b) and a MPS (Fig. 2c, d). After implantation of a BRS, the curvature changed from 0.58 to 0.49 cm^{-1} whereas after the MPS was implanted, the curvature changed from 0.85 to 0.23 cm^{-1}. *BRS* bioresorbable scaffold, *MPS* metallic platform stent

percentage diameter stenosis in both groups. Pretreatment curvature was similar between the BRS and MPS groups in both systole and diastole phases [systole: 0.290 (0.155–0.639) cm^{-1} vs. 0.283 (0.125–0.519) respectively, p = 0.803 and diastole: 0.305 (0.193–0.580) cm^{-1} vs. 0.257 (0.151–0.518) cm^{-1} respectively, p = 0.803].

Geometric changes within and between groups

Table 2 shows the changes in curvature in both systole and diastole of the treated vessel in the BRS and MPS groups. After implantation of MPS, there was a significant decrease in median diastolic curvature (from 0.257 to 0.199 cm^{-1}, p = 0.001) and median systolic curvature (0.283–0.194 cm^{-1}, p < 0.001) representing a percentage reduction of 16.0 and 28.6% respectively. Following an absorb scaffold implantation, there was a trend towards a decrease in the median diastolic curvature (from 0.305 to 0.283 cm^{-1}, p = 0.056) and median systolic curvature (from 0.290 to 0.282 cm^{-1}, p = 0.061) which trends towards significance. As a result, the diastolic curvature was significantly higher in the BRS compared with the MPS group post treatment [BRS vs. MPS; 0.283 cm^{-1} (0.150–0.541) vs. 0.199 cm^{-1} (0.089–0.357), p = 0.035] (Fig. 4). Post treatment, Percentage relative reduction in curvature was also smaller in the BRS group compared with MPS group in both the diastole and systole phases [BRS vs. MPS; 7.48 vs. 29.4%, p = 0.013; 9.04 vs. 28.2%, p = 0.010 respectively]. Cyclic changes in curvature (i.e. between systole and diastole) were similar between the BRS and the MPS (p = 0.271).

Predictive factors of modifying curvature

In univariate analysis, the use of MPS predicts a greater reduction in curvature with a coefficient of 23.33 (95% confidence interval 3.81–42.85, p = 0.02).

Discussion

In summary, the major finding of this study showed that in the deployment of long coronary devices (28 mm in length), BRS showed a non-significant decrease in curvature in the post treated vessel compared with a significant reduction in curvature of the treated vessel with deployment of a MPS.

Table 1 Baseline clinical and angiographic characteristics

	BRS (N = 32)	MPS (N = 32)	p value
Age (years)	59.6 (52.5, 67.8)	64.9 (57.7, 70.7)	0.453
Men	22 (68.8)	22 (68.8)	1.000
Hypertension	18 (56.2)	20 (62.5)	0.611
Hypercholesterolemia	15 (46.9)	17 (53.1)	0.617
Diabetes mellitus	5 (15.6)	8 (25.0)	0.351
Smoker (active)	12 (37.5)	7 (21.9)	0.391
Family history			
Previous CVA	2 (6.2)	2 (6.2)	1.000
Previous AMI	6 (18.8)	12 (37.5)	0.095
Previous PCI	5 (15.6)	9 (28.1)	0.226
Previous CABG	0	0	
Clinical presentation			
Stable or silent angina	10 (31.3)	18 (56.3)	0.074
Unstable angina	1 (3.1)	4 (12.5)	0.355
STEMI	4 (12.5)	0	0.155
NSTEMI	17 (53.1)	9 (28.1)	0.074
Other	0	1 (3.1)	1.000
Target vessel			0.857
LAD	15 (46.9)	13 (40.6)	
LCX	6 (18.8)	6 (18.8)	
RCA	11 (34.4)	13 (40.6)	
RVD (mm)	2.90 (2.49, 3.18)	2.91 (2.29, 3.26)	0.803
MLD (mm)	0.92 (0.77, 1.57)	1.20 (0.75, 1.55)	0.453
Diameter stenosis (%)	60.00 (47.25, 72.75)	56.00 (46.00, 76.75)	0.452
Bifurcation	12 (37.5)	7 (21.9)	0.274
AHA type			0.149
A	2 (6.3)	0	
B1	19 (59.4)	14 (43.8)	
B2	6 (18.8)	13 (40.6)	
C	5 (15.6)	5 (15.6)	
Calcification			
Mild	19 (59.4)	12 (37.5)	
Moderate/severe	13 (40.6)	20 (62.5)	
Pre-treatment region length (mm)	22.19 (17.67, 25.08)	20.38 (17.05, 25.75)	0.803
Procedural details			
Predilation performed	29	18	0.004
Predilation balloon diameter	2.50 (2.50, 2.50)	2.00 (2.00, 2.50)	0.03
Postdilation	18	13	0.317
Postdilation diameter	3.00 (2.94, 3.50)	3.50 (2.75, 4.00)	0.253

Values are presented as number (%) or median (interquartile range)

AMI acute myocardial infarct, *BRS* bioresorbable scaffold, *CABG* coronary artery bypass graft, *CVA* cerebrovascular accident, *LAD* left anterior descending artery, *LCX* left circumflex artery, *MLD* minimal luminal diameter, *MPS* metallic platform stent, *PCI* percutaneous coronary intervention, *RCA* right coronary artery, *RVD* reference vessel diameter, *STEMI* ST elevation myocardial infarct

Use of MPS was an independent predictor of vessel curvature change post deployment.

Stent conformability is dependent on both the material and design of the stent and differs between the commercial devices that are available [14–16]. An open cell stent design would have higher conformability compared to a closed cell design. The difference in curvature post treatment between BRS and MPS could be attributed to the difference

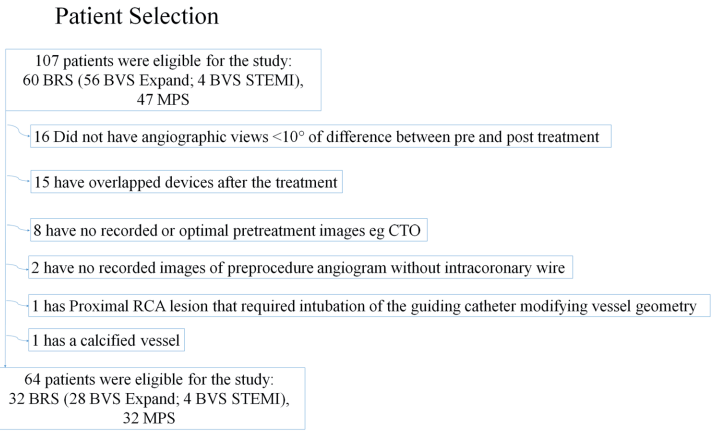

Fig. 3 Flow chart of patient selection. *BRS* bioresorbable scaffold, *CTO* chronic total occlusion, *MPS* metallic platform stents, *STEMI* ST elevation myocardial infarct

Table 2 Changes in curvature of the study population

	BRS (N = 32)	MPS (N = 32)	p value
Pre-treatment curvature (cm^{-1})			
Systole	0.290 (0.155, 0.639)	0.283 (0.125, 0.519)	0.648
Diastole	0.305 (0.193, 0.580)	0.257 (0.151, 0.518)	0.460
Post-treatment curvature (cm^{-1})			
Systole	0.282 (0.147, 0.549)	0.194 (0.097, 0.407)	0.077
Diastole	0.283 (0.150, 0.541)	0.199 (0.089, 0.357)	0.035
Percentage reduction in curvature post-pretreatment[a]			
Systole	2.76	28.6*	
Diastole	7.21	16.0*	
Absolute reduction in curvature (cm^{-1})			
Systole	0.024 (0.015, 0.087)	0.064 (0.010, 0.230)	0.034
Diastole	0.021 (0.025, 0.098)	0.090 (0.011, 0.192)	0.066
Percentage relative change in curvature (cm^{-1})			
Systole	−9.035 (−22.128, 7.911)	−28.17 (−46.22, −6.64)	0.010
Diastole	−7.484 (−23.193, 8.355)	−29.43 (−50.31, −3.55)	0.013
Pre-treatment cyclic change in curvature (cm^{-1})	−0.021 (−0.072, 0.061)	0.002 (−0.086, 0.096)	0.398
Post-treatment cyclic change in curvature (cm^{-1})	−0.026 (−0.054, 0.023)	−0.041 (−0.04, 0.125)	0.271

Values are presented as numbers or median (interquartile range)

[a]For BRS, the p values for comparison between pre and post curvature for systole and diastole are 0.061 and 0.056 respectively. For MPS, the p values for comparison between pre and post curvature for systole and diastole are <0.001(*) and 0.001(*) respectively

BRS bioresorbable scaffold, *MPS* metallic platform stent

in underlying material composition of the devices in that a polymeric bioresorbable scaffold has better conformability to vessel geometry compared to metallic stents. In a study evaluating the bending stiffness of the BRS compared to the MPS in-vitro, the maximum compressive load of a BRS from ABSORB COHORT B trial was significantly lower compared to the XIENCE^{R} stent which signifies better conformability of the BRS (Fig. 5) [17]. This is despite the fact that the strut thickness of the ABSORB Cohort B stent is thicker than that of the XIENCE^{R} stent (strut thickness

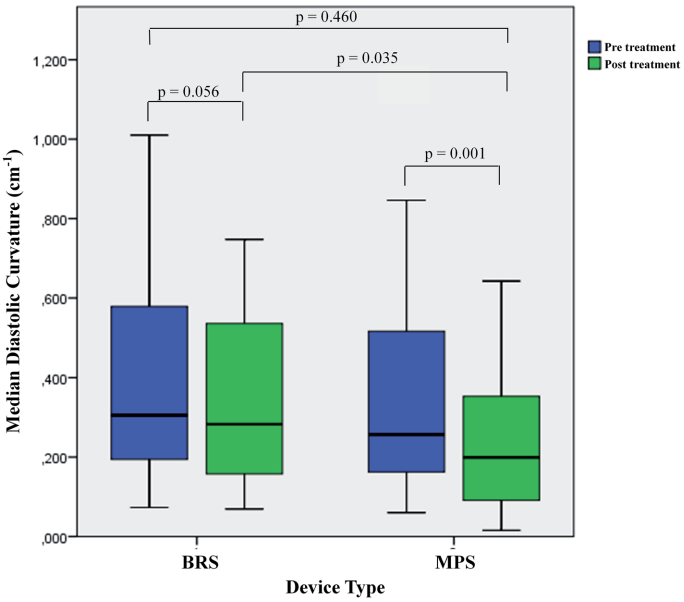

Fig. 4 Change in curvature post treatment in BRS and MPS. This *boxplot* illustrates the difference in median diastolic curvature post treatment in the BRS compared to the MPS group

152.4 vs. 81.3 μm). A previous study had shown that the use of relatively shorter (18 mm) BRS and MPS devices modify baseline vessel curvature but the change was more marked in the MPS compared with the BRS [6]. In this study, the median pretreatment lesion length was 16.3 and 16.8 mm in the BRS and MPS groups respectively which are comparatively shorter compared to our study population. To our knowledge, this is the first in vivo study that shown that BRS does not affect the curvature of the treated vessel significantly in the deployment of long scaffolds. This might be of useful significance as we treat longer lesions with overlap scaffold required.

Though OCT has been widely described in existing methodology [18–21] to evaluate scaffold performance, OCT by itself is not able to measure curvature of the vessel, whereas QCA is available pre and post in almost all patients. From fluid dynamics and the resulting shear stress we know curvatures do have an impact on plaque formation in the following years where it is important to minimize the distortion of the natural vessel course post stent or scaffold implantation. As vascular geometry is the most important determinant of local wall shear stress, any beneficial effect on the conformability of the blood vessel might have clinical implications. Studies have demonstrated that low wall shear stress promotes atherosclerosis and plaque progression in native arteries [22] and greater intimal hyperplasia

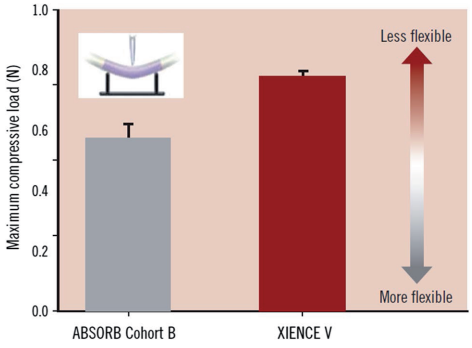

Fig. 5 Maximum compressive force of ABSORB Cohort B scaffold and XIENCE V stent. This figure shows the maximum compressive force applied to deflect the ABSORB Cohort B and XIENCE V 3.0×18 mm devices by 1.1 mm using 3 point- bend test (n=5). Statistical analysis yielded p=0.004 using One- way ANOVA and Tukey- Kramer HSD. Tests were performed by and data are on file at Abbott Vascular. (Reprinted from EuroIntervention Supplement (2009) Vol.5 Supplement F; Oberhauser JP, Hossainy S, Rapoza RJ. Design principles and performance of bioresorbable polymeric vascular scaffolds. F15-22, Copyright, with permission from Europa Digital and Publishing)

after stent deployment [23]. Metallic stents deployed in curved porcine coronary arteries were noted to cause vessel straightening in the stented segment and increased curvature at the stent edges [2]. A study by Gyongyosi et al. had further showed that a longitudinal straightening of stents is an additional predictor of major adverse events [24]. There are possible physiological and clinical benefits arising from the improvement in conformability in the BRS. An increased conformability of the BRS platform may result in physiological wall shear stress at the stent edges due to less vessel distortion. This may translate to clinical benefits such as reduced risk of scaffold edge restenosis. However, the clinical benefits associated with better conformability still needs further evaluation. This has become more relevant in the setting of recent data that showed a potential lack of benefits up to 3 years [25] particular certain lesion subsets such as smaller vessels with the BRS compared with best in class DES, with the BRS showing either similar or increased risk of TLR and increased risks of scaffold thrombosis compared to DES [26, 27].

Stent flexibility (and conformability) is also one of the key determinants of stent fracture, a common cause of late stent failure. Hinge motion (i.e. rocking back and forth on a bend) was one of the factors that can increase the risk of stent strut fracture. Our results suggest that there is a subtle but certain cyclic change of curvature after device implantation in both groups. Although there is no difference between groups, one can speculate that this cyclic movement repeating greater than 86,400 times a day (based on average heart rate of 60 beats per minute) can cause mechanical failure at the metallic struts. In a study looking at predictors of stent fracture, stent fracture was identified in 2.9% of 1339 lesions treated with the XIENCE^{R} stent in only 6–9 months after placement [28]. In that study, the three major determinants of stent fracture in order of importance were hinge motion, ostial location and tortuosity. Since the BRS is programmed to get dismantled in the due course of the bioresorption, this might cause fewer problems with BRS than with MPS.

The impact of procedural factors such as predilation on conformability is still unknown. Although lesion pre and postdilation may potentially impact on outcome by its impact on lesion expansion (concentricity, eccentricity, final MLD/MLA, remaining DS% and AS%), changes in curvature is ultimately mostly influenced by the remaining implanted material characteristics and the design of the stent/scaffold (Number of longitudinal connectors). In clinical practice this is manifested by the straightening of the vessel during balloon inflations and increase in vessel curvatures directly after balloon deflation.

Limitations

We acknowledge the following limitations. The study is non-randomized and population in each group is relatively small. 2D angiographic analysis may also not be the most optimal imaging modality to assess the geometry of coronary vessels. However the differences between the pre and post treatment angiographic views were less than 10°, indicating that the analysis were mainly performed in the same angiographic view. In addition, the precise impact of subsequent procedural steps (predilation, stent implantation, postdilation) on vascular curvature could not be entirely captured due to the inherent retrospective nature of our study and there was no specific protocol for operators to include the necessary angiographic or cinefluroscopic projections. Potentially this issue is best addressed in a future prospective study with dedicated research protocol ensuring the angiographic projections are obtained at the procedural steps of predilation, stent implantation and postdilation.

Conclusion

In the deployment of long coronary scaffolds/stents (28 mm in length), bioresorbable scaffolds provides better conformability compared with MPS. The findings of this study and its clinical significance merits further evaluation.

Compliance with ethical standards

Conflict of interest One or more of the authors have disclosed potential conflicts of interest regarding the content herein. The BVS Expand and BVS STEMI First registries are supported by research grants from Abbott Vascular. Prof Robert-Jan van Geuns received speaker's fees from Abbott Vascular. Yoshinobu Onuma is a member of the advisory board of Abbott Vascular.

References

1. Sarno G, Bruining N, Serruys PW et al (2012) Morphological and functional evaluation of the bioresorption of the bioresorbable everolimus-eluting vascular scaffold using IVUS, echogenicity and vasomotion testing at two year follow-up: a patient level insight into the ABSORB A clinical trial. Int J Cardiovasc Imaging 28:51–58

2. Wentzel JJ, Whelan DM, van der Giessen WJ et al (2000) Coronary stent implantation changes 3-D vessel geometry and 3-D shear stress distribution. J Biomech 33:1287–1295
3. Colombo A, Stankovic G, Moses JW (2002) Selection of coronary stents. J Am Coll Cardiol 40:1021–1033
4. Ormiston JA, Dixon SR, Webster MW et al (2000) Stent longitudinal flexibility: a comparison of 13 stent designs before and after balloon expansion. Catheter Cardiovasc Interv 50:120–124
5. Onuma Y, Serruys PW, Ormiston JA et al (2010) Three-year results of clinical follow-up after a bioresorbable everolimus-eluting scaffold in patients with de novo coronary artery disease: the ABSORB trial. EuroIntervention 6:447–453
6. Gomez-Lara J, Garcia-Garcia HM, Serruys PW et al (2010) A comparison of the conformability of everolimus-eluting bioresorbable vascular scaffolds to metal platform coronary stents. J Am Coll Cardiol Intv 3:1190–1198
7. Gomez-Lara J, Brugaletta S, Serruys PW et al (2011) Angiographic geometric changes of the lumen arterial wall after bioresorbable vascular scaffolds and metallic platform stents at 1 year follow up. JACC Cardiovasc Interv 4(7):789–799
8. Felix CM, Fam JM, Diletti R, Ishibashi Y, Karanasos A, Everaert BR, van Mieghem NM, Daemen J, de Jaegere PP, Zijlstra F, Regar ES, Onuma Y, van Geuns RJ (2016) Mid- to long-term clinical outcomes of patients treated with the everolimus-eluting bioresorbable vascular scaffold: the BVS expand registry. JACC Cardiovasc Interv 9(16):1652–1663
9. Fam JM, Felix C, van Geuns RJ, Onuma Y, Van Mieghem NM, Karanasos A, van der Sijde J, De Paolis M, Regar E, Valgimigli M, Daemen J, de Jaegere P, Zijlstra F, Diletti R (2016) Initial experience with everolimus-eluting bioresorbable vascular scaffolds for treatment of patients presenting with acute myocardial infarction: a propensity-matched comparison to metallic drug eluting stents 18-month follow-up of the BVS STEMI first study. EuroIntervention 12(1):30–37
10. Onuma Y, Kukreja N, Serruys PW, On behalf of the Interventional Cardiologists of the Thoraxcenter (2000 to 2007) et al (2009) The everolimus-eluting stent in real world patients: 6 month follow up of the X-SEARCH (Xience V Stent Evaluated at Rotterdam Cardiac Hospital) registry. J Am Coll Cardiol 54(3):269–276
11. Stone GW, Teirstein PS, Dawkins KD et al (2011) A prospective, randomized evaluation of a novel everolimus-eluting coronary stent The PLATINUM (a prospective, randomized, multicenter trial to assess an everolimus-eluting coronary stent system [PROMUS element] for the treatment of up to two de novo coronary artery lesions) trial for the PLATINUM TRIAL investigators. J Am Coll Cardiol 57:1700–1708
12. Tanimoto S, Serruys PW, Thuesen L et al (2007) Comparison of in vivo acute stent recoil between the bioabsorbable everolimus-eluting coronary stent and the everolimus-eluting cobalt chromium coronary stent: insights from the ABSORB and SPIRIT trials. Catheter Cardiovasc Interv 70:515–523
13. Choi G, Cheng CP, Wilson NM, Taylor CA (2009) Methods for quantifying three-dimensional deformation of arteries due to pulsatile and nonpulsatile forces: implications for the design of stents and stent grafts. Ann Biomed Eng 37:14–33
14. Schmidt W, Lanzer P, Behrens P, Topoleski LD, Schmitz KP (2009) A comparison of the mechanical performance characteristics of seven drug-eluting stent systems. Catheter Cardiovasc Interv 73:350–360
15. Sangiorgi G, Melzi G, Agostoni P et al (2007) Engineering aspects of stents design and their translation into clinical practice. Ann Ist Super Sanita 43:89–100
16. Rieu R, Barragan P, Sainsous J et al (2003) Assessment of the trackability, flexibility and conformability of coronary stents: a comparative analysis. Catheter Cardiovasc Interv 59(4):496–503
17. Oberhauser JP, Hossainy S, Rapoza RJ (2009) Design principles and performance of bioresorbable polymeric vascular scaffolds. EuroInterv Suppl 5(Supplement F):F15–F22
18. Serruys PW, Onuma Y, Ormiston JA et al (2010) Evaluation of the second generation of a bioresorbable everolimus drug-eluting vascular scaffold for treatment of de novo coronary artery stenosis: six-month clinical and imaging outcomes. Circulation 122:2301–2312
19. Serruys PW, Onuma Y, Garcia-Garcia HM et al (2014) Dynamics of vessel wall changes following the implantation of the absorb everolimus-eluting bioresorbable vascular scaffold: a multi-imaging modality study at 6, 12, 24 and 36 months. EuroIntervention 9:1271–1284
20. Diletti R, Karanasos A, Muramatsu T et al (2014) Everolimus-eluting bioresorbable vascular scaffolds for treatment of patients presenting with ST-segment elevation myocardial infarction: BVS STEMI first study. Eur Heart J 35:777–786
21. Garcia-Garcia HM, Serruys PW, Campos CM et al (2014) Assessing bioresorbable coronary devices: methods and parameters. JACC Cardiovasc Imaging 7:1130–1148
22. Samady H, Eshtehardi P, Giddens DP et al (2011) Coronary artery wall shear stress is associated with progression and transformation of atherosclerotic plaque and arterial remodeling in patients with coronary artery disease. Circulation 124(7):779–788
23. Wentzel JJ, Krams R, Schuurbiers JC et al (2001) Relationship between neointimal thickness and shear stress after Wallstent implantation in human coronary arteries. Circulation 103:1740–1745
24. Gyöngyösi M, Yang P, Glogar D et al (2000) Austrian Wiktor Stent Study Group and European Paragon Stent Investigators. Longitudinal straightening effect of stents is an additional predictor for major adverse cardiac events. JACC 35(6):1580–1589
25. Serruys PW, Chevalier B, Sotomi Y, Cequier A, Carrié D, Piek JJ, Van Boven AJ, Dominici M, Dudek D, McClean D, Helqvist S, Haude M, Reith S, de Sousa Almeida M, Campo G, Iñiguez A, Sabaté M, Windecker S, Onuma Y (2016) Comparison of an everolimus-eluting bioresorbable scaffold with an everolimus-eluting metallic stent for the treatment of coronary artery stenosis (ABSORB II): a 3 year, randomised, controlled, single-blind, multicentre clinical trial. Lancet 388(10059):2479–2491. doi:10.1016/S0140-6736(16)32050-5
26. Ellis SG, Kereiakes DJ, Metzger DC, Caputo RP, Rizik DG, Teirstein PS, Litt MR, Kini A, Kabour A, Marx SO, Popma JJ, McGreevy R, Zhang Z, Simonton C, Gregg W, Stone for the ABSORB III Investigators (2015) Everolimus-eluting bioresorbable scaffolds for coronary artery disease. N Engl J Med 373:1905–1915. doi:10.1056/NEJMoa1509038
27. JJ Wykrzykowska, RP Kraak, SH Hofma, RJ van der Schaaf, EK Arkenbout, AJ IJsselmuiden, J Elias, IM van Dongen, RYG Tijssen, KT Koch, J Baan, MM Vis, RJ de Winter, JJ Piek, JGP Tijssen, Jose PS, Henriques for the AIDA Investigators* (2017). Bioresorbable scaffolds versus metallic stents in routine PCI. NEJM. doi:10.1056/NEJMoa1614954
28. Kuramitsu S, Iwabuchi M, Hyodo M et al (2012) Incidence and clinical impact of stent fracture after everolimus-eluting stent implantation. Circ Cardiovasc Interv 5(5):663–671

20

CHAPTER

ARE BVS SUITABLE FOR ACS PATIENTS? SUPPORT FROM A LARGE SINGLE CENTER REAL LIVE REGISTRY

Felix Cordula, Onuma Yoshinobu, **Fam Jiang Ming**, Diletti Roberto, Ishibashi Yuki, Karanasos Antonis, Everaert Bert, van Mieghem Nicolas M, Daemen Joost, de Jaegere Peter P, Zijlstra, Felix, Regar Evelyn, van Geuns Robert-Jan.

Int J Cardiol. 2016 Sep 1; 218: 89-97.

Are BVS suitable for ACS patients? Support from a large single center real live registry

C.M. Felix, Y. Onuma, J.M. Fam, R. Diletti, Y. Ishibashi, A. Karanasos, B.R.C. Everaert, N.M.D.A. van Mieghem, J. Daemen, P.P.T. de Jaegere, F. Zijlstra, E.S. Regar, R.J.M. van Geuns *

Thoraxcenter, Erasmus MC, s-Gravendijkwal 230, 3015 CE, Rotterdam, the Netherlands

ARTICLE INFO

Article history:
Received 2 December 2015
Received in revised form 5 April 2016
Accepted 12 May 2016
Available online 13 May 2016

Keywords:
Coronary artery disease
Percutaneous coronary intervention
Bioresorbable vascular scaffold
BVS
Acute coronary syndrome
Stable angina

ABSTRACT

Objectives: To investigate one-year outcomes after implantation of a bioresorbable vascular scaffold (BVS) in patients presenting with acute coronary syndrome (ACS) compared to stable angina patients.
Background: Robust data on the outcome of BVS in the setting of ACS is still scarce.
Methods: Two investigator initiated, single-center, single-arm BVS registries have been pooled for the purpose of this study, namely the BVS Expand and BVS STEMI registries.
Results: From September 2012–October 2014, 351 patients with a total of 428 lesions were enrolled. 255 (72.6%) were ACS patients and 99 (27.4%) presented with stable angina/silent ischemia. Mean number of scaffold/patient was 1.55 ± 0.91 in ACS group versus 1.91 ± 1.11 in non-ACS group (P = 0.11). Pre- and post-dilatation were performed less frequent in ACS patients, 75.7% and 41.3% versus 89.0% and 62.0% respectively (P = 0.05 and P = 0.001). Interestingly, post-procedural acute lumen gain and percentage diameter stenosis were superior in ACS patients, 1.62 ± 0.65 mm (versus 1.22 ± 0.49 mm, P < 0.001) and 15.51 ± 8.47% (versus 18.46 ± 9.54%, P = 0.04). Major adverse cardiac events (MACE) rate at 12 months was 5.5% in the ACS group (versus 5.3% in stable group, P = 0.90). One-year definite scaffold thrombosis rate was comparable: 2.0% for ACS population versus 2.1% for stable population (P = 0.94), however, early scaffold thromboses occurred only in ACS patients.
Conclusions: One-year clinical outcomes in ACS patients treated with BVS were similar to non-ACS patients. Acute angiographic outcomes were better in ACS than in non-ACS, yet the early thrombotic events require attention and further research.

1. Introduction

Drug-eluting stents (DES) are the first choice devices in percutaneous coronary interventions (PCI). Despite recent advantages, shortcomings related to the use of DES still are present such as delayed arterial healing, late stent thrombosis (ST), neo-atherosclerosis and hypersensitivity reactions to the polymer [1,2].

To overcome these limitations, coronary devices made of fully bioresorbable material were developed to provide mechanical support and drug-delivery within the first year, followed by complete resorption. The first bioresorbable vascular scaffold (BVS) was commercially introduced in September 2012 as the Absorb BVS (Abbott Vascular, Santa Clara, CA). The BVS provides transient vessel support and gradually elutes the anti-proliferative drug everolimus. After degradation of the polymer (after approximately two to three years) no foreign material remains and need for late reintervention triggered by foreign material should thus be reduced [3].

First-in-man trials have proven the safety of the BVS up to five years [4,5] with a fully completed bioresorption process, a late luminal enlargement due to plaque reduction and a persistent restoration of vasomotion [6–8]. The 1-year results of the larger ABSORB II, ABSORB Japan, ABSORB China and ABSORB III randomized controlled trials comparing BVS with DES (Xience V), confirmed the safety in relatively simple coronary lesions with similar clinical event rates for both devices [9–12].

In all these early studies, ACS patients were largely excluded while BVS would comprise a more attractive choice in this setting as ACS patients are in general younger with a longer life expectancy, less previous

Abbreviations: ACS, acute coronary syndrome; BMS, bare metal stent; BVS, bioresorbable vascular scaffold; BRS, bioresorbable scaffold; CABG, coronary artery bypass grafting; CAD, coronary artery disease; CEC, clinical events committee; DES, drug-eluting stent; ITT, intention-to-treat; IVUS, intravascular ultrasound; LM, left main; MACE, major adverse cardiac events; MI, myocardial infarction; MLD, minimal lumen area; Non-TVR, non-target vessel revascularization; NSTEMI, non-ST elevation myocardial infarction; OCT, optical coherence tomography; PCI, percutaneous coronary intervention; PT, per-treatment; QCA, quantitative coronary angiography; RVD, reference vessel diameter; ST, scaffold thrombosis; STEMI, ST elevation myocardial infarction; TLF, target lesion failure; TLR, target lesion revascularization; TVR, target vessel revascularization; UA, unstable angina pectoris; %DS, percentage diameter stenosis.

* Corresponding author at: Thoraxcenter, Room Ba585, Erasmus Medical Center, s-Gravendijkwal 230, 3015 CE Rotterdam, the Netherlands.
E-mail address: r.vangeuns@erasmusmc.nl (R.J.M. van Geuns).

http://dx.doi.org/10.1016/j.ijcard.2016.05.037

MI and revascularizations with implantation of metallic stents, that would conflict with a therapy aiming at maximal recovery and restoration of normal anatomy of both the coronary artery and myocardium. Furthermore, lesions primarily consisting of soft plaque would be conceptually easy to expand thus facilitating BVS implantation in ACS population. On the other hand, ACS patients are in a much higher prothrombotic state which might accelerate thrombus formation on the larger struts of the BVS impacting much more on shear stress compared to the thinner struts of current metallic DES.

Few registries focused on the performance of the BVS in patients presenting with ACS, mainly ST-elevation myocardial infarction (STEMI). BVS STEMI First examined the procedural and short-term clinical outcomes of 49 STEMI patients, revealing excellent results: procedural success was 97.9% and only 1 patient suffered an event (non-target vessel MI) [13]. Kočka et al. reported similar results in the Prague-19 study [14]. Extending the initial Prague-19 study, the BVS Examination is currently the largest registry on BVS in STEMI with encouraging MACE rates (Device oriented clinical endpoint: 4.1% at one year for both the BVS and the DES), although with a not negligible definite/probable scaffold thrombosis rate (2.4% at one year for the BVS) [15].

The recently published TROFI II randomized trial investigated arterial healing in 90 STEMI patients treated with a BVS compared to those treated with an everolimus-eluting stent (EES). Based on OCT, arterial healing at 6 months after BVS implantation was non-inferior to that after EES implantation [16].

In general, the previous studies on BVS in ACS are limited in size and procedural details and there is a need for more data on the efficacy of BVS in the setting of PCI for ACS. The aim of this study was to compare the angiographic and clinical outcomes of BVS in ACS patients with stable patients.

2. Material and methods

2.1. Population

Two investigator-initiated, prospective, single-center, single-arm studies performed in an experienced, tertiary PCI center have been pooled for the purpose of this investigation. Patients presenting with NSTEMI, stable or unstable angina (UA), or silent ischemia caused by a *de novo* stenotic lesion in a native previously untreated coronary artery with intention to treat with a BVS were included in BVS Expand registry. Angiographic inclusion criteria were lesions with a Dmax (proximal and distal maximal lumen diameter) within the upper limit of 3.8 mm and the lower limit of 2.0 mm by online quantitative coronary angiography (QCA). Complex lesions such as bifurcation, calcified (as assessed by angiography), long and thrombotic lesions were not excluded. Exclusion criteria were patients with a history of coronary bypass grafting (CABG), presentation with cardiogenic shock, bifurcation lesions requiring kissing balloon post-dilatation, ST-elevation myocardial infarction (STEMI) patients, allergy or contra-indications to antiplatelet therapy, fertile female patients not taking adequate contraceptives or currently breastfeeding and patients with expected survival of less than one year. As per hospital policy patients with a previously implanted metal DES in the intended target vessel were also excluded. Also, although old age was not an exclusion criterion, BVS were in general reserved for younger patients, and left to operator's interpretation of biological age.

Patients presenting with STEMI, were approached to participate in the BVS STEMI Registry, which started two months after the BVS Expand registry. The study design has been described elsewhere [13]. The most important inclusion criteria were presentation with STEMI and complaints <12 h. The remaining inclusion criteria were similar to the BVS-EXPAND registry.

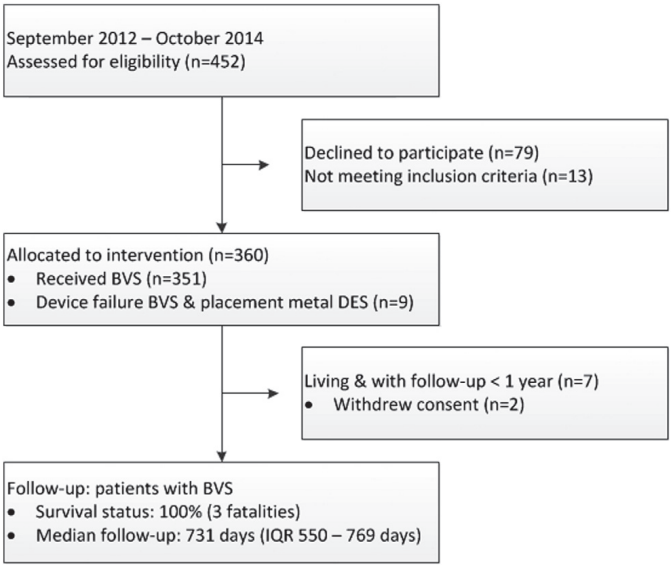

Fig. 1. Flowchart study.

2.2. Ethics

This is an observational study, performed based on international regulations, including the declaration of Helsinki. Approval of the ethical board of the Erasmus MC was obtained. All patients undergoing clinical follow-up provided written informed consent to be contacted regularly during the follow-up period of the study.

2.3. Procedure

PCI was performed according to current clinical practice standards. The radial or femoral approach using 6 or 7 French catheters were the principal route of vascular access. Pre-dilatation was recommended with a balloon shorter than the planned study device length. Advanced lesion preparation was left to the operator's discretion. Post-dilatation was recommended with a non-compliant balloon without overexpanding the scaffold beyond its limits of expansion (by >0.5 mm larger than nominal diameter). Intravascular imaging with the use of Intravascular Ultrasound (IVUS) or Optical Coherence Tomography (OCT) was used for pre-procedural sizing and optimization of scaffold deployment on the discretion of the operator. All patients were treated with unfractionated heparin (at a dose of 70–100 UI/kg). Patients with stable angina were preloaded with 300 mg of aspirin and 600 mg of clopidogrel. Patients presenting with ACS were preloaded with 300 mg of aspirin and 60 mg of prasugrel or 180 mg of ticagrelor.

2.4. Angiographic analysis

The angiographic analysis was performed by three independent investigators (YI, JF and YO). Coronary angiograms were analyzed with the CAAS 5.10 QCA software (Pie Medical BV, Maastricht, the Netherlands). The QCA measurements provided reference vessel diameter (RVD), percentage diameter stenosis (%DS), minimal lumen diameter (MLD), and maximal lumen diameter (Dmax). Acute gain was defined as post-procedural MLD minus pre-procedural MLD (in an occluded vessel MLD value was zero by default).

2.5. Follow-up

Survival status of all patients was obtained from municipal civil registries. Follow-up information specific for hospitalization and cardiovascular events was obtained through questionnaires. If needed, medical records or discharge letters from other hospitals were collected. Events were adjudicated by an independent clinical events committee (CEC).

2.6. Definitions

The primary endpoint was MACE, defined as the composite endpoint of cardiac death, myocardial infarction (MI) and target lesion revascularization (TLR). Deaths were considered cardiac unless a non-cardiac cause was definitely identified. TLR was described as any repeated revascularization of the target lesion. Target vessel revascularization (TVR) was defined as any repeat percutaneous intervention or surgical bypass of any segment of the target vessel. Non-target vessel revascularization was described as any revascularization in a vessel other than the vessel(s) of the target lesion(s). Target lesion failure (TLF) was defined as a composite endpoint of cardiac death, target vessel MI and TLR. Scaffold thrombosis (ST) and MI were classified according to the Academic Research Consortium (ARC) [17]. Clinical device success was defined as successful delivery and deployment of the first study scaffold/stent at the intended target lesion and successful withdrawal of the delivery system with attainment of final in-scaffold/stent residual stenosis of <30% as evaluated by QCA. Clinical procedure success was described as device success without major peri-procedural complications or in-hospital MACE (maximum of 7 days).

Table 1
Patient characteristics.

	ACS patients	Non-ACS patients	P value
Number of patients (%)	255 (72.6)	96 (27.4)	
Mean age in years (±SD)	57.9 ± 10.7	63.4 ± 8.9	<0.001
Gender (%)			
Male	191/255 (74.9)	73/96 (76.0)	0.84
Female	64/255 (25.1)	23/96 (24.0)	0.84
Smoking (%)	149/255 (58.4)	44/96 (45.8)	0.03
Hypertension (%)	130/253 (51.0)	55/95 (57.3)	0.29
Dyslipidemia (%)	92/251 (36.1)	49/95 (51.0)	0.01
All diabetes mellitus (%)	33/255 (12.9)	18/98 (18.8)	0.16
Insulin dependent	7/255 (2.7)	3/96 (3.1)	1.00
Family history of CAD (%)	104/252 (40.8)	39/94 (41.5)	0.94
History of MI (%)	25/255 (9.8)	21/96 (21.9)	0.003
History of PCI (%)	12/255 (4.7)	12/96 (12.5)	0.01
Cardiogenic shock (%)	5/255 (2.0)	0/96 (0.0)	0.33
Renal insufficiency (%)	8/255 (3.1)	8/88 (8.3)	0.046
Presentation (%)			<0.001
Stable angina	0/255 (0.0)	95/96 (99.0)	
Unstable angina	40/255 (15.6)	0/96 (0.0)	
STEMI	120/255 (46.9)	0/96 (0.0)	
NSTEMI	95/255 (37.3)	0/96 (0.0)	
Silent ischemia	0/255 (0.0)	1/96 (1.0)	
Single vessel disease (%)	183/255 (71.5)	52/96 (54.2)	0.02
P2Y12 inhibition use			<0.001
Clopidogrel	60/255 (23.5)	86/96 (89.6)	
Prasugrel	164/255 (64.3)	9/96 (9.4)	
Ticagrelor	30/255(11.8)	1/96 (1.0)	

Values are expressed as percentages or mean ± standard deviation when appropriate. P values are based on Chi square test or Fishers' exact test for categorical variables and Student's *t* test for continuous variables. ACS: acute coronary syndrome, CAD: coronary artery disease, MI: myocardial infarction, NSTEMI: non-ST elevation myocardial infarction, PCI: percutaneous coronary intervention, STEMI: ST elevation myocardial infarction.

The intention-to-treat (ITT) group includes all the patients regardless of whether or not the scaffold was successfully implanted. The per-treatment (PT) group consists of all patients in whom the

Table 2
Lesion characteristics.

	ACS patients N = 255, L = 300	**Non-ACS patients N = 96, L = 128**	**P value**
Number of lesions per patient	1.18 ± 0.49	1.33 ± 0.56	
Left anterior descending artery (%)	48.0	54.4	0.23
Left circumflex artery (%)	24.3	20.0	0.38
Right coronary artery (%)	27.7	25.6	0.61
Bifurcation (%)	20.3	30.7	0.009
Calcification (moderate or severe) (%)	31.8	50.4	<0.001
(Chronic) total occlusion(%)	26.2	8.7	<0.001
CTO (%)	1.7	7.0	0.007
ACC/AHA lesion classification (%)			
A	14.1	15.0	0.75
B1	53.4	41.7	0.02
B2	24.2	22.0	0.66
C	7.2	19.7	<0.001
TIMI (%)			
Pre-procedure			<0.001
TIMI 0	25.2	9.4	
TIMI I	4.6	0.8	
TIMI II	16.1	6.3	
TIMI III	52.1	81.9	
Post-procedure			0.61
TIMI 0	0.0	0.0	
TIMI I	0.3	0.0	
TIMI II	4.6	3.1	
TIMI III	93.4	95.3	

Values are expressed as percentages or mean ± standard deviation when appropriate. P values are based on Chi square test or Fishers' exact test for categorical variables and Student's *t* test for continuous variables. ACS: acute coronary syndrome (ST-elevation myocardial infarction, non-ST myocardial infarction and unstable angina), non-ACS: non acute coronary syndrome (stable angina and silent ischemia).

BVS was successfully implanted. All analyses were performed in the PT group.

As a measure of scaffold expansion, the expansion index was calculated as post-procedural MLD divided by nominal device diameter. A cut-off value of <0.70 below was used to define underexpansion.

2.7. Statistical analysis

Categorical variables are reported as counts and percentages, continuous variables as mean ± standard deviation. The Student's *t* test and the chi square test (or Fishers' exact test) were used for comparison of means and percentages. The cumulative incidence of adverse events was estimated according to the Kaplan–Meier method. Patients lost to follow-up were considered at risk until the date of last contact, at which point they were censored. Kaplan–Meier estimates were compared by means of the log-rank test. For the endpoint MACE, a landmark survival analysis was performed with the landmark time point of 30 days. All statistical tests were two-sided and the P value of <0.05 was considered statistically significant. Statistical analyses were performed using SPSS, version 21 (IL, US).

A univariate logistic regression analysis was performed to look for predictors of TLF and probable/definite ST.

3. Results

From September 2012 up to October 2014, 452 patients were intended to be treated with one or more BVS. Thirteen patients were excluded based on protocol related exclusion criteria of the BVS Expand registry and the BVS STEMI registry and 79 patients declined to participate in one of the two follow-up registries. Thus 360 patients (intention-to-treat group) remained for the purpose of this study. There were 9 cases of device failure in which a metallic stent was implanted and the per-treatment group consisted of 351 patients. A flowchart of the study is given in Fig. 1.

3.1. Baseline characteristics

Baseline characteristics are presented in Table 1. Presentation with ACS was present in 72.6% of the patients and 27.4% were stable patients. Mean age was significantly different between the two groups: 57.9 ± 10.7 years for ACS patients and 63.4 ± 8.9 years for non-ACS patients (P < 0.001). Dyslipidemia, history of MI, history of PCI and renal insufficiency were factors that occurred significantly more frequent in stable patients. ACS patients had more single vessel disease (71.5% versus 54.2%, P = 0.02).

Table 3
Procedural and angiographical characteristics.

	ACS N = 255, L = 300	Non-ACS N = 96, L = 128	P value
Procedural characteristics			
Aspiration (%)	34.4	0.0	<0.001
Rotablation (%)	1.0	5.6	0.02
Scoring balloon (%)	1.3	3.9	0.14
Invasive imaging at baseline (%)			
OCT	25.2	36.2	0.10
IVUS	9.9	24.8	<0.001
Pre-dilatation (%)	75.7	89.0	0.05
Pre-dilatation balloon: artery ratio	1.01 ± 0.21	1.05 ± 0.25	0.11
Maximum pre-dilatation balloon diameter (mm)	2.57 ± 0.42	2.60 ± 0.34	0.49
Maximum pre-dilatation inflation pressure (atm)	13.96 ± 3.02	14.01 ± 3.41	0.91
Buddy wire (%)	9.8	10.2	0.74
Daughter catheter (%)	3.6	4.0	0.80
Total number of scaffolds implanted	394	183	
Mean number of scaffolds/patient	1.55 ± 0.91	1.91 ± 1.11	0.11
Mean number of lesions/patient	1.18 ± 0.49	1.33 ± 0.56	0.015
Mean scaffold diameter (mm)	3.14 ± 0.37	3.02 ± 0.38	0.003
Mean scaffold length (mm)	20.35 ± 5.67	20.75 ± 5.99	
Overlap (%)	20.7	31.5	0.04
Post-dilatation (%)	41.3	62.2	0.001
Post-dilation balloon: mean scaffold diameter ratio	1.23 ± 0.21	1.31 ± 0.23	0.11
Maximum post-dilatation balloon diameter (mm)	3.38 ± 0.42	3.19 ± 0.42	0.003
Maximum post-dilatation inflation pressure (atm)	15.40 ± 3.00	16.10 ± 3.31	0.17
Clinical device success (%)	98.0	97.7	0.82
Clinical procedural success (%)	95.4	96.9	0.49
Angiographical characteristics			
Mean lesion length (mm)	22.41 ± 12.24	24.58 ± 14.58	0.35
Pre-procedure, overall			
RVD (mm ± SD)	2.65 ± 0.54	2.57 ± 0.45	0.22
MLD (mm ± SD)	0.69 ± 0.51	1.04 ± 0.40	<0.001
DS (%)	64.82 ± 42.0	47.94 ± 43.48	<0.001
Pre-procedure, non-total occlusion			
RVD (mm ± SD)	2.60 ± 0.48	2.58 ± 0.44	0.72
MLD (mm ± SD)	0.89 ± 0.39	1.06 ± 0.37	0.002
In-scaffold DS (%)	65.45 ± 20.91	58.62 ± 13.84	0.002
Pre-procedure, total occlusion (L = 80 for ACS and L = 11 for non-ACS)			
RVD (mm ± SD)	2.81 ± 0.69	1.78 ± 1.34	<0.001
Post-procedure, overall			
RVD (mm ± SD)	2.79 ± 0.48	2.77 ± 0.43	0.66
MLD (mm ± SD)	2.35 ± 0.42	2.26 ± 0.38	0.05
In-scaffold DS (%)	15.57 ± 8.47	18.46 ± 9.54	0.04
Acute gain (mm ± SD)	1.62 ± 0.65	1.22 ± 0.49	<0.001

Values are expressed as percentages or mean ± standard deviation when appropriate. P values are based on Chi square test or Fishers' exact test for categorical variables and Student's *t* test for continuous variables. ACS: acute coronary syndrome (ST-elevation myocardial infarction, non-ST myocardial infarction and unstable angina), non-ACS: non acute coronary syndrome (stable angina and silent ischemia), %DS: percentage diameter stenosis, IVUS: intravascular imaging, OCT: optical coherence tomography, MLD: minimal lumen diameter, RVD: reference vessel diameter.

Table 4
Clinical outcomes at one year.

	ACS (N = 255)	Non-ACS (N = 96)	P value
All-cause death (%)	0.0 (0)	3.2 (3)	0.05
Cardiac	0.0 (0)	3.2 (3)	0.05
Non-Cardiac	0.0 (0)	0.0 (3)	–
MACE (%)	5.5 (14)	5.3 (5)	0.90
Myocardial infarction (%)	5.1 (13)	2.1 (2)	0.22
Target lesion revascularization (%)	3.1 (8)	3.2 (3)	0.99
Target vessel revascularization (%)	3.5 (9)	3.2 (3)	0.86
Non-target vessel revascularization (%)	3.2 (8)	5.5 (5)	0.35
Overall scaffold thrombosis[a] (%)	2.4 (6)	4.2 (4)	0.37
Definite scaffold thrombosis (%)	2.0 (5)	2.1 (2)	0.94
Acute	1.2 (3)	0.0 (0)	0.29
Subacute	0.4 (1)	0.0 (0)	0.54
Late	0.4 (1)	2.1 (2)	0.12
Definite/probable scaffold thrombosis (%)	2.4 (6)	2.1 (2)	0.88
Acute	1.2 (3)	0.0 (0)	0.29
Subacute	0.4 (1)	0.0 (0)	0.54
Late	0.8 (2)	2.1 (2)	0.30

Event rates are summarized as %. P values are based on log rank test for comparing Kaplan Meier. MACE: major adverse cardiac events (composite endpoint consisting of cardiac death, myocardial infarction and target lesion revascularization).
[a] Includes definite, probable and possible ST.

Lesion characteristics are presented in Table 2. In both groups, the left anterior descending coronary artery (LAD) was most commonly treated (48.0% in ACS group and 54.4% in non-ACS group, P = 0.23). Lesions in stable patients were more complex, with a higher percentage of AHA/ACC type B2/C lesions. Pre-procedural TIMI flow was significantly different (P < 0.001). The mean lesion length was comparable in both groups (24.58 ± 14.58 mm for non-ACS versus 22.41 ± 12.24 mm for ACS, P = 0.35) (Table 3). Pre-procedural QCA analysis revealed significant differences between the groups in MLD: 0.69 ± 0.51 mm for ACS patients versus 1.04 ± 0.40 in stable patients (P < 0.001). After excluding the thrombotic total occlusions, this statistical difference remained (0.89 ± 0.39 mm for ACS versus 1.06 ± 0.37 mm for non-ACS, P = 0.002). Pre-procedural %DS was 65.45 ± 20.91% in the ACS group versus 58.62 ± 13.84% in non-ACS group (P < 0.001). Post-procedural QCA measurements revealed a superior acute performance in the ACS population: remaining %DS was significant lower (15.57 ± 8.47% versus 18.46 ± 9.54%, P = 0.04). Final MLD was larger (2.35 ± 0.42 mm versus 2.26 ± 0.38 mm, P = 0.05) and also acute lumen gain was higher (1.62 ± 0.65 mm versus 1.22 ± 0.49 mm, P < 0.001).

3.2. Procedural details

Procedural and angiographic details are summarized in Table 3. In ACS patients, pre-dilatation was performed in 75.7% of the lesions, compared to 89.0% in stable patients (P = 0.05). Pre-dilatation balloon to artery ratio was comparable (1.01 ± 0.21 versus 1.05 ± 0.25, P = 0.11). Post-dilatation was significantly less frequently performed in the ACS group (41.3% versus 62.2%, P = 0.001). Advanced lesion preparation was less often performed in ACS patients than in stable patients (rotational atherectomy: 1.0% versus 5.6%, P = 0.02; scoring balloon 1.3% versus 3.9%, P = 0.14). A total of 582 BVS were implanted: 399 in the ACS group (with a mean of 1.55 ± 0.91 scaffolds per patient) and 183 in stable patients (with a mean of 1.91 ± 1.11 per patient in stable patients).

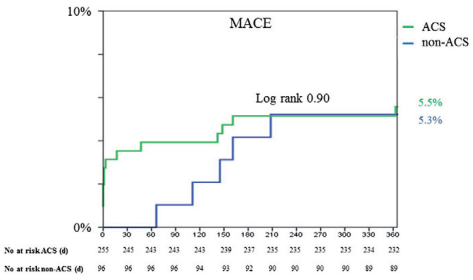

Fig. 2. Kaplan–Meier curve for MACE.

In the ACS population 6 cases of device failure occurred, all due to delivery failure. Main causes of these delivery failures were calcification and angulation (see Table 6 for details). Eight in-hospital MACE were reported. Whereas in the stable population 3 device failures (placement metal DES due to dissection after BVS implantation and delivery failures due to severe calcification and tortuosity) and no in-hospital MACE were documented in stable patients. Clinical device and procedural success were 98.0% and 95.4% for the ACS population and 97.7 and 96.9% respectively for stable patients.

3.3. Clinical outcomes

Data on survival status was available in 100% with a median follow-up period of 731 days (interquartile range [IQR]: 550–769 days). A total of 340 (96.9%) patients had a follow-up duration of at least 365 (±2) days.

Cumulative clinical events rates are summarized in Table 4. Clinical outcomes appeared to be comparable with no significant difference between patients presenting with ACS as compared to stable patients. Rate of death was 0.0% in the ACS group versus 3.1% in the non-ACS group (P = 0.06). Three patients died within the first year. One patient, with extensive cardiovascular disease died at day 166, 4 days after he went through a definite ST and MI, most probably due to a brief interruption of his antithrombotic medication during an elective surgery. The second patient died a few days after his prostate was surgically removed. In this case, dual antiplatelet inhibition therapy (DAPT) was also shortly interrupted causing a MI (probable ST). The last patient died of a sudden cardiac death 66 days after baseline PCI (possible ST).

MACE rate in the ACS population was comparable to the non-ACS population (5.5% versus 5.3%, P = 0.90, Fig. 2). MACE was mainly driven by MI and TLR. TLR rate was comparable in both groups. Rate of TVR was in 3.2% in ACS patients versus 3.5% in stable patients (P = 0.86). Non-TVR rate was 3.2% and 5.5% in respectively ACS and non-ACS patients (P = 0.350). Rate of definite ST was similar in both groups: 2.0% in the ACS group versus 2.1% in stable patients (P = 0.94). Of note, early ST only occurred in the ACS group, late thrombosis was more prevalent in stable patients (Table 4 and Fig. 3B).

A landmark survival analysis of MACE, definite/probable ST, MI and TLR indicated a trend for higher event rates of the ACS population in the short-term (<30 days). Conversely, mid-term event rates were higher in stable patients, although log rank test failed to prove significance (Fig. 3A–D).

In an univariate analysis of TLF the following characteristics tended to be related by at least a twofold increase in odds ratio (OR): renal insufficiency, bifurcation, male gender and age above 65 years (Table 5). The use of intravascular imaging at baseline might be protective for TLF (OR 0.49, P = 0.22).

4. Discussion

The present study reports on the comparative procedural and the one-year clinical outcomes of ACS patients versus non-ACS patients treated with an Absorb bioresorbable scaffold. The main findings of this study are summarized as follows: 1) angiographic outcomes were better in ACS patients despite the fact that less aggressive lesion preparation and less frequent post-dilatation were performed; 2) overall one-year ST rate in ACS patients was similar to the non-ACS patients.

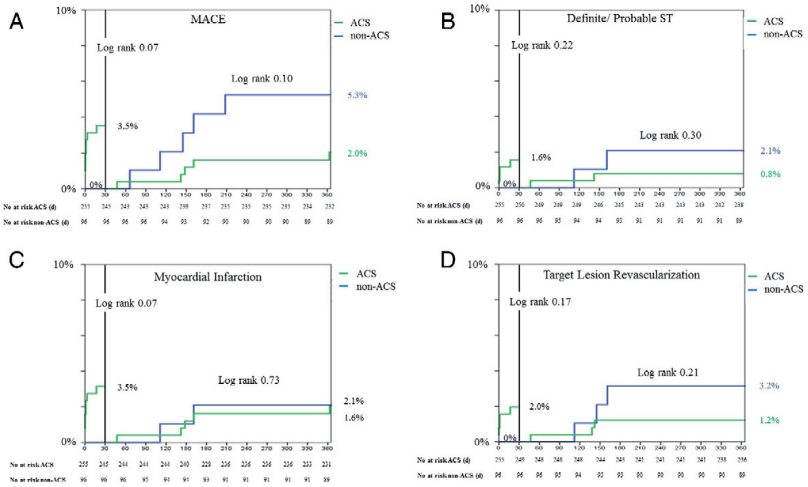

Fig. 3. A–D Landmark survival analysis for MACE, probable/definite ST, MI and TLR.

Interestingly, early definite ST occurred only in the ACS population while late ST seemed more frequent in stable patients; 3) despite the higher rate of early complications in the ACS group, landmark analyses after one month demonstrated that event rates were lower in this group than the stable patient group; and 4) clinical outcomes at one year were comparable among ACS and stable patients.

Differences between ACS patients and stable patients exist at multiple levels. On a patient level, patients presenting with ACS often are younger and thus have a longer life expectancy. Cardiovascular disease in this group is less extensive when compared to stable patients. Additionally, a different plaque composition is present, featured by a lipid-rich necrotic core with a thin fibrous cap. All these factors make ACS patients very attractive for bioresorbable technologies where full expansion is important and acute recoil a concern. Moreover, in ACS patients DAPT pretreatment is usually short (especially in STEMI patients) and frequently not yet resulting in active platelet function inhibition, while the thrombus burden is greater with high platelet activation and a systemic inflammatory response. These factors might amplify the risk of acute thromboses and cause a higher risk of MACE. For these reasons studies like ours are important to investigate the suitability of BVS in ACS patients. To the best of our knowledge, no data is available comparing the performance of BVS in ACS with stable patients compared to stable patients.

Table 5
Univariate analysis of TLF.

	Odds ratio ACS vs. non ACS (95% confidence interval)	P value
Renal insufficiency	3.28 (0.68–15.83)	0.14
Bifurcation	2.68 (0.98–7.36)	0.06
Male gender	2.38 (0.53–10.69)	0.26
Age above 65 years	2.10 (0.77–5.75)	0.15
History of MI	1.57 (0.43–5.73)	0.50
Small vessel (<2.5 mm)	1.54 (0.56–4.20)	0.40
Post-procedural TIMI 0/1	1.45 (0.53–3.99)	0.47
Underexpansion	1.30 (0.46–3.66)	0.62
Calcification	1.26 (0.46–3.46)	0.66
Long lesion (>32 mm)	1.20 (0.33–4.36)	0.78
Smoking	1.07 (0.74–1.54)	0.72
Diabetes mellitus	0.83 (0.18–3.78)	0.81
Presentation with ACS	0.82 (0.28–2.43)	0.72
Intravascular imaging at baseline	0.49 (0.15–1.54)	0.22

ACS: acute coronary syndrome, MI: myocardial infarction, TLF: target lesion failure (cardiac death, target vessel MI, ischemia driven TLR).

The BVS Expand registry and the BVS STEMI registry are two single-center, single-arm registries describing procedural clinical outcomes of patients treated with BVS. At variance of previous studies investigating the Absorb bioresorbable scaffold, all events were adjudicated by an independent clinical event committee (CEC). Also, all angiograms were analyzed using QCA. Lastly, combining the results of the two registries, both handling less restrictive inclusion criteria, we were able to create a study population reflecting a real-world population with a considerable amount of ACS patients.

The superior acute angiographic outcome in ACS patients compared to stable patients is an important observation. In previous studies it was demonstrated that the acute performance of the Absorb scaffold is somewhat inferior to metallic stents for stable angina patients. For example, in-device acute lumen gain in the ABSORB II trial was 1.15 ± 0.38 mm in BVS group versus 1.46 ± 0.38 mm in the EES group ($P < 0.001$). In the ABSORB III trial reported lumen gain was 1.45 ± 0.45 mm versus 1.59 ± 0.44 mm ($P < 0.001$). Finally, in the ABSORB Japan and ABSORB China trials acute lumen gain numbers were as follows: 1.46 ± 0.40 mm versus 1.65 ± 0.40 mm ($P < 0.0001$) and 1.51 ± 0.03 versus 1.59 ± 0.03 ($P = 0.04$) respectively. Remarkably, in STEMI patients no difference in acute gain was observed between BVS and DES (2.16 ± 0.52 mm versus 2.21 ± 0.56 mm, $P = 0.57$). This finding also suggests that the somewhat inferior angiographic results only imply for stable angina patients while the current semi-compliant balloon and wide strut BVS design are sufficient for the general softer plaque composition of ACS patients. In the current study, post-dilatation was significantly less frequently performed in ACS patients, however angiographic outcomes were better. Post-procedural MLD, RVD, %DS and in-scaffold acute lumen gain were all superior compared to post-procedural QCA measurements in stable patients. These promising angiographic results in ACS patients support the use BVS in this setting as they are predictive for clinical events.

Overall, one-year ST rate in ACS patients was similar to the non-ACS patients. The observed rate of early ST in the ACS population might raise some concerns. Previous studies have stated that presentation with ACS is an independent risk factor for the development of (metal) stent

Table 6
Details device failures in ACS population.

	Age (yr.)	Gender	Presentation	Culprit	Location	AHA/ACC	Calc.	Bif.	Ang.	Tort.	Additional device	Treatment
1	71	M	NSTEMI	RCA	RCA	B2	Severe	No	No	No	PT Graphix Super Support	3.0 × 28, 3.0 × 28 Xience
2	37	M	UAP	RCA	LCx	B1	No	No	Yes	No	None	2.5 × 12 Xience
3	60	M	UAP	LCx	LCx	B2	Moderate	No	Yes	No	None	2.5 × 18, 2.25 × 12 Xience
4	47	M	STEMI	LAD	LAD	B2	No	Yes	No	Yes	STO1 Heartrail	3.5 × 23 Xience
5	71	F	UAP	RCA	RCA	B2	Severe	No	No	No	Rotablator	4 Promus stents
6	59	M	UAP	LCx	LCx	B2	Severe	Yes	Yes	No	STO1 Heartrail	3.5 × 8 Xience

Ang = angulation, Bif = bifurcation, Calc = calcification, NSTEMI = non-ST elevation myocardial infarction, STEMI = ST elevation myocardial infarction, Tort = tortuositas, UAP = unstable angina pectoris.

thrombosis [18–20]. Using metal devices, multiple studies have documented that stenting of lesions with appeared plaque rupture are prone to delayed healing, characterized by higher percentages of uncovered, malapposed and protruding stent struts with a subsequent risk of stent thrombosis [21–24]. Furthermore, underexpansion appeared to be an important predictor [25–27]. This is also the case for ST in BVS patients [28,29]. In ACS patients, high thrombus burden, increased platelet activation and vasospasm are mechanisms that trouble optimal sizing resulting in higher rates of malapposition. In the acute setting, lesion preparation using pre-dilatation and intravascular imaging are less frequently performed than in stable patients. Although the acute scaffold expansion is on average better in the ACS population than in the stable population, it is very important to properly size the vessel and to optimize the final scaffold expansion in order to avoid early ST.

The landmark analysis beyond one month up to 12 months showed favorable results with regard to ST and TLR for the ACS patients (0.8% and 1.2% respectively). The somewhat higher event rates in the non-ACS group are a representation of a more complex non-study real world patient population. Therefore, the one-year MACE (composite of cardiac death, MI and TLR) rates of 5.5% (ACS) and 5.3% (non-ACS) are acceptable and comparable to trials using BVS in relatively simple lesions: 5.0% in the ABSORB II trial and 3.8% in the ABSORB China trial [9,12]. A comparable endpoint, target lesion failure (TLF: composite endpoint consisting of cardiac death, target vessel MI and ischemia driven TLR), in the ABSORB III and ABSORB Japan trials were 7.8% and 4.2% respectively [10,11]. In these studies, STEMI patients were excluded. Compared to studies investigating clinical outcomes of metal DES in STEMI patients, event rates in our report are higher than for EES but for lower compared to first-generation DES [30,31].

Recently, few concerns were raised concerning a potentially increased incidence of ST after implantation of a BVS [27,32–34]. Also, in our registry rate of definite ST (2.0% for ACS patients and 2.1% for stable patients) was higher compared to that of currently available metallic DES [35,36]. The importance of patient selection, lesion preparation, pre- and post-dilatation and also the consideration of intra-vascular imaging have to be underlined [37,38]. A pilot imaging study suggested suboptimal implantation as an important cause for BVS ST [28]. Use of intravascular imaging could improve pre-procedural vessel sizing, optimize lesion coverage and eventually reduce adverse events.

Next generation BVS with smaller scaffold struts may reduce the early event rates in ACS patients. For the current design, using more potent P2Y12 inhibitors such as ticagrelor, a direct-acting platelet inhibitor or cangrelor, an intravenous antiplatelet drug, could be valuable. In the ATLANTIC trial, ticagrelor was administered prehospital in the ambulance to STEMI patients, leading to a reduction in ST rate [39]. The CHAMPION PHOENIX trial assessed ischemic complications of PCI after administration of cangrelor and showed a decrease in these complications, with no significant increase in severe bleeding [40]. The upcoming HORIZONS-ABSORB AMI will compare the performance of BVS to DES when cangelor is used on top of heparin or bivalirudin in STEMI patients [41].

Rate of mortality in ACS patients is worse compared with patients who present with stable CAD [42–45]. In our patient cohort, mortality was 0% in the ACS population probably reflecting our exclusion criteria for the STEMI population (exclusion of patients presenting with cardiogenic shock). As shown by our landmark survival analyses, events in the ACS group are especially clustered in the early phase after BVS implantation. On the other hand, one-year Kaplan Meier curves for events are lower in ACS patients. This is probably due to patient selection, where ACS patients present with different patient and lesion factors (younger age, less extensive cardiovascular disease and more often simple lesions), and the higher intake of prasugrel and ticagrelor in these patients (76.1% versus 10.4%).

In summary, our results warrant further confirmation in a large-scale trial with a high number of ACS patients and an optimal implantation strategy tailored at the limitation of this first generation fully bioresorbable scaffolds. Ongoing and upcoming trials such as the AIDA, Compare Absorb (NCT02486068) and HORIZON-ABSORB AMI, will provide data derived from larger patient cohorts and in direct comparison to metallic DES [41,46].

5. Limitations

These results are derived from two single-center, single-arm registries with no direct comparison with metallic DES. The total number of patients in this study was limited.

Baseline differences in patient and lesion characteristics could have led to biased outcome in clinical event rates.

Furthermore, deciding which patient or lesion was suitable for BVS implantation could have led to selection bias. However, there was a fair amount of patients presenting with ACS and with B2/C lesions were included, indicating the complexity of the present study population.

6. Conclusion

Despite the higher rate of early complications due to early ST in the ACS population, the one-year clinical outcomes for BVS implantations in ACS patients versus non-ACS patients are comparable. The early ST rate observed in ACS needs further attention and optimized antiplatelet therapy may play a role. Angiographic outcomes for BVS in ACS patients are at least as good as non-ACS patients. Therefore, ACS patients may be suitable candidates for the treatment with the BVS if early procedural related complications can be avoided.

Conflict of interest

This study was supported by an unrestricted grant from Abbott Vascular. Robert-Jan van Geuns, Nicolas van Mieghem and Yoshinobu Onuma received speaker's fee from Abbott Vascular. The other authors have no conflicts of interest to declare. All authors have approved the final article.

Acknowledgments

We want to thank Isabella Kardys, Martijn Akkerhuis and Johannes Schaar for their appearance in the CEC. We want to thank Nienke van Ditzhuijzen and Saskia Wemelsfelder for her contribution to data management.

References

[1] M. Joner, A.V. Finn, A. Farb, E.K. Mont, F.D. Kolodgie, E. Ladich, et al., Pathology of drug-eluting stents in humans: delayed healing and late thrombotic risk, J. Am. Coll. Cardiol. 48 (1) (2006) 193–202.
[2] F. Otsuka, M. Vorpahl, M. Nakano, J. Foerst, J.B. Newell, K. Sakakura, et al., Pathology of second-generation everolimus-eluting stents versus first-generation sirolimus- and paclitaxel-eluting stents in humans, Circulation 129 (2) (2014) 211–223.
[3] K. Yamaji, T. Kimura, T. Morimoto, Y. Nakagawa, K. Inoue, S. Kuramitsu, et al., Very long-term (15 to 23 years) outcomes of successful balloon angioplasty compared with bare metal coronary stenting, J. Am. Heart Assoc. 1 (5) (2012), e004085.
[4] J.A. Ormiston, P.W. Serruys, E. Regar, D. Dudek, L. Thuesen, M.W. Webster, et al., A bioabsorbable everolimus-eluting coronary stent system for patients with single de-novo coronary artery lesions (ABSORB): a prospective open-label trial, Lancet 371 (9616) (2008) 899–907.
[5] S. Nakatani, Y. Onuma, Y. Ishibashi, T. Muramatsu, J. Iqbal, Y.J. Zhang, et al., Early (before 6 months), late (6–12 months) and very late (after 12 months) angiographic scaffold restenosis in the ABSORB cohort B trial, EuroIntervention (2014).
[6] A. Karanasos, C. Simsek, P. Serruys, J. Ligthart, K. Witberg, R.J. van Geuns, et al., Five-year optical coherence tomography follow-up of an everolimus-eluting bioresorbable vascular scaffold: changing the paradigm of coronary stenting? Circulation 126 (7) (2012) e89–e91.
[7] C. Simsek, A. Karanasos, M. Magro, H.M. Garcia-Garcia, Y. Onuma, E. Regar, et al., Long-term invasive follow-up of the everolimus-eluting bioresorbable vascular scaffold: five-year results of multiple invasive imaging modalities, EuroIntervention (2014).
[8] Y. Onuma, D. Dudek, L. Thuesen, M. Webster, K. Nieman, H.M. Garcia-Garcia, et al., Five-year clinical and functional multislice computed tomography angiographic results after coronary implantation of the fully resorbable polymeric everolimus-eluting scaffold in patients with de novo coronary artery disease: the ABSORB cohort A trial, JACC Cardiovasc. Interv. 6 (10) (2013) 999–1009.
[9] P.W. Serruys, B. Chevalier, D. Dudek, A. Cequier, D. Carrie, A. Iniguez, et al., A bioresorbable everolimus-eluting scaffold versus a metallic everolimus-eluting stent for ischaemic heart disease caused by de-novo native coronary artery lesions (ABSORB II): an interim 1-year analysis of clinical and procedural secondary outcomes from a randomised controlled trial, Lancet (2014).
[10] T. Kimura, K. Kozuma, K. Tanabe, S. Nakamura, M. Yamane, T. Muramatsu, et al., A randomized trial evaluating everolimus-eluting absorb bioresorbable scaffolds vs. everolimus-eluting metallic stents in patients with coronary artery disease: ABSORB Japan, Eur. Heart J. (2015).
[11] S.G. Ellis, D.J. Kereiakes, D.C. Metzger, R.P. Caputo, D.G. Rizik, P.S. Teirstein, et al., Everolimus-eluting bioresorbable scaffolds for coronary artery disease, N. Engl. J. Med. (2015).
[12] R. Gao, Y. Yang, Y. Han, Y. Huo, J. Chen, B. Yu, et al., Bioresorbable vascular scaffolds versus metallic stents in patients with coronary artery disease: ABSORB China trial, J. Am. Coll. Cardiol. (2015).
[13] R. Diletti, A. Karanasos, T. Muramatsu, S. Nakatani, N.M. Van Mieghem, Y. Onuma, et al., Everolimus-eluting bioresorbable vascular scaffolds for treatment of patients presenting with ST-segment elevation myocardial infarction: BVS STEMI first study, Eur. Heart J. 35 (12) (2014) 777–786.
[14] V. Kocka, M. Maly, P. Tousek, T. Budesinsky, L. Lisa, P. Prodanov, et al., Bioresorbable vascular scaffolds in acute ST-segment elevation myocardial infarction: a prospective multicentre study 'Prague 19', Eur. Heart J. 35 (12) (2014) 787–794.
[15] S. Brugaletta, T. Gori, A.F. Low, P. Tousek, E. Pinar, J. Gomez-Lara, et al., Absorb bioresorbable vascular scaffold versus everolimus-eluting metallic stent in ST-segment elevation myocardial infarction: 1-year results of a propensity score matching comparison: the BVS-EXAMINATION study (bioresorbable vascular scaffold-a clinical evaluation of everolimus eluting coronary stents in the treatment of patients with ST-segment elevation myocardial infarction), JACC Cardiovasc. Interv. 8 (1 Pt B) (2015) 189–197.
[16] M. Sabate, S. Windecker, A. Iniguez, L. Okkels-Jensen, A. Cequier, S. Brugaletta, et al., Everolimus-eluting bioresorbable stent vs. durable polymer everolimus-eluting metallic stent in patients with ST-segment elevation myocardial infarction: results of the randomized ABSORB ST-segment elevation myocardial infarction-TROFI II trial, Eur. Heart J. (2015).
[17] D.E. Cutlip, S. Windecker, R. Mehran, A. Boam, D.J. Cohen, G.A. van Es, et al., Clinical end points in coronary stent trials: a case for standardized definitions, Circulation 115 (17) (2007) 2344–2351.
[18] J. Daemen, P. Wenaweser, K. Tsuchida, L. Abrecht, S. Vaina, C. Morger, et al., Early and late coronary stent thrombosis of sirolimus-eluting and paclitaxel-eluting stents in routine clinical practice: data from a large two-institutional cohort study, Lancet 369 (9562) (2007) 667–678.
[19] D.W. Park, S.W. Park, K.H. Park, B.K. Lee, Y.H. Kim, C.W. Lee, et al., Frequency of and risk factors for stent thrombosis after drug-eluting stent implantation during long-term follow-up, Am. J. Cardiol. 98 (3) (2006) 352–356.
[20] D. Planer, P.C. Smits, D.J. Kereiakes, E. Kedhi, M. Fahy, K. Xu, et al., Comparison of everolimus- and paclitaxel-eluting stents in patients with acute and stable coronary syndromes: pooled results from the SPIRIT (a clinical evaluation of the XIENCE V everolimus eluting coronary stent system) and COMPARE (a trial of everolimus-eluting stents and paclitaxel-eluting stents for coronary revascularization in daily practice) trials, JACC Cardiovasc. Interv. 4 (10) (2011) 1104–1115.
[21] L. Raber, T. Zanchin, S. Baumgartner, M. Taniwaki, B. Kalesan, A. Moschovitis, et al., Differential healing response attributed to culprit lesions of patients with acute coronary syndromes and stable coronary artery after implantation of drug-eluting stents: an optical coherence tomography study, Int. J. Cardiol. 173 (2) (2014) 259–267.
[22] G.F. Attizzani, D. Capodanno, Y. Ohno, C. Tamburino, Mechanisms, pathophysiology, and clinical aspects of incomplete stent apposition, J. Am. Coll. Cardiol. 63 (14) (2014) 1355–1367.
[23] G. Nakazawa, A.V. Finn, M. Joner, E. Ladich, R. Kutys, E.K. Mont, et al., Delayed arterial healing and increased late stent thrombosis at culprit sites after drug-eluting stent placement for acute myocardial infarction patients: an autopsy study, Circulation 118 (11) (2008) 1138–1145.
[24] N. Gonzalo, P. Barlis, P.W. Serruys, H.M. Garcia-Garcia, Y. Onuma, J. Ligthart, et al., Incomplete stent apposition and delayed tissue coverage are more frequent in drug-eluting stents implanted during primary percutaneous coronary intervention for ST-segment elevation myocardial infarction than in drug-eluting stents implanted for stable/unstable angina: insights from optical coherence tomography, JACC Cardiovasc. Interv. 2 (5) (2009) 445–452.
[25] E. Cheneau, L. Leborgne, G.S. Mintz, J. Kotani, A.D. Pichard, L.F. Satler, et al., Predictors of subacute stent thrombosis: results of a systematic intravascular ultrasound study, Circulation 108 (1) (2003) 43–47.
[26] K. Fujii, S.G. Carlier, G.S. Mintz, Y.M. Yang, I. Moussa, G. Weisz, et al., Stent underexpansion and residual reference segment stenosis are related to stent thrombosis after sirolimus-eluting stent implantation: an intravascular ultrasound study, J. Am. Coll. Cardiol. 45 (7) (2005) 995–998.
[27] S. Puricel, F. Cuculi, M. Weissner, A. Schmermund, P. Jamshidi, T. Nyffenegger, et al., Bioresorbable coronary scaffold thrombosis: multicenter comprehensive analysis of clinical presentation, mechanisms, and predictors, J. Am. Coll. Cardiol. 67 (8) (2016) 921–931.
[28] A. Karanasos, N. Van Mieghem, N. van Ditzhuijzen, C. Felix, J. Daemen, A. Autar, et al., Angiographic and optical coherence tomography insights into bioresorbable scaffold thrombosis: single-center experience, Circ. Cardiovasc. Interv. 8 (5) (2015).
[29] Y. Ishibashi, S. Nakatani, Y. Onuma, Definite and probable bioresorbable scaffold thrombosis in stable and ACS patients, EuroIntervention (2014).
[30] S.H. Hofma, J. Brouwer, M.A. Velders, A.W. van't Hof, P.C. Smits, M. Quere, et al., Second-generation everolimus-eluting stents versus first-generation sirolimus-eluting stents in acute myocardial infarction. 1-year results of the randomized XAMI (XienceV stent vs. cypher stent in primary PCI for acute myocardial infarction) trial, J. Am. Coll. Cardiol. 60 (5) (2012) 381–387.
[31] C. Simsek, M. Magro, E. Boersma, Y. Onuma, S. Nauta, J. Daemen, et al., Comparison of six-year clinical outcome of sirolimus- and paclitaxel-eluting stents to bare-metal stents in patients with ST-segment elevation myocardial infarction: an analysis of the RESEARCH (rapamycin-eluting stent evaluated at Rotterdam cardiology hospital) and T-SEARCH (taxus stent evaluated at Rotterdam cardiology hospital) registries, J. Invasive Cardiol. 23 (8) (2011) 336–341.
[32] D. Capodanno, T. Gori, H. Nef, A. Latib, J. Mehilli, M. Lesiak, et al., Percutaneous coronary intervention with everolimus-eluting bioresorbable vascular scaffolds in routine clinical practice: early and midterm outcomes from the European multicentre GHOST-EU registry, EuroIntervention 10 (10) (2015) 1144–1153.
[33] R.P. Kraak, M.E. Hassell, M.J. Grundeken, K.T. Koch, J.P. Henriques, J.J. Piek, et al., Initial experience and clinical evaluation of the absorb bioresorbable vascular scaffold (BVS) in real-world practice: the AMC single centre real world PCI registry, EuroIntervention 10 (10) (2015) 1160–1168.
[34] Y. Ishibashi, S. Nakatani, Y. Onuma, Definite and probable bioresorbable scaffold thrombosis in stable and ACS patients, EuroIntervention 11 (3) (2015) e1–e2.
[35] C. Tamburino, P. Capranzano, T. Gori, A. Latib, M. Lesiak, H. Nef, et al., 1-year outcomes of everolimus-eluting bioresorbable scaffolds versus everolimus-eluting stents: a propensity-matched comparison of the GHOST-EU and XIENCE V USA registries, JACC Cardiovasc. Interv. 9 (5) (2016) 440–449.
[36] G.W. Stone, R. Gao, T. Kimura, D.J. Kereiakes, S.G. Ellis, Y. Onuma, et al., 1-year outcomes with the absorb bioresorbable scaffold in patients with coronary artery disease: a patient-level, pooled meta-analysis, Lancet (2016).
[37] B. Everaert, C. Felix, J. Koolen, P. den Heijer, J. Henriques, J. Wykrzykowska, et al., Appropriate use of bioresorbable vascular scaffolds in percutaneous coronary interventions: a recommendation from experienced users: a position statement on the use of bioresorbable vascular scaffolds in the Netherlands, Neth. Heart J. 23 (3) (2015) 161–165.
[38] C. Tamburino, A. Latib, R.J. van Geuns, M. Sabate, J. Mehilli, T. Gori, et al., Contemporary practice and technical aspects in coronary intervention with bioresorbable scaffolds: a European perspective, EuroIntervention 11 (1) (2015) 45–52.
[39] G. Montalescot, A.W. van 't Hof, F. Lapostolle, J. Silvain, J.F. Lassen, L. Bolognese, et al., Prehospital ticagrelor in ST-segment elevation myocardial infarction, N. Engl. J. Med. 371 (11) (2014) 1016–1027.
[40] J.L. Gutierrez-Chico, P.W. Serruys, C. Girasis, S. Garg, Y. Onuma, S. Brugaletta, et al., Quantitative multi-modality imaging analysis of a fully bioresorbable stent: a head-to-head comparison between QCA, IVUS and OCT, Int. J. Cardiovasc. Imaging 28 (3) (2012) 467–478.
[41] G.W. Stone, Rationale for and Design of HORIZONS-ABSORB AMI, 2015.
[42] R.F. Alcock, A.S. Yong, A.C. Ng, V. Chow, C. Cheruvu, B. Aliprandi-Costa, et al., Acute coronary syndrome and stable coronary artery disease: are they so different? Long-term outcomes in a contemporary PCI cohort, Int. J. Cardiol. 167 (4) (2013) 1343–1346.

[43] A. Hirsch, N.J. Verouden, K.T. Koch, J. Baan Jr., J.P. Henriques, J.J. Piek, et al., Comparison of long-term mortality after percutaneous coronary intervention in patients treated for acute ST-elevation myocardial infarction versus those with unstable and stable angina pectoris, Am. J. Cardiol. 104 (3) (2009) 333–337.
[44] G. Montalescot, Z. Ongen, R. Guindy, A. Sousa, S.Z. Lu, D. Pahlajani, et al., Predictors of outcome in patients undergoing PCI. Results of the RIVIERA study, Int. J. Cardiol. 129 (3) (2008) 379–387.
[45] M.L. Fokkema, S.K. James, P. Albertsson, M. Aasa, A. Akerblom, F. Calais, et al., Outcome after percutaneous coronary intervention for different indications: long-term results from the Swedish coronary angiography and angioplasty registry (SCAAR), EuroIntervention 11 (6) (2015).
[46] P. Woudstra, M.J. Grundeken, R.P. Kraak, M.E. Hassell, E.K. Arkenbout, J. Baan Jr., et al., Amsterdam investigator-initiated absorb strategy all-comers trial (AIDA trial): a clinical evaluation comparing the efficacy and performance of ABSORB everolimus-eluting bioresorbable vascular scaffold strategy vs the XIENCE family (XIENCE PRIME or XIENCE Xpedition) everolimus-eluting coronary stent strategy in the treatment of coronary lesions in consecutive all-comers: rationale and study design, Am. Heart J. 167 (2) (2014) 133–140.

21

CHAPTER

INITIAL EXPERIENCE WITH EVEROLIMUS-ELUTING BIORESORBABLE VASCULAR SCAFFOLDS FOR TREATMENT OF PATIENTS PRESENTING WITH ACUTE MYOCARDIAL INFARCTION: A PROPENSITY-MATCHED COMPARISON TO METALLIC DRUG ELUTING STENTS 18-MONTH FOLLOW-UP OF THE BVS STEMI FIRST STUDY

Fam Jiang Ming, Felix Cordula, van Geuns Robert-Jan, Onuma Yoshinobu, Van Mieghem Nicolas M, Karanasos Antonis, van der Sijde Jors, De Paolis Marcella, Regar Evelyn, Valgimigli Marco, Daemen Joost, de Jaegere Peter, Zijlstra Felix, Diletti Roberto.

EuroIntervention. 2016 May 17; 12(1):30-7.

Initial experience with everolimus-eluting bioresorbable vascular scaffolds for treatment of patients presenting with acute myocardial infarction: a propensity-matched comparison to metallic drug eluting stents 18-month follow-up of the BVS STEMI first study

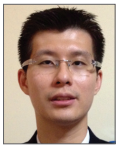

Jiang Ming Fam[1,2], MD; Cordula Felix[1], MD; Robert Jan van Geuns[1], MD, PhD; Yoshinobu Onuma[1], MD, PhD; Nicolas M. Van Mieghem[1], MD, PhD; Antonios Karanasos[1], MD, PhD; Jors van der Sijde[1], MD; Marcella De Paolis[1], MD; Evelyn Regar[1], MD, PhD; Marco Valgimigli[1,3], MD, PhD; Joost Daemen[1], MD, PhD; Peter de Jaegere[1], MD, PhD; Felix Zijlstra[1], MD, PhD; Roberto Diletti[1]*, MD

1. Department of Interventional Cardiology, Thoraxcenter, Erasmus MC, Rotterdam, The Netherlands; 2. National Heart Centre Singapore, Singapore; 3. Swiss Cardiovascular Center Bern, Bern University Hospital, Bern, Switzerland

Jiang Ming Fam and Roberto Diletti contributed equally to this manuscript.

GUEST EDITOR: Tommaso Gori, MD, PhD; *Zentrum für Kardiologie, Universitätsmedizin Mainz, University Medical Center, Mainz and DZHK Rhein-Main, Germany*

KEYWORDS

- bioresorbable vascular scaffolds (BVS)
- percutaneous coronary intervention (PCI)
- ST-segment elevation myocardial infarction

Abstract

Aims: Limited data are currently available on midterm outcomes after implantation of everolimus-eluting bioresorbable vascular scaffolds (BVS) for treatment of acute ST-elevation myocardial infarction (STEMI).

Methods and results: Patients presenting with STEMI and undergoing primary percutaneous coronary intervention in the initial experience with BVS were evaluated and compared with patients treated with everolimus-eluting metal stents (EES) by applying propensity matching. Quantitative coronary angiography analysis, and 18-month clinical follow-up were reported. A total of 302 patients were analysed, 151 with BVS and 151 with EES. Baseline clinical characteristics were similar between groups. Final TIMI 3 flow was 87.4% vs. 86.1%, p=0.296. At 18-month follow-up, all-cause mortality was 2.8% vs. 3.0% in the BVS and EES groups respectively, p=0.99; the MACE rate was higher in the BVS group (9.8% vs. 3.6%, p=0.02); target lesion revascularisation was 5.7% vs. 1.3%, p=0.05. The 30-day MACE rate in BVS patients without post-dilatation was 6.8%, while in patients with post-dilatation it was 3.6%. Scaffold thrombosis (ST) occurred primarily in the acute phase (acute ST 2.1% vs. 0.7%, p=0.29; subacute 0.7% vs. 0.7%, p=0.99; late 0.0% vs. 0.0%; very late 1.5% vs. 0.0%, p=0.18). All three BVS cases with acute ST had no post-dilatation at the index procedure.

Conclusions: STEMI patients treated during the early experience with BVS had similar acute angiographic results as compared with the EES group. Clinical midterm follow-up data showed a higher clinical events rate compared with metal stents. The majority of clinical events occurred in the early phase after implantation and mainly in cases without post-dilatation. Optimisation of the implantation technique in the acute clinical setting is of paramount importance for optimal short and mid-term outcomes.

**Corresponding author: Department of Cardiology, Thoraxcenter, Room Ba-581, Erasmus MC, 's-Gravendijkwal 230, 3015 GE Rotterdam, The Netherlands. E-mail: r.diletti@erasmusmc.nl*

Introduction

Bioresorbable vascular scaffolds (BVS) have recently been introduced as a novel approach for treatment of coronary artery disease, providing transient vascular support and drug delivery, potentially restoring the vascular physiology after device bioresorption[1-4].

The theoretical advantages of this novel technology, such as late lumen enlargement, restoration of coronary vasomotion and plaque sealing, make this device appealing for patients with ruptured thin-capped lipid-rich soft plaques in general[5-7] and thrombotic lesions in acute coronary syndromes and STEMI in particular[8-10]. Due to vasoconstriction and presence of thrombus, the treatment of acute lesions is often associated with device undersizing and the occurrence of malapposition after thrombus resolution. Theoretically, the complete bioresorption of the device would avoid the presence of long-term malapposed struts. In addition, the wider struts of the BVS could entrap thrombotic material and reduce distal embolisation[11]. Futhermore, polymer bioresorption and concomitant formation of a neointimal layer given by connective tissue and smooth muscle cells could stabilise the plaque, creating a neothick fibrous cap, without the long-term permanence of metallic material in the vessel wall[5].

Initial small cohort studies with short follow-up and relatively selected populations reported encouraging results after BVS implantation in acute patients; however, currently only limited data are available on the midterm performance of this novel device in patients presenting with acute myocardial infarction[11-13]. Given this background, we analysed patients presenting with ST-elevation myocardial infarction (STEMI) treated with BVS and we compared angiographic and 18-month clinical results with a matched population implanted with everolimus-eluting stents (EES).

Methods

Patients presenting with ST-segment elevation myocardial infarction and treated with BVS at the Thoraxcenter, Erasmus MC in Rotterdam between November 2012 and December 2014 were evaluated for the present analysis. Subjects included were patients ≥18 years old admitted with STEMI. Culprit lesions were located in vessels within the upper limit of 3.8 mm and the lower limit of 2.0 mm by online quantitative coronary angiography (QCA). The BVS was implanted according to the manufacturer's sizing matrix. The BVS with a nominal diameter of 2.5 mm was implanted in vessels ≥2.0 and ≤3.0 mm by online QCA; the 3.0 mm BVS was implanted in vessels ≥2.5 and ≤3.3 mm by online QCA; and the 3.5 mm BVS was implanted in vessels ≥3.0 and ≤3.8 mm. For each nominal diameter a further expansion of 0.5 mm was allowed. All patients were loaded with unfractionated heparin (70-100 UI/kg for an activated clotting time between 250 and 300 s), and dual antiplatelet therapy after treatment was planned to last 12 months. Exclusion criteria comprised pregnancy, known intolerance to contrast medium, uncertain neurological outcome after cardiopulmonary resuscitation, previous percutaneous coronary intervention (PCI) with the implantation of a metal stent, left main (LM) disease, previous coronary artery bypass grafting (CABG), and participation in another investigational drug or device study before reaching the primary endpoints.

Propensity score analysis was applied to match each STEMI patient treated with BVS to a comparable patient treated with an everolimus-eluting stent (EES) in our institution with an available follow-up of at least two years.

Baseline and post-scaffold/stent implantation quantitative coronary angiographic analyses were performed and clinical outcomes at the 18-month follow-up were evaluated **(Figure 1)**.

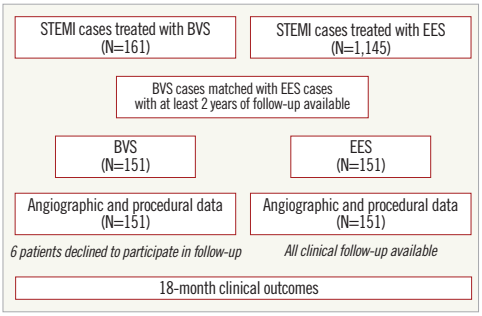

Figure 1. *Flow chart of the study.*

STUDY DEVICE

The second-generation BVS (Absorb BVS; Abbott Vascular, Santa Clara, CA, USA) is a balloon-expandable scaffold consisting of a polymer backbone of poly-L-lactide (PLLA) coated with a thin layer of a 1:1 mixture of an amorphous matrix of poly- D, L-lactide (PDLLA) polymer and 100 μg/cm^2 of the antiproliferative drug everolimus. Two platinum markers located at each BVS edge allow enhanced visualisation of the radiolucent BVS during angiography or other imaging modalities. The PDLLA controls the release of everolimus and 80% of the drug is eluted within the first 30 days. Both PLLA and PDLLA are fully bioresorbable. The polymers are degraded via hydrolysis of the ester bonds, and the resulting lactate and its oligomers are transformed to pyruvate and metabolised in the Krebs cycle. Small particles, less than 2 μm in diameter, have also been shown to be phagocytised and degraded by macrophages. According to preclinical studies[14], complete bioresorption of the polymer backbone occurs from two to three years after implantation[15].

CONTROL DEVICE

The everolimus-eluting coronary stent system is a balloon-expandable metallic platform stent manufactured from a flexible cobalt chromium alloy with a multicellular design and coated with a thin non-adhesive, durable, biocompatible acrylic, and fluorinated everolimus-releasing copolymer.

Quantitative coronary angiographic analysis

Angiographic views with minimal foreshortening of the lesion and limited overlap with other vessels were used whenever possible for all phases of the treatment. Analyses pre- and post-treatment were performed in matched angiographic views. In case of a thrombotic total occlusion, pre-procedure quantitative coronary angiographic analysis was performed as proximally as possible from the occlusion (in case of a side branch distally to the most proximal take-off of the side branch), as previously reported[11]. Intracoronary thrombus was angiographically identified and scored in five grades as previously described[16,17]. Thrombus grade was assessed before procedure and after thombectomy. The two-dimensional angiograms were analysed with the CAAS 5.10 analysis system (Pie Medical BV, Maastricht, The Netherlands). In each patient, the treated region and the peri-treated regions (defined as 5 mm proximal and distal to the device edge) were analysed. The QCA measurements included reference vessel diameter (RVD), percentage diameter stenosis, minimal lumen diameter (MLD), and maximal lumen diameter (Dmax). Acute gain was defined as post-procedural MLD minus pre-procedural MLD (an MLD value equal to zero was applied when the culprit vessel was occluded pre-procedurally).

PROCEDURAL-CLINICAL OUTCOMES AND DEFINITIONS

Device success was defined as successful delivery and deployment of the device with the attainment of <30% final residual stenosis. Procedure success was defined as device success and no major periprocedural complications (emergent CABG, coronary perforation requiring pericardial drainage, residual dissection impairing vessel flow – TIMI flow 2 or less). All deaths were considered cardiac unless an undisputed non-cardiac cause was identified. Target lesion revascularisation (TLR) was defined as clinically driven if at repeat angiography the diameter stenosis was ≥70%, or if a diameter stenosis 50% was present in association with (i) presence of recurrent angina pectoris, related to the target vessel, (ii) objective signs of ischaemia at rest (ECG changes) or during exercise test, related to the target vessel, and (iii) abnormal results of any functional diagnostic test. Scaffold/stent thrombosis was defined according to the Academic Research Consortium definition[18]. Major adverse cardiac events (MACE) were defined as the composite of cardiac death, any re-infarction (Q- or non-Q-wave), emergent bypass surgery (CABG), or clinically driven TLR.

Ethics

This is an observational study, performed according to the privacy policy of the Erasmus MC and to the Erasmus MC regulations for the appropriate use of data in patient-oriented research, which are based on international regulations, including the declaration of Helsinki. The BVS received the CE mark for clinical use, indicated for improving coronary lumen diameter in patients with ischaemic heart disease due to *de novo* native coronary artery lesions with no restriction in terms of clinical presentation. Therefore, the BVS can be currently used routinely in Europe in different settings comprising STEMI without a specific written informed consent in addition to the standard informed consent to the procedure. Given this background, a waiver from the hospital Ethical Committee was obtained for written informed consent, as according to Dutch law written consent is not required, if patients are not subject to acts other than as part of their regular treatment.

On the other hand all the follow-up clinical data reported in the present study are derived from patients who consented to participate in this registry being clinically followed-up. A questionnaire was sent to all living patients with specific queries on rehospitalisation and cardiovascular events. For patients who suffered an adverse event at another centre, medical records or discharge letters from the other institutions were systematically reviewed. General practitioners and referring physicians were contacted for additional information if necessary.

STATISTICAL ANALYSIS

A propensity score matching was performed using a proprietary macro developed and tested for SPSS version 22.0 (IBM Corp., Armonk, NY, USA). First, the programme performed a logistic regression to score all patients according to the treatment (BVS vs. EES), using as covariates clinical and procedural parameters: age (years), sex (male/female), cardiogenic shock (yes/no), hypertension (yes/no), hypercholesterolaemia (yes/no), smoking (yes/no), diabetes mellitus (yes/no), pre-procedure TIMI flow, culprit vessel. Second, the macro searched and selected the best match case of the EES group for every BVS case according to the absolute value of the difference between the propensity score of BVS and EES cases under consideration. Patients in the two groups were matched through a greedy algorithm based on local optimisation[19]. The control selected for a particular case was the one closest to the case in terms of distance. Analyses were then performed on the two matched groups (BVS vs. EES), stratified by pairs to account for propensity score matching. For the study, individual data were pooled on a patient-level basis. Categorical variables are reported as counts and percentages, continuous variables as mean±standard deviation. The Student's t-test and the chi-square test (or Fisher's exact test) were used for comparison of means and percentages. The cumulative incidence of adverse events was estimated according to the Kaplan-Meier method. Patients lost to follow-up were considered at risk until the date of last contact, at which point they were censored. Kaplan-Meier estimates were compared by means of the log-rank test. For the endpoint MACE, a landmark survival analysis was performed with the landmark time point at 30 days. All statistical tests were two-sided and a p-value of <0.05 was considered statistically significant.

Results

A total of 1,306 patients presenting with acute ST-segment elevation myocardial infarction were evaluated for the present analysis (161 patients implanted with BVS and 1,145 patients implanted with EES with at least two-year follow-up available). After matching, 302 patients treated with either BVS or EES (151 patients treated with BVS matched with 151 patients treated with EES)

were analysed. Six patients (3.9%) in the BVS group declined to participate in follow-up.

Baseline clinical characteristics were balanced between the groups, as shown in **Table 1**.

A total of 403 devices (193 BVS) were deployed, and aspiration thrombectomy was performed equally in the two groups (BVS 76.7% vs. 76.8% EES, p=1.000). Predilatation was performed more frequently in the BVS group (54.1% vs. 28.4%, p<0.001) with a higher balloon/artery ratio (1.02±0.24 vs. 0.88±0.21, p=0.002). Post-dilatation was also performed more frequently in the BVS group (39.7% vs. 21.8%, p<0.001, respectively), but with a balloon/scaffold-stent ratio higher in the EES group (1.07±0.09 vs. 1.12±0.12, p=0.031). The BVS group rate of post-dilatation increased over time during the inclusion: in the first 75 patients the rate of post-dilatation was 25.3%, while in the remaining 76 patients it was 53.9%. Device success was similar between groups (98.7% vs. 99.3%, p=1.000) **(Table 2)**.

Baseline culprit vessels, vessel dimensions, percentage of stenosis, TIMI flow and thrombotic burden were similar between patients treated with BVS and those treated with EES **(Table 3)**.

At the end of the procedure, there were no cases of TIMI flow 0, and final TIMI 3 flow was achieved in 87.4% and 86.1% of the BVS and EES groups, respectively (p=0.296), with similar minimal lumen diameter and percentage stenosis.

SIX-MONTH CLINICAL OUTCOMES

All-cause death was observed in 2.1% vs. 2.0% of the cases in the BVS and EES groups respectively, p=0.97; the rate of any myocardial infarction was 5.5% in the BVS group and 1.3% in the EES group, p=0.05. The target lesion revascularisation rate was 3.5% and 1.3%, respectively, p=0.23. Acute scaffold thrombosis occurred in 2.1% of BVS implanted patients and 0.7% of EES implanted patients, p=0.29. In both groups the subacute ST rate was 0.7%, p=0.99. All three acute scaffold thromboses occurred in patients without post-dilatation performed at the index procedure. The overall MACE rate was 7.6% vs. 2.7%, p=0.06. A landmark analysis showed that the 30-day MACE rate in BVS patients without post-dilatation was 6.8%, while in patients with post-dilatation it was 3.6%.

Table 1. Baseline clinical characteristics.

	BVS (N=151)	EES (N=151)	*p*-value
Age, years	56.31±10.22	54.90±11.52	0.263
Male	109/151 (72.2)	113/151 (74.8)	0.696
Active smoker	71/151 (41.0)	89/151 (58.9)	0.050
Diabetes mellitus	17/151 (11.3)	15/151 (9.9)	0.852
Dyslipidaemia	43/151 (28.4)	41/151 (27.1)	0.226
Hypertension	60/151 (39.7)	56/151 (37.1)	0.723
Family history	51/151 (33.8)	52/151 (34.4)	1.000
Target vessel			0.520
LAD	64/151 (42.4)	62/151 (41.1)	
LCX	32/151 (21.2)	40/151 (26.5)	
RCA	51/151 (33.8)	46/151 (30.5)	
Diagonal	2/151 (1.3)	3/151 (2.0)	
Ramus intermedius	2/151 (1.3)	0	
Left main	0	0	
SVG	0	0	

Data are expressed as count and proportion (%) or mean±standard deviation.

Table 2. Procedural characteristics.

	BVS (N=151)	EES (N=151)	*p*-value
Aspiration thrombectomy	115/151 (76.7)	116/151 (76.8)	1.000
Predilatation performed	80/151 (54.1)	42/151 (28.4)	<0.001
Predilatation balloon/artery ratio	1.02±0.24	0.88±0.21	0.002
Maximal diameter balloon predilatation, mm	2.54±0.47	2.40±0.48	0.111
Supportive wire used	18/151 (12.2)	3/151 (2.0)	<0.001
Device failure	2/151 (1.5)	1/151 (0.7)	1.000
Device success	149/151 (98.7)	150/151 (99.3)	1.000
Procedure success	148/151 (98.0)	150/151 (99.3)	0.622
Mean scaffold diameter, mm	3.21±0.33	3.20±0.46	0.827
Mean total nominal scaffold length, mm	26.32±13.27	27.76±14.81	0.378
Number of scaffolds deployed per treated vessel	1.28±0.61	1.39±0.73	0.148
0	2 (1.3)	0	0.398
1	115 (76.2)	108 (71.5)	
2	25 (16.6)	32 (21.2)	
3	8 (5.3)	7 (4.6)	
4	1 (0.7)	3 (2.0)	
5	0	1 (0.7)	
Procedures with overlapping scaffolds	31/151 (20.7)	39/151 (25.8)	0.340
Post-dilatation performed	60/151 (39.7)	33/151 (21.8)	<0.001
Post-dilatation balloon/scaffold or stent ratio	1.07±0.09	1.12±0.12	0.031
Maximal post-dilatation balloon diameter, mm	3.45±0.41	3.54±0.59	0.435
Complications occurring anytime during the procedure			
Any dissection	10/151 (6.7)	8/151 (5.3)	0.809
Thrombosis	0	0	
Perforation	1/151 (0.7)	0	

Data are expressed as count and proportion (%) or mean±standard deviation.

12-MONTH CLINICAL OUTCOMES

From six to 12-month follow-up, one non-cardiac death, one target lesion revascularisation and one non-target vessel revascularisation occurred in the group treated with a bioresorbable vascular scaffold.

18-MONTH CLINICAL OUTCOMES

From 12 to 18 months, two cases of very late scaffold thrombosis were observed in the BVS group, at 416 and 449 days after implantation **(Figure 2)**. In both cases the dual antiplatelet therapy was interrupted (per protocol) at the moment of the event.

Table 3. Angiographic characteristics.

	BVS (N=151)	EES (N=151)	*p*-value
Pre-procedure			
TIMI flow			0.213
0	80/151 (53.0)	85/151 (56.3)	
1	16/151 (10.6)	12/151 (7.9)	
2	31/151 (20.5)	40/151 (26.5)	
3	24/151 (15.9)	14/151 (9.3)	
Thrombus burden			0.551
1	24/148 (16.2)	20/150 (13.3)	
2	21/148 (14.2)	16/150 (10.7)	
3	12/148 (8.1)	9/150 (6.0)	
4	12/148 (8.1)	18/150 (12.0)	
5	79/148 (53.4)	87/150 (58.0)	
Total thrombotic occlusion			
RVD (mm)	2.76±0.72	2.71±0.47	0.608
Non-total thrombotic occlusion			
RVD (mm)	2.60±0.52	2.72±0.54	0.179
MLD (mm)	0.82±0.46	0.91±0.66	0.335
Diameter stenosis (%)	68.07±15.08	66.27±21.57	0.571
Post-procedure			
TIMI flow			0.296
0	0	0	
1	2/151 (1.3)	0/151	
2	17/151 (11.3)	21/151 (13.9)	
3	132/151 (87.4)	130/151 (86.1)	
RVD (mm)	2.63±0.54	2.98±1.76	0.023
MLD (mm)	2.11±0.50	2.22±0.54	0.067
Diameter stenosis (%)	20.64±11.02	22.28±9.92	0.181
Acute lumen gain	1.98±0.67	2.06±0.73	0.398

Data are expressed as count and percentages or mean±standard deviation.

In both cases the review of intravascular imaging showed scaffold malapposition. In the EES group, two additional non-TVR were reported, one of them associated with a myocardial infarction **(Table 4)**.

Discussion

The feasibility of BVS implantation in patients presenting with acute myocardial infarction has recently been reported with preliminary information on short-term clinical outcomes[11-13]. However, data comparing the midterm performance of the bioresorbable technology with the current generation of metal DES in this specific subset are limited. The present study represents an initial experience evaluating the use of the second-generation BVS for the treatment of patients presenting with STEMI in comparison with everolimus-eluting metal stents in terms of acute angiographic results and 18-month clinical outcomes.

The majority of the treated patients presented with TIMI flow 0 or 1, and more than 60% of the lesions had a large thrombus burden (four or five) in the culprit vessel, in line with recent large STEMI trials with minimal exclusion criteria[20,21].

Procedural and angiographic data showed an overall comparable device success rate between the two groups, with a similar intraprocedural complication rate. At the end of the procedure, the restoration of TIMI 3 flow was achieved in a large number of patients and similarly in both groups, with comparable acute lumen gain, percentage diameter stenosis and minimal lumen diameter.

On the other hand, at 18-month follow-up, MACE rate was higher in the BVS group. Importantly, most events occurred in the very early phase after implantation. In particular, three scaffold thromboses occurred within 24 hours following the index procedure and in none of them was a post-dilatation performed.

Notably, this registry enrolled patients at a time when post-dilation was not regarded to be key for optimal implantation and clinical results, especially in the acute subset. Studies reporting pooled BVS data from different European registries performed in the same era showed similar rates of scaffold thrombosis at 30 days[13].

A consortium of experienced European experts has recently emphasised the importance of high-pressure post-dilation with BVS[22] and, in our study, the uptake of post-dilatation with BVS doubled over the course of this registry. Furthermore, an optimised implantation strategy including systematic post-dilatation has been shown to be associated with a reduction in thrombotic events[23].

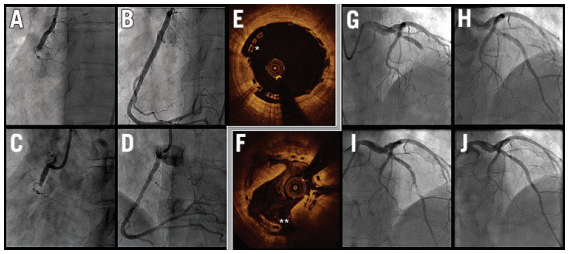

Figure 2. *Cases of very late scaffold thrombosis. Both cases were performed with satisfactory final angiographic results. Case 1 (panels A-E): A) baseline; B) final result of the index procedure; C) thrombosis; D) final result of the event treatment. Post-dilatation was performed during the index intervention, but at the end of the procedure intravascular imaging (E) highlighted the remaining malapposition (*). Case 2 (panels F-J): G) baseline; H) final result of the index procedure; I) thrombosis; J) final result of the event treatment. At the time of the event, intravascular imaging (F) showed persistent malapposition (**).*

Table 4. Clinical outcomes.

	6-month follow-up			12-month follow-up			18-month follow-up		
	BVS (n=145)	EES (n=151)	*p*-value	BVS (n=145)	EES (n=151)	*p*-value	BVS (n=145)	EES (n=151)	*p*-value
All-cause death	3 (2.1)	3 (2.0)	0.97	4 (2.8)	3 (2.0)	0.68	4 (2.8)	4 (3.0)	0.99
Cardiac death	3 (2.1)	2 (1.3)	0.63	3 (2.1)	2 (1.3)	0.63	3 (2.1)	2 (1.3)	0.63
MACE	11 (7.6)	4 (2.7)	0.06	12 (8.1)	4 (2.7)	0.03	14 (9.8)	5 (3.6)	0.03
MI	8 (5.5)	2 (1.3)	0.05	8 (5.5)	2 (1.3)	0.05	9 (6.3)	3 (2.3)	0.07
TLR	5 (3.5)	2 (1.3)	0.23	6 (4.2)	2 (1.3)	0.14	8 (5.7)	2 (1.3)	0.05
Non-TVR	3 (2.1)	3 (2.0)	0.97	4 (2.8)	3 (2.0)	0.67	5 (3.6)	5 (4.0)	0.95
Definite ST	4 (2.8)	2 (1.3)	0.38	4 (2.8)	2 (1.3)	0.38	6 (4.3)	2 (1.3)	0.15
Acute	3 (2.1)	1 (0.7)	0.29	3 (2.1)	1 (0.7)	0.29	3 (2.1)	1 (0.7)	0.29
Subacute	1 (0.7)	1 (0.7)	0.99	1 (0.7)	1 (0.7)	0.99	1 (0.7)	1 (0.7)	0.99
Late	–	–	–	–	–	–	0 (0.0)	0 (0.0)	–
Very late	–	–	–	–	–	–	2 (1.5)	0 (0.0)	0.18

Data are expressed as count and percentages

In the randomised Absorb-TROFI II trial, evaluating short-term imaging results in either BVS or EES in acute myocardial infarction, the rate of subacute scaffold thrombosis was 1.1% at six-month follow-up. In this study, the implantation technique was slightly different from ours, including mandatory thrombus aspiration and post-dilation performed in a slightly higher number of cases[24].

Our study further highlighted the importance of post-dilatation with BVS because patients without post-dilatation had a higher MACE rate in the first month, and both cases of very late scaffold thrombosis were associated with persistent malapposition. We therefore hypothesise that an optimal BVS implantation technique, encompassing adequate pre- and post-dilatation is essential for improving clinical outcomes also in the acute clinical setting.

The minimalist PCI approach in STEMI, focussing on restoration of TIMI 3 flow in the culprit vessel with a minimum of manoeuvres to minimise the risk of distal embolisation, may not be valid with BVS. The observations reported in the present study could support a more frequent use of post-dilatation to optimise scaffold expansion, even in acute patients. Large randomised trials currently in preparation may add to our understanding of the real performance of bioresorbable technologies in the acute setting.

Limitations

The number of subjects evaluated in the present study is limited, and data on clinical outcomes should be considered descriptive and hypothesis-generating. The two study groups were not randomised. Despite the use of propensity matching, unadjusted confounders might remain, possibly having an impact on results. A larger patient population and longer follow-up would be needed for adequate comparison of this novel technology with current-generation metal DES.

Conclusion

STEMI patients treated with PCI and BVS in the early experience had similar acute angiographic results as compared to EES. Clinical midterm follow-up data showed a higher clinical events rate compared with metal stents. The majority of clinical events occurred in the early phase after implantation and mainly in cases without post-dilatation. Optimisation of the implantation technique is relevant in acute patients for achieving optimal short and mid-term clinical outcomes.

Guest Editor

This paper was guest edited by Tommaso Gori, MD, PhD; Zentrum für Kardiologie, Universitätsmedizin Mainz, University Medical Center, Mainz and DZHK Rhein-Main, Germany.

Impact on daily practice

Implantation of bioresorbable vascular scaffolds requires a meticulous lesion preparation and an adequate optimisation of scaffold expansion with a frequent use of high pressure post-dilatation. Our results after early experience in patients presenting with acute myocardial infarction, showed a slightly higher rate of events in patients implanted with bioresorbable vascular scaffolds. Procedural factors might have had a role in these findings and an optimal implantation technique, including high pressure post-dilatation should also be considered in the acute setting when using bioresorbable scaffolds.

Funding

Abbott Vascular is providing an institution research grant for the Erasmus MC.

Conflict of interest statement

R.J. van Geuns received speakers fees from Abbott Vascular. A. Karanasos received funding support from the Hellenic Heart Foundation and St Jude Medical.

The Guest Editor, Tommaso Gori has received speaker's honoraria from multiple companies including Abbott Vascular.

References

1. Serruys PW, Ormiston JA, Onuma Y, Regar E, Gonzalo N, Garcia-Garcia HM, Nieman K, Bruining N, Dorange C, Miquel-Hebert K, Veldhof S, Webster M, Thuesen L, Dudek D. A bioabsorbable everolimus-eluting coronary stent system (ABSORB): 2-year outcomes and results from multiple imaging methods. *Lancet.* 2009;373:897-910.

2. Serruys PW, Onuma Y, Ormiston JA, de Bruyne B, Regar E, Dudek D, Thuesen L, Smits PC, Chevalier B, McClean D, Koolen J, Windecker S, Whitbourn R, Meredith I, Dorange C, Veldhof S, Miquel-Hebert K, Rapoza R, Garcia-Garcia HM. Evaluation of the second generation of a bioresorbable everolimus drug-eluting vascular scaffold for treatment of de novo coronary artery stenosis: six-month clinical and imaging outcomes. *Circulation.* 2010;122: 2301-12.

3. Diletti R, Onuma Y, Farooq V, Gomez-Lara J, Brugaletta S, van Geuns RJ, Regar E, de Bruyne B, Dudek D, Thuesen L, Chevalier B, McClean D, Windecker S, Whitbourn R, Smits P, Koolen J, Meredith I, Li D, Veldhof S, Rapoza R, Garcia-Garcia HM, Ormiston JA, Serruys PW. 6-month clinical outcomes following implantation of the bioresorbable everolimus-eluting vascular scaffold in vessels smaller or larger than 2.5 mm. *J Am Coll Cardiol.* 2011;58:258-64.

4. Serruys PW, Chevalier B, Dudek D, Cequier A, Carrie D, Iniguez A, Dominici M, van der Schaaf RJ, Haude M, Wasungu L, Veldhof S, Peng L, Staehr P, Grundeken MJ, Ishibashi Y, Garcia-Garcia HM, Onuma Y. A bioresorbable everolimus-eluting scaffold versus a metallic everolimus-eluting stent for ischaemic heart disease caused by de-novo native coronary artery lesions (ABSORB II): an interim 1-year analysis of clinical and procedural secondary outcomes from a randomised controlled trial. *Lancet.* 2015;385: 43-54.

5. Brugaletta S, Radu MD, Garcia-Garcia HM, Heo JH, Farooq V, Girasis C, van Geuns RJ, Thuesen L, McClean D, Chevalier B, Windecker S, Koolen J, Rapoza R, Miquel-Hebert K, Ormiston J, Serruys PW. Circumferential evaluation of the neointima by optical coherence tomography after ABSORB bioresorbable vascular scaffold implantation: can the scaffold cap the plaque? *Atherosclerosis.* 2012;221:106-12.

6. Bourantas CV, Serruys PW, Nakatani S, Zhang YJ, Farooq V, Diletti R, Ligthart J, Sheehy A, van Geuns RJ, McClean D, Chevalier B, Windecker S, Koolen J, Ormiston J, Whitbourn R, Rapoza R, Veldhof S, Onuma Y, Garcia-Garcia HM. Bioresorbable vascular scaffold treatment induces the formation of neointimal cap that seals the underlying plaque without compromising the luminal dimensions: a concept based on serial optical coherence tomography data. *EuroIntervention.* 2015;11:746-56.

7. Diletti R, Yetgin T, Manintveld OC, Ligthart JM, Zivelonghi C, Zijlstra F, Ribichini F. Percutaneous coronary interventions during ST-segment elevation myocardial infarction: current status and future perspectives. *EuroIntervention.* 2014;10 Suppl T:T13-22.

8. Farb A, Burke AP, Tang AL, Liang TY, Mannan P, Smialek J, Virmani R. Coronary plaque erosion without rupture into a lipid core. A frequent cause of coronary thrombosis in sudden coronary death. *Circulation.* 1996;93:1354-63.

9. Diletti R, Farooq V, Girasis C, Bourantas C, Onuma Y, Heo JH, Gogas BD, van Geuns RJ, Regar E, de Bruyne B, Dudek D, Thuesen L, Chevalier B, McClean D, Windecker S, Whitbourn RJ, Smits P, Koolen J, Meredith I, Li X, Miquel-Hebert K, Veldhof S, Garcia-Garcia HM, Ormiston JA, Serruys PW. Clinical and intravascular imaging outcomes at 1 and 2 years after implantation of absorb everolimus eluting bioresorbable vascular scaffolds in small vessels. Late lumen enlargement: does bioresorption matter with small vessel size? Insight from the ABSORB cohort B trial. *Heart.* 2013;99:98-105.

10. Serruys PW, Onuma Y, Dudek D, Smits PC, Koolen J, Chevalier B, de Bruyne B, Thuesen L, McClean D, van Geuns RJ, Windecker S, Whitbourn R, Meredith I, Dorange C, Veldhof S, Hebert KM, Sudhir K, Garcia-Garcia HM, Ormiston JA. Evaluation of the second generation of a bioresorbable everolimus-eluting vascular scaffold for the treatment of de novo coronary artery stenosis: 12-month clinical and imaging outcomes. *J Am Coll Cardiol.* 2011;58:1578-88.

11. Diletti R, Karanasos A, Muramatsu T, Nakatani S, Van Mieghem NM, Onuma Y, Nauta ST, Ishibashi Y, Lenzen MJ, Ligthart J, Schultz C, Regar E, de Jaegere PP, Serruys PW, Zijlstra F, van Geuns RJ. Everolimus-eluting bioresorbable vascular scaffolds for treatment of patients presenting with ST-segment elevation myocardial infarction: BVS STEMI first study. *Eur Heart J.* 2014;35:777-86.

12. Kocka V, Maly M, Tousek P, Budesinsky T, Lisa L, Prodanov P, Jarkovsky J, Widimsky P. Bioresorbable vascular scaffolds in acute ST-segment elevation myocardial infarction: a prospective multicentre study 'Prague 19'. *Eur Heart J.* 2014;35:787-94.

13. Brugaletta S, Gori T, Low AF, Tousek P, Pinar E, Gomez-Lara J, Scalone G, Schulz E, Chan MY, Kocka V, Hurtado J, Gomez-Hospital JA, Munzel T, Lee CH, Cequier A, Valdes M, Widimsky P, Serruys PW, Sabate M. Absorb bioresorbable vascular scaffold versus everolimus-eluting metallic stent in ST-segment elevation myocardial infarction: 1-year results of a propensity score matching comparison: the BVS-EXAMINATION Study (bioresorbable vascular scaffold-a clinical evaluation of everolimus eluting coronary stents in the treatment of patients with ST-segment elevation myocardial infarction). *JACC Cardiovasc Interv.* 2015;8: 189-97.

14. Onuma Y, Serruys PW. Bioresorbable scaffold: the advent of a new era in percutaneous coronary and peripheral revascularization? *Circulation.* 2011;123:779-97.

15. Onuma Y, Serruys PW, Perkins LE, Okamura T, Gonzalo N, Garcia-Garcia HM, Regar E, Kamberi M, Powers JC, Rapoza R, van Beusekom H, van der Giessen W, Virmani R. Intracoronary optical coherence tomography and histology at 1 month and 2, 3, and 4 years after implantation of everolimus-eluting bioresorbable vascular scaffolds in a porcine coronary artery model: an attempt to decipher the human optical coherence tomography images in the ABSORB trial. *Circulation.* 2010;122:2288-300.

16. Sianos G, Papafaklis MI, Daemen J, Vaina S, van Mieghem CA, van Domburg RT, Michalis LK, Serruys PW. Angiographic stent thrombosis after routine use of drug-eluting stents in ST-segment elevation myocardial infarction: the importance of thrombus burden. *J Am Coll Cardiol.* 2007;50:573-83.

17. Gibson CM, de Lemos JA, Murphy SA, Marble SJ, McCabe CH, Cannon CP, Antman EM, Braunwald E; TIMI Study Group. Combination therapy with abciximab reduces angiographically evident thrombus in acute myocardial infarction: a TIMI 14 substudy. *Circulation.* 2001;103:2550-4.

18. Cutlip DE, Windecker S, Mehran R, Boam A, Cohen DJ, van Es GA, Steg PG, Morel MA, Mauri L, Vranckx P, McFadden E, Lansky A, Hamon M, Krucoff MW, Serruys PW; Academic Research Consortium. Clinical end points in coronary stent trials: a case for standardized definitions. *Circulation.* 2007;115: 2344-51.

19. Austin PC, Mamdani MM. A comparison of propensity score methods: a case-study estimating the effectiveness of post-AMI statin use. *Stat Med.* 2006;25:2084-106.

20. Jolly SS, Cairns JA, Yusuf S, Meeks B, Pogue J, Rokoss MJ, Kedev S, Thabane L, Stankovic G, Moreno R, Gershlick A, Chowdhary S, Lavi S, Niemela K, Steg PG, Bernat I, Xu Y, Cantor WJ, Overgaard CB, Naber CK, Cheema AN, Welsh RC, Bertrand OF, Avezum A, Bhindi R, Pancholy S, Rao SV, Natarajan MK, ten Berg JM, Shestakovska O, Gao P, Widimsky P, Dzavik V; TOTAL Investigators. Randomized trial of primary PCI with or without routine manual thrombectomy. *N Engl J Med.* 2015;372: 1389-98.

21. Fröbert O, Lagerqvist B, Olivecrona GK, Omerovic E, Gudnason T, Maeng M, Aasa M, Angeras O, Calais F, Danielewicz M, Erlinge D, Hellsten L, Jensen U, Johansson AC, Karegren A, Nilsson J, Robertson L, Sandhall L, Sjogren I, Ostlund O, Harnek J, James SK; TASTE Trial. Thrombus aspiration during ST-segment elevation myocardial infarction. *N Engl J Med.* 2013;369:1587-97.

22. Tamburino C, Latib A, van Geuns RJ, Sabate M, Mehilli J, Gori T, Achenbach S, Alvarez MP, Nef H, Lesiak M, Di Mario C, Colombo A, Naber CK, Caramanno G, Capranzano P, Brugaletta S, Geraci S, Araszkiewicz A, Mattesini A, Pyxaras SA, Rzeszutko L, Depukat R, Diletti R, Boone E, Capodanno D, Dudek D. Contemporary practice and technical aspects in coronary intervention with bioresorbable scaffolds: a European perspective. *EuroIntervention.* 2015;11:45-52.

23. Puricel S, Cuculi F, Weissner M, Schmermund A, Jamshidi P, Nyffenegger T, Binder H, Eggebrecht H, Munzel T, Cook S, Gori T. Bioresorbable Coronary Scaffold Thrombosis: Multicenter Comprehensive Analysis of Clinical Presentation, Mechanisms, and Predictors. *J Am Coll Cardiol.* 2016;67:921-31.

24. Sabate M, Windecker S, Iniguez A, Okkels-Jensen L, Cequier A, Brugaletta S, Hofma SH, Raber L, Christiansen EH, Suttorp M, Pilgrim T, Anne van Es G, Sotomi Y, Garcia-Garcia HM, Onuma Y, Serruys PW. Everolimus-eluting bioresorbable stent vs. durable polymer everolimus-eluting metallic stent in patients with ST-segment elevation myocardial infarction: results of the randomized ABSORB ST-segment elevation myocardial infarction-TROFI II trial. *Eur Heart J.* 2016;37:229-40.

22

CHAPTER

MID- TO LONG-TERM CLINICAL OUTCOMES OF PATIENTS TREATED WITH THE EVEROLIMUS-ELUTING BIORESORBABLE VASCULAR SCAFFOLD: THE BVS EXPAND REGISTRY

Felix Cordula, **Fam Jiang Ming**, Diletti Roberto, Ishibashi Yuki, Karanasos Antonis, Everaert Bert, van Mieghem Nicolas M, Daemen Joost, de Jaegere Peter , Zijlstra Felix , Regar Evelyn, Onuma Yoshinobu, van Geuns Robert-Jan.

JACC Cardiovasc Interv. 2016 Aug 22; 9(16):1652-63.

Mid- to Long-Term Clinical Outcomes of Patients Treated With the Everolimus-Eluting Bioresorbable Vascular Scaffold

The BVS Expand Registry

Cordula M. Felix, MD, Jiang Ming Fam, MD, Roberto Diletti, MD, Yuki Ishibashi, MD, PhD, Antonios Karanasos, MD, PhD, Bert R.C. Everaert, MD, PhD, Nicolas M.D.A. van Mieghem, MD, PhD, Joost Daemen, MD, PhD, Peter P.T. de Jaegere, MD, PhD, Felix Zijlstra, MD, PhD, Evelyn S. Regar, MD, PhD, Yoshinobu Onuma, MD, PhD, Robert-Jan M. van Geuns, MD, PhD

ABSTRACT

OBJECTIVES This study sought to report on clinical outcomes beyond 1 year of the BVS Expand registry.

BACKGROUND Multiple studies have proven feasibility and safety of the Absorb bioresorbable vascular scaffold (BVS) (Abbott Vascular, Santa Clara, California). However, data on medium- to long-term outcomes are limited and available only for simpler lesions.

METHODS This is an investigator-initiated, prospective, single-center, single-arm study evaluating performance of the BVS in a lesion subset representative of daily clinical practice, including calcified lesions, total occlusions, long lesions, and small vessels. Inclusion criteria were patients presenting with non-ST-segment elevation myocardial infarction, stable/unstable angina, or silent ischemia caused by a de novo stenotic lesion in a native previously untreated coronary artery. Procedural and medium- to long-term clinical outcomes were assessed. Primary endpoint was major adverse cardiac events, defined as a composite of cardiac death, myocardial infarction, and target lesion revascularization.

RESULTS From September 2012 to January 2015, 249 patients with 335 lesions were enrolled. Mean number of scaffolds per patient was 1.79 ± 1.15. Invasive imaging was used in 39%. In 38.1% there were American College of Cardiology/American Heart Association classification type B2/C lesions. Mean lesion length was 22.16 ± 13.79 mm. Post-procedural acute lumen gain was 1.39 ± 0.59 mm. Median follow-up period was 622 (interquartile range: 376 to 734) days. Using Kaplan-Meier methods, the MACE rate at 18 months was 6.8%. Rates of cardiac mortality, myocardial infarction, and target lesion revascularization at 18 months were 1.8%, 5.2%, and 4.0%, respectively. Definite scaffold thrombosis rate was 1.9%.

CONCLUSIONS In our study, BVS implantation in a complex patient and lesion subset was associated with an acceptable rate of adverse events in the longer term, whereas no cases of early thrombosis were observed.
(J Am Coll Cardiol Intv 2016;■:■–■) © 2016 by the American College of Cardiology Foundation.

From the Thoraxcenter, Erasmus Medical Center, Rotterdam, the Netherlands. This study was supported by an unrestricted grant from Abbott Vascular. Dr. Karanasos has received research support from St. Jude Medical. Dr. van Mieghem has served as on the Speakers Bureau for and has received speakers fees from Abbott Vascular. Dr. Daemen has received institutional research support from Boston Scientific, St. Jude Medical, Medtronic, and Recor Medical. Dr. Onuma has served as a member of the advisory board for and has received speakers fees from Abbott Vascular. Dr. van Geuns has received speakers fees from Abbott Vascular. All other authors have reported that they have no relationships relevant to the contents of this paper to disclose.

Manuscript received September 22, 2015; revised manuscript received March 30, 2016, accepted April 21, 2016.

ABBREVIATIONS AND ACRONYMS

BVS = bioresorbable vascular scaffold

DES = drug-eluting stent(s)

IVUS = intravascular ultrasound

MACE = major adverse cardiac event

MI = myocardial infarction

MLD = minimal lumen diameter

NSTEMI = non-ST-segment elevation myocardial infarction

OCT = optical coherence tomography

QCA = quantitative coronary angiography

RVD = reference vessel diameter

STEMI = ST-segment elevation myocardial infarction

ST = scaffold thrombosis

TLR = target lesion revascularization

Drug-eluting stents (DES) currently form the mainstay of coronary devices used in percutaneous coronary interventions (PCI) in many parts of the world. Despite advantages in clinical outcomes such as reduction in target lesion revascularization (TLR) rates, shortcomings related to the use of DES still exist such as delayed arterial healing, late scaffold thrombosis, and hypersensitivity reactions to the polymer, with observations of ongoing very late stent failure beyond 1 year (1,2).

In addition, from a physiological point of view, a vessel that is indefinitely caged in a metal stent may not be desirable with both short- and long-term implications and potentially adverse consequences such as impaired endothelial function, the reduced potential for vessel remodeling, interference with the normal arterial healing process, and the risk of occlusion of covered side branches by neointima hyperplasia. Furthermore, interference with noninvasive imaging (cardiac computed tomography or magnetic resonance imaging) during patient follow-up and possible impairment of future treatment options (re-PCI or coronary artery bypass surgery) are drawbacks of metallic stents (3).

To overcome these issues, bioresorbable vascular scaffolds (BVS) were developed. The BVS most studied is the Absorb BVS (Abbott Vascular, Santa Clara, California). The BVS provides transient vessel support and gradually elutes the antiproliferative drug everolimus. After degradation of the polymer (after approximately 3 years) no foreign material remains and the risk for developing very late scaffold thrombosis (ST) is potentially reduced.

Intravascular imaging observations 5 years after BVS implantation in a simple patient and lesion subset have demonstrated late luminal enlargement due to plaque reduction, a persistent restoration of vasomotion and a fully completed bioresorption process (4,5), and a low major adverse cardiac event (MACE) rate (3.4%) (6). This is consistent in randomized controlled trials (ABSORB II and ABSORB Japan), which showed comparable clinical event rates in BVS compared with best in class with metallic DES (Xience V Abbott Vascular, Santa Clara, California) (7,8). However, as these studies included a selected group of patients, extrapolation to a more complex population is limited. Yet, the registry-level clinical data on the outcomes after BVS implantation in more complex patient and lesion subsets have not been well documented that such data are available from registries with a relatively short follow-up of 6 to 12 months, which have shown variable early clinical outcomes (8-10). Thus, the medium- to long-term outcomes beyond 1 year after BVS implantation in such complex real-world lesions remain elusive.

In the current study, we report on extended follow-up beyond 1 year of the BVS Expand Registry. This is a single-center registry initiated in September 2012 that investigates the clinical outcomes after BVS implantation in a more complex real-world population.

METHODS

POPULATION. This is an investigator-initiated, prospective, single-center, single-arm study performed in an experienced, tertiary PCI center. Patients presenting with non-ST-segment elevation myocardial infarction (NSTEMI), stable or unstable angina, or silent ischemia caused by a de novo stenotic lesion in a native previously untreated coronary artery with intention to treat with a BVS were included. Angiographic inclusion criteria included lesions with a proximal and distal maximal lumen diameter within the upper limit of 3.8 mm and the lower limit of 2.0 mm by online quantitative coronary angiography (QCA). Complex lesions such as bifurcation, calcified (as assessed by angiography), long, and thrombotic lesions were not excluded. Exclusion criteria were patients with a history of coronary bypass grafting, presentation with cardiogenic shock, bifurcation lesions requiring kissing balloon post-dilation, ST-segment elevation myocardial infarction (STEMI) patients, allergy or contraindications to antiplatelet therapy, fertile female patients not taking adequate contraceptives or currently breastfeeding, and patients with expected survival of <1 year. As per hospital policy, patients with a previously implanted metal DES in the intended target vessel were also excluded. Also, although old age was not an exclusion criterion, BVS were in general reserved for younger patients, and left to operator's interpretation of biological age.

ETHICS. This is an observational study, performed according to the privacy policy of the Erasmus Medical Center, and to the Erasmus Medical Center regulations for the appropriate use of data in patient-oriented research, which are on the basis of international regulations, including the Declaration of Helsinki. Approval of the ethical board of the Erasmus MC was obtained. All patients undergoing clinical follow-up provided written informed consent for the PCI and to be contacted regularly during the follow-up period of the study.

PROCEDURE. PCI was performed according to current clinical practice standards. The radial or femoral routes were the principal routes of vascular access and 6- or 7-F catheters were used depending on the discretion of the operator. Pre- and post-dilation were recommended with a balloon shorter than the planned study device length and with a noncompliant balloon without overexpanding the scaffold beyond its limits of expansion (0.5 mm > nominal diameter), respectively. Intravascular imaging with the use of intravascular ultrasound (IVUS) or optical coherence tomography (OCT) was used for pre-procedural sizing and optimization of stent deployment on the discretion of the operator. All patients were treated with unfractionated heparin (at a dose of 70 to 100 UI/kg). Patients with stable angina were preloaded with 300 mg of aspirin and 600 mg of clopidogrel. Patients presenting with acute coronary syndrome were preloaded with 300 mg of aspirin and 60 mg of prasugrel or 180 mg of ticagrelor.

ANGIOGRAPHIC ANALYSIS. QCA was performed by 3 independent investigators. Coronary angiograms were analyzed with the CAAS 5.10 QCA software (Pie Medical BV, Maastricht, the Netherlands). The QCA measurements provided reference vessel diameter (RVD), percentage diameter stenosis, minimal lumen diameter (MLD), and maximal lumen diameter. Acute gain was defined as post-procedural MLD minus pre-procedural MLD (in an occluded vessel MLD value was zero by default). For the purpose of this study we defined underexpansion as a ratio of post-procedural MLD to the nominal device diameter of <0.7. The ratio of pre-procedural RVD to the nominal device diameter was used to assess pre-procedural sizing.

FOLLOW-UP. Clinical demographic data of all patients were obtained from municipal civil registries. Follow-up information specific for hospitalization and cardiovascular events was obtained through questionnaires. If needed, medical records or discharge letters from other hospitals were requested. Events were adjudicated by an independent clinical events committee. All information concerning baseline characteristics and follow-up was gathered in a clinical data management system.

DEFINITIONS. The primary endpoint was MACE, defined as the composite endpoint of cardiac death, myocardial infarction (MI) and TLR. Deaths were considered cardiac unless a noncardiac cause was definitely identified. TLR was described as any repeated revascularization of the target lesion. Target vessel revascularization was defined as any repeat percutaneous intervention or surgical bypass of any segment of the target vessel. Non-target vessel revascularization was described as any revascularization in a vessel other than the target lesion. ST and MI were classified according to the Academic Research Consortium (11). Clinical device success (lesion basis) was defined as successful delivery and deployment of all intended scaffolds at the target lesion and successful withdrawal of the delivery system with attainment of final in-scaffold residual stenosis of <30% as evaluated by QCA. When bailout device was used, the success or failure of the bailout device delivery and deployment is not one of the criteria for device success. Clinical procedure success (patient basis) was described as achievement of final in-scaffold residual stenosis of <30% by QCA with successful delivery and deployment of all intended scaffolds at the target lesion and successful withdrawal of the delivery system for all target lesions without major periprocedural complications or in-hospital MACE (maximum of 7 days). In dual target lesion setting, both lesions must meet clinical procedure success criteria to have a patient level procedure success.

The intention-to-treat group includes all the patients regardless of whether or not the scaffold was successfully implanted. The per-treatment group consists of all patients in whom the BVS was successfully implanted. Only events in the per-treatment population were analyzed.

The off-registry population consisted of patients that were excluded in this study, mainly STEMI patients.

STATISTICAL ANALYSIS. Categorical variables are reported as counts and percentages, continuous variables as mean ± SD. Student's *t* test and the chi-square test (or Fisher exact test) were used for comparison of means and percentages. The cumulative incidence of adverse events was estimated according to the Kaplan-Meier method. Patients lost to follow-up were considered at risk until the date of last contact, at which point they were censored. All statistical tests were 2-sided and a p value <0.05 was considered statistically significant. To investigate possible predictors for clinical outcomes MACE and ST, univariate analysis using a Cox regression model was used investigating variables that are frequently present. Statistical analyses were performed using SPSS, version 21 (SPSS Inc., Chicago, Illinois).

RESULTS

From September 2012 up to January 2015, 3,373 patients were treated with PCI in our center.

The majority of patients were considered not suitable for BVS either to their biological age related to comorbidities, indication for stent >3.5 mm or smaller than <2.5 mm, previous coronary bypass grafting, previous PCI with metal DES in the target vessel, or STEMI as indication for PCI shortly after the commercial introduction of BVS in Europe. These patients were in general older (64.5 ± 11.6 years of age) and presented with more risk factors compared to the BVS population (previous coronary bypass grafting 9.5%, previous PCI 31.3%, previous MI 25.6%) and presented more frequently with multivessel disease (57.8%). Finally, 485 patients were treated with 1 or more BVS in the registry period. Most excluded patients (n = 169) presented with STEMI and entered a separate registry starting later, 5 had a previous coronary bypass grafting, 1 needed kissing balloon post-dilation for bifurcation, 2 had a previous implanted metal DES in the target vessel as formal exclusion criteria for this analysis, and 58 did not return their informed consent because they declined to participate, emigrated abroad, or participated in another trial investigating BVS.

A total of 249 signed the informed consent for follow-up and were eligible on the basis of protocol inclusion and exclusion criteria. In 5 patients delivery failure occurred (intention-to-treat group). The per-treatment group thus consisted of 244 patients. The flow chart of the registry is given in **Figure 1**.

BASELINE CHARACTERISTICS. Baseline characteristics of all BVS treated patients are presented in **Table 1**. Mean age was 61.3 ± 10.2 years, 73.5% were male, 18.5% were diabetic, and 59.1% presented with an acute coronary syndrome (NSTEMI or unstable angina; STEMI patients were excluded). Multivessel disease was present in 45.6%. The off-registry patients were younger, with fewer comorbidities, and presented more frequently with STEMI.

Lesion characteristics are presented in **Table 2**. The left anterior descending coronary artery was most commonly treated (50.0% of lesions). Moderate or severe calcification (as assessed by angiography) was present in 42.2% and a chronic total occlusion in 4.2% of the lesions. Bifurcation lesions (involving lesions

FIGURE 1 Flowchart of the Study

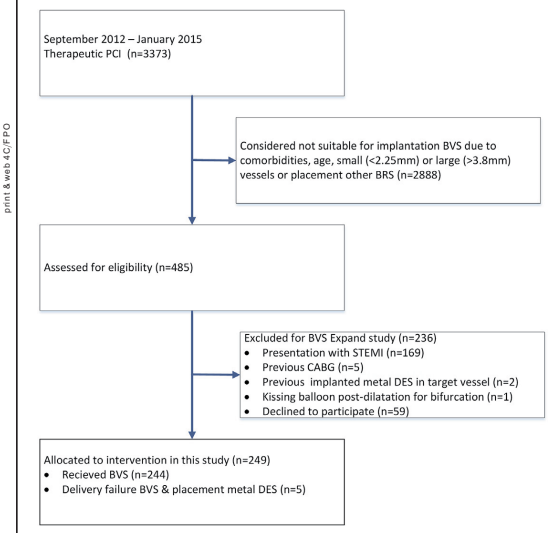

BRS = bioresorbable scaffold; BVS = bioresorbable vascular scaffold; CABG = coronary artery bypass grafting; PCI = percutaneous coronary intervention; STEMI = ST-segment elevation myocardial infarction.

TABLE 1 Patient Characteristics

	ITT Population (n = 249)	Off-Registry Population (n = 236)	p Value
Gender			0.57
Men	73.5	75.6	
Women	26.5	24.4	
Mean, yrs	61.3 ± 10.2	55.4 ± 10.6	<0.001
Smoking	55.0	59.0	0.24
Hypertension	59.4	41.9	<0.001
Dyslipidemia	51.0	29.9	<0.001
Diabetes mellitus	18.5	13.2	0.14
Family history of CAD	44.6	37.6	0.23
Prior MI	17.7	6.0	<0.001
Prior PCI	9.2	4.7	0.05
Prior CABG	0.0	2.6	0.01
Presenting with multiple vessel disease	45.6	28.2	0.07
Indication for PCI			<0.001
Stable angina	40.6	9.8	
Unstable angina	16.1	2.1	
STEMI	0.0	71.4	
NSTEMI	43.0	16.7	
Silent ischemia	0.4	0.0	
Periphery artery disease	8.8	1.7	<0.001
COPD	7.2	3.9	0.10
Heart failure	4.8	0.9	0.01
Renal insufficiency	6.4	2.1	0.02
CVA/TIA	9.6	4.3	0.03

Values are % or mean ± SD.

CAD = coronary artery disease; COPD = chronic obstructive pulmonary disease; CVA = cerebrovascular accident; ITT = intention to treat; MI = myocardial infarction; NSTEMI = non-ST-segment elevation myocardial infarction; PCI = percutaneous coronary intervention; STEMI = ST-segment elevation myocardial infarction; TIA = transient ischemic attack.

TABLE 2 Lesion Characteristics

Target vessel	
LAD	50.0
LCX	23.7
RCA	26.0
Ramus intermedius	0.3
SVG	0.0
Lesion AHA A/B1/B2/C	16.2/45.8/24.3/13.8
Bifurcation	21.3
Medina 1,1,1	15.3
Medina 1,1,0	27.8
Medina 1,0,1	4.2
Medina 0,1,1	12.5
Medina 1,0,0	11.1
Medina 0,1,0	22.2
Medina 0,0,1	6.9
Moderate/severe calcification	42.2
(Chronic) total occlusion	4.2
TIMI	
Pre-procedure	
TIMI 0	8.4
TIMI 1	1.8
TIMI 2	13.8
TIMI 3	75.4
Post-procedure	
TIMI 0	0.0
TIMI 1	0.3
TIMI 2	3.0
TIMI 3	96.4
QCA analysis	
Pre-procedure	
Lesion length, mm	22.10 ± 13.90
RVD, mm	2.42 ± 0.74
MLD, mm	0.91 ± 0.45
Diameter stenosis, %	59.13 ± 20.72
Post-procedure	
RVD, mm	2.77 ± 0.46
MLD, mm	2.30 ± 0.42
Diameter stenosis, %	16.90 ± 9.04
Acute lumen gain, mm	1.39 ± 0.59

Values are % or mean ± SD.

AHA = American Heart Association; LAD = left anterior descending artery; LCX = left coronary artery; MLD = minimal lumen diameter; QCA = quantitative coronary angiography; RCA = right coronary artery; RVD = reference vessel diameter; SVG = saphenous vein graft; TIMI = Thrombolysis In Myocardial Infarction.

within 3 mm of the bifurcation and with side branches ≥2 mm by visual estimation in diameter, treated with implantation of at least 1 BVS) were present in 21.3% with significant side branch involvement (true bifurcations: Medina 1,1,1; 1,0,1; and 0,1,1 lesions) in 32% of these. Overall, 38.1% of lesions were American College of Cardiology/American Heart Association type B2 or C. Mean lesion length was 22.16 ± 13.79 mm. Pre-procedural QCA showed a RVD of 2.42 ± 0.74 mm, a MLD of 0.91 ± 0.45 mm, and a percentage diameter stenosis of 59.12 ± 20.72%.

PROCEDURAL DETAILS. Table 3 shows the procedural characteristics. Pre-dilation was performed in 89.9% (pre-dilation balloon to artery ratio of 1.05 ± 0.23). Post-dilation was performed in 53.3% with a balloon to scaffold ratio of 1.08 ± 0.11. Advanced lesion preparation using rotational artherectomy and scoring balloon was done in 3.1% and 2.7%. Pre-procedural evaluation and device optimization using invasive imaging with IVUS and OCT was done in 14.4% and 24.6% of the procedures, respectively. A total of 445 BVS were implanted with a mean number of 1.34 ± 0.69 scaffolds per lesion and a mean number of 1.79 ± 1.15 scaffolds per patient. For the bifurcation lesions, the provisional side branch treatment was

TABLE 3 Procedural Characteristics (N = 249, 335 Lesions)

Treated lesion per procedure	1.35 ± 0.62
Aspiration thrombectomy	4.2
Rotablation	3.1
Scoring balloon	2.7
Intracoronary imaging	
IVUS	14.4
OCT	24.6
Pre-dilation	89.8
Max pre-dilation diameter, mm	2.61 ± 0.44
Pre-dilation balloon: artery ratio	1.05 ± 0.23
Maximum pre-dilation inflation pressure, atm	12.80 ± 5.91
Buddy wire	8.1
Mean number of scaffolds/lesion	1.34 ± 0.69
Mean number of scaffolds/patient	1.79 ± 1.15
Number of scaffolds	445
1	72.6
2	20.3
3	4.5
4	2.5
Scaffold diameter, mm	3.08 ± 0.35
Scaffold length implanted, mm	28.31 ± 17.06
Lesions with overlapping scaffolds	25.4
Overlapping scaffold diameter 3.5 mm-3.5 mm	24
Overlapping scaffold diameter 3.5 mm-3.0 mm	23
Overlapping scaffold diameter 3.5 mm-2.5 mm	7
Overlapping scaffold diameter 3.0 mm-3.0 mm	21
Overlapping scaffold diameter 3.0 mm-2.5 mm	29
Overlapping scaffold diameter 2.5 mm-2.5 mm	11
Maximum scaffold implantation pressure, atm	15.08 ± 1.82
Post-dilation	53.3
Post-dilation balloon mean scaffold diameter ratio	1.08 ± 0.11
Max post-dilation balloon, mm	3.20 ± 0.46
Maximum post-dilation inflation pressure, atm	15.50 ± 3.42
Procedural complications	
Dissection	5.1
Slow flow/no reflow	2.7
Clinical device success	97.3
Clinical procedural success	96.8

Values are mean ± SD or %.

IVUS = intravascular ultrasound; OCT = optical coherence tomography.

standard in this study. Side branch wiring before main vessel stenting was employed in 37.5%. Side branch dilation after main vessel stent was performed for 31% and bailout stenting only in 1 BVS. Side branch fenestration was performed in 25%. Side branch dilation was followed by mini-kissing post-dilation of just sequential ballooning with proximal optimalization.

Post-procedural QCA characteristics were: RVD 2.77 ± 0.46 mm, MLD 2.30 ± 0.42 mm, and percentage diameter stenosis 16.90 ± 9.04. Acute lumen gain was 1.39 ± 0.59 mm.

Clinical device success was 97.3% and clinical procedural success was 96.8%. In 5 patients delivery failure of the BVS occurred because the scaffold could not pass the lesion, for example due to severe calcification or tortuosity. After multiple attempts, metal DES were placed in these cases.

CLINICAL OUTCOMES. Survival data was available in 100% with a median follow-up period of 622 days (interquartile range: 376 to 734 days). Two patients withdrew their informed consent within a few weeks after the index procedure.

One-year clinical outcomes are reported in **Table 4**. Event rates are described as Kaplan-Meier estimates. **Figures 2A to 2C** give an impression of the event rates during late follow-up. At 18 months, there were 4 fatalities (all cardiac death) with a Kaplan-Meier estimate of 1.8%. In the per-treatment group, MACE rate at 18 months was 6.8%, mainly driven by the rate of MI (5.2%). There were 2 cases of periprocedural MI. TLR at 18 months was performed in 4.0% and target vessel revascularization in 4.0%. Rate of non-target vessel revascularization was 5.4%. Rate of overall ST at 18 months was 2.7%, with a definite ST rate of 1.9%.

Details of ST cases are summarized in **Table 5**. Narratives of each case are presented in the electronic supplement.

In **Figure 3** we present MACE, its components, and definite/probable ST rates in various subgroups. There was no increased rate of both MACE and definite/probable ST in patients presenting with acute coronary syndrome (NSTEMI and unstable angina) compared to the overall population.

Univariate analysis was performed to identify predictors for the occurrence of MACE and definite/probable ST (**Tables 6 and 7**). Due to lack of power, none of the factors was significant. However, regarding MACE, the following characteristics tended to be associated with ≥2 times increased risk of MACE: male (hazard ratio [HR]: 4.079; p = 0.18), more than 2 scaffolds/lesion (HR: 2.41; p = 0.19), underexpansion (HR: 2.25; p = 0.16), and >65 years of age (HR: 2.11; p = 0.20) (**Table 6**). Regarding ST, the following characteristics tended to be associated with ≥3 times increased risk of ST: >65 years of age (HR: 4.49; p = 0.19), long lesions (HR: 3.55; p = 0.27 for lesions of 20 mm; HR: 3.42; p = 0.22 for lesions of 32 mm), calcified lesion (HR: 3.55; p = 0.27), and RVD ≤ 2.5 mm (HR: 3.26; p = 0.31).

TABLE 4 Kaplan-Meier Estimates at 1 Year for Clinical Event Rate

	ITT (n = 249)	PT (n = 244)
MACE	5.5	5.1
All-cause death	1.3	1.3
Cardiac death	1.3	1.3
Noncardiac death	0.0	0.0
All myocardial infarction	3.8	3.4
Target vessel	2.8	2.5
Target lesion revascularization	3.8	3.4
Target vessel revascularization	3.8	3.4
Non-target vessel revascularization	3.9	3.7
Total scaffold thrombosis	2.1	2.1
Definite scaffold thrombosis	1.3	1.3
Acute	0.0	0.0
Subacute	0.0	0.0
Late	1.3	1.3
Probable scaffold thrombosis	0.4	0.4
Acute	0.0	0.0
Subacute	0.0	0.0
Late	0.4	0.4
Possible scaffold thrombosis	0.4	0.4
Acute	0.0	0.0
Subacute	0.0	0.0
Late	0.4	0.4
Bleeding (Gusto)	2.1	2.2
CVA/TIA	0.9	0.9

Values are %.
PT = per treatment; other abbreviations as in **Table 1**.

Concerning intravascular imaging at baseline, patients who did not undergo baseline imaging had a TLR rate of 4.0%, compared to 2.3% in patients who did undergo baseline imaging (log-rank p = 0.29). Intravascular imaging was performed more often in patients who had a complex lesion (American Heart Association classification type B2/C lesion): 44.5% versus 31.1% (p = 0.03).

To examine the relationship between underexpansion, sizing and MACE, a scatterplot of the preprocedural sizing and post-procedural expansion divided by nominal diameter was created on the basis of QCA (**Figure 4**). When a cutoff value of MLD post-procedure/nominal device diameter of <0.70 is applied, the scaffold was underexpanded in 26% of the lesions. Patients, in whom underexpansion occurred, tended to have an increased rate of MACE: 8.0% versus 3.8% (p = 0.15, log-rank test).

DISCUSSION

To the best of our knowledge this is the first registry reporting on the extended follow-up beyond 1 year, with a median follow-up duration of 622 days. The main findings of our study are that: 1) 12-month MACE incidence for the per-treatment group was 5.1%, mainly driven by rate of MI (approximately 70% due to target vessel MI), with a further flattening of Kaplan-Meier after 1 year (6.8% at 18 months); 2) the rate of definite/probable ST at 1 year was 1.7%, which is higher compared to second generation metal DES (12); 3) patients with acute coronary syndrome did not have increased risk of MACE and ST; and 4) underexpansion of the BVS was a rather frequent finding and there was a trend for an increased rate of MACE.

The BVS Expand registry describes the procedural and medium to long-term clinical outcomes of BVS in patients with native, de novo coronary artery disease. Other studies investigating clinical outcomes of BVS were often characterized by small sample size and inclusion of patients with noncomplex lesions. In this single-center study we report event rates in a more complex lesions including long lesions (mean lesion length 22.10 ± 13.90 mm), calcified and bifurcated lesions, with a relatively high proportion of American College of Cardiology/American Heart Association type B2 or C lesions (38.1%). Furthermore and different from other registries (10), all events were adjudicated by an independent clinical events committee and all angiograms were analyzed using QCA, creating a complete QCA database. Finally, in the present registry there were limited angiographic exclusion criteria that allowed a study population that is more reflective of a real-world population.

Taking into account the complexity of the treated lesions, the 1-year MACE rate of 5.1% observed in the current registry is low and in line with previous trials using BVS in relatively simple lesions: 5% in the ABSORB II (A bioresorbable everolimus-eluting scaffold versus a metallic everolimus-eluting stent for ischaemic heart disease caused by de-novo native coronary artery lesions) trial (7), 5.0% in the ASSURE BVS registry (Beyond the early stages: insights from the ASSURE registry on bioresorbable vascular scaffolds.) (9), 4.3% in the BVS Extend trial (ABSORB EXTEND study: preliminary report of the twelve-month clinical outcomes in the first 512 patients enrolled) (13). Recently, several European registries reported on the 6-month clinical outcomes after implantation of BVS in all-comer settings (**Table 8**). In our registry, 6-month MACE rate was 4.7%, which is comparable to the other registries.

FIGURE 2 Kaplan-Meier Curves for Adverse Events at 18 Months

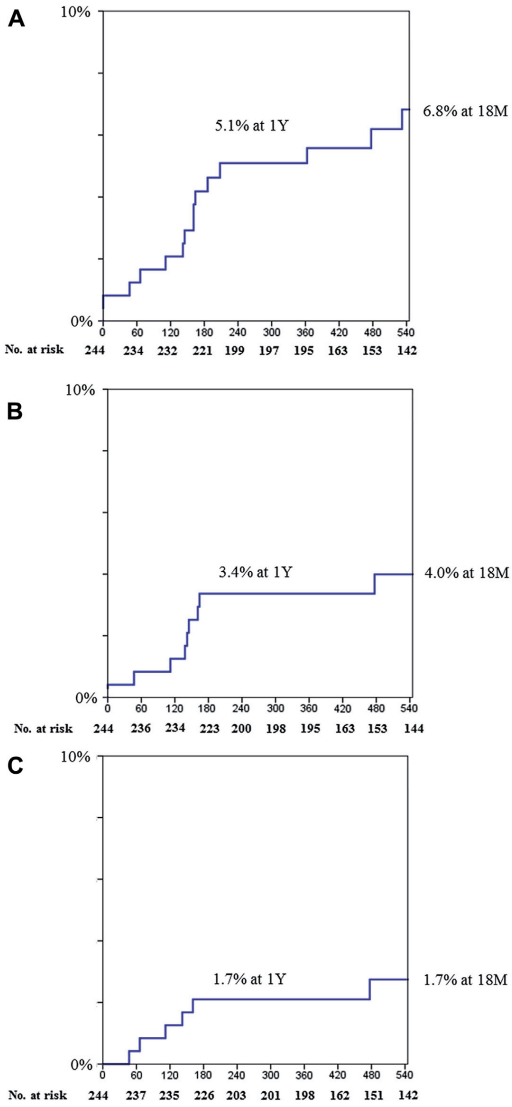

Cumulative rates of **(A)** major adverse cardiac event, **(B)** target lesion revascularization, and **(C)** definite/probable scaffold thrombosis up to 18 months using Kaplan-Meier estimation.

TABLE 5 Overview Cases ST

Case #	Time (days)	Type ST	Age (yrs)	Presentation at Baseline	Vessel	BVS, mm	Pre-Dil	Post-Dil	Baseline Imaging	Patient-Related Factor	DAPT	Possible Mechanism ST	Treatment During Event
1	47	Def	69	NSTEMI	LAD	3.0 × 28, 3.5 × 18, 3.5 × 18	Yes	Yes	Yes	Yes (PCI for ACS)	Yes	Residual thrombus, total occlusion, long lesion, calcification, bifurcation	Thrombectomy, eptifibatide, Xience (3.5 × 38 mm)
2	66	Poss	76	SAP	LAD	3.0 × 18	Yes	Yes	Yes	Yes (KD, SM)	Yes	Bifurcation, calcification	None, sudden death
3	112	Def	58	SAP	LAD	3.5 × 28	Yes	Yes	Yes	Yes (SM, ↓LVF)	Yes	NIH, calcification, underexpansion, long lesion, small vessel	Thrombectomy, Promus (3.5 × 32 mm), eptifibatide
4	142	Prob	65	NSTEMI	LAD	3.0 × 18	Yes	Yes	No	Yes (PCI for ACS, SM)	Yes	Geographical miss, edge restenosis, trifurcated lesion	Thrombectomy, Promus (3.5 × 38 mm)
5	161	Def	70	Decreased LVF	LAD	2.5 × 18 3.0 × 18	Yes	Yes	Yes	Yes (KD, SM, ↓LVF)	No	Interruption anticoagulants due to surgery, calcification, long lesion, small vessel	POBA, eptifibatide

ACS = acute coronary syndrome; BVS = bioresorbable vascular scaffold; DAPT = dual antiplatelet therapy; Def = definite; DM = diabetes mellitus; KD = kidney disease; LAD = left anterior descending; LVF = left ventricular function; NIH = neointima hyperplasia; PCI = percutaneous coronary intervention; POBA = plain old balloon angioplasty; Poss = possible; Post-dil = post-Dilation; Pre-Dil = pre-dilation; Prob = probable; SAP = stable angina pectoris; SM = smoking; ST = scaffold thrombosis.

FIGURE 3 Rate of MACE and Definite/Probable ST, Divided by Subgroups

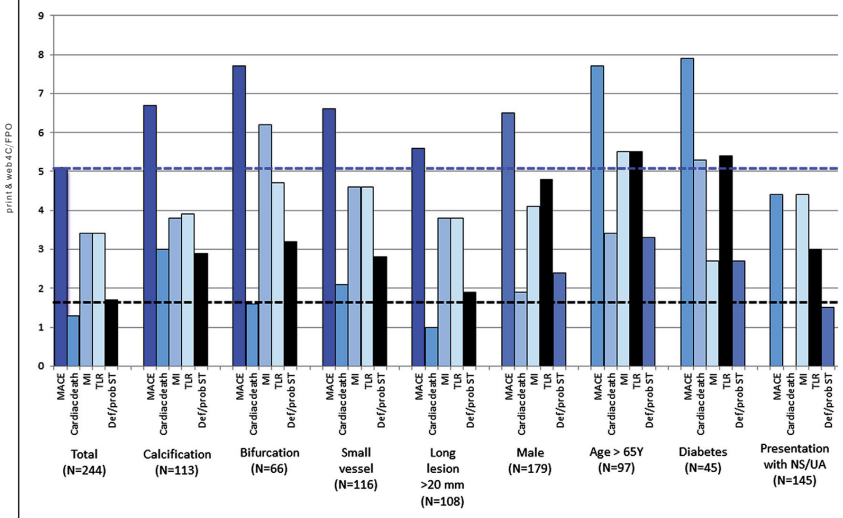

Bar graphs demonstrating the rate of major cardiac adverse event (MACE) rate, its components, and scaffold thrombosis in subgroups of population (e.g., calcification, bifurcation, small vessel). MI = myocardial infarction; NS = non-ST-segment elevation myocardial infarction; ST = scaffold thrombosis; TLR = target lesion revascularization; UA = unstable angina.

TABLE 6 Univariate Analysis of MACE

	Hazard Ratio (95% Confidence Interval)	p Value
Male	4.07 (0.53-31.51)	0.18
>2 scaffolds/lesion	2.41 (0.66-8.84)	0.19
Underexpansion	2.25 (0.73-6.98)	0.16
>65 yrs of age	2.11 (0.67-6.64)	0.20
Bifurcation lesion	1.97 (0.63-6.21)	0.25
Long lesion (>32 mm)	1.73 (0.52-5.76)	0.37
Long lesion (>20 mm)	1.67 (0.53-5.27)	0.38
Calcified lesion	1.64 (0.52-5.17)	0.39
Overlap	1.59 (0.49-5.17)	0.44
RVD ≤2.5 mm	1.56 (0.49-4.91)	0.45
Diabetes mellitus	1.51 (0.41-5.57)	0.54
Presentation with ACS	0.71 (0.23-2.20)	0.55
Imaging at baseline	0.55 (0.15-2.03)	0.37

Underexpansion was defined as PostMLD/nominal device diameter <0.7.
ACS = acute coronary syndrome; MACE = major adverse cardiac events; MLD = minimal lumen diameter; RVD = reference vessel diameter.

FIGURE 4 Relation of BVS Underexpansion and MACE

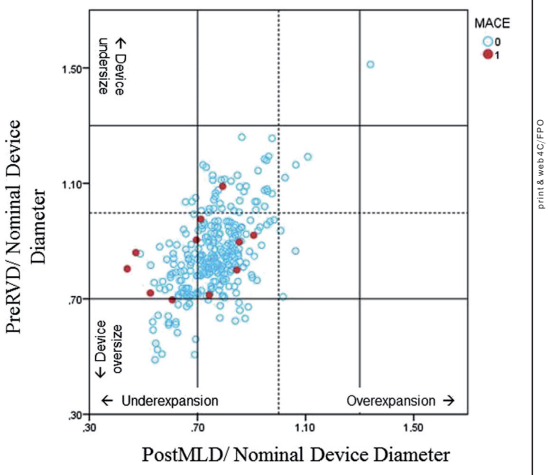

BVS = bioresorbable vascular scaffold; MACE = major adverse cardiac events; MLD = minimal lumen diameter; RVD = reference vessel diameter.

Recently, some concerns were raised regarding a potentially increased rate of ST after implantation of the Absorb BVS (10,14,15). Scaffold thrombosis in the case of metallic DES is an entity with complex multifactorial pathomechanisms, something that probably applies to the case of BVS (16). The importance of patient selection, lesion preparation, pre- and post-dilation, and the consideration of invasive imaging for optimal device deployment have to be emphasized (17,18), whereas dual antiplatelet therapy continuation for at least 1 year is recommended. Pilot imaging observations in real-world patients with BVS thrombosis suggest suboptimal implantation with underexpansion, malapposition, and incomplete lesion coverage, often in combination with dual antiplatelet therapy discontinuation, to be the major substrate both for acute and late events (19). Although it is not clear why this complication is observed in high incidence with BVS, a potential explanation could be the increased thickness of the BVS struts, which can cause convective flow patterns, potentially triggering platelet deposition and subsequent thrombosis, especially in settings with suboptimal flow conditions (20). For this reason, BVS with thinner struts are currently being developed and animal studies are ongoing.

TABLE 7 Univariate Analysis of Probable/Definite Scaffold Thrombosis

	Hazard Ratio (95% Confidence Interval)	p Value
>65 yrs of age	4.49 (0.47-43.15)	0.19
Long lesion (>20 mm)	3.55 (0.37-34.13)	0.27
Calcified lesion	3.55 (0.37-34.13)	0.27
Long lesion (>32 mm)	3.42 (0.48-24.26)	0.22
RVD ≤2.5 mm	3.26 (0.34-31.34)	0.31
Bifurcation lesion	2.72 (0.38-19.31)	0.32
Overlap	2.20 (0.30-15.92)	0.44
Underexpansion	2.19 (0.31-15.53)	0.43
>2 scaffolds/lesion	1.74 (0.21-14.70)	0.61
Diabetes mellitus	1.52 (0.16-14.64)	0.72
Presentation with ACS	0.70 (0.10-4.96)	0.72

Underexpansion was defined as PostMLD/nominal device diameter <0.7.
Abbreviations as in Table 6.

Rate of definite ST in the AMC (Initial experience and clinical evaluation of the Absorb bioresorbable vascular scaffold [BVS] in real-world practice: the AMC Single Centre Real World PCI Registry) registry was 3.0% at 6 months (14). However, in the latter trial, STEMI patients were also included. The annual rate of definite/probable ST in the GHOST-EU (Percutaneous coronary intervention with everolimus-eluting bioresorbable vascular scaffolds in routine clinical practice: early and midterm outcomes from the European multicentre GHOST-EU registry) trial was 3.4% and 70% of the ST cases occurred in the first 30 days. In our study, there were 3 cases of definite ST (1.3%) within 1 year (**Table 5**, Online Appendix). In most of these cases, suboptimal implantation in complex lesions was the main finding, with also inadequate

TABLE 8 Overview of BVS Registries

	ABSORB A	ABSORB B	ABSORB II	BVS EXTEND	ASSURE	ABSORB FIRST	AMC	Milan	GHOST-EU	Robaei et al. (23)	Polish National Registry	BVS EXPAND
N	30	101	355	512	183	800	135	92	1189	100	591	249
Sites	4	9	46	56	6	95	1	2	10	2	30	1
Period	03/06-07/06	03/09-11/09	11/11-06/13	1/10-12/12	4/12-3/13	1/13-3/14	8/12-8/13	5/12-8/13	11/11-1/14	12/10-10/13	10/12-11/13	9/12-01/15
ACS	27%	–	20%	0%	21.3%	38%	48.8%	10.9%	47.4%	44%	52%	59.1%
Single-vessel PCI	100%	99%	–	93%	–	90.7%	81.1%	–	–	85%	–	76.7%
Lesions/patient	1.0	1.0	1.0	1.1	1.1	1.2	1.2	1.5	1.2	1.5	–	1.4
Lesion length	8.2 mm	9.7 mm	21.1 mm	11.9 mm	15 mm	18.3 mm	–	36.5 mm	19.4 mm	20.9 mm	–	22.1 mm
Calcification	–	–	13%	15%	15.7%	20.4%	11.3%	20.4%	–	–	–	45.8%
B2	40%	53.5%	44.0%	41%	43.4%	23.1%	42.1%	83.9%	23.6%	19%	–	24.3%
C	0.0%	5.9%	2.0%	2%	21.2%	23.6%	25.2%		27.6%	37%	–	13.8%
Baseline imaging	100% (IVUS documentary)	100% (IVUS, documentary)	100% (IVUS documentary)	–	–	–	25.0%	?	28.2%	15.8%	–	39.0%
Device success	94%	100%	99.0%	98.6%	–	98.9%	96.0%	–	99.7%	98.8%	100%	97.3%
TLR	3.3% at 1 yr	3.6% at 1 yr	1% at 1 yr	1.8% at 1 yr	2.8% at 1 yr	–	5.0% at 6 months	3.3% at 6 months	2.5% at 6 months	0% at 30 days	–	3.1% at 1 year
TVR	–	–	2% at 1 yr	–	–	–	6.6% at 6 months	3.3% at 6 months	4.0% at 6 months	0% at 30 days	–	3.1% at 1 year
Definite scaffold thrombosis	0% at 1 yr	0% at 1 yr	0.6% at 1 yr	0.8% at 1 yr	0% at 1 yr	0.3% at 30 days	3.2% at 6 months	0% at 6 months	1.7% at 6 months	0% at 30 days	–	1.3% at 1 year
Acute definite ST	0% at 1 yr	0% at 1 yr	0.3% at 1 yr	0.0% at 1 yr	0% at 1 yr	–	0.0% at 6 months	0% at 6 months	1.2% (definite/probable ST) at 6 months	0% at 30 days	–	0% at 1 year
Subacute definite ST	0%	0%	0.3%	0.4%	0%	–	2.4%	0%	1.2% (definite/probable ST)	0%	–	0%
Late definite ST	0%	0%	0%	0.4%	0%	–	0.8%	0%	0.5%	0%	–	1.3%
MACE	3.4% at 5 yrs	9.9% at 3 yrs	5.0% at 1 yr	4.3% at 1 yr	5% at 1 yr	–	–	3.3% at 6 months	TLF: 4.4% at 6 months	4% at 30 days	–	5.3% at 1 year

ACS = acute coronary syndrome; BVS = bioresorbable vascular scaffold; IVUS = intravascular ultrasound; MACE = major adverse cardiac events; PCI = percutaneous coronary intervention; ST = scaffold thrombosis; TLF = target lesion failure; TLR = target lesion revascularization; TVR = target vessel revascularization.

dual antiplatelet therapy duration in 1 case. Notably and in contrast to the other registries, no cases of acute or subacute ST occurred. The lower rate of ST in the BVS Expand registry could presumably be due to the good procedural performance: usage of invasive imaging in almost 40% and pre-dilation in 89%. Unlike the previously mentioned registries, STEMI patients were excluded in our study. The enrolled patients were all appropriately preloaded with P2Y12 inhibitors, which could attribute to the absence of acute and subacute ST, whereas this is not always the case in STEMI patients.

In this study, the presence of with NSTEMI/unstable angina was not associated with an additional risk of MACE or ST. Theoretically, the lesions in patients with acute coronary syndrome are generally lipid rich with or without thrombus, which hinder neither the deployment nor the expansion of the BVS.

Our analysis shows that underexpansion of BVS occurs frequently and had a nonsignificant association with an increased risk of MACE and probable/definite ST. Compared to other BVS registries rate of post-dilation in our study is somewhat low (53.3%) and this could partly explain the frequent occurrence of underexpansion. This low post-dilation rate was an extension of the ABSORB-EXTEND (The ABSORB EXTEND study: preliminary report of the twelve-month clinical outcomes in the first 512 patients enrolled.) and ABSORB II (A bioresorbable everolimus-eluting scaffold versus a metallic everolimus-eluting stent for ischaemic heart disease caused by de-novo native coronary artery lesions) studies, where post-dilation was discouraged as a reflex to a single case where strut fractures were observed due to severe undersizing and post-dilation with an oversized balloon beyond the expansion limits of the scaffold. This is a different situation compared to underexpansion due to atherosclerotic disease where struts are still apposed but the initial lesions are difficult to dilate. It is now clear that for underexpansion high-pressure post-dilation does not result in strut fractures as long as noncompliant post-dilation balloons are used within the maximum expansion limit of the implanted device.

Nevertheless, the arbitrary definition of underexpansion we used for this manuscript was partly on the basis of QCA measurements, which are known to underestimate vessel dimensions when compared to invasive imaging methods such as IVUS and OCT, which is considered the standard at the moment (21,22). The difference for IVUS might be even larger compared to OCT, with an underestimation of approximately of QCA of 0.2 mm versus OCT and 0.3 mm versus IVUS. Use of intravascular imaging might improve pre-procedural vessel sizing, whereas a more liberal use of post-dilation has to be underlined, with the aim of minimizing BVS underexpansion and, eventually, improving the clinical outcome.

STUDY LIMITATIONS. This is a single-center, single-arm registry with no direct comparison with metallic DES. The total number of patients in this study was limited. Thus, these findings warrant further confirmation in a large-scale trial. Ongoing and upcoming trials such as the ABSORB III, ABSORB IV, and the Compare Absorb (ABSORB Bioresorbable Scaffold vs. Xience Metallic Stent for Prevention of Restenosis in Patients at High Risk of Restenosis) will provide data derived from larger patient cohorts and in direct comparison to metallic DES.

Furthermore, deciding which patient or lesion was suitable for BVS implantation could have led to selection bias. Almost 80% of the patients returned their study informed consent and thus follow-up was only investigated in these patients. The event rate is unknown in the remaining patients.

CONCLUSIONS

In our study, BVS implantation in a more complex patient and lesion subset was associated with an acceptable rate of adverse events at the longer term, comparable to rates reported with contemporary second-generation metallic DES, whereas no cases of early thrombosis were observed. This study supports a more extensive use of BVS and launch of randomized trials aiming to demonstrate superiority in the longer term, when optimal implantation strategies are used.

ACKNOWLEDGMENTS The authors want to thank Isabella Kardys, Martijn Akkerhuis, and Johannes Schaar for their contribution in the event adjudication. They also want to thank Nienke van Ditzhuijzen and Saskia Wemelsfelder for their contribution to data management.

REPRINT REQUESTS AND CORRESPONDENCE: Dr. Prof. dr. Robert-Jan M. van Geuns, Thoraxcenter, Room Ba585, Erasmus Medical Center, 's-Gravendijkwal 230, 3015 CE Rotterdam, the Netherlands. E-mail: r.vangeuns@erasmusmc.nl.

PERSPECTIVES

WHAT IS KNOWN? Multiple studies, mainly registries, have proven feasibility and safety of the Absorb BVS. However, data on medium- to long-term outcomes are limited and available only for simpler lesions.

WHAT IS NEW? At a median follow-up duration of 622 days, MACE rate in a regular cath lab population was reasonable with a warning signal for scaffold thrombosis potentially linked to underexpansion.

WHAT IS NEXT? Large randomized controlled trials comparing BVS with metal DES in a more real-world patient population with strict and dedicated BVS implantation strategies are coming up to establish the value of BVS in this setting.

REFERENCES

1. Joner M, Finn AV, Farb A, et al. Pathology of drug-eluting stents in humans: delayed healing and late thrombotic risk. J Am Coll Cardiol 2006; 48:193–202.

2. Raber L, Magro M, Stefanini GG, et al. Very late coronary stent thrombosis of a newer-generation everolimus-eluting stent compared with early-generation drug-eluting stents: a prospective cohort study. Circulation 2012;125:1110–21.

3. Iqbal J, Onuma Y, Ormiston J, Abizaid A, Waksman R, Serruys P. Bioresorbable scaffolds: rationale, current status, challenges, and future. Eur Heart J 2014;35:765–76.

4. Karanasos A, Simsek C, Gnanadesigan M, et al. OCT Assessment of the long-term vascular healing response 5 years after everolimus-eluting bioresorbable vascular scaffold. J Am Coll Cardiol 2014;64:2343–56.

5. Simsek C, Karanasos A, Magro M, et al. Long-term invasive follow-up of the everolimus-eluting bioresorbable vascular scaffold: five-year results of multiple invasive imaging modalities. EuroIntervention 2016;11:996–1003.

6. Onuma Y, Dudek D, Thuesen L, et al. Five-year clinical and functional multislice computed tomography angiographic results after coronary implantation of the fully resorbable polymeric everolimus-eluting scaffold in patients with de novo coronary artery disease: the ABSORB cohort A trial. J Am Coll Cardiol Intv 2013;6:999–1009.

7. Serruys PW, Chevalier B, Dudek D, et al. A bioresorbable everolimus-eluting scaffold versus a metallic everolimus-eluting stent for ischaemic heart disease caused by de-novo native coronary artery lesions (ABSORB II): an interim 1-year analysis of clinical and procedural secondary outcomes from a randomised controlled trial. Lancet 2015;385:43–54.

8. Kimura T, Kozuma K, Tanabe K, et al. A randomized trial evaluating everolimus-eluting Absorb bioresorbable scaffolds vs. everolimus-eluting metallic stents in patients with coronary artery disease: ABSORB Japan. Eur Heart J 2015; 36:3332–42.

9. Wohrle J, Naber C, Schmitz T, et al. Beyond the early stages: insights from the ASSURE registry on bioresorbable vascular scaffolds. EuroIntervention 2015;11:149–56.

10. Capodanno D, Gori T, Nef H, et al. Percutaneous coronary intervention with everolimus-eluting bioresorbable vascular scaffolds in routine clinical practice: early and midterm outcomes from the European multicentre GHOST-EU registry. EuroIntervention 2015;10:1144–53.

11. Cutlip DE, Windecker S, Mehran R, et al. Clinical end points in coronary stent trials: a case for standardized definitions. Circulation 2007;115: 2344–51.

12. Hermiller JB, Rutledge DR, Gruberg L, et al. Sustained low clinical event rates in real-world patients receiving everolimus-eluting coronary stent system from a large, prospective, condition of approval study: 2-year clinical outcomes from the XIENCE V USA Study. J Interv Cardiol 2012;25:565–75.

13. Abizaid A, Ribamar Costa J Jr., Bartorelli AL, et al. The ABSORB EXTEND study: preliminary report of the twelve-month clinical outcomes in the first 512 patients enrolled. EuroIntervention 2015;10:1396–401.

14. Kraak RP, Hassell ME, Grundeken MJ, et al. Initial experience and clinical evaluation of the Absorb bioresorbable vascular scaffold (BVS) in real-world practice: the AMC Single Centre Real World PCI Registry. EuroIntervention 2015;10:1160–8.

15. Ishibashi Y, Nakatani S, Onuma Y. Definite and probable bioresorbable scaffold thrombosis in stable and ACS patients. EuroIntervention 2015;11: e1–2.

16. Capodanno D, Joner M, Zimarino M. What about the risk of thrombosis with bioresorbable scaffolds? EuroIntervention 2015;11:V181–4.

17. Everaert B, Felix C, Koolen J, et al. Appropriate use of bioresorbable vascular scaffolds in percutaneous coronary interventions: a recommendation from experienced users : A position statement on the use of bioresorbable vascular scaffolds in the Netherlands. Neth Heart J 2015;23:161–5.

18. Tamburino C, Latib A, van Geuns RJ, et al. Contemporary practice and technical aspects in coronary intervention with bioresorbable scaffolds: a European perspective. EuroIntervention 2015;11:45–52.

19. Karanasos A, Van Mieghem N, van Ditzhuijzen N, et al. Angiographic and optical coherence tomography insights into bioresorbable scaffold thrombosis: single-center experience. Circ Cardiovasc Interv 2015;8:002369.

20. Kolandaivelu K, Swaminathan R, Gibson WJ, et al. Stent thrombogenicity early in high-risk interventional settings is driven by stent design and deployment and protected by polymer-drug coatings. Circulation 2011;123: 1400–9.

21. Okamura T, Onuma Y, Garcia-Garcia HM, et al. First-in-man evaluation of intravascular optical frequency domain imaging (OFDI) of Terumo: a comparison with intravascular ultrasound and quantitative coronary angiography. EuroIntervention 2011;6:1037–45.

22. Tu S, Xu L, Ligthart J, et al. In vivo comparison of arterial lumen dimensions assessed by co-registered three-dimensional (3D) quantitative coronary angiography, intravascular ultrasound and optical coherence tomography. Int J Cardiovasc Imaging 2012;28:1315–27.

23. Robaei D, Back LM, Ooi SY, Pitney MR, Jepson N. Everolimus-eluting bioresorbable vascular scaffold implantation in real world and complex coronary disease: procedural and 30-day outcomes at two Australian centres. Heart Lung Circ 2015;24:854–9.

KEY WORDS Absorb bioresorbable vascular scaffold, BVS, coronary artery disease, follow-up, mid- to long-term, percutaneous coronary intervention

APPENDIX For an expanded Discussion section, please see the online version of this article.

Mid- to Long-Term Clinical Outcomes of Patients Treated With the Everolimus-Eluting Bioresorbable Vascular Scaffold: The BVS Expand Registry

Cordula M. Felix, Jiang Ming Fam, Roberto Diletti, Yuki Ishibashi, Antonios Karanasos, Bert R.C. Everaert, Nicolas M.D.A. van Mieghem, Joost Daemen, Peter P.T. de Jaegere, Felix Zijlstra, Evelyn S. Regar, Yoshinobu Onuma, Robert-Jan M. van Geuns

oooo

Medium- to long-term outcomes of Absorb bioresorbable vascular scaffold (BVS) (Abbott Vascular, Santa Clara, California) during coronary interventions are limited and available only for simpler lesions. The authors report 12- and 18-month major adverse cardiac event (MACE) rates after implantation of BVS in a large single-center registry including 249 patients with 335 lesions. Using Kaplan-Meier methods, the MACE rate at 18 months was 6.8%. Rates of cardiac mortality, myocardial infarction, and target lesion revascularization at 18 months were 1.8%, 5.2%, and 4.0%, respectively. Definite scaffold thrombosis rate was 1.9%. These data support the potential use of BVS for complex lesions.

23

CHAPTER

EVEROLIMUS-ELUTING BIORESORBABLE VASCULAR SCAFFOLDS IMPLANTED IN CORONARY BIFURCATION LESIONS: IMPACT OF POLYMERIC WIDE STRUTS ON SIDE-BRANCH IMPAIRMENT

De Paolis Marcella, Felix Cordula, van Ditzhuijzen Nienke, **Fam Jiang Ming**, Karanasos Antonis, de Boer Sanneke, van Mieghem Nicolas M, Daemen Joost, Costa Francesco, Bergoli Luis Carlos, Jurgen M.R. Ligthart, Regar Evelyn, de Jaegere Peter , Zijlstra Felix, van Geuns Robert-Jan, Diletti Roberto.

Int J Cardiol. 2016 Oct 15; 221: 656-64.

Everolimus-eluting bioresorbable vascular scaffolds implanted in coronary bifurcation lesions
Impact of polymeric wide struts on side-branch impairment

Marcella De Paolis [1], Cordula Felix, Nienke van Ditzhuijzen, Jiang Ming Fam, Antonis Karanasos, Sanneke de Boer, Nicolas M. van Mieghem, Joost Daemen, Francesco Costa, Luis Carlos Bergoli, Jurgen M.R. Ligthart, Evelyn Regar, Peter P. de Jaegere, Felix Zijlstra, Robert Jan van Geuns, Roberto Diletti *,[1]

Department of Interventional Cardiology, Thoraxcenter, Erasmus MC, Rotterdam, The Netherlands

ARTICLE INFO

Article history:
Received 6 April 2016
Accepted 24 June 2016
Available online 25 June 2016

Keywords:
Bifurcations
Bioresorbable vascular scaffold
Side-branch
Quantitative coronary angiography
Optical coherence tomography

ABSTRACT

Background: Limited data are available on bioresorbable vascular scaffolds (BVS) performance in bifurcations lesions and on the impact of BVS wider struts on side-branch impairment.
Methods: Patients with at least one coronary bifurcation lesion involving a side-branch ≥2 mm in diameter and treated with at least one BVS were examined. Procedural and angiographic data were collected and a dedicated methodology for off-line quantitative coronary angiography (QCA) in bifurcation was applied (eleven-segment model), to assess side-branch impairment occurring any time during the procedure. Two- and three-dimensional QCA were used. Optical coherence tomography (OCT) analysis was performed in a subgroup of patients and long-term clinical outcomes reported.
Results: A total of 102 patients with 107 lesions, were evaluated. Device- and procedural-successes were 99.1% and 94.3%, respectively. Side-branch impairment occurring any time during the procedure was reported in 13 bifurcations (12.1%) and at the end of the procedure in 6.5%. Side-branch minimal lumen diameter (Pre: 1.45 ± 0.41 mm vs Final: 1.48 ± 0.42 mm, p = 0.587) %diameter-stenosis (Pre: 26.93 ± 16.89% vs Final: 27.80 ± 15.57%, p = 0.904) and minimal lumen area (Pre: 1.97 ± 0.89 mm^2 vs Final: 2.17 ± 1.09 mm^2, p = 0.334), were not significantly affected by BVS implantation. Mean malapposed struts at the bifurcation polygon-of-confluence were 0.63 ± 1.11.
Conclusions: The results of the present investigation suggest feasibility and relative safety of BVS implantation in coronary bifurcations. BVS wide struts have a low impact on side-branch impairment when considering bifurcations with side-branch diameter ≥ 2 mm.

1. Introduction

Coronary artery bifurcation treatment is a frequent and challenging subset in interventional cardiology. The introduction of first generation drug eluting stents (DES) was associated with a reduction in main vessel restenosis rate compared with balloon angioplasty or bare metal stent implantation [1,2], but without a clear benefit in terms of side branch ostium impairment and restenosis regardless the technique used [3–5]. Data on second-generation DES, extrapolated from post-hoc analyses of randomized trials are encouraging, with similar long-term mortality after zotarolimus and everolimus DES implantation in bifurcation and non-bifurcation lesions [6]; On the other hand the presence of permanent metallic material at the side-branch ostia could be associated with delayed vascular healing and incomplete neointimal coverage [7] with a possible impact on late thrombotic events [8]. Given this background bioresorbable vascular scaffolds (BVS) could provide a novel paradigm for bifurcation treatment possibly overcoming some of the long-term limitation of metallic DES, avoiding after bioresorption side-branch ostium caging and long-term malapposition. A possible drawback of the BVS usage in such lesions, could be represented by the theoretical risk of an increased acute side-branch impairment due to the wider BVS struts, as previously hypothesized and demonstrated for very small (<0.5 mm) side-branches [9]. Despite the presence of recently reported analyses in relatively simple lesions, [10] at the current state of the art, very limited data are available on BVS performance in bifurcation lesions [11,12] especially when evaluating the impact of BVS

* Corresponding author at: Department of Cardiology, Thoraxcenter, Room Ba-581, Erasmus University Medical Centre, 's-Gravendijkwal 230, 3015 GE Rotterdam, The Netherlands.
E-mail address: r.diletti@erasmusmc.nl (R. Diletti).
[1] MDP and RD equally contributed to this article.

implantation on side-branch impairment in vessels with a visually estimated diameter ≥ 2.0 mm. Therefore, we sought to report feasibility, procedural performance and acute angiographic results after BVS implantation in this specific subgroup with a detailed evaluation of side-branch ostium at pre-and post implantation and describing mid-term clinical outcomes.

2. Methods

The present report is an investigator initiated, single-arm, single-centre study to assess feasibility and performance of the second-generation everolimus-eluting BVS for the treatment of patients with coronary bifurcation lesions.

Patients eligible for the present analysis were ≥ 18 years of age, presenting with stable angina or acute coronary syndromes with at least one *de novo* bifurcation lesion (regardless of morphology, number, length and angulations), involving a side-branch (SB) ≥ 2 mm by visual estimation in diameter treated with at least one BVS implantation. Exclusion criteria were minimal comprising pregnancy, known intolerance to contrast medium and participation to another investigational drug or device study before reaching the primary endpoints. Procedural details, including materials and techniques were collected. Pre- and post-BVS implantation off-line two-dimensional quantitative coronary angiography (QCA) and, if technically feasible, off-line three-dimensional-QCA were performed. Optical coherence tomography (OCT) analyses at post-BVS implantation in a subgroup of patients, and clinical long-term clinical outcomes were evaluated. All patients included in the present analyses were part of the bioresorbable vascular scaffold evaluation program at the Thoraxcenter Rotterdam, The Netherlands and were already included in the EXPAND or in the BVS STEMI FIRST study.

Survival status information was obtained from the national population registry. A questionnaire was sent to all living patients with specific queries on re-hospitalization and cardiovascular events. Patients received the questionnaire on planned follow-up (1-, 6-, 12-month follow-up).

For patients who suffered an adverse event at another center, medical records or discharge letters from the other institutions were systematically reviewed.

In case of death all possible events in that specific patient were investigated by reviewing our hospital records and referring hospitals or general practitioner were contacted to collect as much information as possible.

In case patients did not send back the questionnaires, a second form was sent by post after one month. If this was not returned, patients were contacted by phone.

2.1. Ethics

This is an observational study, performed according to the privacy policy of the Erasmus MC and to the Erasmus MC regulations for the appropriate use of data in patient-oriented research, which are based on international regulations, including the declaration of Helsinki. The BVS received the CE mark for clinical use, indicated for improving coronary lumen diameter in patients with ischaemic heart disease due to *de novo* native coronary artery lesions with no restriction in terms of clinical presentation. Therefore, the BVS can be currently used routinely in Europe in different settings comprising the acute MI without a specific written informed consent in addition to the standard informed consent to the procedure. Given this background, a waiver from the hospital Ethical Committee was obtained for written informed consent, as according to Dutch law written consent is not required, if patients are not subject to acts other than as part of their regular treatment.

2.2. Study procedure

The procedures were performed according to standard practice. The device implantation was performed in accordance with the manufacturer's recommendations, at a rate of 2 atm per 5 s up to burst pressure. Pre- and post-dilatation were encouraged but not mandatory. Wiring of the side-branch before main vessel stenting was performed at the operator's discretion and mainly based on the extension of the disease and anatomical characteristics. A single scaffold approach was encouraged as preferred approach for the majority of cases. Side-branch treatment was recommended only in cases with side-branch impairment or significant atherosclerotic disease. After the procedure, dual antiplatelet therapy was recommended for at least one year followed by aspirin indefinitely.

2.3. Definitions

Device success was defined as the attainment of a residual final stenosis <30% in Main vessel (MV) or side-branch (SB) segment covered by BVS. Procedural success was defined as device success and no major peri-procedural complications (emergent CABG, coronary perforation requiring pericardial drainage, residual dissection impairing vessel flow with final TIMI-flow grade ≤ 2 in MV or SB). Clinical success was defined as procedural success and no in-hospital major adverse cardiac events (MACEs). All deaths were considered cardiac unless an undisputed non-cardiac cause was identified. Myocardial infarction (MI) and scaffold thrombosis were defined according to the Academic Research Consortium definition. Any target bifurcation revascularization was defined as clinically driven if at repeat angiography a diameter stenosis >70% was observed, or if a diameter stenosis >50% was present in the main vessel or in the daughter branches in association with 1) recurrent angina pectoris; 2) objective signs of ischaemia (electrocardiogram changes) at rest or during exercise test, likely to be related to the target vessel; 3) abnormal results of any invasive functional diagnostic test. The target bifurcation failure was defined as the composite of cardiac death, target vessel myocardial infarction, or clinically-driven target bifurcation revascularization. MACEs were defined as the composite of cardiac death, any re-infarction (Q or Non Q-Wave) or clinically-driven target bifurcation revascularization.

To investigate the BVS performance in MV/SB ostium, we adopted the following procedural and angiographic parameters already reported in de the literature [7]:

- "Side-branch impairment", as previously described [7] and defined as a composite of 1) SB TIMI flow grade < 3 after MV stenting, 2) need of guidewire(s) different from the default wire to rewire SB after MV stenting, 3) failure to rewire the SB after MV stenting, or 4) failure to dilate the SB after MV stenting and SB rewiring;
- "SB acute angiographic result", defined as the comparison between the pre- and the post-procedure 2-dimensional QCA–estimated minimal lumen diameter of 3-mm ostial SB sub-segment, according to the modified eleven-segment model analysis [13–15].

2.4. Study device

The second-generation everolimus-eluting BVS (ABSORB; Abbott Vascular, Santa Clara, CA, USA) consist of a backbone of semi crystalline polymer of poly-L-lactide acid, an amorphous matrix of poly-DL-lactide acid which controls the everolimus release (100 micrograms/cm2) and two markers of platinum at proximal and distal edges of scaffold which are radiopaque and facilitate the correct implantation of device. The entire polymer is degraded to carbon dioxide and water.

2.5. Quantitative coronary angiography analysis

Off-line quantitative coronary angiography (QCA) analysis was performed using the Cardiovascular Angiography Analysis System (CAAS; Version 5.10, Pie Medical Imaging, Maastricht, the Netherlands) software packages, according to methodological standards previously described and adopting the modified- eleven-segment model [13–15]. Only matched pre- and post-BVS implantation projections were considered for the analyses. Two-dimensional QCA (2DQCA)was performed using the angiographic image with the largest distal bifurcation angle. 3-dimensional QCA (3DQCA) was performed if at least two projections had been acquired at least 30° apart; The following parameters were included: reference vessel diameter (RVD), minimal lumen diameter (MLD) and percentage diameter stenosis (%DS) of MV, SB and 3-mm ostial SB sub-segment (segment 8 in the eleven segment model), bifurcation proximal angle (between proximal MV and SB) and bifurcation distal angle (between distal MV and SB). If 3DQCA was feasible, minimal lumen area and percentage area stenosis of MV, SB and 3-mm ostial SB sub-segment were added (Fig. 1). Bifurcation lesions were classified according to the Medina classification; AHA/ACC modified lesion criteria, extent of coronary disease, presence of calcification, lesion length, SB and main vessel (MV) thrombolysis in myocardial infarction (TIMI)-flow grade.

2.6. Optical coherence tomography image acquisition and analysis

Intravascular imaging was encouraged but not mandatory and left to the operator discretion. The Optical coherence tomography (OCT) examination was performed with the Illumien or Illumien Optis systems and the corresponding Dragonfly or Dragonfly Duo intravascular imaging catheters (St. Jude Medical, St. Paul, MN, USA). The catheter was advanced into the MV distally to the treated segment and then automated pullback (20 mm/s) and simultaneous contrast injection (flush rate 3–4 mL/s) were performed to acquire the images. Off-line analysis of the OCT images was performed using the QCU-CMS software (Medis Medical Imaging System, Leiden, The Netherlands) at 1-mm longitudinal intervals within the treated coronary segment, including proximal and distal 5-mm edge segments, after exclusion of frames with <75% lumen contour visibility, using previously described methodology for the analysis of bioresorbable scaffolds [16]. Morphometric measurements were performed as previously described, using the abluminal strut points for the delineation of the scaffold contour. A scaffold strut was defined as incompletely apposed when there was no contact between the abluminal border of the strut and the vessel wall. This definition does not include struts located in front of SBs ostia which were defined as SB-related struts and were recorded separately. The bifurcation of interest was identified in the OCT pullback and divided in 3 subsegments: proximal, polygon of confluence and distal (Fig. 2). Strut apposition was calculated separately for each of the sub-segments.

2.7. Statistical analysis

Continuous variables were expressed as mean and standard deviation or as median and interquartile ranges if data were non-normally distributed. Dichotomous variables are presented as count and/or percentages. The paired *t*-test was used for comparison between pre and post-procedure QCA parameters. Statistical analysis was performed using SPSS, version 20.0 for Windows (SPSS Inc., Chicago, IL,US).

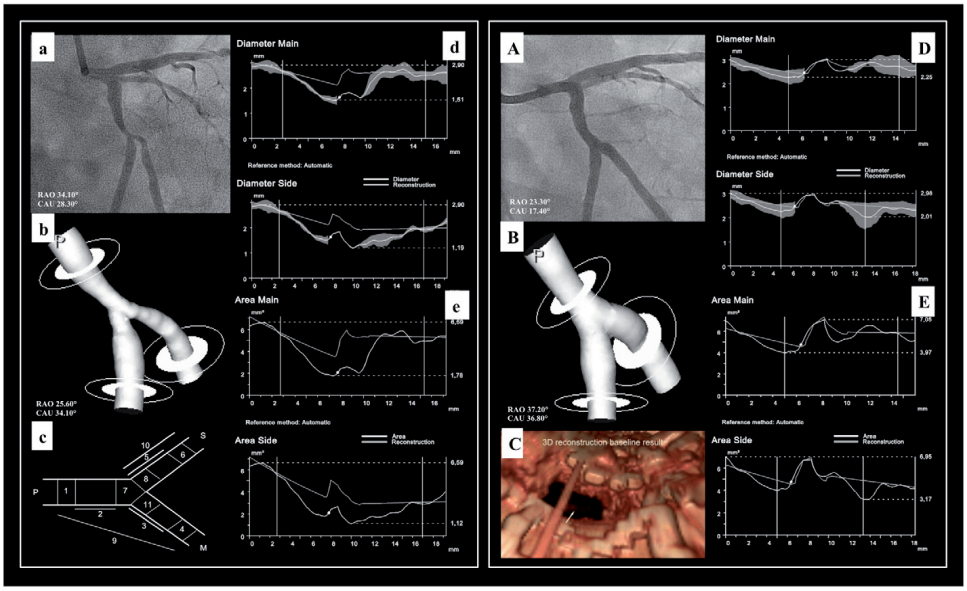

Fig. 1. Quantitative coronary analysis and 3-dimensional reconstruction. – a. Pre-procedural angiogram of treated bifurcation was acquired at RAO34.10°CAU28.30° and LAO51.30°CAU29.70° (not shown). b. 3-dimensional reconstruction is shown in the optimal projection (P = proximal main vessel). **c.** 11-segment model in Cardiovascular Angiography Analysis System (CAAS); P, M and S = proximal main vessel, distal main vessel and side branch, respectively. d and e. Pre-procedural reference vessel diameter and area curve, respectively, for proximal main vessel into distal main vessel and side branch. A. Post-procedural angiogram. B and C. 3-dimensional reconstruction using 3dimensional-QCA and 3-dimensional OCT, respectively (white arrow indicates SB ostium). D and E. Post-procedural reference vessel diameter and area curve, for proximal main vessel into distal main vessel and side branch.

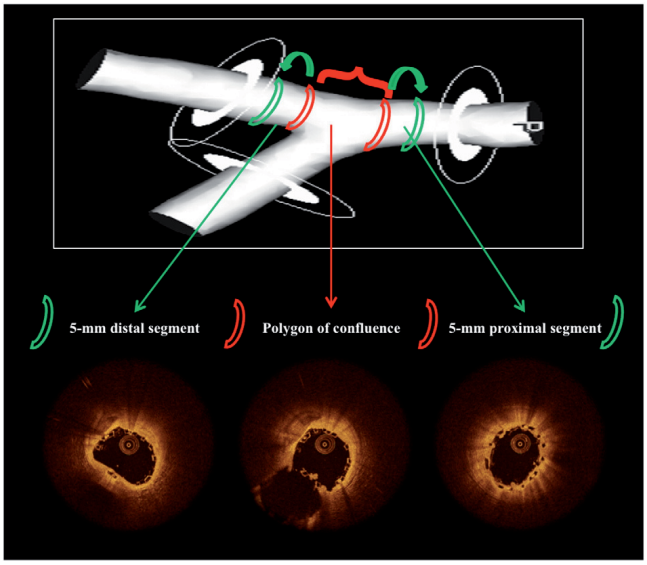

Fig. 2. Sub-segments location in the treated bifurcation lesion. – The bifurcation of interest was identified in the OCT pullback and divided in 3 sub-segments: we defined the polygon of confluence as the sub-segment between the last (distally) and the first (proximally) cross sections (red lines) in which the contorn was not distorced by the side branch. The distal and proximal sub-segments (green lines) were defined as the 5-mm distal and the 5-mm proximal sub-segments from the last and the first cross sections of the polygon of confluence, respectively.

3. Results

A total of 102 patients, with 107 bifurcation lesions, were included in this study. The baseline clinical characteristics are reported in Table 1. Briefly, the average age was 59.61 ± 10.79 years, 81.4% of the patients were male, 43.9% showed a multivessel disease, 57.8% were admitted with an acute coronary syndrome and approximately one third of these acute patients presented with ST-segment elevation myocardial infarction (Table 1).

3.1. Angiographic and procedural characteristics

Angiographic characteristics of bifurcation lesions (N = 107) are listed in Table 2. The most frequently treated lesion was on left anterior descending/diagonal bifurcation (68.2%), a large part of the lesions involved both the main branch and the side-branch (true bifurcation lesions 42.0%), moderate or severe calcification was present in nearly one third of the lesions (28.9%) and long lesions were commonly observed (55.1%). In 10 cases (9.3%) the bifurcation was located in chronically occluded coronary segments.

Reflecting the presence of acute patients TIMI flow 0 or 1 pre-intervention was reported in 17 main vessel lesions (15.9%) and with a similar rate in the side-branch (Table 2).

The most commonly performed technique was the provisional one scaffold approach (93.4%). A crossover from a one-scaffold to two-scaffolds technique occurred in only one case.

Pre-dilation was highly recommended and performed in 84.1% of the main vessels and 23.4% of the side-branches before treatment.

Side-branch wire protection before provisional scaffolding was performed in 38.0% of the cases, in 41 cases (38.3%) a highly supportive wire (Hi-Torque Balance Heavyweight or Hi-Torque Whisper ES) was the default for wiring the MV or the SB (MV 32.7%, SB 9.3%).

Table 1
Baseline clinical characteristics.

Patient characteristics	N = 102
Age, yrs	59.61 ± 10.79
Gender (male)	83 (81.4)
Risk factors	
Family History of CAD	30 (29.4)
Diabetes mellitus	16 (15.7)
Hypercholesterolemia	53 (52.0)
Hypertension	57 (55.9)
Active smoking	42 (41.2)
Kidney disease	6 (5.9)
Clinical history	
Previous MI	23 (22.5)
Previous PCI	15 (14.7)
Previous CABG	2 (2.0)
Previous TIA/stroke	4 (3.9)
Peripheral arterial disease	7 (6.9)
Chronic obstructive pulmonary disease	5 (4.9)
Extent of coronary artery disease	
Single vessel disease	60 (56.1)
2-vessel disease	40 (37.4)
3-vessel disease	6 (5.6)
Left main	1 (0.9)
Clinical presentation	
Acute coronary syndrome	59 (57.8)
STEMI	19 (18.6)
Acute heart failure	2 (2.0)
Out-hospital cardiac arrest	2 (2.0)

Values are expressed as mean ± standard deviation (SD) or count (n) and percentages (%). CABG = coronary artery by-pass; CAD = coronary artery disease; MI = myocardial infarction; PCI = percutaneous coronary intervention; STEMI = ST-segment elevation myocardial infarction; TIA = transient ischemic attack.

Table 2
Angiographic characteristics.

Number of bifurcations	N = 107
Target bifurcation	
Distal left main	2 (1.9)
Left anterior descending/Diagonal	73 (68.2)
Circumflex/Marginal	26 (24.3)
Right posterior descending/posterior lateral	6 (5.6)
ACC/AHA modified lesion classification	
Type B2	73 (68.2)
Type C	34 (31.8)
True bifurcations	45 (42.0)
Moderate or severe calcification	31 (28.9)
Length lesion > 20 mm	59 (55.1)
Chronic total occlusion	10 (9.3)
Medina bifurcation classification	
1.1.1	20 (18.7)
1.1.0	24 (22.4)
1.0.1	11 (10.3)
0.1.1	14 (13.1)
1.0.0	14 (13.1)
0.1.0	18 (16.8)
0.0.1	6 (5.6)
MV TIMI flow pre-procedure	
0	13 (12.1)
1	4 (3.7)
2	3 (2.8)
3	87 (81.3)
SB TIMI flow pre-procedure	
0	9 (8.4)
1	4 (3.7)
2	2 (1.9)
3	92 (85.9)

Values are expressed as count (n) and percentages (%).
ACC/AHA = American College of Cardiology/American Heart Association; MV = main vessel; SB = side branch; TIMI = thrombolysis in myocardial infarction.

Table 3
Procedural characteristics.

Number of bifurcations	N = 107
Technique	
Provisional	100 (93.4)
T-stenting	5 (4.7)
Culotte	1 (0.9)
Mini-crush	1 (0.9)
MV direct stenting	14 (13.1)
MV pre-dilation	90 (84.1)
Semi-compliant balloon	82 (76.6)#
Non-compliant balloon	17 (15.9)#
SB wiring before MV provisional stenting	38 (38.0)*
Default supportive wire	41 (38.3)
MV supportive wire	35 (32.7)
SB supportive wire	10 (9.3)
Cutting balloon	1 (0.9)
Rotablator	2 (1.9)
SB ostium dilation before MV treatment	25 (23.4)
Total number of scaffolds	178
Mean scaffolds per-bifurcation	1.66 ± 0.84
MV Scaffold	104 (97.2)
Scaffold diameter (mm)	3.03 ± 0.4
Scaffold length (mm)	19.95 ± 5.6
SB Scaffold	14 (13.1)
Scaffold diameter (mm)	2.8 ± 0.3
Scaffold length (mm)	16.21 ± 4.8
MV post-dilation	64 (59.8)
Semi-compliant balloon	17 (15.9)#
Non-compliant balloon	52 (48.5)#
POT	38 (35.5)
Final kissing balloon inflation	5 (4.6)
SB ostium dilation after MV stent	39 (36.4)
Balloon diameter (mm)	2.03 ± 0.48
Vascular access	
Radial	66 (61.7)
Femoral	42 (39.2)
Contrast media (ml)	208.15 ± 90.82

Values are expressed as mean ± standard deviation (SD) or count (n) and percentages (%). * % calculated over all provisional approach. # In the same vessel both semi-compliant and non-compliant balloons could have been used.
MV = main vessel; POT = Proximal Optimization Technique; SB = side branch.

One-hundred and seventy-eight Absorb BVS were implanted, with a maximum scaffolded length of 102 mm (4 BVS). To achieve an optimal final angiographic result, the MV post-dilation was performed in 64 cases (59.8%), non-compliant balloons were frequently used (52/64, 81.2%) and a proximal optimization technique (POT) was performed in the 59.4% of overall post-dilations.

SB ostium dilation across MV scaffold struts was performed in 39 bifurcations (36.4%), using balloons with mean diameter of 2.03 mm ± 0.48 and semi-compliant in the 99% of cases (Table 3).

The device success was achieved in 99.1% of the cases (106/107), in one calcified lesion a residual final stenosis not inferior to 30% persisted at the end of the procedure. The procedural success was 94.3%, in one case, a distal edge dissection caused a post-procedure MV TIMI flow grade equal to 1 and in 4 cases the final SB TIMI flow grade was inferior to 3 (TIMI flow 0 in one case, after MV provisional approach without a previous SB wiring). The "SB impairments" occurred in 13 procedures (12.1%). The most frequently reported cause was a SB TIMI flow grade < 3 after MV scaffolding, reported in 10 cases. In 6 of those cases the final SB TIMI flow grade improved after SB ostium post-dilation, with no need for SB treatment (Table 4).

3.2. Quantitative coronary angiography analysis

Two-dimensional and 3-dimensional QCA were performed in 103 patients and 40 patients, respectively (inadequate views either pre- or post- procedure were excluded).

At the end of the procedure, the side-branch was not significantly affected by the BVS implantation the main vessels. In the 2-dimensional and the 3-dimensional QCA analyses, there were no differences between the pre- and post-procedure reference vessel diameter (2D RVD: 1.98 ± 0.33 mm vs 2.03 ± 0.41 mm, p = 0.718 - 3D RVD: 2.00 ± 0.28 mm vs 2.08 ± 0.34 mm, p = 0.28), minimal lumen diameter (2D MLD: 1.45 ± 0.41 mm vs 1.48 ± 0.42 mm, p = 0.587 - 3D MLD: 1.54 ± 0.37 mm vs 1.61 ± 0.41 mm, p = 0.363), and minimal lumen area (3D MLA 1.97 ± 0.89 mm^2 vs 2.17 ± 1.09 mm^2, p = 0.334). In true bifurcation lesions the (2D) diameter stenosis appeared significantly increased (%DS pre PCI 58.7% vs 31.9%, p = 0.0001) after treatment.

Additionally, also in the 3-mm ostial SB sub-segment, no statistically significant pre- and post-procedural variations were reported in terms of reference vessel diameter (2D RVD: 1.99 ± 0.33 mm vs 2.06 ± 0.38 mm, p = 0.309 - 3D RVD: 2.03 ± 0.28 mm vs 2.10 ± 0.32 mm, p = 0.123), minimal lumen diameter (2D MLD: 1.51 ± 0.38 mm vs 1.53 ± 0.44 mm, p = 0.567 - 3D MLD: 1.59 ± 0.35 mm vs 1.62 ±

Table 4
Procedural results.

Number of bifurcations	N = 107
Device success	106 (99.1)
Procedural success	101 (94.3)
Final MV TIMI flow grade 3	106 (99.1)
Final SB TIMI flow grade 3	103 (96.3)
SB impairment	13 (12.1)
SB TIMI flow grade < 3 after MV stenting	10 (9.3)
SB TIMI flow grade = 0 after MV stenting	4 (3.7)
SB TIMI flow grade = 1 after MV stenting	2 (1.9)
SB TIMI flow grade = 2 after MV stenting	4 (3.7)
Need to guidewire(s) different from the default wire to rewire SB after MV stenting	5 (4.7)
Failure to rewire the SB after MV stenting	1 (0.9)
Failure to dilate the SB after MV stenting	1 (0.9)

Values are expressed as count (n) and percentages (%).
MV = main vessel; SB = side branch; TIMI = thrombolysis in myocardial infarction.

Table 5
Pre- and post-procedural vessel diameters 2D-QCA-evaluation.

Number of bifurcations	Pre-PCI (N = 103)	Post-PCI (N = 103)	p value
Main vessel			
Reference diameter (mm)	2.63 ± 0.61	2.77 ± 0.55	0.286
Minimal lumen diameter (mm)	1.30 ± 0.55	2.35 ± 0.52	<0.001
% diameter stenosis	50.13 ± 18.86	15.14 ± 8.40	<0.001
Side branch			
Reference diameter (mm)	1.98 ± 0.33	2.03 ± 0.41	0.718
Minimal lumen diameter (mm)	1.45 ± 0.41	1.48 ± 0.42	0.587
% diameter stenosis	26.93 ± 16.89	27.80 ± 15.57	0.904
3-mm ostial side branch sub-segment			
Reference diameter (mm)	1.99 ± 0.33	2.06 ± 0.38	0.309
Minimal lumen diameter (mm)	1.51 ± 0.38	1.53 ± 0.44	0.567
% diameter stenosis	23.97 ± 15.99	25.82 ± 16.15	0.697
Angle			
Proximal main vessel/side branch (°)	143.58 ± 17.44	143.53 ± 18.04	0.282
Distal main vessel/side branch (°)	53.47 ± 15.65	52.68 ± 17.95	0.764

Values are expressed as mean ± SD. PCI = percutaneous coronary intervention.

0.41 mm, p = 0.760) minimal lumen area (3D MLA 2.10 ± 0.86 mm^2 vs 2.19 ± 1.10 mm^2, p = 0.660) (Tables 5 and 6).

3.3. Optical coherence tomography findings

OCT imaging was performed in 20 bifurcations after BVS implantation (Table 7). Incomplete scaffold apposition (ISA) was observed in 15 patients, with a mean ISA area of 0.12 ± 0.14 mm^2 and a mean percentage of malapposed struts per patient equal to 3.87 ± 4.12%.

The sub-segments analysis was available in 19 cases (one case was excluded owing to incomplete pullback of treated MV). The mean percentages of malapposed struts per patient in distal, polygon of confluence and proximal sub-segments were 1.50 ± 2.59%, 4.08 ± 9.45% and 6.41 ± 16.99% respectively.

In the sub-group of patients in which a proximal optimization technique (POT) was performed, the percentages of malapposed struts in the polygon of confluence and in the proximal sub-segment were numerically lower compared with the sub-group in which POT was not performed (1.54 ± 3.42% vs 6.37 ± 12.49% and 3.31 ± 3.57% vs 8.33 ± 24.29% respectively).

Table 6
Pre- and post-procedural vessels diameters and areas 3DQCA-evaluation.

Number of bifurcations	Pre-PCI (N = 40)	Post-PCI (N = 40)	p value
Main vessel			
Reference diameter (mm)	2.60 ± 0.72	2.77 ± 0.48	0.128
Minimal lumen diameter (mm)	1.48 ± 0.59	2.43 ± 0.46	<0.001
Minimal lumen area (mm^2)	1.99 ± 1.52	4.81 ± 1.70	<0.001
Percentage area stenosis	63.47 ± 21.49	22.15 ± 12.27	<0.001
Side branch			
Reference diameter (mm)	2.00 ± 0.28	2.08 ± 0.34	0.280
Minimal lumen diameter (mm)	1.54 ± 0.37	1.61 ± 0.41	0.363
Minimal lumen area (mm^2)	1.97 ± 0.89	2.17 ± 1.09	0.334
Percentage area stenosis	42.25 ± 21.50	38.62 ± 21.33	0.305
3-mm ostial side branch sub-segment			
Reference diameter (mm)	2.03 ± 0.28	2.10 ± 0.32	0.123
Minimal lumen diameter (mm)	1.59 ± 0.35	1.62 ± 0.41	0.760
Minimal lumen area (mm^2)	2.10 ± 0.86	2.19 ± 1.10	0.660
Percentage area stenosis	34.98 ± 19.98	37.48 ± 20.28	0.798
Angle			
Proximal main vessel/side branch (°)	139.19 ± 15.94	140.86 ± 14.70	0.597
Distal main vessel/side branch (°)	59.02 ± 12.31	55.23 ± 13.34	0.189
Proximal main vessel/distal main vessel (°)	152.40 ± 13.08	155.74 ± 10.27	0.128

Values are expressed as mean ± SD. PCI = percutaneous coronary intervention.

Table 7
Optical coherence tomography (OCT) analysis post-scaffold implantation in bifurcated coronary lesions.

OCT variables	N = 20
In-segment analysis	
Minimum lumen area (mm^2)	5.05 ± 1.05
Mean lumen area (mm^2)	7.36 ± 1.37
Lumen volume (mm^3)	231.49 ± 97.72
Minimum scaffold area (mm^2)	5.68 ± 1.08
Mean scaffold area (mm^2)	7.61 ± 1.45
Scaffold volume (mm^3)	236.88 ± 99.71
Mean ISA area (mm^2)	0.12 ± 0.14
Max ISA area (mm^2)	1.64 ± 1.56
% ISA area	1.71 ± 2.22
Mean prolapse area (mm^2)	0.47 ± 0.27
Max prolapsed area (mm^2)	1.40 ± 0.75
% prolapse	6.27 ± 3.46
Distal dissection (N = 15)	5 (33.3)
Proximal dissection (N = 17)	4 (23.5)
Analyzed struts per patient	292 ± 117.52
Malapposed struts per patient	10.15 ± 8.37
% malapposed struts	3.87 ± 4.12
Side branch struts per bifurcation	3.20 ± 2.31
5-mm proximal MV sub-segment (N = 19)	
Malapposed struts	2.11 ± 4.53
% malapposed struts	6.41 ± 16.99
Polygon of confluence (POC) (N = 19)	
Malapposed struts	0.63 ± 1.11
% malapposed struts	4.08 ± 9.45
SB-related struts	2.0 ± 2.13
5-mm distal MV sub-segment (N = 19)	
Malapposed struts	0.61 ± 1.09
% malapposed struts	1.50 ± 2.59

Values are expressed as mean ± SD, median [IQR] or n (%). ISA = incomplete scaffold apposition. MV = main vessel. OCT = optical coherence tomography. POC = polygon of confluence.

3.4. Clinical outcomes

Survival status was available in 99.0% (101/102). The overall mortality at one year was 2.2% (2/101). Clinical follow-up rate was 91.1% (92/101) with a median follow up duration of 731 days (interquartile range, IQR: 644–762 days). 89 patients had a follow-up of at least one year (2 patients had a follow-up duration of 353 and 332 days respectively. One patient was lost to follow-up with follow-up duration of 202 days).

The remaining 9 out of 101 patients could not be approached for clinical follow-up the cause was refusal to participate and in one case emigration. A total of 5 patients were reported to have major adverse cardiac event (Fig. 4) including 1 cardiac death (and possible ST), 4 MI (2 ST-segment elevation MI, one periprocedural MI caused by a distal-edge scaffold dissection and one occurred after a staged procedure on a non-target vessel, and 2 non ST-segment elevation MI, both due to a late scaffold thrombosis (Table 8), 3 ischemia-driven target bifurcation

Table 8
Clinical outcomes at 1-year follow-up.

Clinical events	N = 102
Major adverse cardiac events	5.5%
All cause death	2.2%
Cardiac death	1.1%
Myocardial infarction	4.4%
Target lesion revascularization	3.3%
Target vessel revascularization	6.6%
Non- target vessel revascularization	3.4%
Scaffold thrombosis	3.3%
Definite ST	2.2%
Probable ST	0.0%
Possible ST	1.1%

Table 9
Cases of definite scaffold thrombosis.

Case #	Type of lesion	Technique	Device size (mm)	Timing (days from index procedure to scaffold thrombosis)	Dual antiplatelet therapy at the time of scaffold thrombosis
1	LAD/1°diagonal Medina 1.1.1 Angulation 78°	"Provisional MV stenting"	3.0 × 18	142	ASA (80 mg) + PRASUGREL (10 mg)
2	LAD/1°diagonal CTO	"Provisional MV stenting"	3.0 × 28 3.5 × 18 3.5 × 18 (2 overlap)	47	ASA (80 mg) + CLOPIDOGREL (75 mg)

ASA = aspirin; CTO = chronic total occlusion; LAD = left anterior descending; MV = main vessel.

revascularizations (due to an in-scaffold restenosis inducing angina). At one year, 2 cases of definite ST (at day 47 and at day 142) occurred. (See Table 9.)

4. Discussion

The initial clinical experience with bioresorbable vascular scaffolds has been focused on simple lesions and relatively stable patients. Recent data, mainly derived from registry, provided additional information on safety, feasibility and performance of BVS in more complex lesions and patients [17,18], however specific challenging subsets such as bifurcation lesions remain poorly investigated.

In the present study we reported the BVS performance after implantation in bifurcation lesions in a wide range clinical scenarios, including patients presenting with acute myocardial infarction or showing multivessel disease (Fig. 3) and coronary chronic total occlusions.

The approach adopted in the vast majority of the cases was a T-provisional scaffolding, a solid amount of evidence suggests this strategy as to be the preferable in most of the bifurcation cases [19,20]. Such evidences are provided from studies performed with metal stents but it is reasonable to apply the same principles to bioresorbable devices, especially considering the fact that a single scaffold technique reduce the amount of polymer at the bifurcation site, avoids overlap and the need for multiple layer of polymer.

The scaffold sizing in bifurcation lesions could be challenging in case of remarkable vessel tapering distally to the side-branch.

Recently Ishibashi et al. reported that oversizing the implanted scaffold compared to both the proximal and distal vascular maximal diameter (Dmax) could be associated with clinical events. On the other hand underexpansion was also shown to increase the risk of scaffold thrombosis [21]. Probably a reasonable approach could be to balance the proximal and distal Dmax, ensuring optimal apposition proximally after postdilatation, without causing high vessel stretch and injury distally.

In the present series the size of the BVS was usually chosen on the basis of the proximal maximal diameter (Dmax) [22] but also taking into account the distal Dmax, often performing low-pressure deployment

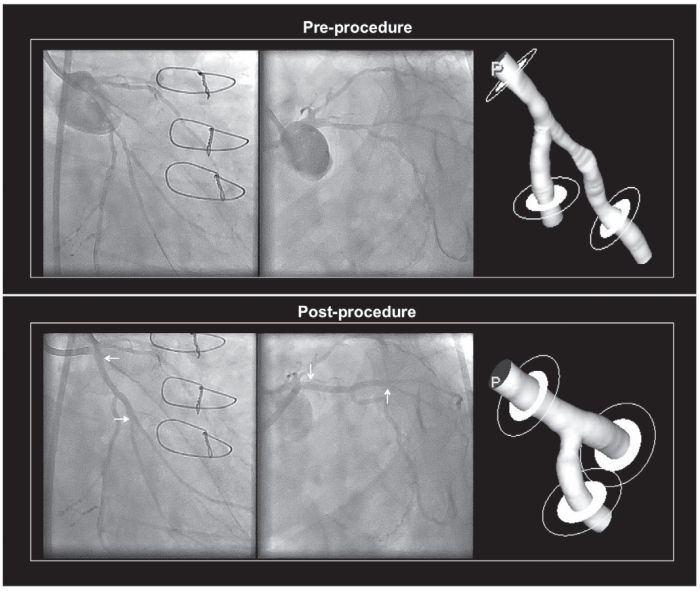

Fig. 3. Treatment of a coronary bifurcation located in a diffusely disease vessel in a patient with previous coronary artery bypass graft. In the upper panel angiographic appearance pre-intervention and 3-dimentional QCA reconstruction of the target bifurcation. In the lower panel post-procedure appearance and 3-dimentional QCA reconstruction with no side-branch impairment.

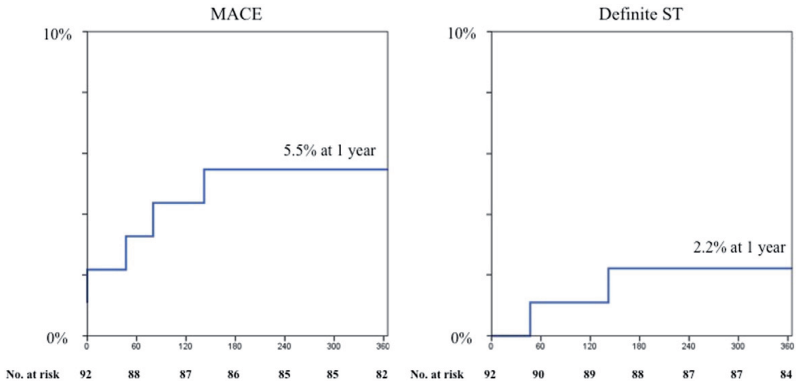

Fig. 4. Kaplan–Meier curves for MACE and scaffold thrombosis.

and thereafter performing proximal optimization. In our report we observed a trend toward a reduction in malapposition at the proximal segment and at the polygon of confluence in the cases with performed proximal optimization.

Taking into consideration the faith of the side-branches after BVS implantation, an initial concern associated with the larger BVS struts width and its possible impact on side-branch impairment has been raised [9]. Maramatsu et al. performed a post-hoc analysis of the ABSORB-EXTEND and SPIRIT First and II Trials [9] to assess the incidence of small SB occlusion (bifurcation lesions involving a SB < 2 mm) after either BVS or everolimus eluting metal stents. BVS demonstrated a higher incidence of post-procedural side branch occlusion compared with EES but only in small side branches with a reference vessel diameter ≤ 0.5 mm.

To investigate the impact of BVS wider struts on side-branch impairment when treating what is most commonly considered a bifurcation lesion (with a side-branch of at least 2 mm in diameter) [20,23–27], we performed a detailed analysis taking into consideration both procedural and angiographic parameters.

We evaluated the composite parameter of "side-branch impairment" observing the TIMI flow, need for dedicated wires, or failure to re-cross or dilate the side-branch and we assessed the 2- and 3-dimentional QCA pre and post BVS implantation of the side-branch.

A side-branch impairment occurred in 13 cases (12.1%) after BVS deployment, the most frequently reported cause was a SB TIMI flow grade < 3 after MV scaffolding, (10 cases). Of note in 6 of those cases the final SB TIMI flow grade improved to grade TIMI flow 3 after SB ostium post-dilation, with no need for SB treatment and reducing the occurrence of final side-branch slow flow to only 4 bifurcations (3.7%). Such data are in line with previous investigations evaluating the impact of first- and second-generation drug eluting metal stents on side-branch impairment [7].

It would therefore appear, that the concern of an increased side-branch damage or occlusion after BVS implantation may not be justified, when considering side-branches with a visually estimated diameter of 2 mm or more.

The OCT analysis although performed in a subgroup of patients showed a low amount of malapposition in the overall bifurcation segment probably also in association with a high rate of postdilatation. Malapposition was distributed with a reduction from the proximal to the distal segment of the bifurcation, highlighting the possible need for proximal optimization.

Finally, although due to the small number of patients and events reported is not possible to reach firm conclusions in terms of clinical outcomes, the overall mortality and the MACE rate suggest a relative safety of BVS implantation in bifurcation lesions given a preferred single scaffold technique and a high rate of pre and post dilatation.

5. Limitations

The present report is an investigator initiated, single center, single arm study and is a retrospective analysis of the BVS evaluation program at Thoraxcenter Rotterdam, The Netherlands. The choice for BVS implantation was left to operator discretion, this could be source of selection bias. The absence of a comparator arm is limiting the interpretation of our data. In the present study side branch vessel with a visual estimated diameter ≥ 2.0 mm was evaluated, by QCA the mean RVD of the side branch was 1.98 mm highlighting the well-known underestimation of vessel size by QCA. Intravascular imaging was encouraged but not mandatory and left to the operator discretion, such approach could be associated with selection bias. The limited number of patients does not allow reaching firm conclusions in terms of clinical outcomes, therefore clinical data should be considered as purely descriptive and hypothesis generating.

6. Conclusion

The present investigation suggest the feasibility and good performance of everolimus-eluting BVS implantation in patients with a native bifurcated coronary lesion, involving a SB ≥ 2 mm in diameter. Further investigations in randomized clinical trials are required to provide the actual impact of this novel technology on safety, efficacy and long-term clinical outcomes, also compared to second-generation DESs.

Conflict of interest

R.J. van Geuns received speakers fees from Abbott Vascular. A. Karanasos received funding support from the Hellenic Heart Foundation and St Jude Medical.

References

[1] P.R. Stella, A. Belkacemi, C. Dubois, H. Nathoe, J. Dens, C. Naber, et al., A multicenter randomized comparison of drug-eluting balloon plus bare-metal stent versus bare-metal stent versus drug-eluting stent in bifurcation lesions treated with a single-stenting technique: six-month angiographic and 12-month clinical results of the drug-eluting balloon in bifurcations trial, Catheter. Cardiovasc. Interv. 80 (2012) 1138–1146.

[2] H. Kelbaek, S. Helqvist, L. Thuesen, L. Klovgaard, E. Jorgensen, K. Saunamaki, et al., Sirolimus versus bare metal stent implantation in patients with total coronary

occlusions: subgroup analysis of the Stenting Coronary Arteries in Non-Stress/Benestent Disease (SCANDSTENT) trial, Am. Heart J. 152 (2006) 882–886.
[3] A. Colombo, J.W. Moses, M.C. Morice, J. Ludwig, D.R. Holmes Jr., V. Spanos, et al., Randomized study to evaluate sirolimus-eluting stents implanted at coronary bifurcation lesions, Circulation 109 (2004) 1244–1249.
[4] K. Tanabe, A. Hoye, P.A. Lemos, J. Aoki, C.A. Arampatzis, F. Saia, et al., Restenosis rates following bifurcation stenting with sirolimus-eluting stents for de novo narrowings, Am. J. Cardiol. 94 (2004) 115–118.
[5] M. Pan, J.S. de Lezo, A. Medina, M. Romero, J. Segura, D. Pavlovic, et al., Rapamycin-eluting stents for the treatment of bifurcated coronary lesions: a randomized comparison of a simple versus complex strategy, Am. Heart J. 148 (2004) 857–864.
[6] R. Diletti, H.M. Garcia-Garcia, C.V. Bourantas, R.J. van Geuns, N.M. Van Mieghem, P. Vranckx, et al., Clinical outcomes after zotarolimus and everolimus drug eluting stent implantation in coronary artery bifurcation lesions: insights from the RESOLUTE all comers trial, Heart 99 (2013) 1267–1274.
[7] F. Burzotta, C. Trani, D. Todaro, L. Mariani, G.P. Talarico, A. Tommasino, et al., Prospective randomized comparison of sirolimus- or everolimus-eluting stent to treat bifurcated lesions by provisional approach, JACC Cardiovasc. Interv. 4 (2011) 327–335.
[8] I. Iakovou, T. Schmidt, E. Bonizzoni, L. Ge, G.M. Sangiorgi, G. Stankovic, et al., Incidence, predictors, and outcome of thrombosis after successful implantation of drug-eluting stents, JAMA 293 (2005) 2126–2130.
[9] T. Muramatsu, Y. Onuma, H.M. Garcia-Garcia, V. Farooq, C.V. Bourantas, M.A. Morel, et al., Incidence and short-term clinical outcomes of small side branch occlusion after implantation of an everolimus-eluting bioresorbable vascular scaffold: an interim report of 435 patients in the ABSORB-EXTEND single-arm trial in comparison with an everolimus-eluting metallic stent in the SPIRIT first and II trials, JACC Cardiovasc. Interv. 6 (2013) 247–257.
[10] Y. Ishibashi, T. Muramatsu, S. Nakatani, Y. Sotomi, P. Suwannasom, M.J. Grundeken, et al., Incidence and potential mechanism(s) of post-procedural rise of cardiac biomarker in patients with coronary artery narrowing after implantation of an everolimus-eluting bioresorbable vascular scaffold or everolimus-eluting metallic stent, JACC Cardiovasc. Interv. 8 (2015) 1053–1063.
[11] M. Pan, M. Romero, S. Ojeda, S. de Lezo J, J. Segura, F. Mazuelos, et al., Fracture of bioresorbable vascular scaffold after side-branch balloon dilation in bifurcation coronary narrowings, Am. J. Cardiol. 116 (2015) 1045–1049.
[12] H. Kawamoto, A. Latib, N. Ruparelia, T. Miyazaki, A. Sticchi, T. Naganuma, et al., Clinical outcomes following bioresorbable scaffold implantation for bifurcation lesions: overall outcomes and comparison between provisional and planned double stenting strategy, Catheter. Cardiovasc. Interv. 86 (2015) 644–652.
[13] S. Ramcharitar, Y. Onuma, J.P. Aben, C. Consten, B. Weijers, M.A. Morel, et al., A novel dedicated quantitative coronary analysis methodology for bifurcation lesions, EuroIntervention 3 (2008) 553–557.
[14] A. Lansky, J. Tuinenburg, M. Costa, M. Maeng, G. Koning, J. Popma, et al., Quantitative angiographic methods for bifurcation lesions: a consensus statement from the European Bifurcation Group, Catheter. Cardiovasc. Interv. 73 (2009) 258–266.
[15] C. Girasis, J.C. Schuurbiers, Y. Onuma, J.P. Aben, B. Weijers, E. Boersma, et al., Two-dimensional quantitative coronary angiographic models for bifurcation segmental analysis: in vitro validation of CAAS against precision manufactured plexiglas phantoms, Catheter. Cardiovasc. Interv. 77 (2011) 830–839.
[16] P.W. Serruys, Y. Onuma, J.A. Ormiston, B. de Bruyne, E. Regar, D. Dudek, et al., Evaluation of the second generation of a bioresorbable everolimus drug-eluting vascular scaffold for treatment of de novo coronary artery stenosis: six-month clinical and imaging outcomes, Circulation 122 (2010) 2301–2312.
[17] D. Capodanno, T. Gori, H. Nef, A. Latib, J. Mehilli, M. Lesiak, et al., Percutaneous coronary intervention with everolimus-eluting bioresorbable vascular scaffolds in routine clinical practice: early and midterm outcomes from the European multicentre GHOST-EU registry, EuroIntervention 10 (2015) 1144–1153.
[18] R. Diletti, A. Karanasos, T. Muramatsu, S. Nakatani, N.M. Van Mieghem, Y. Onuma, et al., Everolimus-eluting bioresorbable vascular scaffolds for treatment of patients presenting with ST-segment elevation myocardial infarction: BVS STEMI first study, Eur. Heart J. 35 (2014) 777–786.
[19] L. Antonsen, M. Maeng, P. Thayssen, E.H. Christiansen, K.N. Hansen, A. Kaltoft, et al., Intimal hyperplasia and vascular remodeling after everolimus-eluting and sirolimus-eluting stent implantation in diabetic patients: the randomized Diabetes and Drug-Eluting Stent (DiabeDES) IV Intravascular Ultrasound trial, Catheter. Cardiovasc. Interv. 83 (2014) 864–872.
[20] D. Hildick-Smith, A.J. de Belder, N. Cooter, N.P. Curzen, T.C. Clayton, K.G. Oldroyd, et al., Randomized trial of simple versus complex drug-eluting stenting for bifurcation lesions: the British Bifurcation Coronary Study: old, new, and evolving strategies, Circulation 121 (2010) 1235–1243.
[21] S. Puricel, F. Cuculi, M. Weissner, A. Schmermund, P. Jamshidi, T. Nyffenegger, et al., Bioresorbable coronary scaffold thrombosis: multicenter comprehensive analysis of clinical presentation, mechanisms, and predictors, J. Am. Coll. Cardiol. 67 (2016) 921–931.
[22] J. Gomez-Lara, R. Diletti, S. Brugaletta, Y. Onuma, V. Farooq, L. Thuesen, et al., Angiographic maximal luminal diameter and appropriate deployment of the everolimus-eluting bioresorbable vascular scaffold as assessed by optical coherence tomography: an ABSORB cohort B trial sub-study, EuroIntervention 8 (2012) 214–224.
[23] M. Niemela, K. Kervinen, A. Erglis, N.R. Holm, M. Maeng, E.H. Christiansen, et al., Randomized comparison of final kissing balloon dilatation versus no final kissing balloon dilatation in patients with coronary bifurcation lesions treated with main vessel stenting: the Nordic-Baltic Bifurcation Study III, Circulation 123 (2011) 79–86.
[24] A. Colombo, E. Bramucci, S. Sacca, R. Violini, C. Lettieri, R. Zanini, et al., Randomized study of the crush technique versus provisional side-branch stenting in true coronary bifurcations: the CACTUS (Coronary Bifurcations: Application of the Crushing Technique Using Sirolimus-Eluting Stents) Study, Circulation 119 (2009) 71–78.
[25] T.K. Steigen, M. Maeng, R. Wiseth, A. Erglis, I. Kumsars, I. Narbute, et al., Randomized study on simple versus complex stenting of coronary artery bifurcation lesions: the Nordic bifurcation study, Circulation 114 (2006) 1955–1961.
[26] J.Y. Hahn, W.J. Chun, J.H. Kim, Y.B. Song, J.H. Oh, B.K. Koo, et al., Predictors and outcomes of side branch occlusion after main vessel stenting in coronary bifurcation lesions: results from the COBIS II Registry (COronary BIfurcation Stenting), J. Am. Coll. Cardiol. 62 (2013) 1654–1659.
[27] S.L. Chen, T. Santoso, J.J. Zhang, F. Ye, Y.W. Xu, Q. Fu, et al., A randomized clinical study comparing double kissing crush with provisional stenting for treatment of coronary bifurcation lesions: results from the DKCRUSH-II (Double Kissing Crush versus Provisional Stenting Technique for Treatment of Coronary Bifurcation Lesions) trial, J. Am. Coll. Cardiol. 57 (2011) 914–920.

24

CHAPTER

EVEROLIMUS-ELUTING BIORESORBABLE VASCULAR SCAFFOLDS FOR TREATMENT OF COMPLEX CHRONIC TOTAL OCCLUSIONS

Fam Jiang Ming, Ojeda S, Garbo R, Latib A, La Manna A, Vaquerizo B, Boukhris M, Vlachojannis GJ, van Geuns RJ, Ezhumalai B, Kawamoto H, van der Sijde J, Felix C, Pan M, Serdoz R, Boccuzzi GG, De Paolis M, Sardella G, Mancone M, Tamburino C, Smits PC, Di Mario C, Seth A, Serra A, Colombo A, Serruys P, Galassi AR, Zijlstra F, Van Mieghem NM, Diletti R.

EuroIntervention. 2017 Jun 20; 13(3):355-363.

Everolimus-eluting bioresorbable vascular scaffolds for treatment of complex chronic total occlusions

Jiang Ming Fam[1], MD; Soledad Ojeda[2], MD, PhD; Roberto Garbo[3], MD; Azeem Latib[4], MD; Alessio La Manna[5], MD; Beatriz Vaquerizo[6], MD; Marouane Boukhris[7], MD; Georgios J. Vlachojannis[8], MD, PhD; Robert-Jan van Geuns[1], MD, PhD; Babu Ezhumalai[9], MD; Hiroyoshi Kawamoto[4], MD; Jors van der Sijde[1], MD; Cordula Felix[1], MD; Manuel Pan[2], MD, PhD; Roberta Serdoz[10], MD; Giacomo Giovanni Boccuzzi[3], MD; Marcella De Paolis[1], MD; Gennaro Sardella[11], MD; Massimo Mancone[11], MD, PhD; Corrado Tamburino[5], MD, PhD; Pieter C. Smits[8], MD, PhD; Carlo Di Mario[10], MD, PhD; Ashok Seth[9], MD; Antonio Serra[6], MD; Antonio Colombo[4], MD; Patrick Serruys[1], MD, PhD; Alfredo R. Galassi[7], MD; Felix Zijlstra[1], MD, PhD; Nicolas M. Van Mieghem[1], MD, PhD; Roberto Diletti[1]*, MD, PhD

1. Department of Interventional Cardiology, Thoraxcenter, Erasmus MC, Rotterdam, the Netherlands; 2. Department of Cardiology, Reina Sofia Hospital, University of Córdoba (IMIBIC), Córdoba, Spain; 3. Department of Cardiology, San Giovanni Bosco Hospital, Turin, Italy; 4. San Raffaele Scientific Institute and EMO-GVM Centro Cuore Columbus, Milan, Italy; 5. Ferrarotto Hospital, University of Catania, Catania, Italy; 6. Cardiology Department, Hospital Sant Pau, Barcelona, Spain; 7. Department of Experimental and Clinical Medicine, University of Catania, Catania, Italy; 8. Department of Cardiology, Maasstad Hospital, Rotterdam, the Netherlands; 9. Fortis Escorts Heart Institute, New Delhi, India; 10. National Institute for Health Research, Cardiovascular BRU Royal Brompton & Harefield NHS Foundation Trust, London, United Kingdom; 11. Department of Cardiovascular, Respiratory, Nephrology, Anesthesiologic and Geriatric Sciences, Policlinico Umberto I, "Sapienza" University of Rome, Rome, Italy

J.M. Fam and R. Diletti contributed equally to this study.

GUEST EDITOR: Holger Thiele, MD; *University Heart Center Lübeck, Medical Clinic II, Lübeck, Germany*

KEYWORDS

- bioresorbable scaffolds
- chronic coronary total occlusion
- stable angina

Abstract

Aims: Bioresorbable vascular scaffolds (BVS) represent a novel therapeutic option for the treatment of coronary artery diseases. The objective of this study was to evaluate the feasibility of BVS implantation in complex chronic total occlusions (CTO).

Methods and results: The present report is a multicentre registry evaluating results after BVS deployment in challenging CTO lesions, defined as J-CTO score ≥2 (difficult or very difficult). A total of 105 patients were included in the present analysis. The mean J-CTO score was 2.61 (difficult 52.4%, very difficult 47.6%). Device success and procedural success rates were 98.1% and 97.1%, respectively. The retrograde approach was used in 25.7% of cases. After wire crossing, predilatation was performed in all cases with a mean predilatation balloon diameter of 2.73±0.43 mm. The mean scaffold length was 59.75±25.85 mm, with post-dilatation performed in 89.5% of the cases and a mean post-dilatation balloon diameter of 3.35±0.44 mm. Post-PCI minimal lumen diameter was 2.50±0.51 mm and percentage diameter stenosis 14.53±10.31%. At six-month follow-up, a total of three events were reported: one periprocedural myocardial infarction, one late scaffold thrombosis and one additional target lesion revascularisation.

Conclusions: The present report suggests the feasibility of BVS implantation in complex CTO lesions, given adequate lesion preparation and post-dilatation, with good acute angiographic results and midterm clinical outcomes.

**Corresponding author: Department of Cardiology, Thoraxcenter, Room Ba-581, Erasmus University Medical Center, 's-Gravendijkwal 230, 3015 GE Rotterdam, the Netherlands. E-mail: r.diletti@erasmusmc.nl*

Abbreviations

BVS	bioresorbable vascular scaffolds
CTO	chronic total occlusions
ISA	incomplete strut apposition
MACE	major adverse cardiac events
MI	myocardial infarction
MLD	minimal lumen diameter
PCI	percutaneous coronary intervention
QCA	quantitative coronary angiography
RVD	reference vessel diameter
ST	scaffold thrombosis
TLR	target lesion revascularisation
%DS	percentage diameter stenosis

Introduction

Recanalisation of chronic total occlusions (CTO) by percutaneous coronary intervention (PCI) is associated with angina relief, improved left ventricular function[1-3], reduction in the rate of myocardial infarction and coronary artery bypass grafting with possibly improved patient survival[4-9], even in patients with well-developed collateral circulation[9].

However, despite recent advances in techniques and materials, the success rate for PCI in CTO is significantly lower compared to other lesion subsets[10,11]. CTO is present in up to 20% of patients with coronary artery disease undergoing elective angiography[12,13], yet this lesion subset represents only a minority of the target lesions treated with PCI[13,14]. In addition, CTO are often long lesions requiring the implantation of multiple metallic stents resulting in a "full metal jacket" treated artery[15], potentially increasing the risk of thrombosis and restenosis[16].

Furthermore, many patients with CTO have extensive coronary disease, requiring multivessel revascularisation[7,17], potentially benefiting from future bypass graft surgery. Given this background, the introduction of bioresorbable vascular scaffolds (BVS) provides a novel therapeutic option for the treatment of chronic total occlusions, allowing revascularisation without permanent caging of long coronary segments, potentially reducing the long-term limitations related to the presence of metallic stents and maintaining the option for future surgical revascularisations.

Bioresorbable technologies have so far mostly been tested in relatively simple coronary lesions[18,19], but there are very limited data and experience with BVS in complex scenarios, especially in CTO lesions[20-22].

Therefore, the objective of the present study was to evaluate the feasibility and midterm performance of BVS in CTO with challenging characteristics according to the J-CTO score[23].

Methods

This was a multicentre single-arm study conducted in the Netherlands, England, Italy, Spain and India from March 2015 to March 2016, to evaluate the feasibility, procedural results and midterm performance of the Absorb™ BVS (Abbott Vascular, Santa Clara, CA, USA) in patients with complex CTO lesions **(Figure 1)**.

Enrolled patients presented with silent ischaemia, stable angina pectoris or acute coronary syndromes. Lesion difficulty was graded according to the J-CTO score; lesions defined as "easy" (J-CTO score 0) or with intermediate difficulty (J-CTO score 1) were excluded from the analysis and only complex cases, defined as those with J-CTO score ≥2 (difficult or very difficult)[23], were evaluated. Exclusion criteria comprised contraindications to antiplatelet medication, maximal vessel diameter >4 mm, female patients with childbearing potential or currently breastfeeding and acute ST-segment elevation myocardial infarction.

Patients were considered suitable for the assessment of success rates after successful wire crossing of the CTO lesions.

Invasive imaging was per operator discretion. After implantation, optical coherence tomography (OCT) was performed in a patient subgroup of 10 patients to assess scaffold expansion and incomplete strut apposition (ISA).

The post-procedural drug regimen included dual antiplatelet therapy for at least 12 months followed by lifelong aspirin.

QUANTITATIVE CORONARY ANGIOGRAPHY

Quantitative coronary angiography (QCA) analyses were performed with the Coronary Angiography Analysis System (CAAS; Pie Medical Imaging, Maastricht, the Netherlands). The QCA measurements were performed pre and post BVS implantation. Angiographic views with minimal foreshortening of the lesion and limited overlap with other vessels were used. Pre-procedure QCA analysis was performed as proximally as possible to the occlusion (in case of a side branch, distally to the most proximal take-off of the side branch), as already described[24]. For each lesion, the following QCA parameters were measured in diastole: minimal lumen diameter (MLD), reference vessel diameter (RVD), percent diameter stenosis (%DS), and occlusion length. The J-CTO score was calculated to estimate lesion complexity and probability of successful guidewire crossing within 30 minutes.

OCT IMAGE ACQUISITION AND ANALYSIS

The C7 system or the ILUMIEN™ OPTIS™ system and the corresponding Dragonfly™ or Dragonfly™ Duo imaging catheters (St. Jude Medical, St. Paul, MN, USA) were used for image acquisition. The OCT catheter was advanced distal to the treated segment, and an automated pullback was performed at 20 mm/s with simultaneous contrast injection at a rate of 3 to 4 ml/s using a power injector. Two sequential pullbacks were performed to enable assessment of the entire scaffolded/stented segment when required.

The OCT measurements were performed offline using the QCU-CMS software (Medis medical imaging systems, Leiden, the Netherlands). Analysis was performed at 1 mm intervals within the entire scaffolded segment and 5 mm proximal and distal to the stent edge. Lumen and scaffold area and diameter measurements were performed in the region of interest (ROI), as appropriate, using standard methodology for the analysis of bioresorbable scaffolds[24,25]. Eccentricity index and symmetry index were additionally calculated as previously reported[26,27].

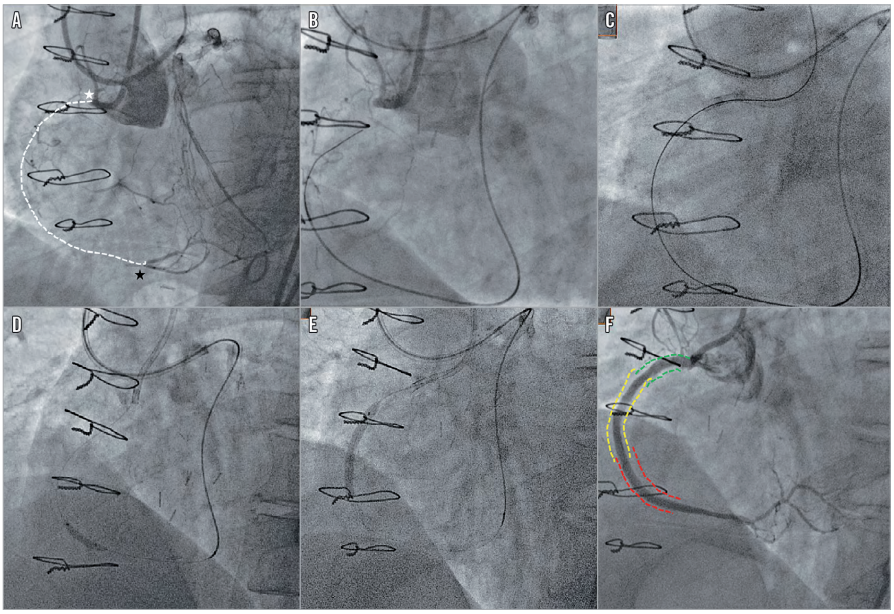

Figure 1. *Successful implantation of bioresorbable vascular scaffolds in a right coronary artery with a chronic total occlusion using a retrograde strategy. The lesion had a blunt stump (white star) with a good distal landing zone (black star) (A). Good septal collaterals were seen from contralateral contrast injection. Successful crossing was achieved with a Conquest Pro wire on a Corsair microcatheter support (Asahi Intecc) (B & C). Predilation (D) was performed before scaffold deployment (two BVS 3.5×28 mm and one 3.0×28 mm in overlap) (E), with a good angiographic result (F).*

STUDY DEFINITIONS

Device success was defined as successful BVS implantation with the attainment of ≤30% final in-segment residual stenosis by angiographic visual estimation after Absorb BVS implantation. Procedure success was defined as device success and no major periprocedural complications (emergent CABG, coronary perforation requiring pericardial drainage, residual dissection impairing vessel flow – TIMI flow 2 or less). Clinical success was defined as procedural success and no in-hospital major adverse cardiac events (MACE). All deaths were considered cardiac unless an undisputed non-cardiac cause was identified. Myocardial infarction (MI) and scaffold thrombosis were defined according to the Academic Research Consortium (ARC) definitions[28]. Any target lesion revascularisation (TLR) was defined as clinically driven if at repeat angiography a diameter stenosis >70% was observed, or if a diameter stenosis >50% was present in association with recurrent angina pectoris, objective signs of ischaemia (ECG changes) at rest or during exercise test likely to be related to the target vessel, or if there were abnormal results of any invasive functional diagnostic test.

MACE was defined as the composite of cardiac death, any reinfarction (Q- or non-Q-wave), emergent bypass surgery (CABG), or clinically driven target lesion revascularisation (TLR).

STATISTICAL ANALYSIS

Categorical variables are reported as counts and percentages and continuous variables as mean±standard deviation. Statistical analyses were performed using SPSS for Windows, Version 20 (IBM Corp., Armonk, NY, USA).

Results

PATIENT DEMOGRAPHICS

Baseline demographics of the patients (N=105) are presented in **Table 1.** Mean age was 59.40±8.96 years, 89.5% of the patients were male, 33.3% had diabetes mellitus, and 68.6% presented with stable angina.

ANGIOGRAPHIC AND LESION CHARACTERISTICS

The most frequently treated vessel was the right coronary artery (44.8%), 35.2% of the CTO were located at the proximal/ostial coronary segment, 28.6% of the cases involved a bifurcation lesion with a side branch ≥2 mm, 56.2% of the cases showed multivessel disease, 74.3% of the lesions had an occlusion length ≥20 mm, and 43.8% had bridging collaterals at the level of the occlusion. Rentrop grade 3 collaterals were present in 29.5% of the lesions.

Table 1. Baseline demographic and clinical characteristics.

Clinical characteristics	N=105
Age, yrs	59.40±8.96
Male gender, %	89.5
History of smoking, %	48.6
Diabetes mellitus, %	33.3
Dyslipidaemia, %	72.4
Hypertension, %	69.5
Family history of CAD, %	21.9
Myocardial infarct, %	29.5
Prior PCI, %	46.7
Prior CABG, %	2.9
Silent ischaemia, %	5.7
Stable angina, %	68.6
Acute coronary syndrome, %	23.8
Congestive cardiac failure, %	1.9

Values specified as percentages or mean with standard deviation.
CABG: coronary artery bypass graft; CAD: coronary artery disease; PCI: percutaneous coronary intervention

Table 2. Baseline lesion and angiographic characteristics.

Lesion characteristics	N=105
Left anterior descending artery, %	41.9
Left circumflex/marginal, %	12.4
Right coronary artery, %	44.8
Ostial-proximal, %	35.2
Mid, %	61.9
Distal, %	2.8
Bifurcation, %	28.6
Single-vessel disease, %	43.8
Two-vessel disease, %	40.0
Three-vessel disease, %	16.2
Severe tortuosity, %	26.7
Blunt stump, %	60.0
Calcification present, %	70.5
Bending >45 degrees, %	49.5
Occlusion ≥20 mm, %	74.3
Retry lesion, %	11.4
(Any) Side branch present, %	65.7
(Any) Bridge collateral present, %	43.8
Rentrop grade 3 collateral, %	29.5
Bad landing zone, %	34.3
Bad distal vessel, %	26.7
Mean J-CTO score	2.61±0.75
Easy (J-CTO score 0), %	0
Intermediate (J-CTO score 1), %	0
Difficult (J-CTO score 2), %	52.4
Very difficult (J-CTO score ≥3), %	47.6
J-CTO score 3	37.1
J-CTO score 4	7.6
J-CTO score 5	2.9
QCA analysis	
Pre-treatment reference vessel diameter, mm	2.71±0.55
Pre-treatment diameter stenosis, %	100.0
Post-treatment minimal lumen diameter, mm	2.50±0.51
Post-treatment reference vessel diameter, mm	2.88±0.51
Post-treatment diameter stenosis, %	14.53±10.31

Values specified as percentages or mean with standard deviation.

The mean J-CTO score was 2.61, with nearly half of the cases (47.6%) having a score ≥3 **(Table 2)**. QCA showed a pre-treatment reference vessel diameter of 2.71±0.55 mm, a post-PCI mean MLD of 2.50±0.51 mm and a percentage diameter stenosis of 14.53±10.31% **(Table 2)**.

PROCEDURAL CHARACTERISTICS

Procedural characteristics are tabulated in **Table 3.** The majority of the cases (62.9%) were performed with a bifemoral approach and contralateral injections. A retrograde strategy occurred in 25.7% of the procedures **(Figure 1)**. Predilatation was performed in every lesion with a mean predilatation balloon diameter of 2.73±0.43 mm. Guidewires used for successful crossing included the Fielder XT-R/FC (23.8%), Conquest Pro 9/12 (12.4%), Gaia First/Second/Third (11.4%), MIRACLEbros 3/6 (8.6%) (all Asahi Intecc, Aichi, Japan) and Pilot® 150/200 (19.0%) (Abbott Vascular/Guidant, Santa Clara, CA, USA). A total of 256 BVS were implanted with a mean number of scaffolds implanted per lesion of 2.44±1.12, including 79 overlaps, a total scaffold length per lesion of 59.75±25.85 mm and a mean scaffold diameter per lesion of 3.00±0.31 mm. Post-dilatation was performed in 89.5% of the cases.

OCT MEASUREMENTS POST SCAFFOLD DEPLOYMENT

Post scaffold deployment, imaging of the scaffolds with OCT was performed in 10 cases. Mean lumen area was 7.31±1.28 mm^2, with a minimum lumen area of 5.35±1.53 mm^2 and residual area stenosis of 6.83±26.44%. Mean ISA area was 0.03±0.04 mm^2. Mean eccentricity index was 0.86±0.04 and symmetry index was 0.37±0.10 **(Table 4)**.

CLINICAL OUTCOMES

Device success and procedural success were 98.1% and 97.1%, respectively. No severe in-hospital adverse events were observed. The six-month follow-up was completed for 96 patients (91.4%). A total of three events were reported, one periprocedural myocardial infarction, one late scaffold thrombosis, and one additional target lesion revascularisation **(Table 5, Figure 2)**.

In particular, the patient who developed late scaffold thrombosis had three Absorb BVS scaffolds (3.0×28 mm; 3.5×18 mm and 3.5×18 mm in an overlapping manner) implanted in the left anterior descending artery (J-CTO score 3). The lesion was predilated with a 3.0 mm balloon and post-dilated with a 3.5 mm non-compliant balloon. On day 47 after the index procedure, the patient was re-admitted with a non-ST-segment elevation myocardial infarction while on DAPT. The coronary angiogram showed

Table 3. Procedural characteristics.

Procedural characteristics		N=105
Single access, femoral		22.8
Single access, radial		9.5
Double access, femoral and radial		4.8
Double access, both femoral		62.9
Contralateral injection		63.8
Intravascular ultrasound		55.2
Optical coherence tomography		9.5
Antegrade strategy		74.3
Retrograde strategy		25.7
Number of guidewires used per lesion		3.27±1.69
Conquest Pro 9/12		12.4
Fielder XT-R/FC		23.8
Gaia First/Second/Third		11.4
MIRACLEbros 3/6		8.6
Pilot 150/200		19.0
Sion/Sion Black/Sion Blue		6.7
Ultimate Bro		5.7
BMW		1.9
Cross-IT 100/200 XT/Progress		8.6
Whisper		1.9
Predilation performed		100
Use of OTW balloon		8.6
Microcatheters used		85.7
Cutting balloon/rotational atherectomy (11/1)		11.4
Maximum predilation balloon diameter, mm		2.73±0.43
Maximum predilation pressure, atm		14.97±2.72
Total number of scaffolds implanted		256
Number of scaffolds per lesion		2.44±1.12
Overlapping scaffolds		79.0
Total scaffold length per lesion, mm		59.75±25.85
Mean scaffold diameter per lesion, mm		3.00±0.31
Maximum scaffold implantation pressure, atm		13.82±2.93
Post-dilation performed		89.5
Maximum post-dilation balloon diameter, mm		3.35±0.44
Procedure time, min		167.06±78.28
Fluoroscopy time, min		60.95±35.16
Contrast volume, ml		334.63±138.01
Antiplatelet therapy	Aspirin	100.0
	Clopidogrel	47.6
	Prasugrel	28.6
	Ticagrelor	23.8
Device success		98.1
Procedural success		97.1

Values specified as percentages or mean with standard deviation. OTW: over the wire.

scaffold thrombosis involving the target vessel which was treated with re-PCI (thrombectomy, implantation of a metal drug-eluting stent and intravenous infusion of eptifibatide).

Table 4. Optical coherence tomography measurements post scaffold deployment.

Number of lesions	N=10
Analysed length, mm	36.64±11.64
Reference lumen area, mm^2	6.00±1.88
Minimum lumen area, mm^2	5.35±1.53
Mean lumen area, mm^2	7.31±1.28
Lumen volume, mm^3	254.02±79.47
Maximum scaffold diameter, mm	3.85±0.45
Minimum scaffold diameter, mm	2.42±0.32
MSA, mm^2	5.84±1.31
Mean scaffold area, mm^2	7.71±1.37
Scaffold volume, mm^3	268.81±93.51
RAS, %	6.83±26.44
EI	0.86±0.04
EI at MSA	0.84±0.06
SI	0.37±0.10
Device with ISA detected	6
Mean ISA area, mm^2	0.03±0.04
Total struts	3,387
Malapposed struts	39
Mean prolapse area, mm^2	0.53±0.42
Edge dissection	8 (80.0)

Values are expressed as mean±standard deviation. EI: eccentricity index; ISA: incomplete strut apposition; MSA: minimum scaffold area; RAS: residual area stenosis; SI: symmetry index

Computed tomography scans were performed at six months in 34 patients **(Figure 3)**, and revealed scaffold restenosis in two patients. One patient was symptomatic and underwent target lesion revascularisation; the other patient was asymptomatic without inducible ischaemia and was managed conservatively. All patients were alive at six-month follow-up.

Discussion

Coronary chronic total occlusions are typically regarded as a challenging subset burdened by low procedural success and poorer clinical outcomes when compared to other lesion types. Even

Table 5. Clinical events at 6-month follow-up.

Outcomes		N=96
Cardiac death		(0/96) 0%
All MI		(2/96) 2.08%
Non-Q-wave MI		(2/96) 2.08%
Q-wave MI		(0/96) 0%
Scaffold thrombosis	Early	(0/96) 0%
	Late	(1/96) 1.04%
Clinically driven TLR		(2/96) 2.08%
Non-TLR		(0/96) 0%

A total of three patients had a clinical event: one periprocedural non-Q-wave myocardial infarction, one late scaffold thrombosis (that was reported as ST, MI and TLR), and one additional target lesion revascularisation. MI: myocardial infarction; TLR: target lesion revascularisation

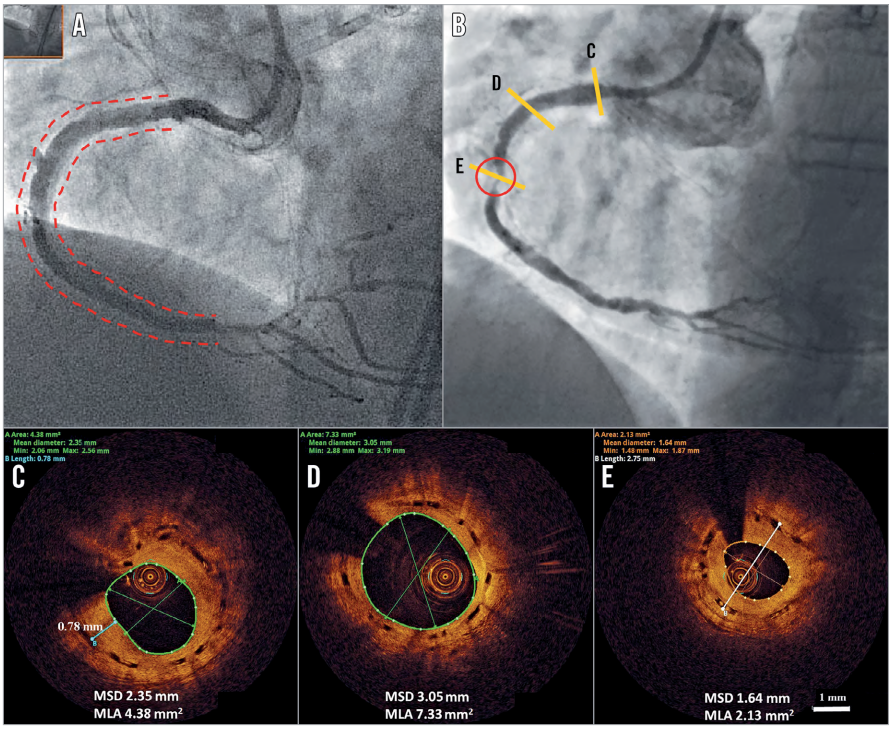

Figure 2. *Subintimal BVS implantation. The final result at the index procedure after subintimal tracking, true lumen re-entry and subintimal BVS implantation (A). Two-year angiographic appearance (B) with an in-scaffold restenosis (circled area). C) In-scaffold restenosis. D) & E) Long-term vascular healing after BVS subintimal implantation. MLA: mean lumen area; MSD: mean scaffold diameter*

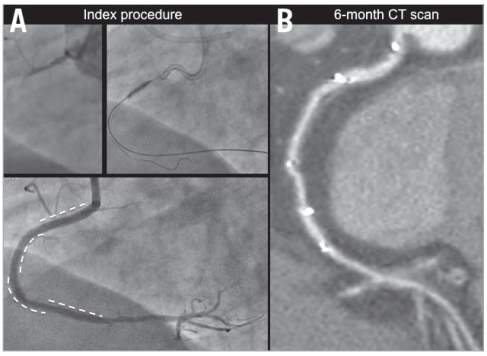

Figure 3. *Computed tomography scans at six-month follow-up. An occluded right coronary artery treated with multiple BVS implantation at the index procedure (A). At six-month follow-up the vessel appears patent on CT scan angiography (B). The position of the implanted BVS is described by the presence of the radiopaque markers.*

though the introduction of drug-eluting stents has reduced the rate of in-stent restenosis, the adoption of these devices is not devoid of limitations, especially in chronically occluded vessels.

Treatment of CTO often implies stenting of long coronary segments with permanent vessel caging of a large part of the artery. This is not only associated with a possible increased risk of restenosis and stent thrombosis, but also precludes future surgical revascularisations in patients who often show diffuse and multivessel atherosclerosis, as is confirmed in the present report with 56.2% of the patients having multivessel disease.

Moreover, a flow-dependent positive vascular remodelling process marks a progressive increase in lumen diameter, external elastic membrane (EEM) diameter, lumen area and EEM area[29-31]. Park and colleagues[29] reported that this increase in lumen dimensions results in more incomplete stent apposition at six-month follow-up in patients treated for CTO lesions. Theoretically, the bioresorption process could eliminate this limitation, as the scaffold remnants can already follow the vessel wall motion between six months and one year after implantation[19].

Recently, small series of BVS in CTO reported similar clinical outcomes but they had overall lower lesion complexity[20-22]. The present investigation focused specifically on complex CTO, illustrated by the fact that half of the CTO were very difficult and we excluded all easy or intermediately difficult CTO as per the J-CTO score. The final angiographic results showed a post-PCI minimal lumen diameter of 2.50±0.51 mm with a low percentage diameter stenosis (14.53±10.31%) and good final TIMI flow. Such promising acute results are in line with angiographic data obtained in previous reports evaluating the BVS as well as metallic DES implantation in CTO lesions[20,22,32].

In our series, advanced BVS implantation techniques were applied, including balloon predilatation with a balloon-to-vessel ratio approaching 1:1, scaffold implantation at nominal pressures and post-dilatation with non-compliant balloons up to 5 mm larger than the nominal scaffold diameter. This approach translated into optimal scaffold apposition and expansion with a very low ISA area by OCT. The mean scaffold eccentricity index and symmetry index were similar to those typically reported for BVS and for metal DES in non-chronically occluded vessels[26,27,33].

Clinical follow-up at six months demonstrated survival and target lesion revascularisation rates comparable to metal stents in CTO lesions[34].

A current limitation of bioresorbable technology is the high strut thickness that could be associated with a delayed vascular healing and endothelialisation, especially at the site of the overlap. In addition, the larger profile of this device compared with previous-generation metallic DES could represent an important obstacle when approaching tortuous, calcified vessels. New delivery systems and reduction in strut thickness and crossing profile may further improve device performance in the future.

Our results support the feasibility of BVS implantation in CTO lesions even in complex scenarios, given an appropriate implantation technique, and justify further research including direct comparison with standard metal drug-eluting stents and analysis of angiographic, intravascular imaging and clinical results at long-term follow-up.

Limitations

This was a single-arm retrospective study. As such, procedural and clinical outcomes cannot be directly compared with lesions treated with metallic drug-eluting stents. Given the limited number of patients and the low rate of events, clinical outcome data should be considered as purely descriptive and hypothesis-generating. The BVS was used as per operator discretion; this methodology may be a source of selection bias. Although personnel trained in an independent core lab performed the QCA analysis, a certified core lab analysis was not available. Invasive imaging was also performed per operator discretion and lacked uniformity.

Conclusions

The present report suggests the feasibility of BVS implantation in complex CTO, given adequate lesion preparation and post-dilatation, with good acute angiographic results and midterm clinical outcomes.

Impact on daily practice

Our observations suggest the feasibility of bioresorbable scaffold implantation in patients with chronic total occlusion and complex anatomies. Optimal antiplatelet regimen, accurate comparison with the current-generation metallic DES and long-term performance remain to be evaluated.

Guest Editor

This paper was guest edited by Holger Thiele, MD; University Heart Center Lübeck, Medical Clinic II, Lübeck, Germany.

Conflict of interest statement

The authors have no conflicts of interest to declare. The Guest Editor has no conflicts of interest to declare.

References

1. Sirnes PA, Myreng Y, Mølstad P, Bonarjee V, Golf S. Improvement in left ventricular ejection fraction and wall motion after successful recanalization of chronic coronary occlusions. *Eur Heart J.* 1998;19:273-81.

2. Chung CM, Nakamura S, Tanaka K, Tanigawa J, Kitano K, Akiyama T, Matoba Y, Katoh O. Effect of recanalization of chronic total occlusions on global and regional left ventricular function in patients with or without previous myocardial infarction. *Catheter Cardiovasc Interv.* 2003;60:368-74.

3. Chadid P, Markovic S, Bernhardt P, Hombach V, Rottbauer W, Wohrle J. Improvement of regional and global left ventricular function in magnetic resonance imaging after recanalization of true coronary chronic total occlusions. *Cardiovasc Revasc Med.* 2015;16:228-32.

4. George S, Cockburn J, Clayton TC, Ludman P, Cotton J, Spratt J, Redwood S, de Belder M, de Belder A, Hill J, Hoye A, Palmer N, Rathore S, Gershlick A, Di Mario C, Hildick-Smith D; British Cardiovascular Intervention Society; National Institute for Cardiovascular Outcomes Research. Long-term follow-up of elective chronic total coronary occlusion angioplasty: analysis from the U.K. Central Cardiac Audit Database. *J Am Coll Cardiol.* 2014;64:235-43.

5. Suero JA, Marso SP, Jones PG, Laster SB, Huber KC, Giorgi LV, Johnson WL, Rutherford BD. Procedural outcomes and long-term survival among patients undergoing percutaneous coronary intervention of a chronic total occlusion in native coronary arteries: a 20-year experience. *J Am Coll Cardiol.* 2001;38:409-14.

6. Aziz S, Stables RH, Grayson AD, Perry RA, Ramsdale DR. Percutaneous coronary intervention for chronic total occlusions: improved survival for patients with successful revascularization compared to a failed procedure. *Catheter Cardiovasc Interv.* 2007;70:15-20.

7. Valenti R, Migliorini A, Signorini U, Vergara R, Parodi G, Carrabba N, Cerisano G, Antoniucci D. Impact of complete revascularization with percutaneous coronary intervention on survival in patients with at least one chronic total occlusion. *Eur Heart J.* 2008;29:2336-42.

8. Christakopoulos GE, Christopoulos G, Carlino M, Jeroudi OM, Roesle M, Rangan BV, Abdullah S, Grodin J, Kumbhani DJ, Vo M, Luna M, Alaswad K, Karmpaliotis D, Rinfret S, Garcia S, Banerjee S, Brilakis ES. Meta-analysis of clinical outcomes of patients who underwent percutaneous coronary interventions for chronic total occlusions. *Am J Cardiol.* 2015; 115:1367-75.

9. Jang WJ, Yang JH, Choi SH, Song YB, Hahn JY, Choi JH, Kim WS, Lee YT, Gwon HC. Long-term survival benefit of revascularization compared with medical therapy in patients with coronary chronic total occlusion and well-developed collateral circulation. *JACC Cardiovasc Interv.* 2015;8:271-9.

10. Abbott JD, Kip KE, Vlachos HA, Sawhney N, Srinivas VS, Jacobs AK, Holmes DR, Williams DO. Recent trends in the percutaneous treatment of chronic total coronary occlusions. *Am J Cardiol.* 2006;97:1691-6.

11. Prasad A, Rihal CS, Lennon RJ, Wiste HJ, Singh M, Holmes DR Jr. Trends in outcomes after percutaneous coronary intervention for chronic total occlusions: a 25-year experience from the Mayo Clinic. *J Am Coll Cardiol.* 2007;49:1611-8.

12. Fefer P, Knudtson ML, Cheema AN, Galbraith PD, Osherov AB, Yalonetsky S, Gannot S, Samuel M, Weisbrod M, Bierstone D, Sparkes JD, Wright GA, Strauss BH. Current perspectives on coronary chronic total occlusions: the Canadian Multicenter Chronic Total Occlusions Registry. *J Am Coll Cardiol.* 2012;59: 991-7.

13. Christofferson RD, Lehmann KG, Martin GV, Every N, Caldwell JH, Kapadia SR. Effect of chronic total coronary occlusion on treatment strategy. *Am J Cardiol.* 2005;95:1088-91.

14. Kahn JK. Angiographic suitability for catheter revascularization of total coronary occlusions in patients from a community hospital setting. *Am Heart J.* 1993;126:561-4.

15. Sharp AS, Latib A, Ielasi A, Larosa C, Godino C, Saolini M, Magni V, Gerber RT, Montorfano M, Carlino M, Michev I, Chieffo A, Colombo A. Long-term follow-up on a large cohort of "full-metal jacket" percutaneous coronary intervention procedures. *Circ Cardiovasc Interv.* 2009;2:416-22.

16. Moreno R, Fernandez C, Hernandez R, Alfonso F, Angiolillo DJ, Sabate M, Escaned J, Banuelos C, Fernandez-Ortiz A, Macaya C. Drug-eluting stent thrombosis: results from a pooled analysis including 10 randomized studies. *J Am Coll Cardiol.* 2005;45:954-9.

17. Olivari Z, Rubartelli P, Piscione F, Ettori F, Fontanelli A, Salemme L, Giachero C, Di Mario C, Gabrielli G, Spedicato L, Bedogni F; TOAST-GISE Investigators. Immediate results and one-year clinical outcome after percutaneous coronary interventions in chronic total occlusions: data from a multicenter, prospective, observational study (TOAST-GISE). *J Am Coll Cardiol.* 2003;41:1672-8.

18. Serruys PW, Chevalier B, Dudek D, Cequier A, Carrie D, Iniguez A, Dominici M, van der Schaaf RJ, Haude M, Wasungu L, Veldhof S, Peng L, Staehr P, Grundeken MJ, Ishibashi Y, Garcia-Garcia HM, Onuma Y. A bioresorbable everolimus-eluting scaffold versus a metallic everolimus-eluting stent for ischaemic heart disease caused by de-novo native coronary artery lesions (ABSORB II): an interim 1-year analysis of clinical and procedural secondary outcomes from a randomised controlled trial. *Lancet.* 2015;385: 43-54.

19. Serruys PW, Onuma Y, Dudek D, Smits PC, Koolen J, Chevalier B, de Bruyne B, Thuesen L, McClean D, van Geuns RJ, Windecker S, Whitbourn R, Meredith I, Dorange C, Veldhof S, Hebert KM, Sudhir K, Garcia-Garcia HM, Ormiston JA. Evaluation of the second generation of a bioresorbable everolimus-eluting vascular scaffold for the treatment of de novo coronary artery stenosis: 12-month clinical and imaging outcomes. *J Am Coll Cardiol.* 2011;58:1578-88.

20. Vaquerizo B, Barros A, Pujadas S, Bajo E, Estrada D, Miranda-Guardiola F, Rigla J, Jimenez M, Cinca J, Serra A. Bioresorbable everolimus-eluting vascular scaffold for the treatment of chronic total occlusions: CTO-ABSORB pilot study. *EuroIntervention.* 2015;11:555-6.

21. Wiebe J, Liebetrau C, Dorr O, Most A, Weipert K, Rixe J, Bauer T, Mollmann H, Elsasser A, Hamm CW, Nef HM. Feasibility of everolimus-eluting bioresorbable vascular scaffolds in patients with chronic total occlusion. *Int J Cardiol.* 2015;179:90-4.

22. Ojeda S, Pan M, Romero M, Suarez de Lezo J, Mazuelos F, Segura J, Espejo S, Morenate C, Blanco M, Martin P, Medina A, Suarez de Lezo J. Outcomes and computed tomography scan follow-up of bioresorbable vascular scaffold for the percutaneous treatment of chronic total coronary artery occlusion. *Am J Cardiol.* 2015;115:1487-93.

23. Morino Y, Abe M, Morimoto T, Kimura T, Hayashi Y, Muramatsu T, Ochiai M, Noguchi Y, Kato K, Shibata Y, Hiasa Y, Doi O, Yamashita T, Hinohara T, Tanaka H, Mitsudo K; J-CTO Registry Investigators. Predicting successful guidewire crossing through chronic total occlusion of native coronary lesions within 30 minutes: the J-CTO (Multicenter CTO Registry in Japan) score as a difficulty grading and time assessment tool. *JACC Cardiovasc Interv.* 2011;4:213-21.

24. Diletti R, Karanasos A, Muramatsu T, Nakatani S, Van Mieghem NM, Onuma Y, Nauta ST, Ishibashi Y, Lenzen MJ, Ligthart J, Schultz C, Regar E, de Jaegere PP, Serruys PW, Zijlstra F, van Geuns RJ. Everolimus-eluting bioresorbable vascular scaffolds for treatment of patients presenting with ST-segment elevation myocardial infarction: BVS STEMI first study. *Eur Heart J.* 2014;35:777-86.

25. Serruys PW, Onuma Y, Ormiston JA, de Bruyne B, Regar E, Dudek D, Thuesen L, Smits PC, Chevalier B, McClean D, Koolen J, Windecker S, Whitbourn R, Meredith I, Dorange C, Veldhof S, Miquel-Hebert K, Rapoza R, Garcia-Garcia HM. Evaluation of the second generation of a bioresorbable everolimus drug-eluting vascular scaffold for treatment of de novo coronary artery stenosis:

six-month clinical and imaging outcomes. *Circulation.* 2010; 122:2301-12.

26. Brugaletta S, Gomez-Lara J, Diletti R, Farooq V, van Geuns RJ, de Bruyne B, Dudek D, Garcia-Garcia HM, Ormiston JA, Serruys PW. Comparison of in vivo eccentricity and symmetry indices between metallic stents and bioresorbable vascular scaffolds: insights from the ABSORB and SPIRIT trials. *Catheter Cardiovasc Interv.* 2012;79:219-28.

27. Shaw E, Allahwala UK, Cockburn JA, Hansen TC, Mazhar J, Figtree GA, Hansen PS, Bhindi R. The effect of coronary artery plaque composition, morphology and burden on Absorb bioresorbable vascular scaffold expansion and eccentricity - A detailed analysis with optical coherence tomography. *Int J Cardiol.* 2015;184:230-6.

28. Cutlip DE, Windecker S, Mehran R, Boam A, Cohen DJ, van Es GA, Steg PG, Morel MA, Mauri L, Vranckx P, McFadden E, Lansky A, Hamon M, Krucoff MW, Serruys PW; Academic Research Consortium. Clinical end points in coronary stent trials: a case for standardized definitions. *Circulation.* 2007;115:2344-51.

29. Park JJ, Chae IH, Cho YS, Kim SW, Yang HM, Seo JB, Kim SY, Oh IY, Yoon CH, Suh JW, Park KW, Chung WY, Youn TJ, Choi DJ, Kim HS. The recanalization of chronic total occlusion leads to lumen area increase in distal reference segments in selected patients: an intravascular ultrasound study. *JACC Cardiovasc Interv.* 2012;5:827-36.

30. Gomez-Lara J, Teruel L, Homs S, Ferreiro JL, Romaguera R, Roura G, Sanchez-Elvira G, Jara F, Brugaletta S, Gomez-Hospital JA, Cequier A. Lumen enlargement of the coronary segments located distal to chronic total occlusions successfully treated with drug-eluting stents at follow-up. *EuroIntervention.* 2014;9:1181-8.

31. Galassi AR, Tomasello SD, Crea F, Costanzo L, Campisano MB, Marza F, Tamburino C. Transient impairment of vasomotion function after successful chronic total occlusion recanalization. *J Am Coll Cardiol.* 2012;59:711-8.

32. Colmenarez HJ, Escaned J, Fernandez C, Lobo L, Cano S, del Angel JG, Alfonso F, Jimenez P, Banuelos C, Gonzalo N, Garcia E, Hernandez R, Macaya C. Efficacy and safety of drug-eluting stents in chronic total coronary occlusion recanalization: a systematic review and meta-analysis. *J Am Coll Cardiol.* 2010;55:1854-66.

33. Mattesini A, Secco GG, Dall'Ara G, Ghione M, Rama-Merchan JC, Lupi A, Viceconte N, Lindsay AC, De Silva R, Foin N, Naganuma T, Valente S, Colombo A, Di Mario C. ABSORB biodegradable stents versus second-generation metal stents: a comparison study of 100 complex lesions treated under OCT guidance. *JACC Cardiovasc Interv.* 2014;7:741-50.

34. Kandzari DE, Kini AS, Karmpaliotis D, Moses JW, Tummala PE, Grantham JA, Orr C, Lombardi W, Nicholson WJ, Lembo NJ, Popma JJ, Wang J, Larracas C, Rutledge DR. Safety and Effectiveness of Everolimus-Eluting Stents in Chronic Total Coronary Occlusion Revascularization: Results From the EXPERT CTO (Evaluation of the XIENCE Coronary Stent, Performance, and Technique in Chronic Total Occlusions) Multicenter Trial. *JACC Cardiovasc Interv.* 2015;8:761-9.

25

CHAPTER

IMPACT OF CALCIUM ON PROCEDURAL AND CLINICAL OUTCOMES IN LESIONS TREATED WITH BIORESORBABLE VASCULAR SCAFFOLDS- A PROSPECTIVE BRS REGISTRY STUDY

Jiang Ming Fam, Cordula Felix, Yuki Ishibashi, Yoshinobu Onuma, Roberto Diletti, Nicolas M van Mieghem, Evelyn Regar, Peter de Jaegere, Felix Zijlstra, Robert J van Geuns.

Int J Cardiol. 2017 Dec 15; 249: 119-126.

Impact of calcium on procedural and clinical outcomes in lesions treated with bioresorbable vascular scaffolds - A prospective BRS registry study

Jiang Ming Fam [a,b], Cordula Felix [a], Yuki Ishibashi [a], Yoshinobu Onuma [a], Roberto Diletti [a], Nicolas M. Van Mieghem [a], Evelyn Regar [c], Peter De Jaegere [a], Felix Zijlstra [a], Robert Jan M. van Geuns [a,*]

[a] Thoraxcenter, Erasmus MC, Rotterdam, The Netherlands
[b] National Heart Centre Singapore, Singapore
[c] University Hospital Zürich, Switzerland

ARTICLE INFO

Article history:
Received 22 April 2017
Received in revised form 11 July 2017
Accepted 14 August 2017
Available online 25 August 2017

Keywords:
Bioresorbable vascular scaffolds
Calcified lesions
Scaffold thrombosis

ABSTRACT

Background: There is limited data on the impact of calcium (Ca) on acute procedural and clinical outcomes in patients with lesions treated with bioresorbable vascular scaffolds (BRS). We sought to evaluate the effect of calcium on procedural and clinical outcomes in a 'real world' population.
Methods: Clinical outcomes were compared between patients with at least 1 moderately or heavily calcified lesion (Ca) and patients with no/mild calcified lesions (non-Ca) enrolled in our institutional BRS registry.
Results: 455 patients (N) with 548 lesions (L) treated with 735 BRS were studied. Patients in the Ca group (N = 160, L = 200) had more complex (AHA B2/C lesion: 69.0% in Ca vs 14.9% in non-Ca, $p < 0.001$) and significantly longer lesions (27.80 ± 15.27 vs 19.48 ± 9.92 mm, $p < 0.001$). Overall device success rate was 99.1% with no significant differences between the groups. Despite more aggressive lesion preparation and postdilation compared to non Ca, acute lumen gain was significantly less in Ca lesions (1.50 ± 0.66 vs 1.62 ± 0.69 mm, $p = 0.040$) with lower final MLD (2.28 ± 0.41 vs 2.36 ± 0.43, $p = 0.046$). There were no significant differences in all-cause mortality, total definite scaffold thrombosis (ST), target lesion revascularization and myocardial infarction between the 2 groups. Late ST was more frequent in the Ca group compared to non Ca group (late ST: 2.1 vs 0%, $p = 0.02$).
Conclusions: Clinical outcomes after BRS implantation in calcified and non-calcified lesions were similar. A remarkable difference in timing of thrombosis was observed, with an increased rate of late thrombosis in calcified lesions.

1. Introduction

Bioresorbable scaffolds (BRS) have been developed as an alternative to metallic stents as the need for mechanical support for the treated vessel is temporary, and beyond the first few months there are potential disadvantages of a permanent metallic prosthesis. In earlier studies to demonstrate Absorb BRS feasibility and safety, severe calcification was an exclusion criterium [1–6]. Calcified lesions may be challenging and encountered in up to 35% of patients who undergo percutaneous coronary intervention (PCI) [7–8]. Lesion calcification has been associated with increased PCI complexity with worse procedural outcomes compared to non-calcified lesions [9]. Wire crossing, delivery of equipment during pre and post dilation and stent delivery may be more cumbersome. In calcific lesions, the effect of acute plaque recoil may affect stent expansion and is associated with adverse clinical and angiographic outcomes [10–11]. Currently there is still limited data on the impact of calcium (Ca) on acute procedural and clinical outcomes in patients with lesions treated with BRS. We sought to determine the impact of calcification on acute angiographic and 2 year clinical outcomes of a large cohort of patients treated solely with the Absorb Bioresorbable Vascular Scaffold (BVS) system (Abbott Vascular, Santa Clara, CA, USA).

2. Methods

This is an investigator-initiated, prospective, single-center, single-arm study evaluating performance of the Absorb BVS in lesions representative of daily clinical practice, including calcified lesions, total occlusions, long lesions and small vessels [12–13]. The study inclusion period was from September 2012 till January 2015. Inclusion criteria were patients presenting with STEMI [12], NSTEMI, stable/unstable angina, or silent ischemia caused by a de novo stenotic lesion in a native previously untreated coronary artery [13]. Procedural and long-term clinical outcomes were assessed. The primary endpoint was major adverse cardiac events, defined as a composite of cardiac death, myocardial infarction and target lesion revascularization.

Abbreviations: BRS, bioresorbable vascular scaffolds; Ca, calcium; DOCE, device oriented composite endpoints; MACE, major adverse cardiovascular events; MI, myocardial infarct; MLD, minimal lumen diameter; PCI, percutaneous coronary intervention; POCE, patient oriented composite endpoints; QCA, Quantitative Coronary Analysis; RVD, reference vessel diameter; ST, scaffold thrombosis; TLR, target lesion revascularization; TVR, target vessel revascularization.

* Corresponding author at: Department of Cardiology, Thoraxcentre, Erasmus University Medical Centre, 's-Gravendijkwal 230, 3015 GE Rotterdam, The Netherlands.
E-mail address: r.vangeuns@erasmusmc.nl (R.J.M. van Geuns).

2.1. Ethics

This is an observational study, performed according to the privacy policy of the Erasmus MC, and to the Erasmus MC regulations for the appropriate use of data in patient-oriented research, which are based on international regulations, including the declaration of Helsinki. Approval of the ethical board of the Erasmus MC was obtained. All patients undergoing clinical follow-up provided written informed consent for the PCI and to be contacted regularly during the follow-up period of the study.

2.2. Quantitative Coronary Analysis (QCA)

The angiographic analysis was performed by three independent investigators. Coronary angiograms were analyzed with the CAAS 5.10 QCA software (Pie Medical BV, Maastricht, the Netherlands). The QCA (Quantitative Coronary Analysis) measurements provided reference vessel diameter (RVD), percentage diameter stenosis and minimal lumen diameter (MLD). Acute gain was defined as post-procedural MLD minus pre-procedural MLD (in an occluded vessel MLD value was zero by default).

2.3. Angiographic assessment of lesion calcification

Lesion calcification was recognized as radio-opacities within the vessel wall at the treated lesion. Calcification was categorized as either none/mild or moderate if the radio-opacities were noted only during the cardiac cycle before contrast injection and further classified as either none/mild or moderate based on visual assessment. Severe calcification was defined as having multiple persisting (that are noted even without cardiac motion) opacifications of the coronary wall and visible in more than one projection, surrounding the complete lumen of the coronary artery at the site of the lesion as per SYNTAX definition (www.syntaxscore.com). Angiographic assessment of calcification was conducted independently by 2 cardiologists. In cases of disagreement, a third independent cardiologist reviewed the films and provided a final diagnosis.

2.4. Follow-up

Clinical demographic data of all patients were obtained from municipal civil registries. Follow-up information specific for hospitalization and cardiovascular events was obtained through questionnaires. If needed, medical records or discharge letters from other hospitals were requested. Events were adjudicated by an independent clinical events committee (CEC). All information concerning baseline characteristics and follow-up was gathered in a clinical data management system. Only patients who had given written consent for follow up were included in the clinical outcome assessments.

2.5. Definitions

The primary endpoint was major adverse cardiovascular events (MACE), defined as the composite endpoint of cardiac death, myocardial infarction (MI) and target lesion revascularization (TLR). The secondary endpoints were device oriented composite endpoints (DOCE: composite of cardiac death, target vessel myocardial infarct and clinically indicated target lesion revascularization) and patient oriented composite endpoints (POCE: composite of all-cause mortality, all-cause myocardial infarct and any revascularization). Deaths were considered cardiac unless a non-cardiac cause was definitely identified. TLR was described as any repeated revascularization of the target lesion. Target vessel revascularization (TVR) was defined as any repeat percutaneous intervention or surgical bypass of any segment of the target vessel. Non-target vessel revascularization was described as any revascularization in a vessel other than the target lesion. Scaffold thrombosis (ST) and MI were classified according to the Academic Research Consortium (ARC) [14]. Clinical device success was defined as successful delivery and deployment of the first study scaffold/stent at the intended target lesion and successful withdrawal of the delivery system with attainment of final in-scaffold/stent residual stenosis of <30% as evaluated by QCA. Clinical procedure success was described as device success without major peri-procedural complications or in-hospital MACE (maximum of 7 days).

2.6. Statistical analysis

Categorical variables are reported as counts and percentages, continuous variables as mean ± standard deviation. The cumulative incidence of adverse events was estimated according to the Kaplan-Meier method. Patients lost to follow-up were considered at risk until the date of last contact, at which point they were censored. A cox regression was performed to investigate clinical outcomes at two years, with the binary variable calcification (yes/no). Adjusted cox regression were performed using fourteen patient and lesion factors (see Online Supplement Table 1) to account for baseline differences between patients with at least 1 moderately or heavily calcified lesion (Ca) and patients with no/mild calcified lesions (non-Ca). Statistical analyses were performed using SPSS, version 21 (IL, US). All statistical tests were two-sided and the p value of <0.05 was considered statistically significant.

3. Results

Baseline clinical characteristics are shown in Table 1A. A total of 548 lesions in 455 patients were studied of which 200 (36.5%) lesions in 160 patients (35.2%) were moderately or heavily calcified (Ca group) (Table 1A). Patients in the Ca group were older, with more hypertension, and kidney disease. In the calcified cohort, there were 1.24 lesions per patient. Lesion and QCA characteristics are as shown in Table 1B. The left anterior descending artery (n = 254, 46.4%) was the most commonly treated vessel in the study population. Lesions in the Ca group were more complex (AHA B2/C lesion: 69.0% in Ca vs 14.9% in non-Ca, p < 0.001) and significantly longer. Compared to non-Ca group, lesions in the Ca groups had smaller RVD and lower percentage diameter stenosis.

Procedural characteristics are as shown in Table 1C. Ca lesions were treated with more aggressive lesion preparation compared to non Ca as evidenced by the more significant use of predilation, rotational atherectomy and scoring balloon. The use of buddy wires was higher in Ca lesions compared to non Ca lesions. Fig. 1A illustrates the satisfactory expansion with minimal eccentricity on OCT of a calcified LAD treated with a BRS. Fig. 1B and C illustrates the acute and 2 year angiographic and IVUS result respectively after rotational atherectomy and lesion preparation followed by BRS implantation in a calcified coronary artery. A total of 735 scaffolds were implanted in the study population with more scaffolds per lesion for Ca lesions (1.58 vs 1.21). Scaffold diameter was similar in the two groups however scaffold length implanted was longer in the Ca group. Postdilation was more frequently used in the Ca group (Ca vs non Ca: 64.8% vs 42.1%, p < 0.001).

Procedural outcomes are shown in Table 2A. Post procedure, acute lumen gain was significantly less in Ca compared to non-Ca lesions (1.50 ± 0.66 vs 1.62 ± 0.69 mm, p = 0.040) with lower final MLD (2.28 ± 0.41 vs 2.36 ± 0.43, p = 0.046). RVD and percentage diameter stenosis were smaller in the Ca group compared to the non Ca group though the differences did not reach statistical significance. Procedural success was high for both patient groups (98.7 and 99.7%, p = 0.25). Overall device success rate and final TIMI 3 flow result were similar in the two groups.

We were able to obtain written consent for the follow up program in 395 patients (86.8%). Clinical outcomes were available in all (100%) of these patients (Table 2B). These patient had similar baseline and procedural characteristics as the total population. Kaplan-Meier curves for

Table 1A
Demographic characteristics of the study population.

	BRS (N = 455; L = 548)		
	Patients with at least 1 calcified lesion (N = 160/35.2%; L = 200/36.5%)	Patients with no calcified lesions (N = 295/64.8%; L = 348/63.5%)	
Age	62.12 ± 10.64	56.54 ± 10.25	<0.001
Male	122/160 (76.3)	220/295 (74.6)	0.734
Ex/active smoker	81/160 (50.7)	181/294(61.6)	0.064
Diabetes mellitus	31/160 (19.4)	40/295 (13.6)	0.107
Dyslipidemia	75/158 (47.5)	109/288 (37.8)	0.056
Hypertension	93/159 (58.5)	139/290 (47.9)	0.038
Family history	55/160 (34.4)	127/295 (43.1)	0.206
CVA/TIA	13/160(8.1)	16/295 (5.4)	0.260
Prior MI	26/160 (16.3)	27/295 (9.2)	0.032
Prior PCI	10/160 (6.3)	20/295 (6.8)	1.000
Prior CABG	1/160 (0.6)	0	0.352
Kidney disease	11/160 (6.9)	8/295 (2.7)	0.048
Heart failure	7/160 (4.4)	7/295 (2.4)	0.262
Clinical presentation			0.002
Stable angina	53/160 (33.1)	63/295 (21.4)	
Unstable angina	14/160 (8.8)	32/295 (10.8)	
STEMI	40/160 (25.0)	118/295 (40.0)	
NSTEMI	51/160 (31.9)	82/295 (27.8)	
CCF/others	2/160 (1.3)	0	
Disease involvement			0.060
SVD	97/160 (60.6)	210/295 (71.2)	
DVD	42/160 (26.3)	63/295 (21.4)	
LM/TVD	21/160 (13.1)	22/295 (7.4)	

Values are expressed in numbers (percentages) or mean ± standard deviation when appropriate.

MACE were parallel throughout the follow-up to two year (Fig. 2A). Crude cumulative event rates at two years for the secondary endpoints, described as Kaplan-Meier estimates are as shown in Table 2B. There was a slight trend for higher events on cardiac death and all-cause mortality for patients with calcified lesions. No difference was observed in POCE and DOCE. Though definite ST rates were similar between the two groups (Fig. 2B), there was a remarkable variation in acute and late definite ST. For acute definite ST, the incidence was higher in the non-Ca lesions; for late definite ST there was a significant increase in Ca group compared to non-Ca group (late ST: 2.1% vs 0, $p = 0.02$) but not for very late ST (Table 2B). After adjusting for difference in baseline characteristics, Ca lesions was not found to be a significant predictor of any clinical events (Table 2C).

4. Discussion

In our study, the key finding was that despite Ca lesions were more complex, required more lesion preparation, and encountered more deliverability issues with lower acute luminal gain and smaller final MLD, acute procedural and 24 month clinical outcomes were similar regardless of the calcification group with the exception of a higher rate of late ST at 2 years in the Ca group compared to non-Ca group. While there have been earlier studies evaluating the use of BRS in calcified lesions. [15–17], this is the first large clinical prospective registry study involving BRS scaffolds that look at the impact of lesion calcification on long term clinical outcomes at 2 years.

Our findings, which showed that Ca lesions were more complex and required more careful and elaborate lesion preparation including rotational atherectomy (in 5.5% of the lesions), were consistent with similar findings published elsewhere [9,18]. The use of intracoronary imaging like IVUS was also increased in Ca lesions compared to non Ca lesions. The more frequent use of buddy wires in the Ca group suggested that difficult deliverability issues may be encountered more commonly in Ca lesions thus potentially prolonging procedure times. Despite the advances in interventional techniques, calcific lesions still pose a challenge for the procedurist. Due to their inherent polymeric structural composition and increased strut thickness, BRS have been shown to have less favorable mechanical characteristics including less deliverability and radial strength compared to current second generation DES [18, 19]. There have been concerns as to whether such mechanical characteristics may result in less optimal stent performance which may be more pronounced in calcified lesions where focal areas of calcification limit expansion of the BRS more compared to DES [18]. This may have practical clinical implications since suboptimal stent expansions has been known to contribute to metallic stent failure [20] and there have been reports of inadequate scaffold expansion in BRS failure [21,22].

Table 1B
Lesion characteristics of the study population.

	BRS (L = 548)		p value
	Calcified lesions (L = 200/36.5%)	Non calcified lesions (L = 348/63.5%)	
Target vessel			
LAD	126/200 (63.0)	128/348 (36.8)	<0.001
LCX	27/200 (13.5)	96/348 (27.6)	<0.001
RCA	42/200 (21.0)	111/348(31.9)	0.007
Diagonal	4/200 (2.0)	13/348(3.7)	0.314
Left main	1/200 (0.5)	0	0.365
SVG	0	0	–
Lesion AHA			<0.001
A	5/200 (2.5)	71/348 (20.4)	
B1	60/200 (30.0)	226/348 (64.9)	
B2	85/200 (42.5)	46/348 (13.2)	
C	53/200 (26.5)	6/348 (1.7)	
Bifurcation	61/199 (31.7)	58/347 (16.7)	<0.001
CTO	13/200 (6.5)	4/348 (1.1)	0.001
TIMI			
Pre-procedure			0.074
TIMI 0	35/200 (17.5)	87/344 (25.0)	
TIMI 1	6/200 (3.0)	17/344 (4.9)	
TIMI 2	50/200 (14.4)	50/344 (14.4)	
TIMI 3	125/200 (62.5)	190/344 (54.6)	
QCA analysis			
Pre-procedure			
Treatment length	27.80 ± 15.27	19.48 ± 9.92	<0.001
RVD (mm)	2.52 ± 0.57	2.62 ± 0.57	0.053
MLD (mm)	0.85 ± 0.47	0.75 ± 0.55	0.036
Diameter stenosis (%)	65.39 ± 18.68	70.78 ± 20.98	0.004

Values are expressed in numbers (percentages) or mean ± standard deviation when appropriate.

Our findings are also consistent with clinical [23,24] data addressing the feasibility of BRS in calcified lesions. In a recent study looking at specific procedural outcomes in 62 calcified lesions by Panoulas et al. [23], expansion of BRS as measured in terms of lumen gain on QCA and intravascular ultrasound (IVUS) was similar between calcified and non-calcified lesions. Acute luminal gain (1.83 ± 0.6 vs 1.86 ± 0.6 mm, $p = 0.732$) and angiographic success were similar (98% non-calcific vs 95.2% calcific, $p = 0.369$), whereas procedural success was reduced in patients with calcific lesions (94.1% vs 83.9%, $p = 0.034$) due to higher rates of periprocedural myocardial infarction (MI) (5% vs 13.1%, $p = 0.067$). MACE rates (10.9% non-calcific vs 12.9% calcific, p log-rank = 0.546) were similar in the median follow-up time of 14 months. However a greater degree of lesion preparation in calcified lesions was also required. OCT was not used and a comparison of the expansion of BRS compared with DES was not performed. In our study, we report 2 year clinical outcomes in a larger study population which showed MACE rates were similar between Ca and non-Ca groups. In another study conducted by Kawamoto et al. [24], though eccentric calcium distribution resulted in asymmetric expansion of BRS, the final MSA was still comparable irrespective of calcium distribution, and the use of IVUS for scaffold optimization led to favorable clinical outcomes even in calcified lesions. Earlier OCT findings published from our center [25] also suggest that regardless of the degree of angiographic calcification, BRS can achieve a similar expansion as DES, in the context of an imaging-guided strategy with adequate lesion preparation. Our findings were also consistent with recent published literature showing that the presence of moderate or severe lesion calcification does not negatively affect angiographic outcomes at both post-procedure and 13-month follow-up after BVS implantation [26]. However, in this study [26], heavily calcified lesions or those requiring extensive lesion preparation such as rotational atherectomy were excluded according to the study protocol whereas our study included "all comers" lesions with various degrees of calcification or that require rotational atherectomy.

However, BRS deployment requires more lesion preparation and decalcification strategy particularly for moderately or heavily calcified lesions. Further studies are needed to ascertain if in such lesions the use of such a strategy may impact on long term clinical outcomes such as increased TLR rates such as seen in DES deployment after lesion debulking or decalcification using rotational atherectomy [27,28]. In addition, the postdilation rate reported in our study (Table 1C) was comparable to other studies considering that systematic postdilation was implemented on average in <50% of previously published studies [29]. It is still debatable if pursuing a systematic postdilation strategy will have an impact on long term results particularly the risk of very late ST (VLST). Given the results of this study, an analysis of BRS specific implantation technique such as PSP (Prepare the lesion to be reengineered; Size the vessel appropriately; Postdilate to embed scaffold struts into the vessel wall) would be timely and of interest [30]. Though the lesions treated in the Ca group were more complex, requiring longer and more overlapping scaffolds and the post dilatation rate of 64.8% was considered relatively low for calcific lesions, the procedural and clinical results were still similar between the Ca and non Ca groups. This may be reassuring since the current practice suggest a large use of postdilation especially in stable patients with complex lesions.

BRS offers several unique potential advantages over DES. The future bioresorption of BRS permits potential future grafting of treated

Table 1C
Procedural characteristics of the study population.

	BRS (L = 548)		p value
	Calcified lesions (L = 200/36.5%)	Non calcified lesions (L = 348/63.5%)	
Number of treated lesions per procedure	1.24 ± 0.48	1.17 ± 0.48	0.133
Aspiration thrombectomy	34/200 (17.1)	106/348 (30.5)	0.001
Rotational atherectomy	11/200 (5.5)	0/348	0.002
Scoring balloon	9/200 (4.5)	1/348 (0.3)	0.001
Intracoronary imaging			
IVUS	30/199 (15.1)	30/348 (8.6)	0.023
OCT	62/200 (31.0)	95/348 (27.3)	0.378
Predilation performed	177/200 (88.5)	265/348 (76.1)	<0.001
Max predilation diameter	2.66 ± 0.36	2.53 ± 0.42	0.002
Predilation balloon: artery ratio	1.08 ± 0.25	1.01 ± 0.23	0.005
Maximum predilation inflation pressure, atm	14.25 ± 3.35	13.56 ± 3.01	0.067
Buddy wire	23/199 (11.6)	22/347 (6.3)	0.036
Additional daughter catheter	3/199 (1.5)	3/348 (0.9)	0.673
Mean number of scaffold	1.58 ± 0.823	1.21 ± 0.53	<0.001
Number of scaffolds (total 735)	315	420	<0.001
0	1/200 (0.5)	1/348 (0.3)	
1	117/200 (58.5)	289/348 (83.0)	
2	56/200 (28.0)	47/348 (13.5)	
3	18/200 (9.0)	7/348 (2.0)	
4	8/200 (4.0)	4/348 (1.1)	
Scaffold diameter, mm	3.11 ± 0.32	3.12 ± 0.38	0.615
Scaffold length implanted, mm	34.65 ± 19.94	23.84 ± 12.20	<0.001
Overlapping scaffolds	80/200 (40.0)	52/348 (15.0)	<0.001
Maximum scaffold implantation pressure, atm	14.99 ± 1.88	14.86 ± 1.97	0.510
Postdilation performed	129/199 (64.8)	146/347 (42.1)	<0.001
Postdilation balloon: mean scaffold diameter ratio	1.06 ± 0.15	1.07 ± 0.10	0.422
Max postdilation balloon, mm	3.31 ± 0.43	3.31 ± 0.44	0.906
Maximum postdilation inflation pressure, atm	16.27 ± 3.63	15.83 ± 3.97	0.496

Values are expressed as numbers (percentages) or mean ± standard deviation when appropriate.

segments, allows potential reopening of "jailed" side branches and potential recovery of vasomotor function and vessel remodeling. These benefits would be more pertinent in patients with calcific lesions, who often have widespread disease resulting in long stented segments. However whether these will translate into long term clinical benefits in more complex lesions such as those with significant calcifications would

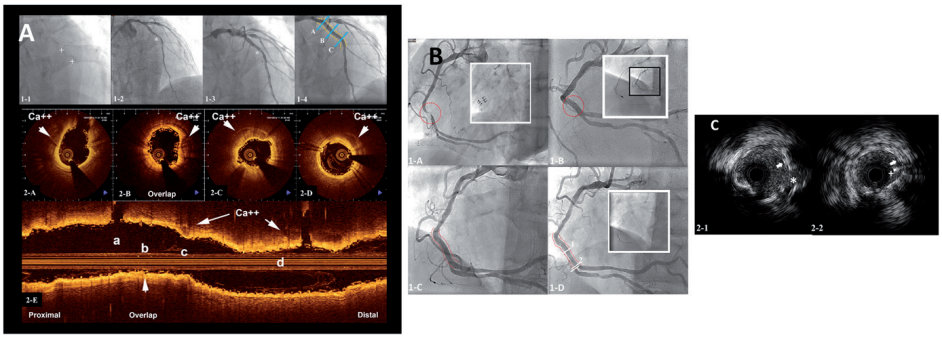

Fig. 1. A. Implantation of Bioresorbable vascular scaffold (BRS in calcified left anterior descending artery (LAD). Panel 1. Implantation of bioresorbable vascular scaffolds (two 3.0 × 28 mm Absorb™ BVS deployed in an overlapping manner-indicated in yellow) in a calcified left anterior descending artery (LAD). Calcification marked '+' in Panel 1-1. Target lesion marked '*' preprocedure (Panel 1-2), after predilation with a 2.5 mm balloon at (Panel 1-3) and after postdilation with a noncompliant 3.0 mm balloon at high pressure (Panel 1-4).Panel 2A–E: Final OCT performed showed that the scaffold was well expanded and apposed with no significant dissection seen. Proximal and distal reference areas were 7.21 mm^2 and 5.52 mm^2 respectively. The minimal lumen area (MLA) was 4.5 mm^2 (2.83 × 1.81 mm) with an eccentricity index (EI) of 0.63. Panel 2-A–C showed the corresponding segments of the treated vessel in Panel 1-4. Panel 2-D showed the BRS implanted in a calcified segment of the treated vessel with satisfactory expansion with minimal eccentricity. Panel 2-E showed the longitudinal pullback of the treated vessel. B. Angiogram and intravascular ultrasound (IVUS) of the right coronary artery (RCA). Angiogram and intravascular ultrasound (IVUS) of the right coronary artery (RCA). Panel 1-A shows the preprocedural angiogram at baseline with a severely tight lesion (circled) in the mid segment of the RCA which is heavily calcified (see insert). Panel 1-B shows the RCA post rotational artherectomy with 1.5 mm burr (see insert) and predilation with a Trek NC 3.25 mm balloon. Panel 1-C shows the RCA after deployment of a BRS (BVS Absorb 3.0 × 28 mm - outlined in red). The borderline lesions in the ostium and mid right posterior descending artery (RPDA) was managed conservatively (white arrow). Panel 1-D shows the RCA at 2 years follow up which demonstrates that the previously deployed scaffold in the mid RCA was still widely patent with no significant restenosis (outlined red). C. IVUS images of the RCA. The figure shows IVUS images of the corresponding segments of the RCA in Fig. 1B Panel 1-D at 2 years follow up demonstrating that the scaffold struts (white arrow) remained visible in the mid RCA with good apposition and expansion with side branch (*-RPDA) patency and confirmed the scaffolded vessel remained widely patent with no significant restenosis (Panels 2-1 and 2-2). + - Guidewire.

still require further evaluation. Previous studies have highlighted a higher rate of ST related to the use of BRS [4,31–33], but did not provide details on the effect of calcification. In our study, we see an observation pattern of higher early ST cases in the non-Ca group followed by a significantly higher rate of late ST in the Ca group. To the best of our knowledge, we believe the difference in timing on ST observed in the two groups is notable and interesting which warrant further studies. The observation of early ST in the non-Ca group (a group with a higher number of acute coronary syndromes; ACS) patients might be related to scaffold under sizing and to increased platelets activation. Predisposing factors of scaffold undersizing include the increased thrombus burden and vasoconstriction in the setting of acute STEMI leading to underestimation of the actual size of the infarct-related artery, thus increasing the risk of the implantation of undersized scaffolds which can be seen even in the setting of metallic drug eluting stents [34]. Implantation of a relatively small scaffold in a relatively larger vessel can result in incomplete apposition, predisposing to ST [35]. Higher rates of ST were also previously noted in patients with ACS which could be due to reduction of early neointimal growth and strut coverage [36,37]. Reasons for the increase in late ST in the Ca compared to the non Ca group include a role for technical factors such as suboptimal implantation with incomplete lesion coverage, underexpansion and malapposition [35,38] and possibly greater impact on the scaffold endothelization and resorption process from a reduced MLD in the Ca group. The additional risks of late ST in the Ca lesions may arise from either the loss of radial strength after scaffold resorption (which typically commences 6 months to >1 year after scaffold implantation) or the scaffold 'dismantling' around calcified lesions which will have forces localized at the edge of the calcified areas where expansion tends to be asymmetrical [24]. Scaffold 'dismantling' might result in rapid changes in vessel wall architecture and therefore exert localized forces on the neointimal coverage potentially resulting in microdissections, triggering the thrombosis.

In our current study, though the event rate is similar between the Ca and non Ca groups, this may also be partially attributed to a higher ACS population in the non Ca group which is known to have higher risk of clinical events at follow up. In an earlier study evaluating the one-year outcomes in patients presenting with ACS compared to stable angina patients after implantation of a BRS from our center, one-year clinical outcomes in ACS patients treated with BRS were similar to non-ACS patients. One-year definite ST rate was comparable: 2.0% for ACS population versus 2.1% for stable population ($p = 0.94$), however, early ST occurred only in ACS patients [39]. Comparatively, overall ST rates were similar between the two groups in this study and further analysis did not show that Ca lesions were a significant predictor of ST (Table 2C). Of note, there was no difference in VLST between the Ca and non-Ca groups.

Though recent guidelines have supported a shift towards a shorter duration of DAPT [40], our findings on an increased late ST rate in Ca lesions may suggest that a longer duration of DAPT may still be necessary if BRS is to be implanted before the patient is to derive the potential benefits of BRS resorption. In our study, data on the use of dual antiplatelets therapy (DAPT) were available in the 395 patients whose follow up were available. All patients were prescribed aspirin during the duration of the study. Second generation $P2Y_{12}$ antiplatelet medications were used; clopidogrel ($n = 157$, 39.7%), prasugrel ($n = 187$, 47.3%) and ticagrelor ($n = 51$, 12.9%). The median duration of DAPT was 365.00 (IQR 364.00–394.50) days and was similar between the 2 groups. In a study to evaluate the impact of DAPT termination on late and very late ST in patients treated with the Absorb BRS, the incidence of ST was low while on DAPT but potentially higher when DAPT was terminated before 18 months [41,42]. Further studies may be required to evaluate the effect of a prolonged duration of DAPT on the rate of late ST.

The findings showing a lesser acute lumen gain and similar 2 year MACE were consistent with previous research involving metallic DES in calcified versus non calcified lesions [8]. Moussa et al. reported in a subanalysis of the TAXUS IV trial [8] a significant reduction in late lumen loss in calcific lesions ($n = 247$) treated with PES vs BMS (0.26 ± 0.56 vs 0.51 ± 0.48 mm, $p = 0.015$). In a study from the SPIRIT II trial by Onuma et al. [43], the efficacy of EES in patients with at least one angiographically defined moderate calcific lesion (68 patients), was compared to those without any calcific lesion (144 patients). Late lumen loss was similar between the two groups at two years. No significant difference in two-year MACE rates was observed between the two groups (calcific vs non-calcific: 10.9% vs 4.4%, $p = 0.12$). The numerically increased MACE rate was attributed to an increased ischemia-driven TLR (7.8% vs 1.5%, $p = 0{,}03$). However TLR rates were similar between the Ca and non Ca groups in our study.

Table 2A
Procedural outcomes of the study population.

	BRS (L = 548)		p value
	Calcified lesions (L = 200/36.5%)	Non-calcified lesions (L = 348/63.5%)	
TIMI postprocedure			0.850
TIMI 0	0	0	
TIMI 1	1/200 (0.5)	2/348 (0.6)	
TIMI 2	12/200 (6.0)	17/348 (4.9)	
TIMI 3	187/200 (93.5)	329/348 (94.5)	
QCA analysis post-procedure			
RVD (mm)	2.75 ± 0.48	2.78 ± 0.45	0.401
MLD (mm)	2.28 ± 0.41	2.36 ± 0.43	0.046
Diameter stenosis (%)	16.71 ± 8.89	15.30 ± 8.61	0.069
Acute lumen gain	1.50 ± 0.66	1.62 ± 0.69	0.040
Procedural outcomes			
Device success	197/200 (98.5)	346/348 (99.4)	0.208
Bailout by scaffold	6/200 (3.0)	5/348 (1.4)	0.439
Bailout by metallic stent	4/200 (2.0)	5/348 (1.4)	0.547
Intraprocedural thrombosis	1/200 (0.5)	1/348 (0.3)	1.000
Significant dissection	14/200 (7.0)	16/348 (4.6)	0.444
Significant no reflow/slow flow	9/200 (4.5)	9/348 (2.6)	0.272

MLD: minimal lumen diameter; QCA: Quantitative Coronary Analysis; RVD: reference vessel diameter. Values are expressed as numbers (percentages) or mean ± standard deviation when appropriate.

In summary, clinical outcomes of calcified and non-calcified lesions treated with BRS are in general similar except for late ST. Overall two-year MACE rates appear acceptable in patients with and without calcific lesions treated with BRS. Further larger randomized controlled trials comparing clinical outcomes of DES to BRS in calcified lesions may be required to evaluate the full impact of calcium on BRS outcomes compared to DES.

4.1. Study limitations

This is a single-center, single-arm registry with no direct comparison with metallic DES. The total number of patients in this study was still limited. In addition, calcification assessment was based on angiographic classification alone rather than characterization of coronary calcification using alternative imaging modality such as intravascular ultrasound. Thus, these findings warrant further confirmation in a large-scale trial. Furthermore, deciding which patient or lesion was suitable for treatment with BRS could have resulted in selection bias. The event rate is unknown in the patients ($n = 60$, 13.2%) who did not agree to participate in further follow up and hence excluded from clinical outcome analysis. We further evaluated the population who did not agree to further follow up and compared the baseline demographic, lesion and procedural characteristics between the cases with calcified lesions and non-calcified lesions. There were significant differences in terms of age and use of predilation between the 2 groups which were similarly observed in the main population. Overall, the results are similar which provide support to our inference that the clinical outcomes reported in our study may be extrapolated to the patients whose clinical outcomes were not available. In addition, as our study was not powered to study clinical outcomes in relation to DAPT, we believe that further

Table 2B
Clinical endpoints at two years, described as Kaplan-Meier estimates.

	Ca (n = 143)	Non-Ca (n = 252)	p value
MACE (%)	11.7 (17)	8.0 (19)	0.351
DOCE (%)	9.0 (12)	7.3 (17)	0.564
Cardiac death (%)	3.8 (5)	0.8 (2)	0.052
Target vessel MI	5.3 (7)	5.1 (12)	0.945
Clinically indicated TLR (%)	4.7 (6)	5.9 (14)	0.544
Definite ST (%)	2.1 (3)	2.4 (6)	0.856
Acute	0.0	1.2 (3)	0.191
Subacute	0.0	0.4 (1)	0.450
Late	2.1 (3)	0.0	0.020
Very late	0.0	0.8 (2)	0.287
Probable ST (%)	0.7 (1)	0.4 (1)	0.682
Acute	0.0	0.0	
Subacute	0.0	0.0	
Late	0.7 (1)	0.4 (1)	0.682
Very late	0.0	0.0	
Definite/probable ST (%)	2.9 (4)	2.8 (7)	0.993
Acute	0.0	1.2 (3)	0.191
Subacute	0.0	0.4 (1)	0.450
Late	2.9 (4)	0.4 (1)	0.039
Very late	0.0	0.8 (2)	0.287
POCE (%)	12.2 (23)	17.2 (29)	0.211
All-cause mortality (%)	3.8 (6)	0.8 (3)	0.052
Any revascularization	12.2 (16)	10.3 (25)	0.714
TVR (%)	5.3 (7)	6.5 (16)	0.544
Non-TVR (%)	7.7 (10)	4.7 (11)	0.260
All cause MI (%)	8.3 (11)	6.5 (15)	0.509

DOCE: device oriented composite endpoints (composite of cardiac death, target vessel myocardial infarct and clinically indicated target lesion revascularization); POCE: patient oriented composite endpoints (composite of all - cause mortality, all cause myocardial infarct and any revascularization). (Number of composite endpoints does not add up as any patient may have multiple events.) Ca - calcified lesions; non-Ca - non calcified lesions.

Table 2C
Predictors for clinical outcomes at two years follow-up (using Cox regression), calcified vs non-calcified lesions.

	Unadjusted HR (95% CI)	p-Value	Adjusted[a] HR (95% CI)	p value
All-cause death				
Ca vs non-Ca	4.428 (0.859–22.822)	0.075	1.7 (0.263–10.994)	0.578
Cardiac death				
Ca vs non-Ca	4.428 (0.859–22.822)	0.075	1.7 (0.263–10.994)	0.578
MACE				
Ca vs non-Ca	1.378 (0.700–2.712)	0.353	0.850 (0.382–1.895)	0.692
MI				
Ca vs non-Ca	1.393 (0.632–3.068)	0.411	0.944 (0.366–2.433)	0.905
TLR				
Ca vs non-Ca	0.754 (0.290–1.963)	0.564	0.644 (0.225–1.845)	0.644
TVR				
Ca vs non-Ca	0.762 (0.314–1.853)	0.549	0.629 (0.236–1.674)	0.353
Non-TVR				
Ca vs non-Ca	1.627 (0.691–3.831)	0.265	0.950 (0.342–2.634)	0.921
Definite ST				
Ca vs non-Ca	0.880 (0.220–3.518)	0.856	0.930 (0.206–4.234)	0.930
Probable ST				
Ca vs non-Ca	1.771 (0.111–28.307)	0.686	0.917 (0.039–21.720)	0.957
Def/prob ST				
Ca vs non-Ca	1.005 (0.294–3.434)	0.993	0.935(0.242–3.610)	0.922
DOCE				
Ca vs non-Ca	1.242 (0.593–2.600)	0.566	0.961 (0.416–2.218)	0.926
POCE				
Ca vs non-Ca	1.416 (0.819–2.448)	0.213	1.045 (0.556–1.963)	0.891

To account for baseline differences between patients with at least 1 moderately or heavily calcified lesion (Ca) and patients with no/mild calcified lesions (non-Ca), covariate adjustment using fourteen patient and lesion factors were used (see Online Supplement).
[a] Adjusted for gender, age, presentation with ACS, multivessel disease, diabetes mellitus, dyslipidemia, smoking, hypertension, peripheral artery disease, small vessel, bifurcation, average scaffold diameter per patient, total scaffold length per patient. DOCE: device oriented composite endpoints (composite of cardiac death, target vessel myocardial infarct and clinically indicated target lesion revascularization); POCE: patient oriented composite endpoints (composite of all - cause mortality, all cause myocardial infarct and any revascularization). (Number of composite endpoints does not add up as any patient may have multiple events.) Ca - calcified lesions; non-Ca - non calcified lesions; MACE - major adverse cardiovascular events; MI - myocardial infarct; TLR - target lesion revascularization; TVR - target vessel revascularization; ST - scaffold thrombosis.

studies may be required to evaluate if a prolonged duration of DAPT may reduce late onset ST in calcified lesions.

5. Conclusion

Careful more elaborate lesion preparation and the use of dedicated devices, such as scoring balloons and rotational atherectomy and intracoronary imaging were more likely encountered in Ca lesions. Even after more lesion preparation, acute gain and resulting final MLD by BRS implantation was less compared to non-calcified lesion. Clinical outcomes of calcified and non-calcified lesions treated with BRS were otherwise similar. However this is accomplished in the setting of appropriate case selection, adequate lesion preparation and scaffold optimization with attention to an adequate duration of dual antiplatelet in line with guideline recommendations. Interestingly, a different pattern of timing of ST was observed with no early ST but an increased late ST rate when implanted in calcified lesions.

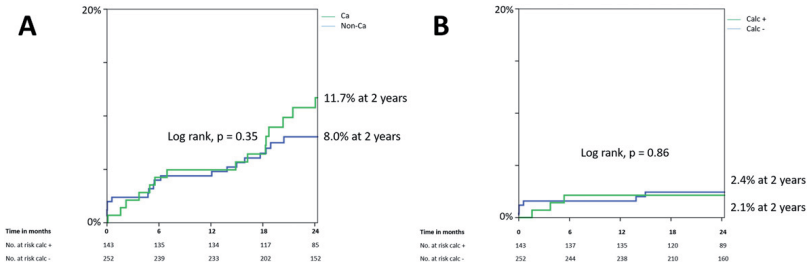

Fig. 2. Kaplan-Meier curve showing no significant difference in A) MACE and B) definite ST at 2 years in patients with calcified (Ca) and non-calcified (non-Ca) lesions treated with bioresorbable vascular scaffolds (BRS). The primary endpoint was major adverse cardiovascular events (MACE), defined as the composite endpoint of cardiac death, myocardial infarction (MI) and target lesion revascularization (TLR). Of note while the incidence of acute ST was higher in the non-Ca group compared to Ca group, there was a significant increase in late ST in calcified lesions compared to non-Ca lesions. ST - scaffold thrombosis.

5.1. Clinical perspectives

Data on the impact of calcium (Ca) on outcomes in patients with lesions treated with bioresorbable vascular scaffolds (BRS) is limited, particularly in a "real world" study population. Careful more elaborate lesion preparation and the use of dedicated devices, such as scoring balloons and rotational atherectomy and intracoronary imaging were more likely encountered in Ca lesions. Late ST was more frequent in the Ca group compared to non-Ca group and no difference for VLST was observed. The findings merit further evaluation of clinical outcomes of BRS and the impact of implantation techniques in complex calcified lesions.

Supplementary data to this article can be found online at https://doi.org/10.1016/j.ijcard.2017.08.046.

Conflict of interest

The authors acknowledged that BVS Expand and BVS STEMI are supported by research grants from Abbott Vascular. Prof van Geuns and Yoshinobu Onuma received speaker's fee from Abbott Vascular.

References

[1] C. Simsek, A. Karanasos, M. Magro, H.M. Garcia-Garcia, Y. Onuma, E. Regar, E. Boersma, P.W. Serruys, R.J. van Geuns, Long-term invasive follow-up of the everolimus-eluting bioresorbable vascular scaffold: five-year results of multiple invasive imaging modalities, EuroIntervention (Oct 28 2014) https://doi.org/10.4244/EIJY14M10_12.

[2] A. Karanasos, C. Simsek, M. Gnanadesigan, N.S. van Ditzhuijzen, R. Freire, J. Dijkstra, S. Tu, N. Van Mieghem, G. van Soest, P. de Jaegere, P.W. Serruys, F. Zijlstra, R.J. van Geuns, E. Regar, OCT assessment of the long-term vascular healing response 5 years after everolimus-eluting bioresorbable vascular scaffold, J. Am. Coll. Cardiol. 64 (22) (Dec 9 2014) 2343–2356.

[3] P.W. Serruys, J.A. Ormiston, Y. Onuma, E. Regar, N. Gonzalo, H.M. Garcia-Garcia, K. Nieman, N. Bruining, C. Dorange, K. Miquel-Hébert, S. Veldhof, M. Webster, L. Thuesen, D. Dudek, A bioabsorbable everolimus-eluting coronary stent system (ABSORB): 2-year outcomes and results from multiple imaging methods, Lancet 373 (2009) 897–910.

[4] S.G. Ellis, D.J. Kereiakes, D.C. Metzger, R.P. Caputo, D.G. Rizik, P.S. Teirstein, M.R. Litt, A. Kini, A. Kabour, S.O. Marx, J.J. Popma, R. McGreevy, Z. Zhang, C. Simonton, G.W. Stone, ABSORB III Investigators, Everolimus-eluting bioresorbable scaffolds for coronary artery disease, N. Engl. J. Med. 373 (20) (Nov 12 2015) 1905–1915.

[5] R. Gao, Y. Yang, Y. Han, Y. Huo, J. Chen, B. Yu, X. Su, L. Li, H.C. Kuo, S.W. Ying, W.F. Cheong, Y. Zhang, X. Su, B. Xu, J.J. Popma, G.W. Stone, ABSORB China Investigators, Bioresorbable vascular scaffolds versus metallic stents in patients with coronary artery disease: ABSORB China Trial, J. Am. Coll. Cardiol. 66 (21) (Dec 1 2015) 2298–2309.

[6] T. Kimura, K. Kozuma, K. Tanabe, S. Nakamura, M. Yamane, T. Muramatsu, S. Saito, J. Yajima, N. Hagiwara, K. Mitsudo, J.J. Popma, P.W. Serruys, Y. Onuma, S. Ying, S. Cao, P. Staehr, W.F. Cheong, H. Kusano, G.W. Stone, ABSORB Japan Investigators, A randomized trial evaluating everolimus-eluting Absorb bioresorbable scaffolds vs. everolimus-eluting metallic stents in patients with coronary artery disease: ABSORB Japan, Eur. Heart J. 36 (47) (Dec 14 2015) 3332–3342.

[7] R. Kawaguchi, H. Tsurugaya, H. Hoshizaki, T. Toyama, S. Oshima, K. Taniguchi, Impact of lesion calcification on clinical and angiographic outcome after sirolimus-eluting stent implantation in real-world patients, Cardiovasc. Revasc. Med. 9 (2008) 2–8.

[8] I. Moussa, S.G. Ellis, M. Jones, D.J. Kereiakes, D. McMartin, B. Rutherford, R. Mehran, M. Collins, M.B. Leon, J.J. Popma, M.E. Russell, G.W. Stone, Impact of coronary culprit lesion calcium in patients undergoing paclitaxel-eluting stent implantation (a TAXUS-IV sub study), Am. J. Cardiol. 96 (2005) 1242–1247.

[9] C.V. Bourantas, Y.J. Zhang, S. Garg, J. Iqbal, M. Valgimigli, S. Windecker, F.W. Mohr, S. Silber, Vries Td, Y. Onuma, H.M. Garcia-Garcia, M.A. Morel, P.W. Serruys, Prognostic implications of coronary calcification in patients with obstructive coronary artery disease treated by percutaneous coronary intervention: a patient-level pooled analysis of 7 contemporary stent trials, Heart 100 (15) (Aug 2014) 1158–1164.

[10] P. de Jaegere, H. Mudra, H. Figulla, Y. Almagor, S. Doucet, I. Penn, A. Colombo, C. Hamm, A. Bartorelli, M. Rothman, M. Nobuyoshi, T. Yamaguchi, V. Voudris, C. DiMario, S. Makovski, D. Hausmann, S. Rowe, S. Rabinovich, M. Sunamura, G.A. van Es, Intravascular ultrasound-guided optimized stent deployment. Immediate and 6 months clinical and angiographic results from the multicenter ultrasound stenting in coronaries study (MUSIC Study), Eur. Heart J. 19 (1998) 1214–1223.

[11] H. Otake, J. Shite, J. Ako, T. Shinke, Y. Tanino, D. Ogasawara, T. Sawada, N. Miyoshi, H. Kato, B.K. Koo, Y. Honda, P.J. Fitzgerald, K. Hirata, Local determinants of thrombus formation following sirolimus-eluting stent implantation assessed by optical coherence tomography, J. Am. Coll. Cardiol. Intv. 2 (2009) 459–466.

[12] R. Diletti, A. Karanasos, T. Muramatsu, S. Nakatani, N.M. Van Mieghem, Y. Onuma, S.T. Nauta, Y. Ishibashi, M.J. Lenzen, J. Ligthart, C. Schultz, E. Regar, P.P. de Jaegere, P.W. Serruys, F. Zijlstra, R.J. van Geuns, Everolimus-eluting bioresorbable vascular scaffolds for treatment of patients presenting with ST-segment elevation myocardial infarction: BVS STEMI first study, Eur. Heart J. 35 (12) (Mar 2014) 777–786.

[13] C.M. Felix, J.M. Fam, R. Diletti, Y. Ishibashi, A. Karanasos, B.R. Everaert, N.M. van Mieghem, J. Daemen, P.P. de Jaegere, F. Zijlstra, E.S. Regar, Y. Onuma, R. van Geuns, Mid- to long-term clinical outcomes of patients treated with the everolimus-eluting bioresorbable vascular scaffold: the BVS expand registry, JACC Cardiovasc. Interv. 9 (16) (Aug 22 2016) 1652–1663.

[14] D.E. Cutlip, S. Windecker, R. Mehran, A. Boam, D.J. Cohen, G.A. van Es, et al., Clinical end points in coronary stent trials: a case for standardized definitions, Circulation 115 (2007) 2344–2351.

[15] S. Basavarajaiah, T. Naganuma, A. Latib, A. Colombo, Can bioabsorbable scaffolds be used in calcified lesions? Catheter. Cardiovasc. Interv. 84 (1) (Jul 1 2014) 48–52.

[16] A. Seth, V. Ravisekar, U. Kaul, Use of 'Guideliner' catheter to overcome failure of delivery of Absorb™ Bioresorbable Vascular Scaffold in calcified tortuous coronary lesions: technical considerations in 'Real World Patients', Indian Heart J. 66 (4) (Jul–Aug 2014) 453–458.

[17] T. Miyazaki, V.F. Panoulas, K. Sato, A. Latib, Colombo A[1]. Bioresorbable vascular scaffolds for heavily calcified lesions: how to tackle the rugged passage? J. Invasive Cardiol. 27 (8) (Aug 2015) E167–8.

[18] S. Tanimoto, P.W. Serruys, L. Thuesen, D. Dudek, B. de Bruyne, B. Chevalier, J.A. Ormiston, Comparison of in vivo acute stent recoil between the bioabsorbable everolimus-eluting coronary stent and the everolimus-eluting cobalt chromium coronary stent: insights from the ABSORB and SPIRIT trials, Catheter. Cardiovasc. Interv. 70 (2007) 515–523.

[19] J.A. Ormiston, B. Webber, B. Ubod, M.W. Webster, J. White, Absorb everolimus-eluting bioresorbable scaffolds in coronary bifurcations: a bench study of deployment, side branch dilatation and post-dilatation strategies, EuroIntervention 10 (2015) 1169–1177.

[20] S.Y. Choi, B. Witzenbichler, A. Maehara, A.J. Lansky, G. Guagliumi, B. Brodie, M.A. Kellett Jr., O. Dressler, H. Parise, R. Mehran, G.D. Dangas, G.S. Mintz, G.W. Stone, Intravascular ultrasound findings of early stent thrombosis after primary percutaneous intervention in acute myocardial infarction: a harmonizing outcomes with revascularization and stents in acute myocardial infarction (HORIZONS-AMI) substudy, Circ. Cardiovasc. Interv. 4 (3) (Jun 2011) 239–247.

[21] Antonios Karanasos, Nicolas M. Van Mieghem, Nienke van Ditzhuijzen, Cordula Felix, Joost Daemen, Anouchska Autar, Yoshinobu Onuma, Mie Kurata, Roberto Diletti, Marco Valgimigli, Floris Kauer, Heleen van Beusekom, Peter de Jaegere, Felix Zijlstra, Robert-Jan van Geuns, Evelyn Regar, Angiographic and optical coherence tomography insights into bioresorbable scaffold thrombosis. A single-center experience, Circ. Cardiovasc. Interv. 8 (5) (May 2015) https://doi.org/10.1161/CIRCINTERVENTIONS.114.002369.

[22] G. Longo, F. Granata, D. Capodanno, Y. Ohno, C.I. Tamburino, P. Capranzano, A. La Manna, B. Francaviglia, G. Gargiulo, C. Tamburino, Anatomical features and management of bioresorbable vascular scaffolds failure: a case series from the GHOST registry, Catheter. Cardiovasc. Interv. (Jan 8 2015) https://doi.org/10.1002/ccd.25819.

[23] V.F. Panoulas, T. Miyazaki, K. Sato, T. Naganuma, A. Sticchi, H. Kawamoto, F. Figini, A. Chieffo, M. Carlino, M. Montorfano, A. Latib, A. Colombo, Procedural outcomes of patients with calcified lesions treated with bioresorbable vascular scaffolds, EuroIntervention 11 (12) (Mar 2016) 1355–1362.

[24] H. Kawamoto, N. Ruparelia, A. Latib, T. Miyazaki, K. Sato, A. Tanaka, T. Naganuma, A. Sticchi, A. Chieffo, M. Carlino, M. Montorfano, A. Colombo, Expansion in calcific lesions and overall clinical outcomes following bioresorbable scaffold implantation optimized with intravascular ultrasound, Catheter. Cardiovasc. Interv. (Aug 22 2016) https://doi.org/10.1002/ccd.26725.

[25] Ming Jiang Fam, J.N. van Der Sijde, A. Karanasos, C. Felix, R. Diletti, N. van Mieghem, P. de Jaegere, F. Zijlstra, R. Jan van Geuns, E. Regar, Comparison of acute expansion of bioresorbable vascular scaffolds versus metallic drug-eluting stents in different degrees of calcification: an optical coherence tomography study, Catheter. Cardiovasc. Interv. (Oct 7 2016) https://doi.org/10.1002/ccd.26676.

[26] M. Ohya, K. Kadota, Y. Sotomi, K. Kozuma, K. Tanabe, M. Uematsu, T. Kawasaki, Y. Morino, T. Tobaru, K. Nakao, K. Tachibana, K. Kishi, Y. Shibata, S. Ying, H. Kusano, G.W. Stone, J.J. Popma, Y. Onuma, P.W. Serruys, T. Kimura, Impact of lesion calcification on angiographic outcomes after Absorb everolimus-eluting bioresorbable vascular scaffold implantation: an observation from the ABSORB Japan trial, EuroIntervention (Nov 8 2016) https://doi.org/10.4244/EIJ-D-16-00359.

[27] A. Colombo, V.F. Panoulas, After 3 decades, at long last, a new device to deal with calcific lesions, JACC Cardiovasc. Interv. 7 (2014) 519–520.

[28] S. Basavarajaiah, T. Naganuma, A. Latib, A. Colombo, Can bioabsorbable scaffolds be used in calcified lesions? Catheter. Cardiovasc. Interv. 84 (2014) 48–52.

[29] K. Yamaji, L. Räber, S. Windecker, What determines long-term outcomes using fully bioresorbable scaffolds - the device, the operator or the lesion? EuroIntervention (Jan 26 2017) https://doi.org/10.4244/EIJV12I14A277.

[30] Patrick W. Serruys, Yoshinobu Onuma, Dmax for sizing, PSP-1, PSP-2, PSP-3 or OCT guidance: interventionalist's jargon or indispensable implantation techniques for short- and long-term outcomes of Absorb BRS? EuroIntervention (Mar 2 2017) https://doi.org/10.4244/EIJY17M02_01.

[31] S. Cassese, R.A. Byrne, G. Ndrepepa, S. Kufner, J. Wiebe, J. Repp, H. Schunkert, M. Fusaro, T. Kimura, A. Kastrati, Everolimus-eluting bioresorbable vascular scaffolds versus everolimus-eluting metallic stents: a meta-analysis of randomised controlled trials, Lancet 387 (10018) (Feb 6 2016) 537–544.

[32] G.W. Stone, R. Gao, T. Kimura, et al., 1-year outcomes with the Absorb bioresorbable scaffold in patients with coronary artery disease: a patient-level, pooled meta-analysis, Lancet 387 (2016) 1277–1289.

[33] Joanna J. Wykrzykowska, Robin P. Kraak, Sjoerd H. Hofma, Rene J. van der Schaaf, E. Karin Arkenbout, Alexander J. IJsselmuiden, Joëlle Elias, Ivo M. van Dongen, Ruben

Y.G. Tijssen, Karel T. Koch, Jan Baan, Jr., M. Marije Vis, Robbert J. de Winter, Jan J. Piek, Jan G.P. Tijssen, and Jose P.S. Henriques, for the AIDA Investigators". Bioresorbable scaffolds versus metallic stents in routine PCI. N. Engl. J. Med. https://doi.org/10.1056/NEJMoa1614954.

[34] R.J. van Geuns, C. Tamburino, J. Fajadet, et al., Self-expanding versus balloon-expandable stents in acute myocardial infarction: results from the APPOSITION II study: self-expanding stents in ST-segment elevation myocardial infarction, JACC Cardiovasc. Interv. 5 (12) (2012) 1209–1219.

[35] S. Puricel, F. Cuculi, M. Weissner, A. Schmermund, P. Jamshidi, T. Nyffenegger, H. Binder, H. Eggebrecht, T. Münzel, S. Cook, T. Gori, Bioresorbable coronary scaffold thrombosis: multicenter comprehensive analysis of clinical presentation, mechanisms, and predictors, J. Am. Coll. Cardiol. 67 (8) (Mar 1 2016) 921–931.

[36] J.P. Giblett, A.J. Brown, H. Keevil, C. Jaworski, S.P. Hoole, N.E. West, Implantation of bioresorbable vascular scaffolds following acute coronary syndrome is associated with reduced early neointimal growth and strut coverage, EuroIntervention 12 (6) (Aug 20 2016) 724–733.

[37] D. Capodanno, D.J. Angiolillo, Antiplatelet therapy after implantation of bioresorbable vascular scaffolds: a review of the published data, practical recommendations, and future directions, JACC Cardiovasc. Interv. 10 (5) (Mar 13 2017) 425–437.

[38] A. Karanasos, N. Van Mieghem, N. van Ditzhuijzen, C. Felix, J. Daemen, A. Autar, Y. Onuma, M. Kurata, R. Diletti, M. Valgimigli, F. Kauer, H. van Beusekom, P. de Jaegere, F. Zijlstra, R.J. van Geuns, E. Regar, Angiographic and optical coherence tomography insights into bioresorbable scaffold thrombosis: single-center experience, Circ. Cardiovasc. Interv. 8 (5) (May 2015) https://doi.org/10.1161/CIRCINTERVENTIONS.114.002369.

[39] C.M. Felix, Y. Onuma, J.M. Fam, R. Diletti, Y. Ishibashi, A. Karanasos, B.R. Everaert, N.M. van Mieghem, J. Daemen, P.P. de Jaegere, F. Zijlstra, E.S. Regar, R.J. van Geuns, Are BVS suitable for ACS patients? Support from a large single center real live registry, Int. J. Cardiol. 218 (Sep 1 2016) 89–97.

[40] G.N. Levine, E.R. Bates, J.A. Bittl, R.G. Brindis, S.D. Fihn, L.A. Fleisher, C.B. Granger, R.A. Lange, M.J. Mack, L. Mauri, R. Mehran, D. Mukherjee, L.K. Newby, P.T. O'Gara, M.S. Sabatine, P.K. Smith, S.C. Smith Jr., ACC/AHA guideline focused update on duration of dual antiplatelet therapy in patients with coronary artery disease: a report of the American College of Cardiology/American Heart Association Task Force on Clinical Practice Guidelines, J. Am. Coll. Cardiol. 68 (10) (2016) 1082–1115.

[41] C.M. Felix, G.J. Vlachojannis, A.J.J. IJsselmuiden, J.M. Fam, P.C. Smits, W. Lansink, R. Diletti, F. Zijlstra, E.S. Regar, E. Boersma, Y. Onuma, R.J.M. van Geuns, Potentially increased incidence of scaffold thrombosis in patients treated with Absorb BVS who terminated DAPT before 18 months, EuroIntervention 13 (2) (2017) e177–e184.

[42] C.M. Felix, G.J. Vlachojannis, A.J. IJsselmuiden, Y. Onuma, R.J. van Geuns, Very late scaffold thrombosis in Absorb BVS: association with DAPT termination? JACC. Cardiovasc. Interv. 10 (6) (Mar 27 2017) 625–626.

[43] Y. Onuma, S. Tanimoto, P. Ruygrok, J. Neuzner, J.J. Piek, A. Seth, J.J. Schofer, G. Richardt, M. Wiemer, D. Carrie, L. Thuesen, C. Dorange, K. Miquel-Hebert, S. Veldhof, P.W. Serruys, Efficacy of everolimus eluting stent implantation in patients with calcified coronary culprit lesions: two-year angiographic and three-year clinical results from the SPIRIT II study, Catheter. Cardiovasc. Interv. 76 (2010) 634–642.

26

CHAPTER

POTENTIALLY INCREASED INCIDENCE OF SCAFFOLD THROMBOSIS IN PATIENTS TREATED WITH ABSORB BVS WHO TERMINATED DAPT BEFORE 18 MONTHS

Cordula M. Felix, Georgios J. Vlachojannis, Alexander J.J. IJsselmuiden, **Jiang Ming Fam**, Peter C. Smits, Wouter J. Lansink, Roberto Diletti, Felix Zijlstra, Evelyn S. Regar, Eric Boersma, Yoshinobu Onuma, Robert J.M. van Geuns.

EuroIntervention. 2017 Jun 2; 13(2):e177-e184.

Potentially increased incidence of scaffold thrombosis in patients treated with Absorb BVS who terminated DAPT before 18 months

Cordula M. Felix[1], MD; Georgios J. Vlachojannis[2], MD, PhD; Alexander J.J. IJsselmuiden[3], MD, PhD; Jiang M. Fam[4], MD; Peter C. Smits[2], MD, PhD; Wouter J. Lansink[3], Msc; Roberto Diletti[1], MD, PhD; Felix Zijlstra[1], MD, PhD; Evelyn S. Regar[1], MD, PhD; Eric Boersma[1], PhD; Yoshinobu Onuma[1], MD, PhD; Robert J.M. van Geuns[1]*, MD, PhD

1. Thoraxcenter, Erasmus Medical Center, Rotterdam, the Netherlands; 2. Maasstad Hospital, Rotterdam, the Netherlands; 3. Albert Schweitzer Hospital, Dordrecht, the Netherlands; 4. National Heart Centre Singapore, Singapore

KEYWORDS

- adjunctive pharmacotherapy
- bioresorbable scaffolds
- clinical research
- stent thrombosis

Abstract

Aims: The aim of this study was to investigate the impact of dual antiplatelet therapy (DAPT) termination on late and very late scaffold thrombosis (ScT) in patients treated with the Absorb bioresorbable vascular scaffold (BVS).

Methods and results: Data from the registries of three centres were pooled (808 patients). To investigate the effect of DAPT termination on ScT after a minimum of six months, we selected a subgroup ("DAPT study cohort" with 685 patients) with known DAPT status >6 months and excluded the use of oral anticoagulants and early ScT. In this cohort, definite/probable ScT incidence for the period on DAPT was compared to ScT incidence after DAPT termination. ScT incidence was 0.83 ScT/100 py with 95% confidence interval (CI): 0.34-1.98. After DAPT termination, the incidence was higher (1.77/100 py; 95% CI: 0.66-4.72), compared to the incidence on DAPT (0.26/100 py, 95% CI: 0.04-1.86; p=0.12) and increased within the month after DAPT termination (6.57/100 py, 95% CI: 2.12-20.38; p=0.01). No very late ScT occurred in patients who continued on DAPT for a minimum of 18 months.

Conclusions: The incidence of late and very late definite/probable ScT was acceptable. The incidence was low while on DAPT but potentially higher when DAPT was terminated before 18 months.

**Corresponding author: Thoraxcenter, Room Ba585, Erasmus Medical Center, 's-Gravendijkwal 230, 3015 CE Rotterdam, the Netherlands. E-mail: r.vangeuns@erasmusmc.nl*

Abbreviations

ACS acute coronary syndrome
BVS bioresorbable vascular scaffold
CAD coronary artery disease
DAPT dual antiplatelet therapy
DES drug-eluting stent
IVUS intravascular ultrasound
MI myocardial infarction
NOAC new oral anticoagulant
NSTEMI non-ST-elevation myocardial infarction
OAC oral anticoagulant
OCT optical coherence tomography
PCI percutaneous coronary intervention
ScT scaffold thrombosis
ST stent thrombosis
STEMI ST-elevation myocardial infarction
UA unstable angina pectoris
VLScT very late scaffold thrombosis

Introduction

Bioresorbable scaffolds are a new treatment option for coronary interventions with the aim of overcoming some of the limitations of metallic drug-eluting stents (DES), such as very late stent thromboses and reinterventions due to polymer reactions, strut fracture, neoatherosclerosis and inflammation.

The Absorb bioresorbable vascular scaffold (BVS) (Abbott Vascular, Santa Clara, CA, USA) has been the most intensively studied. Multiple meta-analyses have shown comparable one-year outcomes for target lesion failure (TLF) of the BVS versus the cobalt-chromium-based everolimus-eluting XIENCE stent (CoCr-EES) (Abbott Vascular) in selected patients. Numbers of scaffold thrombosis (ScT) and target vessel myocardial infarction (MI) tended to be higher in the BVS group[1-3]. In populations reflecting real-world patients[4-8], ScT occurs more frequently. More recently, concerns have been expressed about the occurrence of very late (>1 year) scaffold thrombosis (VLScT)[9,10]. In randomised controlled trials (RCTs), VLScT rates up to two years were low in one (1.6%) but higher in another (2.0%) at three years[11,12].

Dual antiplatelet therapy (DAPT) reduces the risk of local thrombotic events related to stent implantation, systemic thrombotic events, and cardiovascular mortality. In the current ESC and AHA/ACC guidelines, a minimum DAPT duration of six months after DES implantation is recommended, with prolonged treatment in patients with an increased risk of thrombotic events and low bleeding risks. For BVS, the optimal DAPT duration has not yet been clearly defined[13,14]. The early studies investigating BVS applied a minimum DAPT duration of six months. In the more recent RCTs, a minimum duration of 12 months was implemented[11,15].

Editorial, see page 139 and page 142

To summarise, data on long-term ScT outcomes after BVS implantation in real-world patients are lacking and information on optimal DAPT duration is missing. To fill this gap, we describe here the incidence of ScT and report our investigation into the impact of DAPT termination on late and very late ScT in regular clinical practice.

Methods

POPULATION

Patients were pooled from the registries of three Dutch centres where the Absorb BVS was used as part of daily clinical practice. The decision to treat a patient with BVS was made at the discretion of the interventional cardiologist.

The patients of the Erasmus Medical Center were drawn from two investigator-initiated, single-centre, single-arm registries (BVS Expand and BVS STEMI). Inclusion and exclusion criteria have been described elsewhere[5,6]. Patients included in the other two hospital registries were part of local all-comers registries initiated for the control of quality of standard care following introduction of a new CE-approved device.

Between September 2012 and April 2015, 808 patients treated with at least one BVS were included in this study (total cohort). To investigate specifically the association between DAPT and late events without the interference of oral anticoagulants, the DAPT cohort was selected by including patients with a known DAPT status and with a duration of at least six months, without the occurrence of early ScT and without usage of (new) oral anticoagulants ([N]OAC).

ETHICS

This is an observational study, performed based on international regulations, including the Declaration of Helsinki. Data were collected in an encrypted database with the approval of the local ethics committee. The Absorb BVS has received the CE mark and the BVS can be currently used routinely in Europe in different settings without a specific written informed consent.

PROCEDURE

Percutaneous coronary intervention (PCI) was performed according to current clinical practice standards. The radial and femoral approaches using 6 or 7 Fr catheters were the principal routes of vascular access. All patients were treated with unfractionated heparin (at a dose of 70-100 IU/kg). According to the guidelines, patients with stable angina were preloaded with 300 mg of aspirin and 600 mg of clopidogrel. Patients presenting with ACS were preloaded with 300 mg of aspirin and 60 mg of prasugrel or 180 mg of ticagrelor. Previous guidelines for DES and per hospital policies were used to prescribe DAPT and this was also based on the operator's instructions.

FOLLOW-UP

Survival status was obtained from municipal civil registries. Follow-up information specifically for hospitalisation and major cardiovascular events was obtained through questionnaires which were mailed to individual patients at one, six, 12 and 18 months after the procedure. In the case of an absent response after a reminder mail, patients were called thereafter or information was gathered from general practitioners or hospitals.

Information on DAPT status and the date of stopping the $P2Y_{12}$ inhibitor was collected. When an exact stop date was available (through questionnaires, pharmacies, general practitioners or hospital letters), that date was used to compute the duration of DAPT. When patients did not exactly recall the precise stop date but instead noted that he or she used DAPT for a period of one year, the duration of DAPT was recorded as 365 days. In the case of a patient writing that he/she had visited the hospital, additional medical records and discharge letters were consulted to check if any event had occurred.

DEFINITIONS

ScT was classified as stent thrombosis (ST) according to the Academic Research Consortium (ARC)[16]. Scaffold thromboses were reported as either acute (≤24 hours), subacute (1-30 days), late (30-365 days), or very late (>365 days). DAPT termination was defined as the date on which one of the two components of DAPT (aspirin or $P2Y_{12}$ inhibitor) had been terminated.

ENDPOINTS

The primary endpoint in the DAPT study cohort was the incidence rate of definite or probable ScT beyond six months while the patient either was using DAPT or had terminated DAPT. This time period (six to 18 months) was chosen because we assumed that, based on the healing process, the pathophysiology of scaffold thrombosis in the period between six and 18 months was similar. To investigate the time relation with DAPT in more detail, an additional analysis was performed for the first month after DAPT termination compared to the incidence rate while on DAPT.

STATISTICAL ANALYSIS

Categorical variables are reported as counts and percentages, continuous variables as mean±standard deviation or median (25^{th}-75^{th} percentile). For each time period, the ScT incidence was calculated as the number of events divided by the sum of the follow-up times for each individual. The variable "on DAPT" was computed as the stop date of DAPT minus the date of the index procedure. In case of an ScT while the patient was using DAPT, "on DAPT" was reported as days until the event. "off DAPT" was calculated as 18 months post procedure (or the latest available follow-up date) minus the time period until termination of the $P2Y_{12}$ inhibitor. In the case of ScT while DAPT was terminated, days off DAPT were computed as follows: date of ScT minus date of DAPT termination. The cumulative incidence of study endpoints was estimated according to the Kaplan-Meier method. Patients lost to follow-up were considered at risk until the date of last contact, at which point they were censored. All statistical tests were patient-based, two-sided and a p-value of <0.05 was considered statistically significant. Statistical analyses were performed using SPSS, Version 21 (IBM Corp., Armonk, NY, USA).

Results

Between September 2012 and January 2015, 808 patients were included in the pooled database. The DAPT study cohort consisted of 685 patients **(Figure 1)**. Survival status in this group was known in 100% and the median follow-up duration was 730 (interquartile range [IQR]: 531.8-923.3) days. The median duration of DAPT was 367 (IQR: 365-398) days, with a range from 180 to 1,237 days. One hundred and thirty (19%) patients had a DAPT duration ranging between six months and one year, and 81% had a DAPT duration of at least 365 days. Eighty-nine patients (12.9%) continued DAPT until the last follow-up. **Figure 2A** displays the individual duration of DAPT for the patients.

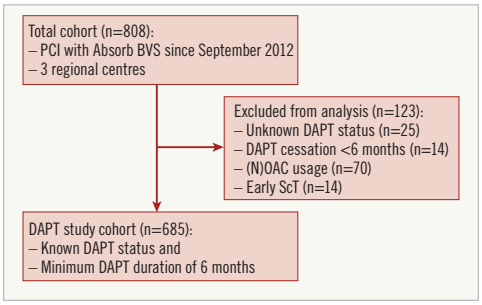

Figure 1. *Study flow chart.*

BASELINE CHARACTERISTICS

Baseline characteristics of both the full cohort and the DAPT study cohort are presented in **Table 1.** In the DAPT study cohort, mean age was 57.9 (±10.6) years, 73.9% were male, 14.3% were diabetic, and 12.4% had a history of myocardial infarction. Most patients (70.3%) presented with ACS. The majority of the patients used a potent $P2Y_{12}$ inhibitor such as prasugrel or ticagrelor (76.6%). The mean number of lesions/patient was 1.19 (±0.45). Moderate or severe lesion calcification, as assessed by angiography, was present in 32.9% and bifurcation in 21.3% of patients. AHA/ACC lesion classification type B2/C was present in 45.7%.

PROCEDURAL DETAILS

Procedural details are described in **Table 2.** In the DAPT study cohort, a total of 964 BVS were implanted. Predilatation was performed in 88.3% of the patients, post-dilatation in 56.7% and intravascular imaging (OCT or IVUS) in 31.3%. A 2.5 mm BVS was used in 21.8% of patients. Mean scaffold diameter and mean scaffold length were 3.1 (±0.4) mm and 20.9 (±5.8) mm, respectively. Device success and procedural success were achieved in 98.3% and 98.0%, respectively.

CLINICAL OUTCOMES

In the total cohort of 808 patients, 26 definite or probable ScT occurred with a cumulative event rate (Kaplan-Meier estimate) of 3.3% (95% CI: 2.1-4.5) at 18 months **(Figure 3)**. The majority (1.7%) were early ScT: the acute ScT rate was 0.2% (95% CI: -0.2-0.6) and the subacute ScT rate was 1.5% (95% CI: 0.7-2.3).

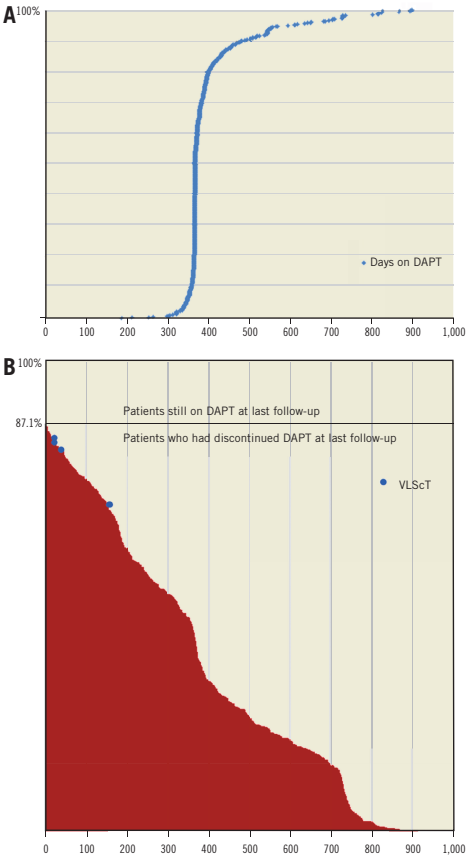

Figure 2. *DAPT duration for all indivudual patients. A) Days on DAPT in the DAPT study cohort. B) Days off DAPT in the DAPT study cohort. Blue dots indicate the ScT timing in relation to the number of days off DAPT. VLScT: very late scaffold thrombosis.*

Late and very late ScT were less frequent: 1.0% (95% CI: 0.2-2.0) and 0.6% (95% CI: 0.02-1.2), respectively. In the DAPT study cohort, Kaplan-Meier estimates for late and very late ScT were similar (0.9% and 0.7%, respectively).

Figure 2B shows the duration in days while off DAPT and the association with very late ScT in the DAPT study cohort. Four cases of very late definite/probable ScT occurred: at 379 days (10 days after DAPT termination), at 416 days (35 days after DAPT termination), at 429 days (20 days after DAPT termination), and at 526 days (149 days after DAPT termination). These cases have been described elsewhere[17]. The four patients were using aspirin but had terminated $P2Y_{12}$ inhibitor use. Their duration of DAPT was a little over 365 days. However, this was not based

Table 1. Patient and lesion characteristics.

		Total cohort N patients=808, N lesions=949	DAPT study cohort N patients=685, N lesions=813
Median follow-up in days (IQR)		729 (516-899.75)	730 (531.8-923.3)
Gender (%)	Male	73.9	73.9
	Female	26.1	26.1
Mean age in years (±SD)		58.46 (10.91)	57.9 (10.6)
Smoking (%)		50.8	51.5
Hypertension (%)		47.9	45.0
Dyslipidaemia (%)		45.9	45.4
Diabetes mellitus (%)		14.2	14.3
Family history of CAD (%)		48.8	49.5
Prior MI (%)		12.8	12.4
Prior PCI/CABG (%)		13.7	13.4
Presentation with multivessel disease (%)		30.8	30.3
Indication for PCI (%)			
Stable angina		26.6	26.1
Unstable angina		10.1	10.0
NSTEMI		30.7	31.2
STEMI		28.6	29.1
Silent ischaemia		3.9	3.6
Peripheral artery disease (%)		3.8	3.2
Heart failure (%)		4.0	2.5
Renal insufficiency (%)		3.3	2.5
ASA+$P2Y_{12}$ inhibitor (%)			
clopidogrel		39.8	38.3
prasugrel		38.2	38.3
ticagrelor		22.0	23.4
Median duration of DAPT in days (IQR)			367 (365-398)
Min and max DAPT duration in days			180-1,237
Number of lesions per patient (±SD)		1.17 (0.44)	1.19 (0.45)
Left anterior descending artery (%)		54.4	54.2
Left circumflex artery (%)		20.9	21.4
Right coronary artery (%)		24.7	24.4
Bifurcation (%)		23.0	21.3
Calcification (moderate or severe) (%)		33.7	32.9
CTO (%)		3.1	3.2
ACC/AHA lesion classification (%)	A	10.3	10.3
	B1	43.5	44.0
	B2	28.4	27.3
	C	17.8	18.4

ACC/AHA: American College of Cardiology/American Heart Association; ASA: acetylsalicylic acid; CABG: coronary artery bypass graft; CAD: coronary artery disease; CTO: chronic total occlusion; DAPT: dual antiplatelet therapy; MI: myocardial infarction; NSTEMI: non-ST-elevation myocardial infarction; PCI: percutaneous coronary intervention; STEMI: ST-elevation myocardial infarction.

Table 2. Procedural characteristics.

	Total cohort N patients=808, N lesions=949	DAPT study cohort N patients=685, N lesions=813
Predilatation (%)	88.4	88.3
Invasive imaging at baseline (%)	30.8	31.3
Total number of scaffolds implanted	1,119	964
2.5 mm BVS (%)	22.7	21.8
3.0 mm BVS (%)	39.2	40.7
3.5 mm BVS (%)	38.1	37.4
Mean scaffold diameter, mm (±SD)	3.08 (0.38)	3.08 (0.38)
Mean scaffold length, mm (±SD)	20.90 (5.83)	20.94 (5.83)
Mean total scaffold length per patient, mm (±SD)	32.48 (20.99)	33.14 (21.60)
Overlap (%)	29.7	30.6
Post-dilatation (%)	55.4	56.7
Clinical device success (%)	98.0	98.3
Clinical procedure success (%)	97.2	98.0

BVS: bioresorbable vascular scaffold.

on a specific reason such as an increased ischaemic risk. The rate of definite/probable ScT in this particular time frame was 0.7%.

For reasons of comparability with the current literature, the incidences per 100 patient-years (py) were computed in the DAPT study cohort **(Figure 4, Table 3)**. For calculating the incidence of ScT in the time period six to 18 months, 607.52 py were available and five events occurred (one late ScT and four very late ScT) with an incidence of 0.83/100 py (95% CI: 0.34-1.98).

For the period on DAPT, 381.90 py were available and one event occurred (at day 208). This resulted in an incidence of 0.26/100 py (95% CI: 0.04-1.86). For the period after DAPT termination, 225.62 py and four events were reported with an ScT incidence of 1.77/100 py (95% CI: 0.66-4.72), numerically 6.8 times higher than the incidence on DAPT but not statistically significant (p=0.12).

For the incidence of ScT in the first month after DAPT termination, 45.64 py were available and three events occurred, which subsequently provided an incidence of 6.57/100 py (95% CI: 2.12-20.38). This was statistically significant when compared to the incidence in the on DAPT period (p=0.01). The incidence of ScT during the last month of DAPT usage was zero.

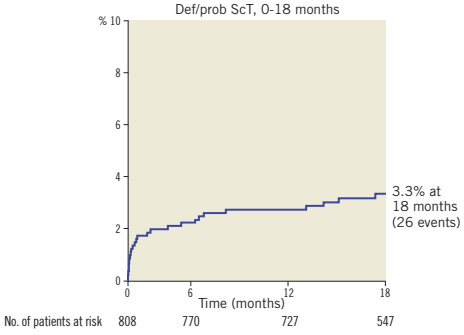

Figure 3. *Cumulative ScT rate in the total cohort from the index procedure up to 18 months post procedure. ScT: scaffold thrombosis.*

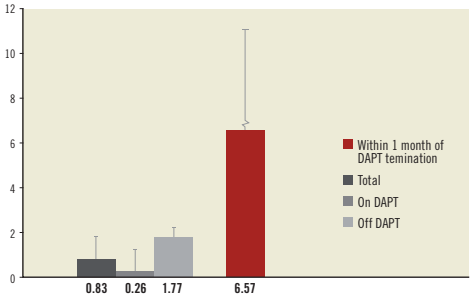

Figure 4. *Incidence densities for the whole DAPT study cohort, in patients on and off DAPT and within the first month of termination in the DAPT study cohort. DAPT: dual antiplatelet therapy.*

Table 3. Incidence of definite/probable ScT per 100 patient-years.

	Incidence rates per 100 patient-years (95% CI) 6-18 months
Total	0.83 (0.34-1.98)
On DAPT period	0.26 (0.04-1.86)
Off DAPT period	1.77 (0.66-4.72)
Within 1 month of DAPT termination	6.57 (2.12-20.38)

DAPT: dual antiplatelet therapy; ScT: scaffold thrombosis

Discussion

To the best of our knowledge, this is the first study that reports on the impact of DAPT termination on the occurrence of definite/probable ScT in Absorb BVS in a clearly defined study cohort, reflecting real-world patients. The main findings of our study are as follows: 1) the incidence of definite or probable late and very late ScT in patients who are on DAPT is low; 2) all cases of very late ScT at 18 months were not using DAPT at the time of the event; 3) the incidence of ScT in patients off DAPT is potentially increased within the first 18 months post implantation, with the highest incidence within one month after termination of DAPT.

OVERALL INCIDENCE OF LATE AND VERY LATE ScT

Overall, the late and very late scaffold thrombosis rates in this multicentre, real-world registry were acceptable and comparable

to the rates in selected populations as included in approval studies for different countries[11,12,15]. In this study, and regardless of DAPT status, the overall incidence density of late and very late def/prob ScT was 1.0 and 1.44 per 100 py, respectively. A large all-comers observational cohort study, investigating ST in metallic DES during four-year follow-up reported a late ST incidence density of 0.4 def/prob ST per 100 py in patients treated with newer-generation EES. For SES and PES, incidence densities were higher for both late (SES: 0.7/100 py and PES: 1.5/100 py) and very late ST (SES: 2.8/100 py and PES: 4.0/100 py). In this regard, late and very late ScT incidence in BVS patients seems comparable to first-generation metallic DES[18].

DAPT AND LATE EVENTS

At 18 months, there were four patients with VLScT, all while not using DAPT during the event. Three out of four cases appeared to be associated with DAPT termination. The incidence density was 1.79/100 py in patients who were not continuously on DAPT. Importantly, the incidence of ScT within one month of DAPT termination was even higher. In the ABSORB EXTEND study, 50% of the ScT cases were related to either premature DAPT termination or resistance to clopidogrel[19]. The ABSORB Japan trial has reported two-year follow-up. Two out of four patients with VLScT were not using DAPT at the time of the event. In the recently published ABSORB II RCT, three-year results revealed six cases of VLScT. Of note, all cases of late and very late ScT occurred in patients off DAPT. Moreover, in patients who did not terminate DAPT up to three years, no cases of ScT were described[12]. In our series, the relationship between the moment of DAPT termination and the occurrence of VLScT was notable, with three out of four cases within 35 days of DAPT termination, a finding not so clear in the ABSORB II and ABSORB Japan trials. Thus, as reported in multiple studies, DAPT termination seems to play an important role in the occurrence of VLScT.

POSSIBLE CAUSES OF LATE ScT

Other factors besides DAPT termination that were associated with ScT were suboptimal implantation technique, late discontinuities, uncovered struts, neoatherosclerosis, high maximum footprint, small minimal lumen diameter, small vessels, higher % diameter stenosis, overlap, ostial lesions and decreased LVEF[11,20-25]. Late and very late ScT while DAPT was terminated might be explained by the high volume of implanted material, in particular to the increased strut thickness, which could cause laminar flow disturbance and subsequently the triggering of platelet deposition[26]. This might be a special problem in small vessels or when full dilatation was not achieved without high-pressure post-dilatation using non-compliant balloons. In early BVS registries, there was a higher risk of malapposition, often induced by undersizing, which occurs regularly[5]. During the first large studies in BVS patients, high-pressure post-dilatation with non-compliant balloons was not mandatory as a result of a case where strut fractures were observed. Nowadays, a different implantation tactic for BVS is used, after an optimal implantation strategy started in January 2014 was associated with a large reduction in ScT incidence[20,27]. Also, thinner-strut BVS are currently being developed, which will mitigate the risk of ScT.

Study limitations

This was a retrospective and registry data-pooled study. As the sample size is limited and the numbers of this low-frequency event are small, these results should be interpreted with caution and considered hypothesis-generating. More data and dedicated studies are needed to confirm our suggestion to prolong DAPT in BVS-treated patients. Lastly, quantitative coronary analysis (QCA) was not available in all patients.

Conclusions

The incidence of probable/definite late and very late ScT in BVS patients who were on DAPT in our study was low. However, the incidence of early ScT and also the occurrence of very late ScT was not negligible. Between six and 18 months, the incidence of ScT in patients who terminated DAPT was potentially increased.

Impact on daily practice

As long as studies with an optimal implantation strategy have not revealed data on safe DAPT termination before 18 months, it would be reasonable to consider extension of DAPT. Prolonging DAPT even up to three years could be a possible solution in patients with an increased risk of ischaemic events and low bleeding risk (the DAPT score can be used for risk assessment[28]), as the resorption process of the Absorb BVS is completed in three years and, until that time, the polymer is still present, and the risk of very late ScT is lurking. The decision as to whether or not to continue DAPT beyond a certain time point cannot be made according to a "one size fits all" principle but should be based on each individual patient.

Acknowledgements

We wish to thank Isabella Kardys for her valuable input and role in event adjudication. We wish to thank Ester Salentijn, Nienke van Ditzhuijzen and Saskia Wemelsfelder for their contribution to data management.

Funding

This research was possible through funding from Abbott Vascular to the Erasmus Medical Center as coordinating centre.

Conflict of interest statement

R. van Geuns, P. Smits, G. Vlachojannis, Y. Onuma, and A. IJsselmuiden have received fees or grants from Abbott Vascular. The other authors have no conflicts of interest to declare.

References

1. Stone GW, Gao R, Kimura T, Kereiakes DJ, Ellis SG, Onuma Y, Cheong WF, Jones-McMeans J, Su X, Zhang Z, Serruys PW. 1-year

outcomes with the Absorb bioresorbable scaffold in patients with coronary artery disease: a patient-level, pooled meta-analysis. *Lancet.* 2016;387:1277-89.

2. Cassese S, Byrne RA, Ndrepepa G, Kufner S, Wiebe J, Repp J, Schunkert H, Fusaro M, Kimura T, Kastrati A. Everolimus-eluting bioresorbable vascular scaffolds versus everolimus-eluting metallic stents: a meta-analysis of randomised controlled trials. *Lancet.* 2016;387:537-44.

3. Kang SH, Chae IH, Park JJ, Lee HS, Kang DY, Hwang SS, Youn TJ, Kim HS. Stent Thrombosis With Drug-Eluting Stents and Bioresorbable Scaffolds: Evidence From a Network Meta-Analysis of 147 Trials. *JACC Cardiovasc Interv.* 2016;9:1203-12.

4. Capodanno D, Gori T, Nef H, Latib A, Mehilli J, Lesiak M, Caramanno G, Naber C, Di Mario C, Colombo A, Capranzano P, Wiebe J, Araszkiewicz A, Geraci S, Pyxaras S, Mattesini A, Naganuma T, Münzel T, Tamburino C. Percutaneous coronary intervention with everolimus-eluting bioresorbable vascular scaffolds in routine clinical practice: early and midterm outcomes from the European multicentre GHOST-EU registry. *EuroIntervention.* 2015;10:1144-53.

5. Felix CM, Fam JM, Diletti R, Ishibashi Y, Karanasos A, Everaert BR, van Mieghem NM, Daemen J, de Jaegere PP, Zijlstra F, Regar ES, Onuma Y, van Geuns RM. Mid- to Long-Term Clinical Outcomes of Patients Treated With the Everolimus-Eluting Bioresorbable Vascular Scaffold: The BVS Expand Registry. *JACC Cardiovasc Interv.* 2016;9:1652-63.

6. Fam JM, Felix C, van Geuns RJ, Onuma Y, Van Mieghem NM, Karanasos A, van der Sijde J, De Paolis M, Regar E, Valgimigli M, Daemen J, de Jaegere P, Zijlstra F, Diletti R. Initial experience with everolimus-eluting bioresorbable vascular scaffolds for treatment of patients presenting with acute myocardial infarction: a propensity-matched comparison to metallic drug eluting stents 18-month follow-up of the BVS STEMI first study. *EuroIntervention.* 2016;12:30-7.

7. Felix CM, Onuma Y, Fam JM, Diletti R, Ishibashi Y, Karanasos A, Everaert BR, van Mieghem NM, Daemen J, de Jaegere PP, Zijlstra F, Regar ES, van Geuns RJ. Are BVS suitable for ACS patients? Support from a large single center real live registry. *Int J Cardiol.* 2016;218:89-97.

8. Kraak RP, Grundeken MJ, Hassell ME, Elias J, Koch KT, Henriques JP, Piek JJ, Baan J Jr, Vis MM, Tijssen JG, de Winter RJ, Wykrzykowska JJ. Two-year clinical outcomes of Absorb bioresorbable vascular scaffold implantation in complex coronary artery disease patients stratified by SYNTAX score and ABSORB II study enrolment criteria. *EuroIntervention.* 2016;12:e557-65.

9. Collet C, Serruys PW. Very late scaffold thrombosis after bioresorbable scaffold implantation: an unexpected new enemy on the horizon... or just a false alarm? *EuroIntervention.* 2016;12:1077-9.

10. Toyota T, Morimoto T, Shiomi H, Yoshikawa Y, Yaku H, Yamashita Y, Kimura T. Very Late Scaffold Thrombosis of Bioresorbable Vascular Scaffold: Systematic Review and a Meta-Analysis. *JACC Cardiovasc Interv.* 2017;10:27-37.

11. Onuma Y, Sotomi Y, Shiomi H, Ozaki Y, Namiki A, Yasuda S, Ueno T, Ando K, Furuya J, Igarashi K, Kozuma K, Tanabe K, Kusano H, Rapoza R, Popma JJ, Stone GW, Simonton C, Serruys PW, Kimura T. Two-year clinical, angiographic, and serial optical coherence tomographic follow-up after implantation of an everolimus-eluting bioresorbable scaffold and an everolimus-eluting metallic stent: insights from the randomised ABSORB Japan trial. *EuroIntervention.* 2016;12:1090-101.

12. Serruys PW, Chevalier B, Sotomi Y, Cequier A, Carrie D, Piek JJ, Van Boven AJ, Dominici M, Dudek D, McClean D, Helqvist S, Haude M, Reith S, de Sousa Almeida M, Campo G, Iniguez A, Sabaté M, Windecker S, Onuma Y. Comparison of an everolimus-eluting bioresorbable scaffold with an everolimus-eluting metallic stent for the treatment of coronary artery stenosis (ABSORB II): a 3 year, randomised, controlled, single-blind, multicentre clinical trial. *Lancet.* 2016;388:2479-91.

13. Bittl JA, Baber U, Bradley SM, Wijeysundera DN. Duration of Dual Antiplatelet Therapy: A Systematic Review for the 2016 ACC/AHA Guideline Focused Update on Duration of Dual Antiplatelet Therapy in Patients With Coronary Artery Disease: A Report of the American College of Cardiology/American Heart Association Task Force on Clinical Practice Guidelines. *J Am Coll Cardiol.* 2016;68:1116-39.

14. Roffi M, Patrono C, Collet JP, Mueller C, Valgimigli M, Andreotti F, Bax JJ, Borger MA, Brotons C, Chew DP, Gencer B, Hasenfuss G, Kjeldsen K, Lancellotti P, Landmesser U, Mehilli J, Mukherjee D, Storey RF, Windecker S, Baumgartner H, Gaemperli O, Achenbach S, Agewall S, Badimon L, Baigent C, Bueno H, Bugiardini R, Carerj S, Casselman F, Cuisset T, Erol Ç, Fitzsimons D, Halle M, Hamm C, Hildick-Smith D, Huber K, Iliodromitis E, James S, Lewis BS, Lip GY, Piepoli MF, Richter D, Rosemann T, Sechtem U, Steg PG, Vrints C, Luis Zamorano J; Management of Acute Coronary Syndromes in Patients Presenting without Persistent ST-Segment Elevation of the European Society of Cardiology. 2015 ESC Guidelines for the management of acute coronary syndromes in patients presenting without persistent ST-segment elevation: Task Force for the Management of Acute Coronary Syndromes in Patients Presenting without Persistent ST-Segment Elevation of the European Society of Cardiology (ESC). *Eur Heart J.* 2016;37:267-315.

15. Gao R, Yang Y, Han Y, Huo Y, Chen J, Yu B, Su X, Li L, Kuo HC, Ying SW, Cheong WF, Zhang Y, Su X, Xu B, Popma JJ, Stone GW; ABSORB China Investigators. Bioresorbable Vascular Scaffolds Versus Metallic Stents in Patients with Coronary Artery Disease: ABSORB China trial. *J Am Coll Cardiol.* 2015;66:2298-309.

16. Cutlip DE, Windecker S, Mehran R, Boam A, Cohen DJ, van Es GA, Steg PG, Morel MA, Mauri L, Vranckx P, McFadden E, Lansky A, Hamon M, Krucoff MW, Serruys PW; Academic Research Consortium. Clinical end points in coronary stent trials: a case for standardized definitions. *Circulation.* 2007;115:2344-51.

17. Felix CM, Vlachojannis GJ, IJsselmuiden AJ, Onuma Y, van Geuns RJ. Very Late Scaffold Thrombosis in Absorb BVS: Association With DAPT Termination? *JACC Cardiovasc Interv.* 2017;10:625-6.

18. Palmerini T, Biondi-Zoccai G, Della Riva D, Stettler C, Sangiorgi D, D'Ascenzo F, Kimura T, Briguori C, Sabate M, Kim HS, De Waha A, Kedhi E, Smits PC, Kaiser C, Sardella G, Marullo A, Kirtane AJ, Leon MB, Stone GW. Stent thrombosis with drug-eluting and bare-metal stents: evidence from a comprehensive network meta-analysis. *Lancet.* 2012;379:1393-402.

19. Ishibashi Y, Onuma Y, Muramatsu T, Nakatani S, Iqbal J, Garcia-Garcia HM, Bartorelli AL, Whitbourn R, Abizaid A, Serruys PW; ABSORB EXTEND Investigators. Lessons learned from acute and late scaffold failures in the ABSORB EXTEND trial. *EuroIntervention.* 2014;10:449-57.

20. Puricel S, Cuculi F, Weissner M, Schmermund A, Jamshidi P, Nyffenegger T, Binder H, Eggebrecht H, Munzel T, Cook S, Gori T. Bioresorbable Coronary Scaffold Thrombosis: Multicenter Comprehensive Analysis of Clinical Presentation, Mechanisms, and Predictors. *J Am Coll Cardiol.* 2016;67:921-31.

21. Ellis SG, Kereiakes DJ, Metzger DC, Caputo RP, Rizik DG, Teirstein PS, Litt MR, Kini A, Kabour A, Marx SO, Popma JJ, McGreevy R, Zhang Z, Simonton C, Stone GW; ABSORB III Investigators. Everolimus-Eluting Bioresorbable Scaffolds for Coronary Artery Disease. *N Engl J Med.* 2015;373:1905-15.

22. Karanasos A, Van Mieghem N, van Ditzhuijzen N, Felix C, Daemen J, Autar A, Onuma Y, Kurata M, Diletti R, Valgimigli M, Kauer F, van Beusekom H, de Jaegere P, Zijlstra F, van Geuns RJ, Regar E. Angiographic and optical coherence tomography insights into bioresorbable scaffold thrombosis: single-center experience. *Circ Cardiovasc Interv.* 2015;8(5).

23. Räber L, Brugaletta S, Yamaji K, O'Sullivan CJ, Otsuki S, Koppara T, Taniwaki M, Onuma Y, Freixa X, Eberli FR, Serruys PW, Joner M, Sabate M, Windecker S. Very Late Scaffold Thrombosis: Intracoronary Imaging and Histopathological and Spectroscopic Findings. *J Am Coll Cardiol.* 2015;66:1901-14.

24. Azzalini L, Al-Hawwas M, L'Allier PL. Very late bioresorbable vascular scaffold thrombosis: a new clinical entity. *EuroIntervention.* 2015;11:e1-2.

25. Sotomi Y, Suwannasom P, Serruys PW, Onuma Y. Possible mechanical causes of scaffold thrombosis: insights from case reports with intracoronary imaging. *EuroIntervention.* 2017;12: 1747-56.

26. Kolandaivelu K, Swaminathan R, Gibson WJ, Kolachalama VB, Nguyen-Ehrenreich KL, Giddings VL, Coleman L, Wong GK, Edelman ER. Stent thrombogenicity early in high-risk interventional settings is driven by stent design and deployment and protected by polymer-drug coatings. *Circulation.* 2011;123:1400-9.

27. Généreux P, Rutledge DR, Palmerini T, Caixeta A, Kedhi E, Hermiller JB, Wang J, Krucoff MW, Jones-McMeans J, Sudhir K, Simonton CA, Serruys PW, Stone GW. Stent Thrombosis and Dual Antiplatelet Therapy Interruption With Everolimus-Eluting Stents: Insights From the Xience V Coronary Stent System Trials. *Circ Cardiovasc Interv.* 2015;8(5).

28. Yeh RW, Secemsky EA, Kereiakes DJ, Normand SL, Gershlick AH, Cohen DJ, Spertus JA, Steg PG, Cutlip DE, Rinaldi MJ, Camenzind E, Wijns W, Apruzzese PK, Song Y, Massaro JM, Mauri L; DAPT Study Investigators. Development and Validation of a Prediction Rule for Benefit and Harm of Dual Antiplatelet Therapy Beyond 1 Year After Percutaneous Coronary Intervention. *JAMA.* 2016;315:1735-49.

27

CHAPTER

LATE AND VERY LATE SCAFFOLD THROMBOSIS

Antonis Karanasos, Bu-Chun Zhang, Jors van der Sijde, **Jiang Ming Fam**, Robert-Jan van Geuns, Evelyn Regar.

Textbook on Bioresorbable Scaffolds: from basic concept to clinical application, Edited by Yoshinobu Onuma and Patrick W. Serruy. Chapter 8.2 pages 421-430. (Textbook chapter)

Late and very late scaffold thrombosis

ANTONIOS KARANASOS, BU-CHUN ZHANG, JORS VAN DER SIJDE, JIANG-MING FAM, ROBERT-JAN M. VAN GEUNS, AND EVELYN REGAR

Late and very late thrombosis in metallic stents 461
Healing response in bioresorbable scaffolds 462
Current experience with late scaffold thrombosis 463
Current experience with very late scaffold thrombosis 464
Imaging observations in late and very late scaffold thrombosis 466
Potential mechanisms—Preventive measures 467
Conclusions 467
References 467

Bioresorbable scaffolds (BRS) are a new treatment for coronary artery disease. As these devices are expected to resorb after providing the mechanical support required the first months after percutaneous coronary intervention (PCI), they could potentially be associated with several long-term advantages over the metallic stents, such as a lack of permanent vessel caging that enables restoration of the vessel vasomotor tone, adaptive shear stress, late luminal enlargement with late expansive remodeling, preservation of long-term side-branch patency, and allowing future revascularization options, while free of complications observed with metallic stents such as neoatherosclerosis and late failure [1]. First-in-human studies of BRS have shown promising results demonstrating a favorable healing response at long-term with complete scaffold resorption, late lumen enlargement, recovery of vasomotion, and a potentially favorable plaque modification [2,3]. Furthermore, initial clinical results were also promising showing a low rate of adverse events and a complete absence of late and very late thrombotic events. Utilization of BRS in more complex lesions and populations was associated with a higher event rate, while several cases of late and very late scaffold thrombosis were reported. In this chapter, we aim to briefly summarize current insights from late and very late metallic stent thrombosis, give basic insights into BVS healing, review current experience on BRS thrombosis, and suggest potential mechanisms and preventive measures for this complication.

LATE AND VERY LATE THROMBOSIS IN METALLIC STENTS

Late thrombosis, defined as the occurrence of stent thrombosis beyond 1 month after baseline implantation, had not received much attention from the interventional community during the first years of metallic stents. However, the report of several angiographically confirmed cases of first-generation metallic drug-eluting stent (DES) thrombosis related to antiplatelet therapy discontinuation brought this issue in the spotlight [4], and intracoronary devices have ever since been scrutinized for the occurrence of this complication. First-generation DES had been considered the main devices associated with this complication, with an annual incidence rate of late and very late (defined as stent thrombosis occurring beyond 1 year since initial implantation) stent thrombosis of 0.6% per year in a large two-center registry [5]. However, accumulating experience has shown that an ongoing thrombotic risk is present with all devices, including bare metal stents (BMS) with cases of thrombosis reported up to 15–20 years postimplantation [6,7]. Similarly, although second-generation drug-eluting stents have been associated with an improved long-term safety profile with lower risk of stent thrombosis in meta-analyses [8], it appears that late thrombosis remains an issue with these devices as well, with an annual incidence rate of definite very late stent thrombosis of 0.2% [9]. It is therefore evident that late and very late stent thrombosis is consistently observed with all metallic stents, although the incidence might vary depending on stent type.

Several factors have been implicated in the pathogenesis of stent thrombosis, including patient-related factors (acute coronary syndrome, diabetes, renal failure, impaired left ventricular function, prior brachytherapy, malignancy), lesion factors (lesion/stent length, vessel/stent diameter, bifurcation, total occlusion, saphenous venous graft lesions), procedural factors (inadequate stent expansion or sizing, malapposition, stent deployment in necrotic core, residual edge dissections), antithrombotic and antiplatelet therapy (premature dual antiplatelet therapy discontinuation,

aspirin or clopidogrel nonresponsiveness), and device-related factors (hypersensitivity to stent polymer or drug, incomplete endothelialization, stent design, covered stents) [10,11].

Pathologic studies were the first to assess the pathomechanisms of metallic stent thrombosis [12,13]. These observations hinted to the underlying plaque as an important substrate in BMS thrombosis, whereas in DES an impaired healing response with high incidence of incomplete strut coverage and stent malapposition was identified as the main mechanism [13]. Namely in first-generation DES, this pattern of healing response has been associated with vessel wall toxicity either due to the released drug or to the polymer [14]. These initial pathologic observations were expanded by *in vivo* optical coherence tomography (OCT) studies which tried to evaluate imaging findings in patients with late and very late metallic stent thrombosis (Figure 8.2.1). As the high resolution of OCT allows for detection of tissue with ~10 μm resolution, strut coverage by OCT has been used to assess strut endothelialization. Although numerous studies have assessed OCT coverage as a surrogate for healing, the percentage of uncovered struts has not been prospectively associated with stent thrombosis thus far [15]. Nevertheless, studies focusing on patients with events have shown a high incidence of incomplete coverage in patients with late and very late metallic DES thrombosis [16–24]. Similarly, stent malapposition has also been suggested to play a role in metallic stent thrombosis. As with incomplete coverage, acute malapposition has not been prospectively associated with stent thrombosis [25]; however, metallic stents with late thrombosis have a very high incidence of malapposition [16–24], while late malapposition has been associated with the presence of local inflammation in first-generation metallic DES and prospectively linked to very late adverse outcome [26]. Importantly, findings of incomplete coverage and malapposition are exaggerated within the stent in segments with thrombus versus segments without thrombus [24].

Overall in these studies, this impaired healing response accounts for approximately half of the very late thrombotic events in metallic DES. In the rest of the cases with very late DES thrombosis and also in the vast majority of very late bare metal stent (BMS) thrombosis, another mechanism, consisting of *de novo* development of atherosclerosis within the stented segment and called neoatherosclerosis, seems to prevail [27–30]. Indeed, several reports have linked neoatherosclerosis to in-stent plaque rupture and subsequent thrombosis within the stent [6], while neoatherosclerotic plaque rupture has been associated with acute coronary syndrome presentation, although it can be also encountered in asymptomatic or stable patients [27]. Finally, a third more rare mechanism is identified in some cases, consisting of a native plaque rupture at the edges of a stent triggering thrombosis within the stented segment [16,21].

It becomes thus apparent that late and very late metallic stent thrombosis is to some extent triggered by the permanent metallic structure of the implanted devices which might be a source of vascular toxicity, while it massively limits the vessel's ability for remodeling, plaque regression, and lumen enlargement, thus leading inevitably to lumen narrowing with or without neoatherosclerosis over time. Conceptually, bioresorbable scaffolds could allow for a different healing response with recovery of the native vessel morphology over time [2] (Figure 8.2.2).

HEALING RESPONSE IN BIORESORBABLE SCAFFOLDS

First-in-human bioresorbable scaffold studies have employed multimodality imaging for evaluating the vascular healing response after BRS implantation [31–34]. Therefore, the healing response of several bioresorbable scaffolds has been well documented. The more extensively studied bioresorbable scaffold is the ABSORB BVS (Abbott Vascular, Santa Clara, CA) with two generations: ABSORB BVS 1.0 evaluated in the ABSORB A study, and ABSORB BVS 1.1, which was evaluated in the ABSORB B study. Invasive imaging follow-up of ABSORB A has documented a favorable healing response of the ABSORB BVS 1.0 with strut integration within the vessel wall and resolution of acute malapposition by 6 months, although accompanied by moderate acute and chronic recoil [35]. Longer-term follow-up, namely 5 years

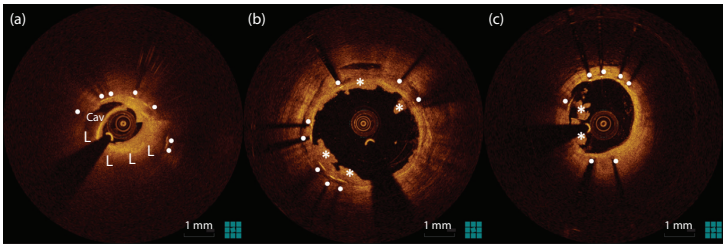

Figure 8.2.1 Different mechanisms of very late stent thrombosis in metallic stents. **(a)** Neointimal rupture with in-stent cavity formation. **(b)** Thrombus attached to malapposed struts. **(c)** Thrombus attached to an uncovered strut. Annotations: L = necrotic core, white bullets = stent struts, white asterisk = white thrombus, Cav = cavity.

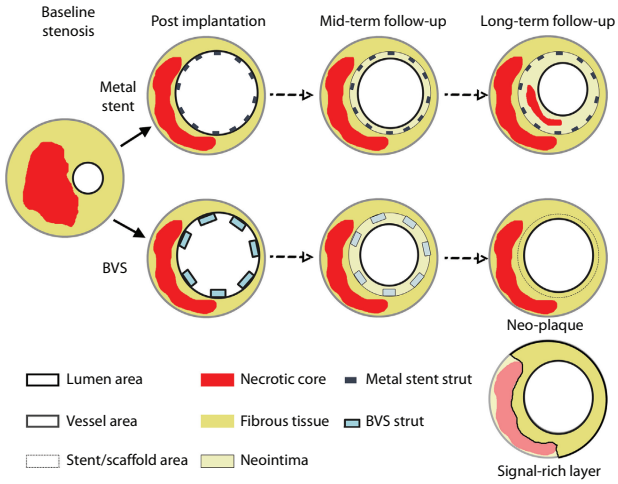

Figure 8.2.2 Long-term vascular healing response in metal stents and bioresorbable scaffolds. After metal stent implantation, struts are preserved and the neointimal area is clearly delineated between stent and lumen contour even at long-term follow-up, with possible development of neoatherosclerosis within the neointima. Conversely, in long-term follow-up of bioresorbable scaffolds, neointimal boundaries are unclear after bioresorption (dotted line), and the intima resembles a native plaque, defined as neoplaque. The signal-rich layer is the layer that separates the underlying plaque components from the lumen. BVS = bioresorbable vascular scaffold. (Adapted from Karanasos et al., *J Am Coll Cardiol* 2014;64:2343–56.)

postimplantation, has demonstrated complete strut resorption, recovery of vasomotion at the scaffolded segment, late luminal enlargement due to plaque regression, increased luminal symmetry, side-branch patency, and development of a signal-rich and low-attenuating by OCT tissue layer covering potentially thrombogenic plaque components [2,3]. Similarly, ABSORB BVS 1.1 has exhibited a favorable healing response with an incidence of ~3% of uncovered struts at 6 months, decreasing to ~1.5% over 3 years, while scaffold-level malapposition decreased from 81% postimplantation to 16% at 3 years [32].

The DESolve BCS (Elixir Medical, Sunnyvale, CA) has also demonstrated a good healing response with 1.32% uncovered struts and 0.04% malapposed struts at 6 months [33], and ongoing bioresorption with 14% reduction in the number of discernible struts by OCT. Likewise, the magnesium bioresorbable platform (DREAMS; Biotronik, Bülach, Switzerland) has demonstrated excellent healing with 100% strut coverage at 6 months and 2.8% malapposed struts at 6 months that diminished to 0.2% at 1 year [34].

CURRENT EXPERIENCE WITH LATE SCAFFOLD THROMBOSIS

These imaging observations suggest a good healing response for bioresorbable scaffolds. However, the main limitation of these imaging studies is that they have mainly focused on relatively simple patient and lesion subsets. As a result, the complication rate was low and no cases of late or very late stent thrombosis have been reported in these first-in-human studies. Nevertheless, vascular healing and also complication rate could differ in more complex lesions. Implantation of overlapping ABSORB BVS in animal models has demonstrated a delayed coverage of segments with strut overlap compared to segments without strut overlap [36]. Similarly, it is known from metallic stents that implantation in myocardial infarction is associated with higher rates of uncovered and malapposed struts compared to implantation in stable patients [37,38].

Recently, the ABSORB BVS and the DESolve BCS have received approval for commercial use in several countries. Consequently, these scaffolds were also implanted in patients and lesions not usually encountered in the context of clinical trials and several registries recording the outcomes in patients treated with bioresorbable scaffolds—mainly with ABSORB BVS—have been published [39–48]. As these registries tend to include more complex patient and lesion subsets, outcome in these registries could differ from the ones reported in the first-in-human studies. Indeed, scaffold thrombosis has been reported, with an incidence that varies across the different series, and comprises mainly cases with acute or subacute thrombosis. In these registries, the reported rate of 6-month definite scaffold thrombosis has ranged from 0% to 2.7% [49]. Additionally to (sub)acute

thrombosis, several cases of late thrombosis have also been reported in these studies.

Due to the limited number of patients included in these registries and the limited available follow-up—as most registries have reported outcomes up to 6 months—it is difficult to make firm estimations for the incidence of a relatively rare complication such as late scaffold thrombosis. Next to the first-in-human studies, only a limited number of studies with follow-up up to 1 year have been reported: ABSORB EXTEND, ABSORB II, ASSURE, POLAR-ACS, and BVS EXAMINATION [42–44,50,51] (Table 8.2.1). The reported 1-year incidence of late scaffold thrombosis in these registries has ranged from 0 to 0.4%.

Thus far, a total of 12 cases of late scaffold thrombosis has been reported in the literature. For the majority of these cases, the etiology was not completely elucidated; however, early discontinuation of antiplatelet therapy has been implicated in some of them. The majority of these cases come from the multicenter GHOST registry. In this registry of 1189 patients at a median follow-up of 184 days, seven cases of definite or probable late scaffold thrombosis occurring from 34 to 239 days since implantation have been reported [41]. A detailed description of the mechanism for the majority of these cases was not provided. High-risk characteristics in this series include baseline implantation performed due to acute coronary syndrome in three out of seven cases, while two of the implantations had been performed in type C lesions. In two of the cases (34 and 149 days post-implantation), DAPT had been discontinued prematurely at the time of the event. Two additional cases have been reported in ABSORB EXTEND registry [52]. One of them occurred three months after implantation in a bifurcation lesion, and in this case platelet function tests revealed a normal ADP-induced platelet aggregation, potentially due to resistance to clopidogrel. The second case occurred 239 days postimplantation without clear identification of the pathomechanism; however, the close temporal correlation of the acute coronary syndrome with a bee sting has raised speculation by the authors regarding a possible participation of spasm in the pathogenesis of this case. One case of probable late scaffold thrombosis at 335 days has also been documented at the 1-year follow-up report of ABSORB II, a randomized comparison of ABSORB BVS with metallic stents [51]. In the AMC registry with 6-month follow-up after ABSORB BVS implantation, one case of late scaffold thrombosis 3 months after implantation was reported, which was associated with DAPT discontinuation due to gastrointestinal bleeding [46]. Finally, one more case of late scaffold thrombosis occurring at 96 days postimplantation has been reported in the BVS EXAMINATION registry, a registry investigating the 1-year outcomes following ABSORB BVS implantation in 290 STEMI patients; however, more details were not available [42].

Table 8.2.1 Studies of bioresorbable scaffolds reporting on 1-year scaffold thrombosis rates

Study	Population size, n	Definite/probable late scaffold thrombosis, n (%)
ABSORB BVS		
ABSORB A [31]	30	0 (0)
ABSORB B [32]	101	0 (0)
ABSORB EXTEND [50]	512	2 (0.4)
ABSORB II [51]	335	1 (0.3)
ASSURE [44]	180	0 (0)
POLAR ACS [43]	98	0 (0)
BVS EXAMINATION [42]	290	1 (0.3)
DESolve BCS		
DESolve First-in-Man [33]	16	0 (0)
DREAMS		
BIOSOLVE-I [62]	43	0 (0)

CURRENT EXPERIENCE WITH VERY LATE SCAFFOLD THROMBOSIS

In line with expectations of a very low incidence of very late scaffold thrombosis with BRS, considering that a significant fraction of the scaffold mass is expected to have been resorbed after 1 year, only four cases of very late scaffold thrombosis have been reported in the literature. In one case from our center, scaffold thrombosis occurred almost 2 years post-initial implantation, soon after dual antiplatelet therapy discontinuation [53] (Figures 8.2.3 and 8.2.4). Imaging findings in this case included extensive scaffold discontinuity with struts protruding into the lumen and thrombus formation. This observed scaffold deformation was possibly caused by a repeat procedure where the scaffolded segment had been subjected to postdilation, performed 1 year after the baseline implantation. As by that time point, the scaffold is expected to have lost a large part of its mechanical support, intervention or catheter manipulation at the scaffolded segment could have resulted in scaffold disruption, which in turn triggered thrombosis soon after antiplatelet therapy discontinuation. Another case of very late scaffold thrombosis which occurred 16 months after implantation, after scheduled dual antiplatelet therapy at 12 months was recently reported [54]. Imaging by intravascular ultrasound revealed the presence of scaffold underexpansion. The underexpansion was attributed to late recoil, although this diagnosis was not supported by intravascular ultrasound measurements at baseline and event demonstrating a reduction in scaffold area. Finally, two more cases of very late scaffold thrombosis have been reported; however, OCT imaging findings have not provided further insight into the mechanisms [55,56]; interestingly, the common link between these two cases is that both these patients were not receiving any antiplatelet therapy at the time of thrombosis.

In our center, we have witnessed two additional cases of very late scaffold thrombosis [57]. The first occurred on day 371 after implantation, 6 days after discontinuation of

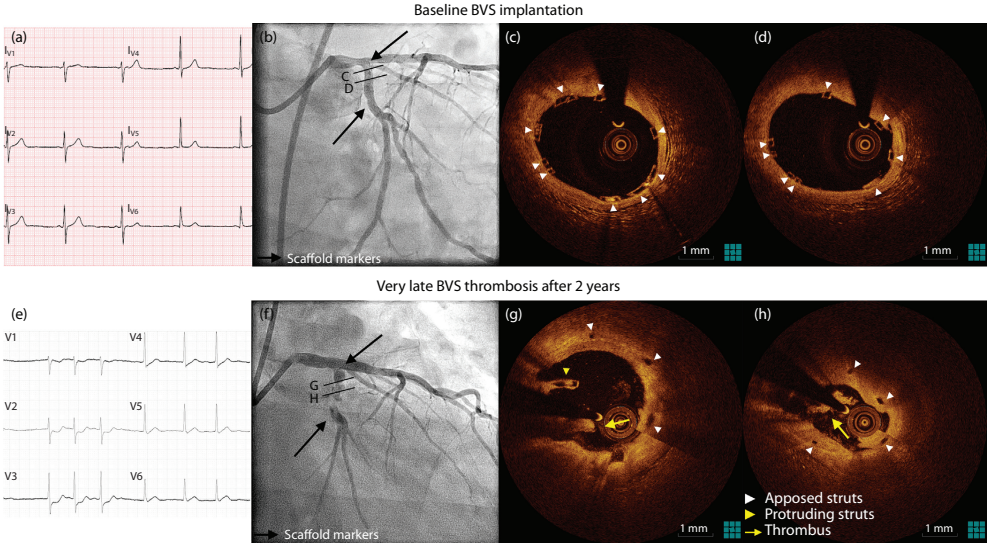

Figure 8.2.3 Very late scaffold thrombosis soon after dual antiplatelet therapy discontinuation. **(a)** ECG prebaseline implantation. **(b–d)** Angiogram and OCT images post-ABSORB BVS implantation in the ostial left circumflex artery (LCx). **(e)** ECG at event 2 years after implantation. **(f)** Coronary angiogram at event showed a filling defect in the scaffolded segment. **(g, h)** OCT at event showing intracoronary thrombus and scaffold discontinuity. (Adapted with permission from Karanasos et al., *Eur Heart J* 2014;35:1781.)

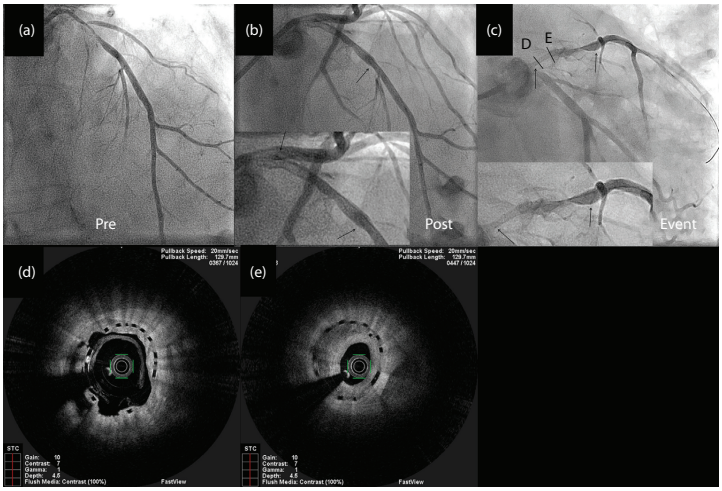

Figure 8.2.4 Late scaffold thrombosis 112 days postimplantation with malapposition and underexpansion. Implantation of a 3.5 × 28 mm ABSORB BVS in an ostial LAD lesion **(a)** with suspected underexpansion by angiography **(b)**. **(c)** Angiogram at event after thrombus aspiration. OCT reveals sites with malapposed struts with thrombus **(d)** and focal restenosis in underexpanded segments (minimal scaffold diameter: 2.71 mm) **(e)**.

both aspirin and clopidogrel, which the patient had been consistently taking since implantation. This patient had a complex BVS implantation for non-ST myocardial infarction in a vessel with heavy calcification by OCT, proximally overlapping a first-generation metallic DES, with extensive malapposition due to intra-scaffold dissections. The other case occurred 478 days after implantation, while the patient was on aspirin alone. The imaging findings included thrombus arising from a site with possible minor late discontinuity and malapposition, and several adjacent uncovered struts.

IMAGING OBSERVATIONS IN LATE AND VERY LATE SCAFFOLD THROMBOSIS

Overall, eight cases with late or very late scaffold thrombosis have been documented in our center up to June 2014 [57]. OCT was performed at the time of the event in seven

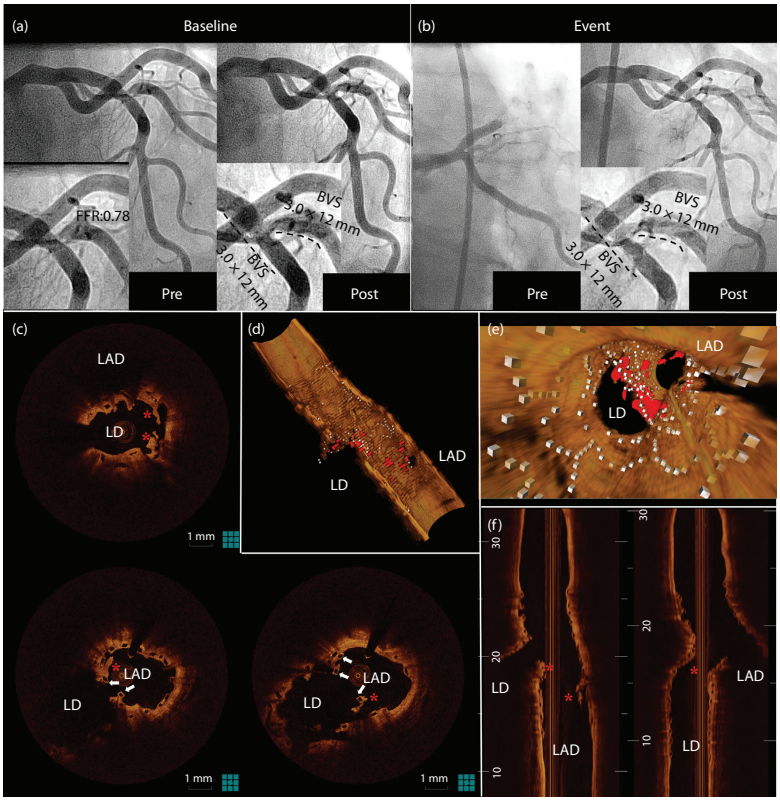

Figure 8.2.5 Late scaffold thrombosis in a patient with complex bifurcation intervention and antiplatelet therapy discontinuation. **(a)** Implantation of two 3.0 × 12 mm ABSORB BVS with T-stenting in a LAD-diagonal bifurcation due to stable angina with fractional flow reserve <0.80. **(b)** The patient had discontinued both antiplatelet agents after an atrial fibrillation-related embolic ischemic cerebrovascular accident and suffered a late scaffold thrombosis 129 days postimplantation, while on oral anticoagulants alone, treated with balloon dilation, rheolytic thrombectomy, and eptifibatide infusion. **(c)** OCT performed after treatment demonstrated reasonable expansion and apposition, but with uncovered struts (arrows) protruding at the bifurcation, and thrombus (asterisks) mainly located at the site of the bifurcation. **(d)** Three-dimensional longitudinal cut-away view demonstrating the localization of the thrombus (red). **(e)** The three-dimensional downstream fly-through view reveals the patency of both vessel ostia, but with the presence of multiple protruding struts proximal to the carina covered with thrombus. The presence of these multiple struts could affect local hemodynamics and comprise a focus for platelet aggregation in the absence of platelet inhibition. **(f)** L-mode OCT images demonstrating the location of the thrombus. Three-dimensional rendering performed with QAngioOCT 1.0 (Medis specials bv, Leiden, the Netherlands). Abbreviations: LAD = left anterior descending artery; LD = diagonal branch.

of them. In most patients, (very) late BVS thrombosis was observed in the presence of regional suboptimal flow conditions, such as underexpansion and strut protrusion into the lumen due to strut malapposition, scaffold fracture, or bifurcation intervention (Figures 8.2.4 and 8.2.5). In BVS thrombosis, expansion was better in nonthrombosed versus thrombosed sites within the scaffolds. In these patients with (very) late scaffold thrombosis, the incidence of malapposed struts was 1.9 ± 2.2% not differing significantly from a control group of patients undergoing OCT during late metallic stent thrombosis. This range was higher than the range reported in follow-up of asymptomatic patients treated with second-generation metallic DES [58]. Likewise, malapposition distance (486 ± 225 μm) was similar to that of the metallic stent control group, and at the range of previously reported values in metallic DES thrombosis (mean value of 350 μm) [19]. These observations suggest a potential involvement of large-scale malapposition that can potentially affect flow conditions, in the mechanism of (very) late scaffold thrombosis. Similarly, in complex bifurcation interventions the presence of struts protruding into the lumen at the level of the bifurcation could be a cause of suboptimal flow conditions [59,60] (Figure 8.2.5). Such flow conditions could also be instigated by strut discontinuity associated with scaffold protrusion into the lumen, a finding observed in two patients in our series.

Importantly, among the eight patients in our series, two of the patients, concomitantly with these potentially impaired flow conditions, were not receiving any antiplatelet therapy at the time of the event, while on oral anticoagulants. This suggests a potential synergistic effect of lack of platelet inhibition with suboptimal flow conditions in the pathogenesis of late scaffold thrombosis.

POTENTIAL MECHANISMS—PREVENTIVE MEASURES

Due to the small number of observations, the mechanisms underlying late and very late BRS thrombosis are poorly understood at this moment. In the case of the ABSORB BVS, its increased strut thickness (150 μm) has been suggested as a potential factor associated with increased thrombogenicity. This hypothesis has been derived from bench observations of increased thrombogenicity of thick struts, which might become exaggerated in the presence of factors potentially affecting flow conditions such as malapposition or overlap [61]. Therefore, the presence of underexpansion or excessive strut protrusion into the lumen, which are factors that potentially affect flow conditions, could comprise an adverse environment associated with higher risk for scaffold thrombosis. Hence, a meticulous implantation technique, possibly including imaging guidance, could help ensure an optimal implantation result without adverse effects on regional flow conditions. In cases where optimal flow conditions are not achieved, as in suboptimal implantation or complex interventions, absence of adequate antiplatelet inhibition could act synergistically in the pathogenesis of scaffold thrombosis. This might dictate the use of platelet reactivity testing, or of more potent antiplatelet therapy in such cases.

Furthermore, the observation that several reported cases of very late scaffold thrombosis have occurred in patients not receiving any antiplatelet therapy supports the notion that patients treated with BRS should receive at least one antiplatelet agent at a minimum until confirmed scaffold resorption and possibly for life.

Finally, as the scaffold loses a part of its mechanical support over time, reintervention in the same vessel several months after initial implantation should be performed with caution in view of a potential scaffold disruption while recrossing with wires or catheters.

CONCLUSIONS

The introduction of bioresorbable scaffolds has held promise for a reduction of late and very late scaffold thrombosis, as these devices are associated with a favorable healing response, while the vascular morphology can be restored after resorption with elimination of the permanent vessel caging. However, use of bioresorbable scaffolds in more complex patient and lesion subsets has given rise to a limited number of late and very late scaffold thrombosis cases. Although the mechanisms of this complication in bioresorbable scaffolds are not completely understood, we speculate based on preliminary observations on a possible role of suboptimal flow conditions in the pathogenesis, while appropriate antiplatelet therapy administration seems to be important in avoiding this complication. The increasing utilization of BRS in clinical practice might enable the elucidation of the mechanisms of this complication, while properly sized prospective studies will help to define the optimal procedural strategy and optimal antiplatelet regimen that can help diminish the risk of late and very late bioresorbable scaffold thrombosis.

REFERENCES

1. Serruys PW, Garcia-Garcia HM, Onuma Y. From metallic cages to transient bioresorbable scaffolds: Change in paradigm of coronary revascularization in the upcoming decade? *Eur Heart J*. 2012;33:16–25b.
2. Karanasos A, Simsek C, Gnanadesigan M, van Ditzhuijzen NS, Freire R, Dijkstra J, Tu S et al. OCT assessment of the long-term vascular healing response 5 years after everolimus-eluting bioresorbable vascular scaffold. *J Am Coll Cardiol*. 2014;64:2343–2356.
3. Simsek C, Karanasos A, Magro M, Garcia-Garcia HM, Onuma Y, Regar E, Boersma E et al. Long-term invasive follow-up of the everolimus-eluting bioresorbable vascular scaffold: Five-year results of multiple invasive imaging modalities. *EuroIntervention*. 2014.

4. McFadden EP, Stabile E, Regar E, Cheneau E, Ong AT, Kinnaird T, Suddath WO et al. Late thrombosis in drug-eluting coronary stents after discontinuation of antiplatelet therapy. *Lancet*. 2004;364:1519–1521.
5. Daemen J, Wenaweser P, Tsuchida K, Abrecht L, Vaina S, Morger C, Kukreja N et al. Early and late coronary stent thrombosis of sirolimus-eluting and paclitaxel-eluting stents in routine clinical practice: Data from a large two-institutional cohort study. *Lancet*. 2007;369:667–678.
6. Karanasos A, Ligthart JM, Regar E. In-stent neoatherosclerosis: A cause of late stent thrombosis in a patient with "full metal jacket" 15 years after implantation: Insights from optical coherence tomography. *JACC Cardiovasc Interv*. 2012;5:799–800.
7. Yamaji K, Kimura T, Morimoto T, Nakagawa Y, Inoue K, Soga Y, Arita T et al. Very long-term (15 to 20 years) clinical and angiographic outcome after coronary bare metal stent implantation. *Circ Cardiovasc Interv*. 2010;3:468–475.
8. Palmerini T, Biondi-Zoccai G, Riva DD, Stettler C, Sangiorgi D, D'Ascenzo F, Kimura T et al. Stent thrombosis with drug-eluting and bare-metal stents: Evidence from a comprehensive network meta-analysis. *Lancet*. 2012;379:1393–1402.
9. Räber L, Magro M, Stefanini GG, Kalesan B, Domburg RT, Onuma Y, Wenaweser P et al. Very late coronary stent thrombosis of a newer-generation everolimus-eluting stent compared with early-generation drug-eluting stents a prospective cohort study. *Circulation*. 2012;125:1110–1121.
10. Holmes Jr DR, Kereiakes DJ, Garg S, Serruys PW, Dehmer GJ, Ellis SG, Williams DO et al. Stent thrombosis. *J Am Coll Cardiol*. 2010;56:1357–1365.
11. Windecker S, Meier B. Late coronary stent thrombosis. *Circulation*. 2007;116:1952–1965.
12. Farb A, Burke AP, Kolodgie FD, Virmani R. Pathological mechanisms of fatal late coronary stent thrombosis in humans. *Circulation*. 2003;108:1701–1706.
13. Finn AV, Joner M, Nakazawa G, Kolodgie F, Newell J, John MC, Gold HK et al. Pathological correlates of late drug-eluting stent thrombosis: Strut coverage as a marker of endothelialization. *Circulation*. 2007;115:2435–2441.
14. Nakazawa G, Finn AV, Vorpahl M, Ladich ER, Kolodgie FD, Virmani R. Coronary responses and differential mechanisms of late stent thrombosis attributed to first-generation sirolimus- and paclitaxel-eluting stents. *J Am Coll Cardiol*. 2011;57:390–398.
15. Gutierrez-Chico JL, Alegria-Barrero E, Teijeiro-Mestre R, Chan PH, Tsujioka H, de Silva R, Viceconte N et al. Optical coherence tomography: From research to practice. *Eur Heart J Cardiovasc Imaging*. 2012.
16. Alfonso F, Dutary J, Paulo M, Gonzalo N, Perez-Vizcayno MJ, Jimenez-Quevedo P, Escaned J et al. Combined use of optical coherence tomography and intravascular ultrasound imaging in patients undergoing coronary interventions for stent thrombosis. *Heart*. 2012;98:1213–1220.
17. Amabile N, Souteyrand G, Ghostine S, Combaret N, Slama MS, Barber-Chamoux N, Motreff P et al. Very late stent thrombosis related to incomplete neointimal coverage or neoatherosclerotic plaque rupture identified by optical coherence tomography imaging. *Eur Heart J Cardiovasc Imaging*. 2014;15:24–31.
18. Davlouros PA, Karantalis V, Xanthopoulou I, Mavronasiou E, Tsigkas G, Toutouzas K, Alexopoulos D. Mechanisms of non-fatal stent-related myocardial infarction late following coronary stenting with drug-eluting stents and bare metal stents. Insights from optical coherence tomography. *Circ J*. 2011;75:2789–2797.
19. Guagliumi G, Sirbu V, Musumeci G, Gerber R, Biondi-Zoccai G, Ikejima H, Ladich E et al. Examination of the in vivo mechanisms of late drug-eluting stent thrombosis: Findings from optical coherence tomography and intravascular ultrasound imaging. *JACC Cardiovasc Interv*. 2012;5:12–20.
20. Kang S-J, Lee CW, Song H, Ahn J-M, Kim W-J, Lee J-Y, Park D-W et al. OCT analysis in patients with very late stent thrombosis. *JACC Cardiovasc Interv*. 2013;6:695–703.
21. Karanasos A, Witberg K, Van Geuns RJ, Schultz C, Van Mieghem N De Jaegere P, Bruining N et al. Morphological characteristics by optical coherence tomography of ruptured neoatherosclerotic plaques in patients with very late stent thrombosis. *Eur Heart J*. 2012;33:176.
22. Ko Y-G, Kim D-M, Cho JM, Choi SY, Yoon JH, Kim J-S, Kim B-K et al. Optical coherence tomography findings of very late stent thrombosis after drug-eluting stent implantation. *Int J Cardiovasc Imaging*. 2012;28:715–723.
23. Miyazaki S, Hiasa Y, Takahashi T, Yano Y, Minami T, Murakami N, Mizobe M et al. In vivo optical coherence tomography of very late drug-eluting stent thrombosis compared with late in-stent restenosis. *Circ J*. 2012;76:390–398.
24. Parodi G, La Manna A, Di Vito L, Valgimigli M, Fineschi M, Bellandi B, Niccoli G et al. Stent-related defects in patients presenting with stent thrombosis: Differences at optical coherence tomography between subacute and late/very late thrombosis in the Mechanism Of Stent Thrombosis (MOST) study. *EuroIntervention*. 2013;9:936–944.
25. Karanasos A, Regar E. Standing on solid ground?: Reassessing the role of incomplete strut apposition in drug-eluting stents. *Circ Cardiovasc Interv*. 2014;7:6–8.

26. Cook S, Eshtehardi P, Kalesan B, Raber L, Wenaweser P, Togni M, Moschovitis A et al. Impact of incomplete stent apposition on long-term clinical outcome after drug-eluting stent implantation. *Eur Heart J*. 2012;33:1334–1343.
27. Karanasos A, Ligthart J, Witberg K, Toutouzas K, Daemen J, Van Soest G, Gnanadesigan M et al. Association of neointimal morphology by optical coherence tomography with rupture of neoatherosclerotic plaque very late after coronary stent implantation. *Progress in Biomedical Optics and Imaging—Proceedings of SPIE*. 2013;8565:856542.
28. Karanasos A, Witberg K, Ligthart J, Toutouzas K, Daemen J, Van Soest G, Gnanadesigan M et al. In-stent neoatherosclerosis: Are first generation drug eluting stents different than bare metal stents? An optical coherence tomography study. *Progress in Biomedical Optics and Imaging—Proceedings of SPIE*. 2013;8565:856543.
29. Nakazawa G, Otsuka F, Nakano M, Vorpahl M, Yazdani SK, Ladich E, Kolodgie FD et al. The pathology of neoatherosclerosis in human coronary implants bare-metal and drug-eluting stents. *J Am Coll Cardiol*. 2011;57:1314–1322.
30. Otsuka F, Vorpahl M, Nakano M, Foerst J, Newell JB, Sakakura K, Kutys R et al. Pathology of second-generation everolimus-eluting stents versus first-generation sirolimus- and paclitaxel-eluting stents in humans. *Circulation*. 2014;129:211–223.
31. Onuma Y, Dudek D, Thuesen L, Webster M, Nieman K, Garcia-Garcia HM, Ormiston JA et al. Five-year clinical and functional multislice computed tomography angiographic results after coronary implantation of the fully resorbable polymeric everolimus-eluting scaffold in patients with de novo coronary artery disease: The ABSORB Cohort A Trial. *JACC Cardiovasc Interv*. 2013;6:999–1009.
32. Serruys PW, Onuma Y, Garcia-Garcia HM, Muramatsu T, van Geuns RJ, de Bruyne B, Dudek D et al. Dynamics of vessel wall changes following the implantation of the absorb everolimus-eluting bioresorbable vascular scaffold: A multi-imaging modality study at 6, 12, 24 and 36 months. *EuroIntervention*. 2014;9:1271–1284.
33. Verheye S, Ormiston JA, Stewart J, Webster M, Sanidas E, Costa R, Costa Jr JR et al. A next-generation bioresorbable coronary scaffold system—From bench to first clinical evaluation: Six- and 12-month clinical and multimodality imaging results. *JACC Cardiovasc Interv*. 2014;7:89–99.
34. Waksman R, Prati F, Bruining N, Haude M, Bose D, Kitabata H, Erne P et al. Serial observation of drug-eluting absorbable metal scaffold: Multi-imaging modality assessment. *Circ Cardiovasc Interv*. 2013;6:644–653.
35. Ormiston JA, Serruys PW, Regar E, Dudek D, Thuesen L, Webster MW, Onuma Y et al. A bioabsorbable everolimus-eluting coronary stent system for patients with single de-novo coronary artery lesions (ABSORB): A prospective open-label trial. *Lancet*. 2008;371:899–907.
36. Farooq V, Serruys PW, Heo JH, Gogas BD, Onuma Y, Perkins LE, Diletti R et al. Intracoronary optical coherence tomography and histology of overlapping everolimus-eluting bioresorbable vascular scaffolds in a porcine coronary artery model: The potential implications for clinical practice. *JACC Cardiovasc Interv*. 2013;6:523–532.
37. Gonzalo N, Barlis P, Serruys PW, Garcia-Garcia HM, Onuma Y, Ligthart J, Regar E. Incomplete stent apposition and delayed tissue coverage are more frequent in drug-eluting stents implanted during primary percutaneous coronary intervention for ST-segment elevation myocardial infarction than in drug-eluting stents implanted for stable/unstable angina: Insights from optical coherence tomography. *JACC Cardiovasc Interv*. 2009;2:445–452.
38. Diletti R, Karanasos A, Muramatsu T, Nakatani S, Van Mieghem NM, Onuma Y, Nauta ST et al. Everolimus-eluting bioresorbable vascular scaffolds for treatment of patients presenting with ST-segment elevation myocardial infarction: BVS STEMI first study. *Eur Heart J*. 2014;35:777–786.
39. Azzalini L, L'Allier PL. Bioresorbable vascular scaffold thrombosis in an all-comer patient population: Single-center experience. *J Invasive Cardiol*. 2015;27:85–92.
40. Costopoulos C, Latib A, Naganuma T, Miyazaki T, Sato K, Figini F, Sticchi A et al. Comparison of early clinical outcomes between ABSORB bioresorbable vascular scaffold and everolimus-eluting stent implantation in a real-world population. *Catheter Cardiovasc Interv*. 2015;85:E10–E15.
41. Capodanno D, Gori T, Nef H, Latib A, Mehilli J, Lesiak M, Caramanno G,. Percutaneous coronary intervention with everolimus-eluting bioresorbable vascular scaffolds in routine clinical practice: Early and midterm outcomes from the European multicentre GHOST-EU registry. *EuroIntervention*. 2015;10:1144–1153.
42. Brugaletta S, Gori T, Low AF, Tousek P, Pinar E, Gomez-Lara J, Scalone G et al. Absorb bioresorbable vascular scaffold versus everolimus-eluting metallic stent in ST-segment elevation myocardial infarction: 1-year results of a propensity score matching comparison: The BVS-EXAMINATION Study (Bioresorbable Vascular Scaffold-A Clinical Evaluation of Everolimus Eluting Coronary Stents in the Treatment of Patients With ST-segment Elevation Myocardial Infarction). *JACC Cardiovasc Interv*. 2015;8:189–197.

43. Dudek D, Rzeszutko Ł, Zasada W, Depukat R, Siudak Z, Ochała A, Wojakowski W et al. Bioresorbable vascular scaffolds in patients with acute coronary syndromes: The POLAR ACS study. *Pol Arch Med Wewn*. 2014;124:669–677.
44. Wohrle J, Naber C, Schmitz T, Schwencke C, Frey N, Butter C, Brachmann J et al. Beyond the early stages: Insights from the ASSURE registry on bioresorbable vascular scaffolds. *EuroIntervention*. 2014.
45. Sato K, Latib A, Panoulas VF, Kawamoto H, Naganuma T, Miyazaki T, Colombo A. Procedural feasibility and clinical outcomes in propensity-matched patients treated with bioresorbable scaffolds vs new-generation drug-eluting stents. *Can J Cardiol*. 2015;31:328–334.
46. Kraak RP, Hassell ME, Grundeken MJ, Koch KT, Henriques JP, Piek JJ, Baan J, Jr. et al. Initial experience and clinical evaluation of the Absorb bioresorbable vascular scaffold (BVS) in real-world practice: The AMC Single Centre Real World PCI Registry. *EuroIntervention*. 2015;10:1160–1168.
47. Van Geuns RJ, De Jaegere P, Diletti R, Karanasos A, Muramatsu T, Nauta ST, Onuma Y et al. Short- and intermediate- term clinical outcomes after implantation of everolimus-eluting bioresorbable scaffold in complex lesions: A prospective single-arm study—ABSORB Expand trial. *J Am Coll Cardiol*. 2013;62:B133–B133.
48. Ielasi A, Cortese B, Varricchio A, Tespili M, Sesana M, Pisano F, Loi B et al. Immediate and mid-term outcomes following primary PCI with bioresorbable vascular scaffold implantation in patients with ST-segment myocardial infarction: Insights from the multicentre "Registro ABSORB Italiano" (RAI registry). *EuroIntervention*. 2014.
49. Ishibashi Y, Nakatani S, Onuma Y. Definite and probable bioresorbable scaffold thrombosis in stable and ACS patients. *EuroIntervention*. 2014.
50. Abizaid A, Costa JR, Jr., Bartorelli AL, Whitbourn R, van Geuns RJ, Chevalier B, Patel T et al. The ABSORB EXTEND study: Preliminary report of the twelve-month clinical outcomes in the first 512 patients enrolled. *EuroIntervention*. 2014;10:1396–1401.
51. Serruys PW, Chevalier B, Dudek D, Cequier A, Carrié D, Iniguez A, Dominici M et al. A bioresorbable everolimus-eluting scaffold versus a metallic everolimus-eluting stent for ischaemic heart disease caused by de-novo native coronary artery lesions (ABSORB II): An interim 1-year analysis of clinical and procedural secondary outcomes from a randomised controlled trial. *Lancet*. 2015;385:43–54.
52. Ishibashi Y, Onuma Y, Muramatsu T, Nakatani S, Iqbal J, Garcia-Garcia HM, Bartorelli AL et al. Lessons learned from acute and late scaffold failures in the ABSORB EXTEND trial. *EuroIntervention*. 2014;10:449–457.
53. Karanasos A, van Geuns RJ, Zijlstra F, Regar E. Very late bioresorbable scaffold thrombosis after discontinuation of dual antiplatelet therapy. *Eur Heart J*. 2014;35:1781.
54. Cortese B, Piraino D, Ielasi A, Steffenino G, Orrego PS. Very late bioresorbable vascular scaffold thrombosis due to late device recoil. *Int J Cardiol*. 2015;189:132–133.
55. Sato T, Abdel-Wahab M, Richardt G. Very late thrombosis observed on optical coherence tomography 22 months after the implantation of a polymer-based bioresorbable vascular scaffold. *Eur Heart J*. 2015.
56. Timmers L, Stella PR, Agostoni P. Very late bioresorbable vascular scaffold thrombosis following discontinuation of antiplatelet therapy. *Eur Heart J*. 2015;36:393–393.
57. Karanasos A, Van Mieghem N, Van Ditzhuijzen NS, Felix C, Daemen J, Autar A, Onuma Y et al. Angiographic and optical coherence tomography insights into bioresorbable scaffold thrombosis. A single-center experience. *Circ Cardiovasc Interv*. 2015; in press.
58. Papayannis AC, Cipher D, Banerjee S, Brilakis ES. Optical coherence tomography evaluation of drug-eluting stents: A systematic review. *Catheter Cardiovasc Interv*. 2013;81:481–487.
59. Capranzano P, Francaviglia B, Tamburino CI, Gargiulo G, Longo G, Capodanno D, Tamburino C. One-year coverage by optical coherence tomography of a bioresorbable scaffold neocarina: Is it safe to discontinue dual antiplatelet therapy? *Can J Cardiol*.
60. Karanasos A, Li Y, Tu S, Wentzel JJ, Reiber JHC, van Geuns R-J, Regar E. Is it safe to implant bioresorbable scaffolds in ostial side-branch lesions? Impact of 'neo-carina' formation on main-branch flow pattern. Longitudinal clinical observations. *Atherosclerosis*. 2015;238:22–25.
61. Kolandaivelu K, Swaminathan R, Gibson WJ, Kolachalama VB, Nguyen-Ehrenreich KL, Giddings VL, Coleman L et al. Stent thrombogenicity early in high-risk interventional settings is driven by stent design and deployment and protected by polymer-drug coatings. *Circulation*. 2011;123:1400–1409.
62. Haude M, Erbel R, Erne P, Verheye S, Degen H, Böse D, Vermeersch P et al. Safety and performance of the drug-eluting absorbable metal scaffold (DREAMS) in patients with de-novo coronary lesions: 12 month results of the prospective, multicentre, first-in-man BIOSOLVE-I trial. *Lancet*. 2013;381:836–844.

28

CHAPTER

MID-TERM OUTCOMES OF THE ABSORB BVS VERSUS SECOND-GENERATION DES: A SYSTEMATIC REVIEW AND META-ANALYSIS

Cordula Felix, Victor .J. van den Berg, Sanne .E. Hoeks, **Jiang Ming Fam**, Mattie. Lenzen, Eric Boersma, Peter C. Smits, Patrick. W. Serruys, Yoshinobu Onuma, Robert Jan M. van Geuns.

PLoS One (in press).

Mid-term Outcomes of the ABSORB BVS Versus Second-Generation DES

A Systematic Review and Meta-Analysis

Cordula M. Felix[1], MD; Victor J. van den Berg[1], MD; Sanne E. Hoeks[1], PhD; Jiang Ming Fam[2], MD; Mattie Lenzen[1], PhD; Eric Boersma[1], PhD; Peter C. Smits[3], MD, PhD; Patrick W. Serruys[4], MD, PhD; Yoshinobu Onuma[1], MD, PhD; Robert Jan M. van Geuns[1,5], MD, PhD

From the [1]Thorax centre, Erasmus Medical Centre, Rotterdam, the Netherlands; [2]National Heart Centre Singapore, Singapore; [3]Maasstad Hospital, Rotterdam, the Netherlands; [4]The National Heart and Lung Institute, Imperial College London, London, United Kingdom; [5]Radboud UMC, Nijmegen, the Netherlands

Corresponding author: Prof. Robert Jan M. van Geuns, MD, PhD, Thoraxcenter, Room Ba585, Erasmus Medical Centre, 's-Gravendijkwal 230, 3015 CE Rotterdam, the Netherlands

Tel.: +31 10 4635260. Fax: +31 10 4369154

E-mail address: r.vangeuns@erasmusmc.nl

Text word count: 4994

Funding: None

Disclosures: RJG and YO received research grants and speakers fees from Abbott. PCS received fees from Abbott. PWS and YO are members of International Advisory Board of Abbott. All other authors have no conflicts of interest to declare.

ABSTRACT

BACKGROUND Bioresorbable Vascular Scaffolds (BVS) were introduced to overcome some of the limitations of drug-eluting stent (DES) for PCI. Data regarding the clinical outcomes of the BVS versus DES beyond 2 years are emerging.

OBJECTIVE To study mid-term outcomes.

METHODS We searched online databases (PubMed/Medline, Embase, CENTRAL), several websites, meeting presentations and scientific session abstracts until August 8th, 2017 for studies comparing Absorb BVS with second-generation DES. The primary outcome was target lesion failure (TLF). Secondary outcomes were all-cause mortality, myocardial infarction, target lesion revascularization (TLR) and definite/probable device thrombosis. Odds ratios (ORs) with 95% confidence intervals (CIs) were derived using a random effects model.

RESULTS Ten studies, seven randomized controlled trials and three propensity-matched observational studies, with a total of 7320 patients (BVS n=4007; DES n=3313) and a median follow-up duration of 30.5 months, were included. Risk of TLF was increased for BVS-treated patients (OR 1.34 [95% CI: 1.12-1.60], p=0.001, I^2=0%). This was also the case for all myocardial infarction (1.58 [95% CI: 1.27-1.96], p<0.001, I^2=0%), TLR (1.48 [95% CI: 1.19-1.85], p=0< 0.001, I^2=0%) and definite/probable device thrombosis (2.82 [95% CI: 1.86-4.26], p<0.001, I^2=0%). This did not result in a difference in all-cause mortality (0.78 [95% CI: 0.58-1.04], p=0.09, I^2=0%). OR for very late (>1 year) device thrombosis was 6.10 [95% CI: 1.40-26.65], p=0.02).

CONCLUSION At mid-term follow-up, BVS was associated with an increased risk of TLF, MI, TLR and definite/probable device thrombosis, but this did not result in an increased risk of all-cause mortality.

KEYWORDS: BVS, DES, meta-analysis, mid-term outcomes

CONDENSED ABSTRACT

Pooled 1-year results of RCTs in selected patients showed non-inferiority of target lesion failure (TLF) for bioresorbable vascular scaffolds (BVS). Meta-analyses that included more complex patients revealed an increased risk for TLF and scaffold thrombosis in BVS-treated patients. This meta-analysis reports on mid-term outcomes from 10 studies comparing Absorb BVS versus second-generation drug-eluting stents. At a weighted median FU of 30.5 months, risks of TLF, all myocardial infarction, target lesion revascularization and definite/probable device thrombosis were increased in BVS-treated patients, which did not result in higher all-cause mortality.

ABBREVIATIONS AND ACRONYMS

BVS	Bioresorbable vascular scaffold
CI	Confidence interval
DAPT	Dual antiplatelet therapy
DES	Drug-eluting stent
OR	Odds ratio
RCT	Randomized controlled trials
STEMI	ST-segment elevation myocardial infarction
TLF	Target lesion failure
TLR	Target lesion revascularization
TSA	Trial sequential analysis

INTRODUCTION

Bioresorbable scaffolds, developed to overcome some of the (late) adverse events of metallic drug-eluting stents (DES), are the latest innovation in the treatment of coronary artery disease. The Absorb bioresorbable vascular scaffold (BVS, Abbott Vascular, Santa Clara, CA, USA) is the most intensively studied. The first-in-man study in 2006 revealed promising results and this new device received a CE-mark in 2011 and became commercially available in Europe in September 2012. FDA approval followed in 2016 [1].

The concept of the Absorb BVS consists of treatment of obstructive coronary artery disease with temporary support of the vessel wall while avoiding the acute complications of balloon angioplasty. It was hypothesized that complete resorption would result in restoration of vasomotion, a reduction in angina, and the avoidance of caging of the vessels or interference with non-invasive imaging. In addition, vessel geometry would be less affected after implantation of a BVS. This should result in better outcomes for patients, with reduced late event rates. Pooled individual data from the four largest randomized controlled trials (RCTs) comparing BVS with second-generation DES did support the concept of temporary support of the artery and showed non-inferiority of the device during the first year [2]. However, several meta-analyses that included data beyond 1 year revealed higher event rates of myocardial infarction, target lesion revascularization and scaffold thrombosis [3, 4]. Data on the performance of BVS beyond 1 year primarily came from small registries, propensity-matched observational studies and a few RCTs. These raised concerns about the occurrence of very late (after 1 year) scaffold thrombosis [5], whereas RCTs assessed only the mid-term time points. We therefore undertook this systematic review and meta-analysis, and report the mid-term clinical outcomes of the Absorb BVS compared with second-generation DES.

METHODS

DATA SOURCES AND STUDY SELECTION. Inclusion criteria for our study were RCTs comparing the Absorb BVS with the Xience CoCr-EES, a second-generation DES, in patients with coronary artery disease with > 12 months of follow-up available. As randomized mid- to long-term data are scarce, we also allowed propensity-matched observational studies comparing BVS with second-generation DES. Both full-length manuscripts and meeting presentations (containing unpublished data) were included. All studies had to report on the outcomes of interest and be written in English. Exclusion criteria were non-human studies, single-arm studies, imaging-only studies, studies with short follow-up (≤ 12 months), studies in <100 patients, review articles, case series, trial design articles, comparisons other than Absorb BVS versus second-generation DES, studies with duplicate data, and those where the scaffold or stent was implanted elsewhere than in the coronary artery. This meta-analysis was conducted in accordance with the Preferred Reporting Items for Systematic Reviews and Meta-analysis guidelines [6] (**Table 1**).

DATA EXTRACTION AND QUALITY ASSESSMENT. On August 8th , 2017, a medical librarian (WB) conducted a systematic search of the online databases Medline/PubMed, Embase and Cochrane Central Register of Controlled Trials (CENTRAL), several websites (e.g. www.clinicaltrials.gov) and scientific session abstracts and oral presentations from conferences, with the following keywords and corresponding MeSH terms: “drug-eluting stent(s)”, “everolimus-eluting stent”, “bioresorbable vascular stent”, “bioresorbable scaffold”. On October 31th, during the 2017 TCT congress, ABSORB II, III and TROFI II presented their 3- and 4-year outcomes, which we also included in our analysis. The bibliographic records retrieved were imported and de-duplicated in Endnote bibliographic software. Two physician reviewers (CF and

VB) independently screened the records for eligibility at title or abstract level. Records that were relevant were downloaded and full text manuscripts or meeting presentations were reviewed. Differences between reviewers regarding study selection or data extraction were resolved by consensus. If one study had multiple publications with different follow-up lengths, the most recent follow-up record was used.

Quality and risk of bias in reporting data were assessed according to the Cochrane Handbook of Systematic Reviews [7] and by using the Newcastle-Ottawa Quality Assessment scale for case-control studies (maximum score = 9, meaning low risk of bias). Publication bias for the primary endpoint was assessed using funnel plot.

OUTCOMES AND DEFINITIONS. The primary outcome for this analysis was target lesion failure (TLF), a composite endpoint that consists of cardiac death, target-vessel myocardial infarction and ischemia-driven TLR. Secondary outcomes were all-cause mortality, all myocardial infarction, ischemia-driven TLR and definite or probable device thrombosis. Deaths were considered cardiac unless a non-cardiac cause was identified. TLR was described as any repeated revascularization of the target lesion. Device thrombosis was classified according to the Academic Research Consortium [8]. To investigate the effect of the intended bioresorption of the device, we examined outcomes during the first and second years separately. Definitions of clinical outcomes per study are described in **Supplemental Table 1**.

STATISTICAL ANALYSIS. Odds ratios (ORs) with 95% confidence intervals (CIs) were used as summary statistics across all studies and were calculated using a random effects model (Dersimonian and Laird). We also provide results of the fixed-effect model. Treatment effect was not assessed in studies in which no events were reported. Heterogeneity was assessed using Cochran Q and Higgins I^2. I^2 values of <25%, 25-50% or >50% indicate low, moderate or high

heterogeneity. Cochran Q P<0.10 and I^2>50% were considered to be indicative of significant heterogeneity. All analyses were conducted with Revman software (version 5.3).

Primary and secondary outcomes are reported for all included studies in which the outcome of interest was provided. A sensitivity analysis was performed, as detailed in the online supplement. In this analysis, the treatment effect was investigated in studies that included low-risk patients (ABSORB II, ABSORB III, ABSORB Japan, ABSORB China) versus studies that included more complex population (TROFI II, AIDA, EVERBIO and the observational studies, including higher percentage of STEMI, bifurcation, calcification, long lesions etc.). Finally, separate subgroup analyses for RCTs (low risk of bias) and propensity-matched studies (low/low-moderate risk of bias) were performed.

The risks of adverse events between 0 – 1 year, 1 – 2 and 2 -3 years were estimated using a landmark population that censored any casualty and lost to follow-up preceding each specific time point.

TRIAL SEQUENTIAL ANALYSIS. Meta-analyses may results in type 1 errors due to systematic errors (several forms of bias) or random errors (play of chance) due to sparse data and repeated significance testing when a meta-analysis is updated with new trials [9]. This can result in spurious significant results [10]. Trial sequential analysis (TSA) was introduced to minimize random errors. TSA provides the necessary information for meta-analyses and boundaries that determine whether the evidence is reliable and conclusive. We calculated required information size allowing for a type 1 error of 0.05, type 2 error of 0.20, the control event proportions and effect size calculated from the included trials, and heterogeneity estimated by the diversity (D2) in the included trials. We constructed TSA boundaries based on the O'Brien-Fleming alpha-

spending function. Trial Sequence Analysis Software (Copenhagen Trial Unit's TSA Software; Copenhagen, Sweden) was used.

RESULTS

The de-duplicated results yielded 1305 records. **Figure 1** shows a flow diagram of the selection process. Based on the exclusion criteria, 1278 records were excluded after title/abstract review. Twenty-seven records remained for full-text analysis, of which 17 were eliminated (short follow-up or editorials). Ultimately, we included 7 RCTs (3 full-length manuscripts, 4 meeting presentations) with a total of 5578 patients: 3258 received the Absorb BVS and 2320 received a second-generation DES. We also included 3 observational studies (2 manuscripts and 1 meeting presentation) with 1742 patients: 749 were implanted with a BVS and 993 with a DES. Weighted median FU was 30.5 months. **Table 2** summarizes the main characteristics of the included studies.

BASELINE CHARACTERISTICS. Across all studies in this meta-analysis, the mean age of patients ranged from 56.0 to 67.3 years; the percentage of men between 70.1% and 81.4%; diabetic patients between 12.8% and 36.1%; and the percentage of patients that presented with an acute coronary syndrome between 9.8% and 100%. In all studies except ABSORB II and EVERBIO, the per protocol prescribed duration of dual antiplatelet therapy (DAPT) was at least 12 months. The percentage of BVS patients using DAPT at 2 years ranged from 5.5% to 66%. The rate of post-dilatation ranged from 15.2% to 82.2% (**Table 3**).

CLINICAL OUTCOMES. All studies but one (BVS Expand) reported on TLF. Overall, TLF occurred in 617 patients during the mid-term follow-up, with a significantly higher risk in BVS-treated patients (OR 1.34 [95% CI: 1.12-1.60], p=0.001 and I^2=0%) (**Figure 3A**). A subanalysis

of RCTs showed only a significantly similar increased OR (1.31 [95% CI: 1.08-1.58], p=0.005 and I^2=0%). The pooled OR across the observational studies was numerically higher, but with a larger 95% CI (OR 1.57 [95% CI: 0.92-2.68, p=0.10, I^2=0%). In the TSA for the primary endpoint, the cumulative Z-curve did cross the TSA monitoring boundary, indicating that there were a sufficient number of patients to consider this a valid analysis (**Figure 2A**).

See **Supplemental Figure 1** for the sensitivity analysis.

SECONDARY ENDPOINTS. All-cause mortality occurred in 207 patients, without a statistically significant difference between both patient groups (OR 0.78 [95% CI: 0.56-1.37], p=0.09, I^2=0%). Results for the pooled RCT and pooled observational study subgroups were similar (**Figure 3B**).

The risks of myocardial infarction and TLR were significantly increased for BVS compared with DES (**Figures 3C and 3D**). Finally, patients with BVS had a higher risk for definite or probable device thrombosis, with ORs of 2.82 (95% CI: 1.86-3.89], p<0.001 and I^2=40.3%), 3.48 (95% CI: 2.06-5.87, p<0.001 and I^2=0%) and 2.82 (95% CI: 1.86-4.26, p<0.001 and I^2=0%), respectively, for the total cohort, RCTs only and observational data only (**Figure 3E**).

LANDMARK ANALYSIS. **Table 4** summarizes event rates and ORs in the periods up to 1 year, 1-2 years and 2-3 years (for those studies that reported 1- and 2-year and 3-year results of the outcomes of interest: ABSORB II, ABSORB Japan, ABSORB China, ABSORB III). In the first year, the risks of myocardial infarction and device thrombosis were significantly increased in BVS patients. During the second year, all event rates for both BVS and DES were lower, but the increased risk for BVS remained. The OR for late device thrombosis was quadrupled in BVS-treated patients. In the third year, events rates remained lower and no significant differences

between the 2 groups existed anymore. However, the OR for device thrombosis in BVS patients continued to be high.

DEFINITE/PROBABLE DEVICE THROMBOSIS. For the secondary endpoint definite or probable device thrombosis, we specifically investigated early (0-30 days), late (31 days-1 year) and very late (> 1 year) device thrombosis (for studies that reported the outcome of interest at these three time points). Event rates for early thrombosis were 1.07% for BVS versus 0.51% for DES. This resulted in an increased risk for BVS (OR 1.96 [95% CI: 1.01-3.81], p=0.05). Late device thrombosis event rates were 0.53% for BVS versus 0.09% for DES (OR 3.14 [95% CI: 0.83-11.82, p=0.09). Rates of very late device thrombosis up to three years were 1.09% for BVS compared to 0.0% for DES (OR 6.10 [95% CI: 1.40-26.65], p=0.02).

The sensitivity analysis results can be found in **Online Figure and 3.**

QUALITY ASSESSMENT. Quality assessments for both RCTs and observational studies are provided in the **Supplemental Tables 2A, 2B and 3**. All RCTs had a low risk of bias, while the observational studies had a low/low-moderate risk of bias (all scored 7 out of 9). To assess a possible publication bias, a funnel plot for TLF was derived (**Supplemental material**).

DISCUSSION

This study is the largest systematic review and meta-analysis, including 7320 patients, to report on the mid-term clinical outcomes of the Absorb BVS compared with second-generation DES. The main findings of this meta-analysis are: 1) BVS-treated patients were at higher risk for TLF, MI, TLR and device thrombosis compared with second-generation DES, across all studies included in this meta-analysis; 2) this did not result in an increased risk of all-cause mortality; 3) based on studies that have reported clinical outcomes of interest at 1, 2 and 3 years of follow-up,

risks of TLF, MI, TLR and especially the risk of very late device thrombosis, continued to be higher for BVS in following years after device implantation,

Initial study designs for BVS, based on the concept of temporary vascular support, hypothesized non-inferiority at one year and a reduction in TLF of approximately 50% beyond the first year. In this analysis, we demonstrated that event rates were highest during the first year after PCI and, for all endpoints except all-cause mortality; the use of BVS was associated with significantly higher risks of events. The mid-term results in this meta-analysis are in line with previous results [11-17]. Beyond 1 year, event rates were lower than during the first year, but outcomes such as device thrombosis, myocardial infarction and the primary endpoint – TLF – remained not in favour of BVS.

Four RCT's reported their three-year results and one RCT presented four-year results. All revealed continued higher event rates for BVS. During the EuroPCR 2017 congress, longer term data of several large single-arm registries, that included higher percentages of complex patients, was presented and with varying results [18].

DEFINITE/ PROBABLE DEVICE THROMBOSIS. In our study, we demonstrated that the risk of definite device thrombosis was almost three times higher for BVS. Meta-analyses investigating device thrombosis in BVS compared with DES have reported an increased risk of device thrombosis for BVS [5, 19, 20]. Multiple factors have been reported to be associated with scaffold thrombosis, such as a suboptimal implantation strategy, overlap, ostial lesions and decreased left ventricular ejection fraction [21]. Moreover, the first-generation BVS has a strut thickness considerably larger than the competitor metallic DES and similar to first-generation metallic DES. Scaffold thrombosis might be triggered by the smaller minimum lumen diameter and minimum lumen area at the end of the procedure, as previously demonstrated [22]. This has the

most impact on smaller vessels (with a diameter <2.5 mm visual or 2.25 mm by quantitative coronary analysis (QCA).

Early device thrombosis is generally considered to be procedure-related, when the characteristics of the device and operators experience are important factors.

The resorption process of the BVS might influence the mechanisms for very late scaffold thrombosis. It has been postulated that the disintegration of uncovered and malapposed struts (due to resorption-related scaffold discontinuity) might trigger the inflammatory process and thrombus formation, potentially for up to 3 years (18, 26, 27).

RECENT SETBACK. Recently, the ABSORB BVS suffered a setback after the 3-year results of the ABSORB II trial demonstrated similar vasomotion between BVS and everolimus-eluting DES and a greater late lumen loss for BVS. [23, 24] The FDA came with a safety alert after the 2-year results of the largest RCT, the ABSORB III, were presented during the ACC congress in March 2017. The AIDA trial even published their 2-year results earlier than expected after the safety monitoring board recommended to release the preliminary data due to safety concerns (hazard ratio of 3.87 for device thrombosis at 2 years; 95% CI: 1.78 – 8.42; p=<0.001). As a consequence, the current generation BVS has been taken out of the market. Just recently, a Task Force of ESC and EAPCI stated that bioresorbable scaffolds should not be preferred above the current used metallic DES [25]. These unfavourable findings were again confirmed during the 2017 TCT congress in Denver, USA on October the 31th. [26-28]

POSSIBLE SOLUTIONS AND FUTURE OUTLOOK. It remains uncertain whether implantation technique could improve outcomes. The basic concept of optimal implantation includes proper lesion preparation, adequate sizing (avoiding small vessels <2.5 mm) and high-pressure post-dilatation, also known as PSP. In retrospective analyses, this implantation strategy

showed a reduction in TLF [21] [18, 29, 30]. Also, the 30-day ABSORB IV results revealed lower device thrombosis rates, when implantation of stents/ scaffolds in small vessels was minimalized. [31] Furthermore, whether DAPT prolongation could prevent late occurrence of scaffold thrombosis was to be investigated. DAPT termination is a risk factor for device thrombosis, and a possible relationship between scaffold thrombosis and DAPT termination has been described [32]. However, information on the precise duration of DAPT after BVS implantation is lacking and, up to this moment, no dedicated studies exist on this important issue. A recently published review has suggested several considerations for DAPT duration in BVS patients [33]. In metal stents, prolongation of DAPT up to 30 months showed to reduce thrombotic events [34]. The new generation device should have thinner struts, better mechanical properties and shorter resorption time to facilitate easy implantation strategies and to prevent intraluminal dismantling [35].

LIMITATIONS

The most important limitation is the use of unpublished data in the form of meeting presentations. Secondly, the meta-analysis was performed using study-level data rather than patient-level data, so time-to-event curves were not possible. Thirdly, heterogeneity existed in baseline characteristics of included patients and also in protocols, study designs and definitions across the studies. Furthermore, the patients included in the RCTs (which provided most patients) were highly selected (except for AIDA) and, therefore, extrapolation to the real world is difficult. Besides, we were not able to completely exclude potential confounders in the observational registries. However these studies were based on propensity matching. Fourthly, the large AIDA RCT had a median follow-up duration of 1.93 years (range 1−3.3 years); thus this trial did not report outcomes at exactly 2 years.

To assess possible publication bias, we provided a funnel plot in **Online Figure 1**. However, this plot should be interpreted with caution as we included ten studies. There was also a lack of important information on DAPT status (duration of DAPT, reasons for interruption or early termination, type of $P2Y_{12}$ inhibitor). Lastly, the current data only apply for the Absorb BVS and not for other bioresorbable devices.

CONCLUSION

At mid-term follow-up, patients treated with Absorb BVS showed a higher risk of TLF, myocardial infarction, TLR and definite or probable device thrombosis. Beyond 1 year, it was mainly the risk of late device thrombosis that was increased. However, this did not result in a higher risk of all-cause mortality. Despite these unfavourable mid-term outcomes, long-term follow-up will be necessary to investigate any potential late benefits of BVS over DES as this device was not able to show any clinical benefit up to 3 years. Specific registries and post-hoc analyses of larger RCTs identified potential improvements in patient and lesion selection. A device specific implantation strategy is another factor that can result in better outcomes. As long as this has not been demonstrated in prospective and dedicated studies such as ABSORB III (NCT01751906), ABSORB IV (NCT02173379) and Compare Absorb (NCT02486068) operators should not use this version in routine practice.

Acknowledgements: We would like to thank Wichor Bramer and Taulant Muka for their valuable help.

REFERENCES

1. Steinvil A, Rogers T, Torguson R, Waksman R. Overview of the 2016 U.S. Food and Drug Administration Circulatory System Devices Advisory Panel Meeting on the Absorb Bioresorbable Vascular Scaffold System. JACC Cardiovasc Interv 2016;9(17):1757-64.
2. Stone GW, Gao R, Kimura T, Kereiakes DJ, Ellis SG, Onuma Y, Cheong WF, Jones-McMeans J, Su X, Zhang Z, Serruys PW. 1-year outcomes with the Absorb bioresorbable scaffold in patients with coronary artery disease: a patient-level, pooled meta-analysis. Lancet 2016.
3. Banach M, Serban MC, Sahebkar A, Garcia-Garcia HM, Mikhailidis DP, Martin SS, Brie D, Rysz J, Toth PP, Jones SR, Hasan RK, Mosteoru S, Al Rifai M, Pencina MJ, Serruys PW. Comparison of clinical outcomes between bioresorbable vascular stents versus conventional drug-eluting and metallic stents: a systematic review and meta-analysis. EuroIntervention 2016;12(2):e175-89.
4. Cassese S, Byrne RA, Ndrepepa G, Kufner S, Wiebe J, Repp J, Schunkert H, Fusaro M, Kimura T, Kastrati A. Everolimus-eluting bioresorbable vascular scaffolds versus everolimus-eluting metallic stents: a meta-analysis of randomised controlled trials. Lancet 2016;387(10018):537-44.
5. Toyota T, Morimoto T, Shiomi H, Yoshikawa Y, Yaku H, Yamashita Y, Kimura T. Very Late Scaffold Thrombosis of Bioresorbable Vascular Scaffold: Systematic Review and a Meta-Analysis. JACC Cardiovasc Interv 2017;10(1):27-37.
6. Moher D, Liberati A, Tetzlaff J, Altman DG, Group P. Preferred reporting items for systematic reviews and meta-analyses: the PRISMA statement. Int J Surg 2010;8(5):336-41.
7. Higgings JPY GS. *Cochrane Handbook for Systematic Reviews of Interventions Version 5.1.0 [updated March 2011]*; 2011.
8. Cutlip DE, Windecker S, Mehran R, Boam A, Cohen DJ, van Es GA, Steg PG, Morel MA, Mauri L, Vranckx P, McFadden E, Lansky A, Hamon M, Krucoff MW, Serruys PW, Academic Research C. Clinical end points in coronary stent trials: a case for standardized definitions. Circulation 2007;115(17):2344-51.
9. Thorlund K, Devereaux PJ, Wetterslev J, Guyatt G, Ioannidis JP, Thabane L, Gluud LL, Als-Nielsen B, Gluud C. Can trial sequential monitoring boundaries reduce spurious inferences from meta-analyses? Int J Epidemiol 2009;38(1):276-86.
10. Wetterslev J, Thorlund K, Brok J, Gluud C. Trial sequential analysis may establish when firm evidence is reached in cumulative meta-analysis. J Clin Epidemiol 2008;61(1):64-75.
11. Nairooz R, Saad M, Sardar P, Aronow WS. Two-year outcomes of bioresorbable vascular scaffold versus drug-eluting stents in coronary artery disease: a meta-analysis. Heart 2017.
12. Mahmoud AN, Barakat AF, Elgendy AY, Schneibel E, Mentias A, Abuzaid A, Elgendy IY. Long-Term Efficacy and Safety of Everolimus-Eluting Bioresorbable Vascular Scaffolds Versus Everolimus-Eluting Metallic Stents: A Meta-Analysis of Randomized Trials. Circ Cardiovasc Interv 2017;10(5).
13. Sorrentino S, Giustino G, Mehran R, Kini AS, Sharma SK, Faggioni M, Farhan S, Vogel B, Indolfi C, Dangas GD. Everolimus-Eluting Bioresorbable Scaffolds versus Metallic Everolimus-Eluting Stents: Meta-Analysis of Randomized Controlled Trials. J Am Coll Cardiol 2017.
14. Cassese S, Robert BA, Juni P, Wykrzykowska JJ, Puricel S, Ndrepepa G, Schunkert H, Fusaro M, Cook S, Kimura T, Henriques JPS, Serruys PW, Windecker S, Kastrati A. Mid-term clinical outcomes with everolimus-eluting bioresorbable scaffolds versus everolimus-eluting metallic stents for percutaneous coronary interventions: a meta-analysis of randomized trials. EuroIntervention 2017.
15. Ali ZA, Serruys PW, Kimura T, Gao R, Ellis SG, Kereiakes DJ, Onuma Y, Simonton C, Zhang Z, Stone GW. 2-year outcomes with the Absorb bioresorbable scaffold for treatment of coronary artery disease: a systematic review and meta-analysis of seven randomised trials with an individual patient data substudy. Lancet 2017.
16. Montone RA, Niccoli G, De Marco F, Minelli S, D'Ascenzo F, Testa L, Bedogni F, Crea F. Temporal Trends in Adverse Events After Everolimus-Eluting Bioresorbable Vascular Scaffold Versus Everolimus-

Eluting Metallic Stent Implantation: A Meta-Analysis of Randomized Controlled Trials. Circulation 2017;135(22):2145-2154.
17. Ha FJ, Nerlekar N, Cameron JD, Bennett MR, Meredith IT, West NE, Brown AJ. Midterm Safety and Efficacy of ABSORB Bioresorbable Vascular Scaffold Versus Everolimus-Eluting Metallic Stent: An Updated Meta-Analysis. JACC Cardiovasc Interv 2017;10(3):308-310.
18. Serruys PW, Katsikis A, Onuma Y. Long-term data of BRS presented at EuroPCR 2017 (Friday, 19 May). EuroIntervention 2017;13(5):e515-e521.
19. Lipinski MJ, Escarcega RO, Baker NC, Benn HA, Gaglia MA, Jr., Torguson R, Waksman R. Scaffold Thrombosis After Percutaneous Coronary Intervention With ABSORB Bioresorbable Vascular Scaffold: A Systematic Review and Meta-Analysis. JACC Cardiovasc Interv 2016;9(1):12-24.
20. Kang SH, Chae IH, Park JJ, Lee HS, Kang DY, Hwang SS, Youn TJ, Kim HS. Stent Thrombosis With Drug-Eluting Stents and Bioresorbable Scaffolds: Evidence From a Network Meta-Analysis of 147 Trials. JACC Cardiovasc Interv 2016;9(12):1203-12.
21. Puricel S, Cuculi F, Weissner M, Schmermund A, Jamshidi P, Nyffenegger T, Binder H, Eggebrecht H, Munzel T, Cook S, Gori T. Bioresorbable Coronary Scaffold Thrombosis: Multicenter Comprehensive Analysis of Clinical Presentation, Mechanisms, and Predictors. J Am Coll Cardiol 2016;67(8):921-31.
22. Ellis SG, Kereiakes DJ, Metzger DC, Caputo RP, Rizik DG, Teirstein PS, Litt MR, Kini A, Kabour A, Marx SO, Popma JJ, McGreevy R, Zhang Z, Simonton C, Stone GW, Investigators AI. Everolimus-Eluting Bioresorbable Scaffolds for Coronary Artery Disease. N Engl J Med 2015.
23. Ellis S, Kereiakes D, Stone GW. Everolimus-eluting Bioresorbable Vascular Scaffolds in Patients with Coronary Artery Disease: ABSORB III Trial 2-Year Results. American College of Cardiology Congress 2017 2017;Oral presentation.
24. Serruys PW, Chevalier B, Sotomi Y, Cequier A, Carrie D, Piek JJ, Van Boven AJ, Dominici M, Dudek D, McClean D, Helqvist S, Haude M, Reith S, de Sousa Almeida M, Campo G, Iniguez A, Sabate M, Windecker S, Onuma Y. Comparison of an everolimus-eluting bioresorbable scaffold with an everolimus-eluting metallic stent for the treatment of coronary artery stenosis (ABSORB II): a 3 year, randomised, controlled, single-blind, multicentre clinical trial. Lancet 2016.
25. Byrne RA, Stefanini GF, Capodanno D, Onuma Y, Baumbach A, Escaned J, Haude M, James S, Joner M, Ju Ni P, Kastrati A, Oktay S, Wijns W, Serruys PW, Windecker S. Report of an ESC-EAPCI Task Force on the evaluation and use of bioresorbable scaffolds for percutaneous coronary intervention: executive summary. EuroIntervention 2017.
26. Sabate M, Asano T. Comparison of the ABSORB Everolimus Eluting Bioresorbable Vascular Scaffold System With a Drug-Eluting Metal Stent (Xience) in Acute ST-Elevation Myocardial Infarction: 3-year results of TROFI II Study and correlations with the 6-month OCT findings. Oral presentation at TCT congress 2017;October 31th 2017.
27. Ellis SG, Kereiakes DJ, Stone GW. Three-Year Clinical Outcomes with Everolimus-Eluting Bioresorbable Scaffolds: Results from the Randomized ABSORB III Trial. Oral presentation at TCT congress 2017;October 31th 2017.
28. Chevalier B, Serruys PW. The 4-year Clinical Outcomes of the ABSORB II Trial: First Randomized Comparison between the Absorb Everolimus Eluting Bioresorbable Vascular Scaffold and the XIENCE Everolimus Eluting Stent. Oral presentation at TCT congress 2017;October 31th 2017.
29. Ortega-Paz L, Capodanno D, Gori T, Nef H, Latib A, Caramanno G, Di Mario C, Naber C, Lesiak M, Capranzano P, Wiebe J, Mehilli J, Araszkiewicz A, Pyxaras S, Mattesini A, Geraci S, Naganuma T, Colombo A, Munzel T, Sabate M, Tamburino C, Brugaletta S. Predilation, sizing and post-dilation scoring in patients undergoing everolimus-eluting bioresorbable scaffold implantation for prediction of cardiac adverse events: development and internal validation of the PSP score. EuroIntervention 2017.
30. Tanaka A, Latib A, Kawamoto H, Jabbour RJ, Sato K, Miyazaki T, Naganuma T, Mangieri A, Pagnesi M, Montalto C, Chieffo A, Carlino M, Montorfano M, Colombo A. Clinical outcomes of a real

world cohort following bioresorbable vascular scaffold implantation utilizing an optimized implantation strategy. EuroIntervention 2016.
31. Stone GW. Outcomes of Absorb Bioresorbable Scaffolds with Improved Technique in an Expanded Patient Population: The ABSORB IV Randomized Trial. Oral presentation at TCT congress 2017;October 31th 2017.
32. Felix CM, Vlachojannis GJ, IJsselmuiden AJJ, Fam JM, Smits PC, Lansink WJ, Diletti R, Zijlstra F, Regar ES, Boersma E, Onuma Y, van Geuns RJM. Potentially increased incidence of scaffold thrombosis in patients treated with Absorb BVS who terminated DAPT before 18 months. EuroIntervention 2017; 2017 Jun 2;13(2):e177-e184.
33. Capodanno D, Angiolillo DJ. Antiplatelet Therapy After Implantation of Bioresorbable Vascular Scaffolds: A Review of the Published Data, Practical Recommendations, and Future Directions. JACC Cardiovasc Interv 2017;10(5):425-437.
34. Mauri L, Kereiakes DJ, Yeh RW, Driscoll-Shempp P, Cutlip DE, Steg PG, Normand SL, Braunwald E, Wiviott SD, Cohen DJ, Holmes DR, Jr., Krucoff MW, Hermiller J, Dauerman HL, Simon DI, Kandzari DE, Garratt KN, Lee DP, Pow TK, Ver Lee P, Rinaldi MJ, Massaro JM, Investigators DS. Twelve or 30 months of dual antiplatelet therapy after drug-eluting stents. N Engl J Med 2014;371(23):2155-66.
35. Seth A, Onuma Y, Costa R, Chandra P, Bahl VK, Manjunath CN, Mahajan AU, Kumar V, Goel PK, Wander GS, Kalarickal MS, Kaul U, Kumar VKA, Rath PC, Trehan V, Sengottuvelu G, Mishra S, Abizaid A, Serruys PW. First-in-human evaluation of a novel poly-L-lactide based sirolimus-eluting bioresorbable vascular scaffold for the treatment of de novo native coronary artery lesions: MeRes-1 trial. EuroIntervention 2017;13(4):415-423.
36. Kozuma K, Tanabe K, Kimura T. 3-year Clinical and Angiographic Results of a Randomized trial Evaluating the Absorb Bioresorbable Vascular Scaffold vs. Metallic Drug-eluting Stent in de novo Native Coronary Artery Lesions. EuroPCR congress 2017;Oral presentation on May 16.
37. Gao R. Randomized comparison of everolimus-eluting bioresorbable vascular scaffold vs. everolimus-eluting metallic stents in patients with coronary artery disease: 3-year clinical outcomes from ABSORB China. EuroPCR congress 2017;Oral presentation on May 16.
38. Arroyo D, Gendre G, Schukraft S, Kallinikou Z, Muller O, Baeriswyl G, Stauffer JC, Goy JJ, Togni M, Cook S, Puricel S. Comparison of everolimus- and biolimus-eluting coronary stents with everolimus-eluting bioresorbable vascular scaffolds: Two-year clinical outcomes of the EVERBIO II trial. Int J Cardiol 2017.
39. Wykrzykowska JJ, Kraak RP, Hofma SH, van der Schaaf RJ, Arkenbout EK, AJ IJ, Elias J, van Dongen IM, Tijssen RYG, Koch KT, Baan J, Jr., Vis MM, de Winter RJ, Piek JJ, Tijssen JGP, Henriques JPS, Investigators A. Bioresorbable Scaffolds versus Metallic Stents in Routine PCI. N Engl J Med 2017;376(24):2319-2328.
40. Imori Y, D'Ascenzo F, Gori T, Munzel T, Fabrizio U, Campo G, Cerrato E, Napp LC, Iannaccone M, Ghadri JR, Kazemian E, Binder RK, Jaguszewski M, Csordas A, Capasso P, Biscaglia S, Conrotto F, Varbella F, Garbo R, Gaita F, Erne P, Luscher TF, Moretti C, Frangieh AH, Templin C. Impact of postdilatation on performance of bioresorbable vascular scaffolds in patients with acute coronary syndrome compared with everolimus-eluting stents: A propensity score-matched analysis from a multicenter "real-world" registry. Cardiol J 2016.
41. Brugaletta S, Gori T, Low AF, Tousek P, Pinar E, Gomez-Lara J, Ortega-Paz L, Schulz E, Chan MY, Kocka V, Hurtado J, Gomez-Hospital JA, Giacchi G, Munzel T, Lee CH, Cequier A, Valdes M, Widimsky P, Serruys PW, Sabate M. ABSORB bioresorbable vascular scaffold vs. everolimus-eluting metallic stent in ST-segment elevation myocardial infarction (BVS EXAMINATION study): 2-Year results from a propensity score matched comparison. Int J Cardiol 2016;214:483-4.

42. Felix CM, FAM JM, Diletti R, Regar ES, van Mieghem NM, Onuma Y, van Geuns RJ. Two-years Clinical Outcomes Of The ABSORB BVS Compared EES: A Propensity Matched Analysis Of The BVS Expand Registry. Presented during LBCT of CRT 2017.

FIGURE LEGENDS

Figure 1. Flowchart

Figure 2. Trial Sequential Analysis for (A) Primary Endpoint Target Lesion Failure and Definite/Probable Device Thrombosis (B)

The red dotted line represents the trial sequential monitoring boundaries and the futility boundaries. The solid dark red line illustrates the conventional level of significance (p=0.05). The cumulative Z score (solid blue line) crosses both the conventional boundary and the trial sequential monitoring boundary, indicating sufficient and conclusive evidence.

Figure 3. Forest Plots for Primary and Secondary Endpoint of Bioresorbable Vascular Scaffolds Versus Drug-Eluting Stents

A Target lesion failure.

B All-cause mortality.

C All myocardial infarction.

D Target lesion revascularization. RCTs reported ischemia-driven TLR and observational studies reported all TLR.

E Definite/ probable device thrombosis.

CI, confidence interval; M-H, Mantel-Haenszel; OR, odds ratio.

Table 1 Checklist for PRISMA Guidelines

Section/topic	#	Checklist item	Reported on page #
TITLE			
Title	1	Identify the report as a systematic review, meta-analysis, or both.	1
ABSTRACT			
Structured summary	2	Provide a structured summary including, as applicable: background; objectives; data sources; study eligibility criteria, participants, and interventions; study appraisal and synthesis methods; results; limitations; conclusions and implications of key findings; systematic review registration number.	2
INTRODUCTION			
Rationale	3	Describe the rationale for the review in the context of what is already known.	3
Objectives	4	Provide an explicit statement of questions being addressed with reference to participants, interventions, comparisons, outcomes, and study design (PICOS).	6, 7
METHODS			
Protocol and registration	5	Indicate if a review protocol exists, if and where it can be accessed (e.g., Web address), and, if available, provide registration information including registration number.	NA
Eligibility criteria	6	Specify study characteristics (e.g., PICOS, length of follow-up) and report characteristics (e.g., years considered, language, publication status) used as criteria for eligibility, giving rationale.	6
Information sources	7	Describe all information sources (e.g., databases with dates of coverage, contact with study authors to identify additional studies) in the search and date last searched.	6
Search	8	Present full electronic search strategy for at least one database, including any limits used, such that it could be repeated.	S
Study selection	9	State the process for selecting studies (i.e., screening, eligibility, included in systematic review, and, if applicable, included in the meta-analysis).	6, 7
Data collection process	10	Describe method of data extraction from reports (e.g., piloted forms, independently, in duplicate) and any processes for obtaining and confirming data from investigators.	6, 7
Data items	11	List and define all variables for which data were sought (e.g., PICOS, funding sources) and any assumptions and simplifications made.	6
Risk of bias in individual studies	12	Describe methods used for assessing risk of bias of individual studies (including specification of whether this was done at the study or outcome level), and how this information is to be used in any data synthesis.	6, 7
Summary measures	13	State the principal summary measures (e.g., risk ratio, difference in means).	7
Synthesis of results	14	Describe the methods of handling data and combining results of studies, if done, including measures of consistency (e.g., I^2) for each meta-analysis.	7

Table 2. Major characteristics of included studies

Study	Year	Centres, n	BVS/ DES treated Patients, n	Study type	Clinical presentation	Primary Endpoint	Follow-up, yrs.
ABSORB II [28]	2016	46	335/ 166	RCT	SAP, established ACS	Vasomotion & LLL (at 3 yrs.)	1, 2, 3, 4
ABSORB III [27]	2017	193	1322/ 686	RCT	SAP, established ACS	TLF (at 1 yr.)	1, 2, 3
ABSORB Japan [36]	2016	38	266/ 134	RCT	SAP, established ACS	TLF (at 1 yr.)	1, 2, 3
ABSORB China [37]	2016	24	238/ 237	RCT	SAP, established ACS	LLL (at 1 yr.)	1, 2, 3
TROFI II [26]	2016	8	95/ 96	RCT	STEMI	HS (at 6 months)	1, 2, 3
EVERBIO [38]	2017	1	78/ 80	RCT	SAP, ACS, silent ischemia	LLL (at 9 months)	9 months, 2 yrs.
AIDA [39]	2017	5	924/ 921	RCT	SAP, ACS	TVF (at 2 yrs.)	Median of 707 days
Imori et al. [40]	2016	8	214/ 215	Propensity matched	ACS	MACE	2
BVS-Examination [41]	2016	6	290/ 290	Propensity matched	STEMI	POCE (at 1 yr.)	1, 2
BVS Expand [42]	2017	1	244/ 488	Propensity matched	SAP, UA, NSTEMI, silent ischemia	MACE	2

ACS: acute coronary syndrome; DOCE: device oriented composite endpoint; HS: healing score; LLL: late lumen loss; MACE: major adverse cardiac events; RCT: randomized controlled trial; SAP: stable angina pectoris; STEMI: ST-elevation myocardial infarction; TLF: target lesion failure; LLL: late lumen loss; TVF: target vessel failure; UAP: unstable angina pectoris

Table 3. Baseline characteristics (presented as BVS versus EES)

	ABSORB II	ABSORB III	ABSORB Japan	Absorb China	TROFI II	EVERBIO	AIDA	Imori et al.	BVS-Examination	BVS Expand
Patients										
Randomized, n	355/ 166	1322/ 686	266/ 134	238/ 237	95/ 96	78/ 80	924/ 921	214/ 215	290/ 290	244/ 488
Age, years	61.5/ 60.9	63.5/ 63.6	67.1/ 67.3	57.2/ 57.6	59.1/ 58.2	65/ 65	64.3/ 64.0	59.7/ 61.5	56.0/ 57.6	61.3/ 61.9
Male sex (%)	76/ 80	70.7/ 70.1	78.9/ 73.9	71.8/ 72.6	76.8/ 87.5	80/ 78	72.5/ 76.0	79.4/ 80.5	81.4/ 79.7	73.4/ 73.6
Diabetes (%)	24/ 24	31.5/ 32.7	36.1/ 35.8	25.2/ 23.2	18.9/ 14.7	16/ 22	18.5/ 16.6	14/ 16.7	12.8/ 12.8	18.4/ 20.7
Hypertension (%)	69/ 72	84.9/ 85.0	78.2/ 79.9	58.8/ 60.3	44.1/ 36.5	64/ 55	50.9/ 50.5	56.1/ 54.4	49.7/ 43.8	60.1/ 63.7
Dyslipidaemia (%)	75/ 80	86.2/ 86.3	82/ 81.1	42.4/38.4	63.8/ 57.3	63/ 64	37.6/ 38.3	41.1/ 42.8	41.7/ 45.5	50.6/ 54.7
ACS at presentation (%)	23/ 25	26.9/ 24.5	9.8/ 16.4	72.3/ 75.9	100/ 100 (only STEMI)	34/ 37	53.6/ 54.6	100/100	100/100 (only STEMI)	59.1/ NA
Previous MI (%)	28.0/ 29.0	21.5/ 22.0	16/ 23.9	16.8/ 16.0	2.1/ 3.1	18/ 14	18/ 18.7	NA	3.5/ 3.5	17.2/ 18.1
Previous PCI (%)	12.0/ 9.0	NA	3.4/ 5.2	9.7/8.0	4.2/ 3.1	31/ 32	21.9/ 20.0	NA	3.4/ 3.8	9.4/ 15.2
DAPT per protocol	At least 6 months	At least 1 year	At least 1 year	At least 1 year	At least 1 year	At least 6 months	At least 1 year	1 year	1 year	1 year
On DAPT at 2 yrs. (%)	36.2/ 34.3	66/ 65.6	52.3/ 50.7	NA	NA	21/ 15	17.5/ 15.6	NA	5.8/ 17.0	5.7/ NA
Lesions										
Randomized, n	364/ 182	1385/ 713	275/ 137	251/252	95/ 98	112/ 96	1237/ 1209	NA	NA	355/ NA
ACC/ AHA B2/C (%)	46/ 49	68.7/ 72.5	76/ 75.9	74.9/ 72.1	NA	35/ 29	55.0/ 51.0	48/42 (C)	NA	38.1/ NA
Calcification (moderate/ severe, %)	13/ 15.5	NA	34.6/ 43.7	17.5/15.5	NA	NA	30.0/ 28.0	NA	NA	42.2/ NA
Bifurcation (%)	0/ 0	0/ 0	0/ 0	50.2/ 48.6	NA	NA	5.0/6.0	NA	NA	21.3/ NA
Lesion length (mm)	13.8/ 13.8	12.6/ 13.1	13.5/ 13.3	14.1/ 13.9	12.88/ 13.41	NA	19.1/ 18.8	NA	NA	22.10/ NA
Pre-procedural RVD (mm)	2.6/ 2.6	2.67/ 2.65	2.72/ 2.79	2.81/ 2.82	2.86/ 2.76	2.77/ 2.39	2.67/ NA	NA	NA	2.42/ NA
Pre-procedural DS (%)	59/ 60	65.3/ 65.9	64.6/ 64.7	65.3/ 64.5	89.5/ 89.9	NA	NA	NA	NA	59.13/ NA

Pre-dilatation (%)	100/ 99	100/ 100	100/ 100	99.6/ 98.0	55.8/ 51.0	97/ 86	97.0/ 91.0	NA	81.0/ 29.0	89.8/ NA
Intravascular imaging (%)	100/ 100	11.2/ 10.8	68.8/ 68.7	0.4/ 0.4	NA	NA	NA	23/ NA	NA	39.0/ NA
Post-dilatation (%)	61/ 59	65.5/ 51.2	82.2/ 77.4	63.0/ 54.4	50.5/ 25.5	31/ 34	74.0/ 49.0	55.2/ NA	36.3/ 15.2	53.3/ NA
Maximum pressure (atm)	14.2/ 15.0	15.4/ 15.4	14.7/ 15.1	16.8/ 16.9	15.8/ 18.6	13.6/ 14.6	15.4/ 15.6	20/ NA	NA/ NA	15.5/ NA
In-device MLD (mm)	2.22/ 2.50	2.37/ 2.49	2.42/ 2.64	2.48/ 2.59	2.46/ 2.46	2.56/ 2.62	NA	NA	NA	2.30/ NA
Post-procedural DS (%)	16/ 10	11.6/ 6.4	11.8/ 7.1	12.2/ 8.7	14.1/ 13.4	9.3/ 8.1	17.0/ NR	NA	NA	16.90/ NA

Values are presented as means or percentages and are described as BVS/ DES. ACS: acute coronary syndrome; DAPT: dual antiplatelet therapy; DS: diameter stenosis; MLD: minimum lumen diameter; NA: not available; RVD: reference vessel diameter.

Table 4. Outcomes of interest at 0 -1 year, 1 -2 years and 2 -3 years (for included studies that presented outcomes at these time points*)

Outcome	Up to 1 year				1 up to 2 years				2 up to 3 years			
	BVS	DES	OR (95% CI)	P	BVS	DES	OR (95% CI)	P	BVS	DES	OR (95% CI)	P
TLF (%)	6.39	5.15	1.24 (0.97 – 1.58)	0.09	4.43	2.55	1.55 (0.98 – 2.46)	0.06	1.20	0.34	2.75 (0.97 - 7.78)	0.06
All-cause mortality (%)	1.17	1.49	0.90 (0.33 – 2.43)	0.83	1.10	1.73	0.65 (0.4 – 1.05)	0.08	0.20	1.88	0.14 (0.01 – 1.46)	0.10
Myocardial infarction (%)	5.15	3.50	1.38 (1.04 – 1.83)	0.03	2.20	1.01	2.17 (1.30 - 3.62)	0.003	1.36	0.94	1.18 (0.59 - 2.37)	0.64
ID-TLR (%)	3.08	2.57	1.26 (0.90 – 1.77)	0.18	2.87	1.59	1.67 (0.97 – 2.87)	0.06	2.11	1.02	1.79 (0.62 – 5.15)	0.28
Def/ prob device thrombosis (%)	1.60	0.61	2.45 (1.35 – 4.46)	0.03	0.86	0.10	4.75 (1.63 – 13.82)	0.004	0.53	0.00	3.79 (0.67 – 21.37)	0.13

*ABSORB II, ABSORB III, ABSORB China, ABSORB Japan. Def/ prob: definite/probable; OR: Odds ratio; ID-TLR: ischemia driven target lesion revascularization; TLF: target lesion failure

Supplemental material

Online Figure 1. Funnel Plot for the Primary Endpoint

Online Figure 2. Sensitivity Analysis for TLF and Device Thrombosis, Non-Complex Studies Versus Complex Studies

Online Figures 3A –E Fixed-effect Forest Plots for Primary and Secondary Endpoint of Bioresorbable Vascular Scaffolds Versus Drug-Eluting Stents

A Target lesion failure.

B All-cause mortality.

C Myocardial infarction.

D Target lesion revascularization.

E Definite/ probable device thrombosis.

Literature search in the most important online databases

Online Table 1A. 1B Definitions of Clinical Outcomes Per Study

Online Table 2A. Assessment of Risk of Bias for Randomized Controlled Trials

Online Table 2B. Quality Assessment for Observational Studies

Figure 1 TLF Funnel plot

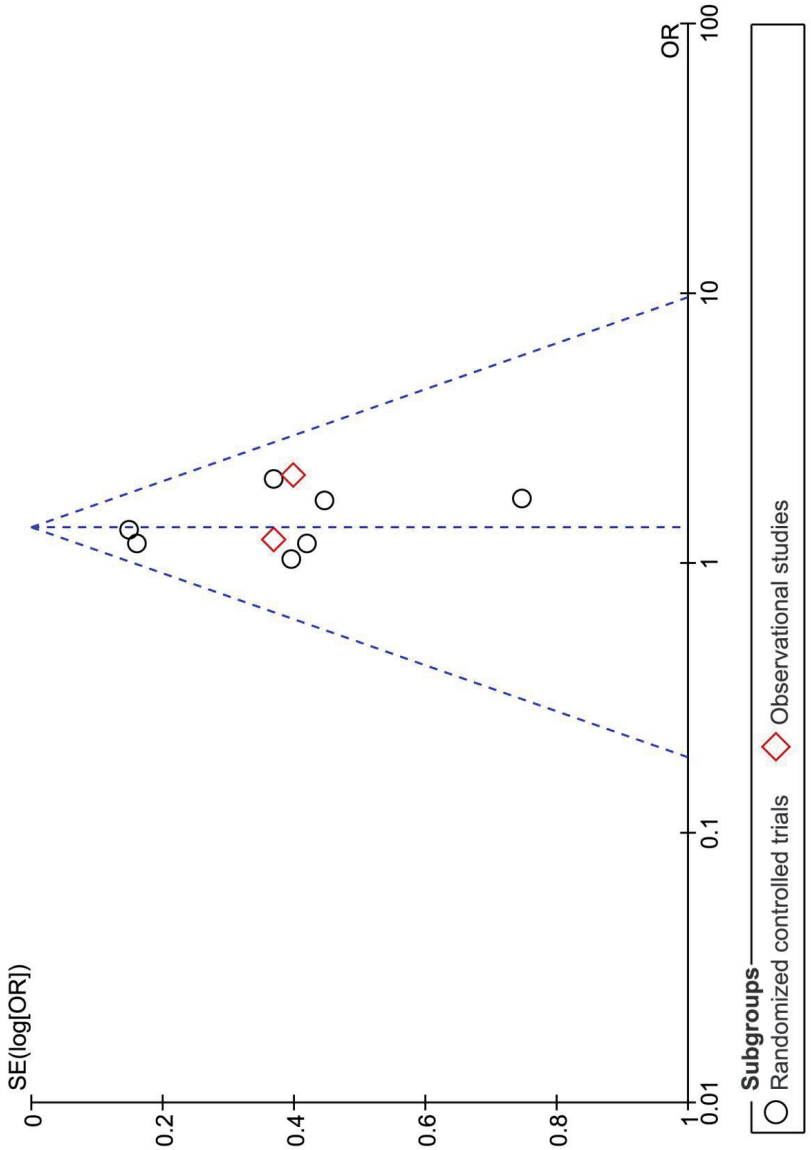

Online Figure 2 Sensitivity analysis for TLF and Device Thrombosis, Non-Complex Studies vs. Complex Studies

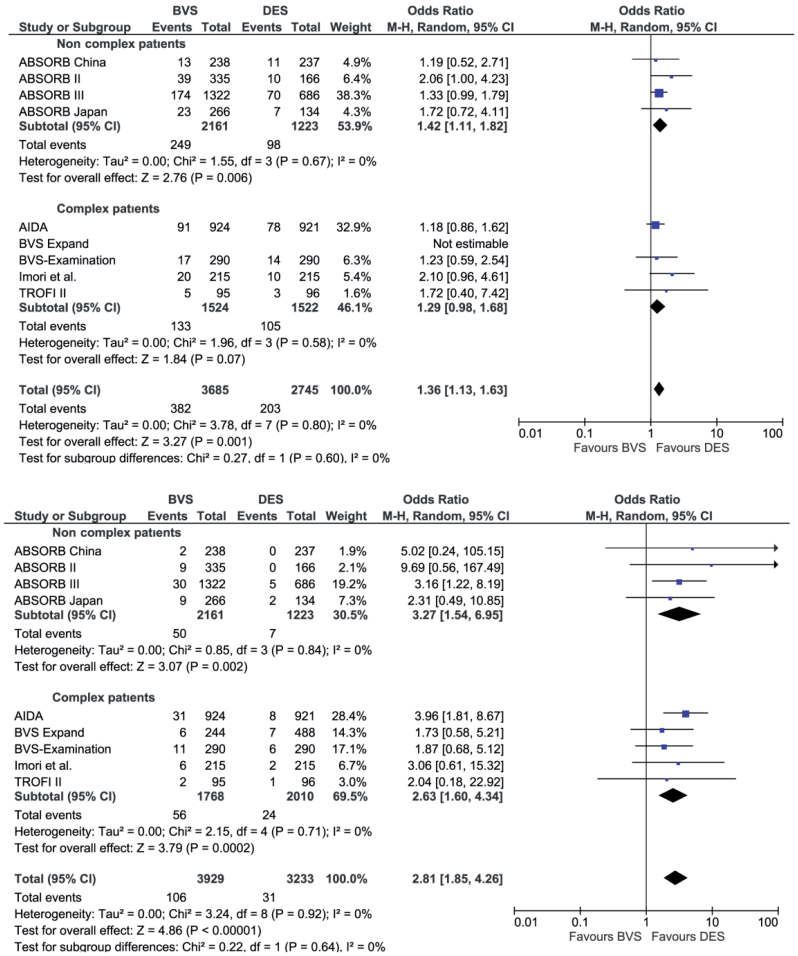

Figure 3A Target lesion failure.

Online Figure 3A

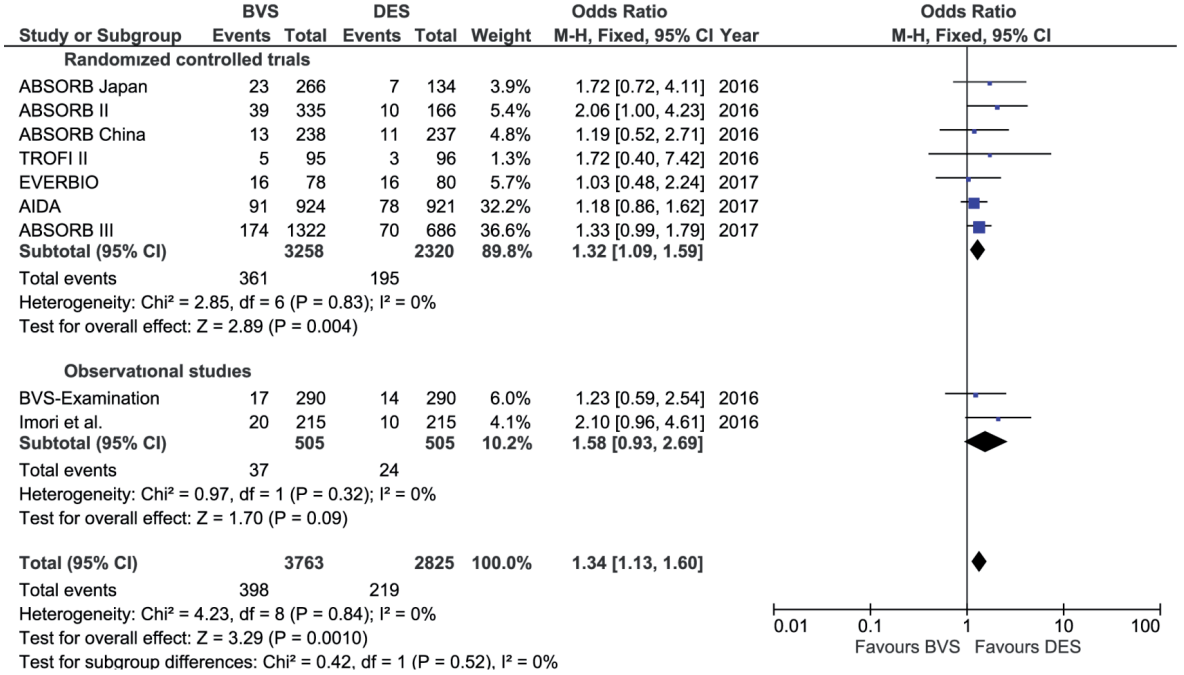

Figure B All-cause mortality.

Online Figure 3B

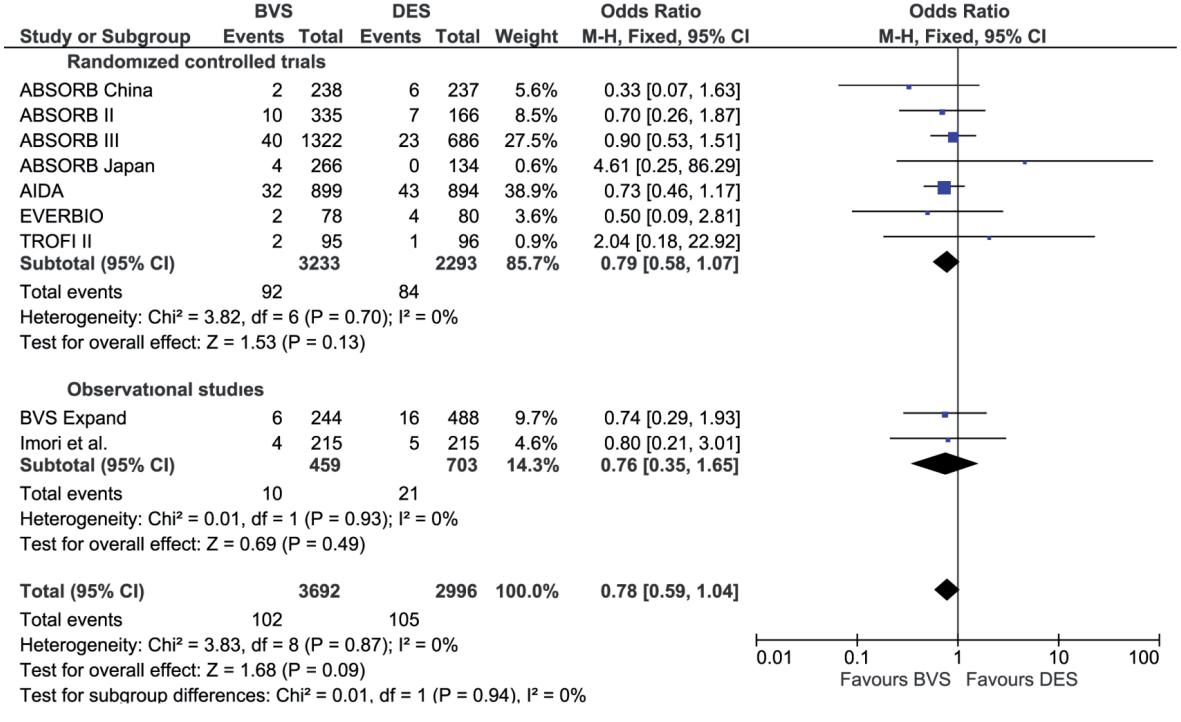

Figure 3C Myocardial infarction.

Online Figure 3C

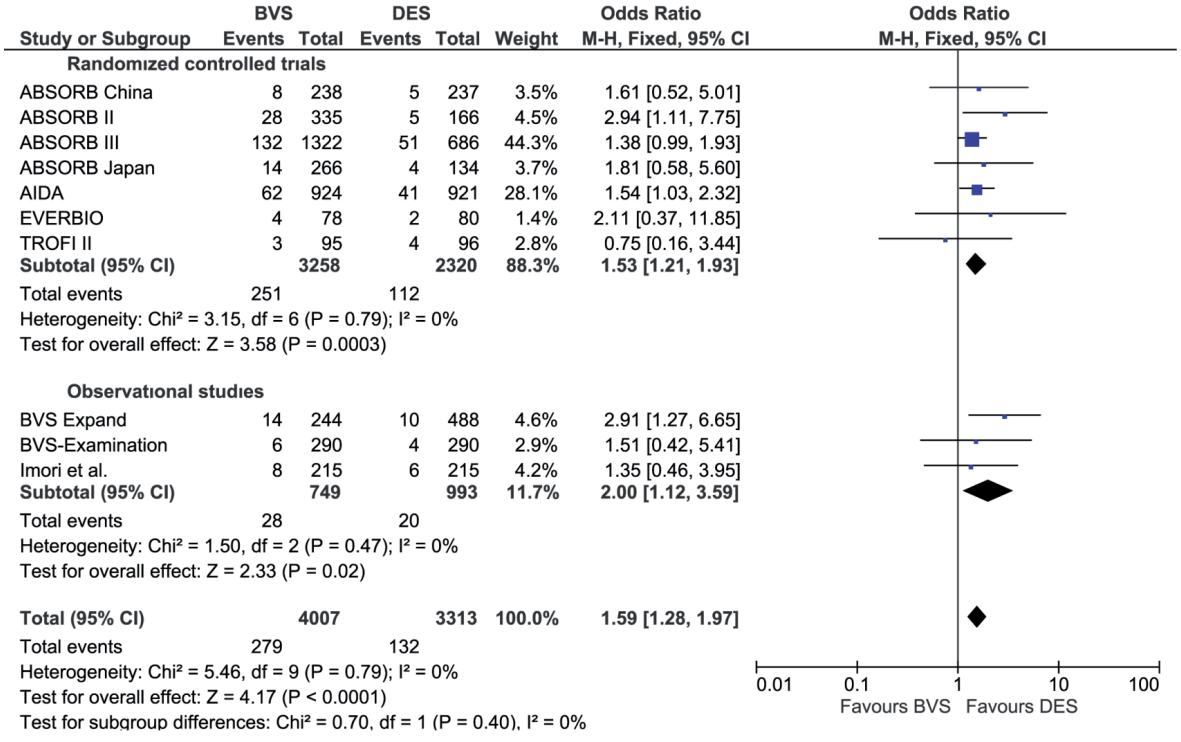

Figure 3D Target lesion revascularization.

Online Figure 3D

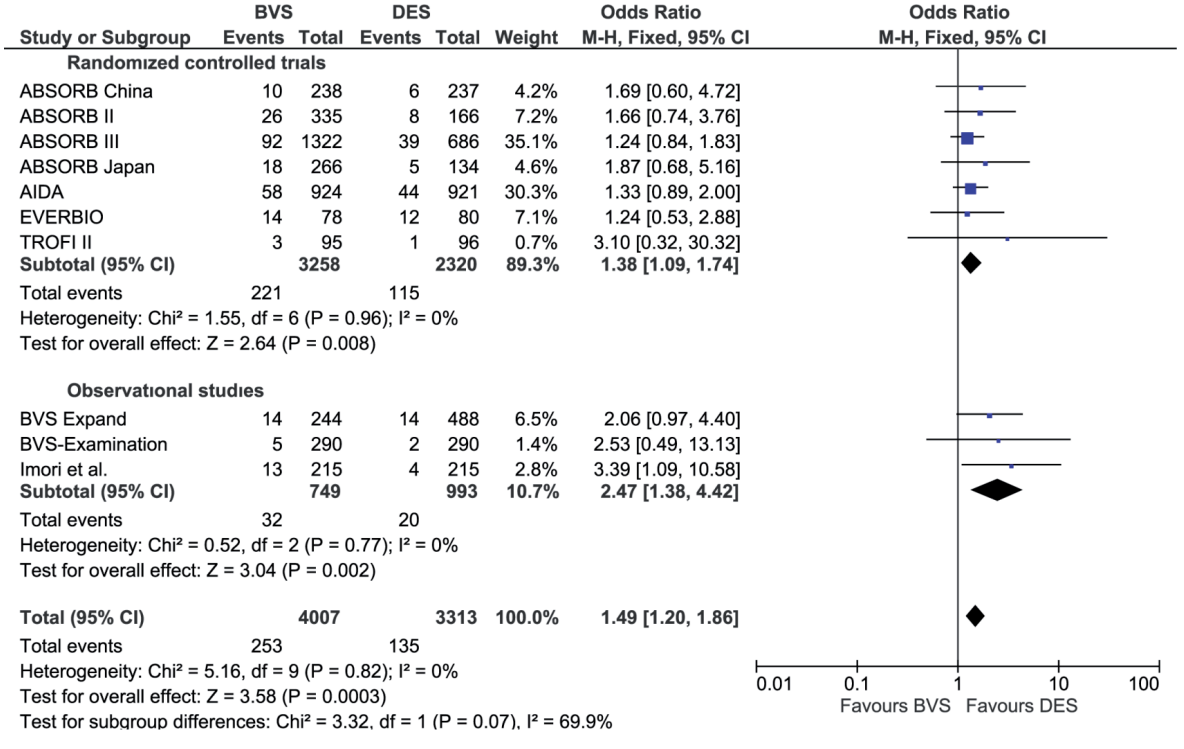

Figure 3E Definite or probable device thrombosis.

Online Figure 3E

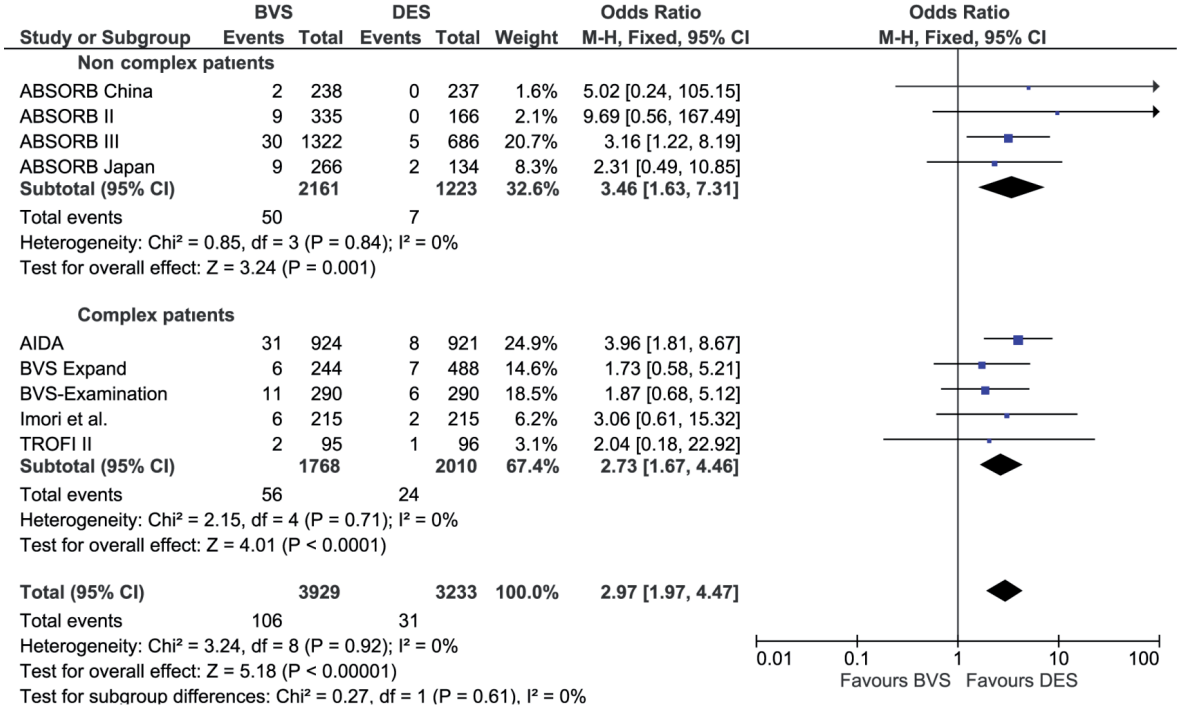

Literature searches in most important databases

Embase.com

('bioresorbable vascular stent'/exp OR 'bioresorbable scaffold'/exp OR (((bioresorbab* OR bioabsorbab* OR bvs OR fully-resorbab*) NEAR/3 (stent* OR scaffold*)) OR (Absorb* NEAR/10 (stent* OR bvs))):ab,ti) AND ('everolimus eluting coronary stent'/exp OR 'drug eluting stent'/mj OR (('drug eluting stent'/de OR 'drug eluting coronary stent'/de OR 'metal stent'/de OR stent/de) AND everolimus/de) OR (((everolimus OR ees) NEAR/3 (stent* OR des)) OR XIENCE-Xpedition* OR Xience OR ((second-generation OR 2nd-generation OR 2-nd-generation OR non-BVS OR non-bioabsorbable OR non-bioresorbable OR conventional OR current-generation*) NEAR/6 (eluting OR des OR coated*) NEAR/6 stent*)):ab,ti OR 'drug eluting stent*':ti)

Medline Ovid

((((bioresorbab* OR bioabsorbab* OR bvs OR fully-resorbab*) ADJ3 (stent* OR scaffold*)) OR (Absorb* ADJ10 (stent* OR bvs))).ab,ti.) AND (*"Drug-Eluting Stents" OR (("Drug-Eluting Stents"/ OR stents/) AND everolimus/) OR (((everolimus OR ees) ADJ3 (stent* OR des)) OR XIENCE-Xpedition* OR Xience OR ((second-generation OR 2nd-generation OR 2-nd-generation OR non-BVS OR non-bioabsorbable OR non-bioresorbable OR conventional OR current-generation*) ADJ6 (eluting OR des OR coated*) ADJ6 stent*)).ab,ti. OR "drug eluting stent*".ti.)

Cochrane

((((bioresorbab* OR bioabsorbab* OR bvs OR fully-resorbab*) NEAR/3 (stent* OR scaffold*)) OR (Absorb* NEAR/10 (stent* OR bvs))):ab,ti) AND ((((everolimus OR ees) NEAR/3 (stent* OR des)) OR XIENCE-Xpedition* OR Xience OR ((second-generation OR 2nd-generation OR 2-nd-generation OR non-BVS OR non-bioabsorbable OR non-bioresorbable OR conventional OR current-generation*) NEAR/6 (eluting OR des OR coated*) NEAR/6 stent*)):ab,ti OR 'drug eluting stent*':ti)

Table 1A. Definitions of Clinical Outcomes Per Study (A) RCTs and (B) registries

	ABSORB II	ABSORB III	ABSORB Japan	ABSORB China	TROFI II	EVERBIO II	AIDA
Target lesion failure	Cardiac death, target-vessel MI, ID-TLR	Cardiac death, target-vessel MI, ID-TLR	Cardiac death, target-vessel MI, ID-TLR	Cardiac death, target-vessel MI, ID-TLR	Cardiac death, MI (not clearly attributable to a non-target vessel), ID-TLR	Cardiac death, target-vessel MI, CD-TLR	Cardiac death, target-vessel MI, CD-TLR
Device thrombosis	ARC definitions	ARC definitions	ARC definitions	ARC definitions	ARC definitions	ARC definitions	ARC definitions
Myocardial infarction	New pathological Q-wave or CK rise > 2 of ULN accomplice by CK-MB rise	*Periprocedural:* CK-MB to >5x ULN within 48 hours in cases in which the baseline CK-MB value is <ULN *Spontaneous:* defined as elevation of troponin >ULN or CK-MB >ULN and ≥ of the following: ischemic symptoms, ischemic ECG changes, development of pathological Q waves, or imaging findings of acute MI	*Periprocedural:* CK-MB >5x ULN. *Spontaneous:* Troponin>ULN or CK-MB>ULN and ≥ of the following: ischemic symptoms, ischemic ECG changes, development of pathological Q waves, or imaging findings of acute MI	*Periprocedural:* CK-MB >5× ULN *Spontaneous:* defined as elevation of troponin >ULN or CK-MB >ULN and ≥ of the following: ischemic symptoms, ischemic ECG changes, development of pathological Q waves, or imaging findings of acute MI	New pathological Q-waves in ≥ 2 contiguous leads (as assessed by the ECG core laboratory) with or without post-procedure troponin, CK or CK-MB levels elevated above normal; Detection of a rise and/or fall of cardiac biomarker values (preferably cardiac troponin) with at least one value above the 99 percentile ULN and ≥ of the following: ischemic symptoms, ischemic ECG changes, development of pathological Q waves, or imaging/ autopsy findings of	*Periprocedural:* According to Global MI Task Force for the Universal definition of Myocardial Infarction [35] *Spontaneous::* Development of new pathological Q waves ≥0.04 s in duration in ≥2 contiguous leads or an elevation of creatine phosphokinase levels to >2 times normal with positive creatine phosphokinase–MB or troponin I levels	'Third Universal Myocardial infarction' definitions[35]

					acute MI		
Target lesion revascularization	Any clinically indicated repeat PCI of the target lesion or CABG of the target vessel	Any repeat PCI of the target lesion or CABG of the target vessel	Any repeat PCI of the target lesion or CABG of the target vessel	Any repeat PCI of the target lesion or CABG of the target vessel	Any repeat PCI of the target lesion or CABG of the target vessel	Repeat revascularization within the stent or the 5-mm boarders proximal and distal to the stent.	Any repeat PCI of the target lesion or CABG of the target vessel
Death	All deaths were considered cardiac unless an unequivocal non-cardiac cause was established	All deaths were considered cardiac unless an unequivocal non-cardiac cause was established	All deaths were considered cardiac unless an unequivocal non-cardiac cause was established	All deaths were considered cardiac unless an unequivocal non-cardiac cause was established	All deaths were considered cardiac unless an unequivocal non-cardiac cause was established	All deaths were considered cardiac unless an unequivocal non-cardiac cause was established	All deaths were considered cardiac unless an unequivocal non-cardiac cause was established

CABG: coronary artery bypass grafting; CK: creatine kinase; CK-MB: creatine kinase myoglobulin; ID-TLR: ischemia-driven target lesion revascularization; MI: myocardial infarction, ULN: upper limit of normal

Table 1B.

	BVS-Examination	Imori et al.	BVS Expand
Target lesion failure	Cardiac death, target-vessel MI, TLR	NA	Cardiac death, target-vessel MI, ID-TLR
Patient oriented endpoint	All-cause death, any MI, any revascularization	NA	NA
Device thrombosis	ARC definitions	ARC definitions	ARC definitions
Myocardial infarction	Based on Historical Extended Definition of MI (modified ARC Definition according to Vranckx *et al.* [33])	NR	Based on Historical Extended Definition of MI (modified ARC Definition according to Vranckx *et al.* [33]) and per protocol definition of MI also known as the World Health Organization Definition of MI.

ID-TLR: ischemia-driven target lesion revascularization; MI: myocardial infarction; NA: not applicable; ULN: upper limit of normal

Table 2A. Assessment of Risk of Bias for Randomized Controlled Trials

Trial	Random sequence generation	Allocation concealment	Blinding of participants	Blinding of outcome assessment	Incomplete outcome data	Selective outcome reporting	Sample size calculation	Sponsor
ABSORB II	IWRS	Yes	Yes	Yes (independent CEC)	Yes	No	Yes	Industry
ABSORB III	IWRS	Yes	Yes	Yes (independent CEC)	Yes	No	Yes	Industry
ABSORB Japan	IWRS	Yes	Yes	Yes (independent CEC)	Yes	No	Yes	Industry
ABSORB China	IWRS	Yes	No	Yes (independent CEC)	Yes	No	Yes	Industry
AIDA	IWRS	Yes	Yes	Yes (independent CEC)	Yes	No	Yes	Investigator
TROFI II	IWRS	Yes	No	Yes (independent CEC)	Yes	No	Yes	Investigator
EVERBIO II	IWRS	Yes	Yes	Yes (independent CEC)	Yes	No	Yes	Investigator

CEC: clinical event committee; IWRS: interactive web-based response system

Study	Selection	Comparability on basis of design and analysis	Outcome
Imori et al.	****	*	***
BVS Examination	****	*	***
BVS Expand	****	*	***

Table 2B. New Castle-Ottawa scale for case-control studies

Score of nine is maximum score (= lowest risk of bias)

29

CHAPTER

MID-TERM CCTA RESULTS FOR ABSORB BIORESORBABLE VASCULAR SCAFFOLD IN CLINICAL PRACTICE - A BVS EXPAND PROJECT

Cordula Felix, Haroun. El Addouli, Adriaan. Coenen, Marissa M. Lubbers, Yoshinobu. Onuma, **Jiang Ming Fam**, Evelyn Regar, Roberto. Diletti, Felix Zijlstra, Ricardo PJ Budde, Koen Nieman, Robert-Jan.M. van Geuns.

Submitted for publication.

Mid-term CCTA Results for ABSORB Bioresorbable Vascular Scaffold in clinical practice- A BVS EXPAND project

C.M. Felix[1], MD; H. El Addouli[1], MD; A. Coenen[1, 2], MD; M.M. Lubbers[1], MD; Y. Onuma[1], MD, PhD; JM Fam[1,5], MD; E. S. Regar[1], MD, PhD; R. Diletti[1], MD, PhD; F. Zijlstra[1], MD, PhD; RPJ Budde[1], MD, PhD; K. Nieman[1,3], MD, PhD; R.J.M. van Geuns[1, 4], MD, PhD

[1] Thoraxcenter, Erasmus MC, Rotterdam, the Netherlands
[2] Department of Radiology, Erasmus MC, Rotterdam, the Netherlands
[3] Departments of Cardiovascular Medicine and Radiology, Stanford University, School of Medicine, Stanford, CA, USA
[4]Department of Cardiology, Radboud UMC, Nijmegen, the Netherlands
[5]Department of Cardiology, National Heart Centre Singapore, Singapore

Abbreviated title: Mid-term CCTA outcomes of the ABSORB BVS. A BVS Expand project

Total word count: 4975

Corresponding author

Prof. dr. Robert Jan M. van Geuns MD, PhD

Thoraxcenter, Room Ba585, Erasmus Medical Centre

's-Gravendijkwal 230

3015 CE Rotterdam, the Netherlands

Tel.: +31 10 4635260

Fax: +31 10 4369154

E-mail address: r.vangeuns@erasmusmc.nl

Aim: To evaluate the mid-term coronary computed tomography angiography (CCTA) outcomes of the Absorb bioresorbable vascular scaffold (BVS) by non-invasive CT imaging in combination with CT perfusion.

Methods: BVS-EXPAND, a single-centre study includes selected, real-world patients. Complex lesions such as bifurcation and long lesions were not excluded. Eighteen to 24 months after index procedure, consecutive suitable patients underwent CT. Main exclusion criteria were: contrast medium allergy, severe renal insufficiency, TLR before CCTA. Additional CT perfusion was performed when a significant non-occlusive stenosis (> 50%) in the target lesion was identified on CCTA. CT-defined BVS success was defined as: stenosis< 50% on CCTA or CT perfusion without perfusion deficits.

Results: The CCTA cohort consisted of 164 patients. CCTA's were assessable in 160 patients with 215 lesions and within that group, rate of BVS patency was 98.6% of the lesions. CT perfusion was necessary in 9 patients (lesions) with degree of stenosis > 50% and ruled out functionally significant restenosis in five. CT-defined BVS success was achieved in 207 lesions (96.7%); CT-derived failure occurred in 7 lesions (3.3%). Complete quantitative CCTA measures were available in 144 patients with in-scaffold MLA of 4.16 (± 1.67) mm^2, % area stenosis 10.32 ± 32.11%. Post-CCTA follow-up with a median of 679 (IQR: 448-746.50) days, identified three TLR cases. No TLR occurred in CT-defined BVS success cases.

Conclusions: CCTA was able to evaluate most BVS treated patients at mid-term follow-up, where additional perfusion imaging was a valuable addition, needed only in a small group of patients.

Key words: BVS, CCTA, PCI, follow-up

ABBREVIATIONS AND ACRONYMS

BVS	Bioresorbable vascular scaffold
CAD	Coronary artery disease
CCTA	Coronary computed tomography angiography
DES	Drug-eluting stent
ICA	Invasive coronary angiography
FFR	Fractional flow reserve
MLA	Minimal lumen area
PCI	Percutaneous coronary intervention
RVA	Reference vessel area
ScT	Scaffold thrombosis
TLR	Target lesion revascularization

1. Introduction

Currently, percutaneous coronary intervention (PCI) with drug-eluting stents (DES) is the gold standard for the treatment of coronary artery disease (CAD). In comparison with balloon angioplasty alone or PCI using bare metal stents (BMS), PCI with DES drastically decreased the rate of restenosis and revascularization. However on the long-term, DES with their permanent presence of foreign material are not devoid of drawbacks and have a stable average rate of reintervention of 2-4% after the first year. (1,2) In an attempt to eliminate the potential (late) limitations of DES (neoatherosclerosis, very late stent thrombosis), bioresorbable scaffolds have been developed. The concept consists of a temporary device that restores the blood flow and temporally supports the vessel but that will fully resorb over time. The bioresorbable device most intensely investigated, is the ABSORB bioresorbable vascular scaffold (BVS. Abbott vascular, Santa Clara, CA, USA), which received both CE mark and FDA approval. It is a fully resorbable everolimus-eluting device made of a poly-L-lactide backbone with a poly-D, L-lactide coating. With the exception of two platinum markers at each end of the scaffold, this device is radiolucent and therefore does not interfere with non-invasive computed tomography of the coronary arteries. This is in contrast to metal stents, which cause blooming artefacts with subsequent hampering of luminal assessment. (3) Recently, mid-term outcomes RCTs that compared BVS with Xience, a second generation everolimus eluting metal DES, showed that the BVS was associated with worse outcomes.(4) (5-7) These results were mainly driven by early scaffold thrombosis, triggered by the relatively thick struts of the first generation. Development of thin strut BVS is complex and expensive which first requires positive signals from long-term imaging and clinical follow-up.

Coronary computed tomography angiography (CCTA) could be such a technology and greatly improved over the last 20 years with an important increase in spatial and temporal resolution. The enhancement in CT technology enabled a reliable visualisation of the vessel lumen and also detection of significant coronary lesions.

A study by Collet and colleagues investigated the diagnostic accuracy of CCTA in ABSORB II and reported that accuracy regarding identification of presence and severity of obstructive CAD was similar between CCTA and coronary angiography at three years of follow-up. (8)

The aim of our study was to report mid-term CCTA outcomes to describe the mid-term performance of the Absorb BVS in more complex coronary lesions when examined by means of CCTA.

2. Methods

2.1 Population

The BVS Expand registry is an investigator-initiated, prospective, single-centre, single-arm study performed in an experienced, tertiary PCI centre. In- and exclusion criteria have been described elsewhere. (9) In brief, patients presenting with NSTEMI, stable or unstable angina (UA), or silent ischemia caused by a *de novo* stenotic lesion in a native coronary artery treated with a BVS were included. Main exclusion criteria were patients with a history of coronary bypass grafting (CABG), presentation with ST-elevation myocardial infarction (STEMI) and patients with expected survival of less than one year. Complex lesions such as bifurcation, calcified (as assessed by angiography), long and thrombotic lesions were not excluded. As per hospital policy patients with a previously implanted metal DES in the intended target vessel were

also excluded. Also, although old age was not an exclusion criterion, BVS were in general reserved for younger patients, and left to operator's interpretation of biological age.

For hospital quality control purposes of this new technique within the field of interventional cardiology, CCTA at mid-term follow-up (between 18 months and two years) was offered to all consecutive suitable patients. Exclusion criteria for undergoing a CCTA were contrast medium allergy, severe renal insufficiency, target lesion revascularization (TLR) performed before CCTA, severe calcification and patients who underwent cardiac imaging during the same time point.

2.2 Ethics

This is an observational study, performed according to the privacy policy of the Erasmus MC, and to the Erasmus MC regulations for the appropriate use of data in patient-oriented research, which are based on international regulations, including the declaration of Helsinki. Approval of the ethical board of the Erasmus MC was obtained. All patients undergoing clinical follow-up provided written informed consent for the PCI and to be contacted regularly during the follow-up period of the study.

2.3 Procedure

PCI was performed according to current clinical practice standards. The radial or femoral routes were the principal routes of vascular access and 6 or 7 French catheters were used depending on the discretion of the operator. Pre-dilatation and post dilation were recommended with a balloon shorter than the planned study device length and with a non-compliant balloon without overexpanding the scaffold beyond its limits of expansion (0.5mm > nominal diameter) respectively. Intravascular imaging with the use of Intravascular Ultrasound (IVUS) or Optical

Coherence Tomography (OCT) was used for pre-procedural sizing and optimization of stent deployment on the discretion of the operator.

2.4 Angiographic analysis

Baseline quantitative Coronary Analysis (QCA) was performed by a total of three different independent investigators. Coronary angiograms were analysed with the CAAS 5.10 QCA software (Pie Medical BV, Maastricht, the Netherlands). The QCA measurements provided reference vessel diameter (RVD), percentage diameter stenosis and minimal lumen diameter (MLD).

2.5 CCTA

Second and third-generation dual source CT scanners (SOMATOM Definition Flash and SOMATOM Force, Siemens Medical Solutions, Forchheim, Germany) were used. Standard acquisition techniques for coronary techniques were used: Sublingual nitroglycerin was given to all patients. Beta-blockers were optional in patients with a fast heart rate.

A prospective electrocardiographically triggered axial scan mode was used, with an exposure window during diastole and/or systole depending on the heart rate. Tube current and tube voltage were selected semi-automatically on the basis of body size. For CTA imaging, a contrast bolus of approximately 50 to 60 ml (depending on iodine concentration and expected scan duration) was injected, followed by a saline bolus chaser. Images were reconstructed with a medium smooth kernel (B26, Bv40) and a slice thickness of 0.5-0.7 mm at 5% intervals of the acquired R-R segment. (10)

Scaffold patency was described as a scaffolded tract with a visible lumen and the possibility to evaluate contrast attenuation. First and according to normal practice, the CCTA was evaluated by a radiologist. Lesions were then divided into three groups: no abnormalities identified in target lesion, abnormalities seen but non-significant, significant stenosis (suspected) or total occlusion.

CT perfusion

Experienced CT readers (KN or RB) evaluated the CT angiograms, using PCI procedural information on BVS sizes and location but blinded to all other modalities. They set indication for any additional CT myocardial perfusion scans in case of a significant, non-occlusive stenosis on CCTA. This CT myocardial perfusion scan was performed in a separate session.

The dynamic CT myocardial perfusion scan was performed to further determine the functional significance of a morphological significant stenosis detected on CCTA. In a dynamic CT myocardial perfusion scan a series of acquisitions is made during the first pass of a contrast bolus, while the patient is in a hyperaemia state. After 3 min of adenosine infusion (at 140 μg/kg/min) the dynamic CT myocardial perfusion scan was started. Fifty ml of contrast medium (Ultravist, 370 mgI/ml; Bayer, Berlin, Germany) was injected at 6 ml/s, followed by a saline bolus of 40 ml. A shuttle mode was used to cover the left ventricle acquiring images in alternating cranial and caudal table positions. CT dynamic myocardial perfusion acquisition was started 5 seconds after the start of the contrast medium injection and patients were asked to hold their breath during the entire acquisition (30-35 seconds) (10,11). The change in attenuation of the myocardium due to the first pass of the contrast bolus was used to compute myocardial blood flow maps using a hybrid deconvolution model. A functionally significant coronary (re)stenosis would result in a reduction of the myocardial blood flow in the associated myocardial territory

(12). By visual inspection, the myocardial blood flow maps in combination with the CTA potential ischemia causing (re)stenosis of the BVS were identified by an expert CCTA reader (KN).

Quantitative CCTA analysis

In a subgroup of patients, quantitative data of the lesion of interest were analysed off-line by a radiologist on a dedicated workstation using commercially available software Syngo.Via (Siemens, Forchheim, Germany) to perform a quantitative CTA analysis. The optimal imaging phase and the centre lumen line through the treated vessel was automatically selected by the software and manually adjusted when needed. Cross-sections of the vessel were reconstructed, extending approximately 5 mm beyond the device (proximal and distal segments), using the platinum scaffold markers as landmarks. Every BVS was evaluated at three locations: 1. the proximal scaffold segment (defined as the segment extending from the platinum marker to five mm proximal to the marker, was evaluated first by using Syngo.Via to detect the minimal lumen and to determine the lumen areas. An automatic tracer was used and in case of insufficient contrast lumen opacification, it was manually adjusted; 2. the distal scaffold segment (defined as the segment extending from the platinum marker to five mm distal to the marker), was evaluated in the same fashion; 3. the minimal scaffold lumen was assessed by visually selecting the minimal lumen area inside the scaffold (**Figure 1**). At each location the cross-sectional lumen area surface was measured. If multiple overlapping scaffolds were inserted, they were considered as one lesion; if none were overlapping, they were considered as separate. Reference vessel area was calculated as the average of the proximal and distal lumen reference area segments. The lumen area stenosis was calculated as follows: reference lumen area minus the minimal lumen area as a percentage of reference lumen area. In case of a bifurcation lesion with

a large side branch elucidating a significant step down, the reference lumen diameter was based on measures of the distal end only.

Quantitative CTA analysis could not (completely) be performed in case of poor image quality (motion artefacts, insufficient contrast lumen opacification), ostial lesion, too small vessel calibre and total occlusion.

2.6 Follow-up.

Follow-up information specific for hospitalization and cardiovascular events was obtained through questionnaires or telephone interviews after different time points (1 month, 6 months, 1, 2, 3 and in the end: 4 and 5 years). If needed, medical records or discharge letters from other hospitals were requested. Events were adjudicated by an independent clinical events committee (CEC). All information concerning baseline characteristics and follow-up was gathered in a clinical data management system.

2.7 Definitions

CCTA feasibility was the percentage of patients with sufficient image quality to assess the target lesion on CCTA. BVS patency was defined as an open vessel at the site of BVS implantation. CT-defined BVS success was described as no stenosis of target lesion, diameter stenosis of < 50% on CCTA or (possible) stenosis of ≥ 50% but with normal additional perfusion CT myocardial perfusion scan. CT-defined BVS failure was defined as stenosis ≥ 50% on CCTA combined with perfusion deficits during perfusion CT or complete occlusion on CCTA. Definitions of events were as described before. (9)

2.8 Statistical analysis

Categorical variables are reported as counts and percentages, continuous variables as mean ± standard deviation. Quantitative CCTA measures are described as median with interquartile range (IQR). The cumulative incidence of adverse events was estimated according to the Kaplan-Meier method. Patients lost to follow-up were considered at risk until the date of last contact, at which point they were censored. All statistical tests were two-sided and the P value of < 0.05 was considered statistically significant. Statistical analyses were performed using SPSS, version 21 (IL, US).

3. Results

After applying the exclusion criteria, 195 consecutive patients were invited as suitable for follow-up CCTA, of which 164 accepted the offer. In four patients, poor CCTA quality made any image assessment impossible and thus 160 patients with 215 lesions remained for analysis (**Figure 2**). In one lesion, patency was assessable but detailed information of degree of stenosis could not be provided.

Figure 3 is an example of a patient with two sequential lesions in the RCA treated with two 28 mm long overlapping BVS with excellent acute outcome. Follow-up CCTA identified an excellent result, even at the location of the overlap.

3.1 Baseline characteristics

Table 1 summarizes baseline characteristics of patients, lesions and certain procedural factors of the whole CCTA cohort (n=160). Mean age was 59.9 ±10.0 years, 76.3% were male, 11.9% diabetics and 60.0 % presented with ACS.

The LAD was the coronary artery most frequently treated (53.2%). AHA/ ACC lesion type B2/ C was present in 37.2%, bifurcation in 22.5%, calcification (moderate or severe on angiography) in 39.0%. Pre-dilatation was performed in almost 90%, with a balloon to artery ratio of 1.07. Intravascular imaging using OCT or IVUS was carried out in 58%. Post-dilatation was performed in 51.8% with a maximum post-dilatation balloon inflation pressure of 15.5 (±3.24) atm. Post-procedural MLD was 2.3 (±0.4) mm, post-procedural % diameter stenosis was 16.5 (±9.3) %.

3.2 CCTA

Median duration from index procedure until CCTA was 714 (IQR: 639 – 754) days. See **Table 2** for median dose length product (DLP) and effective dose.

When assessed by CCTA, in 98.6 % of the 215 lesions BVS patency was achieved. In one lesion, degree of stenosis could not be assessed.

In 154/ 214 lesions (72%) no target lesion abnormalities were seen on CCTA. In 53 lesions (24.7%) some non-significant changes, representing minor neo-intima hyperplasia, were seen. In 12 lesions (5.6%, 12 patients) an anatomical significant stenosis of the target lesion was reported. Three of them showed total occlusion.

3.3 CT Perfusion

In four patients, BVS failure was identified by additional CT perfusion. **Figure 4** demonstrates an example of a patient with two BVS (2.5*28mm) in the LAD for spontaneous coronary artery dissection. CCTA showed ISR at level of the second scaffold and the additional CT perfusion

revealed a small area of ischemia. Therefore, CT-defined BVS success was 96.7% of the lesions (**Figure 2**).

Two patients were subsequently treated by PCI. The other patients were initially treated conservatively, of whom one was treated through PCI during follow-up (> two years post-CCTA). However, during this re-intervention, only a non-target vessel was treated. FFR of the target-vessel was negative and the BVS was patent. In patients who did not have anatomically or functionally significant stenosis, no events occurred during follow-up.

3.4 Quantitative CCTA

Complete quantitative analysis was available in a subgroup of 144/160 patients with 194 lesions (**Table 3**). Quantitative analysis of the lesion was not possible in case of the presence of total occlusion (n= 3 patients), vessel calibre of too small diameter (n=3), too much calcification (n=3), insufficient amount of contrast (n=4) or moving artefacts (n=8).

In-scaffold minimal lumen area was 4.16 ± 1.67 mm^2. In-scaffold percentage area stenosis was 10.32 ± 32.11. In-segment area stenosis was 30.60 ± 25.24 %. Lesions that showed significant abnormalities on CCTA had smaller but non-significant reference areas: 4.28 vs 5.78 mm^2, p=0.69. Out of the seven patients with CT-defined BVS failure, five had MLD < 2.4 mm at baseline. Patients with a suboptimal result post-PCI (MLD <2.4 mm), showed smaller MLA during follow-up CT: 3.88 vs 4.69 mm^2 (p=0.03).

3.5 Clinical outcomes

Clinical outcomes (reported as Kaplan-Meier estimates) are described in **Table 4**. Median duration of follow-up after baseline PCI was 1456.50 (IQR: 1098.25 – 1472.50) days and follow-

up of at least three years post-PCI was available in 85.6%. We focussed on events that took place after CCTA and up to three years after baseline PCI. Those event rates were as follows: rate of death was 0.7% (one patient, non-cardiac cause); rate of MI was 0% and TLR rate was 3.5%. There were no cases of scaffold thrombosis. In three patients, TLR occurred after CCTA

4. Discussion

In this sub-cohort of the BVS Expand registry, we have reported on the mid-term CCTA and clinical outcomes of patients treated with the ABSORB BVS for a variety of lesion complexity. The main findings were as follows: 1) CCTA was a successful tool to establish non-invasively CT-derived BVS success at mid-term follow-up in almost all patients including more complex. 2). Additional CT perfusion imaging provides important functional information in moderate or severe restenotic lesions. 3) Non-clinical CT-derived BVS failure is a rare event. 4) Patients with CT-derived BVS success at mid-term, were free from thrombosis or TLR during follow-up after CT imaging.

Our study demonstrated that even in patients with more complex anatomy, CCTA could be routinely used to follow-up the patients after BRS implantation. Patency was 98.6% and the rate of adverse events after CT, was low. When compared to the ABSORB Cohort A and B studies in which CCTA was also performed (13,14), the percentage of calcification, longer lesion length and AHA/ ACC lesion classification type B2/C illustrates the higher complexity of our patient population. Polymeric BRS technology, through its radiolucency and complete resorption, could be very suitable for non-invasive follow-up. Evaluation of newly introduced technologies in medicine after initial approval is essential. Patients in routine practice differ importantly from patients studied in approval studies where success rates reported in first-in-man studies and RCT

including highly selected patients, are generally higher. Most post-approval investigator-initiated studies rely only on clinical follow-up specific protocols and, in the best case, independent event adjudication by experienced investigators. Invasive coronary angiography has been the objective standard to establish metallic stent patency and presence of in-stent restenosis. Due to the invasiveness, costs of angiography and excellent performance of second-generation DES, routine follow-up after index PCI by invasive coronary angiography (ICA) has disappeared from the spectrum. CCTA is a non-invasive image modality with a high sensitivity and relatively low specificity, particularly for identification of hemodynamically significant CAD. Evaluation of BVS using CCTA was described in several publications and appeared to have a high diagnostic accuracy. (8,13,15) (16) Our study lacked validation with angiography; however, a recent study concluded that the accuracy of the Absorb BVS to detect in-scaffold luminal obstruction, when angiography and IVUS were used as references, was high. (17)

Investigation of efficacy after local introduction of new technology with the best feasible techniques should be routine for every hospital. (18)

In our cohort, in only four patients image quality was not sufficient to assess scaffold patency, let alone severity of stenosis or even quantitative CT measures. Rate of patency and also mid-term CT-defined BVS success were high. Our study showed that when a CT perfusion was performed, perfusion deficits were seen in approximately 50% of the cases. The advantage of CT perfusion is the possibility to perform it on-site and in the same session as CCTA. CT perfusion improves the performance of CCTA in the identification of functionally significant CAD and also improves specificity. (10,19)

In order to discriminate between lesions that are hemodynamically significant and those who are not and with the aim of diminishing unnecessary referrals for ICA, physiological assessment of the target lesion is of importance. One of the possibilities is by using quantitative vessel analysis (20) or MR perfusion(21) and CT-derived fractional flow reserve (FFR_{CT}).(10,19) Quantitative CTA analysis improved specificity from 41% - 76% for percentage area stenosis (22) and accuracy from 49% - 71% for percentage diameter stenosis. (20)

FFR_{CT} has been advocated as additional technology to improve specificity of CCTA, revealing good diagnostic accuracy. (23) Several studies have investigated FFR_{CT}. (19,24-27) Currently, the HeartFlow FFR_{CT} is the only the FDA-approved CCTA derived FFR platform, which can be used off-site only and at significant costs. As so, we selected CT perfusion for our research.

Post-CCTA adverse events up to three years after baseline PCI occurred in only three patients. In all of the other patients, no adverse events of the target lesion were reported after CCTA was performed and therefore this appeared as a rare event. In comparison to other mid-term clinical results (28), outcomes at three years are good with a low rate of death and no cases of ScT.

Findings of our study show that CCTA is feasible in patients treated with Absorb BVS, which can be useful information also for other bioresorbable devices, as the current generation BVS has been taken out of the market.

5. Conclusion

CCTA was able to evaluate most BVS-treated patients at mid-term follow-up. Rates of patency and CT-defined BVS success were high. Additional perfusion imaging was a valuable addition, needed only in a small group of patients. Clinical outcomes at three years were promising without cases of scaffold thrombosis and no TLR post-CT when CCTA results were good.

6. Limitations

The size of our CCTA cohort was relatively limited. There might have been selection bias at the moment patients were included in the CCTA cohort. Quantitative assessment was not possible in all of the patients. Variations in image quality occurred due to calcification and platinum markers causing blooming, motion artefacts. Lastly, there was no validation with angiography or intravascular imaging.

Figures and figure legends

1) Example QCT measurement

2) Flowchart of the study

3) Case 1

Figure 3 A 53-year old female patient presented with an anterior STEMI based on an intramural haematoma. (A) For TIMI I flow, initial balloon angioplasty did not result in stable TIMI III flow due to acute recoil for which two overlapping 2.5 x 28 mm BVS scaffolds were implanted (B). Follow-up CTCA (C and D for 3D image) showed a well patent proximal scaffold with minimal contrast in the distal scaffold suggestive for scaffold failure. CT-perfusion (E) demonstrated localised ischemia in the territory of the distal LAD. Subsequent angiography (F) confirmed target lesion failure, mainly due to late recoil and minimal neo-intima on IVUS which was successfully treated with balloon angioplasty only. Subsequent follow-up for one year was without recurrent events.

4) Case 2

Figure 4 is an example of a successful case. It concerns a 40-year old male, smoking patient with diabetes, dyslipidaemia and a positive family history for CAD. He presented with NSTEMI due to two-vessel disease of the RCA (A) and LAD. The RCA was treated with pre-dilatation, BVS (2x 3.5*28) and post-dilatation (B) The LAD showed a positive FFR (0.75) and one 2.5*18mm BVS was implanted, followed by post-dilatation. He underwent his CCTA 861 days after baseline PCI and all BVS were patent without signs of stenosis (See C for CCTA result of RCA during follow-up).

Tables

1 Baseline characteristics (patient, lesion and procedural)

2 CCTA (perfusion) acquisitions

3 Quantitative CCTA assessments

4 Post-CCTA clinical outcomes, described as Kaplan-Meier estimates

Figure 1

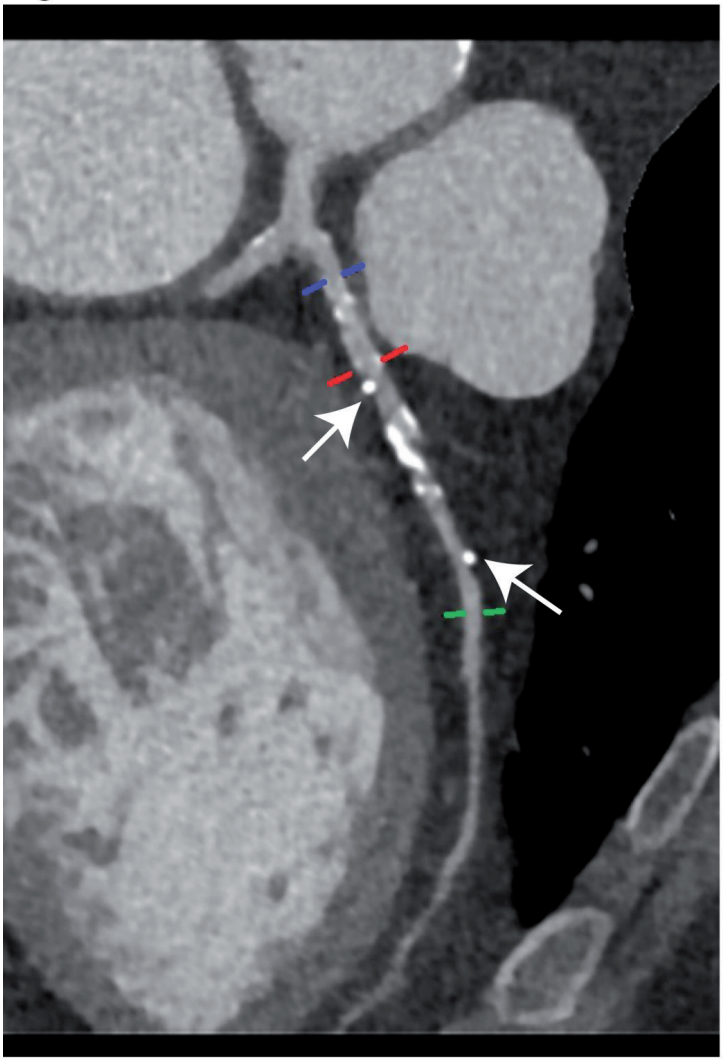

Example of a normal QCT measurement: the blue line shows the proximal reference (5 mm distance from scaffold), the red line indicates the proximal scaffold border (0.3mm distance from proximal scaffold edge). The green line is the distal reference. The white arrows indicate the two pairs of platinum scaffold markers.

Figure 2. Flowchart

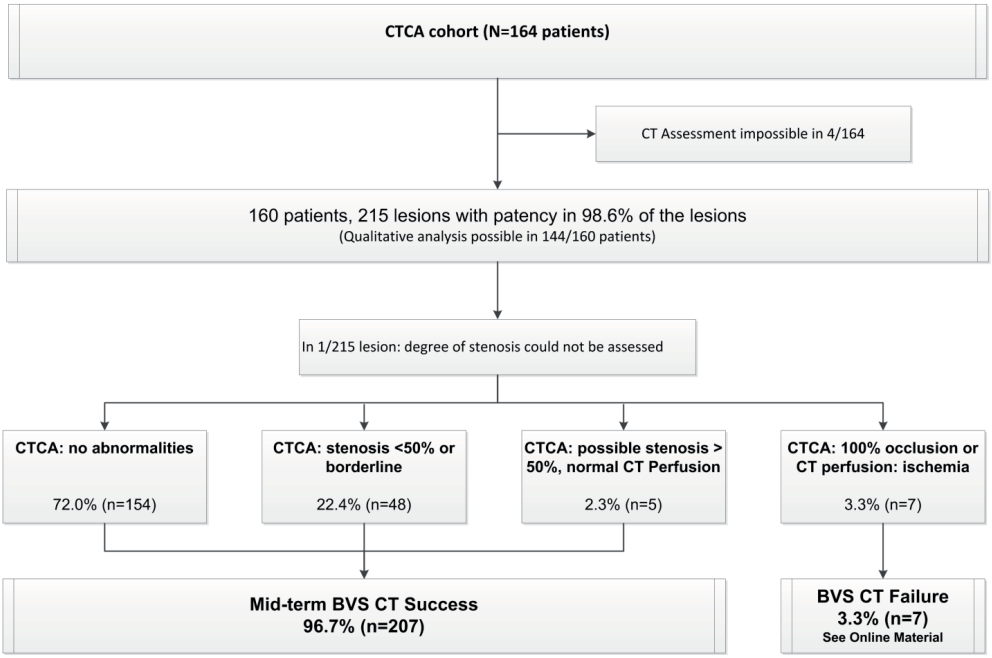

Figure 3

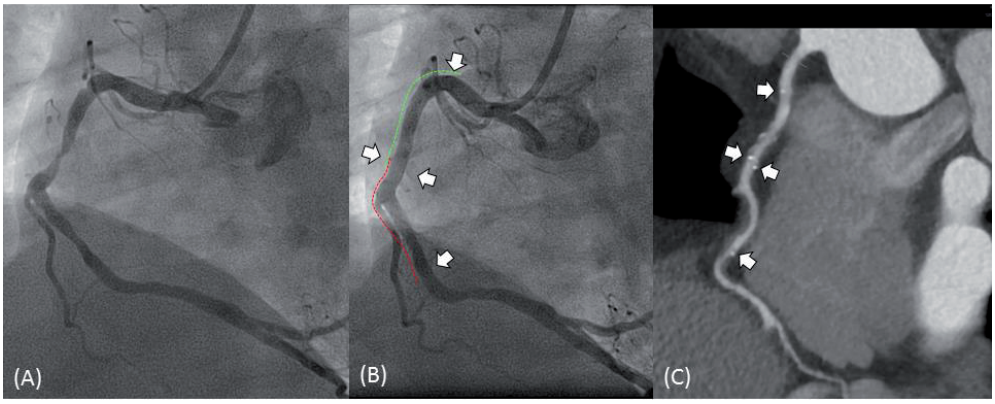

Figure 4

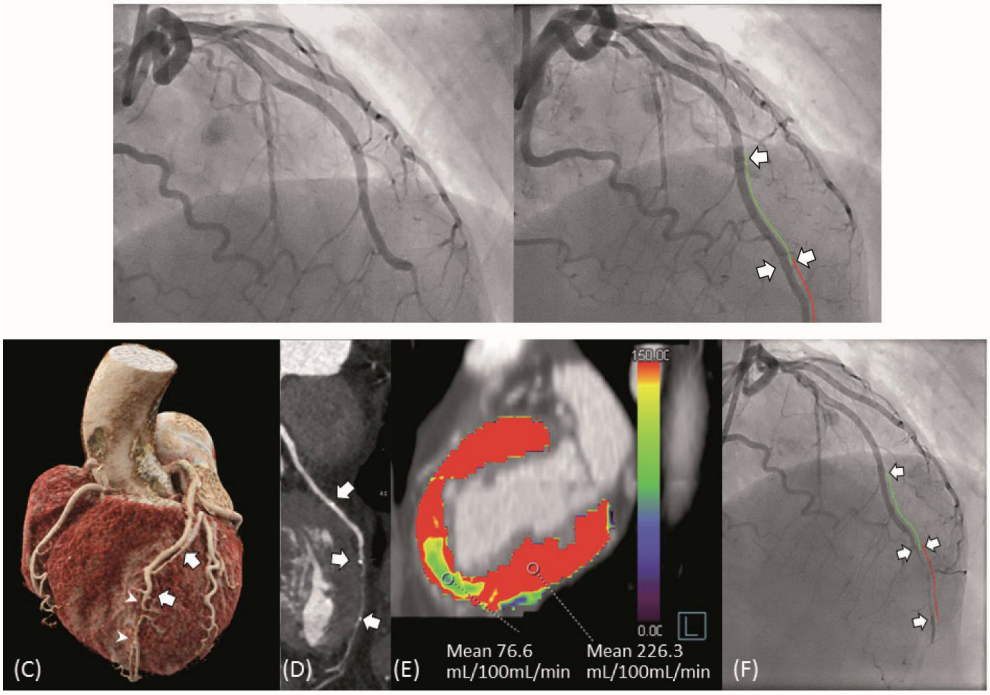

Table 1. Baseline characteristics

Patient (n=160)	
Age (mean ± SD), years	59.86 (±10.0)
Male gender, %	76.3
Diabetes mellitus, %	11.9
Current smoker, %	33.8
Dyslipidaemia, %	51.9
Hypertension, %	55.0
Family history of CAD, %	46.9
Prior myocardial infarction, %	17.5
Prior PCI, %	10.6
Presentation with ACS, %	60.0
Lesion (n= 215 lesions)	
Treated vessel , %	
LAD	53.2
LCX	22.5
RCA	24.3
AHA/ ACC lesion classification type B2 /C, %	37.2
Calcification	39.0
Bifurcation	22.5
CTO	4.1
Procedure	
Pre-dilatation (%)	89.4

Max pre-dilation balloon diameter (mean ± SD), mm	2.62 (±0.39)
Pre-dilation balloon: artery ratio	1.07 (±0.23)
Post-dilatation (%)	51.8
Maximum post-dilatation inflation pressure (mean ± SD), atm	15.50 (±3.24)
Intravascular imaging (%)	58.1
Pre-procedural RVD (mean ± SD), mm	2.54 (±0.47)
Post-procedural MLD (mean ± SD), mm	2.30 (±0.40)
Post-procedural diameter stenosis, %	16.54 (±9.25)
Lesion length (mean ± SD), mm	23.97 (±13.10)

CAD: coronary artery disease, CTO: chronic total occlusion, MLD: minimum lumen diameter, PCI: percutaneous coronary intervention, RVD: reference vessel diameter. Values are mean (±SD) or median (interquartile range)

Table 2. CCTA (perfusion) acquisition

CCTA (n= 160)	
CTDIvol (mGy)	19.52 (13.36 – 35.17)
DLP (mGy-cm)	288.15 (186.15 – 473.55)
Radiation effective dose (mSv)	4.09 (2.63 – 6.73)
CT perfusion (n = 9)	
CTDIvol (mGy)	37.24 (25.00 – 45.06)
DLP (mGy-cm)	338.10 (238.93 – 441.83)
Radiation effective dose (mSv)	5.51 (3.70 – 6.44)
Tube voltage (KV)	70 (70 – 70)

CCTA: Computed tomography coronary angiography, CTDI: CT dose index, DLP: dose length product. Values expressed as median (interquartile range)

Table 3. Quantitative CCTA Assessment

In-scaffold, mm^2	
Minimal lumen area (mean ± SD)	4.16 ± 1.67
Median reference area (mean ± SD)	5.04 ± 2.10
Area stenosis, % (mean ± SD)	10.32 ± 32.11
In-segment, mm^2	
Area stenosis, % (mean ± SD)	30.60 ± 25.24

Values described as mean ± standard deviation (SD) or median (interquartile range [IQR])

Table 4. Clinical outcomes Post-CCTA, described as Kaplan-Meier estimates (n =160 patients)

Death, % (n)	0.7 (1)
Cardiac death, % (n)	0.0 (0)
Myocardial infarction, % (n)	0.0 (0)
Target lesion revascularization % (n)	3.5 (3)
Target vessel revascularization, % (n)	3.5 (3)
Non-target vessel revascularization, % (n)	2.8 (4)
Definite/ probable scaffold thrombosis, % (n)	0.0 (0)

References

1. Vlachojannis GJ, Smits PC, Hofma SH et al. Biodegradable Polymer Biolimus-Eluting Stents Versus Durable Polymer Everolimus-Eluting Stents in Patients With Coronary Artery Disease: Final 5-Year Report From the COMPARE II Trial (Abluminal Biodegradable Polymer Biolimus-Eluting Stent Versus Durable Polymer Everolimus-Eluting Stent). JACC Cardiovasc Interv 2017;10:1215-1221.
2. Taniwaki M, Stefanini GG, Silber S et al. 4-year clinical outcomes and predictors of repeat revascularization in patients treated with new-generation drug-eluting stents: a report from the RESOLUTE All-Comers trial (A Randomized Comparison of a Zotarolimus-Eluting Stent With an Everolimus-Eluting Stent for Percutaneous Coronary Intervention). J Am Coll Cardiol 2014;63:1617-25.
3. Tanabe K, Popma JJ, Kozuma K et al. Multi-slice Computed Tomography Assessment of Everolimus-Eluting Absorb Bioresorbable Scaffold in Comparison with Metallic Drug-Eluting Stents from the ABSORB Japan randomized Trial. EuroIntervention 2017.
4. Wykrzykowska JJ, Kraak RP, Hofma SH et al. Bioresorbable Scaffolds versus Metallic Stents in Routine PCI. N Engl J Med 2017;376:2319-2328.
5. Chevalier B, Cequier A, Dudek D et al. Four-year follow-up of the randomised comparison between an everolimus-eluting bioresorbable scaffold and an everolimus-eluting metallic stent for the treatment of coronary artery stenosis (ABSORB II trial). EuroIntervention 2017.
6. Kereiakes DJ, Ellis SG, Metzger C et al. 3-Year Clinical Outcomes With Everolimus-Eluting Bioresorbable Coronary Scaffolds: The ABSORB III Trial. J Am Coll Cardiol 2017.
7. Ali ZA, Gao RF, Kimura T et al. Three-Year Outcomes With the Absorb Bioresorbable Scaffold: Individual-Patient-Data Meta-Analysis From the ABSORB Randomized Trials. Circulation 2017.
8. Collet C, Sotomi Y, Cavalcante R et al. Accuracy of coronary computed tomography angiography for bioresorbable scaffold luminal investigation: a comparison with optical coherence tomography. Int J Cardiovasc Imaging 2017;33:431-439.
9. Felix CM, Fam JM, Diletti R et al. Mid- to Long-Term Clinical Outcomes of Patients Treated With the Everolimus-Eluting Bioresorbable Vascular Scaffold: The BVS Expand Registry. JACC Cardiovasc Interv 2016.
10. Coenen A, Rossi A, Lubbers MM et al. Integrating CT Myocardial Perfusion and CT-FFR in the Work-Up of Coronary Artery Disease. JACC Cardiovasc Imaging 2017;10:760-770.
11. Bamberg F, Klotz E, Flohr T et al. Dynamic myocardial stress perfusion imaging using fast dual-source CT with alternating table positions: initial experience. European radiology 2010;20:1168-73.
12. Rossi A, Merkus D, Klotz E, Mollet N, de Feyter PJ, Krestin GP. Stress myocardial perfusion: imaging with multidetector CT. Radiology 2014;270:25-46.
13. Onuma Y, Collet C, van Geuns RJ et al. Long-term serial non-invasive multislice computed tomography angiography with functional evaluation after coronary implantation of a bioresorbable everolimus-eluting scaffold: the ABSORB cohort B MSCT substudy. Eur Heart J Cardiovasc Imaging 2017.
14. Onuma Y, Dudek D, Thuesen L et al. Five-year clinical and functional multislice computed tomography angiographic results after coronary implantation of the fully resorbable polymeric everolimus-eluting scaffold in patients with de novo coronary artery disease: the ABSORB cohort A trial. JACC Cardiovasc Interv 2013;6:999-1009.
15. Nieman K, Serruys PW, Onuma Y et al. Multislice computed tomography angiography for noninvasive assessment of the 18-month performance of a novel radiolucent bioresorbable

vascular scaffolding device: the ABSORB trial (a clinical evaluation of the bioabsorbable everolimus eluting coronary stent system in the treatment of patients with de novo native coronary artery lesions). J Am Coll Cardiol 2013;62:1813-4.
16. Regazzoli D, Latib A, Tanaka A et al. Is Multislice Computed Tomography a Feasible Option for Follow-Up of Complex Coronary Lesions Treated With Bioresorbable Scaffolds? JACC Cardiovasc Interv 2016;9:2578-2581.
17. Collet C, Chevalier B, Cequier A et al. Diagnostic Accuracy of Coronary CT Angiography for the Evaluation of Bioresorbable Vascular Scaffolds. JACC Cardiovasc Imaging 2017.
18. Everaert B, Wykrzykowska JJ, Koolen J et al. Recommendations for the use of bioresorbable vascular scaffolds in percutaneous coronary interventions : 2017 revision. Neth Heart J 2017.
19. Coenen A, Lubbers MM, Kurata A et al. Fractional flow reserve computed from noninvasive CT angiography data: diagnostic performance of an on-site clinician-operated computational fluid dynamics algorithm. Radiology 2015;274:674-83.
20. Meijboom WB, Van Mieghem CA, van Pelt N et al. Comprehensive assessment of coronary artery stenoses: computed tomography coronary angiography versus conventional coronary angiography and correlation with fractional flow reserve in patients with stable angina. J Am Coll Cardiol 2008;52:636-43.
21. Kirschbaum SW, Nieman K, Springeling T et al. Non-invasive diagnostic workup of patients with suspected stable angina by combined computed tomography coronary angiography and magnetic resonance perfusion imaging. Circ J 2011;75:1678-84.
22. Rossi A, Papadopoulou SL, Pugliese F et al. Quantitative computed tomographic coronary angiography: does it predict functionally significant coronary stenoses? Circ Cardiovasc Imaging 2014;7:43-51.
23. Tesche C, De Cecco CN, Albrecht MH et al. Coronary CT Angiography-derived Fractional Flow Reserve. Radiology 2017;285:17-33.
24. Curzen NP, Nolan J, Zaman AG, Norgaard BL, Rajani R. Does the Routine Availability of CT-Derived FFR Influence Management of Patients With Stable Chest Pain Compared to CT Angiography Alone?: The FFRCT RIPCORD Study. JACC Cardiovasc Imaging 2016;9:1188-1194.
25. Douglas PS, Pontone G, Hlatky MA et al. Clinical outcomes of fractional flow reserve by computed tomographic angiography-guided diagnostic strategies vs. usual care in patients with suspected coronary artery disease: the prospective longitudinal trial of FFR(CT): outcome and resource impacts study. Eur Heart J 2015;36:3359-67.
26. Hlatky MA, De Bruyne B, Pontone G et al. Quality-of-Life and Economic Outcomes of Assessing Fractional Flow Reserve With Computed Tomography Angiography: PLATFORM. J Am Coll Cardiol 2015;66:2315-2323.
27. Min JK, Leipsic J, Pencina MJ et al. Diagnostic accuracy of fractional flow reserve from anatomic CT angiography. Jama 2012;308:1237-45.
28. Anadol R, Lorenz L, Weissner M et al. Characteristics and outcome of patients with complex coronary lesions treated with bioresorbable scaffolds Three years follow-up in a cohort of consecutive patients. EuroIntervention 2017.

30

CHAPTER

SUMMARY AND CONCLUSION

SUMMARY AND CONCLUSION

This thesis aims to investigate the outcomes and limitations of DES with bioresorbable polymer or even completely bioresorbable stents (frequently referred to as scaffolds) in the different clinical scenarios and lesions subsets. In Part I, I first used a highly sensitive imaging modality which can be used to investigate specific clinical settings and procedural optimisation when new coronary devices are introduced. In Part II and III, I studied novel metallic stents for left main disease and implantation techniques for completely bioresorbable vascular scaffolds (BRS) using different surrogate endpoints. Finally in Part IV outcomes of BRS in larger clinical registries and specific lesion subsets were investigated.

PART 1. OPTICAL COHERENCE TOMOGRAPHY (OCT) FOR EVALUTATION OF NEW THERAPIES AND IN CLINICAL PRACTICE

Since the introduction of percutaneous coronary intervention (PCI), coronary angiography has been the standard tool for the assessment of the severity of coronary artery lesions and evaluation of the outcome of coronary stent implantation. OCT is a light-based intravascular imaging method that has the additional advantage by providing high resolution (5–15 μm) images of the vascular wall and intracoronary devices. The development of the second generation, frequency domain OCT allowed for a widespread implementation of this imaging modality in the clinical practice, by simplifying the procedure of image acquisition facilitating direct assessment of plaque and vessel morphology and the evaluation of the vessel wall response to stenting.

In Chapter 2, we showed in a prospective single registry study comparing 1142 OCT and 2476 IVUS procedures that OCT is as safe as IVUS in an unselected and heterogeneous groups of patients with varying clinical settings. In the following chapters, we describe the diverse clinical applications of OCT in PCI such as preprocedural sizing (Chapter 3) and

evaluation of acute device (BRS) performance after implantation (Chapter 4). In Chapter 4, OCT was used to evaluate the impact of calcium on acute expansion of BRS compared to metallic DES in coronary lesions of different degrees of calcification. We observed that with adequate lesion preparation, implantation of BRS in a population reflective of clinical practice, resulted in a similar luminal gain compared to DES as measured by OCT, regardless of the degree of angiographic calcification. The expansion of BRS was similar to that of DES (in terms of scaffold/stent area, lumen area and Percentage Residual Area Stenosis %RAS) but with higher eccentricity; and these findings were consistent across the calcification subgroups. Tissue prolapse was significantly higher in the DES compared to BRS; and incomplete strut apposition (ISA) was lower in the BRS group compared to DES, a difference observed mainly in moderately and heavily calcified lesions. In this section, we also described the roles OCT play in providing insights into the pathomechanisms of device thrombosis (Chapters 8-9) and the clinical applications of the use of OCT in grafts (Chapter 10). The relatively large vessel size of a venous graft may make accurate angiographic assessment, due to geometric distortion, difficult. OCT can provide high quality images of the vessel lumen with lumen area measurements obtained intraprocedure, allowing thorough preprocedural lesion assessment and proper selection of implantation strategy.

PART II. PERFORMANCE AND OUTCOMES OF NOVEL METALLIC STENTS FOR LEFT MAIN STENTING

With improvements made in interventional techniques and coronary stents, PCI has emerged as a safe option for revascularisation in selected patients with unprotected left main disease with good long term outcomes [1]. However key procedural challenges to achieve adequate stent expansion while maintaining minimal malapposition remain. The average diameter of a left main artery may reach over 5.5mm [2]. Since most contemporary DES are not provided

in suitable sizes for such anatomy and dimension, overexpansion with 2 common postdilatation techniques; Proximal Optimisation Technique (POT) and Final Kissing Balloon Dilation (FKBD) are widely performed to minimize stent malapposition. In Chapter 11, the overexpansion capabilities of contemporary DES (i.e. Synergy, Xience Xpedition, Ultimaster, Orsiro, Resolute Onyx and Biomatrix Alpha) were investigated in a bench testing study looking at the stent measurements obtained after the stents were deployed *in vitro* and further postdilated with a series of noncompliant 5.0mm and 6.0mm balloons in a stepwise manner. The study results emphasised the need for careful selection of stent size so as to avoid implanting stent sizes with too limited expansion capacity which may result in malapposition and overstretching of the stent. Although DES can be oversized, this does not imply it is safe to do so as overexpansion can induce changes in mechanical stiffness and drug delivery therefore altering the performance of the stents. In chapter 12, we showed 1) how in PCI involving relatively larger vessel diameters such as left main stenting, POT but not FKBD can safely expand the Synergy® platinum chromium 4.00mm stent beyond the overexpansion limit to 6.00mm with optimal stent apposition and performance and 2) why POT may be the technique of first choice to achieve optimal stent expansion in left main stenting. In addition, radial strength, which is a key factor in minimizing acute elastic recoil post stenting, was still maintained despite overexpansion.

In Chapter 13, we investigated the early clinical outcomes and stent performance using intravascular ultrasound (IVUS) of a dedicated Tryton® side branch stent in left main bifurcation stenting which showed that there were satisfactory angiographic and IVUS results at the main vessel at 6 months. Six-month angiographic late loss at the proximal and distal main vessel treated with DES was 0.28±0.41mm and 0.17±0.37mm respectively. In the side branch treated only with a BMS, angiographic late loss was 0.65±0.46mm. Using IVUS, minimal lumen area in the proximal left main vessel was stable (11.08 ± 1.97 mm^2 and 11.59

± 2.48 mm^2 at baseline and at 6 months respectively, p= 0.697). Minimal and mean lumen area in the side-branch decreased significantly (Minimal lumen area: 6.68±1.80 mm^2 and 5.10±2.01 mm^2 at baseline and at 6 months respectively, p =0.004; Mean lumen area: 7.79±2.15 mm^2 and 6.53±2.31 mm^2 at baseline and at 6 months respectively, p=0.002) respectively as a result of 1.59±0.77 mm^2 neointimal area. These data suggest that the result of this approach could improve if a drug-eluting version is developed.

PART III. IMPLANTATION TECHNIQUE OF BIORESORBABLE VASCULAR SCAFFOLDS

BRS represent a novel approach in the treatment of coronary artery lesions by allowing device resorption and restoration of vascular physiology. The Absorb BVS® is composed of a backbone of bioresorbable poly-L-lactide (PLLA) polymer structured in a crystalline fashion and have unique structural characteristics such as limited overexpansion capabilities and larger strut thickness which are not present in permanent metallic DES. Thus traditional metallic DES implantation strategies may not be suitably applied to BRS and procedure- and lesion-related factors can play a greater role in influencing acute procedural success. For example oversized scaffold implantation may be associated with scaffold underexpansion which could be related to higher rate of adverse clinical events. Chapter 14 discussed about the technical considerations that result from the unique structural characteristics of the Absorb BVS® and how these considerations may impact on the type of implantation technique. An optimal implantation technique may be summarised as having adequate lesion preparation, optimal sizing of the vessel and implantation of the scaffold bearing in mind the expansion limits of the scaffold, followed by postdilation with a properly sized non-compliant balloon and where possible supported by the use of intravascular imaging such as OCT.

A complex interaction of factors during the scaffold implantation and subsequent vascular healing process may drive some of the pathology behind late acquired scaffold malapposition. Late acquired scaffold malapposition is more commonly seen when there is vessel- scaffold size mismatch, in certain clinical scenarios such as acute coronary syndromes and certain anatomic subsets such as CTOs and large calibre vessels. Chapter 15 covers the possible risk factors and pathomechanisms behind late acquired scaffold malapposition and possible ways to prevent its development.

There has been limited data on the impact of postdilation on acute procedural and late clinical outcomes in patients with lesions treated with BRS. In Chapters 16, we described the potential impact of postdilation on procedural and clinical outcomes in patients treated with the Absorb BVS®. In a group of 294 patients treated with BRS (387 lesion, postdilation 54%), postdilation resulted in 6% increase in minimal lumen diameter (MLD; after BRS implantation 2.18 ± 0.43mm vs Final 2.32 ± 0.35mm; Δ 0.14 ± 0.32mm, $p<0.001$) and an increase in proportion of final MLD > 2.4mm (28.2% vs 41.9%, $p<0.001$). However at 2 years there was no difference in clinical outcomes. (Major adverse cardiovascular events; post dilation vs non postdilation: 9.9% vs 6.9% respectively, p= 0. 402).

PART IV. TREATMENT OF CORONARY ARTERY DISEASE WITH BIORESORBABLE VASCULAR SCAFFOLDS- OUTCOMES AND LIMITATIONS IN DIFFERENT CLINICAL AND LESION SUBSETS

The contemporary 2nd generation DES are devices which are have generally good clinical outcomes. Despite this, metallic DES are not devoid of significant long term limitations. The metallic implant creates a permanent caging effect of the vessel, preventing facilitating late lumen enlargement and vessel remodelling, jailing of side branches, precluding non-invasive imaging and further revascularisation of stented segments [3-4].

BRS represent a novel treatment for obstructive coronary lesions, with the ultimate aim to eradicate permanent metallic caging of the treated vessel, promising to restore physiological function of the treated vessels [5]. The Absorb BVS® was shown to have good short term clinical outcomes in relatively simple non- complex lesions and was shown to be noninferior to second-generation DES in terms of clinical outcomes [6-7]. BRS offers several theoretical unique potential advantages over DES in range of clinical conditions and anatomic subsets (Chapter 17)**.** The complete bioresorption of BRS permits potential future grafting of treated segments, allows potential reopening of "jailed" side branches and potential recovery of vasomotor function, vessel remodelling and improved conformability particularly in long lesions (Chapter 19). The device received CE Mark approval in 2011 for clinical use for in patients with ischaemic heart disease due to de novo native coronary artery disease with no restriction in clinical presentation or complexity initially. Since then, the Absorb BVS® have been used routinely in Europe and elsewhere in different clinical settings and various lesion subsets of varying complexity. In this section, we report on the clinical outcomes and limitations of the Absorb BVS® scaffold in an expanded range of clinical conditions (Chapter 18). In Chapter 20, an acute coronary syndrome substudy of BVS Expand showed that one year clinical outcomes in ACS patients treated with BVS were similar with non ACS patients (1 year MACE: 5.5% vs 5.3% respectively, p=0.90; 1 year scaffold thrombosis (ScT): 2.0% vs 2.1%, p=0.94); however early ScT cases occurred only in ACS cases. Our institution was among the first to report results after BVS implantation in STEMI [8] with early analysis supporting feasibility of the BVS implantation in STEMI patients with high rate of final TIMI III flow and good scaffold apposition. Beyond 12 months, we look at mid to long term outcomes of the Absorb BVS® in acute (Chapter 21) and more stable patients (Chapter 22). In Chapter 21, we report on the 18 month follow up of STEMI patients treated with Absorb BVS® and used propensity score analysis to match each STEMI patient treated with BVS

with a comparable patient treated with everolimus eluting stents (EES) and compared their clinical outcomes. Though STEMI patients treated during the early experience with BVS had similar acute angiographic results as compared with the EES group, clinical midterm follow-up data showed a higher clinical events rate compared with metal stents. At 18 months, the MACE rate was higher in the BVS group (9.8% vs. 3.6%, p=0.02); target lesion revascularisation was 5.7% vs. 1.3%, p=0.05. ScT occurred primarily in the acute phase (acute ST 2.1% vs. 0.7%, p=0.29; subacute 0.7% vs. 0.7%, p=0.99; late 0.0% vs. 0.0%; very late 1.5% vs. 0.0%, p=0.18). The majority of clinical events occurred in the early phase after implantation and mainly in cases without post-dilatation. Our findings suggest that the optimisation of the implantation technique in the acute clinical setting is of paramount importance for optimal short and mid-term outcomes. In stable patients treated with Absorb BVS® and recruited in the BVS Expand registry (Chapter 22), 249 patients with 335 lesions were followed up. The study showed that Absorb BVS® implantation in a complex patient and lesion subset was associated with an acceptable rate of adverse events in the mid to longer term and no cases of early thrombosis was observed. At 18 months, the MACE rate was 6.8%. Rates of cardiac mortality, myocardial infarct and target lesion revascularisation at 18 months were 1.8%, 5.2% and 4.0% respectively. Definite ScT at 18 months was 1.9%.

While the implantation of the Absorb BVS® in an entire range of complex lesions is still a manner of debate, we report preliminary results supporting the feasibility of Absorb BVS® implantation in bifurcation lesions (Chapter 23) and Chronic Total Occlusions (CTOs) (Chapter 24). In Chapter 23, 102 patients with 107 lesions with at least one coronary bifurcation involving a side branch ≥ 2mm in diameter and treated with at least one Absorb BVS® were studied. There was a high device and procedural success rate of 99.1% and 94.3% respectively. Side branch impairment occurring at any time during the procedure was reported in 12.1% (n=13) and at the end of the procedure in 6.5%. The results of the study

suggest feasibility and relative safety of Absorb BVS® implantation in coronary bifurcations. Despite the thickness of the Absorb BVS® struts, the struts pose a low impact on side branch impairment in coronary bifurcations with side branch ⩾ 2mm in diameter. In a multicentre European study involving 105 patients with complex CTOs (mean J-CTO score was 2.61), the device and procedural success of treatment with Absorb BVS® was 98.1% and 97.1% respectively (Chapter 24). At 6 months follow up, 3 events occurred; 1 periprocedural myocardial infarct, one late ScT and 1 target lesion revascularisation (see below). No cases of mortality were reported. Computed tomography follow up scans were performed at 6 months in 34 of these patients which revealed scaffold restenosis in 2 patients. One patient was symptomatic and underwent target lesion revascularisation and the other was asymptomatic with no ischaemia inducible and hence managed conservatively.

Another lesion subset that can pose interesting challenges for interventionists is fibrocalcific atheromatous plaques, which account for 17-35% of patients undergoing PCI [9-10]. PCI with metallic DES already faced limitations with lesion calcification with worse procedural outcomes reported compared to non-calcified lesions in metallic DES [11]. The presence of calcification can impact on the interventions involving BRS implantation such as during lesion crossing with a guide wire, lesion preparation, device delivery and deployment. However clinical and procedural data with regards to scaffold performance and clinical results in calcified (Ca) lesions are limited. The effect of calcium on acute procedural and clinical outcomes in patients with lesions treated with BRS was discussed in Chapter 25. 455 patients with 548 lesions treated with 735 Absorb BVS® were studied. Overall device success rate was 99.1% with no significant differences between the groups. Despite more aggressive lesion preparation and postdilation, Ca lesions exhibited significantly less acute lumen gain compared to non Ca lesions (acute lumen gain: 1.50 ±0.66 vs 1.62 ±0.69mm, p= 0.040) with lower final MLD (2.28± 0.41 vs 2.36±0.43mm, p=0.046). There were no significant

differences in all-cause mortality, total definite ScT, target lesion revascularization and myocardial infarction between the 2 groups. A remarkable difference in timing of thrombosis was observed with an increased risk of late thrombosis in Ca lesions. Late ScT was more frequent in the Ca group compared to non Ca group (Late ST: 2.1 vs 0%, p=0.02). Overall, clinical outcomes after BRS in Ca and non-Ca groups were similar suggesting that BRS implantation in a complex lesion subset may still be feasible provided there is adherence to procedural recommendations using adequate lesion reparation and postdilation supported by a judicious use of intracoronary imaging.

In this section, we also discussed the issue of extending the duration of dual antiplatelet therapy (DAPT) after the implantation of BRS beyond guideline recommendations of 12 months [12] in view of the risks of late ScT (Chapter 26). Patients pooled from 3 hospitals, comprising of 808 patients with 949 lesions treated with 1,119 BRS with a median follow up of 729 days were evaluated. In this cohort, 26 definite/ probable ScT occurred representing a cumulative event rate (Kaplan-Meier estimate) of 3.3% at 18 months. Majority were early ScT (1.7%). Late and very late ScT rate were less frequent at 1.0% and 0.6% respectively. No very late ScT occurred in patients who continued on DAPT for a minimum of 18 months. The study showed that between six and 18 months, the incidence of ScT in patients who terminated DAPT was potentially increased. Looking at ScT incidence in the time period of six to 18 months for a subgroup of patients with known DAPT status > 6 months (n= 685), ScT was higher within the month after DAPT termination (6.57/100 patient-years) compared to the incidence on DAPT (0.26/100 patient-years).

Continued research in this area is vital to the understanding of the long term clinical results of the Absorb BVS®. In a systematic review and meta-analysis (Chapter 28) involving a total of 7320 patients (BVS n=4007; DES n=3313) followed up with a median duration of 30.5 months, patients treated with Absorb BVS® showed a higher risk of target lesion failure (OR

1.34 [95% CI: 1.12-1.60], p=0.001), myocardial infarct (1.58 [95% CI: 1.27-1.96], p<0.001), target lesion revascularisation (1.48 [95% CI: 1.19-1.85], p=0< 0.001) and definite device thrombosis (2.82 [95% CI: 1.86-4.26], p<0.001). OR for very late (> 1 year) device thrombosis was 6.10 (95% CI: 1.40- 26.65, p=0.02). However, this did not result in an increased risk of all-cause mortality (0.78 [95% CI: 0.58-1.04], p=0.09). Recent data have showed a potential lack of benefits up to 3 years [13], with the BRS compared with best in class DES, in particular certain lesion subsets such as smaller vessels; with the BRS showing either similar or increased risks of TLR and increased risks of ScT compared to DES [14]. The results of ABSORB II and ABSORB III and other results elsewhere [13-16] had also highlighted cautionary findings such as increased risk of scaffold thrombosis particularly in small size vessels.

Recently, the FDA have issued out an advisory on the use of BRS in selected lesion subsets in the United States [17]. Abbott Vascular has also voluntarily restricted the use of the device to institutions involved in research registries in Europe [18]. Main postulated pathological causes behind ScT include incomplete lesion coverage, underexpansion of the scaffold and late structural discontinuities after implantation of the BRS. The reported findings of slightly higher thrombosis rates in particular early ScT seem to be related to procedural factors such as implantation technique necessary to compensate for the relative thicker scaffold struts found in BRS and may therefore be potentially preventable. Indeed, the importance of a dedicated implantation protocol for BRS including preimplantation plaque modification, routine high pressure scaffold post-dilatation with non-compliant balloons, and liberal use of intracoronary imaging such as optical coherence tomography (OCT) to evaluate scaffold apposition and coverage was highlighted in a recent study that ScT rates can be reduced by approximately 70% using a specific implantation technique [19].

CONCLUSION

OCT has been used to evaluate emerging technologies such as BRS and has become a safe and standard imaging modality to evaluate acute stent or scaffold performance. While OCT has been used in the treatment of several types of complex lesions such as calcified lesions, its use in left main PCI has been relatively limited due to concerns over penetration. IDEAL-LM is a prospective, randomized, multicenter study that will enrol over 800 patients undergoing left main PCI designed to assess the safety and efficacy of the novel Synergy® stent followed by 4 months of DAPT vs the Xience® stent followed by 12 months of DAPT in patients after left main stenting. A subset of 100 patients will undergo OCT at 3 months. Results from this study may potentially provide new insights in the capabilities of OCT to support PCI in left main stenting. Given the unique mechanical properties of the polymeric scaffold, certain limitations remain which necessitates it be treated not like just another stent in the interventional arena but as a class of its own. The key to improving clinical outcomes for future BRS may very well lie in a multi-pronged strategy of following a dedicated implantation technique with emphasis on appropriate lesion selection and preparation and aggressive post scaffold postdilation supported by judicious use of intracoronary imaging and possibly extended duration of dual antiplatelets and a renewed focus on newer iterations or next generation of BRS such as Falcon Absorb BVS® or Reva scaffolds with thinner struts. The impact of a dedicated implantation technique on clinical outcomes may be seen in newer prospective Absorb BVS® trials such as Absorb IV and COMPARE ABSORB. Till then, it remains highly likely that OCT and registry based studies would once again play a fundamental role in the evaluation of the next generation of BRS and help determine the optimal implantation strategy for future use.

References

1. Stone GW, Sabik JF, Serruys PW, Simonton CA, Généreux P, Puskas J, Kandzari DE, Morice MC, Lembo N, Brown WM 3rd, Taggart DP, Banning A, Merkely B, Horkay F, Boonstra PW, van Boven AJ, Ungi I, Bogáts G, Mansour S, Noiseux N, Sabaté M, Pomar J, Hickey M, Gershlick A, Buszman P, Bochenek A, Schampaert E, Pagé P, Dressler O, Kosmidou I, Mehran R, Pocock SJ, Kappetein AP; EXCEL Trial Investigators. Everolimus-Eluting Stents or Bypass Surgery for Left Main Coronary Artery Disease. N Engl J Med. 2016 Dec 8;375(23):2223-2235. Epub 2016 Oct 31.

2. James A. Shand, Sharma D, Hanratty C, McClelland A, Menown IB, Spence MS, Richardson G, Herity NA, Walsh SJ. A prospective Intravascular Ultrasound Investigation of the Necessity for and Efficacy of Postdilation Beyond Nominal diameter of 3 Current Generation DES Platforms for the percutaneous Treatment of the Left Main Coronary Catheter Cardiovasc Interv. 2014 Sep 1; 84:351-8.

3. Serruys PW, Katagiri Y, Sotomi Y, Zeng Y, Chevalier B, van der Schaaf RJ, Baumbach A, Smits P, van Mieghem NM, Bartorelli A, Barragan P, Gershlick A, Kornowski R, Macaya C, Ormiston J, Hill J, Lang IM, Egred M, Fajadet J, Lesiak M, Windecker S, Byrne RA, Räber L, van Geuns RJ Mintz GS, Onuma Y.Arterial Remodeling After Bioresorbable Scaffolds and Metallic Stents. J Am Coll Cardiol. 2017 Jul 4;70(1):60-74. doi: 10.1016/j.jacc.2017.05.028.

4. Serruys PW, Garcia-Garcia HM, Onuma Y. From metallic cages to transient bioresorbable scaffolds: change in paradigm of coronary revascularization in the upcoming decade? Eur Heart J. 2012 Jan;33(1):16-25b. doi: 10.1093/eurheartj/ehr384. Epub 2011 Oct 31.

5. Simsek C, Karanasos A, Magro M et al. Long-term invasive follow-up of the everolimus-eluting bioresorbable vascular scaffold: five-year results of multiple invasive imaging modalities. EuroIntervention 2014.

6. Karanasos A, Simsek C, Gnanadesigan M, van Ditzhuijzen NS, Freire R, Dijkstra J, Tu S, Van Mieghem N, van Soest G, de Jaegere P, Serruys PW, Zijlstra F, van Geuns RJ, Regar E. OCT assessment of the long-term vascular healing response 5 years after everolimus-eluting bioresorbable vascular scaffold. J Am Coll Cardiol. 2014 Dec 9;64(22):2343-56

7. Serruys PW, Ormiston JA, Onuma Y, Regar E, Gonzalo N, Garcia-Garcia HM, Nieman K, Bruining N, Dorange C, Miquel-Hébert K, Veldhof S, Webster M, Thuesen L, Dudek D. A bioabsorbable everolimus-eluting coronary stent system (ABSORB): 2-year outcomes and results from multiple imaging methods. Lancet 2009;373: 897–910

8. Diletti R, Karanasos A, Muramatsu T, Nakatani S, Van Mieghem NM, Onuma Y, Nauta ST, Ishibashi Y, Lenzen MJ, Ligthart J, Schultz C, Regar E, de Jaegere PP, Serruys PW, Zijlstra F, van Geuns RJ. Everolimus-eluting bioresorbable vascular scaffolds for treatment of patients presenting with ST-segment elevation myocardial infarction: BVS STEMI first study. Eur Heart J. 2014 Mar;35(12):777-86. doi: 10.1093/eurheartj/eht546. Epub 2014 Jan 6.

9. Kawaguchi R, Tsurugaya H, Hoshizaki H, Toyama T, Oshima S, Taniguchi K. Impact of lesion calcification on clinical and angiographic outcome after sirolimus-eluting stent implantation in real-world patients. Cardiovasc Revasc Med. 2008;9:2-8.

10. Moussa I, Ellis SG, Jones M, Kereiakes DJ, McMartin D, Rutherford B, Mehran R, Collins M, Leon MB, Popma JJ, Russell ME, Stone GW. Impact of coronary culprit lesion calcium in patients undergoing paclitaxel-eluting stent implantation (a TAXUS-IV sub study). Am J Cardiol. 2005;96:1242-7

11. Bourantas CV, Zhang YJ, Garg S, Iqbal J, Valgimigli M, Windecker S, Mohr FW, Silber S, Vries Td, Onuma Y, Garcia-Garcia HM, Morel MA, Serruys PW. Prognostic implications of coronary calcification in patients with obstructive coronary artery disease treated by percutaneous coronary intervention: a patient-level pooled analysis of 7 contemporary stent trials. Heart. 2014 Aug;100(15):1158-64.

12. Capodanno D, Angiolillo DJ. Antiplatelet Therapy After Implantation of Bioresorbable Vascular Scaffolds: A Review of the Published Data, Practical Recommendations, and Future Directions. JACC Cardiovasc Interv. 2017 Mar 13;10(5):425-437. doi: 10.1016/j.jcin.2016.12.279.

13. Serruys PW, Chevalier B, Sotomi Y, Cequier A, Carrié D, Piek JJ, Van Boven AJ, Dominici M, Dudek D, McClean D, Helqvist S, Haude M, Reith S, de Sousa Almeida M, Campo G, Iñiguez A, Sabaté M, Windecker S, Onuma Y. Comparison of an everolimus-eluting bioresorbable scaffold with an everolimus-eluting metallic stent for the treatment of coronary artery stenosis (ABSORB II): a 3 year, randomised, controlled, single-blind, multicentre clinical trial. Lancet. 2016 Nov 19;388(10059):2479-2491. doi: 10.1016/S0140-6736(16)32050-5. Epub 2016 Oct 30.

14. Stephen G. Ellis, M.D., Dean J. Kereiakes, M.D., D. Christopher Metzger, M.D., Ronald P. Caputo, M.D., David G. Rizik, M.D., Paul S. Teirstein, M.D., Marc R. Litt, M.D., Annapoorna Kini, M.D., Ameer Kabour, M.D., Steven O. Marx, M.D., Jeffrey J. Popma, M.D., Robert McGreevy, Ph.D., Zhen Zhang, Ph.D., Charles Simonton, M.D., and Gregg W. Stone, M.D., for the ABSORB III Investigators. Everolimus-Eluting Bioresorbable Scaffolds for Coronary Artery Disease. N Engl J Med 2015; 373:1905-1915 November 12, 2015DOI: 10.1056/NEJMoa1509038

15. Wykrzykowska JJ, Kraak RP, Hofma SH, van der Schaaf RJ, Arkenbout EK, IJsselmuiden AJ, Elias J, van Dongen IM, Tijssen RYG, Koch KT, Baan J Jr, Vis MM, de Winter RJ, Piek JJ, Tijssen JGP, Henriques JPS; AIDA Investigators. Bioresorbable Scaffolds versus Metallic Stents in Routine PCI. N Engl J Med. 2017 Jun 15;376(24):2319-2328. doi: 10.1056/NEJMoa1614954. Epub 2017 Mar 29.

16. Cassese S, Byrne RA, Ndrepepa G, Kufner S, Wiebe J, Repp J, Schunkert H, Fusaro M, Kimura T, Kastrati A. Everolimus-eluting bioresorbable vascular scaffolds versus everolimus-eluting metallic stents: a meta-analysis of randomised controlled trials. Lancet. 2016 Feb 6;387(10018):537-44. doi: 10.1016/S0140-6736(15)00979-4. Epub 2015 Nov 17.

17. US Food and Drug Administration (FDA)- Letter to Health Care Providers dated 03/18/2017.

18. Abbott Vascular Europe Field safety notice/physician advisory dated March 31 2017.

19. Serban Puricel, MD Florim Cuculi, MD, Melissa Weissner, MTA, Axel Schmermund, MD, Peiman Jamshidi, MD, Tobias Nyffenegger, MD, Harald Binder, PHD, Holger Eggebrecht, MD, Thomas Münzel, MD, Stephane Cook, MD, Tommaso Gori, DOTT MED CHIR, PHDMulticenter Comprehensive Analysis of Clinical Presentation, Mechanisms, and Predictors.. J Am Coll Cardiol 2016;67:921–31.

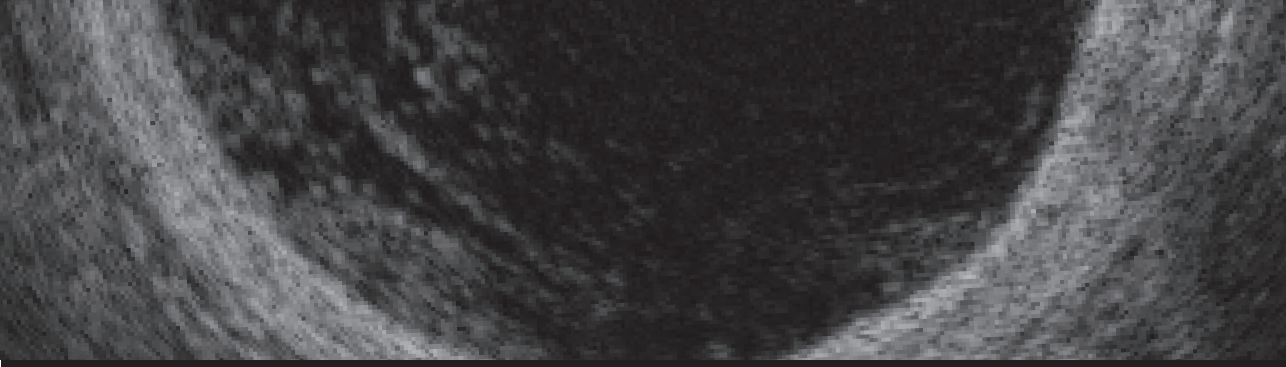

SAMENVATTING EN CONCLUSIE

SAMENVATTING EN CONCLUSIE

Dit proefschrift heeft als doel de resultaten en beperkingen van drug eluting stents (DES) met resorbeerbare polymeer of zelfs volledig bioresorbeerbare stents (ook vaak aangeduid als scaffolds) in de verschillende klinische scenario's en verschillende type vernauwingen in de kransslagaders (Coronaire arteriën) te onderzoeken. In deel I, beschrijf ik de mogelijkheden en onderzoek ik de risico's van een zeer gevoelige beeldvorminingstechniek die kan worden gebruikt voor het evalueren van nieuwe type kranslagaders stents. Vervolgens gebruik ik deze techniek om het implantatie resultaat van deze nieuwe stents in specifieke complex coronaire vernauwingen te onderzoeken en te optimaliseren. In deel II en III bestudeerde ik mogelijkheden van nieuwe metalen stents in de positie van de linker hoofdkransslagader en implantatie technieken voor volledig bioresorbeerbare vasculaire stents (BRS) met behulp van verschillende surrogaateindpunten. Ten slotte werden in deel IV resultaten van BRS in uitgebreide klinische registraties en specifieke subtypes van vernauwing binnen deze registraties onderzocht.

DEEL 1. OPTISCHE COHERENTIE TOMOGRAFIE (OCT) VOOR HET EVALUEREN VAN NIEUWE TYPE KRANSSLAGADERS STENTS EN IN DE KLINISCHE PRAKTIJK

Coronaire Angiografie is sinds de invoering van percutane coronaire interventie (PCI), de standaard techniek voor de beoordeling van de ernst van letsels van de kransslagader en evaluatie van de resultaten van coronaire stent implantatie. OCT is een licht-gebaseerde intravasculaire beeldvormingmethode die de mogelijkheid heeft om hoge resolutie (5 – 15 μm) beelden van de vaatwand en geïmplanteerde stents te creëren. De ontwikkeling van de tweede generatie, zogenaamde frequentie domein OCT, heeft geleid tot een wijdverbreide implementatie van deze beeldvormingsmodaliteit in de klinische praktijk, door

vereenvoudiging van de procedure met simpele beoordeling van de plaque en vaatwand morfologie en de evaluatie van het resultaat van stent plaatsing.

In hoofdstuk 2, toonden we in een prospectieve één centrum studie met 1142 OCT en 2476 IVUS procedures dat OCT net zo veilig is als IVUS in een niet-geselecteerde en heterogene groepvan patiënten met uiteenlopende klinische indicaties. In de volgende hoofdstukken beschrijven we de diverse klinische toepassingen van OCT in PCI zoals preprocedurele stentmaat bepaling (hoofdstuk 3) en evaluatie van acute BRS prestaties na implantatie (hoofdstuk 4). In hoofdstuk 4, werd OCT gebruikt voor de evaluatie van het effect van calcium op acute ontplooiing van BRS vergeleken met metalen DES in coronaire vernauwingen met de verschillende graden van verkalking. Wij constateerden dat met voldoende voorbereiding, implantatie van BRS resulteerde in een soortgelijke luminale winst in vergelijking met DES zoals gemeten door de OCT, ongeacht de mate van verkalking op de angiografie. De ontplooiing van de BRS was vergelijkbaar met dat van een DES (in termen van scaffold of stent oppvervlak, lumen oppervlak en percentage resterende oppervlak stenose (%RAS)) maar met een hogere excentriciteit,deze bevindingen zijn consistent over de subgroepen met verschillende mate van verkalking. Weefsel prolaps was significant hoger in de DES ten opzichte van BRS; en onvolledige strut appositie (incomplete strut apposition area, ISA) was minder in de BRS groep ten opzichte van de DES, een verschil voornamelijk waargenomen in matig en sterk kalkhoudend vernauwingen. In dit deel van het proefschrift beschreven we ook de rol die OCT kan spelen in het verstrekken van inzicht in de mechanismen van stent of scaffold trombose (hoofdstukken 8-9) en de klinische toepassingen van het gebruik van OCT in coronaire bypasses (hoofdstuk 10). OCT kan verschillend bekende oorzaken van stent thrombose zoals onvoldoende ontplooiing, ontstane ruimte tussen stent en vaatwand en hernieuwde atherosclerose binnen de geplaatste stents identificeren.

Ook in coronaire bypasses OCT kan de oorzaak van nieuwe vernauwingen opsporen en behulpzaam zijn bij het optimaal plaatsten van stents in de bypass.

DEEL II. PRESTATIES EN RESULTATEN VAN NIEUWE METALEN STENTS IN DE LINKER HOOFDKRANSSLAGADER

Met de verbeteringen in de interventie technieken en coronaire stents, heeft PCI zich ontpopt als een veilige optie voor revascularisatie bij geselecteerde patiënten met onbeschermde linker hoofdkransslagader ziekte met goede lange termijn resultaten [1]. Toch blijven er belangrijke procedurele uitdagingen om voldoende stent ontplooiing met minimale malappositie te verkrijgen. De gemiddelde diameter van de linker hoofdkransslagader kan oplopen tot meer dan 5,5 mm [2]. Omdat de meeste hedendaagse DES niet voorzien in geschikte maten voor dergelijke dimensies, worden twee verschillende technieken om de benodigde overexpansie te bereiken vaak gebruikt; Proximale Optimalisatie Techniek (POT) en simultane dubbele ballon dilatatie (final kissing balloon dilatation, FKBD). In hoofdstuk 11, werden de overexpansie mogelijkheden van de hedendaagse DES (dat wil zeggen Synergy, Xience Xpedition, Ultimaster, Orsiro, Resolute Onyx en Biomatrix Alpha) in een testopstelling onderzocht om te kijken naar de stent afmetingen na overexpansie met 5.0 en 6.0 mm ballonnen op een stapsgewijze manier. De studieresultaten benadrukten de noodzaak voor de zorgvuldige selectie van de grootte van de stent om het implanteren van stentmaten met te beperkte uitbreidingscapaciteit te voorkomen, aangezien dit kan leiden tot malappositie en overstrekking van de stent. Hoewel DES kan worden overrekt, betekent dit niet dat het is veilig omdat overexpansie veranderingen in mechanische stijfheid kan veroorzaken en de coating voor medicatie afgifte kan beschadigen met mogelijk gevolgen voor de prestaties van de stents. In hoofdstuk 12, toonden we aan dat: 1) dat POT in PCI voor in diameter relatief groter vaten zoals de linker hoofdkransslagader, maar niet FKBD de

platinum-chromium Synergy® stent van 4.00 mm voorbij de limiet van de overexpansie veilig kon ontplooien tot 6.00 mm met optimale stent appositie en prestaties en 2) waarom POT mogelijk de techniek van eerste keuze is voor het bereiken van optimale stent expansie van de linker hoofdkransslagader. Bovendien, is de radiale sterkte, die is een belangrijke factor bij het minimaliseren van acute elastische terugslag na stenting, nog steeds gelijk is ondanks de overexpansion.

In hoofdstuk 13, hebben we de vroege klinische resultaten en intravasculaire echografie (IVUS) prestaties van een voor vaatsplitsingen speciaal ontwikkelde stent (Tryton stent®) wanneer gebruikt in de linker hoofdkransslagader onderzocht. Hieruit bleek dat er uitstekende angiografische en IVUS resultaten waren voor het hoofdvat op 6 maanden. Zes maanden angiografische vermindering van de proximale en distale diameter behandeld met een DES waren 0.28±0.41 en 0.17±0.37 mm respectievelijk. In de zijtak, behandeld slechts met een BMS, was angiografische afname van de diameter met 0.65±0.46 mm. Met behulp van IVUS, was het minimale lumen oppervlak in de proximale linker hoofdkransslagader stabiel (11.08 ± 1.97 mm^2 en 11.59 ± 2,48 mm^2 na implanatatie en bij 6 maanden controle meting respectievelijk, p = 0.697). Minimale en gemiddelde lumen oppervlak in de zijtak waren aanzienlijk gedaald (minimale lumen gebied: 6.68±1.80 $mm,^2$ en 5.10±2.01 mm^2 na implantatie en bij 6 maanden controlemeting respectievelijk, p = 0.004; terwijl de metingen voor de zijtak bij controle meting duidelijk afgenomen waren: 5.10±2.01 $mm,^2$ en 6.53±2.31 mm^2 voor gemiddelde en minimale lumen oppervlakte als gevolg van 1.59±0.77 mm^2 neointima ontwikkeling. Deze gegevens duiden erop dat het resultaat van deze aanpak zou kunnen verbeteren als een medicatie afgevende versie wordt ontwikkeld.

DEEL III. IMPLANTATIE TECHNIEK VAN BIORESORBEERBARE VASCULAIRE STENTS

BRS vertegenwoordigen een nieuwe aanpak in de behandeling van coronaire vernauwingen door resorptie het materiaal en daarbij de mogelijkheid van herstel van de vasculaire fysiologie. The Absorb BVS® is de eerste veel toegepaste BRS en bestaat uit een kern van bioresorbeerbare poly-L-lactide (PLLA) polymeer gestructureerd in een kristallijne samenstelling welke unieke structurele kenmerken oplevert zoals beperkte overexpansie capaciteiten en grotere stent dikte dan in permanente metalen DES aanwezig zijn. Hierdoor kunnen klassieke metalen DES implantatie strategieën niet zomaar worden toegepast op BRS en procedure- en laesie gerelateerde factoren kunnen een grotere rol spelen in het acute succes. Bijvoorbeeld oversized stent implantatie kan gepaard gaan met onvoldoende expansie die tot slechtere klinische uitkomsten kan lijden. Hoofdstuk 14 bespreekt de technische overwegingen die voortvloeien uit de unieke structurele kenmerken van de Absorb BVS® en hoe deze overwegingen invloed kunnen hebben op de implantatie techniek. Een optimale implantatie techniek kan worden samengevat als voldoende laesie voorbewerking, optimale maatvoering van de stent rekening houdend met de beperkte overexpansie mogelijkheden van de stent gevolgd door nadilatie met een ballon van de juiste afmeting en waar mogelijk ondersteund door het gebruik van intravasculaire beeldvorming zoals OCT.

Een complexe interactie van factoren tijdens de BVS implantatie en het daarop volgende vasculaire genezingsproces kan lijden tot laat optredende stent malapposition. Laat verworven stent malapposition wordt meer gezien als er een mismatch is tussen de grootte van het vat en de geselecteerde stent, in bepaalde klinische scenario's zoals acute coronaire syndromen en bij bepaalde anatomische subtypes zoals CTO en grote kaliber bloedvaten. Hoofdstuk 15 behandelt de mogelijke risicofactoren en pathofysiologische mechanismen

achter laat verworven stent malappositie en mogelijke manieren om de ontwikkeling hiervan te voorkomen.

Er zijn beperkte gegevens over het effect van nadilatie op acute procedurele en late klinische resultaten bij patiënten met letsels behandeld met BRS. In hoofdstuk 16, beschreven we de impact van nadilation op procedurele en klinische resultaten in patiënten die behandeld werden met de bioresorbeerbare BVS®. In een groep van 294 patiënten behandeld met BRS (387 laesies, nadilation 54%), resulteerde nadilatie in een 6% stijging van de minimale diameter van het bloedvat (MLD; na BRS implantatie 2.18 ± 0,43 mm vs. definitief 2.32 ± 0.35 mm; Δ 0.14 ± 0,32 mm, $p < 0.001$) en een toename van het percentage met een definitieve MLD > 2.4mm (28,2% vs. 41,9%, $p < 0,001$). Echter na 2 jaar vervolg van de patiënten was er geen verschil in de klinische resultaten. (Major Adverse Cardiac Events (MACE); nadilatatie vs. geen nadilation: 9,9% vs. 6,9% respectievelijk, $p = 0.402$).

DEEL IV. BEHANDELING VAN CORONAIRE VERNAUWINGEN MET BIORESORBEERBARE VASCULAIRE STENTS -RESULTATEN EN BEPERKINGEN IN VERSCHILLENDE KLINISCHE EN ANATOMISCHE SUBGROEPEN

De hedendaagse 2de generatie DES hebben over het algemeen goede klinische resultaten. Ondanks dit zijn de metalen DES niet verstoken van belangrijke lange termijn beperkingen. Het metalen implantaat creëert een permanente kooi rondom het lumen van het bloedvat, dit verhinderd een latere lumen groei en bloedvatwand structuur reorganisatie, leidt tot het afknellen van zijtakken, de onmogelijkheid tot niet-invasieve beeldvorming middels CT-scans en beperkt verdere revascularisatie van het behandelde segmenten [3-4].

BRS vertegenwoordigen een nieuwe behandeling mogelijkheid voor obstructieve coronaire letsels, met het uiteindelijke doel om permanente inkooien van het behandelde vat te

voorkomen, en mogelijkerwijs tot het herstellen van de fysiologische functie van de behandelde bloedvaten [5]. De bioresorbeerbare BVS® bleek goede korte termijn klinische resultaten te hebben in relatief eenvoudige letsels en bleek niet inferieur aan de tweede generatie DES in termen van klinische resultaten [6-7]. BRS biedt verschillende unieke theoretische voordelen ten opzichte van DES in verschillende klinische omstandigheden en anatomische subtypen (hoofdstuk 17)**.** De volledige bioresorptie van BRS laat toekomstige bypass behandeling toe van de behandelde segmenten, levert mogelijk heropening van afgeknelde zijtakken op en een mogelijke herstel van vasomotorisch functie, bloevatwand structuur reorganisatie en verbeterd conformabiliteit met name in lange letsels (hoofdstuk 19). De stent heeft in 2011 het CE-keurmerk voor klinisch gebruik bij patiënten met ischemische hartziekte gekregen zonder beperking in klinische presentatie of complexiteit van de vernauwingen. Sindsdien, zijn de Absorb BVS® routinematig gebruikt in Europa en elders in de wereld in verschillende klinische omstandigheden en letsel subtypen van uiteenlopende complexiteit. In dit deel van het proefschrift, rapporteer ik de klinische resultaten en beperkingen van de Absorb BVS® in een uitgebreide waaier van klinische omstandigheden (hoofdstuk 18). In hoofdstuk 20, toonde een acuut coronair syndroom substudie van BVS-EXPAND dat één jaar klinische resultaten in ACS-patiënten die behandeld werden met BVS vergelijkbaar waren met niet-ACS-patiënten (1 jaar MACE: 5,5% vs 5,3% respectievelijk, p = 0,90; 1 jaar stent trombose (ST): 2,0% vs. 2,1% p = 0.94); maar trad vroege ST alleen op in ACS procedures. Ons centrum was een van de eerste om vroege resultaten van BVS implantatie in STEMI te rapporteren[8], dateen ondersteuning gaf van het concept van BVS implantatie in STEMI patiënten op basis van een hoog percentage TIMI III flow in het vat na afloop en goede stent appositie zoals gemeten met OCT. Na meer dan 12 maanden, heb ik ook gekeken naar de middellange tot lange termijn resultaten van de Absorb BVS® in acute (hoofdstuk 21) en meer stabiele patiënten (hoofdstuk 22). In hoofdstuk 21, rapporteer ik de

18 maanden follow-up van STEMI patiënten behandeld met Absorb BVS® en gebruik propensity score analyse om aan elke STEMI patiënt met behandeld BVS een vergelijkbare patiënt behandeld met Everolimus afgevende metalen stents (EES) te koppelen en hun klinische resultaten te vergelijken. Hoewel de STEMI patiënten behandeld werden terwijl er nog weinig ervaring was met BVS hadden zij vergelijkbare acute angiografische resultaten als EES behandelde patiënten, maar middellange termijn klinische analyse gaf een hoger aantal ongunstigeklinische gebeurtenissen in vergelijking met metalen stents. Bij 18 maanden, werd de MACE incidentie hoger in de BVS groep (9,8% vs. 3,6%, p = 0,02) en ook de hernieuwde letsel revascularisatie was hoger (5,7% vs. 1,3%, p = 0.05). ST kwam vooral voor in de acute fase (ST binnen 24 uur: 2,1% versus 0,7%, p = 0,29; subacute ST tussen 24 uur en 30 dagen: 0,7% versus 0,7%, p = 0,99; late ST na 30 dagen: 0,0% vs. 0.0%; erg late ST na 1 jaar: 1,5% vs. 0,0%, p = 0.18). De meerderheid van de klinische gebeurtenissen hebben plaatsgevonden in de vroege fase na implantatie en vooral in gevallen zonder nadilatatie. Onze bevindingen suggereren dat optimalisering van de implantatietechniek in de acute klinische setting van het allergrootste belang is voor goede korte en middellange termijn resultaten. Stabiele patiënten behandeld met Absorb BVS® werden geïncludeerd in de BVS-EXPAND studie (hoofdstuk 22), waarbij uiteindelijk 249 patiënten met 335 laesies werden vervolgd. De studie toonde aan dat Absorb BVS® implantatie in een complexe patiënt en letsel subset een acceptabel aantal ongunstige uitkomsten liet zien op middellange termijn en er geen gevallen van vroege trombose werden waargenomen. Bij 18 maanden was de incidentie van de MACE 6,8%. Incidentie van cardiale sterfte, myocard infarct en hernieuwde letsel revascularisatie op 18 maanden waren respectievelijk: 1,8% , 5,2% en 4,0%. Bewezen ST op 18 maanden was 1,9%.

Terwijl de inplanting van de Absorb BVS® in algemeen complexe laesies nog steeds onderwerp van discussie was, rapporteren wij de voorlopige resultaten ter ondersteuning van

de haalbaarheid van Absorb BVS® implantatie in bifurcatie laesies (hoofdstuk 23) en chronische totale occlusies (CTO) (hoofdstuk 24). In hoofdstuk 23, werden 102 patiënten met 107 letsels met ten minste één vernauwing ter plaatse van een coronaire splitsing (bifurcatie) waarbij de zijtak tenminste 2mm in diameter is en behandeld Absorb BVS® geanalyseerd. Er was een stent en procedure slagingspercentage van 99,1% en 94,3% respectievelijk. Bedreiging van het open houden van de zijtak op enig moment tijdens de procedure werd gemeld in 12,1% (n = 13) en aan het einde van de procedure in 6,5% van de gevallen. De resultaten van deze studie suggereerden de haalbaarheid en de relatieve veiligheid van Absorb BVS® implantatie in coronaire bifurcaties. Ondanks de dikte van de Absorb BVS® stents, hebben deze dus een laag risico op zijtak afsluiting in coronaire bifurcaties. In een multicenter Europese studie waarbij 105 patiënten met complexe chronische totale occlusie (CTO, met een gemiddelde J-CTO score van 2.61) waren stent en procedure succes 98,1% en 97,1% respectievelijk (hoofdstuk 24). Bij 6 maanden controle, waren er 3 belangrijk gebeurtenissen geweest; 1 periprocedureel myocard infarct, een late ST en 1 hernieuwde letsel revascularisatie. Geen gevallen van sterfte werden gemeld. Computertomografie (CT) follow-up-scans werden uitgevoerd op 6 maanden in 34 van deze patiënten welke een hernieuwde vernauwing liet zien in 2 patiënten. Eén patiënt was symptomatisch en onderging een revascularisatie en de ander was asymptomatische zonder aantoonbare ischemie en werd conservatief behandeld.

Een ander letsel subtype dat een interessante uitdagingen voor interventiecardiologen vormt zijn gecalcificeerde atherosclerotische letsels, die goed zijn voor 17-35% van de patiënten die een PCI ondergaan[9-10]. PCI in gecalcificeerde letsels met metalen DES laat altijd al slechtere procedurele resultaten zien in vergelijking met PCI van niet-verkalkt letsels [11]. De aanwezigheid van verkalking kan gevolgen hebben voor de interventies waarbij BRS gebruikt worden zoals tijdens het inbrengen van de geleide draad, voorbewerking van de

vernauwing met ballonen, stent positionering en implantatie. Klinische en procedurele gegevens met betrekking tot de prestaties van BRS en klinische resultaten in gecalcificeede (Ca) laesies zijn echter beperkt.

Het effect van calcium op acute procedurele en klinische resultaten bij patiënten met letsels behandeld met BRS wordt besproken in hoofdstuk 25. 455 patiënten met 548 letsels behandeld met 735 Absorb BVS® werden bestudeerd. Algemene stent slagingspercentage was 99.1% zonder significante verschillen tussen de groepen. Ondanks meer agressieve laesie voorbereiding en nadilation, toonde Ca laesies aanzienlijk minder directe winst in bloedvat diameter in vergelijking met niet-Ca laesies (directe toename in bloedvatdiameter: 1,50 ±0.66 vs. 1.62 ±0.69 mm, p = 0.040) met lagere definitieve minimale diameter (MLD:2.28± 0,41 vs. 2.36±0.43 mm, p = 0.046). Er waren geen significante verschillen in totale sterfte, bewezen ST, hernieuwde letsel revascularisatie en myocard infarct tussen de 2 groepen. Een opmerkelijk verschil in tijdstip van trombose werd vastgesteld met een verhoogd risico van late trombose in Ca laesies. Late ST was vaker gezien in de Ca-groep in vergelijking met niet-Ca-groep (Late ST: 2.1 versus 0%, p = 0,02). Algemene, klinische uitkomsten na BRS in Ca en niet-Ca groepen waren vergelijkbaar wat suggereert dat BRS implantatie in dit subtype van het complexe letsels nog steeds haalbaar kan zijn mits procedurele aanbevelingen met behulp van adequate laesie voorbewerking en nadilatie ondersteund door een weloverwogen gebruik van intracoronaire beeldvorming worden nageleefd.

In dit deel van het proefschrift, wordt ook gekeken naar de duur van de dubbele plaatjes remmers therapie (DAPT) na de inplanting van BRS die mogelijk anders is dan de aanbevelingen van 12 maanden voor tweede generatie DES [12] met het oog op de risico's van late en erg late ST (hoofdstuk 26). Patiënten uit 3 ziekenhuizen in de regio Rotterdam werden gebundeld, resulterend in een groep bestaande uit 808 patiënten met 949 letsels behandeld met gemiddeld 1,1 BRS met een gemiddelde follow-up van 729 dagen. Kaplan

Meier schattingen voor late en zeer late ST waren 1,0% en 0,6% respectievelijk. Van de groep die DAPT voor tenminste 6 maanden gebruikte was de ST incidentie in de periode van zes tot 18 maanden 0,83/100 patiënt-jaren met een incidentie 0% voor diegene die helemaal niet stopten voor 18 maanden.

Verder onderzoek op dit gebied is van vitaal belang voor het begrip van de klinische resultaten op de lange termijn van de Absorb BVS®. In een systematische review en meta-analyse (hoofdstuk 28) met betrekking tot een totaal van 7320 patiënten (BVS n = 4007; DES n = 3313) die werden vervolgt met een mediane duur van 30.5 maanden, toonde dat patiënten die behandeld werden met Absorb BVS® een hoger risico hadden op enig falen van de stent (Oddsratio 1.34 [95% CI: 1.12-1,60], p = 0,001), myocard infarct (1,58 [95% CI: 1,27-1.96], p < 0,001), hernieuwde letsel revascularisatie (1.48 [95% CI: 1.19-1.85], p = 0 < 0.001) en bewezen stent trombose (2.82 [95% CI: 1,86-4.26], p < 0,001). De OR voor zeer late (> 1 jaar) stent trombose was 6.10 (95% CI: 1.40-26.65, p = 0,02). Echter, dit leidde niet tot een verhoogd risico op algehele sterfte (0.78 [95% CI: 0,58-1.04], p = 0,09). Recente studies hebben een gebrek aan voordelen tot en met 3 jaar van BRS ten opzichte van de beste DES laten zien[13], in het bijzonder bepaalde subtype zoals kleinere vaten vertonen of vergelijkbare of hogere risico op hernieuwde letsel revascularisatie en een verhoogd risico van ST ten opzichte van DES [14] wanneer BRS worden gebruikt. De resultaten van ABSORB II en ABSORB III en andere studies [13-16] hadden ook zorgwekkende bevindingen gerapporteerd zoals een verhoogd risico van stent trombose, vooral in kleine vaten.

Onlangs, heeft de FDA een advies uitgegeven over het gebruik van BVS in specifieke letsel typen in de Verenigde Staten [17]. Abbott Vascular heeft ook vrijwillig het gebruik van de BVS beperkt tot ziekenhuizen die deelnemen aan lopende onderzoeken in Europa [18]. De belangrijkste pathologische oorzaken benoemd van ST omvatten onvolledig letsel afdekking,

onvoldoende uitvouwen van de stent en late ongelijkmatige desintegratie van BRS na implantatie. De gerapporteerde bevindingen van een iets hogere trombose incidentie, met name vroege ST, lijken gerelateerd te kunnen worden aan procedurele factoren zoals de implantatietechniek die nodig is om te compenseren voor de relatieve dikkere stent onderdelen van BRS en kunnen daarom potentieel voorkomen worden. Het belang van een speciale implantatie protocol voor BRS met inbegrip van adequate letsel voorbereiding, routine hogedruk stent nadilatatie met ballonnen en liberaal gebruik van intracoronaire beeldvorming zoals optische coherentie tomografie (OCT) om te evalueren van de stent appositie werd benadrukt in een recente studie waarbij ST incidentie kon worden verminderd met ongeveer 70 procent met behulp van een specifieke implantatie protocol [19].

CONCLUSIE

OCT wordt gebruikt voor het evalueren van opkomende technologieën zoals BRS en is uitgegroeid tot een veilige en standaard beeldvormingsmodaliteit om acute stent prestaties te evalueren. Terwijl OCT is gebruikt bij de behandeling van verschillende soorten complexe vernauwingen zoals kalkhoudend laesies, is het gebruik ervan tijdens linker hoofdkransslagader behandelingen relatief beperkt gebleven als gevolg van de bezorgdheid over het doordringende vermogen. IDEAL-LM is een prospectieve, gerandomiseerde multicenter studie waarin bij meer dan 800 patiënten die behandelingen ondergaan van de linker hoofdkransslagader de veiligheid en de werkzaamheid van de nieuwe Synergy® stent gevolgd door 4 maanden van DAPT wordt vergeleken met de Xience® stent gevolgd door 12 maanden van DAPT. Een subset van 100 patiënten zal OCT ondergaan op 3 maanden. Resultaten van deze studie kunnen de mogelijkheden van OCT tijdens PCI van de linker hoofdkransslagader verder verduidelijken.

Gezien de unieke mechanische eigenschappen van de bioresorbeerbare polymere stent, blijven er bepaalde beperkingen die er voor zorgen dat deze niet als zomaar een stent kan

worden beschouwd maar als een aparte klasse behandeld moet blijven worden. De sleutel tot verbetering van de klinische resultaten voor toekomstige BRS zal op meerdere fronten liggen waarbij een specifieke implantatie techniek wordt gebruikt met nadruk op selectie van de juiste letsels, goede letsel voorbewerking en krachtige stent nadilatie ondersteund door verstandig gebruik van intracoronaire beeldvorming en eventueel verlenging van de duur van de dubbele plaatjesremmers en een hernieuwde focus op volgende generatie van BRS zoals Falcon Absorb BVS® of Reva stents van dunner materiaal. De invloed van een specifieke implantatie techniek op klinische uitkomsten zal worden onderzocht in nieuwe prospectieve Absorb BVS® studies zoals de ABSORB IV en COMPARE ABSORB. Tot dan, blijft het zeer waarschijnlijk dat OCT en specifieke klinische databases nogmaals een fundamentele zullen rol spelen bij de evaluatie van de volgende generatie van BRS en zullen helpen bij het bepalen van de optimale implantatie strategie voor toekomstig gebruik.

Verwijzingen

1. Stone GW , Sabik JF , Serruys PW , Simonton CA , Généreux P , Puskas J , Kandzari DE , Morice MC , Lembo N , Bruin WM 3e , Taggart DP , Verbod op A , Merkely B , Horkay F , Boonstra PW , van Boven AJ , Ik Ungi , Bogáts G , Mansour S , Noiseux N , Sabaté M , Pomar J , Hickey M , Gershlick A , Buszman P , Bochenek A , Schampaert E , Pagé P , Dressler O , Kosmidou ik , Mehran R , Pocock SJ , Kappetein AP ; EXCEL Trial onderzoekers . Everolimus-eluerende Stents of Bypass chirurgie voor linker belangrijkste coronaire hartziekte. N Engl J Med. 2016 Dec 8; 375 (23): 2223-2235. EPUB 2016 Oct 31.

2. James A. Shand, Sharma D, Hanratty C, McClelland A, Menown IB , Spence MS, Richardson G, Herity NA, Walsh SJ . Een potentiële intravasculaire echografie onderzoek naar de noodzaak en doeltreffendheid van Postdilation buiten nominale diameter van 3 huidige generatie DES Platforms voor de percutane behandeling van de links Main coronaire katheter Cardiovasc Interv. 2014-Sep 1; 84:351-8.

3. Serruys PW, Katagiri Y, Sotomi Y, Zeng Y, Chevalier B , van der Schaaf RJ , Baumbach A , Smits P , van Mieghem NM , Bartorelli A , Barragan P , Gershlick A , Kornowski R , Macaya C , Ormiston J , Hill J , Lang IM , Egred M , Fajadet J , Lesiak M , Windecker S , Byrne RA , Räber L , van Geuns RJ Mintz GS, Onuma Y. Arteriële remodelleren na Bioresorbable steigers en metalen Stents. J ben Coll Cardiol. 2017 4 Jul; 70 (1): 60-74. doi: 10.1016/j.jacc.2017.05.028.

4. Serruys PW, Garcia-Garcia HM, Onuma Y. Van metalen kooien om voorbijgaande bioresorbable steigers: verandering in paradigma van coronaire revascularisatie in het komende decennium? Eur hart J. 2012 Jan; 33 (1): 16-25b. doi: 10.1093/eurheartj/ehr384. EPUB 2011 Oct 31.

5. Simsek C, Karanasos A, Magro M et al. langdurig invasieve follow-up van de everolimus-eluerende bioresorbable vasculaire steiger: vijf jaar resultaten van meerdere invasieve beeldvormende modaliteiten. EuroIntervention 2014.

6. Karanasos A, Gnanadesigan M, Simsek C van Ditzhuijzen NS, Freire R Dijkstra J, Tu-S, Van Mieghem N, van Soest G, de Jaegere P, Serruys PW, Zijlstra F, van Geuns RJ, Regar E. OCT beoordeling van de lange termijn vasculaire helende reactie 5 jaar na everolimus-eluerende bioresorbable vasculaire steiger. J Am Coll Cardiol. 2014 Dec 9; 64 (22): 2343-56

7. Serruys PW, Ormiston JA, Onuma Y, E Regar, Gonzalo N , Garcia-Garcia HM , Nieman K , Bruining N , Dorange C , Miquel-Hébert K , Veldhof S , Webster M , Thuesen L , Dudek D . Een bioabsorbable everolimus-eluerende coronaire stent systeem (ABSORB): 2 jaar uitkomsten en resultaten van meerdere beeldvormende methoden. Lancet 2009; 373: 897-910

8. Diletti R, Karanasos A, Muramatsu T, Nakatani S, Van Mieghem NM, Onuma Y, Nauta ST, Ishibashi Y , Lenzen MJ , Ligthart J , Schultz C , Regar E , de Jaegere PP , Serruys PW , Zijlstra F , van Geuns RJ . Everolimus-eluerende bioresorbable vasculaire steigers voor behandeling van patiënten presenteren met ST-segment elevatie myocardinfarct: BVS STEMI eerste studie. Eur hart J. 2014 Mar; 35 (12): 777-86. doi: 10.1093/eurheartj/eht546. EPUB 2014 Jan 6.

9. Kawaguchi R, Tsurugaya H, Hoshizaki H, Toyama T, Oshima S, Taniguchi K. Impact van verkalking van de laesie op klinische en angiographic resultaat na sirolimus-eluerende stent implantatie in levensechte patiënten. Cardiovasc Revasc Med. 2008; 9:2-8.

10. Moussa I, Ellis SG, Jones M, Kereiakes DJ, McMartin D, Rutherford B, Mehran R, Collins M, Leon MB, Popma JJ, Russell ME, steen GW. Gevolgen van coronaire boosdoener laesie calcium in patiënten die een paclitaxel-eluerende stent implantatie (een studie van de sub TAXUS-IV). Ben J Cardiol. 2005; 96:1242-7

11. Bourantas CV, Zhang YJ, Garg S, Iqbal J, Valgimigli M , Windecker S , Mohr FW , Silber S , Vries Td , Onuma Y , Garcia-Garcia HM , Morel MA , Serruys PW . Prognostische implicaties van coronaire verkalking in patiënten met obstructieve coronaire hartziekte behandeld door percutane coronaire interventie: een patiënt-niveau gebundeld analyse van 7 hedendaagse stent proeven. Hart. 2014 Aug; 100 (15): 1158-64.

12. Capodanno D, Angiolillo DJ. Antiplatelet therapie na implantatie van Bioresorbable vasculaire steigers: een overzicht van de gepubliceerde gegevens, praktische aanbevelingen, and Future Directions. JACC Cardiovasc Interv. 2017 13 Mar; 10 (5): 425-437. doi: 10.1016/j.jcin.2016.12.279.

13. Serruys PW, Chevalier B, Sotomi Y, Cequier A, Carrié D, Piek JJ, Van Boven AJ, Dominici M, Dudek D, McClean D, Helqvist S, Haude M, Reith S, de Sousa Almeida M, Campo G, Iñiguez A , Sabaté M , Windecker S , Onuma Y . Vergelijking van een everolimus-eluerende bioresorbable steigerwerk met een everolimus-eluerende metalen stent voor de behandeling van coronaire stenose (ABSORBEREN II): een van 3 jaar, gerandomiseerde, gecontroleerde, single-blind, multicentrische klinische proef. Lancet. 2016 Nov 19; 388 (10059): 2479-2491. doi: 10.1016/S0140-6736 (16) 32050-5. EPUB 2016 Oct 30.

14. Stephen G. Ellis, M.D., Dean J. Kereiakes, M.D., D. Christopher Metzger, M.D., Ronald P. Caputo, M.D., David G. Rizik, M.D., Paul S. Teirstein, M.D., Marc R. Litt, M.D., Annapoorna Kini, M.D., Ameer Kabour, M.D., Steven O. Marx , M.D., Jeffrey J. Popma, M.D., Robert McCreevy, Ph.D., Zhen Zhang, Ph.D., Charles Simonton, M.D., en Gregg W. Stone, M.D., voor de III onderzoekers ABSORBEREN. Everolimus-eluerende Bioresorbable steigers voor coronaire hartziekten. N Engl J Med 2015; 373:1905-1915 November 12, 2015 DOI: 10.1056/NEJMoa1509038

15. Wykrzykowska JJ, Kraak RP, Hofma SH, van der Schaaf RJ , Arkenbout EK , IJsselmuiden AJ , Elias J , van Dongen IM , RYG Tijssen , Koch KT , Baan J Jr , Vis MM , de Winter RJ , Piek JJ , Tijssen JGP , Henriques JPS ; AIDA onderzoekers . Bioresorbable steigers versus metalen Stents in Routine PCI. N Engl J Med. 2017 Jun 15; 376 (24): 2319-2328. doi: 10.1056/NEJMoa1614954. EPUB 2017 Mar 29.

16. cassese S, Byrne RA, Ndrepepa G, Kufner S, Wiebe J, Repp J, Schunkert H, Fusaro M, Kimura T, Tare A. Everolimus-eluerende bioresorbable vasculaire steigers versus everolimus-eluerende metalen stents: een meta-analyse van gerandomiseerde gecontroleerde proeven. Lancet. 2016 6 februari; 387 (10018): 537-44. DOI: 10.1016/S0140-6736 (15) 00979-4. EPUB 2015 Nov 17.

17. US Food and Drug Administration (FDA)- brief aan aanbieders van gezondheidszorg gedateerd 03/18/2017.

18. Abbott Vascular Europa Fgebied veiligheid aankondiging/arts Raadgevend gedateerd 31 maart 2017.

19. Serban Puricel, MD Florim Cuculi, MD, Melissa Weissner, MTA, Axel Schmermund, MD, Peiman Jamshidi, MD, Tobias Nyffenegger, MD, Harald Binder, PHD, Holger Eggebrecht, MD, Thomas Münzel, MD, Stephane Cook, MD, Tommaso Gori, DOTT MED CHIR, PHDMulticenter uitgebreide analyse van de klinische presentatie, mechanismen en voorspellers. . J Am Coll Cardiol 2016; 67:921 – 31.

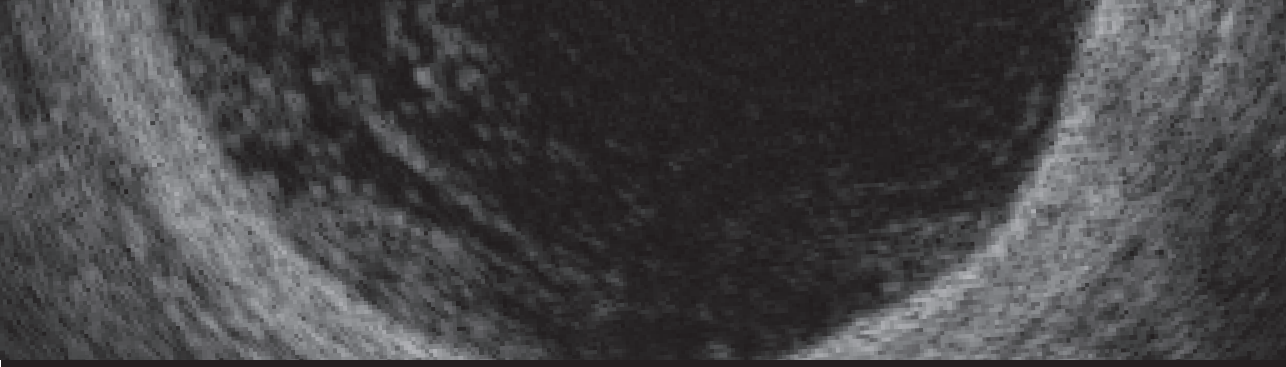

CURRICULUM VITAE

CV

(1) Personal Particulars

Full Name (complete with degrees) : Fam Jiang Ming, MBBS (Singapore), MMED, MRCP (UK)
Gender: Male
Nationality : Singaporean
Office Address : National Heart Centre Singapore 5 Hospital Drive, 169609
Email : fam.jiang.ming@singhealth.com.sg

(2) Brief Biography

Dr Fam Jiang Ming is a Consultant in the Department of Cardiology at the National Heart Centre, Singapore (NHCS). He completed his advanced specialist training in the field of cardiology following which he completed his advanced subspecialty training in Interventional Cardiology in Thorax centre, Erasmus Medical Centre, Rotterdam, the Netherlands in June 2015. He is currently a full time interventional cardiologist and has participated in interventional conferences such as ASIA-PCR and NHCS CTO Live as a live case operator since 2014.

Dr Fam is also actively involved in education and research. He is a lecturer in the Singapore Polytechnic Diploma in Cardiac Technology Course and is part of the faculty of DUKE-NUS medical school and the Singhealth residency program. His research interests include intravascular physiology and imaging as well as clinical outcomes in patients with percutaneous coronary intervention. He has presented his research findings in local and international conferences and is first/coauthor of numerous research papers in local and international peer reviewed journals.

(3) Current Appointment Details

Institution of primary appointment: National Heart Centre Singapore

Present rank(s) and title(s): Consultant

(4) Educational & Training Qualifications

	Institution	Qualification obtained	Year
Basic Degree(s):	National University of Singapore	MBBS	2002
Post Basic Degree(s):	National University of Singapore	MRCP (UK); MMED (Internal Medicine)	2009

(5) Certification & Licensure

(A) Medical Professional License

Licensing Board	Month / Year
Singapore Medical Council	May 2003

(B) Specialty Certificate

Certifying Board	Month / Year
Singapore Accreditation Board	May 2013
Singapore Medical Council	May 2013

(6) Membership in Professional & Academic Societies

Organisation	Rank / Title/ Position	Month / Year
Singapore Cardiac Society	Associate Member	2012
European Society of Cardiology	Fellow	November 2017
American College of Cardiology	Fellow	January 2018

(7) Editorship

Reviewer role: Catheterization and Cardiovascular Interventions, EuroIntervention, International Journal of Cardiology, International Journal of the Health Sciences Center, Journal of Interventional Cardiology, Proceedings of Singapore Healthcare.

(8) Faculty of Courses / Conferences Attended and Speaking Invitations

- Faculty of AsiaPCR and CTO – LIVE; NHCS 2014, 2016-2017
- Guest faculty of EuroPCR 2017-18

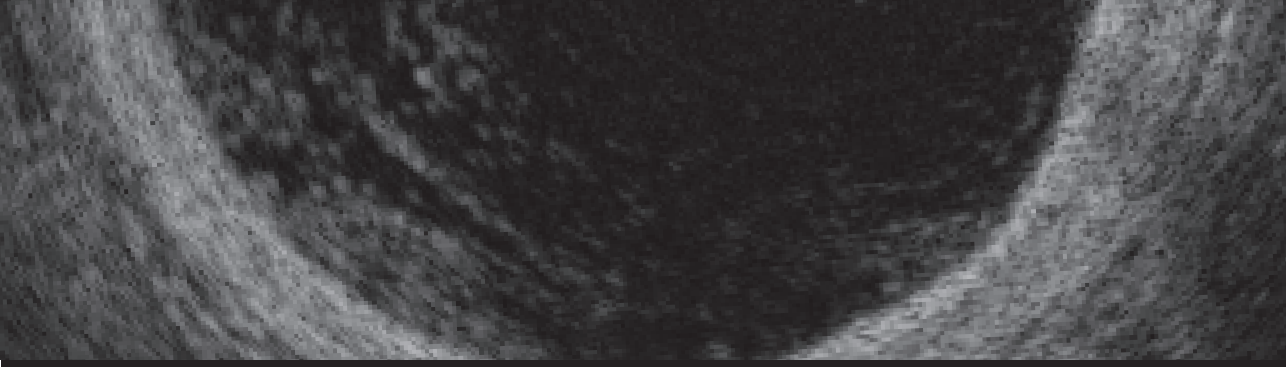

PHD PORTFOLIO

Portfolio

Conferences and Seminars Attended

2014 April TCTAP- Faculty (Best Poster award)

2014 August- ESC Congress (Participant)

2015 January- ASIAPCR (Presenter)

2015 February- CRT (Presenter)

2015 March- Optics Conference (Participant)

2015 May- EuroPCR (Presenter)

2015 October- CCT (Participant)

2016 March- ACC (Participant)

2016 April- TCTAP (Attendee)

2016 May- EuroPCR (Participant)

2016 July- TOPIC (Participant)

2017 April- TCTAP (Attendee)

2017 May- EuroPCR (Faculty)

2017 August- ESC (Participant)

2018 April- TCTAP (Attendee)

2018 May- EuroPCR (Faculty)

COEUR Courses and Seminars Attended

2014 October Symposium: Transcatheter Heart Therapies from Niche to Mainstream

2015 February- COEUR Cardiovascular Imaging and Diagnostics Course

2015 February Symposium: Costs, Quality and Value in Cardiovascular Interventions- Implications for clinical decision-making and policy development

2015 April- COEUR Antithrombotic Symposium

2016 May Symposium: Bioresorbable Scaffolds in Contemporary Clinical Practice

Other Courses Attended

2015 April- Basic Hands-on Cardiac Computed Tomography Course (Towards Level 1 ACC/AHA certification)

2015 April- Advanced Hands-on Cardiac Computed Tomography Course (Towards Level 2 ACC/AHA certification)

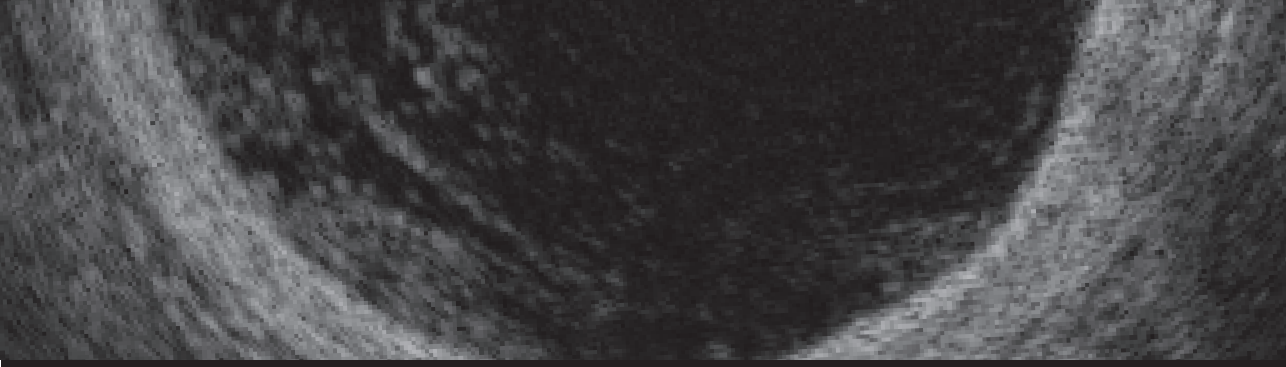

LIST OF PUBLICATIONS

List of Publications

(A) Refereed Journals

1. Cordula Felix, Victor .J. van den Berg, Sanne .E. Hoeks, **Jiang Ming Fam**, Mattie. Lenzen, Eric Boersma, Peter C. Smits, Patrick. W. Serruys, Yoshinobu Onuma, Robert Jan M. van Geuns. **Mid-term outcomes of the ABSORB BVS Versus Second-Generation DES: A Systematic Review and Meta-Analysis.** *PLoS One (in press).*

2. Jun-Mei Zhang, Dongsi Shuang, Lohendran Baskaran, Weijun Wu, Soo Kng Teo, Weimin Huang, Like Gobeawan, John Carson Allen, Ru San Tan, Xi Su, Nasrul Bin Ismail, Min Wan, Boyang Su, Hua Zou, Ris Low, Xiaodan Zhao, Yanling Chi, Jiayin Zhou, Yi Su, Aileen Mae Lomarda, Chee Yang Chin, **Jiang Ming Fam**, Felix Yung Jih Keng, Aaron Sung Lung Wong, Jack Wei Chieh Tan, Khung Keong Yeo, Philip En Hou Wong, Chee Tang Chin, Kay Woon Ho, Jonathan Yap, Ghassan S. Kassab, Terrance Siang Jin Chua, Tian Hai Koh, Swee Yaw Tan, Soo Teik Lim, Zhong Liang. **Advanced Analyses of Computed Tomography Coronary Angiography can Help Discriminate Ischemic Lesions.** Int J Cardiol. 2018 (in press).

3. Seng, Michael CH; Shen, Xiayan; Wang, Kangjie; Chong, Daniel TT; **Fam, Jiang Ming**; Hamid, Nadira; Amanullah, Mohammed Rizwan; Yeo, Khung Keong; Ewe, See Hooi; Chua, Terrance SJ; Ding, Zee Pin; Sahlen, Anders. **Allometric Relations for Cardiac Size and Longitudinal Function in Healthy Chinese Adults: Normal Ranges and Clinical Correlates.** Circulation Journal (in press).

4. **Jiang Ming Fam**, Cordula Felix, Yuki Ishibashi, Yoshinobu Onuma, Roberto Diletti, Nicolas M van Mieghem, Evelyn Regar, Peter de Jaegere, Felix Zijlstra, Robert J van Geuns **Impact of calcium on procedural and clinical outcomes in lesions treated with bioresorbable vascular scaffolds- A prospective BRS registry study.** Int J Cardiol. 2017 Dec 15;249:119-126. doi: 10.1016/j.ijcard.2017.08.046. Epub 2017 Aug 25.

5. **Jiang Ming Fam**, Peter Mortier, Matthieu De Beule, Tim Dezutter, Nicolas van Mieghem, Roberto Diletti, Bert Everaert , Soo Teik Lim, Felix Zijlstra, Robert-Jan van Geuns. **Defining optimal stent overexpansion strategies for left main stenting: insights from bench testing.** *AsiaIntervention 2017;3: 111-120, DOI: 10.4244/AIJ-D-16-00012.*

6. **Jiang Ming Fam**, Yuki Ishibashi, Cordula Felix, Bu Chun Zhang, Roberto Diletti, Nicolas van Mieghem, Evelyn Regar, Ron van Domburg, Yoshinobu Onuma, Robert-Jan van Geuns. **Conformability in everolimus-eluting bioresorbable scaffolds compared with metal platform coronary stents in long lesions.** *Int J Cardiovasc Imaging. 2017 Jul 6. doi: 10.1007/s10554-017-1193-0. [Epub ahead of print].*

7. C.M. Felix; G. J. Vlachojannis; A.J.J. IJsselmuiden; **J.M. Fam**,; P.C. Smits; W. Lansink; R. Diletti; F. Zijlstra; E.S. Regar; Eric Boersma; Y. Onuma; R.J.M van Geuns. **Potentially increased incidence of scaffold thrombosis in patients treated with Absorb BVS who terminated DAPT before 18 months.** *EuroIntervention. 2017 Jun 2;13(2):e177-e184. doi: 10.4244/EIJ-D-17-00119.*

8. **Jiang Ming Fam**, Marcella De Paolis, Roberto Garbo, Alfredo R. Galassi, Nicolas M. van Mieghem MD, Jors van der Sijde, Cordula Felix, Giacomo Giovanni Boccuzzi, Boukhris Marouane, Gennaro Sardella, Felix Zijlstra, Robert Jan van Geuns, Roberto Diletti. **Everolimus-eluting bioresorbable vascular scaffolds for treatment of complex chronic total occlusions.** *EuroIntervention. 2017 Jun 20;13(3):355-363. doi: 10.4244/EIJ-D-16-00253.*

9. Diletti R, Ishibashi Y, Felix C, Onuma Y, Nakatani S, van Mieghem NM, Regar E, Valgimigli M, de Jaegere PP, van Ditzhuijzen N, **Fam JM**, Ligthart JM, Lenzen MJ, Serruys PW, Zijlstra F, Jan van Geuns R. **Expanded clinical use of everolimus eluting bioresorbable vascular scaffolds for treatment of coronary artery disease.** Catheter Cardiovasc Interv. 2017 Jul;90(1):58-69. doi: 10.1002/ccd.26832. Epub 2016 Nov 29.

10. Bulluck H, Foin N, Carbrera-Fuentes HA, Yeo KK, Wong AS, **Fam JM**, Wong PE, Tan JW, Low AF, Hausenloy DJ. **Index of Microvascular Resistance and Microvascular Obstruction in Patients With Acute Myocardial Infarction.** JACC Cardiovasc Interv. 2016 Oct 24;9(20):2172-2174. doi: 10.1016/j.jcin.2016.08.018.

11. **Ming Fam J**, van Der Sijde JN, Karanasos A, Felix C, Diletti R, van Mieghem N, de Jaegere P, Zijlstra F, Jan van Geuns R, Regar E. **Comparison of acute expansion of bioresorbable vascular scaffolds versus metallic drug-eluting stents in different degrees of calcification: An Optical Coherence Tomography Study.** Catheter Cardiovasc Interv. 2017 Apr;89(5):798-810. doi: 10.1002/ccd.26676. Epub 2016 Oct 7. Erratum in: Catheter Cardiovasc Interv. 2017 Sep 1;90(3):530.

12. Felix CM, **Fam JM**, Diletti R, Ishibashi Y, Karanasos A, Everaert BR, van Mieghem NM, Daemen J, de Jaegere PP, Zijlstra F, Regar ES, Onuma Y, van Geuns RJ. **Mid- to Long-Term Clinical Outcomes of Patients Treated With the Everolimus-Eluting Bioresorbable Vascular Scaffold: The BVS Expand Registry.** JACC Cardiovasc Interv. 2016 Aug 22;9(16):1652-63. doi: 10.1016/j.jcin.2016.04.035.

13. Teo JC, Foin N, Otsuka F, Bulluck H, **Fam JM**, Wong P, Low FH, Leo HL, Mari JM, Joner M, Girard MJ, Virmani R. **Optimization of coronary optical coherence tomography imaging using the attenuation-compensated technique: a validation study.** Eur Heart J Cardiovasc Imaging. 2017 May 1;18(8):880-887. doi: 10.1093/ehjci/jew153.

14. De Paolis M, Felix C, van Ditzhuijzen N, **Fam JM**, Karanasos A, de Boer S, van Mieghem NM, Daemen J, Costa F, Bergoli LC, Ligthart JM, Regar E, de Jaegere PP, Zijlstra F, van Geuns RJ, Diletti R. **Everolimus-eluting bioresorbable vascular scaffolds implanted in coronary bifurcation lesions: Impact of polymeric wide struts on side-branch impairment.** Int J Cardiol. 2016 Oct 15;221:656-64. doi: 10.1016/j.ijcard.2016.06.153.

15. Ng J, Foin N, Ang HY, **Fam JM**, Sen S, Nijjer S, Petraco R, Di Mario C, Davies J,

Wong P. **Over-expansion capacity and stent design model: An update with contemporary DES platforms.** Int J Cardiol. 2016 Oct 15;221:171-9. doi: 10.1016/j.ijcard.2016.06.097.

16. Diletti R, van der Sijde J, Karanasos A, **Fam JM**, Felix C, van Mieghem NM, Regar E, Rapoza R, Zijlstra F, van Geuns RJ. **Differential thrombotic prolapse burden in either bioresorbable vascular scaffolds or metallic stents implanted during acute myocardial infarction: The snowshoe effect: Insights from the maximal footprint analysis.** Int J Cardiol. 2016 Oct 1;220:802-8. doi: 10.1016/j.ijcard.2016.06.077.

17. Felix CM, Onuma Y, **Fam JM**, Diletti R, Ishibashi Y, Karanasos A, Everaert BR, van Mieghem NM, Daemen J, de Jaegere PP, Zijlstra F, Regar ES, van Geuns RJ. **Are BVS suitable for ACS patients? Support from a large single center real live registry.** Int J Cardiol. 2016 Sep 1;218: 89-97. doi: 10.1016/j.ijcard.2016.05.037.

18. Zhang JM, Zhong L, Luo T, Lomarda AM, Huo Y, Yap J, Lim ST, Tan RS, Wong AS, Tan JW, Yeo KK, **Fam JM**, Keng FY, Wan M, Su B, Zhao X, Allen JC, Kassab GS, Chua TS, Tan SY. **Simplified Models of Non-Invasive Fractional Flow Reserve Based on CT Images.** PLoS One. 2016 May 17;11(5):e0153070. doi: 10.1371/journal.pone.0153070.

19. Sahlén A, Hamid N, Amanullah MR, **Fam JM**, Yeo KK, Lau YH, Lam CS, Ding ZP. **Impact of aortic root size on left ventricular afterload and stroke volume.** Eur J Appl Physiol. 2016 Jul;116(7):1355-65. doi: 10.1007/s00421-016-3392-0.

20. **Fam JM**, Felix C, van Geuns RJ, Onuma Y, Van Mieghem NM, Karanasos A, van der Sijde J, De Paolis M, Regar E, Valgimigli M, Daemen J, de Jaegere P, Zijlstra F, Diletti R. **Initial experience with everolimus-eluting bioresorbable vascular scaffolds for treatment of patients presenting with acute myocardial infarction: a propensity-matched comparison to metallic drug eluting stents 18-month follow-up of the BVS STEMI first study.** EuroIntervention. 2016 May 17;12(1):30-7. doi: 10.4244/EIJV12I1A6.

21. van der Sijde JN, Karanasos A, van Ditzhuijzen NS, Okamura T, van Geuns RJ, Valgimigli M, Ligthart JM, Witberg KT, Wemelsfelder S, **Fam JM**, Zhang B, Diletti R, de Jaegere PP, van Mieghem NM, van Soest G, Zijlstra F, van Domburg RT, Regar E. **Safety of optical coherence tomography in daily practice: a comparison with intravascular ultrasound.** Eur Heart J Cardiovasc Imaging. 2017 Apr 1;18(4):467-474. doi: 10.1093/ehjci/jew037.

22. **Fam JM**, den Dekker W, de Graaf P, Regar E. **An Unusual Case of Stent-in-Stent Thrombosis.** JACC Cardiovasc Interv. 2015 Dec 28;8(15):e261-2. doi: 10.1016/j.jcin.2015.07.039. No abstract available.

23. **Fam JM**, van der Sijde JN, Karanasos A, Zhang B, van Geuns RJ, Regar E. **Use of intracoronary imaging in ST Elevation Myocardial Infarction with coronary artery aneurysm and very late stent thrombosis.** Int J Cardiol. 2015 Oct 15;197:296-9. doi: 10.1016/j.ijcard.2015.05.087.

24. **Fam JM**, Karanasos A, Regar E, van Geuns RJ. **Bioresorbable vascular scaffold for ST elevation myocardial infarction: optical coherence tomography observations at the 2-year follow-up.** Coron Artery Dis. 2015 Sep;26(6):545-7. doi: 10.1097/MCA.0000000000000256.

25. Loh JP, Liu YC, Chew SW, Ong ES, **Fam JM**, Ng YY, Taylor MB, Ooi EE. **The rapid identification of Clostridium perfringens as the possible aetiology of a diarrhoeal outbreak using PCR.** Epidemiol Infect. 2008 Aug;136(8):1142-6.

(B) Non-refereed publications

(i) Reviews Articles

1. **Fam JM**, Ching CK et al. **Review on noninvasive risk stratification of Sudden Cardiac Death.** Singhealth Proceedings. 2011;20(4).

2. Ma YF, **Fam JM**, Zhang BC. **Critical analysis of the correlation between optical coherence tomography versus intravascular ultrasound and fractional flow reserve in the management of intermediate coronary artery lesion.** Int J Clin Exp Med. 2015 May 15;8(5):6658-67. Review.

3. Bu-Chun Zhang, **Jiang-Ming Fam**, Cheng Wang. **Clinical and angiographic outcomes of rotational atherectomy for patients with calcified coronary lesions: a meta-analysis of randomized and observational studies.** Int J Clin Exp Med 2016;9(2). Review.

4. **Jiang Ming Fam**; Robert-Jan van Geuns. **Implantation technique for Bioresorbable Scaffolds.** *Cardiac Interventions Today January 2017.*

(ii) Books & Chapters

1. **Jiang Ming Fam**, Nienke Simone van Ditzhuijzen, Jors van der Sjide, Antonios Karanasos, Robert-Jan van Geuns, Evelyn Regar. **Optical Coherence Tomography is the way to go.** Status: Published; Textbook on Bioresorbable Scaffolds: from basic concept to clinical application, Edited by Yoshinobu Onuma and Patrick W. Serruys Chapter 5.7 pages 177-187. (Textbook chapter).

2. Antonios Karanasos, Bu-Chun Zhang, Jors van der Sijde, **Jiang Ming Fam**, Robert-Jan van Geuns, Evelyn Regar. **Late and very late scaffold thrombosis.** Status: Published;

Textbook on Bioresorbable Scaffolds: from basic concept to clinical application, Edited by Yoshinobu Onuma and Patrick W. Serruys. Chapter 8.2 pages 421-430. (Textbook chapter).

3. MN AL-Qezweny, JN van der Sijde, **Jiang Ming Fam**, A Karanasos, BC Zhang, E Regar. **Optical Coherence Tomography in grafts.** Status: Published; Textbook on Coronary Graft Failure pp 539-554 In: Ţintoiu I., Underwood M., Cook S., Kitabata H., Abbas A. (eds). Springer, Cham. (Textbook chapter).

4. **Jiang Ming Fam**, Khung Keong Yeo. **Complex case: Severe Diffuse LAD Disease.** Status: Published; Clinical Cases in Coronary Rotational Atherectomy: Complex Cases and Complications (edited by Reginald Low and Khung Keong Yeo). (Textbook chapter).

5. **Jiang Ming Fam**, Khung Keong Yeo. **Complication: No Reflow.** *Status: Published;* Clinical Cases in Coronary Rotational Atherectomy: Complex Cases and Complications (edited by Reginald Low and Khung Keong Yeo). (Textbook chapter).

(iii) Selected abstracts

1. **Fam JM**, Lay Wai Khin, David Kheng Leng Sim, Kah Leng Ho, Reginald Liew, Wee Siong Teo, Chi Keong Ching. **A descriptive prevalence study on patients with reduced ejection fraction in Singapore.** Poster abstract. Asian Congress of Heart Failure October 2010, Busan Korea.

2. **Fam JM**, Tan BY, Reginald Liew, Daniel Chong, Teo WS, David Sim, Ching CK. **Predictors of 2-year mortality rate and cumulative MACE in Asian patients with ejection fraction ≤ 40%.** Poster abstract. Asian Congress of Heart Failure October 2010 Busan, Korea.

3. **Fam JM**, Tan BY, Reginald Liew, Daniel Chong, Teo WS, Ching CK. **Electrophysiological Characteristics of Patients who undergo Two or more ablations for Atrial Fibrillation.** Poster abstract. Asia Pacific Heart Rhythm Society October September 2011 Fukuoka, Japan.

4. **Fam JM**, Tan BY, Reginald Liew, Daniel Chong, Ching CK, Teo WS. **Magnetic stereotaxis in complex congenital heart disease (CHD) and tachyarrthymias- a single centre experience.** Oral abstract. Singapore Cardiac Society Annual Scientific Meeting January 2012.

5. **Fam JM**, Tan BY, Reginald Liew, Daniel Chong, Ching CK, Teo WS. **Effect of magnetic stereotaxis on procedure and fluoroscopy times in catheter based electrophysiological ablation of atrial flutter in atrial septal defects- a single centre experience.** Poster abstract. Asia Pacific Heart Rhythm Society October 2012 Taipei, Taiwan.

6. **Fam JM**, Tan BY, Reginald Liew, Daniel Chong, Ching CK, Teo WS. **Remote Magnetic Navigation and ablation in patients with congenital heart disease (CHD) and tachyarrhythmias.** Poster abstract. Asia Pacific Heart Rhythm Society October 2012 Taipei, Taiwan.

7. **Fam JM**, KK Yeo, YH Lau, James Cai, LL Sim, ST Lim, T SJ Chua, TH Koh. **Clinical characteristics and 1-year readmission rates, length of stay, cost and mortality for men and women undergoing percutaneous coronary intervention.** Abstract. ASIA-PCR 2012, Singapore.

8. KK Yeo, **Fam JM**, YH Lau, James Cai, LL Sim, ST Lim, T SJ Chua, TH Koh. **Comparison of clinical characteristics, 1-year readmission rates, cost and mortality amongst patients undergoing percutaneous coronary intervention for stable angina, acute coronary syndromes and ST-elevation myocardial infarction.** Abstract. ASIA-PCR 2012, Singapore.

9. **Fam JM**, KK Yeo, YH Lau, James Cai, LL Sim, ST Lim, T SJ Chua, TH Koh. **Outcomes, outpatient costs and adherence to guideline guided therapy in SAP, ACS and STEMI patients undergoing percutaneous coronary intervention (PCI).** Poster abstract. European Society of Congress (ESC), Munich, Germany. Aug 2012.

10. James Cai, KK Yeo, **Fam JM**, YH Lau, , LL Sim, ST Lim, T SJ Chua, TH Koh. **Ethnicity, outcomes, outpatient costs and adherence to guideline guided therapy in patients undergoing percutaneous coronary intervention (PCI).** Poster abstract. European Society of Congress (ESC), Munich, Germany. Aug 2012.

11. **Fam JM**, KK Yeo, YH Lau, James Cai, LL Sim, ST Lim, T SJ Chua, TH Koh. **Outcomes, outpatient costs and adherence to guideline guided therapy in patients with left ventricular ejection fraction <=40% undergoing percutaneous coronary intervention (PCI).** International Academy of Cardiology, 17th World Congress on Heart Disease, Annual Scientific Sessions, Toronto, ON, Canada. Poster abstract. July 2012.

12. **Fam JM**, KK Yeo, YH Lau, James Cai, LL Sim, ST Lim, T SJ Chua, TH Koh. **Predictors of nonadherence to guideline recommended therapy and outcomes in patients undergoing PCI.** International Academy of Cardiology, 17th World Congress on Heart Disease, Annual Scientific Sessions,Toronto, ON, Canada. Poster abstract. July 2012.

13. **Fam JM**, KK Yeo, YH Lau, James Cai, LL Sim, ST Lim, T SJ Chua, TH Koh. **Impact of subsidy level on outcomes and adherence to guideline recommended therapy in patients undergoing PCI.** Poster abstract. Duke-NUS Scientific Congress, Singapore. Aug 2012.

14. James Cai, KK Yeo, **Fam JM**, YH Lau, , LL Sim, ST Lim, T SJ Chua, TH Koh. **Ethnicity, outcomes, outpatient costs and adherence to guideline recommended therapy in patients undergoing percutaneous coronary intervention.** Poster abstract. Duke-NUS Scientific Congress, Singapore. Aug 2012.

15. **Fam JM**, KK Yeo, YH Lau, James Cai, LL Sim, ST Lim, T SJ Chua, TH Koh. **Guideline recommended therapy and outcomes in patients undergoing PCI in**

Singapore. Poster abstract. Asean Federation of Cardiology Congress, Singapore. 12-15 July 2012.

16. **Fam JM**, KK Yeo, YH Lau, James Cai, LL Sim, ST Lim, TH Koh, T SJ Chua. **Outcomes and predictors of 1 year all-cause mortality in patients undergoing percutaneous coronary intervention (PCI).** Abstract. ASIA- PCR January 2013.

17. **Fam JM**, KK Yeo, YH Lau, James Cai, LL Sim, ST Lim, TH Koh, T SJ Chua. **Racial differences in outcomes and predictors of 1 year all-cause mortality in patients undergoing percutaneous coronary intervention (PCI).** Poster abstract. ASIA- PCR January 2013.

18. Xinzhe James Cai, KK Yeo, **JM Fam**, YH, Lau, LL So,, ST Lim, TH Koh, T Chua SJ. **Gender differences in outcomes and predictors of 1 year all-cause mortality in patients undergoing percutaneous coronary intervention (PCI).** Abstract. ASIA- PCR January 2013.

19. **Fam JM**, KK Yeo, YH Lau, James Cai, LL Sim, ST Lim, TH Koh, T SJ Chua. **Angiographic characteristics of patients who underwent percutaneous coronary intervention- a single registry experience.** Poster abstract. SGH Annual Scientific Meeting April 2013.

20. **Jiang Ming Fam**, Chun Yuan Khoo, Jonathan Yap, Khung Keong Yeo, Xinzhe James Cai, Yee How Lau, Ling Ling Sim, Soo Teik Lim, Terrance Siang Jin Chua, Tian Hai Koh. **Clinical outcome in dialysis patients who underwent percutaneous coronary intervention.** Poster abstract. WCC Melbourne 2014.

21. **Jiang Ming Fam**, Rena Lim Cai Zuan, Yee How Lau, Kay Woon Ho, Chee Tang Chin, Paul Toon Lim Chiam, Khung Keong Yeo, Jack Wei Chieh Tan, Soo Teik Lim, Tian Hai Koh, Aaron Sung Lung Wong. **Angiographic Characteristics and Clinical outcomes of the use of Dual Therapy Stent.** Poster abstract. TCTAP 2014. (Best poster award).

22. **Jiang Ming Fam**, Paul Lim, Lohendran Baskaran, Daniel Chong, Boon Yew Tan, Kah Leng Ho, Reginald Liew, Wee Siong Teo, Chi Keong Ching. **Prevalence of high DFT (Defibrillation Threshold) in Singapore.** Poster abstract. Asia Pacific Heart Rhythm Society October 2012 Taipei, Taiwan.

23. Paul Lim, **Jiang Ming Fam**, Lohendran Baskaran, Daniel Chong, Boon Yew Tan, Kah Leng Ho, Reginald Liew, Wee Siong Teo, Chi Keong Ching. **Defibrillation threshold testing using a step up, one shock testing protocol commencing at 10J shock energy.** Poster abstract. Asia Pacific Heart Rhythm Society October 2012 Taipei, Taiwan.

24. **Jiang Ming Fam**, Paul Lim, Lohendran Baskaran, Daniel Chong, Boon Yew Tan, Kah Leng Ho, Reginald Liew, Wee Siong Teo, Chi Keong Ching. **Defibrillation threshold testing using a step up, one shock testing protocol commencing at 10J shock energy in patients with low ejection fraction.** Poster abstract. Asia Pacific Heart Rhythm Society October 2012 Taipei, Taiwan.

25. **Jiang Ming Fam**, Antonios Karanasos, Roberto Dilleti, Nicolas van Mighem, Marco Valgimigli, Floris Kauer, Peter de Jaegere, Felix Zijlstra , Robert Jan van Geuns, Evelyn Regar. **Does lesion calcification affect expansion of bioresorbable scaffolds? - An optical coherence tomography study in calcified and non-calcified lesions.** Oral abstract. ASIAPCR 2015.

26. **Jiang Ming Fam**, Peter Mortier, Matthieu De Beule, Tim Dezutter, Nicolas van Mieghem, Roberto Diletti, Bert Everaert , Soo Teik Lim, Felix Zijlstra, Robert-Jan van Geuns. **Defining Optimal Stent Overexpansion Strategies for Left Main PCI- Insights from bench testing.** Poster abstract. CRT 2015.

27. **Jiang Ming Fam**, Yuki Ishibashi, Cordula Felix, Bu Chun Zhang, Roberto Diletti, Nicolas van Mieghem, Evelyn Regar, Ron van Domburg, Yoshinobu Onuma, Robert- Jan van Geuns. **A Study Of Conformability in Everolimus-eluting Bioresorbable Vascular Scaffolds to Metal Platform Coronary Stents in Long Lesions.** Poster abstract. CRT 2015.

28. **Jiang Ming Fam**, Jors N. Van der Sijde, Antonios Karanasos, Roberto Dilleti, Nicolas van Mighem, Marco Valgimigli, Floris Kauer, Peter de Jaegere, Felix Zijlstra , Robert Jan van Geuns, Evelyn Regar. **Differences in stent/scaffold expansion between everolimus-eluting bioresorbable scaffolds and metallic drug-eluting stents in calcified lesions- An optical coherence tomography study.** Oral abstract. EuroPCR 2015.

29. Antonios Karanasos, Nicolas M. Van Mieghem, Hector Garcia-Garcia, Roberto Diletti, Cordula Felix, Jors N. van der Sijde, **Jiang-Ming Fam**, Yuki Ishibashi,Peter De Jaegere, Patrick W. Serruys, Yoshinobu Onuma, Felix Zijlstra, Evelyn Regar, Robert J. Van Geuns. **Incidence of persistent, resolved, and late incomplete scaffold apposition after bioresorbable scaffold implantation in ST-segment elevation myocardial infarction. A BVS-STEMI-first substudy.** Poster abstract. *Oct 2015. TCT* **J Am Coll Cardiol**. *2015;66(15_S):. doi:10.1016/j.jacc.2015.08.546.*

30. **Jiang-Ming Fam**, Yoshinobu Onuma, Cordula Felix, Roberto Diletti, Nicolas M. Van Mieghem, Evelyn Regar, Peter De Jaegere, Felix Zijlstra, Robert J. Van Geuns . **Impact of postdilation on procedural and clinical outcomes in long and complex lesions treated with bioresorbable vascular scaffolds- a prospective registry study.** Poster abstract. *TCT, Oct 2015.* **J Am Coll Cardiol**. *2015;66(15_S):. doi:10.1016/j.jacc.2015.08.557.*

31. Cordula Felix, **Jiang-Ming Fam**, Yoshinobu Onuma, Yuki Ishibashi, Bert Everaert, Roberto Diletti, Evelyn Regar, Nicolas M. Van Mieghem, Joost Daemen, Peter De Jaegere, Felix Zijlstra, Robert J. Van Geuns. **Long-term Clinical Outcomes of Patients Treated With The Everolimus-eluting Bioresorbable Vascular Scaffold. The BVS Expand Study**. Poster abstract. *TCT · Oct 2015.* **J Am Coll Cardiol**. 2015;66(15_S):. doi:10.1016/j.jacc.2015.08.544.

32. De Paolis, **Fam JM**, Felix , Karanasos, Van mieghem N., Daemen, Costa, Bergoli, Ligthart J., De jaegere P., Regar , Zijlstra , Van geuns , Diletti R.. **Everolimus-eluting BRS implanted in coronary bifurcation lesions: impact of polymeric**

wide struts on side-branch impairment. Oral Abstract. *EuroPCR 2016.*

33. **Fam JM**, De paolis, Garbo, Ojeda, Galassi A., Van Mieghem, Van der sijde, Cordula Felix, Pan, Boccuzzi, Marouane, Mardella, Zijlstra, Van geuns, Diletti R. **Everolimus-eluting BRS for treatment of complex CTO.** Oral Abstract. *EuroPCR 2016.*

34. **Fam JM**, Van der sijde, Karanosos, Van mieghem N., Onuma, Felix, De paolis, Regar, Valgimigli, Daemen, De jaegere, Rapoza , Zijlstra, Van geuns, Diletti R. **Everolimus-eluting BRS vs. metallic DES for treatment of patients presenting with acute myocardial infarction: insights from the maximal footprint analysis.** Oral Abstract. EuroPCR 2016.

35. SB. Tai, WR. Lau, **JM. Fam**, N. Hamid, MR. Amanullah, YH. Lau, KK. Yeo, ZP. Ding, A. Sahlen. **Prediction of short-term mortality in ST-elevation myocardial infarction: the echocardiographic index E/e' is robust, powerful and specific.** Poster abstract. ESC 2016.

36. Tomaniak M, Felix C, **Fam JM**, van Geuns RJ, Van Mieghem Nicolas M, Regar E, Daemen J, de Jaegere P, Zijlstra F, Diletti R. **Feasibility of direct scaffolding in acute coronary syndromes patients with relatively simple non-calcified culprit lesions. A pooled analysis of BVS STEMI First and BVS Expand Studies.** Poster Abstract. TCT 2016.

37. Tomaniak M, **Fam JM**, Felix C, van Geuns RJ, Van Mieghem Nicolas M, Regar E, Daemen J, de Jaegere P, Zijlstra F, Diletti R. **Impact of scaffold oversizing, under-expansion and post-dilatation on acute angiographic and one year clinical outcomes in patients with ACS treated with bioresorbable vascular scaffolds.** Poster Abstract. TCT 2016.

38. Tomaniak M, Felix C, **Fam JM**, van Geuns RJ, Van Mieghem Nicolas M, Regar E, Daemen J, de Jaegere P, Zijlstra F, Diletti R. **Impact of optimal implantation technique on bioresorbable scaffold expansion and one-year clinical outcomes in patients presenting with acute coronary syndromes and calcified lesions. A pooled analysis of BVS STEMI First and BVS Expand Studies.** Poster abstract. TCT 2016.

39. Tomaniak M, **Fam JM**, Felix C, van Geuns RJ, Van Mieghem Nicolas M, Regar E, Daemen J,de Jaegere P, Zijlstra F, Diletti R. **Long-term clinical outcomes after implantation of everolimus-eluting bioresorbable vascular scaffold in patients with acute myocardial infarction. 24-month clinical follow-up of the BVS STEMI First Study**. Poster abstract. TCT 2016.

40. Tomaniak M, **Fam JM**, Felix C, Yoshinobu Ouma, van Geuns RJ, Joost Daemen, de Jaegere P, Van Mieghem Nicolas M, Zijlstra F, Diletti R. **Impact of bioresorbable scaffold-specific implantation technique on device expansion in acute coronary syndromes. A pooled analysis from BVS STEMI First and BVS EXPAND studies.** Poster abstract. EuroPCR 2017.

41. Tomaniak M, Felix C**, Fam JM**, Yoshinobu Ouma, van Geuns RJ, Joost Daemen, de Jaegere P, Van Mieghem Nicolas M, Zijlstra F, Diletti R. **BRS expansion impact on acute and one-year clinical outcomes in ACS. A pooled analysis from BVS STEMI First and BVS EXPAND studies.** Oral abstract EuroPCR 2017.

42. Zhang JM, Wu W, Chin CY, Fam JM, Keng FYJ, Ismail NB, Yap J, Wong ASL, Chin CT, Ho KW, Koh TH, Tan JWC, Yeo KK, Zhao X, Leng S, Wong PEH, Chua TSJ, Tan RS, Tan SY, Lim ST, Zhong L. **Diagnostic performance of non-invasive fractional flow reserve with reduced-order computational fluid dynamics simulation on detecting ischemic coronary lesions.** Abstract. APSC 2017.

43. CM. Felix, A. Coenen, MM. Lubbers, Y. Onuma, **JM. Fam**, R. Diletti, E. Regar, F. Zijlstra, H. El Addouli, KN Nieman, R-J M. Van Geuns. **Computed Tomography Coronary Angiography Long-term Results of Bioresorbable Vascular Scaffold in clinical practice.** A BVS-Expand project. Oral Abstract ESC 2017.

44. CM. Felix, **JM. Fam**, R. Diletti, Y Ishibashi, A Karanasos, BRS Everaert, NM van Mieghem, J Daemen, PPT de Jaegere, F. Zijlstra, ES Regar, Y Onuma, R-J M. Van Geuns. **Three-year Clinical Outcomes of the BVS Expand Registry.** Oral Abstract ESC 2017.

45. Mariusz Tomaniak, Cordula Felix, **Jiang Ming Fam**, Nicolas Van Mieghem, Evelyn Regar, Joost Daemen, Jeroen Wilschut, Peter P.T. De Jaegere, Felix Zijlstra, Yoshinobu Onuma, Roberto Diletti, Robert-Jan van Geuns. **Angina frequency and quality of life after implantation of bioresorbable scaffold implantation in complex lesions.** Poster Abstract.TCT 2017.

46. Mariusz Tomaniak, Cordula Felix, **Jiang Ming Fam**, Nicolas Van Mieghem, Evelyn Regar, Joost Daemen, Jeroen Wilschut, Peter P.T. De Jaegere, Felix Zijlstra, Yoshinobu Onuma, Roberto Diletti, Robert-Jan van Geuns. **Impact of diabetes on angina frequency and health status outcomes after bioresorbable scaffold implantation.** Poster abstract. TCT 2017.

47. Lai Heng Lee, Ming Chai Kong, Isabelle Teo, Shun Wei Lim, Jin Shing Hon, Kelly Bee Ling Chng, Sing Lin Tee, Elicia Purnata, Clifton You Xuan Liew , Xin Hui Loh, Cui Mei Fong, Nirmali Ruth Sivapragasam, Yiong Huak Chan, **Jiang Ming Fam**, Heng Joo Ng, Marcus Ong, David Bruce Matchar. **Optimal International Normalized Ratio Range for Asian Patients on Anticoagulation Therapy.** Poster abstract. American Society of Haematology 2017.

48. **Jiang-Ming Fam**, Cordula Felix, Yuki Ishibashi, Yoshinobu Onuma, Roberto Diletti, Nicolas M Van Mieghem, Evelyn Regar, Peter De Jaegere, Felix Zijlstra, Robert J Van Geuns. **Impact of postdilation on procedural and clinical outcomes in complex lesions treated with bioresorbable vascular scaffolds- a prospective registry study.** Poster abstract. EuroPCR 2018.

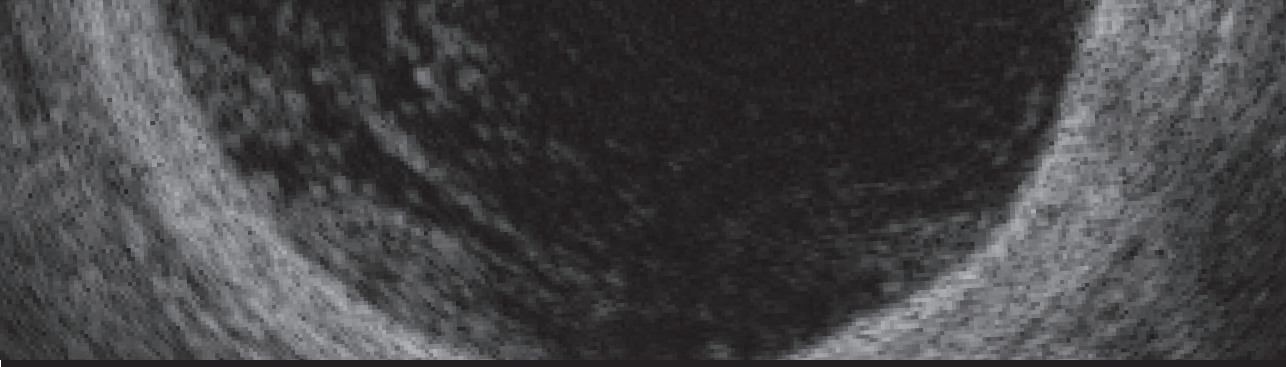

ACKNOWLEDGEMENTS

Acknowledgements

It's almost 4 years to the day since I first set foot here in Netherlands from my tiny island nation of Singapore for my fellowship in interventional cardiology and indeed it was one of the most amazing and fulfilling years I have ever experienced. I have learnt so much from everyone and I am truly grateful beyond words for all the help and guidance given to me.

Prof Robert-Jan, Many thanks for believing in me and giving me the opportunity to complete my fellowship at this world renowned academic centre of excellence. It was my blessing and good fortune to have the greatest mentor anyone can ever wished for. Because of your extraordinarily intellect and clinical and scientific experience, you were always able to give the right insights in difficult situations. You have been a solid beacon of hope as I embark on this unpredictable journey. I shall never forget the long hours in the office discussing our research and the hours on skype in unearthly hours separated by distance and space. I deeply appreciate the program you have set up for me- the scope of research (left main intervention, intravascular imaging, bioresorbable vascular scaffolds etc) and clinical exposure (be it CCU rotation, clinical and cath rounds, clinic sessions or MRI/CT imaging rounds) is beyond anything I can dream of or ask for. The Erasmus program allowed me to strengthen my interventional experience and enable me to acquire new insights into how imaging has developed so much to be a distinct yet integral part of interventional cardiology. I am truly humbled by your intellect, depth of knowledge in both imaging and interventional related fields and keen sense of judgement and perspective during your paper review sessions. With the benefit of your guidance and perspicacity, the ideas and concepts I learnt from working on the projects in left main intervention/ BRS/ intracoronary imaging really transformed my way of looking at interventional research in such a profound and arcane manner beyond my imagination. Indeed I have learnt a great deal from the fellowship and you are indeed the best mentor any fellow can have.

Herewith, I would also like to introduce my boss, mentor Prof Lim Soo Teik (National Heart Centre, Singapore). I must thank you for giving me the chance to move to Rotterdam from Singapore. I shall never forget the long hours we spent together in the Cath Lab and how your patience and skill inspired me to be a better operator. My next goal is to further improve three important components of NHCS (ie clinical work, acaedemic research and education).

Dr Regar, I consider myself extremely fortunate to be given the chance to learn from you through our OCT research project in calcified lesions and I cannot think of anyone else more suitable and better to learn intravascular imaging from. She was immediately friendly and she explained to me the concepts of OCT and interpretation. I learnt from her the fundamentals of intravascular imaging and how to make presentations to bring our messages across. Prior to my fellowship, I had minimal experience in OCT and now through working on the project, the book chapter and a series of short papers, I have learnt and understood more about the potential of what this innovative technology can bring. I look forward to working with you in other related

projects in the near future. I shall never forget the weekly tutorials we had in which through your patience and teachings, I now learnt more about OCT and feel more confident in OCT image interpretation.

Dr Diletti, you are an amazing person to work with and one of the best research mentors any fellow can ask for. I am truly inspired by your enthusiasm, never give up attitude and belief in always striving for the very best. Many thanks for giving me the opportunity to collaborate on the CTO and STEMI projects. I shall look back, will recall and miss fondly those late evening and weekend sessions which in retrospect were among the most memorable times of the posting when we discuss how to push through our projects in a way I never thought was possible. Hope to keep in touch and continue our collaboration anytime (including weekends).

Dr Yoshi, you have been most helpful and friendly helping me to settle in quickly during the first few weeks in Cardialysis and Thorax centre and I really appreciate your time and willingness to help in my projects despite your most hectic schedule in managing your work in both Cardialysis and Thorax centre. I have learnt a great deal from statistics and will miss those times with you and Yuki in Cardialysis.

Drs Antonios, Jors, Marcella, Cordula, Buchun and Nienke, you guys are the best bunch of fellows to work with. No words of gratitude can fully express my deepest appreciation for the countless times I had to ask you guys for help especially Antonios and Jors. Be it from the most basic stuff in Dutch translation of medical reports and writing my own resume in Dutch (and we now learnt the difference between solitary and lonesome nodules...!), to more complex requests such as SPSS tips, excel macros and programs and even photoshop editing skills, I can always count on you guys for support. You guys are one the most helpful group of fellows to work with - and it is no exaggeration to state that virtually each time I request for assistance, you guys managed to sacrifice your precious time to deliver on my requests despite your own challenges and difficulties to finish your own projects- for that I am truly grateful and deeply appreciative. I will also miss those lunch breaks, late night dinners and drink sessions as well. I have a fond recollection of the light hearted batter and conversation topics we engage in during lunch breaks and the occasional office tea break chats- I will always remember the enjoyment and laughter we have in between the monotony of work. Buchun, I will miss those weekend sessions and chats we have over projects! To an overseas fellow like me, you guys form a close social circle of friends I have and this really form an integral and memorable time of a fellowship experience. All the best to your thesis and your residencies too. Nienke, it was great to work with you in the beginning too; all the best to your medical education and I look forward to hearing of your graduation.

Marcella, it was great to work and collaborate with you during the last few months and I am grateful for your help in translating the Italian reports! Thank you for your dinner- you were a great cook and all the best to your fellowship too.

Cordula, you are a great lady to work with and despite your own challenges of managing your family, I can always count on you for speedy and reliable support for our databases and related projects. You are an inspiration for young working mothers who can show it is possible to have a successful career in medicine while balancing the demands of a young family. All the best for your thesis and starting your young family.

Jurghen and Karen, you guys are a great and friendly bunch to work with and I am always in awe and humbled by your wealth of experience as you wax lyrical about the events that occurred in intravascular imaging. Many thanks for helping me to settle in quickly when I started my office as well as for your patience and keenness in your teachings while guiding me in IVUS and OCT image interpretation.

I would like to thank all the fellows and young cardiologists that have worked in the cath lab in Erasmus Medical Centre as well as National Heart Centre Singapore. It is my honour and joy to be able to share with you what I know about our wonderful profession. As I teach, I still learn and you make me a better operator because I always try to give you the best example to follow.

I would like to thank the people I met in Cardialysis, Professor Serruys, Drs Yuki, Pannipa and Shimpei. They were very friendly and patient in teaching and guiding me from the first few days I stepped foot in Rotterdam.

I would like to thank Elles and Yee How who has so patiently helped me with the necessary documentation, biostatistical support and logistics for the thesis though I was already back in Singapore.

Finally my special thanks to my parents, spouse and children especially Joyce, and my mother in law, who were so dedicated and had to fulfil so many roles while looking after our children while I was away. Our three precious ones -- Enrui, Enyi and Enqi are my most profound joy and I dare say among the best things that have ever occurred to me. All my problems vanish instantly when I return home and I see them smiling and running. I hope I will be a good father for them as they represent the true meaning of my life.

Best Regards

Jiang Ming Fam
May 2018